3 Overconstrained *T3*-type TPMs with coupled motions

T3-type TPMs are translational parallel robotic manipulators with three degrees of connectivity between the moving and fixed platforms $S_F = 3$. They give three translational velocities $\boldsymbol{v}_1$, $\boldsymbol{v}_2$ and $\boldsymbol{v}_3$ in the basis of the *operational* velocity *vector space* $(R_F) = (\boldsymbol{v}_1,\boldsymbol{v}_2,\boldsymbol{v}_3)$ along with a constant *orientation* of the moving platform.

Equation (1.16) indicates that *overconstrained* solutions of *T3*-type translational parallel robots with coupled motions and q independent loops meet the condition $\sum_1^p f_i < 3 + 6q$. Various solutions fulfil this condition along with $S_F = 3$, $(R_F) = (\boldsymbol{v}_1,\boldsymbol{v}_2,\boldsymbol{v}_3)$ and the number of overconstraints $N_F \geq 1$.

T3-type translational parallel robots may have identical limbs or limbs with different structures and could be actuated by linear or rotating motors. The limbs can be simple or complex kinematic chains and can combine idle mobilities.

In these solutions, the three *operational velocities* given by Eq. (1.19) depend, in the general case, on the three actuated joint velocities: $v_i = v_i(\dot{q}_1,\dot{q}_2,\dot{q}_3)$, $i = 1,2,3$. In some specific solutions, each operational velocity depends on at least two actuated joints. We note that, in this particular case, the Jacobian matrix in Eq. (1.19) is not triangular and the parallel robot always has *coupled motions*. They have just a few partially decoupled motions.

The actuators can be mounted on the fixed base or on a moving link. The first solution has the advantage of reducing the moving masses and large workspace. The second solution would be more compact.

Basic and derived solutions are presented in this section. No idle mobilities exist in the *basic solutions*. The *derived solutions* are obtained from the basic solutions by combining various idle mobilities.

We limit our presentation in this section to the solutions with just three limbs. A large set of solutions with an additional unactuated limb can also be obtained by combining an unactuated limb presented in Figs. 7.1–7.11 – Part 1 with other three limbs with $4 \leq M_{Gi} = S_{Gi} \leq 6$ that integrate velocities $\boldsymbol{v}_1$, $\boldsymbol{v}_2$ and $\boldsymbol{v}_3$ in the basis of their operational space.

G. Gogu, *Structural Synthesis of Parallel Robots: Part 2: Translational Topologies with Two and Three Degrees of Freedom,* Solid Mechanics and Its Applications 159, 107–363.

3.1 Basic solutions with linear actuators

In the *basic solutions* of the *T3*-type TPMs with *linear actuators* and coupled motions $F \leftarrow G_1$–G_2–G_3, the moving platform $n \equiv n_{Gi}$ ($i = 1, 2, 3$) is connected to the reference platform $1 \equiv 1_{Gi} \equiv 0$ by three limbs with three or four degrees of connectivity. No idle mobilities exist in these basic solutions and the linear actuators are combined in a prismatic pair of each limb.

The various types of limbs with three degrees of connectivity are systematized in Fig. 3.1. They integrate one (Fig. 3.1a–d) or two (Fig. 3.1e–g) parallelogram loops or a prism mechanism (Fig. 3.1h). These limbs are actuated by linear motors mounted on the fixed base. We recall that the parallelogram loop Pa^{cc} and the prism mechanism *Pr* have two degrees of mobility.

The various types of limbs with four degrees of connectivity are systematized in Figs. 3.2 and 3.3. They are simple (Fig. 3.2) or complex (Fig. 3.3) kinematic chains and can be actuated by linear motors mounted on the fixed base.

Examples of simple or complex limbs with four degrees of connectivity that can be actuated by linear actuators mounted on a moving link are presented in Figs. 3.4 and 3.5. The prismatic joints between links 2 and 3 (Fig. 3.4a, b and e–g) and 3 and 4 (Fig. 3.4c, d) must be actuated to obtain solutions with coupled motions. If the prismatic joint adjacent to the fixed base (Fig. 3.4c, d) or between links 2 and 3 (Fig. 3.4d) is actuated, solutions with uncoupled motions can be obtained as shown in the following sections. The same is true when the translation in the cylindrical joint is actuated in Fig. 3.4f. The prismatic joint can be actuated in Fig. 3.5a–d.

The cylindrical joint in Figs. 3.2e, f, 3.4e, f and 3.5e replaces the combination of two successive revolute and the prismatic joints with the same axis/direction of types $R||P$ and $P||R$ (see Figs. 3.2a–d, 3.4a–d and 3.5c, d). The limbs in Figs. 3.3 and 3.5 combine a *Pa*-type parallelogram loop.

Various solutions of translational parallel robots with coupled motions and no idle mobilities can be obtained by using three limbs with identical or different topology presented in Figs. 3.1–3.5. We only show solutions with identical limb type as illustrated in Figs. 3.6–3.23. The limb topology and connecting conditions in these solutions are systematized in Tables 3.1 and 3.2.

The actuated prismatic joints adjacent to the fixed base in the three limbs have orthogonal directions (Figs. 3.6–3.11) in the solutions using the limbs systematized in Fig. 3.1. The structural parameters of the solutions in Figs. 3.6–3.11 are systematized in Table 3.3.

The directions of the three actuated prismatic joints adjacent to the fixed base can be orthogonal (Fig. 3.12) or parallel (Figs. 3.13 and 3.14) when the limbs in Fig. 3.2 are used. They can be coplanar (Fig. 3.15a) or orthogonal in space (Fig. 3.15b) when the limbs in Fig. 3.3a, b are used. The axes of the three unactuated revolute or cylindrical joints adjacent to the moving platform can be orthogonal in space (Figs. 3.12 and 3.15b) or coplanar (Figs. 3.13, 3.14 and 3.15a). The three coplanar axes can form a planar star (Fig. 3.15a), a triangle (Figs. 3.13a, 3.14a and 3.15a), or can be situated on three sides of a rectangle (Figs. 3.13b and 3.14b). The axes of the unactuated joints adjacent to the moving platform form a configuration called a spatial star, if they are orthogonal in space, and planar star, Δ or $\amalg$ if they are coplanar. The structural parameters of the solutions in Figs. 3.12–3.17 are systematized in Tables 3.4 and 3.5.

The solutions based on the use of limb topologies presented in Figs. 3.4 and 3.5 have the linear actuators non adjacent to the fixed base. In these solutions, the axes/directions of the first unactuated joint in the three limbs can be orthogonal in space (Figs. 3.18, 3.21–3.23) or coplanar (Figs. 3.19 and 3.20). The three coplanar axes can also be in a Δ (Figs. 3.19a and 3.20) or a $\amalg$ (Fig. 3.19b) configuration. The first unactuated joint can be a revolute (Figs. 3.18a and 3.19), a prismatic (Fig. 3.21) or a cylindrical joint (Figs. 3.18b and 3.20). The structural parameters of the solutions in Figs. 3.18–3.23 are systematized in Table 3.6.

Table 3.1. Limb topology and connecting conditions of the TPM with no idle mobilities and linear actuators mounted on the fixed base presented in Figs. 3.6–3.17

No.	TPM type	Limb topology	Connecting conditions
1	*3-$\underline{P}$PaP* (Fig. 3.6)	$\underline{P} \perp Pa \| \| P$ (Fig. 3.1a)	Actuated $\underline{P}$ joints with orthogonal directions
2	*3-$\underline{P}$PPa* (Fig. 3.7)	$\underline{P} \perp P \| \| Pa$ (Fig. 3.1b)	Idem No. 1
3	*3-$\underline{P}Pa^{cc}$* (Figs. 3.8 and 3.9)	$\underline{P} \perp Pa^{cc}$ (Fig. 3.1c, d)	Idem No. 1
4	*3-$\underline{P}$PaPa* (Fig. 3.10a)	$\underline{P} \perp Pa \perp^{\perp} Pa$ (Fig. 3.1e)	Idem No. 1
5	*3-$\underline{P}$PaPa* (Fig. 3.10b)	$\underline{P} \perp Pa \perp^{\|} Pa$ (Fig. 3.1f)	Idem No. 1
6	*3-$\underline{P}$PaPa* (Fig. 3.11a)	$\underline{P} \| \| Pa \perp Pa$ (Fig. 3.1g)	Idem No. 1
7	*3-$\underline{P}$Pr* (Fig. 3.11b)	$\underline{P}$-*Pr* (Fig. 3.1h)	Idem No. 1
8	*3-$\underline{P}$RC* (Fig. 3.12a)	$\underline{P} \perp R \| \| C$ (Fig. 3.2e)	Idem No. 1
9	*3-$\underline{P}$CR* (Fig. 3.12b)	$\underline{P} \perp C \| \| R$ (Fig. 3.2f)	Idem No. 1
10	*3-$\underline{P}$RC* (Fig. 3.13a, b)	$\underline{P} \perp R \| \| C$ (Fig. 3.2e)	Actuated $\underline{P}$ joints with parallel directions
11	*3-$\underline{P}$CR* (Fig. 3.14a, b)	$\underline{P} \perp C \| \| R$ (Fig. 3.2f)	Idem No. 10
12	*3-$\underline{P}$RPaR* (Fig. 3.15a)	$\underline{P} \| \| R \perp Pa \perp^{\|} R$ (Fig. 3.3a)	Actuated $\underline{P}$ joints with coplanar directions (planar star configuration)
13	*3-$\underline{P}$RPaR* (Fig. 3.15b)	$\underline{P} \perp R \perp Pa \perp^{\|} R$ (Fig. 3.3b)	Idem No. 1
14	*3-$\underline{P}$RRPa* (Fig. 3.16a)	$\underline{P} \perp R \| \| R \perp^{\|} Pa$ (Fig. 3.3c)	Idem No. 1
15	*3-$\underline{P}$RRPa* (Fig. 3.16b)	$\underline{P} \| \| R \| \| R \perp Pa$ (Fig. 3.3d)	Idem No. 1
16	*3-$\underline{P}$PaRR* (Fig. 3.17a)	$\underline{P} \perp Pa \perp^{\perp} R \| \| R$ (Fig. 3.3e)	Idem No. 1
17	*3-$\underline{P}$PaRR* (Fig. 3.17b)	$\underline{P} \| \| Pa \perp R \| \| R$ (Fig. 3.3f)	Idem No. 1

Table 3.2. Limb topology and connecting conditions of the TPM with no idle mobilities and linear actuators mounted on a moving link presented in Figs. 3.18–3.23

No.	TPM type	Limb topology	Connecting conditions
1	*3-R$\underline{P}$C* (Fig. 3.18a)	$R \perp \underline{P} \perp^{\parallel} C$ (Fig. 3.4e)	Actuated $\underline{P}$ joints non adjacent to the fixed base and the moving platform in a spatial star configuration
2	*3-C$\underline{P}$R* (Fig. 3.18b)	$C \perp \underline{P} \perp^{\parallel} R$ (Fig. 3.4f)	Idem No. 1
3	*3-R$\underline{P}$C* (Fig. 3.19a)	$R \perp \underline{P} \perp^{\parallel} C$ (Fig. 3.4e)	Actuated $\underline{P}$ joints non adjacent to the fixed base and the moving platform in a Δ configuration
4	*3-R$\underline{P}$C* (Fig. 3.19b)	$R \perp \underline{P} \perp^{\parallel} C$ (Fig. 3.4e)	Actuated $\underline{P}$ joints non adjacent to the fixed base and the moving platform in a $\coprod$ configuration
5	*3-C$\underline{P}$R* (Fig. 3.20a)	$C \perp \underline{P} \perp^{\parallel} R$ (Fig. 3.4f)	Idem 3
6	*3-C$\underline{P}$R* (Fig. 3.20b)	$C \perp \underline{P} \perp^{\parallel} R$ (Fig. 3.4f)	Idem 4
7	*3-P$\underline{P}$RR* (Fig. 3.21)	$P \perp \underline{P} \perp^{\parallel} R \parallel R$ (Fig. 3.4g)	Idem 1
8	*3-RPa$\underline{P}$R* (Fig. 3.22a)	$R \perp Pa \perp^{\perp} \underline{P} \perp^{\perp} R$ (Fig. 3.5a)	Idem 1
9	*3-RPa$\underline{P}$R* (Fig. 3.22b)	$R \perp Pa \perp^{\parallel} \underline{P} \parallel R$ (Fig. 3.5c)	Idem 1
10	*3-RPaR$\underline{P}$* (Fig. 3.23a)	$R \perp Pa \perp^{\parallel} R \perp^{\perp} \underline{P}$ (Fig. 3.5b)	Idem 1
11	*3-RPaR$\underline{P}$* (Fig. 3.23b)	$R \perp Pa \perp^{\parallel} R \parallel \underline{P}$ (Fig. 3.5d)	Idem 1

Table 3.3. Structural parameters[a] of translational parallel mechanisms in Figs. 3.6–3.11

No.	Structural parameter	Solution *3-PPaP* (Fig. 3.6a, b) *3-PPPa* (Fig. 3.7a, b)	*3-PPa*^{cc} (Fig. 3.8a, b) (Fig. 3.9a, b)	*3-PPaPa* (Fig. 3.10a, b) (Fig. 3.11a)	*3-PPr* (Fig. 3.11b)
1	m	14	11	20	14
2	p_1	6	5	9	7
3	p_2	6	5	9	7
4	p_3	6	5	9	7
5	p	18	15	27	21
6	q	5	5	8	8
7	k_1	0	0	0	0
8	k_2	3	3	3	3
9	k	3	3	3	3
10	(R_{G1})	$(\boldsymbol{v}_1,\boldsymbol{v}_2,\boldsymbol{v}_3)$	$(\boldsymbol{v}_1,\boldsymbol{v}_2,\boldsymbol{v}_3)$	$(\boldsymbol{v}_1,\boldsymbol{v}_2,\boldsymbol{v}_3)$	$(\boldsymbol{v}_1,\boldsymbol{v}_2,\boldsymbol{v}_3)$
11	(R_{G2})	$(\boldsymbol{v}_1,\boldsymbol{v}_2,\boldsymbol{v}_3)$	$(\boldsymbol{v}_1,\boldsymbol{v}_2,\boldsymbol{v}_3)$	$(\boldsymbol{v}_1,\boldsymbol{v}_2,\boldsymbol{v}_3)$	$(\boldsymbol{v}_1,\boldsymbol{v}_2,\boldsymbol{v}_3)$
12	(R_{G3})	$(\boldsymbol{v}_1,\boldsymbol{v}_2,\boldsymbol{v}_3)$	$(\boldsymbol{v}_1,\boldsymbol{v}_2,\boldsymbol{v}_3)$	$(\boldsymbol{v}_1,\boldsymbol{v}_2,\boldsymbol{v}_3)$	$(\boldsymbol{v}_1,\boldsymbol{v}_2,\boldsymbol{v}_3)$
13	S_{G1}	3	3	3	3
14	S_{G2}	3	3	3	3
15	S_{G3}	3	3	3	3
16	r_{G1}	3	4	6	10
17	r_{G2}	3	4	6	10
18	r_{G3}	3	4	6	10
19	M_{G1}	3	3	3	3
20	M_{G2}	3	3	3	3
21	M_{G3}	3	3	3	3
22	(R_F)	$(\boldsymbol{v}_1,\boldsymbol{v}_2,\boldsymbol{v}_3)$	$(\boldsymbol{v}_1,\boldsymbol{v}_2,\boldsymbol{v}_3)$	$(\boldsymbol{v}_1,\boldsymbol{v}_2,\boldsymbol{v}_3)$	$(\boldsymbol{v}_1,\boldsymbol{v}_2,\boldsymbol{v}_3)$
23	S_F	3	3	3	3
24	r_1	9	12	18	30
25	r_F	15	18	24	36
26	M_F	3	3	3	3
27	N_F	15	12	24	12
28	T_F	0	0	0	0
29	$\sum_{j=1}^{p_1} f_j$	6	7	9	13
30	$\sum_{j=1}^{p_2} f_j$	6	7	9	13
31	$\sum_{j=1}^{p_3} f_j$	6	7	9	13
32	$\sum_{j=1}^{p} f_j$	18	21	27	39

[a]See footnote of Table 2.1 for the nomenclature of structural parameters

Table 3.4. Structural parameters[a] of translational parallel mechanisms in Figs. 3.12–3.17

No.	Structural parameter	Solution *3-PRC* (Figs. 3.12a, 3.13, 3.14) *3-PCR* (Fig. 3.12b)	 *3-PRPaR* (Fig. 3.15) *3-PRRPa* (Fig. 3.16) *3-PPaRR* (Fig. 3.17)
1	m	8	17
2	p_1	3	7
3	p_2	3	7
4	p_3	3	7
5	p	9	21
6	q	2	5
7	k_1	3	0
8	k_2	0	3
9	k	3	3
10	(R_{Gi}) $(i = 1,2,3)$	See Table 3.5	See Table 3.5
11	S_{G1}	4	4
12	S_{G2}	4	4
13	S_{G3}	4	4
14	r_{G1}	0	3
15	r_{G2}	0	3
16	r_{G3}	0	3
17	M_{G1}	4	4
18	M_{G2}	4	4
19	M_{G3}	4	4
20	(R_F)	$(\boldsymbol{v}_1, \boldsymbol{v}_2, \boldsymbol{v}_3)$	$(\boldsymbol{v}_1, \boldsymbol{v}_2, \boldsymbol{v}_3)$
21	S_F	3	3
22	r_1	0	9
23	r_F	9	18
24	M_F	3	3
25	N_F	3	12
26	T_F	0	0
27	$\sum_{j=1}^{p_1} f_j$	4	7
28	$\sum_{j=1}^{p_2} f_j$	4	7
29	$\sum_{j=1}^{p_3} f_j$	4	7
30	$\sum_{j=1}^{p} f_j$	12	21

[a]See footnote of Table 2.1 for the nomenclature of structural parameters

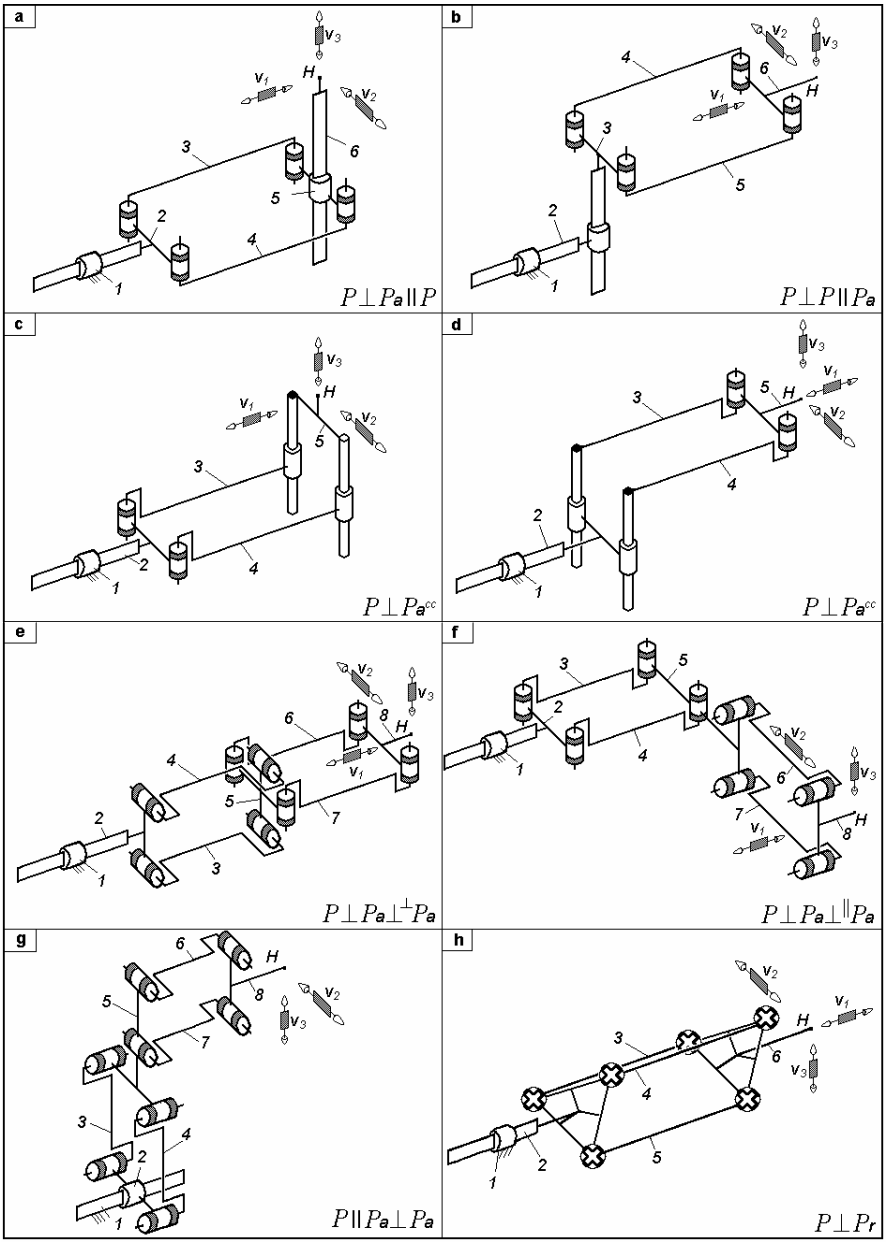

Fig. 3.1. Complex limbs for TPMs with coupled motions defined by $M_G = S_G = 3$, $(R_G) = (\boldsymbol{v}_1, \boldsymbol{v}_2, \boldsymbol{v}_3)$ and actuated by linear motors mounted on the fixed base

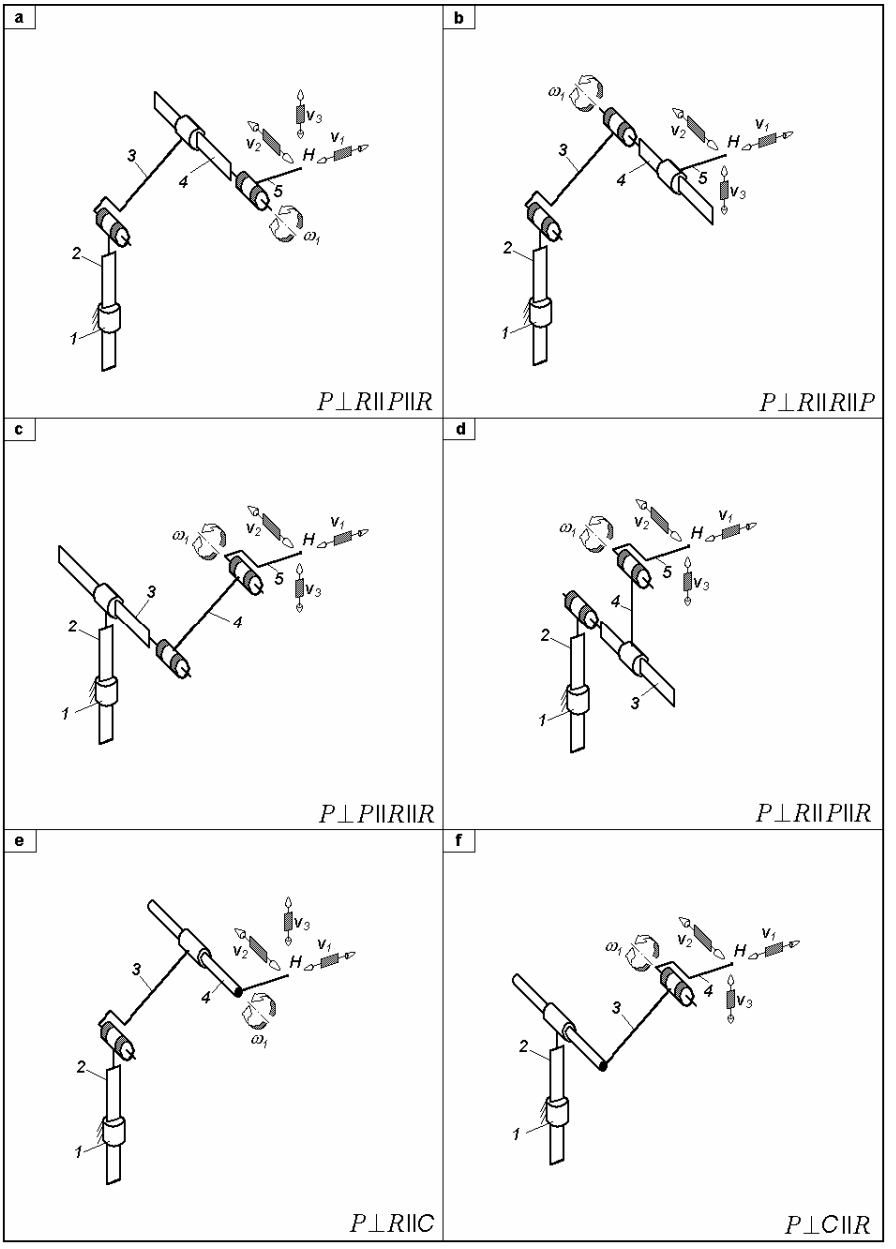

Fig. 3.2. Simple limbs for TPMs with coupled motions defined by $M_G = S_G = 4$, $(R_G) = (\boldsymbol{v}_1, \boldsymbol{v}_2, \boldsymbol{v}_3, \boldsymbol{\omega}_1)$ and actuated by linear motors mounted on the fixed base

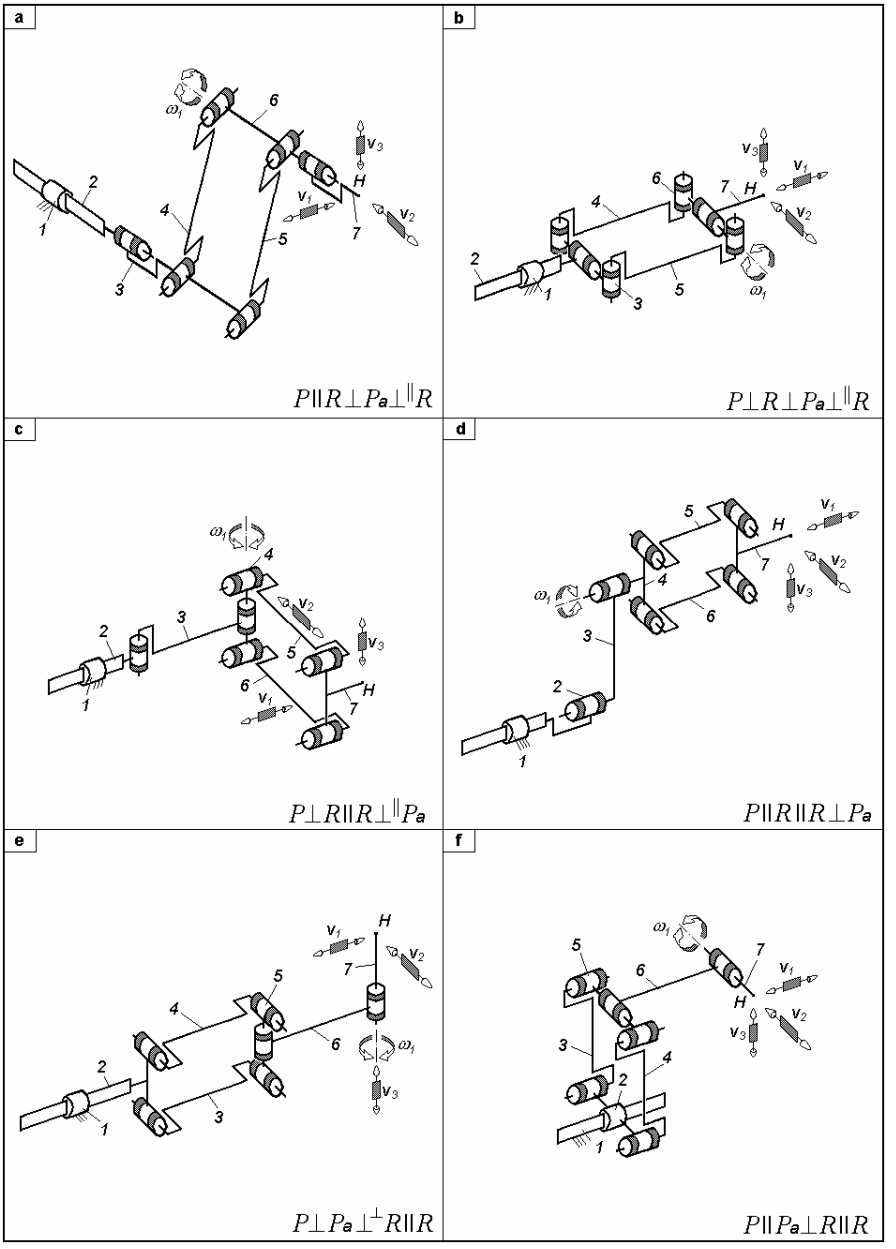

Fig. 3.3. Complex limbs for TPMs with coupled motions defined by $M_G = S_G = 4$, $(R_G) = (\boldsymbol{v}_1, \boldsymbol{v}_2, \boldsymbol{v}_3, \boldsymbol{\omega}_1)$ and actuated by linear motors mounted on the fixed base

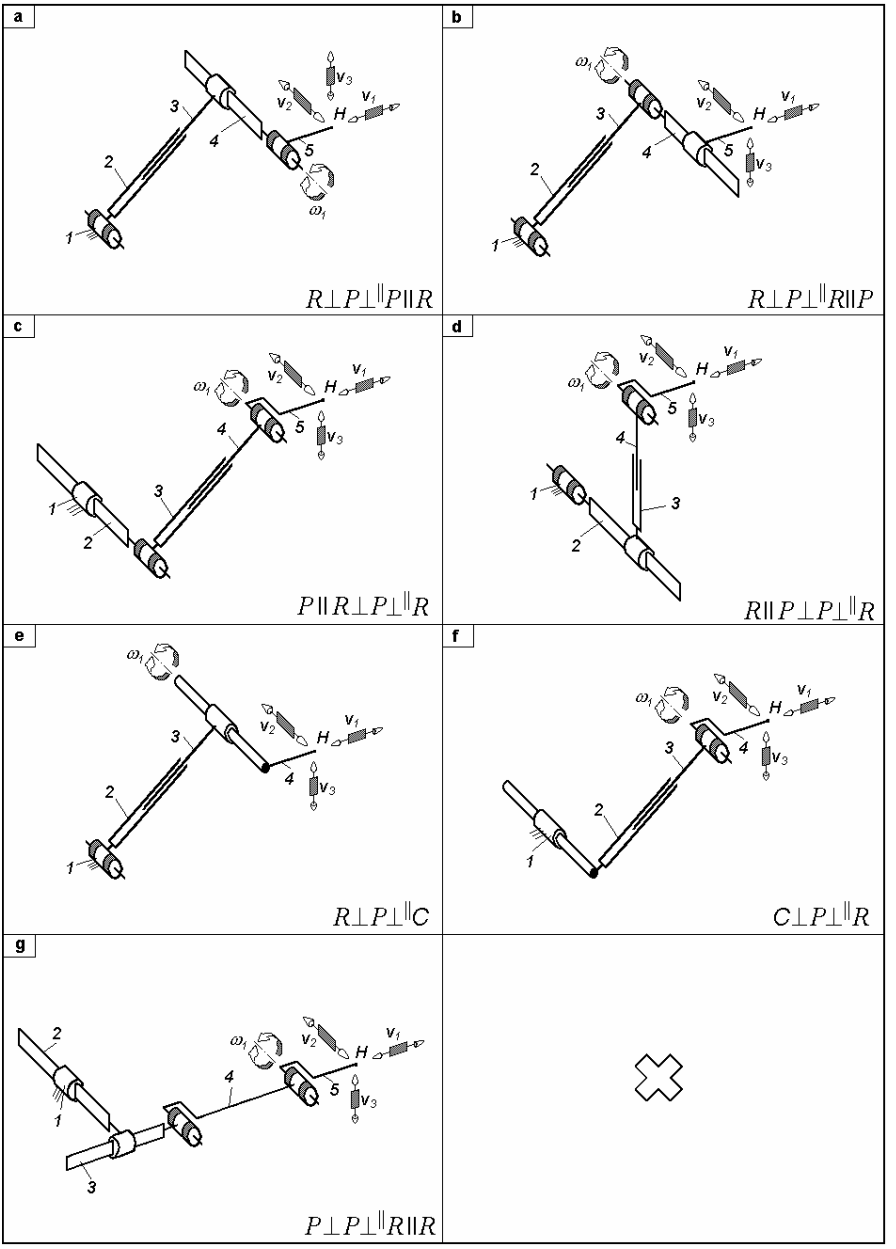

Fig. 3.4. Simple limbs for TPMs with coupled motions defined by $M_G = S_G = 4$, $(R_G) = (\boldsymbol{v}_1, \boldsymbol{v}_2, \boldsymbol{v}_3, \boldsymbol{\omega}_1)$ and actuated by linear motors mounted in the prismatic joint between links 2, 3 (**a**, **b**, **e**–**g**) and 3, 4 (**c**, **d**)

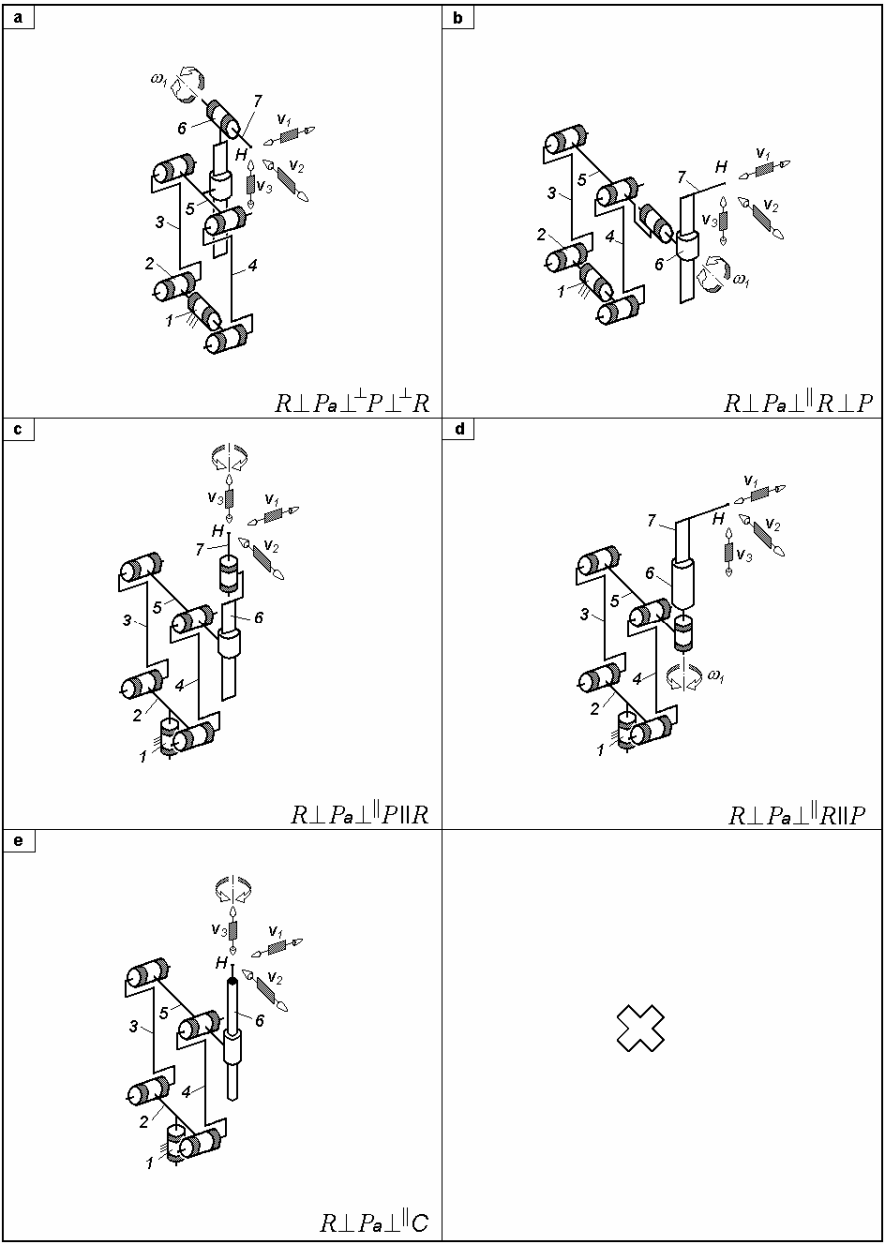

Fig. 3.5. Complex limbs for TPMs with coupled motions defined by $M_G = S_G = 4$, $(R_G) = (\boldsymbol{v}_1, \boldsymbol{v}_2, \boldsymbol{v}_3, \boldsymbol{\omega}_1)$ and actuated by linear motors mounted in the prismatic or cylindrical joint non adjacent to the fixed base

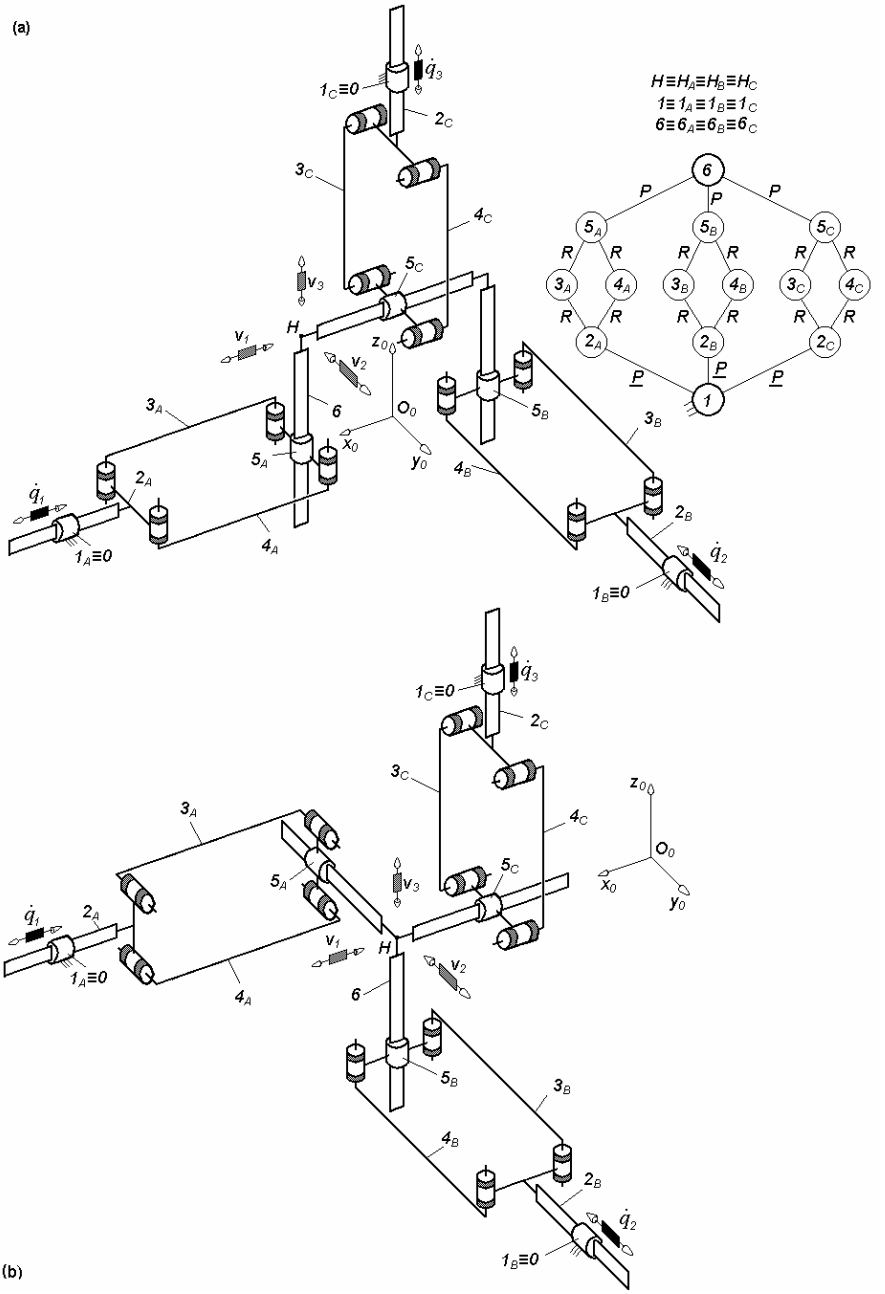

Fig. 3.6. *3-<u>P</u>PaP*-type overconstrained TPMs with coupled motions and linear actuators on the fixed base, defined by $M_F = S_F = 3$, $(R_F) = (\boldsymbol{v}_1, \boldsymbol{v}_2, \boldsymbol{v}_3)$ $T_F = 0$, $N_F = 15$, limb topology $\underline{P} \perp Pa \| P$

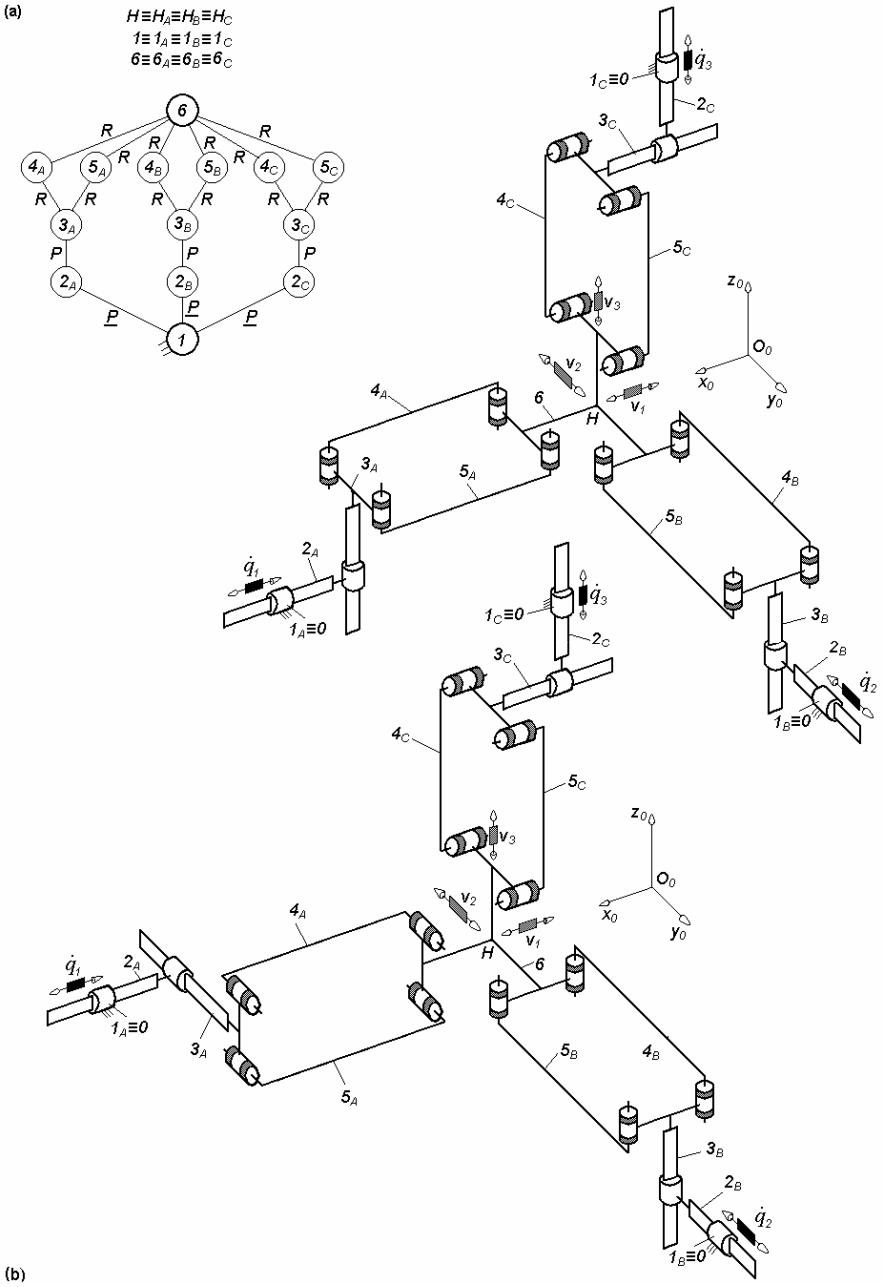

Fig. 3.7. *3-PPPa*-type overconstrained TPMs with coupled motions and linear actuators on the fixed base, defined by $M_F = S_F = 3$, $(R_F) = (\boldsymbol{v}_1, \boldsymbol{v}_2, \boldsymbol{v}_3)$ $T_F = 0$, $N_F = 15$, limb topology $\underline{P} \perp P || Pa$

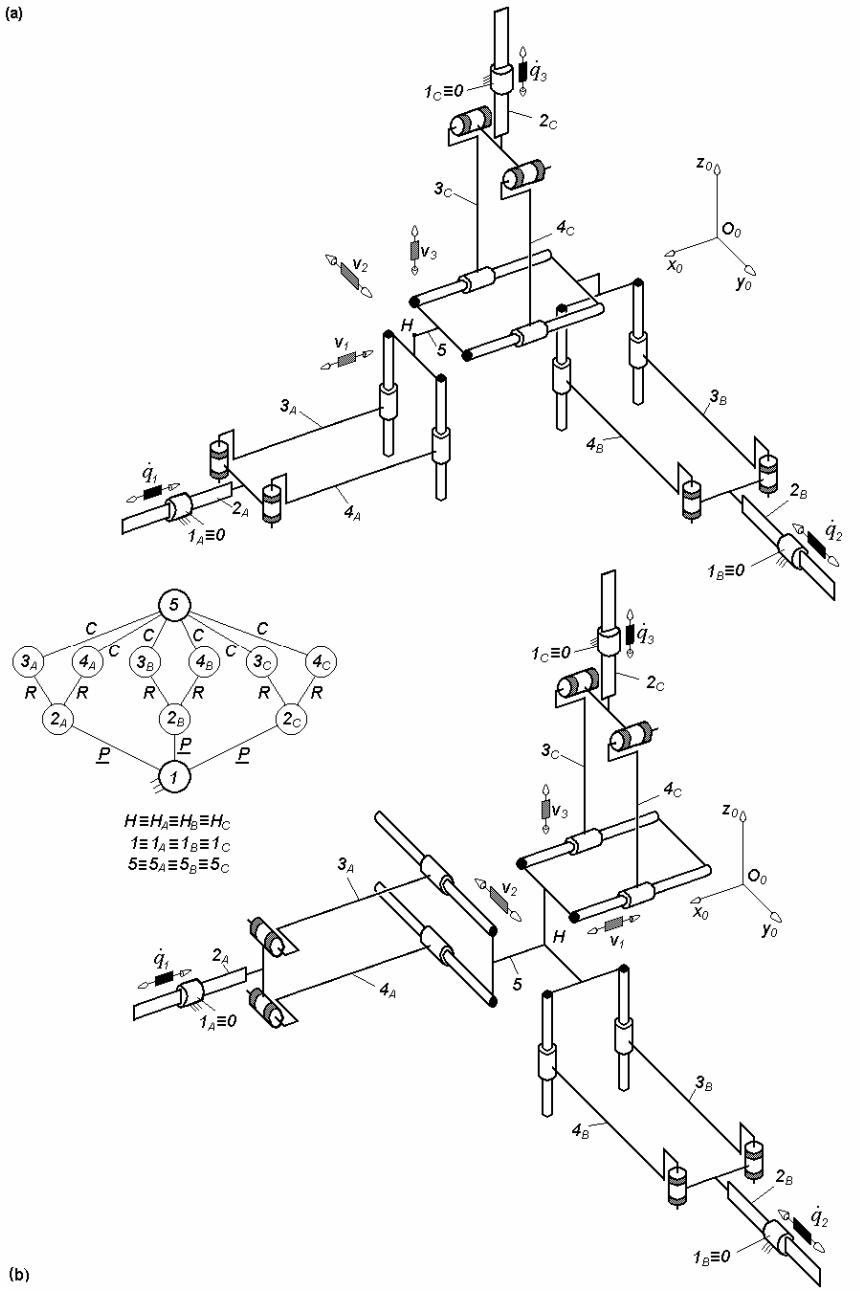

Fig. 3.8. *3-<u>P</u>Pa^{cc}*-type overconstrained TPMs with coupled motions defined by $M_F = S_F = 3$, $(R_F) = (\boldsymbol{v}_1, \boldsymbol{v}_2, \boldsymbol{v}_3)$, $T_F = 0$, $N_F = 12$, linear actuators on the fixed base and six cylindrical joints adjacent to the moving platform, limb topology $\underline{P} \perp Pa^{cc}$

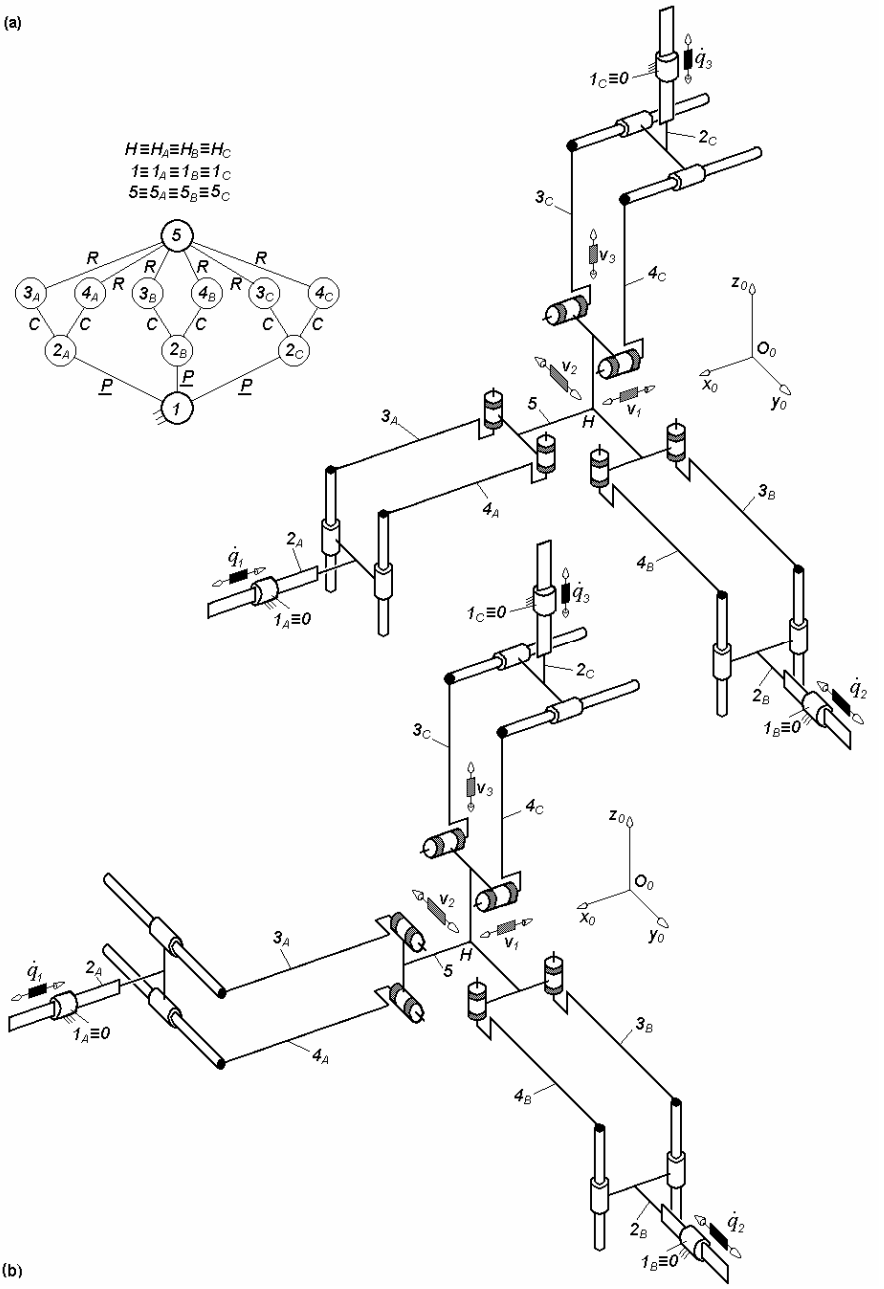

Fig. 3.9. *3-*$\underline{P}$*P*a^{cc}-type overconstrained TPMs with coupled motions defined by $M_F = S_F = 3$, $(R_F) = (\boldsymbol{v}_1, \boldsymbol{v}_2, \boldsymbol{v}_3)$, $T_F = 0$, $N_F = 12$, linear actuators on the fixed base and six revolute joints adjacent to the moving platform, limb topology $\underline{P} \perp Pa^{cc}$

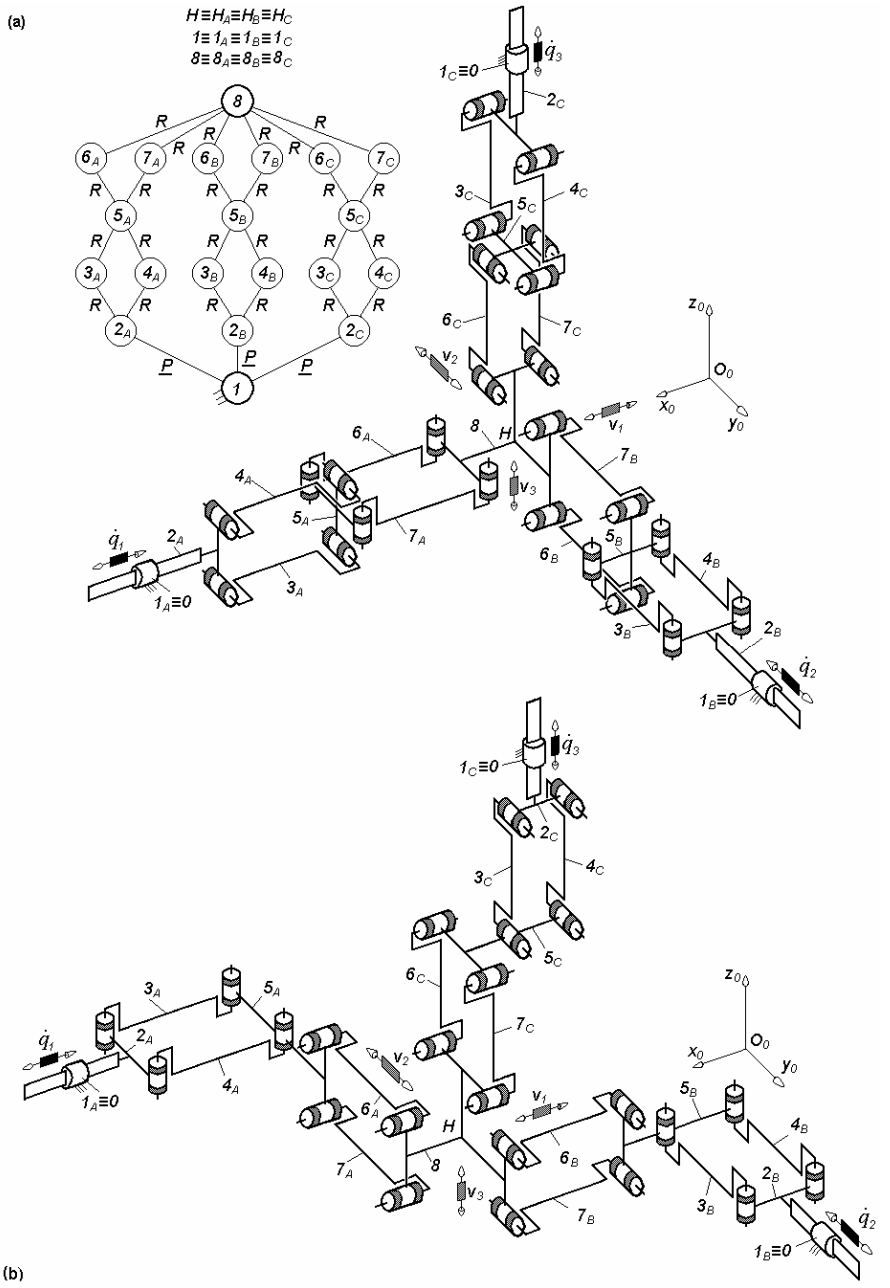

Fig. 3.10. *3-<u>P</u>PaPa*-type overconstrained TPMs with coupled motions and linear actuators on the fixed base, defined by $M_F = S_F = 3$, $(R_F) = (\boldsymbol{v}_1, \boldsymbol{v}_2, \boldsymbol{v}_3)$, $T_F = 0$, $N_F = 24$, limb topology $\underline{P} \perp Pa \perp^{\perp} Pa$ (**a**) and $\underline{P} \perp Pa \perp^{\parallel} Pa$ (**b**)

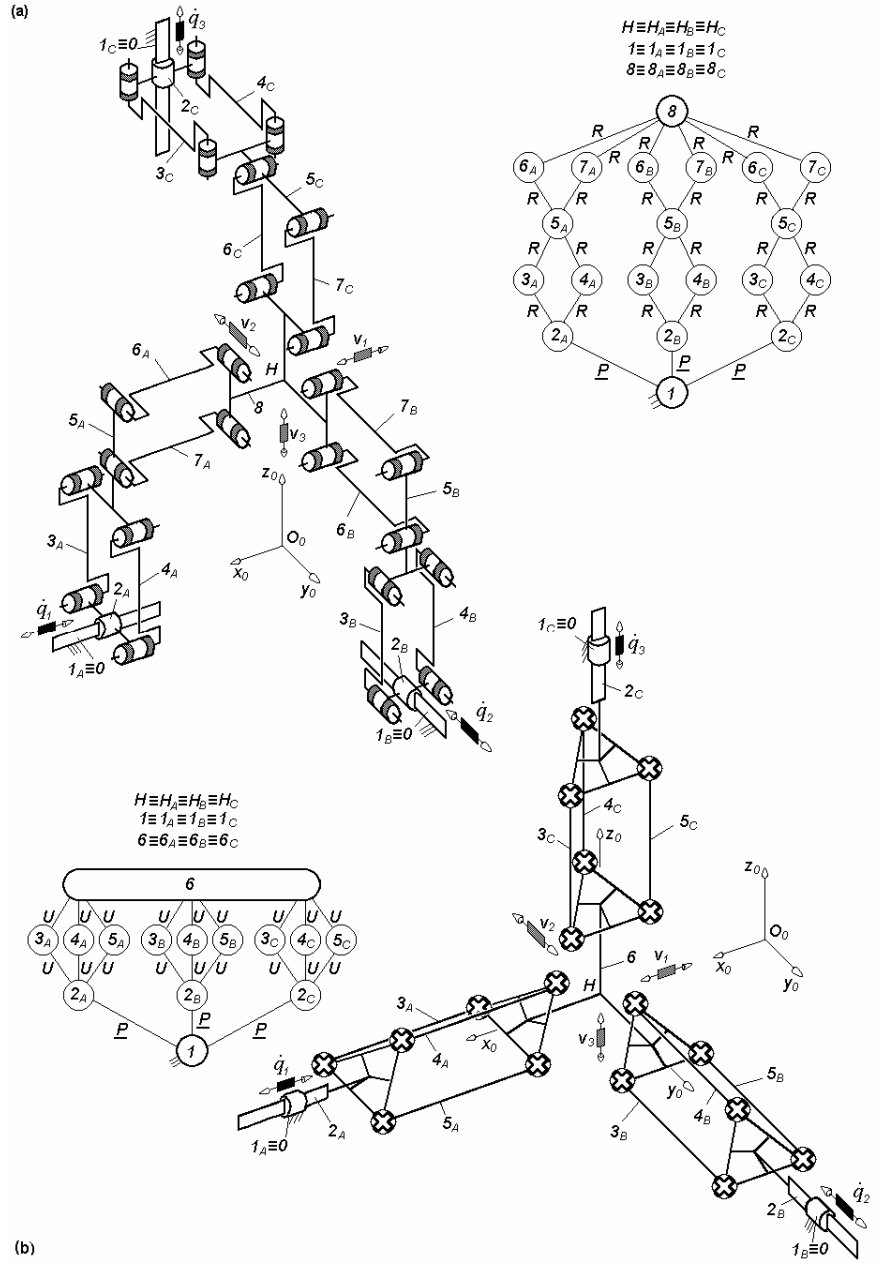

Fig. 3.11. Overconstrained TPMs of types *3-PPaPa* (**a**) and *3-PPr* (**b**) with coupled motions and linear actuators on the fixed base, defined by $M_F = S_F = 3$, $(R_F) = (\boldsymbol{v}_1, \boldsymbol{v}_2, \boldsymbol{v}_3)$, $T_F = 0$ and $N_F = 24$ (**a**), $N_F = 12$ (**b**), limb topology $\underline{P}||Pa \perp Pa$ (**a**) and $\underline{P} \perp Pr$ (**b**)

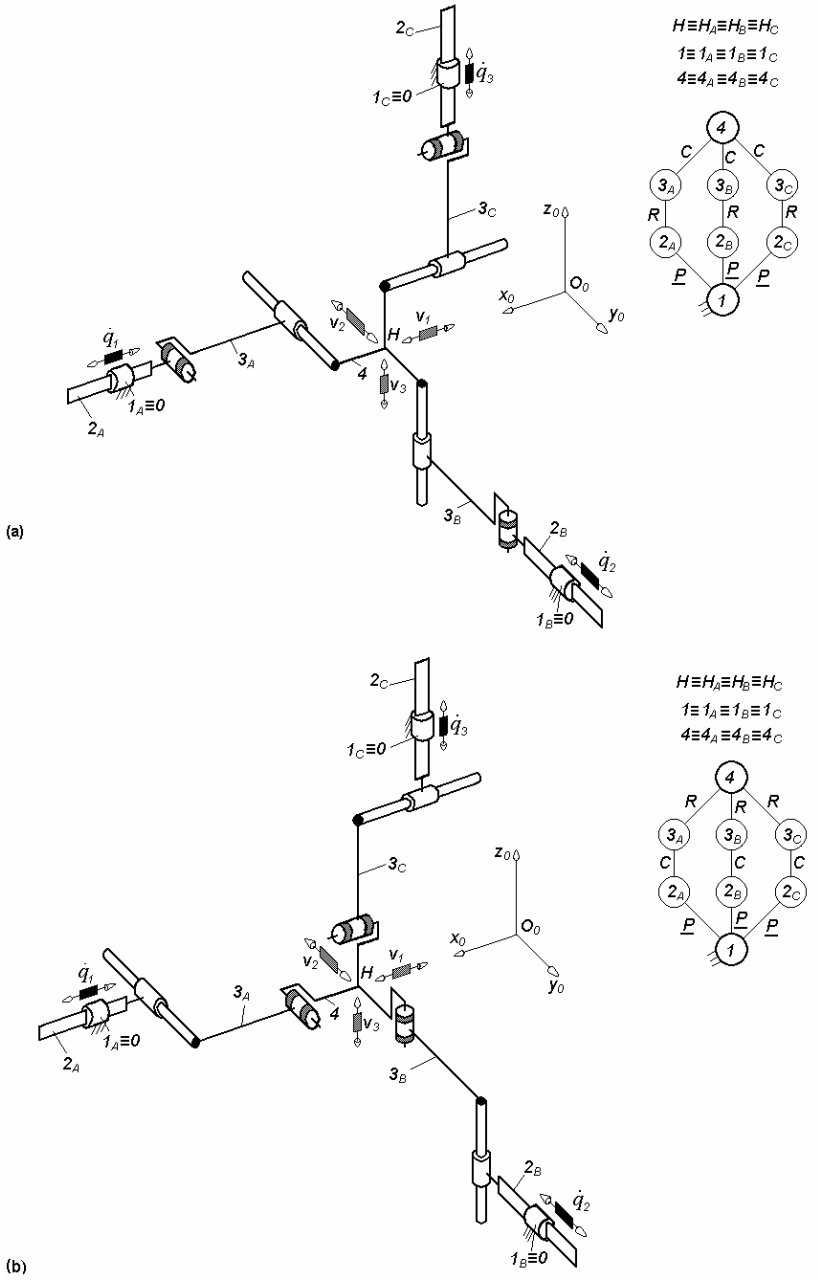

Fig. 3.12. Overconstrained TPMs of types *3-*$\underline{P}$*RC* (**a**) and *3-*$\underline{P}$*CR* (**b**) with coupled motions and linear actuators on the fixed base, defined by $M_F = S_F = 3$, $(R_F) = (\boldsymbol{v}_1, \boldsymbol{v}_2, \boldsymbol{v}_3)$, $T_F = 0$, $N_F = 3$, limb topology $\underline{P} \perp R||C$ (**a**) and $\underline{P} \perp C||R$ (**b**)

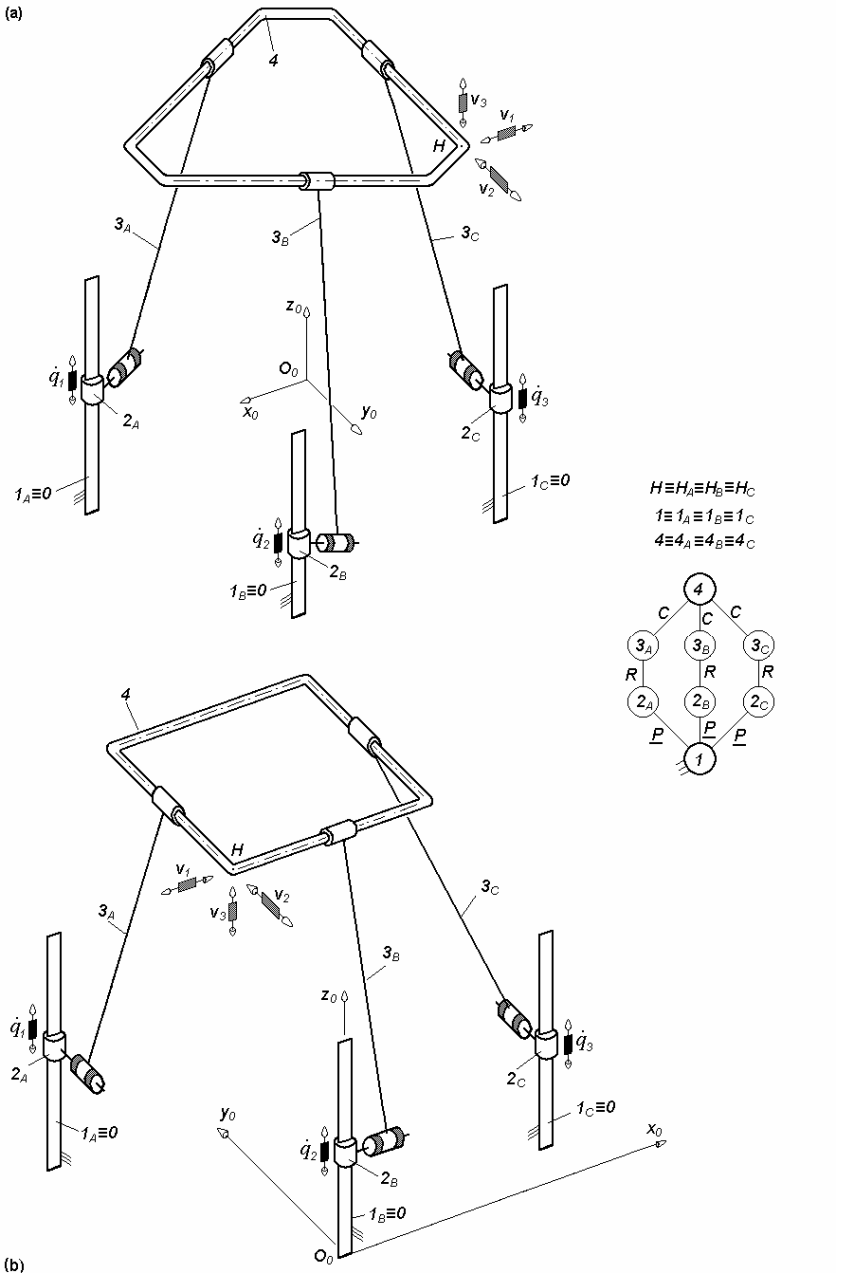

Fig. 3.13. *3-PRC*-type overconstrained TPMs with coupled motions and linear actuators of parallel directions mounted on the fixed base, defined by $M_F = S_F = 3$, $(R_F) = (\boldsymbol{v}_1, \boldsymbol{v}_2, \boldsymbol{v}_3)$, $T_F = 0$, $N_F = 3$, limb topology $\underline{P} \perp R \| C$

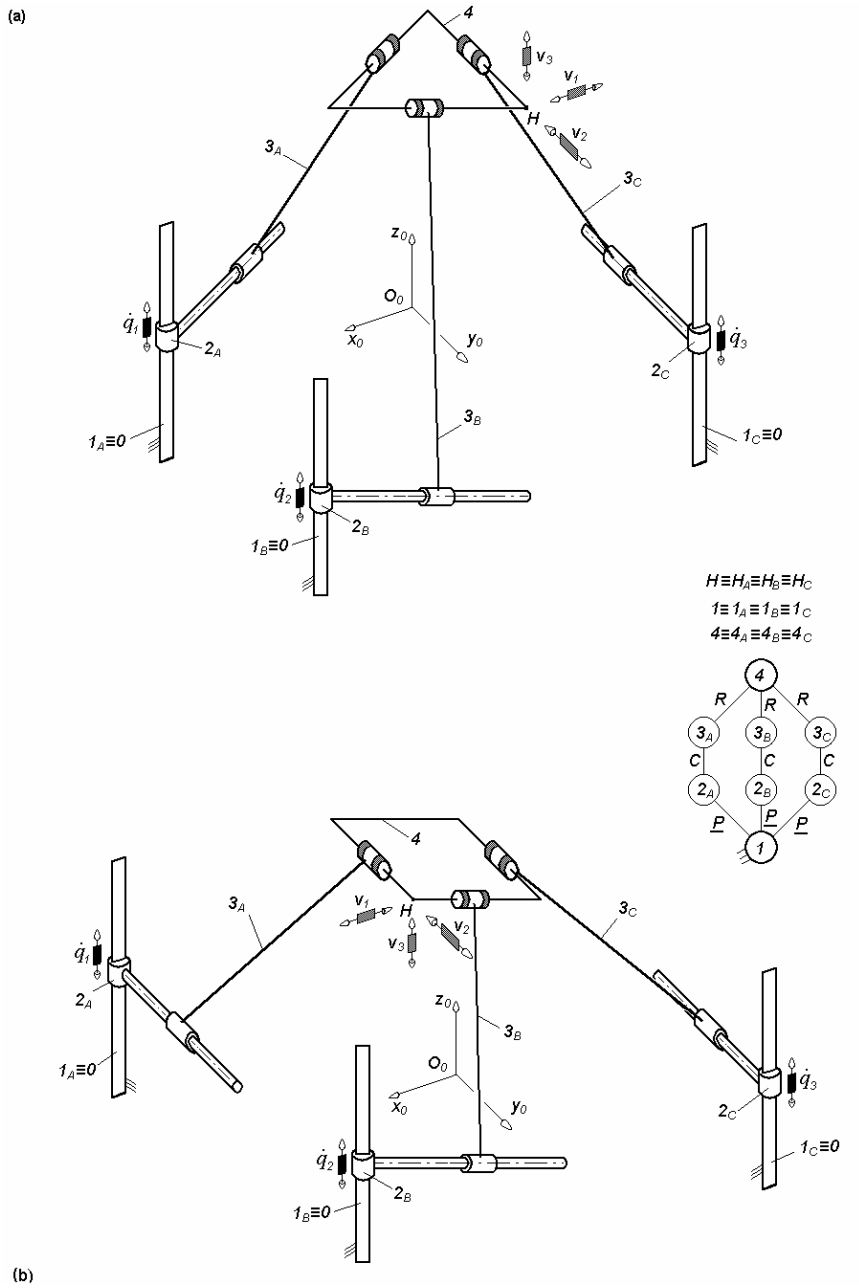

Fig. 3.14. *3-PCR*-type overconstrained TPMs with coupled motions and linear actuators of parallel directions mounted on the fixed base, defined by $M_F = S_F = 3$, $(R_F) = (\boldsymbol{v}_1, \boldsymbol{v}_2, \boldsymbol{v}_3)$, $T_F = 0$, $N_F = 3$, limb topology $\underline{P} \perp C \| R$

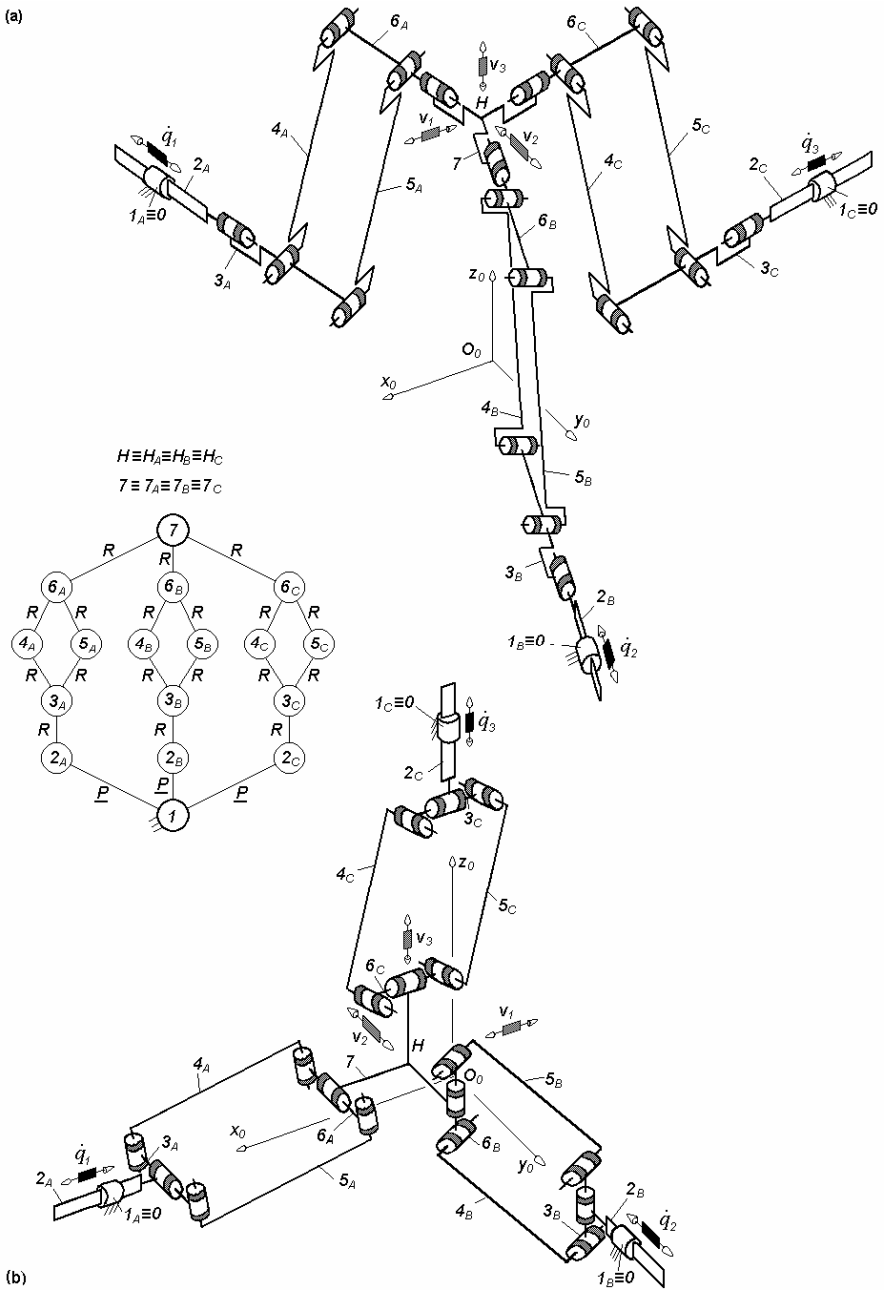

Fig. 3.15. *3-*$\underline{P}$*RPaR*-type overconstrained TPMs with coupled motions and linear actuators on the fixed base, defined by $M_F = S_F = 3$, $(R_F) = (\boldsymbol{v}_1, \boldsymbol{v}_2, \boldsymbol{v}_3)$, $T_F = 0$, $N_F = 12$, limb topology $\underline{P}||R \perp Pa \perp {}^{||}R$ (**a**) and $\underline{P} \perp R \perp Pa \perp {}^{||}R$ (**b**)

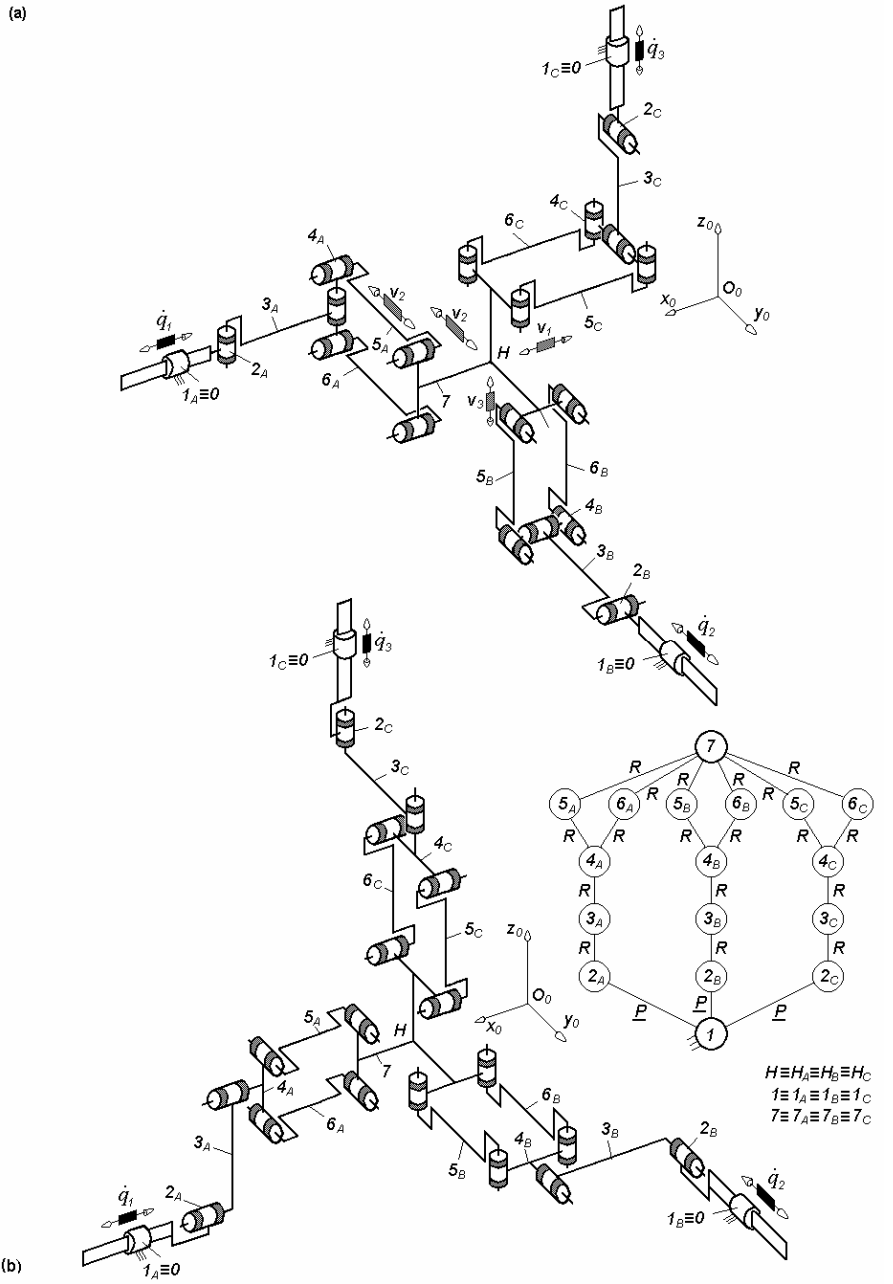

Fig. 3.16. *3-PRRPa*-type overconstrained TPMs with coupled motions and linear actuators on the fixed base, defined by $M_F = S_F = 3$, $(R_F) = (\boldsymbol{v}_1, \boldsymbol{v}_2, \boldsymbol{v}_3)$, $T_F = 0$, $N_F = 12$, limb topology $\underline{P} \perp R \| R \perp {}^{\|}Pa$ (**a**) and $\underline{P} \| R \| R \perp Pa$ (**b**)

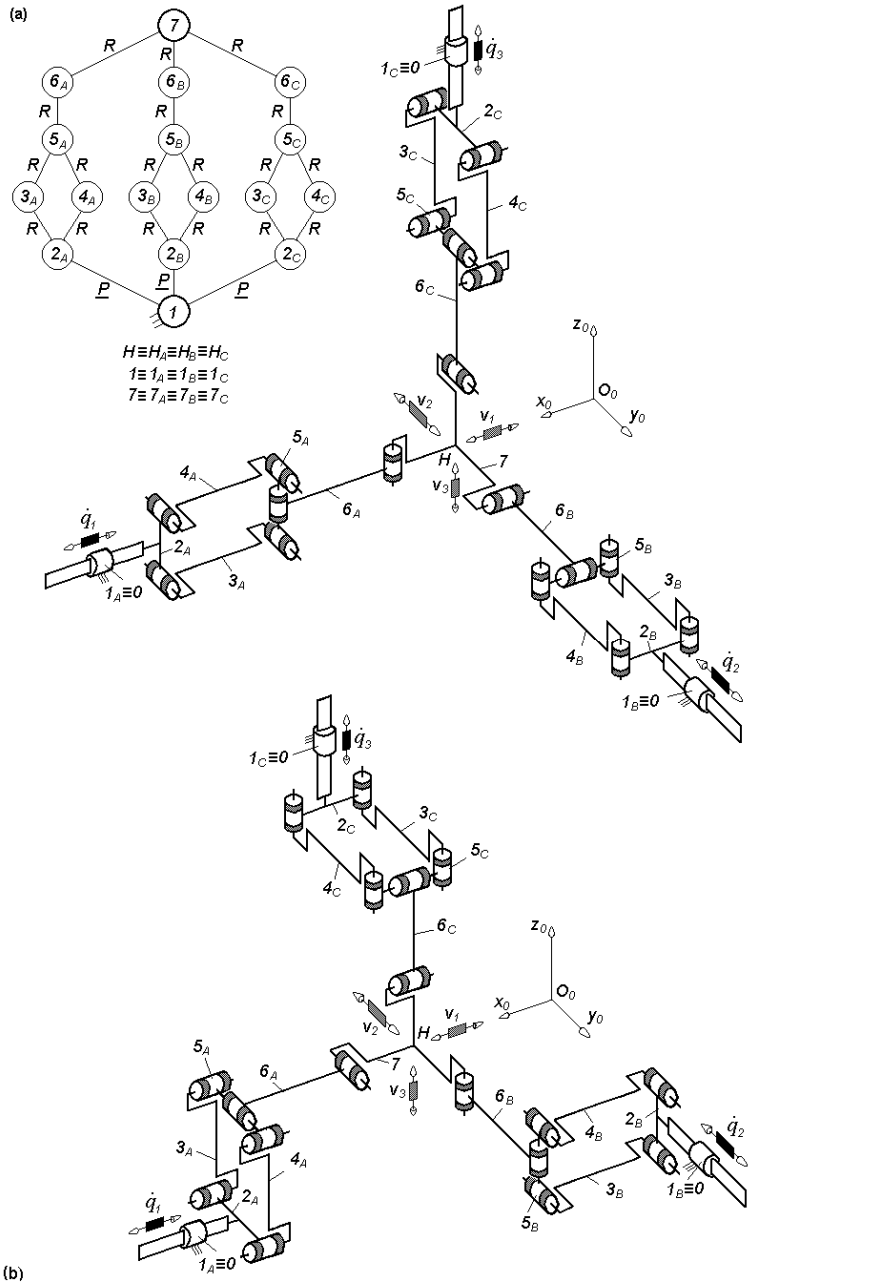

Fig. 3.17. *3-PPaRR*-type overconstrained TPMs with coupled motions and linear actuators on the fixed base, defined by $M_F = S_F = 3$, $(R_F) = (\boldsymbol{v}_1, \boldsymbol{v}_2, \boldsymbol{v}_3)$, $T_F = 0$, $N_F = 12$, limb topology $\underline{P} \perp Pa \perp^{\perp} R||R$ (**a**) and $\underline{P}||Pa \perp R||R$ (**b**)

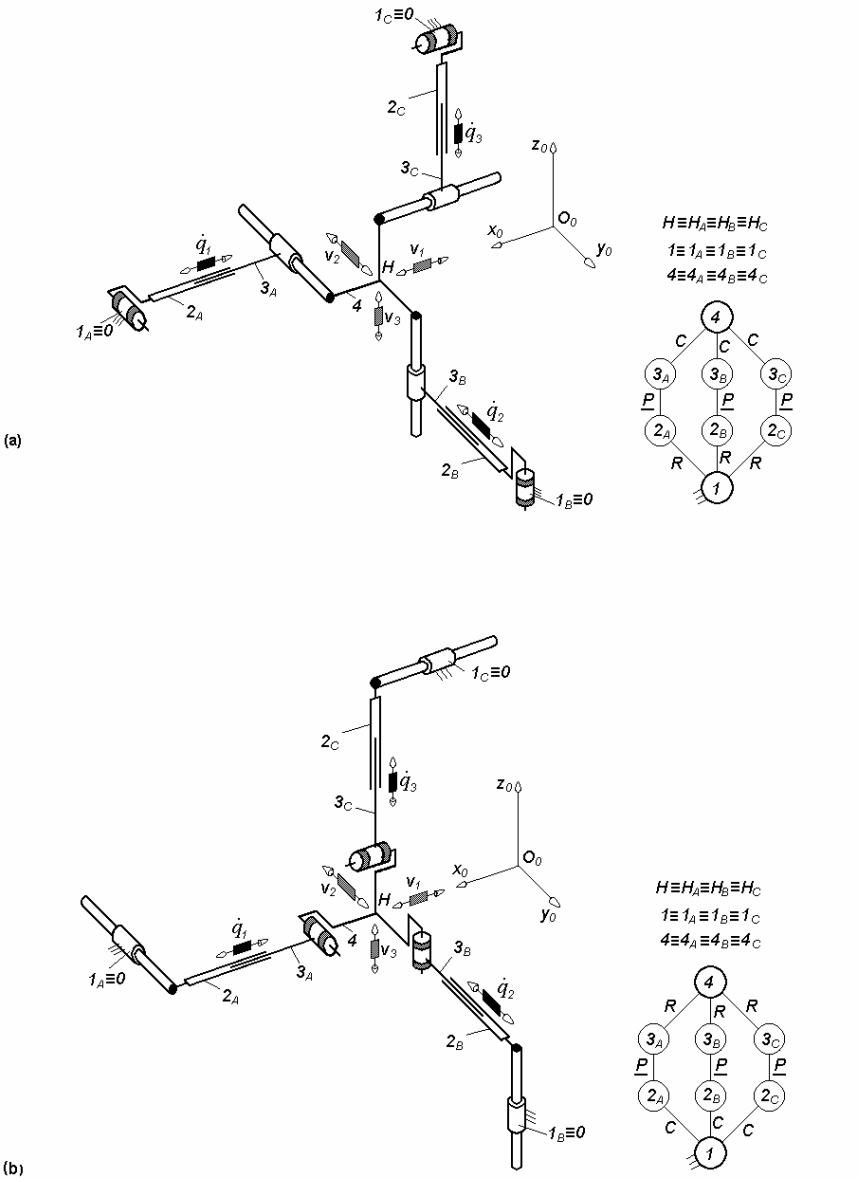

Fig. 3.18. Overconstrained TPMs of types *3-RPC* (**a**) and *3-CPR* (**b**) with coupled motions and linear actuators non adjacent to the fixed base, defined by $M_F = S_F = 3$, $(R_F) = (\boldsymbol{v}_1, \boldsymbol{v}_2, \boldsymbol{v}_3)$, $T_F = 0$, $N_F = 3$, limb topology $R \perp P \perp {}^{\parallel}C$ (**a**) and $C \perp P \perp {}^{\parallel}R$ (**b**)

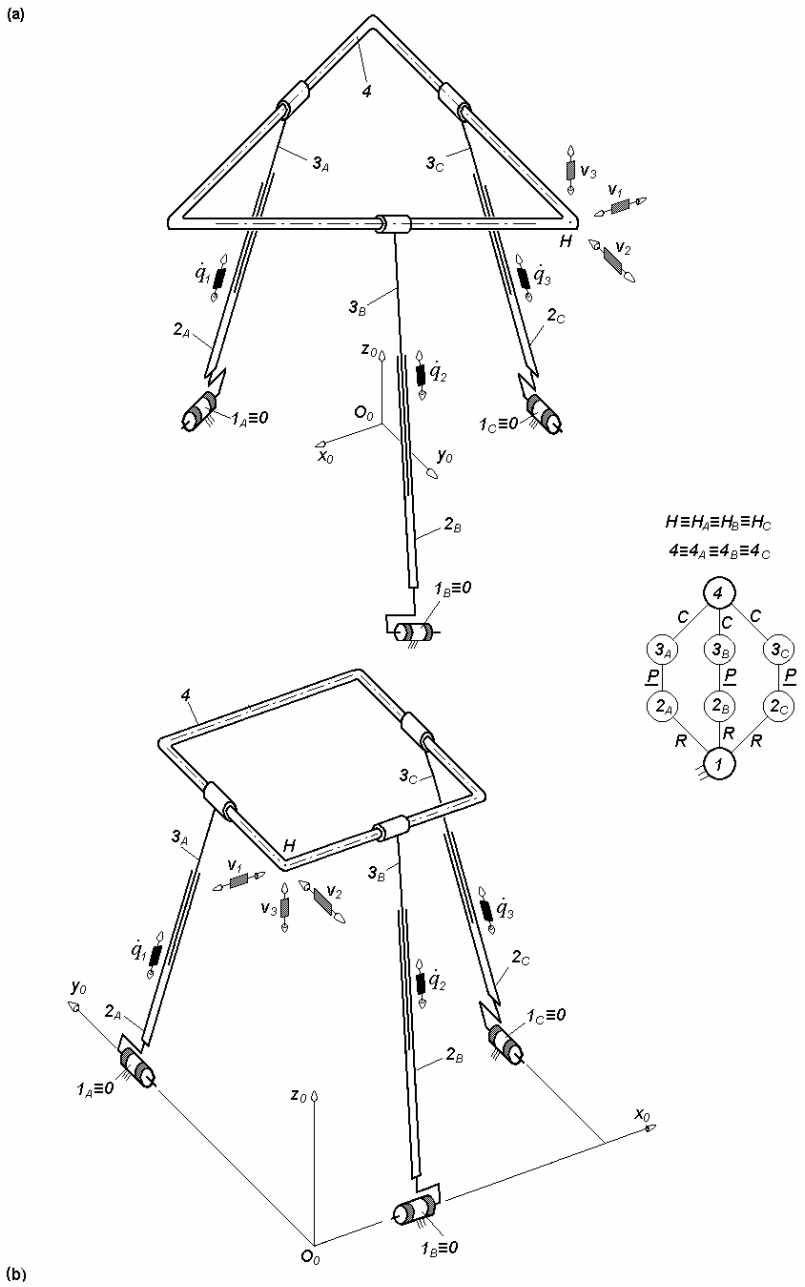

Fig. 3.19. *3-RPC*-type overconstrained TPMs with coupled motions and linear actuators non adjacent to the fixed base in Δ (**a**) and $\coprod$ (**b**) configurations defined by $M_F = S_F = 3$, $(R_F) = (\boldsymbol{v}_1, \boldsymbol{v}_2, \boldsymbol{v}_3)$, $T_F = 0$, $N_F = 3$, limb topology $R \perp \underline{P} \perp {}^{\parallel}C$

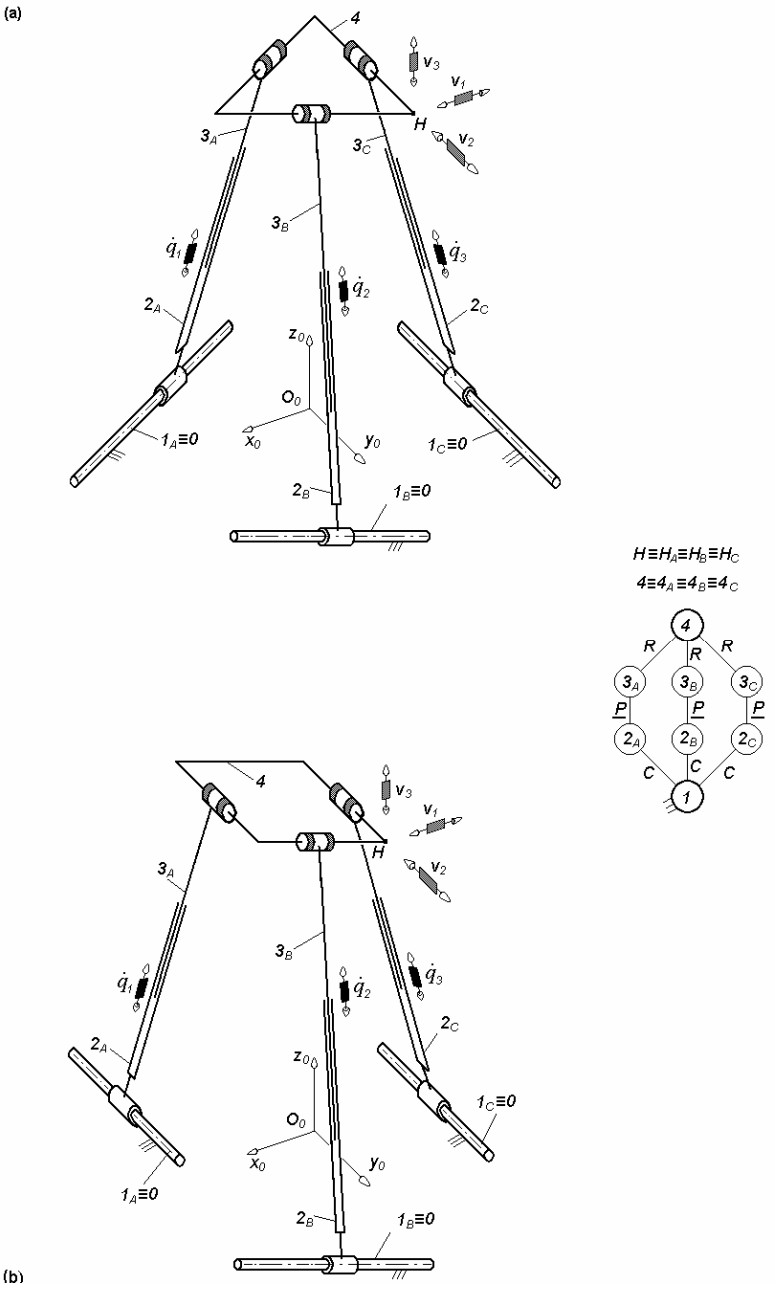

Fig. 3.20. *3-CPR*-type overconstrained TPMs with coupled motions and linear actuators non adjacent to the fixed base in Δ (**a**) and $\amalg$ (**b**) configurations defined by $M_F = S_F = 3$, $(R_F) = (\boldsymbol{v}_1, \boldsymbol{v}_2, \boldsymbol{v}_3)$, $T_F = 0$, $N_F = 3$, limb topology $C \perp \underline{P} \perp {}^{\|}R$

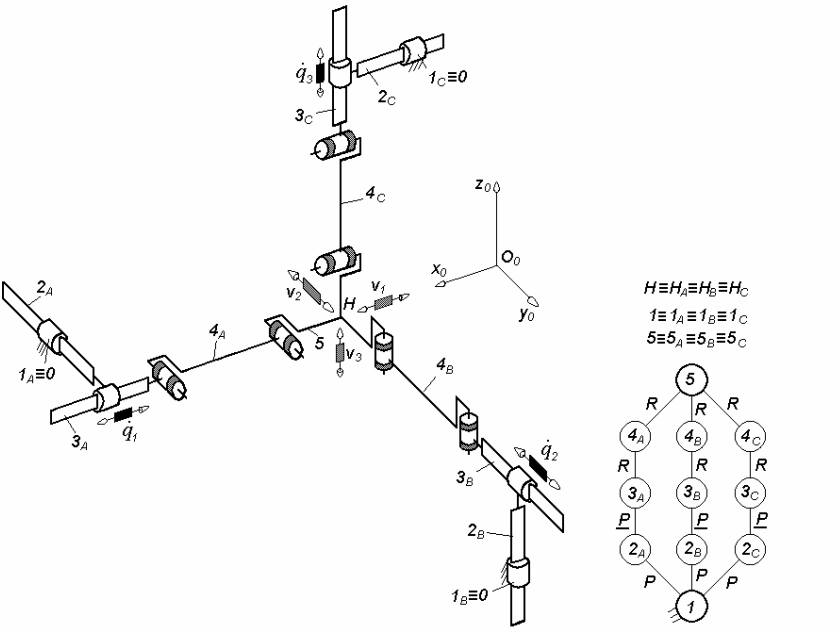

Fig. 3.21. *3-PPRR*-type overconstrained TPMs with coupled motions and linear actuators non adjacent to the fixed base, defined by $M_F = S_F = 3$, $(R_F) = (\boldsymbol{v}_1, \boldsymbol{v}_2, \boldsymbol{v}_3)$, $T_F = 0$, $N_F = 3$, limb topology $P \perp \underline{P} \perp {}^{\|}R \| R$

Table 3.5. Bases of the operational velocities spaces of the limbs isolated from the parallel mechanisms presented in Figs. 3.12–3.23

No.	Parallel mechanism	Basis (R_{G1})	(R_{G2})	(R_{G3})
1	Fig. 3.12	$(\boldsymbol{v}_1, \boldsymbol{v}_2, \boldsymbol{v}_3, \boldsymbol{\omega}_\beta)$	$(\boldsymbol{v}_1, \boldsymbol{v}_2, \boldsymbol{v}_3, \boldsymbol{\omega}_\delta)$	$(\boldsymbol{v}_1, \boldsymbol{v}_2, \boldsymbol{v}_3, \boldsymbol{\omega}_\alpha)$
2	Figs. 3.13, 3.14, 3.15a, 3.19, 3.20	$(\boldsymbol{v}_1, \boldsymbol{v}_2, \boldsymbol{v}_3, \boldsymbol{\omega}_\beta)$	$(\boldsymbol{v}_1, \boldsymbol{v}_2, \boldsymbol{v}_3, \boldsymbol{\omega}_\alpha)$	$(\boldsymbol{v}_1, \boldsymbol{v}_2, \boldsymbol{v}_3, \boldsymbol{\omega}_\beta)$
3	Figs. 3.15b, 3.17b, 3.18, 3.21, 3.22a, 3.23a	$(\boldsymbol{v}_1, \boldsymbol{v}_2, \boldsymbol{v}_3, \boldsymbol{\omega}_\beta)$	$(\boldsymbol{v}_1, \boldsymbol{v}_2, \boldsymbol{v}_3, \boldsymbol{\omega}_\delta)$	$(\boldsymbol{v}_1, \boldsymbol{v}_2, \boldsymbol{v}_3, \boldsymbol{\omega}_\alpha)$
4	Figs. 3.16a, 3.17a, 3.22b, 3.23b	$(\boldsymbol{v}_1, \boldsymbol{v}_2, \boldsymbol{v}_3, \boldsymbol{\omega}_\delta)$	$(\boldsymbol{v}_1, \boldsymbol{v}_2, \boldsymbol{v}_3, \boldsymbol{\omega}_\alpha)$	$(\boldsymbol{v}_1, \boldsymbol{v}_2, \boldsymbol{v}_3, \boldsymbol{\omega}_\beta)$
5	Fig. 3.16b	$(\boldsymbol{v}_1, \boldsymbol{v}_2, \boldsymbol{v}_3, \boldsymbol{\omega}_\alpha)$	$(\boldsymbol{v}_1, \boldsymbol{v}_2, \boldsymbol{v}_3, \boldsymbol{\omega}_\beta)$	$(\boldsymbol{v}_1, \boldsymbol{v}_2, \boldsymbol{v}_3, \boldsymbol{\omega}_\delta)$

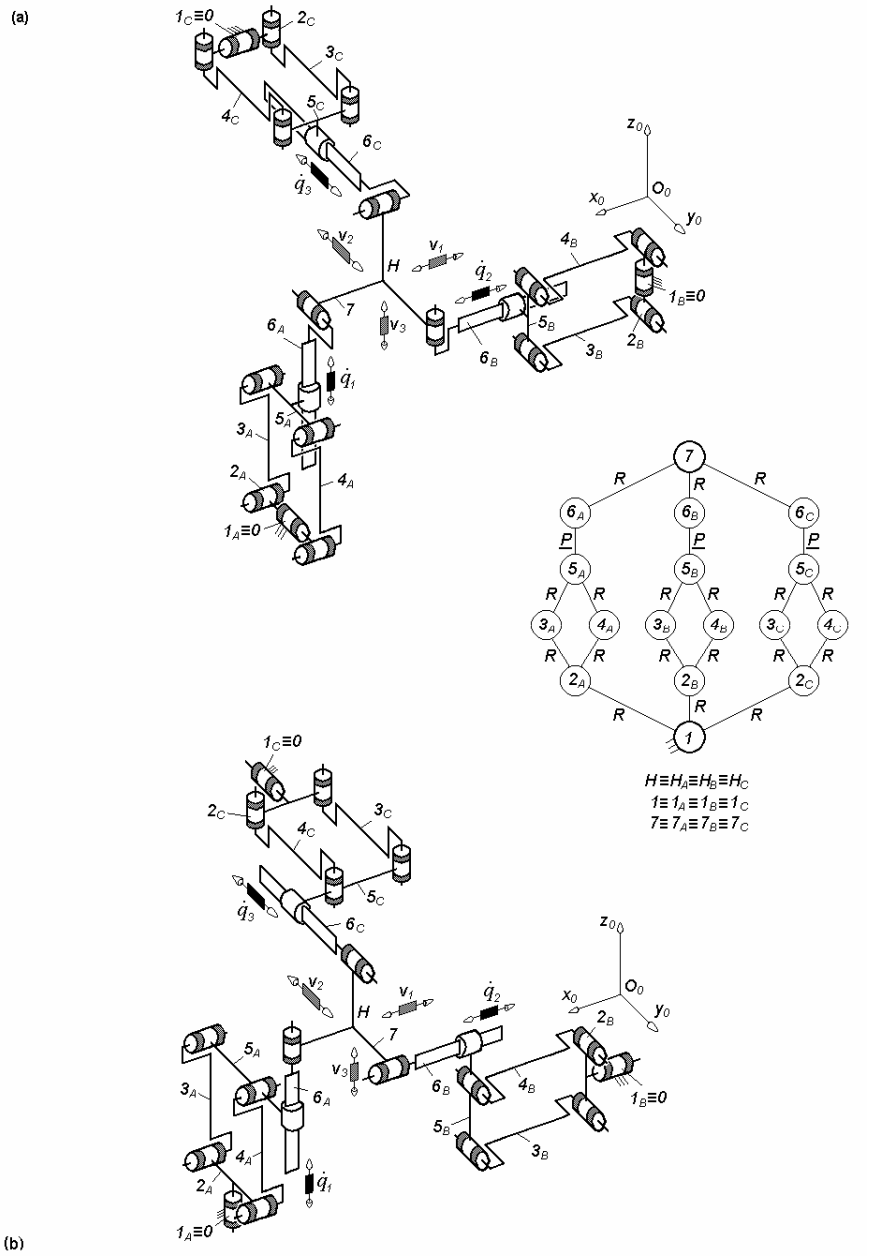

Fig. 3.22. *3-RPa*$\underline{P}$*R*-type overconstrained TPMs with coupled motions and linear actuators non adjacent to the fixed base, defined by $M_F = S_F = 3$, $(R_F) = (\boldsymbol{v}_1, \boldsymbol{v}_2, \boldsymbol{v}_3)$, $T_F = 0$, $N_F = 12$, limb topology $R \perp Pa \perp^{\perp} \underline{P} \perp^{\perp} R$ (**a**) and $R \perp Pa \perp^{||} \underline{P} || R$ (**b**)

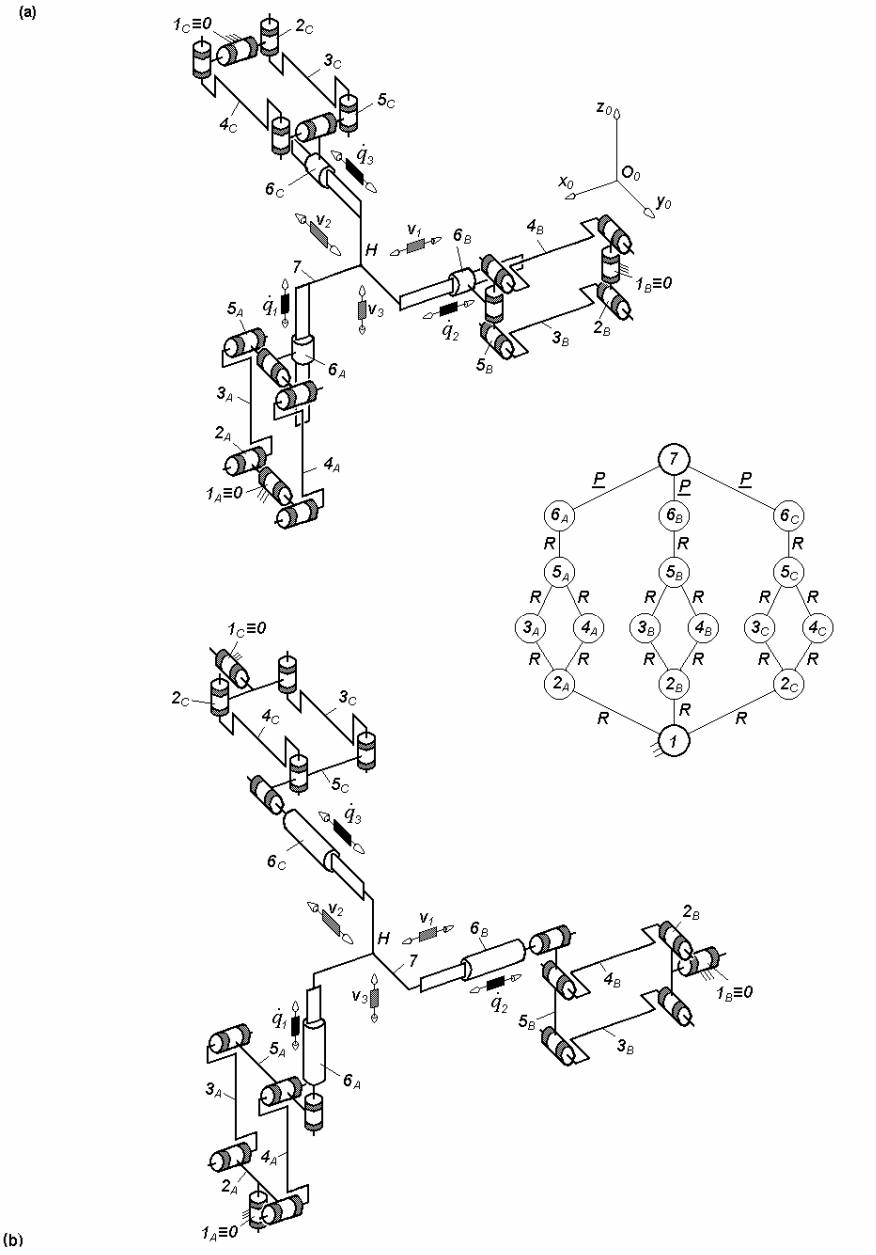

Fig. 3.23. *3-RPaR*$\underline{P}$-type overconstrained TPMs with coupled motions and linear actuators non adjacent to the fixed base, defined by $M_F = S_F = 3$, $(R_F) = (\boldsymbol{v}_1, \boldsymbol{v}_2, \boldsymbol{v}_3)$, $T_F = 0$, $N_F = 12$, limb topology $R \perp Pa \perp^{\parallel} R \perp^{\perp} \underline{P}$ (**a**) and $R \perp Pa \perp^{\parallel} R \| \underline{P}$ (**b**)

Table 3.6. Structural parameters[a] of translational parallel mechanisms in Figs. 3.18–3.23

No.	Structural parameter	Solution *3-RPC* (Figs. 3.18a, 3.19) *3-CPR* (Figs. 3.18b, 3.20)	*3-PPRR* (Fig. 3.21)	*3-RPaPR* (Fig. 3.22) *3-RPaRP* (Fig. 3.23)
1	m	8	11	17
2	p_1	3	4	7
3	p_2	3	4	7
4	p_3	3	4	7
5	p	9	12	21
6	q	2	2	5
7	k_1	3	3	0
8	k_2	0	0	3
9	k	3	3	3
10	(R_{Gi}) $(i = 1,2,3)$	See Table 3.5	See Table 3.5	See Table 3.5
11	S_{G1}	4	4	4
12	S_{G2}	4	4	4
13	S_{G3}	4	4	4
14	r_{G1}	0	0	3
15	r_{G2}	0	0	3
16	r_{G3}	0	0	3
17	M_{G1}	4	4	4
18	M_{G2}	4	4	4
19	M_{G3}	4	4	4
20	(R_F)	$(\boldsymbol{v}_1, \boldsymbol{v}_2, \boldsymbol{v}_3)$	$(\boldsymbol{v}_1, \boldsymbol{v}_2, \boldsymbol{v}_3)$	$(\boldsymbol{v}_1, \boldsymbol{v}_2, \boldsymbol{v}_3)$
21	S_F	3	3	3
22	r_1	0	0	9
23	r_F	9	9	18
24	M_F	3	3	3
25	N_F	3	3	12
26	T_F	0	0	0
27	$\sum_{j=1}^{p_1} f_j$	4	4	7
28	$\sum_{j=1}^{p_2} f_j$	4	4	7
29	$\sum_{j=1}^{p_3} f_j$	4	4	7
30	$\sum_{j=1}^{p} f_j$	12	12	21

[a]See footnote of Table 2.1 for the nomenclature of structural parameters

3.2 Derived solutions with linear actuators

Solutions with lower degrees of overconstraint can be derived from the basic solutions in Figs. 3.6–3.23 by using joints with idle mobilities. A large set of solutions can be obtained by introducing one or two rotational idle mobilities outside the parallelogram loops and up to three idle mobilities (two rotations and one translation) in the parallelogram loop. The joints combining idle mobilities are denoted by an asterisk. The idle mobilities combined in a parallelogram loop (see Fig. 6.3 – Part 1) are systematized in Table 3.7.

For example, the solutions of overconstrained TPMs with identical limbs derived from the basic solution *3-*$\underline{P}$*PaP* in Fig. 3.6a are systematized in Tables 3.8–3.10. One rotational idle mobility is combined in each cylindrical joint *C** outside the parallelogram loop. The rotational mobility of the revolute joint denoted by *R** is an idle mobility. In the same way, a large set of overconstrained solutions can be derived from each solution in Figs. 3.6–3.11.

Examples of solutions with identical limbs and three to twelve degrees of overconstraint derived from the basic solutions in Figs. 3.6–3.11, 3.15–3.17, 3.22 and 3.23 are illustrated in Figs. 3.24–3.42. The limb topology and the number of overconstraints of these solutions are systematized in Tables 3.11 and 3.12, and the structural parameters in Tables 3.13–3.17. Two idle rotational mobilities are introduced in the spherical joint of the parallelogram loops denoted by Pa^{ccs} and Pa^{scc} which combines two cylindrical, one revolute and one spherical joint (see Fig. 3.34).

Solutions with non identical limbs can be also obtained by various combinations of the idle mobilities in the three limbs. Examples of overconstrained solutions with idle mobilities and non identical limbs derived from the basic solutions in Figs. 3.12–3.15 and 3.18–3.21 are presented in Figs. 3.43–3.59. The limb topology and the number of overconstraints of these solutions are systematized in Tables 3.18 and 3.19, and the structural parameters in Tables 3.20–3.24. The linear actuators are mounted on the fixed base in the solutions in Figs. 3.43–3.52 and on a moving link in the solutions in Figs. 3.53–3.59. In the cylindrical joint denoted by $\underline{C}$* in Figs. 3.53–3.58, the translation is the actuated motion and the rotation is the idle mobility.

Table 3.7. Parallelogram loops with idle mobilities

No.	Parallelogram loop	Idle mobilities
1	Pa^{c} (Fig. 6.3b – Part 1)	One translational idle mobility combined in a cylindrical joint
2	Pa^{u} (Fig. 6.3c – Part 1)	One rotational idle mobility combined in a universal joint
3	Pa^{s} (Fig. 6.3d – Part 1)	Two rotational idle mobilities combined in a spherical joint
4	Pa^{uu} (Fig. 6.3e – Part 1)	Two rotational idle mobilities combined in two universal joints
5	Pa^{cu} (Fig. 6.3f – Part 1)	One translational idle mobility combined in a cylindrical joint and one rotational idle mobilities combined in a universal joint
6	Pa^{cs}, Pa^{*} (Fig. 6.3g – Part 1)	One translational idle mobility combined in a cylindrical joint and two rotational idle mobilities combined in a spherical joint
7	Pa^{ss} (Fig. 6.3h – Part 1)	Three idle mobilities combined in two spherical joints adjacent to the same link with a complementary rotational mobility

Table 3.8. Overconstrained TPMs with idle mobilities in the parallelogram loop derived from the basic solution *3-PPaP* in Fig. 3.6a

No.	Derived TPM	Limb topology	N_F
1	$3\text{-}\underline{P}Pa^{c}P$	$\underline{P} \perp Pa^{c}\|\|P$	12
2	$3\text{-}\underline{P}Pa^{u}P$	$\underline{P} \perp Pa^{u}\|\|P$	12
3	$3\text{-}\underline{P}Pa^{s}P$	$\underline{P} \perp Pa^{s}\|\|P$	9
4	$3\text{-}\underline{P}Pa^{uu}P$	$\underline{P} \perp Pa^{uu}\|\|P$	9
5	$3\text{-}\underline{P}Pa^{cu}P$	$\underline{P} \perp Pa^{cu}\|\|P$	9
6	$3\text{-}\underline{P}Pa^{cs}P$	$\underline{P} \perp Pa^{cs}\|\|P$	6

Table 3.9. Overconstrained TPMs with idle mobilities outside the parallelogram loop derived from the basic solution *3-PPaP* in Fig. 3.6a

No.	Derived TPM	Limb topology	N_F
1	*3-PPaPR**	$\underline{P} \perp Pa \| \| P \perp^{\perp} R$ (Fig. 8.13b – Part 1)	12
2		$\underline{P} \perp Pa \| \| P \perp {}^{\|\|} R$ (Fig. 8.13c – Part 1)	12
3		$\underline{P} \perp Pa \| \| P \| \| R$ (Fig. 8.13h – Part 1)	12
4	*3-PPaR*P*	$\underline{P} \perp Pa \perp^{\perp} R \perp {}^{\|\|} P$ (Fig. 8.11h – Part 1)	12
5		$\underline{P} \perp Pa \perp {}^{\|\|} R \perp {}^{\|\|} P$ (Fig. 8.11g – Part 1)	12
6		$\underline{P} \perp Pa \| \| R \| \| P$ (Fig. 8.12h – Part 1)	12
7	*3-PPaC** (Fig. 3.24)	$\underline{P} \perp Pa \| \| C$	12
8	*3-PR*PaP* (Fig. 3.25a)	$\underline{P} \perp R \perp^{\perp} Pa \| \| P$ (Fig. 8.11c – Part 1)	12
9		$\underline{P} \perp R \| \| Pa \| \| P$ (Fig. 8.11f – Part 1)	12
10		$\underline{P} \| \| R \perp Pa \| \| P$ (Fig. 8.8d – Part 1)	12
11	*3-R*PPaP*	$R \perp \underline{P} \perp^{\perp} Pa \| \| P$ (Fig. 8.21f – Part 1)	12
12		$R \perp \underline{P} \perp {}^{\|\|} Pa \| \| P$ (Fig. 8.21d – Part 1)	12
13		$R \| \| \underline{P} \perp Pa \| \| P$ (Fig. 8.21e – Part 1)	12
14	*3-PPaPR*R**	$\underline{P} \perp Pa \| \| P \perp^{\perp} R \perp {}^{\|\|} R$ (Fig. 9.30f – Part 1)	9
15		$\underline{P} \perp Pa \| \| P \| \| R \perp^{\perp} R$ (Fig. 9.30i – Part 1)	9
16	*3-PPaR*PR**	$\underline{P} \perp Pa \| \| R \| \| P \perp^{\perp} R$ (Fig. 9.31h – Part 1)	9
17	*3-PPaC*R**	$\underline{P} \perp Pa \| \| C \perp^{\perp} R$	9
18	*3-PR*PaPR**	$\underline{P} \perp R \perp^{\perp} Pa \| \| P \| \| R$ (Fig. 9.19n – Part 1)	9
19	*3-PR*PaC**	$\underline{P} \perp R \perp^{\perp} Pa \| \| C$	9
20	*3-R*PPaPR**	$R \perp \underline{P} \perp^{\perp} Pa \| \| P \| \| R$	9
21	*3-R*PPaC**	$R \perp \underline{P} \perp^{\perp} Pa \| \| C$	9
22	*3-PR*PaR*P*	$\underline{P} \perp R \perp^{\perp} Pa \| \| R \| \| P$ (Fig. 9.19q – Part 1)	9
23	*3-R*PPaR*P*	$R \perp \underline{P} \perp^{\perp} Pa \| \| R \| \| P$	9
24	*3-PR*R*PaP*	$\underline{P} \perp R \perp^{\perp} R \| \| Pa \| \| P$ (Fig. 9.24g – Part 1)	9
25		$\underline{P} \perp R \perp^{\perp} R \perp {}^{\|\|} Pa \| \| P$ (Fig. 9.24b – Part 1)	9
26	*3-R*R*PPaP*	$R \perp R \perp^{\perp} P \perp^{\perp} Pa \| \| P$ (Fig. 9.56e – Part 1)	9

Table 3.10. Overconstrained TPMs with idle mobilities inside and outside the parallelogram loop derived from the basic solution *3-PPaP* in Fig. 3.6a

No.	Derived TPM	Limb topology	N_F
1	*3-PPa^{c}PR**	$\underline{P} \perp Pa^c \| P \perp^{\perp} R$	9
2		$\underline{P} \perp Pa^c \| P \perp^{\|} R$	9
3		$\underline{P} \perp Pa^c \| P \| R$	9
4	*3-PPa^{u}PR**	$\underline{P} \perp Pa^u \| P \perp^{\perp} R$	9
5		$\underline{P} \perp Pa^u \| P \perp^{\|} R$	9
6		$\underline{P} \perp Pa^u \| P \| R$	9
7	*3-PPa^{c}R*P*	$\underline{P} \perp Pa^c \perp^{\perp} R \perp^{\|} P$	9
8		$\underline{P} \perp Pa^c \perp^{\|} R \perp^{\|} P$	9
9		$\underline{P} \perp Pa^c \| R \| P$	9
10	*3-PPa^{u}R*P*	$\underline{P} \perp Pa^u \perp^{\perp} R \perp^{\|} P$	9
11		$\underline{P} \perp Pa^u \perp^{\|} R \perp^{\|} P$	9
12		$\underline{P} \perp Pa^u \| R \| P$	9
13	*3-PPa^{c}C**	$\underline{P} \perp Pa^c \| C$	9
14	*3-PPa^{u}C**	$\underline{P} \perp Pa^u \| C$	9
15	*3-PR*Pa^{c}P*	$\underline{P} \perp R \perp^{\perp} Pa^c \| P$	9
16		$\underline{P} \perp R \| Pa^c \| P$	9
17		$\underline{P} \| R \perp Pa^c \| P$	9
18	*3-PR*Pa^{u}P*	$\underline{P} \perp R \perp^{\perp} Pa^u \| P$	9
19		$\underline{P} \perp R \| Pa^u \| P$	9
20		$\underline{P} \| R \perp Pa^u \| P$	9
21	*3-R*PPa^{c}P*	$R \perp \underline{P} \perp^{\perp} Pa^c \| P$	9
22		$R \perp \underline{P} \perp^{\|} Pa^c \| P$	9
23		$R \| \underline{P} \perp Pa^c \| P$	9
24	*3-R*PPa^{u}P*	$R \perp \underline{P} \perp^{\perp} Pa^u \| P$	9
25		$R \perp \underline{P} \perp^{\|} Pa^u \| P$	9
26		$R \| \underline{P} \perp Pa^u \| P$	9
27	*3-PPa^{c}PR*R**	$\underline{P} \perp Pa^c \| P \perp^{\perp} R \perp^{\|} R$	6
28		$\underline{P} \perp Pa^c \| P \| R \perp^{\perp} R$	6
29	*3-PPa^{u}PR*R**	$\underline{P} \perp Pa^u \| P \perp^{\perp} R \perp^{\|} R$	6
30		$\underline{P} \perp Pa^u \| P \| R \perp^{\perp} R$	6
31	*3-PPa^{c}R*PR**	$\underline{P} \perp Pa^c \| R \| P \perp^{\perp} R$	6
32	*3-PPa^{u}R*PR**	$\underline{P} \perp Pa^u \| R \| P \perp^{\perp} R$	6
33	*3-PPa^{c}C*R**	$\underline{P} \perp Pa^c \| C \perp^{\perp} R$	6
34	*3-PPa^{u}C*R**	$\underline{P} \perp Pa^u \| C \perp^{\perp} R$	6
35	*3-PR*Pa^{c}PR**	$\underline{P} \perp R \perp^{\perp} Pa^c \| P \| R$	6
36	*3-PR*Pa^{u}PR**	$\underline{P} \perp R \perp^{\perp} Pa^u \| P \| R$	6
37	*3-PR*Pa^{c}C**	$\underline{P} \perp R \perp^{\perp} Pa^c \| C$	6
38	*3-PR*Pa^{u}C**	$\underline{P} \perp R \perp^{\perp} Pa^u \| C$	6
39	*3-R*PPa^{c}PR**	$R \perp \underline{P} \perp^{\perp} Pa^c \| P \| R$	6

Table 3.10. (cont.)

40	$3\text{-}R^*\underline{P}Pa^uPR^*$	$R \perp \underline{P} \perp^{\perp} Pa^u \| \| P \| \| R$	6
41	$3\text{-}R^*\underline{P}Pa^cC^*$	$R \perp \underline{P} \perp^{\perp} Pa^c \| \| C$	6
42	$3\text{-}R^*\underline{P}Pa^uC^*$	$R \perp \underline{P} \perp^{\perp} Pa^u \| \| C$	6
43	$3\text{-}\underline{P}R^*Pa^cR^*P$	$\underline{P} \perp R \perp^{\perp} Pa^c \| \| R \| \| P$	6
44	$3\text{-}\underline{P}R^*Pa^uR^*P$	$\underline{P} \perp R \perp^{\perp} Pa^u \| \| R \| \| P$	6
45	$3\text{-}R^*\underline{P}Pa^cR^*P$	$R \perp \underline{P} \perp^{\perp} Pa^c \| \| R \| \| P$	6
46	$3\text{-}R^*\underline{P}Pa^uR^*P$	$R \perp \underline{P} \perp^{\perp} Pa^u \| \| R \| \| P$	6
47	$3\text{-}\underline{P}R^*R^*Pa^cP$	$\underline{P} \perp R \perp^{\perp} R \| \| Pa^c \| \| P$	6
48		$\underline{P} \perp R \perp^{\perp} R \perp^{\|} Pa^c \| \| P$	6
49	$3\text{-}\underline{P}R^*R^*Pa^uP$	$\underline{P} \perp R \perp^{\perp} R \| \| Pa^u \| \| P$	6
50		$\underline{P} \perp R \perp^{\perp} R \perp^{\|} Pa^u \| \| P$	6
51	$3\text{-}R^*R^*\underline{P}Pa^cP$	$R \perp R \perp^{\perp} P \perp^{\perp} Pa^c \| \| P$	6
52	$3\text{-}R^*R^*\underline{P}Pa^uP$	$R \perp R \perp^{\perp} P \perp^{\perp} Pa^u \| \| P$	6
53	$3\text{-}\underline{P}Pa^sPR^*$	$\underline{P} \perp Pa^s \| \| P \perp^{\perp} R$	6
54		$\underline{P} \perp Pa^s \| \| P \perp^{\|} R$	6
55		$\underline{P} \perp Pa^s \| \| P \| \| R$	6
56	$3\text{-}\underline{P}Pa^{uu}PR^*$	$\underline{P} \perp Pa^{uu} \| \| P \perp^{\perp} R$	6
57		$\underline{P} \perp Pa^{uu} \| \| P \perp^{\|} R$	6
58		$\underline{P} \perp Pa^{uu} \| \| P \| \| R$	6
59	$3\text{-}\underline{P}Pa^{cu}PR^*$	$\underline{P} \perp Pa^{cu} \| \| P \perp^{\perp} R$	6
60		$\underline{P} \perp Pa^{cu} \| \| P \perp^{\|} R$	6
61		$\underline{P} \perp Pa^{cu} \| \| P \| \| R$	6
62	$3\text{-}\underline{P}Pa^sR^*P$	$\underline{P} \perp Pa^s \perp^{\perp} R \perp^{\|} P$	6
63		$\underline{P} \perp Pa^s \perp^{\|} R \perp^{\|} P$	6
64		$\underline{P} \perp Pa^s \| \| R \| \| P$	6
65	$3\text{-}\underline{P}Pa^{uu}R^*P$	$\underline{P} \perp Pa^{uu} \perp^{\perp} R \perp^{\|} P$	6
66		$\underline{P} \perp Pa^{uu} \perp^{\|} R \perp^{\|} P$	6
67		$\underline{P} \perp Pa^{uu} \| \| R \| \| P$	6
68	$3\text{-}\underline{P}Pa^{cu}R^*P$	$\underline{P} \perp Pa^{cu} \perp^{\perp} R \perp^{\|} P$	6
69		$\underline{P} \perp Pa^{cu} \perp^{\|} R \perp^{\|} P$	6
70		$\underline{P} \perp Pa^{cu} \| \| R \| \| P$	6
71	$3\text{-}\underline{P}Pa^sC^*$	$\underline{P} \perp Pa^s \| \| C$	6
72	$3\text{-}\underline{P}Pa^{uu}C^*$	$\underline{P} \perp Pa^{uu} \| \| C$	6
73	$3\text{-}\underline{P}Pa^{cu}C^*$	$\underline{P} \perp Pa^{cu} \| \| C$	6
74	$\underline{P}R^*Pa^sP$	$\underline{P} \perp R \perp^{\perp} Pa^s \| \| P$	6
75		$\underline{P} \perp R \| \| Pa^s \| \| P$	6
76		$\underline{P} \| \| R \perp Pa^s \| \| P$	6
77	$\underline{P}R^*Pa^{uu}P$	$\underline{P} \perp R \perp^{\perp} Pa^{uu} \| \| P$	6
78		$\underline{P} \perp R \| \| Pa^{uu} \| \| P$	6
79		$\underline{P} \| \| R \perp Pa^{uu} \| \| P$	6

Table 3.10. (cont.)

80	$\underline{P}R{*}Pa^{cu}P$	$\underline{P} \perp R \perp^{\perp} Pa^{cu} \| \| P$	6
81		$\underline{P} \perp R \| \| Pa^{cu} \| \| P$	6
82		$\underline{P} \| \| R \perp Pa^{cu} \| \| P$	6
83	$3\text{-}R{*}\underline{P}Pa^{s}P$	$R \perp \underline{P} \perp^{\perp} Pa^{s} \| \| P$	6
84		$R \perp \underline{P} \perp^{\|} Pa^{s} \| \| P$	6
85		$R \| \| \underline{P} \perp Pa^{s} \| \| P$	6
86	$3\text{-}R{*}\underline{P}Pa^{uu}P$	$R \perp \underline{P} \perp^{\perp} Pa^{uu} \| \| P$	6
87		$R \perp \underline{P} \perp^{\|} Pa^{uu} \| \| P$	6
88		$R \| \| \underline{P} \perp Pa^{uu} \| \| P$	6
89	$3\text{-}R{*}\underline{P}Pa^{cu}P$	$R \perp \underline{P} \perp^{\perp} Pa^{cu} \| \| P$	6
90		$R \perp \underline{P} \perp^{\|} Pa^{cu} \| \| P$	6
91		$R \| \| \underline{P} \perp Pa^{cu} \| \| P$	6
92	$3\text{-}\underline{P}Pa^{ss}P$ (Fig. 3.25a)	$\underline{P} \perp Pa^{ss} \| \| P$	3
93	$3\text{-}\underline{P}Pa^{cs}PR{*}$	$\underline{P} \perp Pa^{cs} \| \| P \perp^{\perp} R$	3
94		$\underline{P} \perp Pa^{cs} \| \| P \perp^{\|} R$	3
95		$\underline{P} \perp Pa^{cs} \| \| P \| \| R$	3
96	$3\text{-}\underline{P}Pa^{cs}PR{*}$	$\underline{P} \perp Pa^{cs} \| \| P \perp^{\perp} R$	3
97		$\underline{P} \perp Pa^{cs} \| \| P \perp^{\|} R$	3
98		$\underline{P} \perp Pa^{cs} \| \| P \| \| R$	3
99	$3\text{-}\underline{P}Pa^{cs}R{*}P$	$\underline{P} \perp Pa^{cs} \perp^{\perp} R \perp^{\|} P$	3
100		$\underline{P} \perp Pa^{cs} \perp^{\|} R \perp^{\|} P$	3
101		$\underline{P} \perp Pa^{cs} \| \| R \| \| P$	3
102	$3\text{-}\underline{P}Pa^{cs}R{*}P$	$\underline{P} \perp Pa^{cs} \perp^{\perp} R \perp^{\|} P$	3
103		$\underline{P} \perp Pa^{cs} \perp^{\|} R \perp^{\|} P$	3
104		$\underline{P} \perp Pa^{cs} \| \| R \| \| P$	3
105	$3\text{-}\underline{P}Pa^{cs}C{*}$	$\underline{P} \perp Pa^{cs} \| \| C$	3
106	$3\text{-}\underline{P}Pa^{cs}C{*}$	$\underline{P} \perp Pa^{cs} \| \| C$	3
107	$3\text{-}\underline{P}R{*}Pa^{cs}P$	$\underline{P} \perp R \perp^{\perp} Pa^{cs} \| \| P$	3
108		$\underline{P} \perp R \| \| Pa^{cs} \| \| P$	3
109		$\underline{P} \| \| R \perp Pa^{cs} \| \| P$	3
110	$3\text{-}\underline{P}R{*}Pa^{cs}P$	$\underline{P} \perp R \perp^{\perp} Pa^{cs} \| \| P$	3
111		$\underline{P} \perp R \| \| Pa^{cs} \| \| P$	3
112		$\underline{P} \| \| R \perp Pa^{cs} \| \| P$	3
113	$3\text{-}R{*}\underline{P}Pa^{cs}P$	$R \perp \underline{P} \perp^{\perp} Pa^{cs} \| \| P$	3
114		$R \perp \underline{P} \perp^{\|} Pa^{cs} \| \| P$	3
115		$R \| \| \underline{P} \perp Pa^{cs} \| \| P$	3
116	$3\text{-}R{*}\underline{P}Pa^{cs}P$	$R \perp \underline{P} \perp^{\perp} Pa^{cs} \| \| P$	3
117		$R \perp \underline{P} \perp^{\|} Pa^{cs} \| \| P$	3
118		$R \| \| \underline{P} \perp Pa^{cs} \| \| P$	3
119	$3\text{-}\underline{P}Pa^{s}PR{*}R{*}$	$\underline{P} \perp Pa^{s} \| \| P \perp^{\perp} R \perp^{\|} R$	3
120		$\underline{P} \perp Pa^{s} \| \| P \| \| R \perp^{\perp} R$	3

Table 3.10. (cont.)

121	$3\text{-}\underline{P}Pa^{uu}PR^*R^*$	$\underline{P}\perp Pa^{uu}\|\|P\perp^{\perp} R\perp^{\|} R$	3
122		$\underline{P}\perp Pa^{uu}\|\|P\|\|R\perp^{\perp} R$	3
123	$3\text{-}\underline{P}Pa^{cu}PR^*R^*$	$\underline{P}\perp Pa^{cu}\|\|P\perp^{\perp} R\perp^{\|} R$	3
124		$\underline{P}\perp Pa^{cu}\|\|P\|\|R\perp^{\perp} R$	3
125	$3\text{-}\underline{P}Pa^{s}R^*PR^*$	$\underline{P}\perp Pa^{s}\|\|R\|\|P\perp^{\perp} R$	3
126	$3\text{-}\underline{P}Pa^{uu}R^*PR^*$	$\underline{P}\perp Pa^{uu}\|\|R\|\|P\perp^{\perp} R$	3
127	$3\text{-}\underline{P}Pa^{cu}R^*PR^*$	$\underline{P}\perp Pa^{cu}\|\|R\|\|P\perp^{\perp} R$	3
128	$3\text{-}\underline{P}Pa^{s}C^*R^*$	$\underline{P}\perp Pa^{s}\|\|C\perp^{\perp} R$	3
129	$3\text{-}\underline{P}Pa^{uu}C^*R^*$	$\underline{P}\perp Pa^{uu}\|\|C\perp^{\perp} R$	3
130	$3\text{-}\underline{P}Pa^{cu}C^*R^*$	$\underline{P}\perp Pa^{cu}\|\|C\perp^{\perp} R$	3
131	$3\text{-}\underline{P}R^*Pa^{s}PR^*$	$\underline{P}\perp R\perp^{\perp} Pa^{s}\|\|P\|\|R$	3
132	$3\text{-}\underline{P}R^*Pa^{uu}PR^*$	$\underline{P}\perp R\perp^{\perp} Pa^{uu}\|\|P\|\|R$	3
133	$3\text{-}\underline{P}R^*Pa^{cu}PR^*$	$\underline{P}\perp R\perp^{\perp} Pa^{cu}\|\|P\|\|R$	3
134	$3\text{-}\underline{P}R^*Pa^{s}C^*$	$\underline{P}\perp R\perp^{\perp} Pa^{s}\|\|C$	3
135	$3\text{-}\underline{P}R^*Pa^{uu}C^*$	$\underline{P}\perp R\perp^{\perp} Pa^{uu}\|\|C$	3
136	$3\text{-}\underline{P}R^*Pa^{cu}C^*$	$\underline{P}\perp R\perp^{\perp} Pa^{cu}\|\|C$	3
137	$3\text{-}R^*\underline{P}Pa^{s}PR^*$	$R\perp \underline{P}\perp^{\perp} Pa^{s}\|\|P\|\|R$	3
138	$3\text{-}R^*\underline{P}Pa^{uu}PR^*$	$R\perp \underline{P}\perp^{\perp} Pa^{uu}\|\|P\|\|R$	3
139	$3\text{-}R^*\underline{P}Pa^{cu}PR^*$	$R\perp \underline{P}\perp^{\perp} Pa^{cu}\|\|P\|\|R$	3
140	$3\text{-}R^*\underline{P}Pa^{s}C^*$	$R\perp \underline{P}\perp^{\perp} Pa^{s}\|\|C$	3
141	$3\text{-}R^*\underline{P}Pa^{uu}C^*$	$R\perp \underline{P}\perp^{\perp} Pa^{uu}\|\|C$	3
142	$3\text{-}R^*\underline{P}Pa^{cu}C^*$	$R\perp \underline{P}\perp^{\perp} Pa^{cu}\|\|C$	3
143	$3\text{-}\underline{P}R^*Pa^{s}R^*P$	$\underline{P}\perp R\perp^{\perp} Pa^{s}\|\|R\|\|P$	3
144	$3\text{-}\underline{P}R^*Pa^{uu}R^*P$	$\underline{P}\perp R\perp^{\perp} Pa^{uu}\|\|R\|\|P$	3
145	$3\text{-}\underline{P}R^*Pa^{cu}R^*P$	$\underline{P}\perp R\perp^{\perp} Pa^{cu}\|\|R\|\|P$	3
146	$3\text{-}R^*\underline{P}Pa^{s}R^*P$	$R\perp \underline{P}\perp^{\perp} Pa^{s}\|\|R\|\|P$	3
147	$3\text{-}R^*\underline{P}Pa^{uu}R^*P$	$R\perp \underline{P}\perp^{\perp} Pa^{uu}\|\|R\|\|P$	3
148	$3\text{-}R^*\underline{P}Pa^{cu}R^*P$	$R\perp \underline{P}\perp^{\perp} Pa^{cu}\|\|R\|\|P$	3
149	$3\text{-}\underline{P}R^*R^*Pa^{s}P$	$\underline{P}\perp R\perp^{\perp} R\|\|Pa^{s}\|\|P$	3
150		$\underline{P}\perp R\perp^{\perp} R\perp^{\|} Pa^{s}\|\|P$	3
151	$3\text{-}\underline{P}R^*R^*Pa^{uu}P$	$\underline{P}\perp R\perp^{\perp} R\|\|Pa^{uu}\|\|P$	3
152		$\underline{P}\perp R\perp^{\perp} R\perp^{\|} Pa^{uu}\|\|P$	3
153	$3\text{-}\underline{P}R^*R^*Pa^{cu}P$	$\underline{P}\perp R\perp^{\perp} R\|\|Pa^{cu}\|\|P$	3
154		$\underline{P}\perp R\perp^{\perp} R\perp^{\|} Pa^{cu}\|\|P$	3
155	$3\text{-}R^*R^*\underline{P}Pa^{s}P$	$R\perp R\perp^{\perp} P\perp^{\perp} Pa^{s}\|\|P$	3
156	$3\text{-}R^*R^*\underline{P}Pa^{uu}P$	$R\perp R\perp^{\perp} P\perp^{\perp} Pa^{uu}\|\|P$	3
157	$3\text{-}R^*R^*\underline{P}Pa^{cu}P$	$R\perp R\perp^{\perp} P\perp^{\perp} Pa^{cu}\|\|P$	3

Table 3.11. Limb topology and the number of overconstraints N_F of the derived TPMs with idle mobilities and linear actuators mounted on the fixed base presented in Figs. 3.24–3.38

No.	Basic TPM type	N_F	Derived TPM type	N_F	Limb topology
1	*3-PPaP* (Fig. 3.6a)	*15*	*3-PPaC** (Fig. 3.24a)	*12*	$\underline{P} \perp Pa \| \| C^*$
2			*3-PR*PaP* (Fig. 3.25a)	*12*	$\underline{P} \perp R^* \perp^{\perp} Pa \| \| P$
3			*3-PPa^{ss}P* (Fig. 3.26a)	*3*	$\underline{P} \perp Pa^{ss} \| \| P$
4	*3-PPPa* (Fig. 3.7a)	*15*	*3-PC*Pa* (Fig. 3.24b)	*12*	$\underline{P} \perp C^* \| \| Pa$
5			*3-PPR*Pa* (Fig. 3.25b)	*12*	$\underline{P} \perp P \perp^{\perp} R^* \perp^{\|} Pa$
6			*3-PPPa^{ss}* (Fig. 3.26b)	*3*	$\underline{P} \perp P \| \| Pa^{ss}$
7	*3-PPa^{cc}* (Fig. 3.8a)	*12*	*3-PR*Pa^{cc}* (Fig. 3.28a)	*9*	$\underline{P} \perp R^* \perp^{\perp} Pa^{cc}$
8			*3-PR*Pa^{scc}* (Fig. 3.27a)	*3*	$\underline{P} \perp R^* \perp^{\perp} Pa^{scc}$
9	*3-PPa^{cc}* (Fig. 3.9a)	*12*	*3-PR*Pa^{cc}* (Fig. 3.28b)	*9*	$\underline{P} \perp R^* \perp^{\perp} Pa^{cc}$
10			*3-PR*Pa^{ccs}* (Fig. 3.27b)	*3*	$\underline{P} \perp R^* \perp^{\perp} Pa^{ccs}$
11	*3-PPaPa* (Fig. 3.10a)	*24*	*3-PPaPa^{ss}* (Fig. 3.29a)	*12*	$\underline{P} \perp Pa \perp^{\perp} Pa^{ss}$
12			*3-PPa^{ss}Pa* (Fig. 3.30a)	*12*	$\underline{P} \perp Pa^{ss} \perp^{\perp} Pa$
13	*3-PPaPa* (Fig. 3.10b)	*24*	*3-PPaPa^{ss}* (Fig. 3.29b)	*12*	$\underline{P} \perp Pa \perp^{\|} Pa^{ss}$
14			*3-PPa^{ss}Pa* (Fig. 3.30b)	*12*	$\underline{P} \perp Pa \perp^{\|} Pa^{ss}$
15	*3-PPaPa* (Fig. 3.11a)	*24*	*3-PPaPa^{ss}* (Fig. 3.31a)	*12*	$\underline{P} \| \| Pa \perp Pa^{ss}$
16			*3-PPa^{ss}Pa* (Fig. 3.31b)	*12*	$\underline{P} \| \| Pa^{ss} \perp Pa$
17	*3-PPr* (Fig. 3.11b)	*12*	*3-PPr^{ss}* (Fig. 3.34a)	*6*	$\underline{P} \perp Pr^{ss}$
18			*3-PPr^{ss}R** (Fig. 3.34b)	*3*	$\underline{P} \perp Pr^{ss} \perp^{\|} R^*$
19	*3-PRPaR* (Fig. 3.15a)	*12*	*3-PR*RPaR* (Fig. 3.32a)	*9*	$\underline{P} \perp R^* \perp^{\|} R \perp Pa \perp^{\|} R$
20			*3-PRPa^{ss}* (Fig. 3.33a)	*3*	$\underline{P} \| \| R \perp Pa^{ss}$

Table 3.11. (cont.)

21	*3-<u>P</u>RPaR* (Fig. 3.15b)	*12*	*3-<u>P</u>R*RPaR* (Fig. 3.32b)	*9*	$\underline{P}\|\|R^* \perp R \perp Pa \perp {}^{\|\|}R$
22			*3-<u>P</u>RPa^{ss}* (Fig. 3.33b)	*3*	$\underline{P} \perp R \perp Pa^{ss}$
23	*3-<u>P</u>RRPa* (Fig. 3.16a)	*12*	*3-<u>P</u>RRPaR** (Fig. 3.35a)	*9*	$\underline{P} \perp R\|\|R \perp {}^{\|\|}Pa\|\|R^*$
24			*3-<u>P</u>RPa^{ss}* (Fig. 3.36a)	*3*	$\underline{P} \perp R \perp {}^{\|\|}Pa^{ss}$
25	*3-<u>P</u>RRPa* (Fig. 3.16b)	*12*	*3-<u>P</u>RRPaR** (Fig. 3.35b)	*9*	$\underline{P}\|\|R\|\|R \perp Pa\|\|R^*$
26			*3-<u>P</u>RRPa^{cs}* (Fig. 3.36b)	*3*	$\underline{P}\|\|R\|\|R \perp Pa^{cs}$
27	*3-<u>P</u>PaRR* (Fig. 3.17a)	*12*	*3-<u>P</u>R*PaRR* (Fig. 3.37a)	*9*	$\underline{P} \perp R^*\|\|Pa \perp^{\perp} R\|\|R$
28			*3-<u>P</u>Pa^{ss}R* (Fig. 3.38a)	*3*	$\underline{P} \perp Pa^{ss} \perp^{\perp} R$
29	*3-<u>P</u>PaRR* (Fig. 3.17b)	*12*	*3-<u>P</u>R*PaRR* (Fig. 3.37b)	*9*	$\underline{P}\|\|R^*\|\|Pa \perp R\|\|R$
30			*3-<u>P</u>Pa^{ss}R* (Fig. 3.38b)	*3*	$\underline{P}\|\|Pa^{ss} \perp R$

Table 3.12. Limb topology and the number of overconstraints N_F of the derived TPMs with idle mobilities and linear actuators mounted on a moving link presented in Figs. 3.39–3.42

No.	Basic TPM type	N_F	Derived TPM type	N_F	Limb topology
1	*3-RPa<u>P</u>R* (Fig. 3.22a)	*12*	*3-RPa<u>P</u>RR** (Fig. 3.39a)	*9*	$R \perp Pa \perp^{\perp} \underline{P} \perp^{\perp} R \perp R^*$
2			*3-RPa^{cs}<u>P</u>R* (Fig. 3.40a)	*3*	$R \perp Pa^{cs} \perp^{\perp} \underline{P} \perp^{\perp} R$
3	*3-RPa<u>P</u>R* (Fig. 3.22b)	*12*	*3-RPa<u>P</u>RR** (Fig. 3.39b)	*9*	$R \perp Pa \perp {}^{\|\|}\underline{P}\|\|R \perp R^*$
4			*3-RPa^{cs}<u>P</u>R* (Fig. 3.40b)	*3*	$R \perp Pa^{cs} \perp {}^{\|\|}\underline{P}\|\|R$
5	*3-RPaR<u>P</u>* (Fig. 3.23a)	*12*	*3-RPaRR*<u>P</u>* (Fig. 3.41a)	*9*	$R \perp Pa \perp {}^{\|\|}R \perp R^* \perp^{\perp} \underline{P}$
6			*3-RPa^{ss}<u>P</u>* (Fig. 3.42a)	*3*	$R \perp Pa^{ss} \perp^{\perp} \underline{P}$
7	*3-RPaR<u>P</u>* (Fig. 3.23b)	*12*	*3-RPaR<u>P</u>R** (Fig. 3.41b)	*9*	$R \perp Pa \perp {}^{\|\|}R\|\|\underline{P} \perp R^*$
8			*3-RPa^{cs}R<u>P</u>* (Fig. 3.42b)	*3*	$R \perp Pa^{cs} \perp {}^{\|\|}R\|\|\underline{P}$

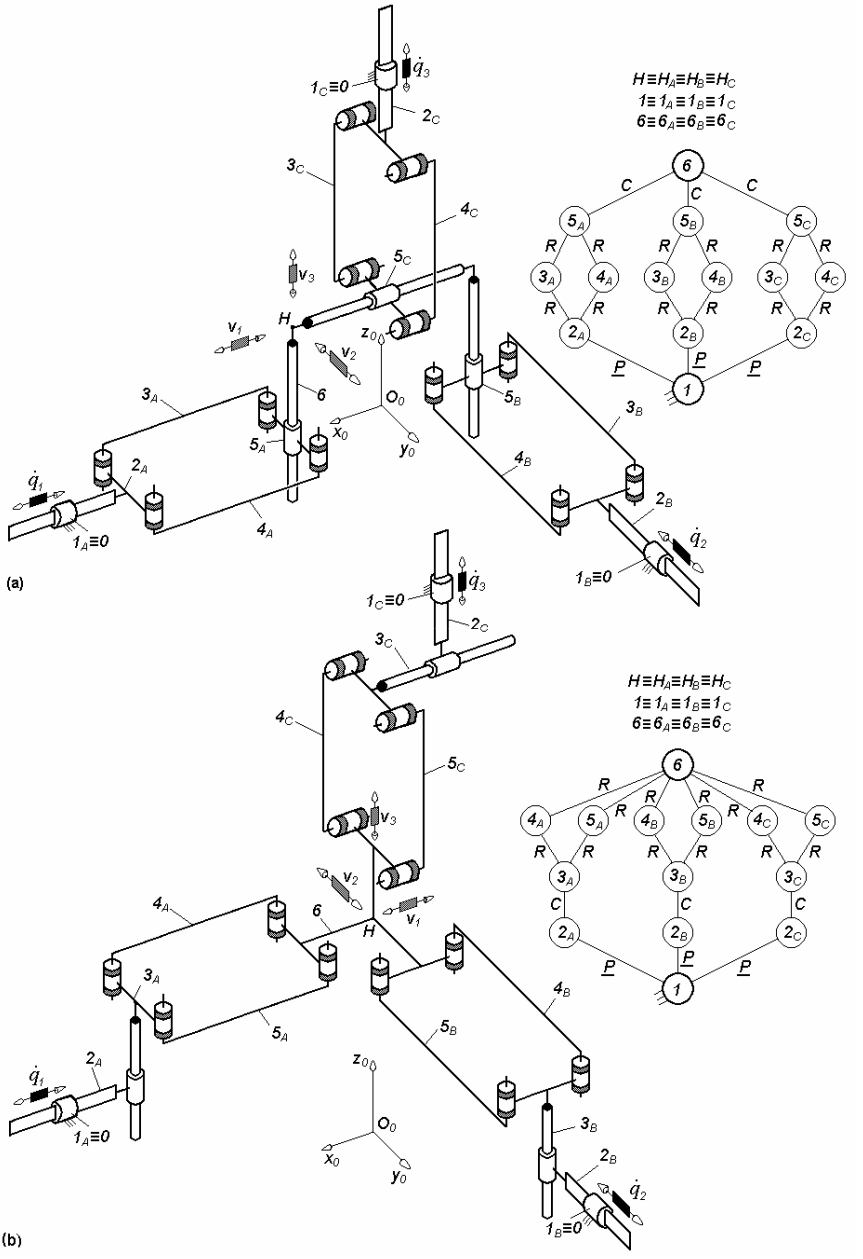

Fig. 3.24. Overconstrained TPMs of types *3-PPaC** (**a**) and *3-PC*Pa* (**b**) with coupled motions and linear actuators on the fixed base, defined by $M_F = S_F = 3$, $(R_F) = (\boldsymbol{v}_1, \boldsymbol{v}_2, \boldsymbol{v}_3)$ $T_F = 0$, $N_F = 12$, limb topology $\underline{P} \perp Pa || C^*$ (**a**) and $\underline{P} \perp C^* || Pa$ (**b**)

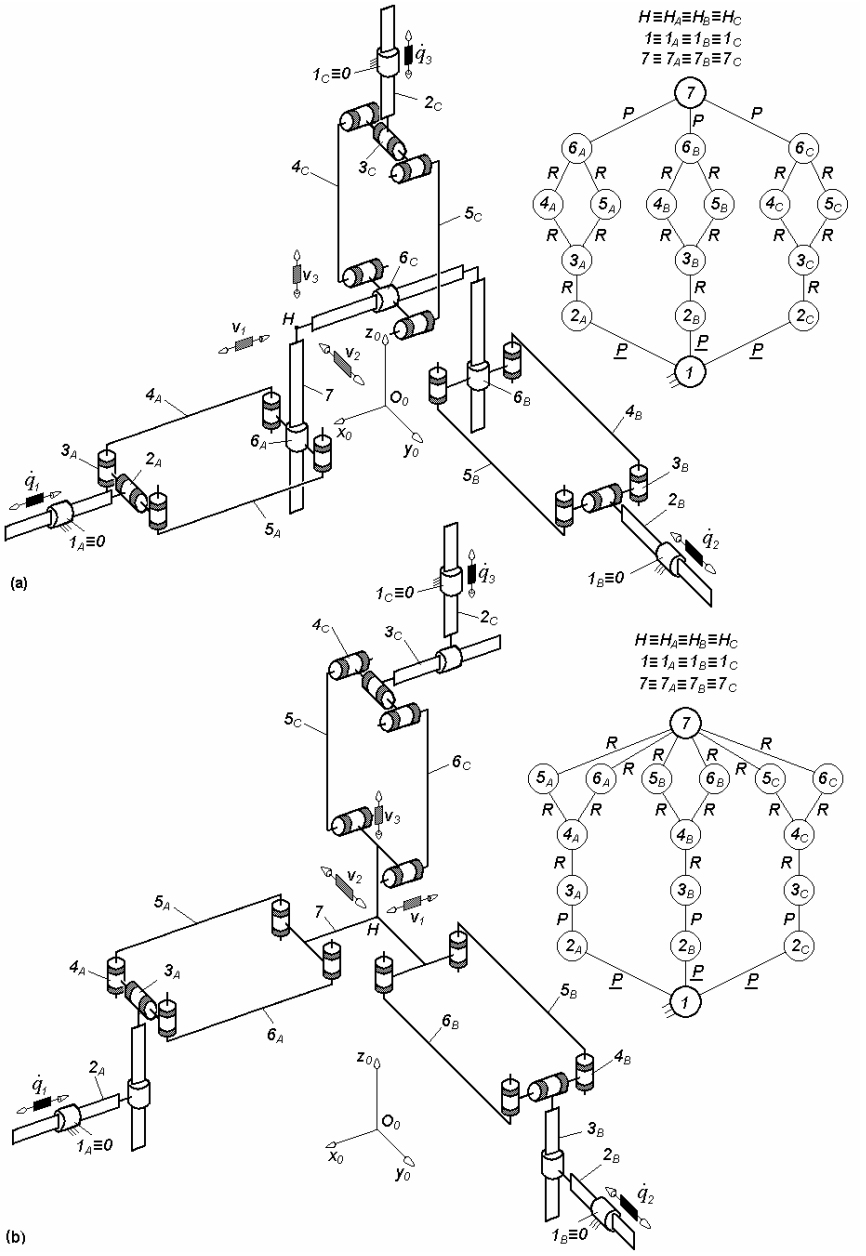

Fig. 3.25. Overconstrained TPMs of types *3-PR*PaP* (**a**) and *3-PPR*Pa* (**b**) with coupled motions and linear actuators on the fixed base, defined by $M_F = S_F = 3$, $(R_F) = (\boldsymbol{v}_1, \boldsymbol{v}_2, \boldsymbol{v}_3)$ $T_F = 0$, $N_F = 12$, limb topology $\underline{P} \perp R^* \perp^{\perp} Pa \| P$ (**a**) and $\underline{P} \perp P \perp^{\perp} R^* \perp^{\|} Pa$ (**b**)

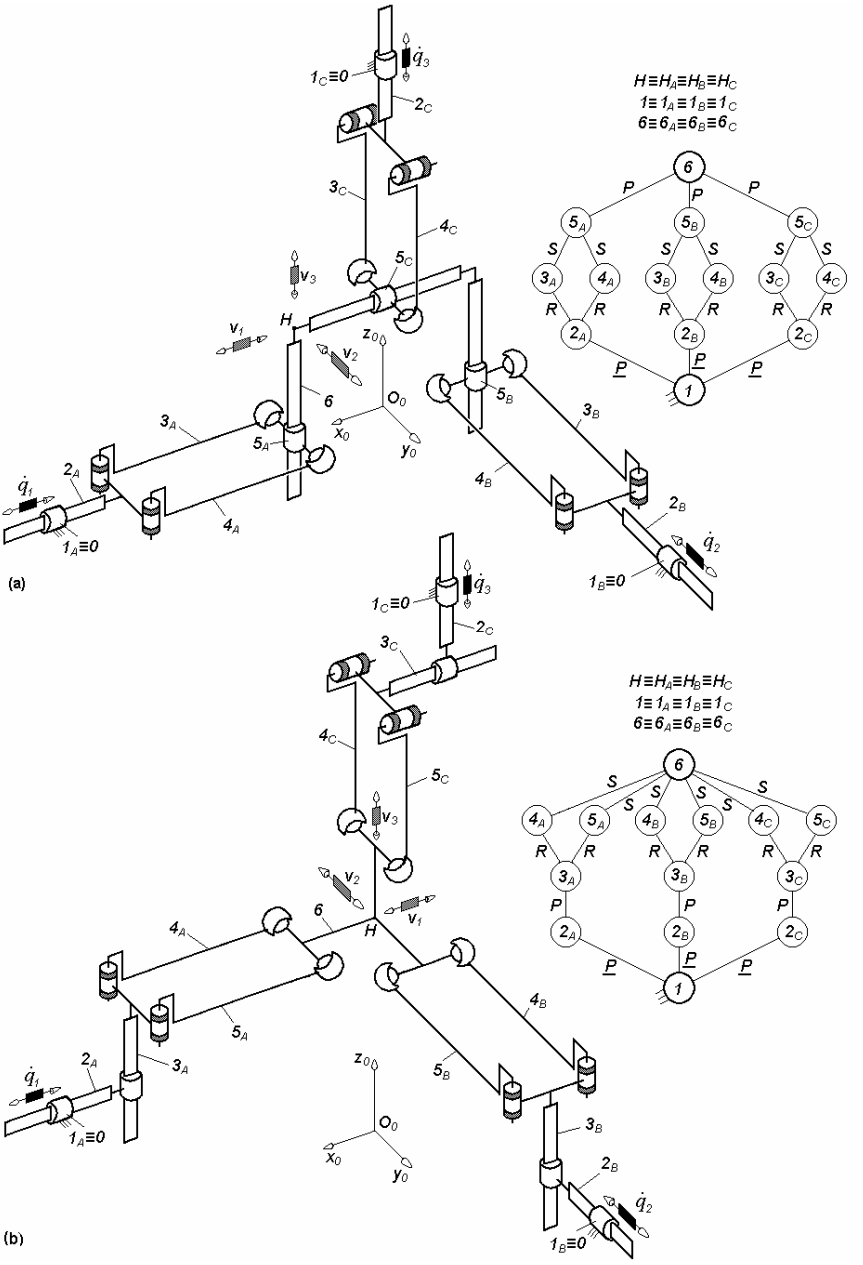

Fig. 3.26. Overconstrained TPMs of types *3-*$\underline{P}$*Pa*^{ss}*P* (**a**) and *3-*$\underline{P}$*PPa*^{ss} (**b**) with coupled motions and linear actuators on the fixed base, defined by $M_F = S_F = 3$, $(R_F) = (\boldsymbol{v}_1, \boldsymbol{v}_2, \boldsymbol{v}_3)$ $T_F = 0$, $N_F = 3$, limb topology $\underline{P} \perp Pa^{ss}||P$ (**a**) and $\underline{P} \perp P||Pa^{ss}$ (**b**)

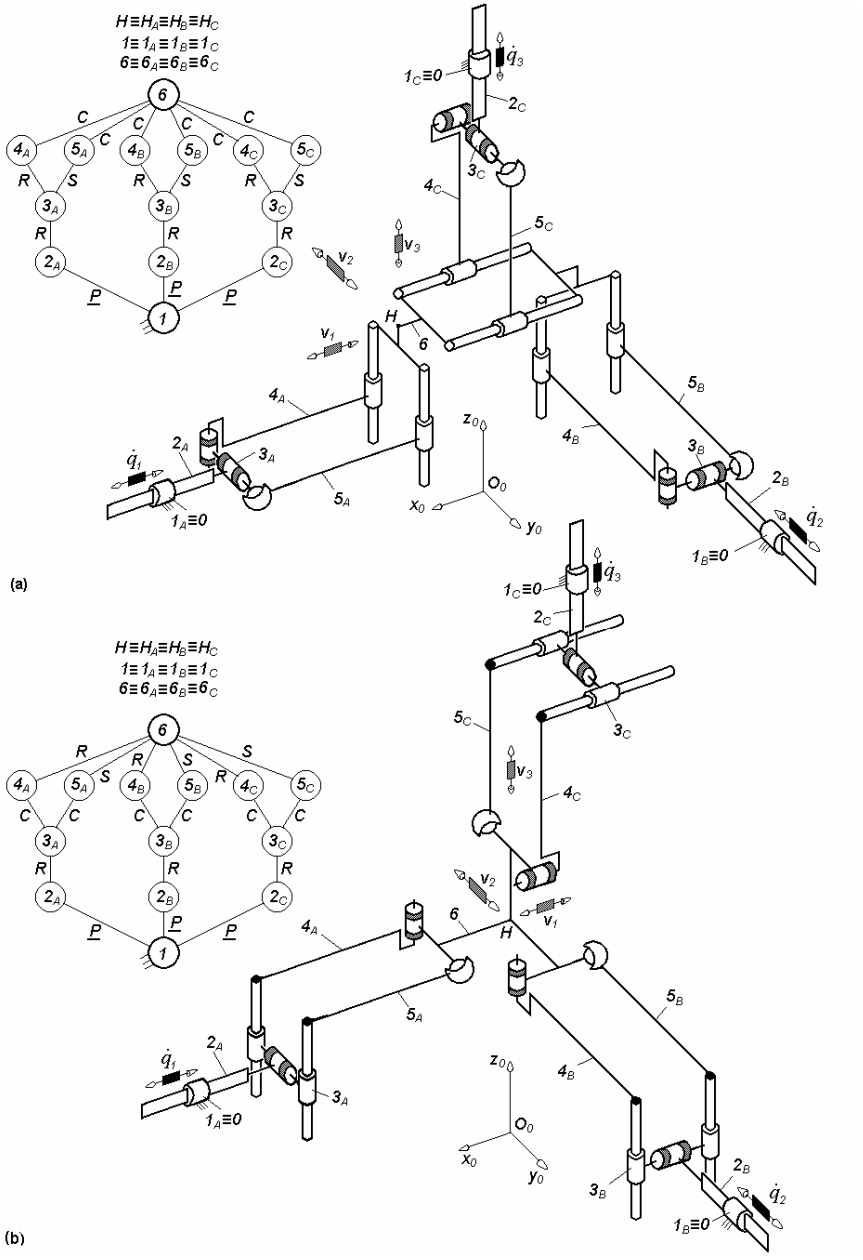

Fig. 3.27. Overconstrained TPMs of types *3-*$\underline{P}$*R*Pa*^{scc} (**a**) and *3-*$\underline{P}$*R*Pa*^{ccs} (**b**) with coupled motions and linear actuators on the fixed base, defined by $M_F = S_F = 3$, $(R_F) = (\boldsymbol{v}_1, \boldsymbol{v}_2, \boldsymbol{v}_3)$ $T_F = 0$, $N_F = 3$, limb topology $\underline{P} \perp R^* \perp^{\perp} Pa^{scc}$ (**a**) and $\underline{P} \perp R^* \perp^{\perp} Pa^{ccs}$ (**b**)

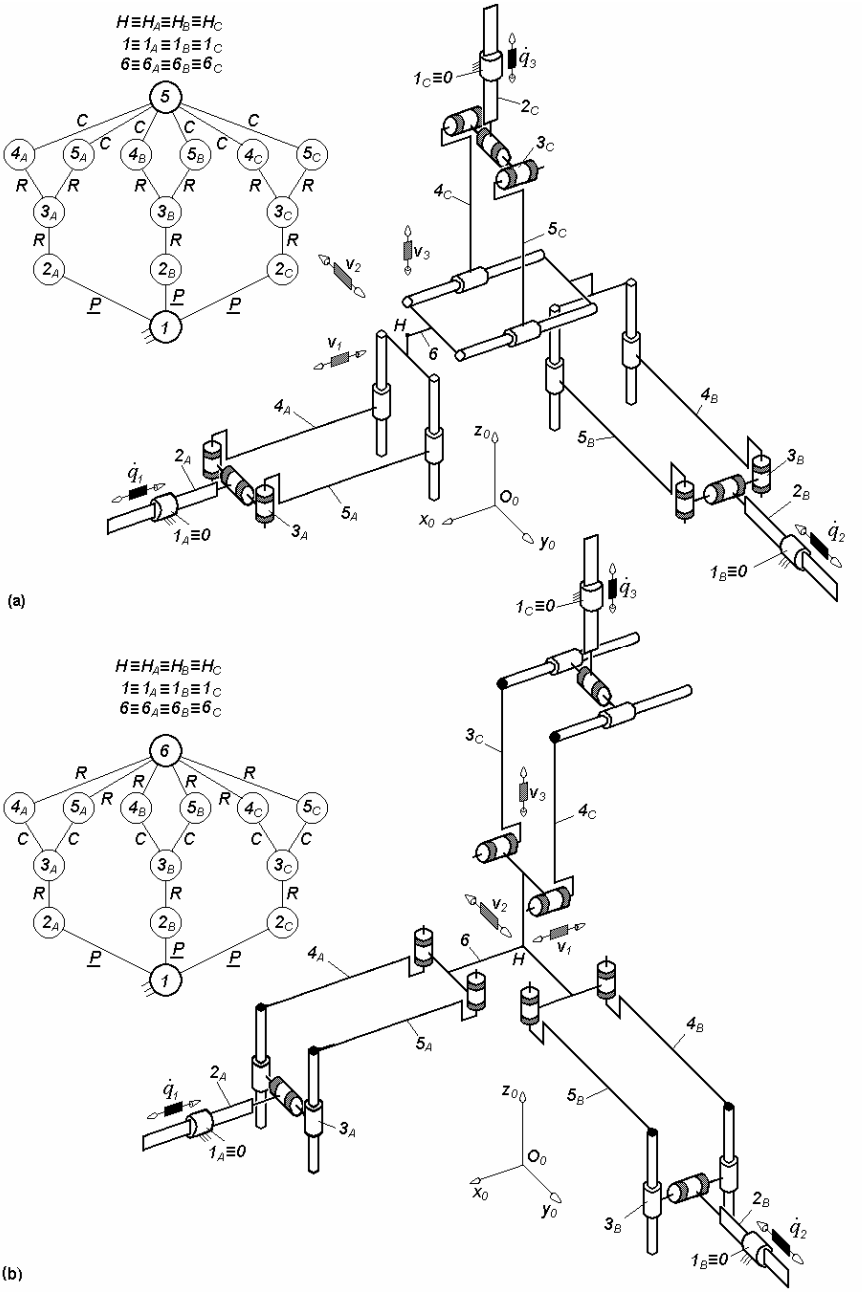

Fig. 3.28. *3-<u>P</u>R*Pa*^{cc}-type overconstrained TPMs with coupled motions and linear actuators on the fixed base, defined by $M_F = S_F = 3$, $(R_F) = (\boldsymbol{v}_1, \boldsymbol{v}_2, \boldsymbol{v}_3)$ $T_F = 0$, $N_F = 9$, limb topology $\underline{P} \perp R^* \perp^{\perp} Pa^{cc}$

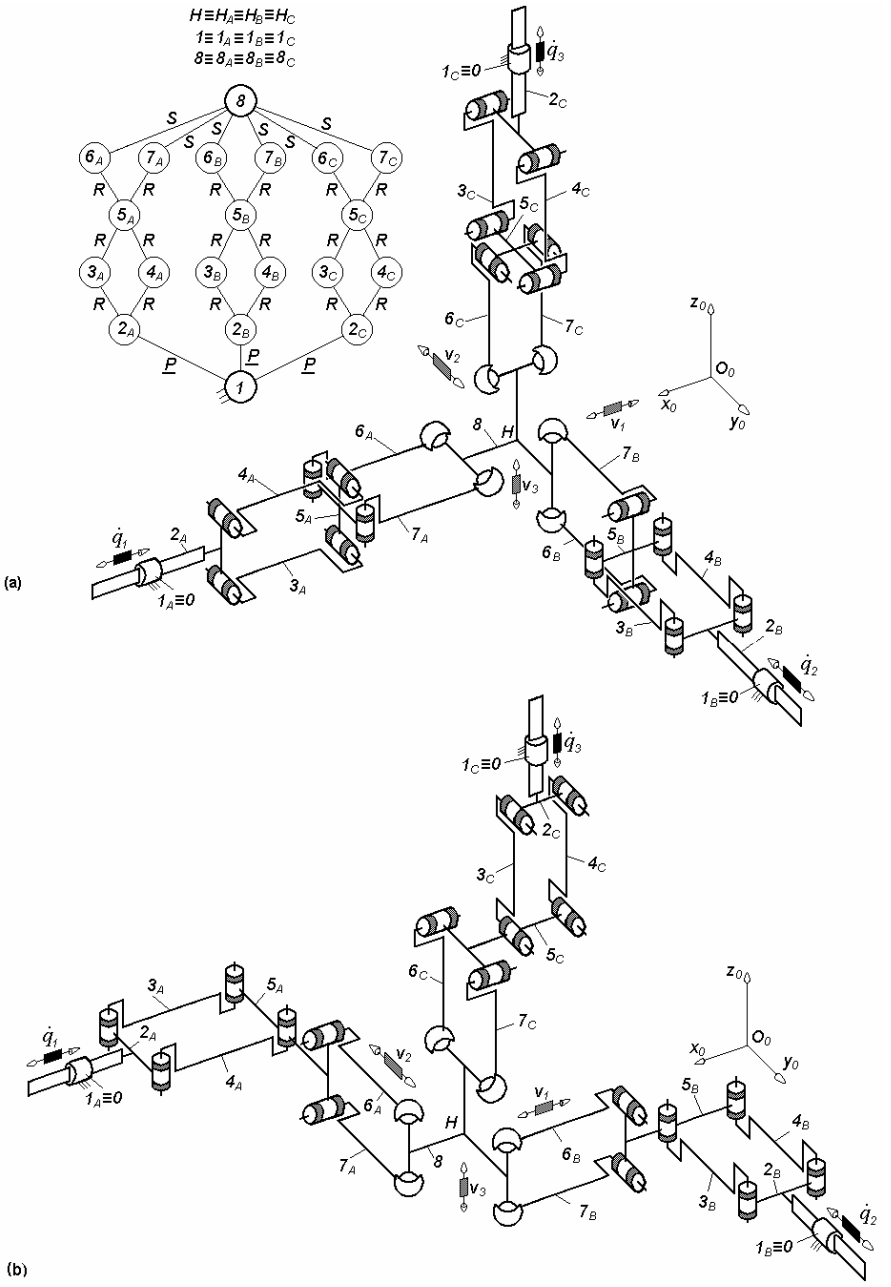

Fig. 3.29. *3-*$\underline{P}$*PaPa*^{ss}-type overconstrained TPMs with coupled motions and linear actuators on the fixed base, defined by $M_F = S_F = 3$, $(R_F) = (\boldsymbol{v}_1, \boldsymbol{v}_2, \boldsymbol{v}_3)$ $T_F = 0$, $N_F = 12$, limb topology $\underline{P} \perp Pa \perp^{\perp} Pa^{ss}$ (**a**) and $\underline{P} \perp Pa \perp^{||} Pa^{ss}$ (**b**)

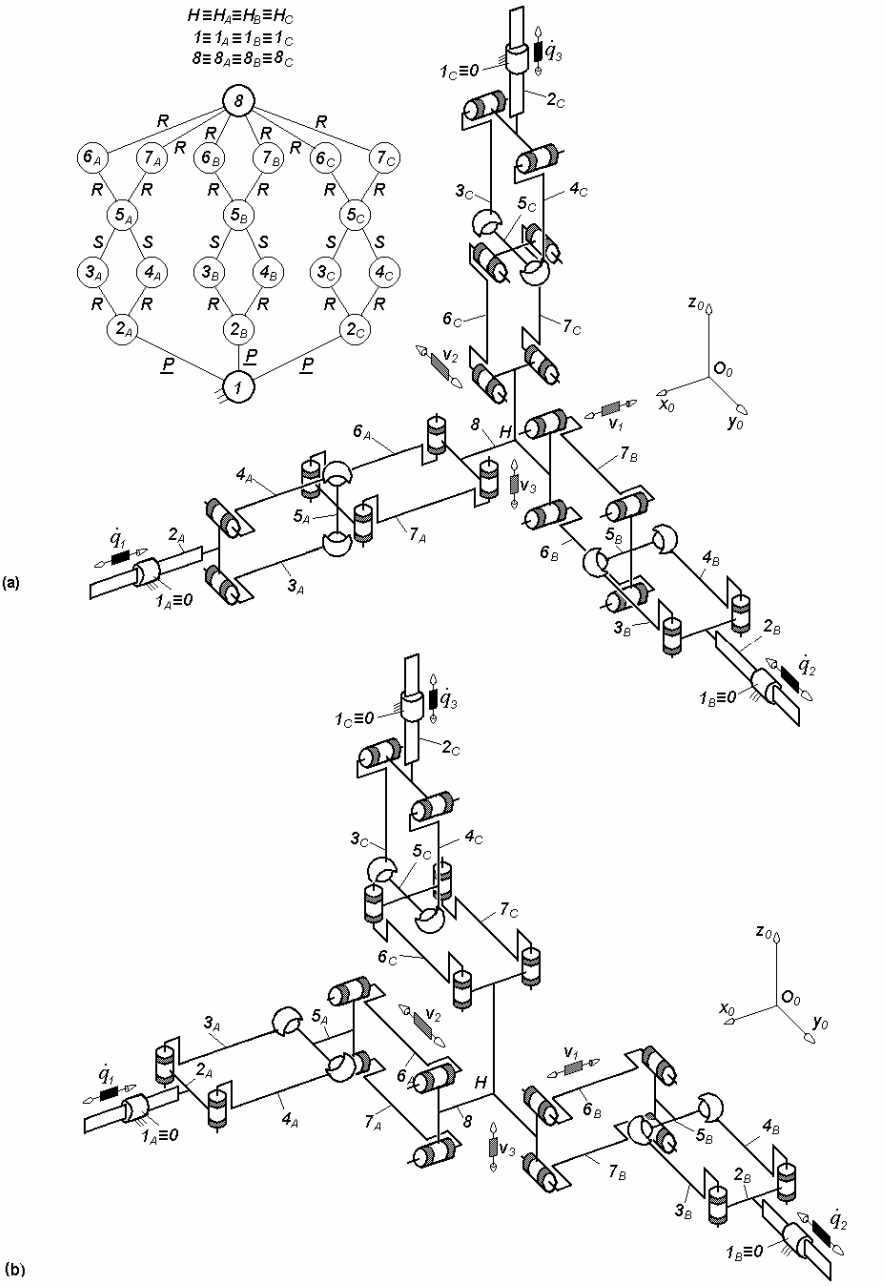

Fig. 3.30. *3-*$\underline{P}$*P*Pa^{ss}*Pa*-type overconstrained TPMs with coupled motions and linear actuators on the fixed base, defined by $M_F = S_F = 3$, $(R_F) = (\boldsymbol{v}_1, \boldsymbol{v}_2, \boldsymbol{v}_3)$ $T_F = 0$, $N_F = 12$, limb topology $\underline{P} \perp Pa^{ss} \perp^{\perp} Pa$ (**a**) and $\underline{P} \perp Pa^{ss} \perp^{\parallel} Pa$ (**b**)

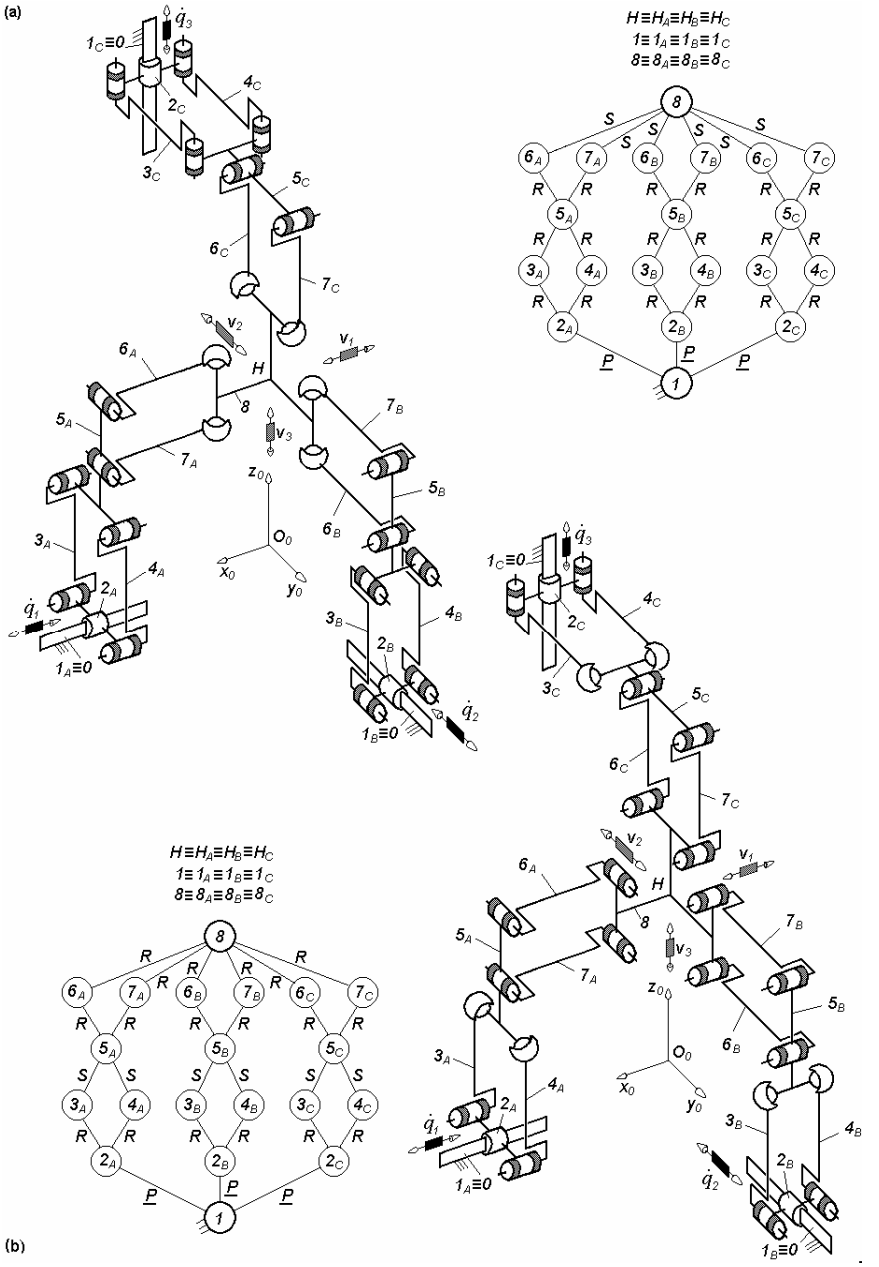

Fig. 3.31. Overconstrained TPMs of types *3-*$\underline{P}$*PaPa*^{ss} (**a**) and *3-*$\underline{P}$*Pa*^{ss}*Pa* (**b**) with coupled motions and linear actuators on the fixed base, defined by $M_F = S_F = 3$, $(R_F) = (\boldsymbol{v}_1, \boldsymbol{v}_2, \boldsymbol{v}_3)$ $T_F = 0$, $N_F = 12$, limb topology $\underline{P}||Pa \perp Pa^{ss}$ (**a**) and $\underline{P}||Pa^{ss} \perp Pa$ (**b**)

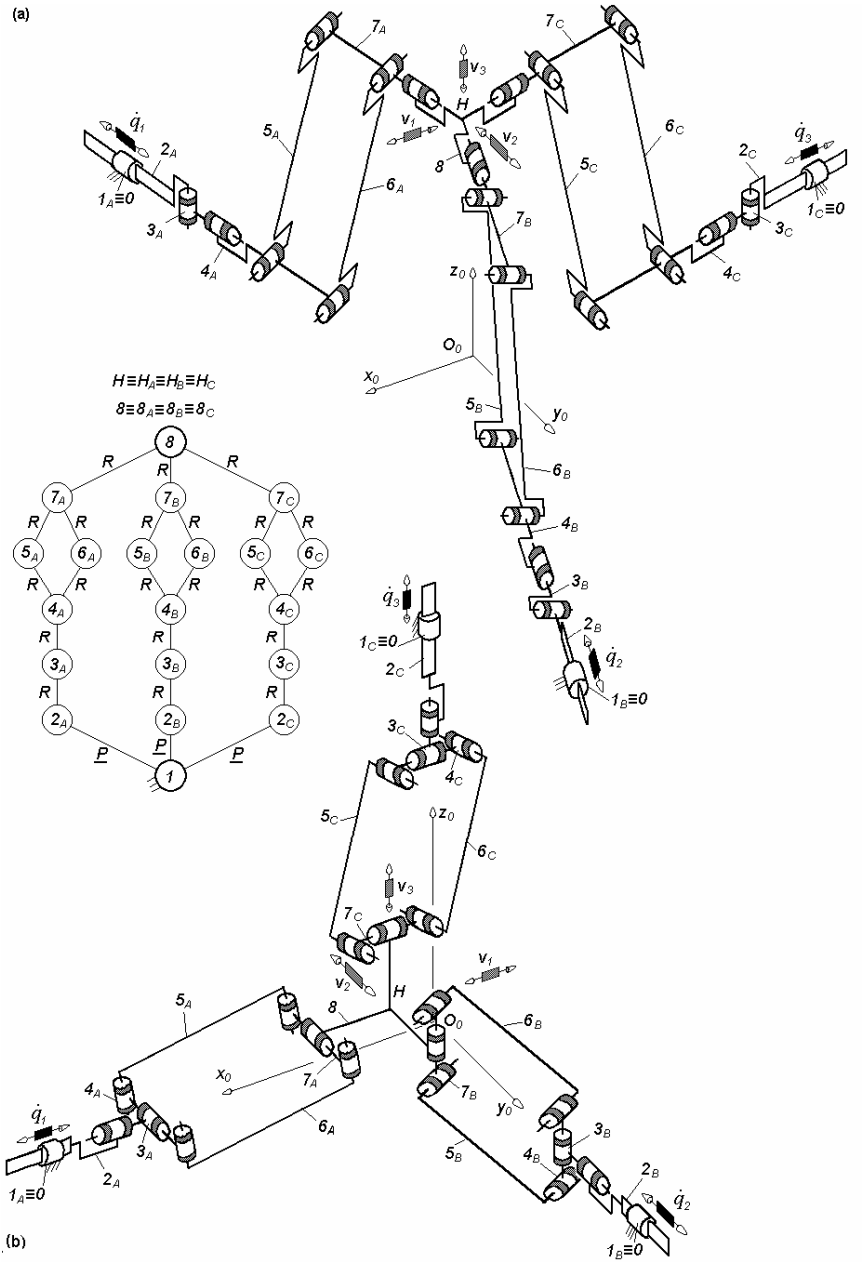

Fig. 3.32. *3-PR*RPaR*-type overconstrained TPMs with coupled motions and linear actuators on the fixed base, defined by $M_F = S_F = 3$, $(R_F) = (\boldsymbol{v}_1, \boldsymbol{v}_2, \boldsymbol{v}_3)$ $T_F = 0$, $N_F = 9$, limb topology $\underline{P} \perp R^* \perp {}^{\parallel}R \perp Pa \perp {}^{\parallel}R$ (**a**) and $\underline{P} \| R^* \perp R \perp Pa \perp {}^{\parallel}R$ (**b**)

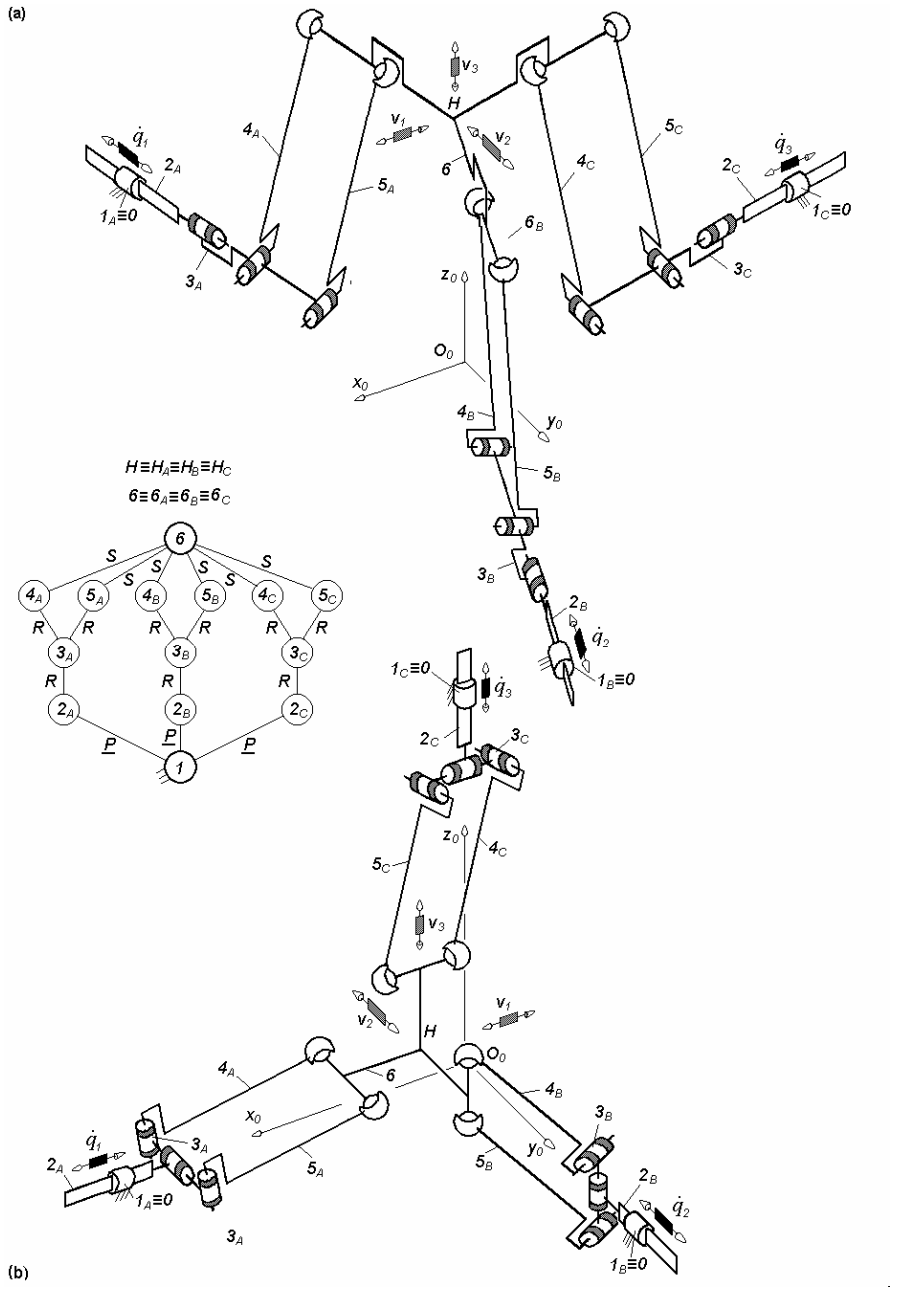

Fig. 3.33. *3-*$\underline{P}$*RPa*^{ss}-type overconstrained TPMs with coupled motions and linear actuators on the fixed base, defined by $M_F = S_F = 3$, $(R_F) = (\boldsymbol{v}_1, \boldsymbol{v}_2, \boldsymbol{v}_3)$ $T_F = 0$, $N_F = 3$, limb topology $\underline{P}||R \perp Pa^{ss}$ (**a**) and $\underline{P} \perp R \perp Pa^{ss}$ (**b**)

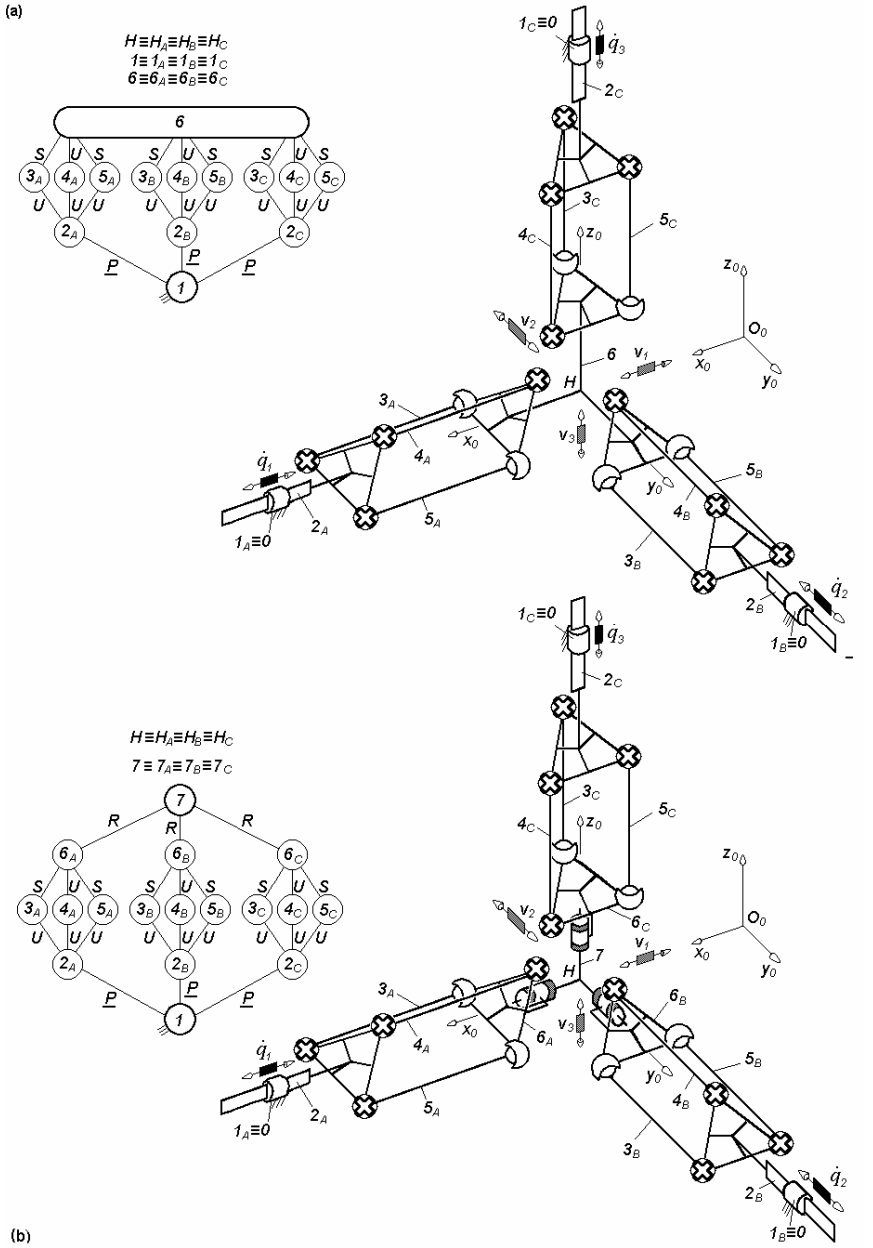

Fig. 3.34. Overconstrained TPMs of types 3-$\underline{P}Pr^{ss}$ (**a**) and 3-$\underline{P}Pr^{ss}R^*$ (**b**) with coupled motions and linear actuators on the fixed base, defined by $M_F = S_F = 3$, $(R_F) = (\boldsymbol{v}_1, \boldsymbol{v}_2, \boldsymbol{v}_3)$ $T_F = 0$, $N_F = 6$ (**a**), $N_F = 3$ (**b**), limb topology $\underline{P} \perp Pr^{ss}$ (**a**) and $\underline{P} \perp Pr^{ss} \perp {}^{\parallel}R^*$ (**b**)

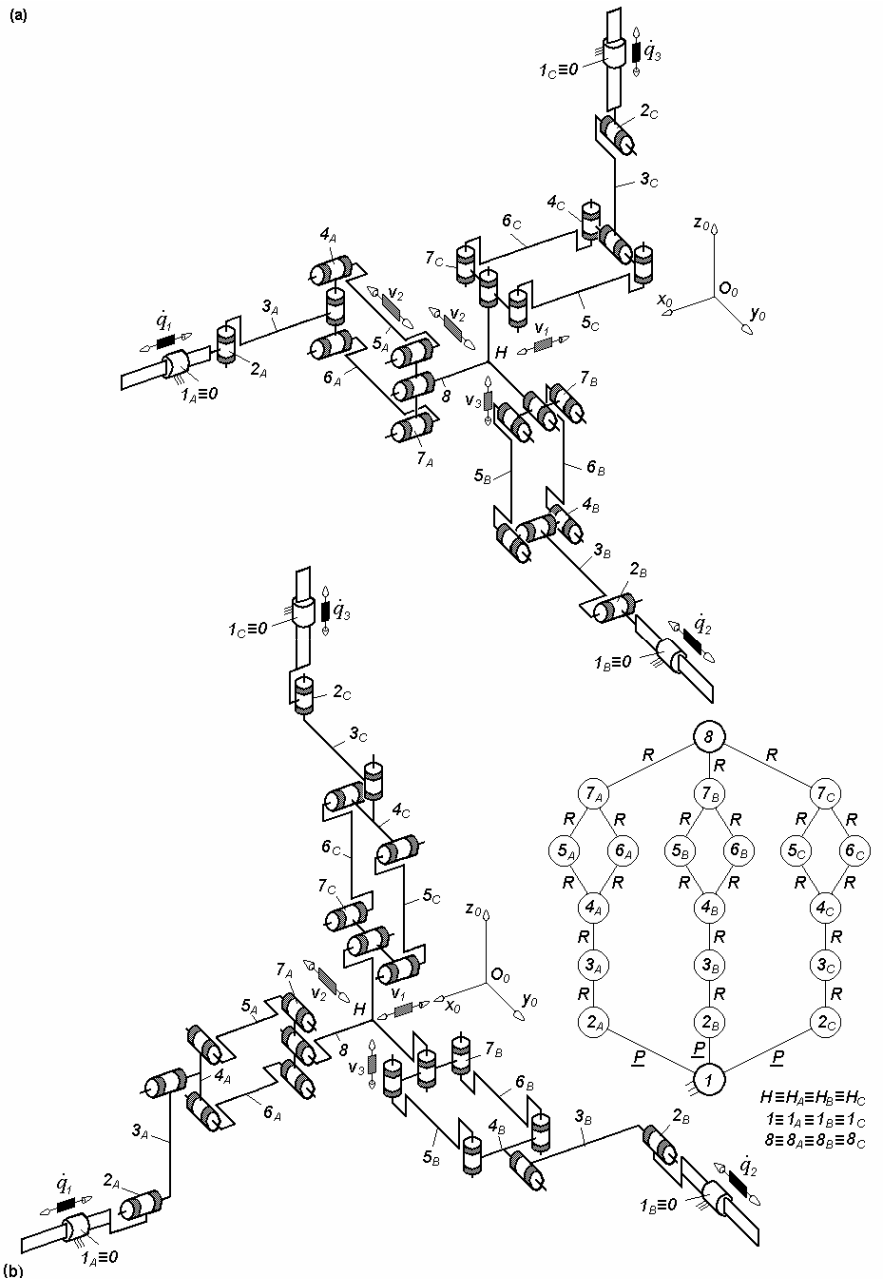

Fig. 3.35. *3-PRRPaR**-type overconstrained TPMs with coupled motions and linear actuators on the fixed base, defined by $M_F = S_F = 3$, $(R_F) = (\boldsymbol{v}_1, \boldsymbol{v}_2, \boldsymbol{v}_3)$ $T_F = 0$, $N_F = 9$, limb topology $\underline{P} \perp R||R \perp {}^{||}Pa||R^*$ (**a**) and $\underline{P}||R||R \perp Pa||R^*$ (**b**)

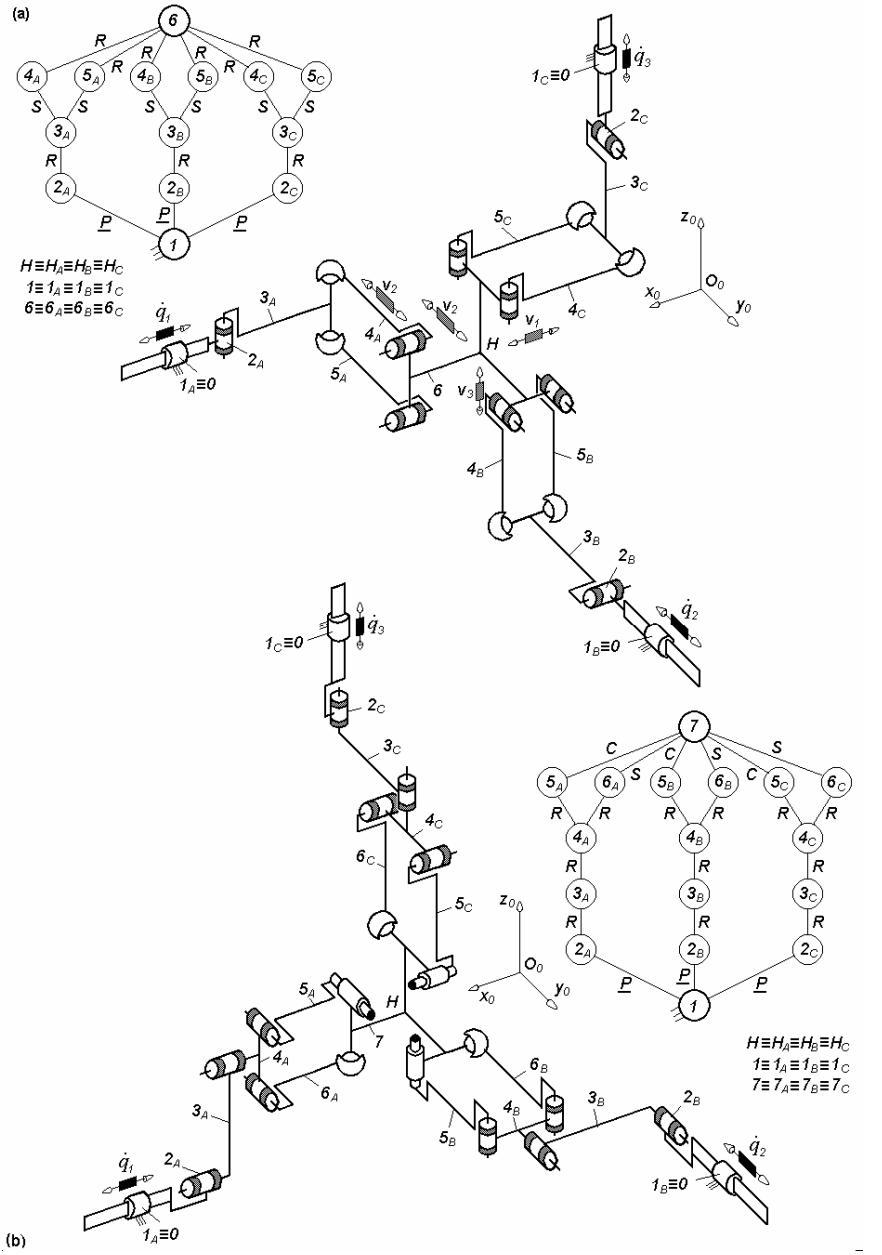

Fig. 3.36. Overconstrained TPMs of types *3-<u>P</u>RPa*^{ss} (**a**) and *3-<u>P</u>RRPa*^{cs} (**b**) with coupled motions and linear actuators on the fixed base, defined by $M_F = S_F = 3$, $(R_F) = (\boldsymbol{v}_1, \boldsymbol{v}_2, \boldsymbol{v}_3)$ $T_F = 0$, $N_F = 3$, limb topology $\underline{P} \perp R \perp {}^{\parallel}Pa^{ss}$ (**a**) and $\underline{P} \| R \| R \perp Pa^{cs}$ (**b**)

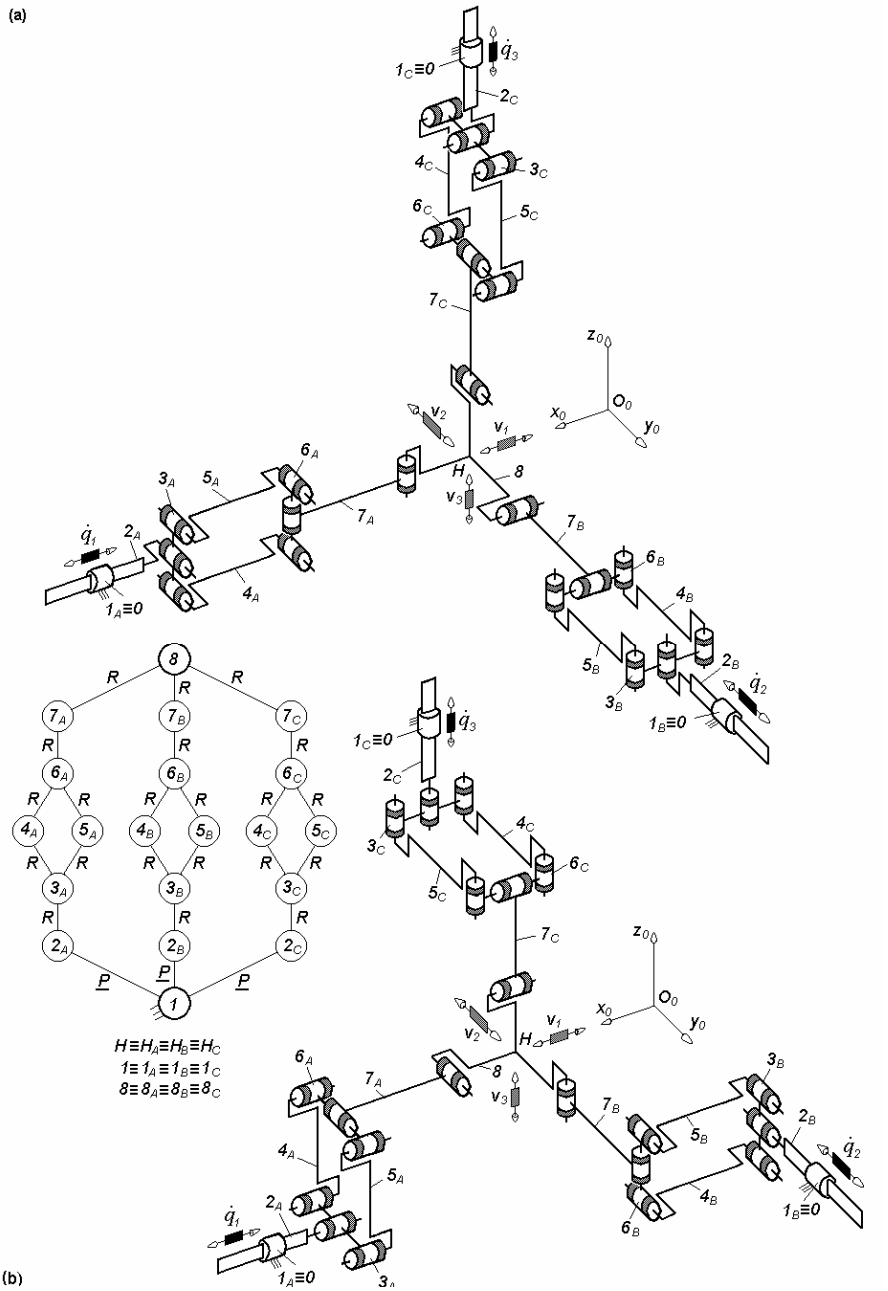

Fig. 3.37. *3-PR*PaRR*-type overconstrained TPMs with coupled motions and linear actuators on the fixed base, defined by $M_F = S_F = 3$, $(R_F) = (\boldsymbol{v}_1, \boldsymbol{v}_2, \boldsymbol{v}_3)$ $T_F = 0$, $N_F = 9$, limb topology $\underline{P} \perp R^* || Pa \perp^{\perp} R || R$ (**a**) and $\underline{P} || R^* || Pa \perp R || R$ (**b**)

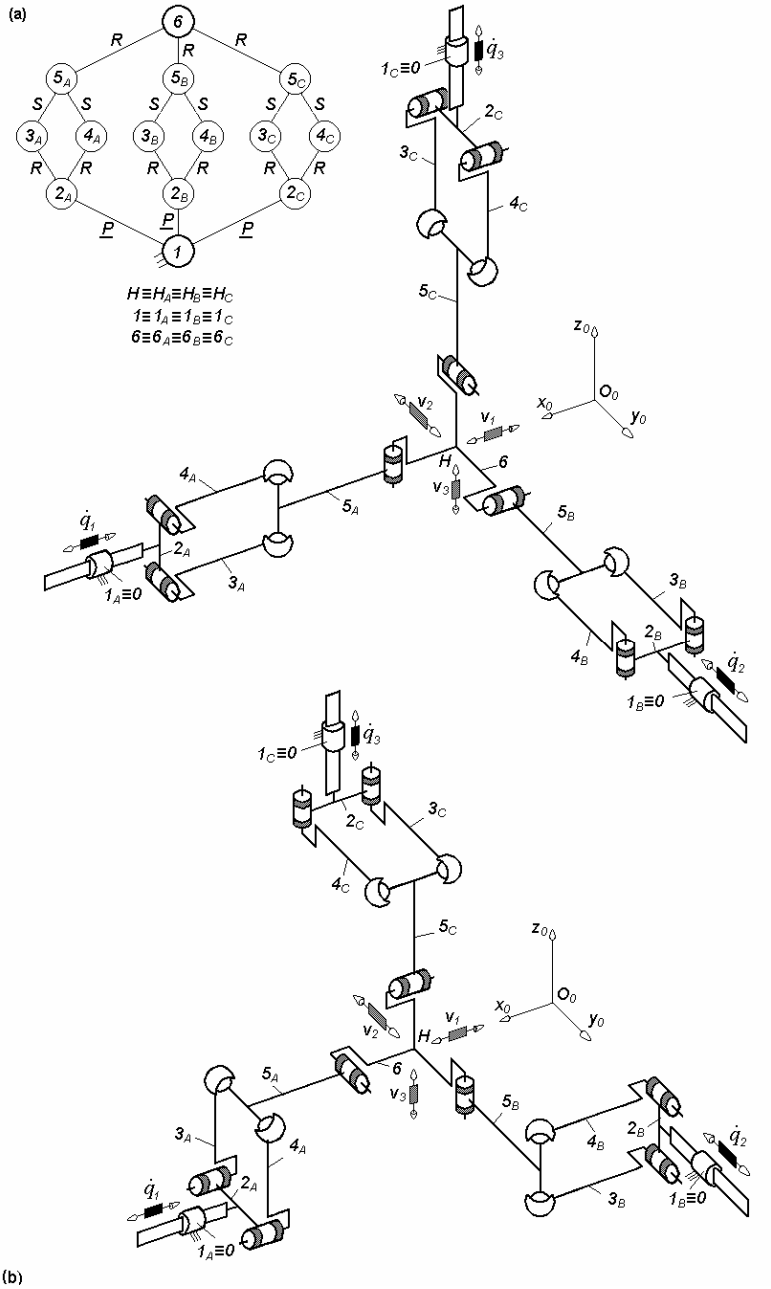

Fig. 3.38. *3-*$\underline{P}$*P*a^{ss}*R*-type overconstrained TPMs with coupled motions and linear actuators on the fixed base, defined by $M_F = S_F = 3$, $(R_F) = (\boldsymbol{v}_1, \boldsymbol{v}_2, \boldsymbol{v}_3)$ $T_F = 0$, $N_F = 3$, limb topology $\underline{P} \perp Pa^{ss} \perp^{\perp} R$ (**a**) and $\underline{P} \| Pa^{ss} \perp R$ (**b**)

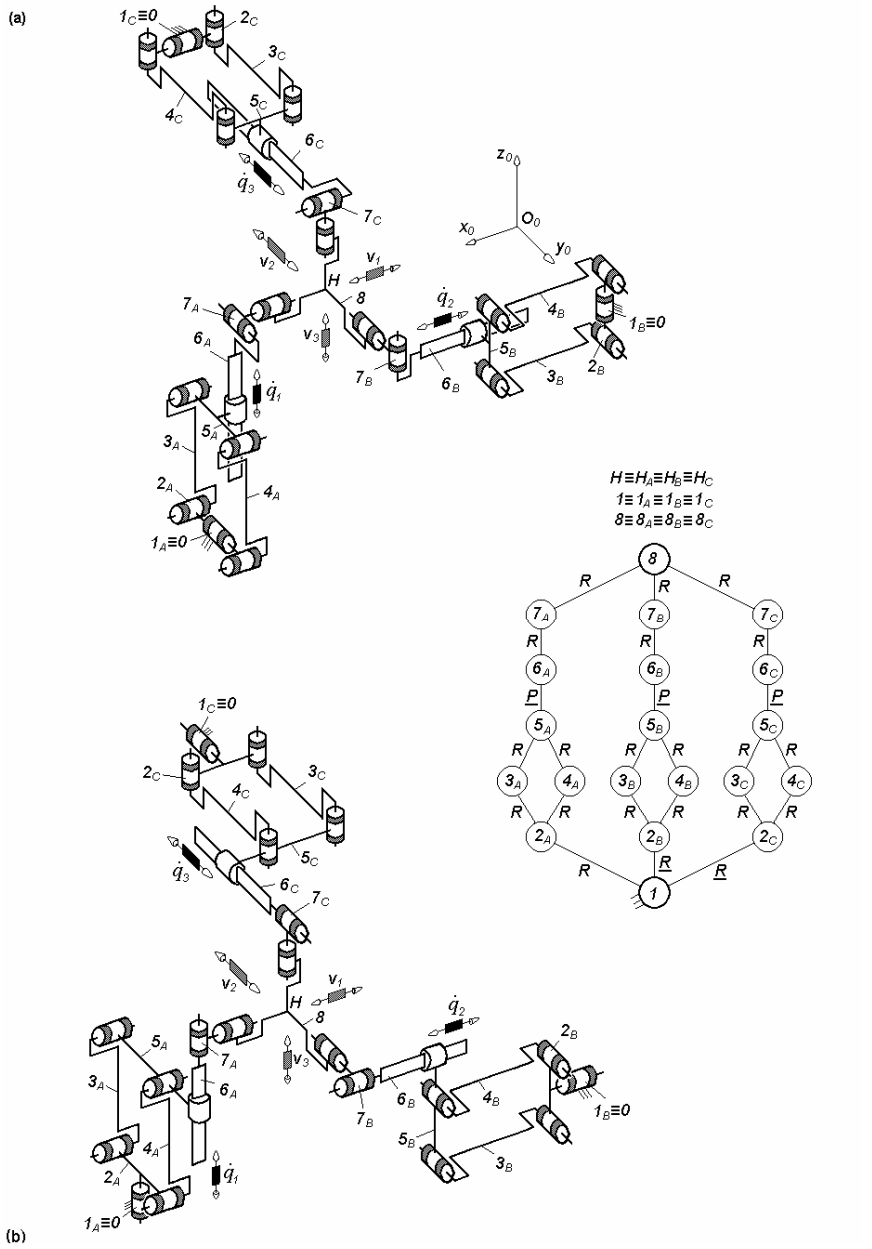

Fig. 3.39. *3-RPa<u>P</u>RR**-type overconstrained TPMs with coupled motions and linear actuators on a moving link, defined by $M_F = S_F = 3$, $(R_F) = (\boldsymbol{v}_1, \boldsymbol{v}_2, \boldsymbol{v}_3)$ $T_F = 0$, $N_F = 9$, limb topology $R \perp Pa \perp^{\perp} \underline{P} \perp^{\perp} R \perp R^*$ (**a**) and $R \perp Pa \perp {}^{||}\underline{P}||R \perp R^*$ (**b**)

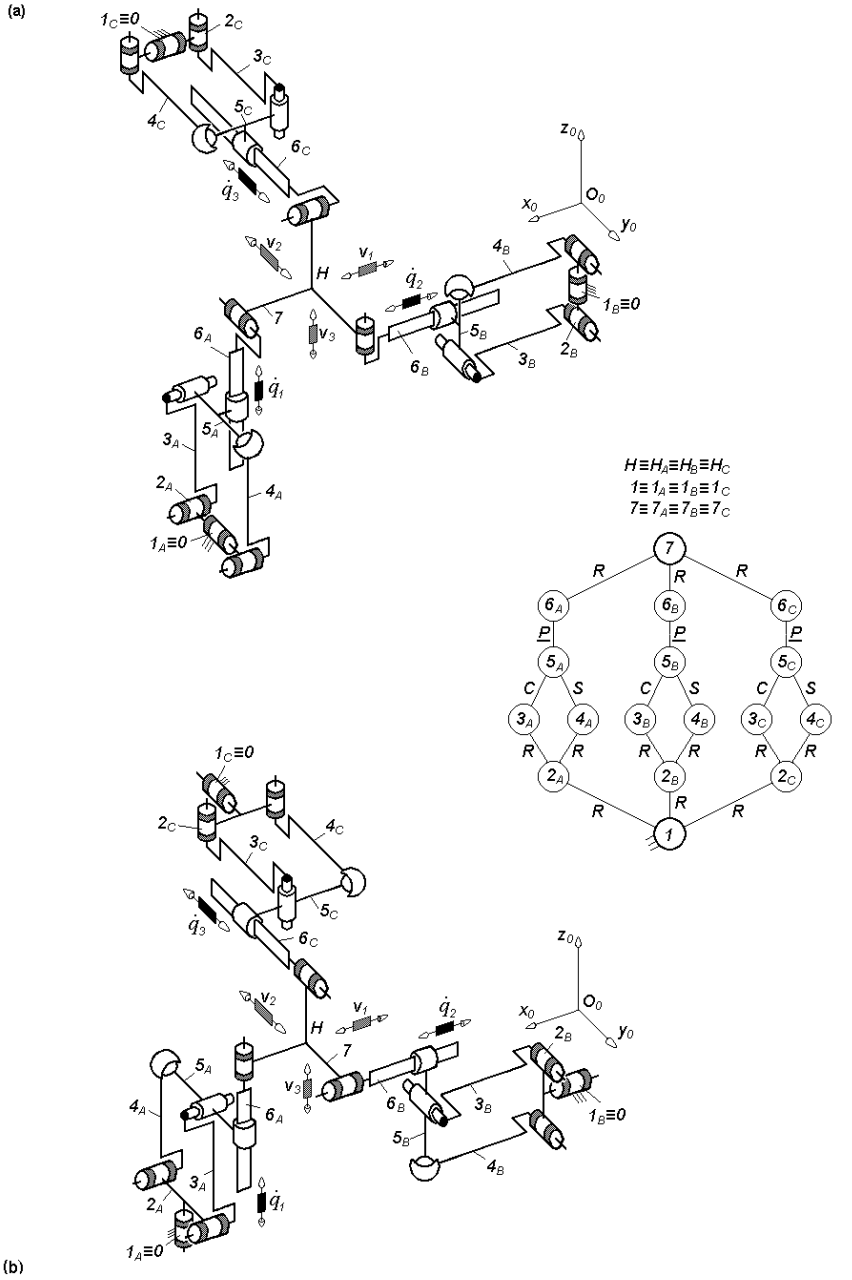

Fig. 3.40. *3-RPa*^{cs}*PR*-type overconstrained TPMs with coupled motions and linear actuators on a moving link, defined by $M_F = S_F = 3$, $(R_F) = (\boldsymbol{v}_1, \boldsymbol{v}_2, \boldsymbol{v}_3)$ $T_F = 0$, $N_F = 3$, limb topology $R \perp Pa^{cs} \perp^{\perp} \underline{P} \perp^{\perp} R$ (**a**) and $R \perp Pa^{cs} \perp {}^{\parallel}\underline{P} \| R$ (**b**)

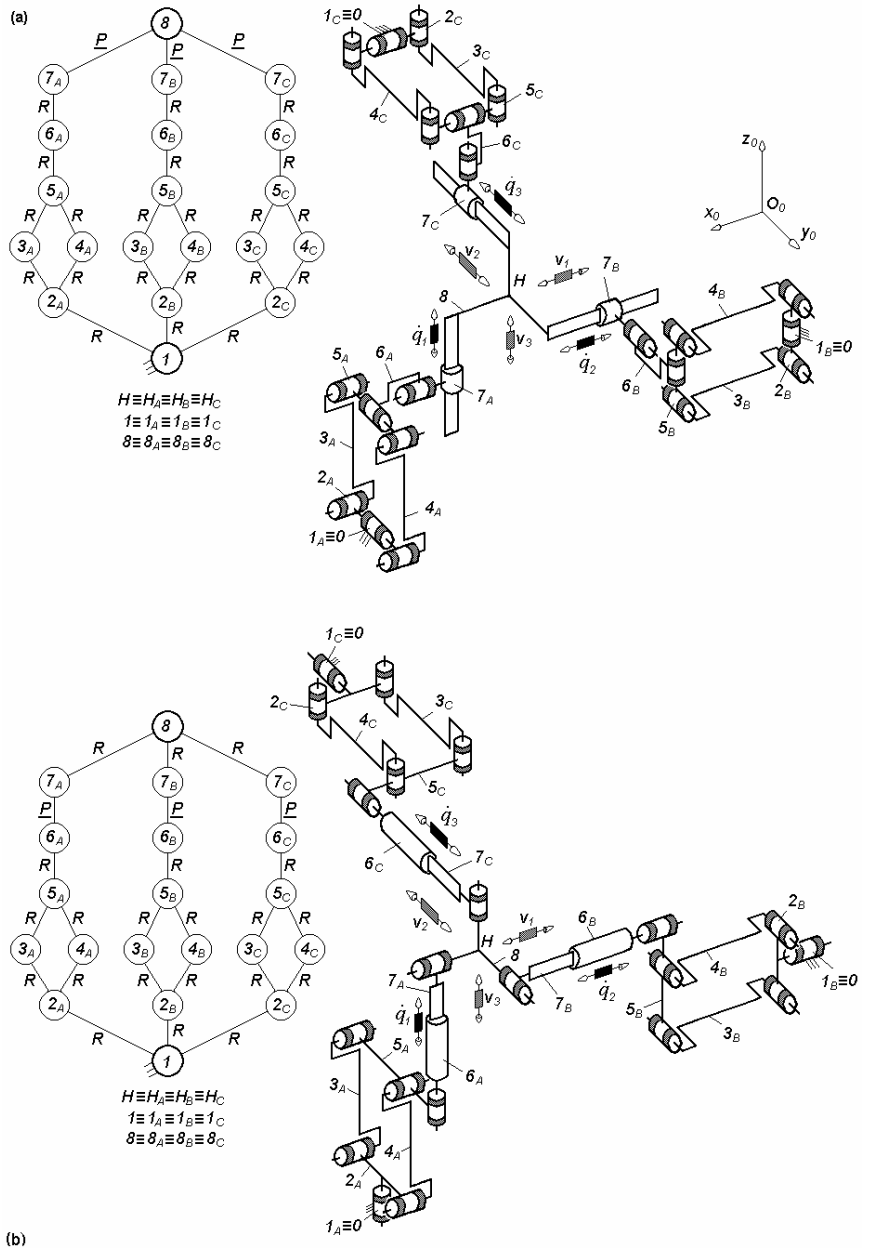

Fig. 3.41. Overconstrained TPMs of types *3-RPaRR*P* (**a**) and *3-RPaRPR** (**b**) with coupled motions and linear actuators mounted on a moving link, defined by $M_F = S_F = 3$, $(R_F) = (\boldsymbol{v}_1, \boldsymbol{v}_2, \boldsymbol{v}_3)$ $T_F = 0$, $N_F = 9$, limb topology $R \perp Pa \perp^{\parallel} R \perp R^* \perp^{\perp} \underline{P}$ (**a**) and $R \perp Pa \perp^{\parallel} R \| \underline{P} \perp R^*$ (**b**)

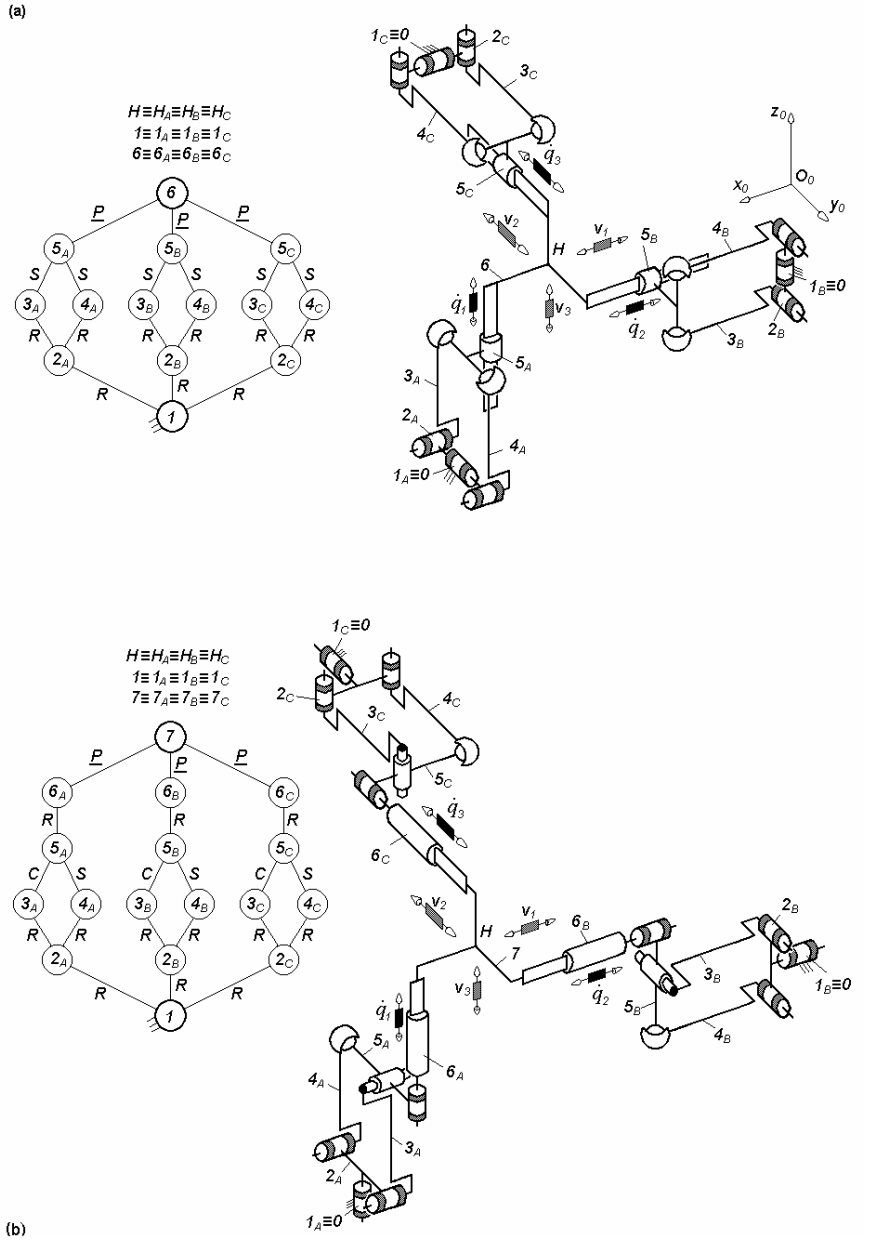

Fig. 3.42. Overconstrained TPMs of types *3-RPa*^{ss}*P* (**a**) and *3-RPa*^{cs}*RP* (**b**) with coupled motions and linear actuators mounted on the moving platform, defined by $M_F = S_F = 3$, $(R_F) = (\boldsymbol{v}_1, \boldsymbol{v}_2, \boldsymbol{v}_3)$ $T_F = 0$, $N_F = 3$, limb topology $R \perp Pa^{ss} \perp^{\perp} P$ (**a**) and $R \perp Pa^{cs} \perp {}^{||}R||P$ (**b**)

Table 3.13. Bases of the operational velocities spaces of the limbs isolated from the parallel mechanisms presented in Figs. 3.24–3.42

No.	Parallel mechanism	Basis (R_{G1})	(R_{G2})	(R_{G3})
1	Fig. 3.24	$(\boldsymbol{v}_1,\boldsymbol{v}_2,\boldsymbol{v}_3,\boldsymbol{\omega}_\delta)$	$(\boldsymbol{v}_1,\boldsymbol{v}_2,\boldsymbol{v}_3,\boldsymbol{\omega}_\delta)$	$(\boldsymbol{v}_1,\boldsymbol{v}_2,\boldsymbol{v}_3,\boldsymbol{\omega}_\alpha)$
2	Figs. 3.25–3.28, 3.30b	$(\boldsymbol{v}_1,\boldsymbol{v}_2,\boldsymbol{v}_3,\boldsymbol{\omega}_\beta)$	$(\boldsymbol{v}_1,\boldsymbol{v}_2,\boldsymbol{v}_3,\boldsymbol{\omega}_\alpha)$	$(\boldsymbol{v}_1,\boldsymbol{v}_2,\boldsymbol{v}_3,\boldsymbol{\omega}_\beta)$
3	Figs. 3.29a, 3.33b, 3.38b, 3.40a, 3.42a	$(\boldsymbol{v}_1,\boldsymbol{v}_2,\boldsymbol{v}_3,\boldsymbol{\omega}_\beta)$	$(\boldsymbol{v}_1,\boldsymbol{v}_2,\boldsymbol{v}_3,\boldsymbol{\omega}_\delta)$	$(\boldsymbol{v}_1,\boldsymbol{v}_2,\boldsymbol{v}_3,\boldsymbol{\omega}_\alpha)$
4	Figs. 3.29b, 3.31a,	$(\boldsymbol{v}_1,\boldsymbol{v}_2,\boldsymbol{v}_3,\boldsymbol{\omega}_\delta)$	$(\boldsymbol{v}_1,\boldsymbol{v}_2,\boldsymbol{v}_3,\boldsymbol{\omega}_\delta)$	$(\boldsymbol{v}_1,\boldsymbol{v}_2,\boldsymbol{v}_3,\boldsymbol{\omega}_\beta)$
5	Figs. 3.30a, 3.36a, 3.38a, 3.40b, 3.42b	$(\boldsymbol{v}_1,\boldsymbol{v}_2,\boldsymbol{v}_3,\boldsymbol{\omega}_\delta)$	$(\boldsymbol{v}_1,\boldsymbol{v}_2,\boldsymbol{v}_3,\boldsymbol{\omega}_\alpha)$	$(\boldsymbol{v}_1,\boldsymbol{v}_2,\boldsymbol{v}_3,\boldsymbol{\omega}_\beta)$
6	Fig. 3.31b	$(\boldsymbol{v}_1,\boldsymbol{v}_2,\boldsymbol{v}_3,\boldsymbol{\omega}_\beta)$	$(\boldsymbol{v}_1,\boldsymbol{v}_2,\boldsymbol{v}_3,\boldsymbol{\omega}_\alpha)$	$(\boldsymbol{v}_1,\boldsymbol{v}_2,\boldsymbol{v}_3,\boldsymbol{\omega}_\alpha)$
7	Figs. 3.32a, 3.35a, 3.39b, 3.41b	$(\boldsymbol{v}_1,\boldsymbol{v}_2,\boldsymbol{v}_3,\boldsymbol{\omega}_\alpha,\boldsymbol{\omega}_\delta)$	$(\boldsymbol{v}_1,\boldsymbol{v}_2,\boldsymbol{v}_3,\boldsymbol{\omega}_\alpha,\boldsymbol{\omega}_\beta)$	$(\boldsymbol{v}_1,\boldsymbol{v}_2,\boldsymbol{v}_3,\boldsymbol{\omega}_\beta,\boldsymbol{\omega}_\delta)$
8	Figs. 3.32b, 3.35b	$(\boldsymbol{v}_1,\boldsymbol{v}_2,\boldsymbol{v}_3,\boldsymbol{\omega}_\alpha,\boldsymbol{\omega}_\beta)$	$(\boldsymbol{v}_1,\boldsymbol{v}_2,\boldsymbol{v}_3,\boldsymbol{\omega}_\beta,\boldsymbol{\omega}_\delta)$	$(\boldsymbol{v}_1,\boldsymbol{v}_2,\boldsymbol{v}_3,\boldsymbol{\omega}_\alpha,\boldsymbol{\omega}_\delta)$
9	Fig. 3.33a	$(\boldsymbol{v}_1,\boldsymbol{v}_2,\boldsymbol{v}_3,\boldsymbol{\omega}_\alpha)$	$(\boldsymbol{v}_1,\boldsymbol{v}_2,\boldsymbol{v}_3,\boldsymbol{\omega}_\beta)$	$(\boldsymbol{v}_1,\boldsymbol{v}_2,\boldsymbol{v}_3,\boldsymbol{\omega}_\beta)$
10	Fig. 3.34a	$(\boldsymbol{v}_1,\boldsymbol{v}_2,\boldsymbol{v}_3)$	$(\boldsymbol{v}_1,\boldsymbol{v}_2,\boldsymbol{v}_3)$	$(\boldsymbol{v}_1,\boldsymbol{v}_2,\boldsymbol{v}_3)$
11	Figs. 3.34b, 3.36b	$(\boldsymbol{v}_1,\boldsymbol{v}_2,\boldsymbol{v}_3,\boldsymbol{\omega}_\alpha)$	$(\boldsymbol{v}_1,\boldsymbol{v}_2,\boldsymbol{v}_3,\boldsymbol{\omega}_\beta)$	$(\boldsymbol{v}_1,\boldsymbol{v}_2,\boldsymbol{v}_3,\boldsymbol{\omega}_\delta)$
12	Fig. 3.37a	$(\boldsymbol{v}_1,\boldsymbol{v}_2,\boldsymbol{v}_3,\boldsymbol{\omega}_\beta,\boldsymbol{\omega}_\delta)$	$(\boldsymbol{v}_1,\boldsymbol{v}_2,\boldsymbol{v}_3,\boldsymbol{\omega}_\alpha,\boldsymbol{\omega}_\delta)$	$(\boldsymbol{v}_1,\boldsymbol{v}_2,\boldsymbol{v}_3,\boldsymbol{\omega}_\alpha,\boldsymbol{\omega}_\beta)$
13	Figs. 3.37b, 3.39a, 3.41a	$(\boldsymbol{v}_1,\boldsymbol{v}_2,\boldsymbol{v}_3,\boldsymbol{\omega}_\alpha,\boldsymbol{\omega}_\beta)$	$(\boldsymbol{v}_1,\boldsymbol{v}_2,\boldsymbol{v}_3,\boldsymbol{\omega}_\beta,\boldsymbol{\omega}_\delta)$	$(\boldsymbol{v}_1,\boldsymbol{v}_2,\boldsymbol{v}_3,\boldsymbol{\omega}_\alpha,\boldsymbol{\omega}_\delta)$

Table 3.14. Structural parameters[a] of translational parallel mechanisms in Figs. 3.24–3.27

No.	Structural parameter	Solution *3-PPaC** (Fig. 3.24a) *3-PC*Pa* (Fig. 3.24b)	*3-PR*PaP* (Fig. 3.25a) *3-PPR*Pa* (Fig. 3.25b)	*3-PPa^{ss}P* (Fig. 3.26a) *3-PPPa^{ss}* (Fig. 3.26b) *3-PR*Pa^{scc}* (Fig. 3.27a) *3-PR*Pa^{ccs}* (Fig. 3.27b)
1	m	14	17	14
2	p_1	6	7	6
3	p_2	6	7	6
4	p_3	6	7	6
5	p	18	21	18
6	q	5	5	5
7	k_1	0	0	0
8	k_2	3	3	3
9	k	3	3	3
10	(R_{Gi}) $(i = 1,2,3)$	See Table 3.13	See Table 3.13	See Table 3.13
11	S_{G1}	4	4	4
12	S_{G2}	4	4	4
13	S_{G3}	4	4	4
14	r_{G1}	3	3	6
15	r_{G2}	3	3	6
16	r_{G3}	3	3	6
17	M_{G1}	4	4	4
18	M_{G2}	4	4	4
19	M_{G3}	4	4	4
20	(R_F)	$(\boldsymbol{v}_1,\boldsymbol{v}_2,\boldsymbol{v}_3)$	$(\boldsymbol{v}_1,\boldsymbol{v}_2,\boldsymbol{v}_3)$	$(\boldsymbol{v}_1,\boldsymbol{v}_2,\boldsymbol{v}_3)$
21	S_F	3	3	3
22	r_1	9	9	18
23	r_F	18	18	27
24	M_F	3	3	3
25	N_F	12	12	3
26	T_F	0	0	0
27	$\sum_{j=1}^{p_1} f_j$	7	7	10
28	$\sum_{j=1}^{p_2} f_j$	7	7	10
29	$\sum_{j=1}^{p_3} f_j$	7	7	10
30	$\sum_{j=1}^{p} f_j$	21	21	30

[a]See footnote of Table 2.1 for the nomenclature of structural parameters

Table 3.15. Structural parameters[a] of translational parallel mechanisms in Figs. 3.28–3.32

No.	Structural parameter	Solution *3-PR*Pa^{cc}* (Fig. 3.28a, b)	*3-PPaPa^{ss}* (Figs. 3.29a, b, 3.31a) *3-PPa^{ss}Pa* (Figs. 3.30a, b, 3.31b)	*3-PR*RPaR* (Fig. 3.32a, b)
1	m	14	20	20
2	p_1	6	9	8
3	p_2	6	9	8
4	p_3	6	9	8
5	p	18	27	24
6	q	5	8	5
7	k_1	0	0	0
8	k_2	3	3	3
9	k	3	3	3
10	(R_{Gi}) $(i = 1,2,3)$	See Table 3.13	See Table 3.13	See Table 3.13
11	S_{G1}	4	4	5
12	S_{G2}	4	4	5
13	S_{G3}	4	4	5
14	r_{G1}	4	9	3
15	r_{G2}	4	9	3
16	r_{G3}	4	9	3
17	M_{G1}	4	4	5
18	M_{G2}	4	4	5
19	M_{G3}	4	4	5
20	(R_F)	$(\boldsymbol{v}_1, \boldsymbol{v}_2, \boldsymbol{v}_3)$	$(\boldsymbol{v}_1, \boldsymbol{v}_2, \boldsymbol{v}_3)$	$(\boldsymbol{v}_1, \boldsymbol{v}_2, \boldsymbol{v}_3)$
21	S_F	3	3	3
22	r_1	12	27	9
23	r_F	21	36	21
24	M_F	3	3	3
25	N_F	9	12	9
26	T_F	0	0	0
27	$\sum_{j=1}^{p_1} f_j$	8	13	8
28	$\sum_{j=1}^{p_2} f_j$	8	13	8
29	$\sum_{j=1}^{p_3} f_j$	8	13	8
30	$\sum_{j=1}^{p} f_j$	24	39	24

[a]See footnote of Table 2.1 for the nomenclature of structural parameters

Table 3.16. Structural parameters[a] of translational parallel mechanisms in Figs. 3.33 and 3.34

No.	Structural parameter	Solution *3-PRPa*^{ss} (Fig. 3.33a, b)	*3-PPr*^{ss} (Fig. 3.34a)	*3-PPr*^{ss}*R** (Fig. 3.34b)
1	m	14	14	17
2	p_1	6	7	8
3	p_2	6	7	8
4	p_3	6	7	8
5	p	18	21	24
6	q	5	8	8
7	k_1	0	0	0
8	k_2	3	3	3
9	k	3	3	3
10	(R_{Gi}) $(i = 1,2,3)$	See Table 3.13	See Table 3.13	See Table 3.13
11	S_{G1}	4	3	4
12	S_{G2}	4	3	4
13	S_{G3}	4	3	4
14	r_{G1}	6	12	12
15	r_{G2}	6	12	12
16	r_{G3}	6	12	12
17	M_{G1}	4	3	4
18	M_{G2}	4	3	4
19	M_{G3}	4	3	4
20	(R_F)	$(\boldsymbol{v}_1, \boldsymbol{v}_2, \boldsymbol{v}_3)$	$(\boldsymbol{v}_1, \boldsymbol{v}_2, \boldsymbol{v}_3)$	$(\boldsymbol{v}_1, \boldsymbol{v}_2, \boldsymbol{v}_3)$
21	S_F	3	3	3
22	r_1	18	36	36
23	r_F	27	42	45
24	M_F	3	3	3
25	N_F	3	6	3
26	T_F	0	0	0
27	$\sum_{j=1}^{p_1} f_j$	10	15	16
28	$\sum_{j=1}^{p_2} f_j$	10	15	16
29	$\sum_{j=1}^{p_3} f_j$	10	15	16
30	$\sum_{j=1}^{p} f_j$	30	45	48

[a]See footnote of Table 2.1 for the nomenclature of structural parameters

Table 3.17. Structural parameters[a] of translational parallel mechanisms in Figs. 3.35–3.42

No.	Structural parameter	Solution *3-PRRPaR** (Fig. 3.35a, b) *3-PR*PaRR* (Fig. 3.37a, b) *3-RPaPRR** (Fig. 3.39a, b) *3-RPaRR*P* (Fig. 3.41a) *3-RPaRPR** (Fig. 3.41b)	*3-PRPa^{ss}* (Fig. 3.36a) *3-PPa^{ss}R* (Fig. 3.38a, b) *3-RPa^{ss}P* (Fig. 3.42a)	*3-PRRPa^{cs}* (Fig. 3.36b) *3-RPa^{cs}PR* (Fig. 3.40a, b) *3-RPa^{cs}RP* (Fig. 3.42b)
1	m	20	14	17
2	p_1	8	6	7
3	p_2	8	6	7
4	p_3	8	6	7
5	p	24	18	21
6	q	5	5	5
7	k_1	0	0	0
8	k_2	3	3	3
9	k	3	3	3
10	(R_{Gi}) (i = *1,2,3*)	See Table 3.13	See Table 3.13	See Table 3.13
11	S_{G1}	5	4	4
12	S_{G2}	5	4	4
13	S_{G3}	5	4	4
14	r_{G1}	3	6	6
15	r_{G2}	3	6	6
16	r_{G3}	3	6	6
17	M_{G1}	5	4	4
18	M_{G2}	5	4	4
19	M_{G3}	5	4	4
20	(R_F)	($\boldsymbol{v}_1,\boldsymbol{v}_2,\boldsymbol{v}_3$)	($\boldsymbol{v}_1,\boldsymbol{v}_2,\boldsymbol{v}_3$)	($\boldsymbol{v}_1,\boldsymbol{v}_2,\boldsymbol{v}_3$)
21	S_F	3	3	3
22	r_1	9	18	18
23	r_F	21	27	27
24	M_F	3	3	3
25	N_F	9	3	3
26	T_F	0	0	0
27	$\sum_{j=1}^{p_1} f_j$	8	10	10
28	$\sum_{j=1}^{p_2} f_j$	8	10	10
29	$\sum_{j=1}^{p_3} f_j$	8	10	10
30	$\sum_{j=1}^{p} f_j$	24	30	30

[a]See footnote of Table 2.1 for the nomenclature of structural parameters

Table 3.18. Limb topology and the number of overconstraints N_F of the derived TPMs with idle mobilities and linear actuators mounted on the fixed base presented in Figs. 3.43–3.52

No.	Basic TPM type	N_F	Derived TPM type	N_F	Topology of the limbs
1	*3-PRC* (Fig. 3.12a)	*3*	*PRCR*-2PRC* (Fig. 3.43a)	*2*	$P \perp R \| \| C \perp {}^{\|\|}R^*$ $P \perp R \| \| C$
2			*2PRCR*-PRC* (Fig. 3.44a)	*1*	
3	*3-PCR* (Fig. 3.12b)	*3*	*PCRR*-2PCR* (Fig. 3.43b)	*2*	$P \perp C \| \| R \perp {}^{\|\|}R^*$ $P \perp C \| \| R$
4			*2PCRR*-PCR* (Fig. 3.44b)	*1*	
5	*3-PRC* (Fig. 3.13a, b)	*3*	*PRR*C-2PRC* (Fig. 3.45a, b)	*2*	$P \perp R \perp R^* \perp {}^{\|\|}C$ $P \perp R \| \| C$
6			*2PRR*C-PRC* (Fig. 3.47a, b)	*1*	
7	*3-PCR* (Fig. 3.14a, b)	*3*	*PCR*R-2PCR* (Fig. 3.46a, b)	*2*	$P \perp C \perp R^* \perp {}^{\|\|}R$ $P \perp C \| \| R$
8			*2PCR*R-PCR* (Fig. 3.48a, b)	*1*	
9	*3-PRPaR* (Fig. 3.15a)	*12*	*PR*RPaR-2PRPaR* (Fig. 3.49a)	*11*	$P \perp R^* \perp {}^{\|\|}R \perp Pa \perp {}^{\|\|}R$ $P \| \| R \perp Pa \perp {}^{\|\|}R$
10			*PRPa^{ss}-2PRPaR* (Fig. 3.50a)	*9*	$P \| \| R \perp Pa^{ss}$ $P \| \| R \perp Pa \perp {}^{\|\|}R$
11			*PR*RPa^{ss}-2PRPa^{ss}* (Fig. 3.51a)	*2*	$P \perp R^* \perp {}^{\|\|}R \perp Pa^{ss}$ $P \| \| R \perp Pa^{ss}$
12			*2PR*RPa^{ss}-PRPa^{ss}* (Fig. 3.52a)	*1*	
13	*3-PRPaR* (Fig. 3.15b)	*12*	*PR*RPaR-2PRPaR* (Fig. 3.49b)	*11*	$P \| \| R^* \perp R \perp Pa \perp {}^{\|\|}R$ $P \perp R \perp Pa \perp {}^{\|\|}R$
14			*PRPa^{ss}-2PRPaR* (Fig. 3.50b)	*9*	$P \perp R \perp Pa^{ss}$ $P \perp R \perp Pa \perp {}^{\|\|}R$
15			*PR*RPa^{ss}-2PRPa^{ss}* (Fig. 3.51b)	*2*	$P \| \| R^* \perp R \perp Pa^{ss}$ $P \perp R \perp Pa^{ss}$
16			*2PR*RPa^{ss}-PRPa^{ss}* (Fig. 3.52b)	*1*	

Table 3.19. Limb topology and the number of overconstraints N_F of the derived TPMs with idle mobilities and linear actuators mounted on a moving link presented in Figs. 3.53–3.59

No.	Basic TPM type	N_F	Derived TPM type	N_F	Topology of the limbs
1	*3-R<u>P</u>C* (Fig. 3.18a	*3*	*R<u>C</u>*C-2R<u>P</u>C* (Fig. 3.53a)	*2*	$R \perp \underline{C}^* \perp {}^{\parallel}C$ $R \perp \underline{P} \perp {}^{\parallel}C$
2			*2R<u>C</u>*C-R<u>P</u>C* (Fig. 3.54a)	*1*	
3	*3-C<u>P</u>R* (Fig. 3.18b)	*3*	*C<u>C</u>*R-2C<u>P</u>R* (Fig. 3.53b)	*2*	$C \perp \underline{C}^* \perp {}^{\parallel}R$ $C \perp \underline{P} \perp {}^{\parallel}R$
4			*2C<u>C</u>*R-C<u>P</u>R* (Fig. 3.54b)	*1*	
5	*3-R<u>P</u>C* (Fig. 3.19a, b)	*3*	*R<u>C</u>*C-2R<u>P</u>C* (Fig. 3.55a, b)	*2*	$R \perp \underline{C}^* \perp {}^{\parallel}C$ $R \perp \underline{P} \perp {}^{\parallel}C$
6			*2R<u>C</u>*C-R<u>P</u>C* (Fig. 3.57a, b)	*1*	
7	*3-C<u>P</u>R* (Fig. 3.20a, b)	*3*	*C<u>C</u>*R-2C<u>P</u>R* (Fig. 3.56a, b)	*2*	$C \perp \underline{C}^* \perp {}^{\parallel}R$ $C \perp \underline{P} \perp {}^{\parallel}R$
8			*2C<u>C</u>*R-C<u>P</u>R* (Fig. 3.58a, b)	*1*	
9	*3-P<u>P</u>RR* (Fig. 3.21)	*3*	*P<u>P</u>RRR*-2P<u>P</u>RR* (Fig. 3.59a)	*2*	$P \perp \underline{P} \perp {}^{\parallel}R \| R \perp {}^{\parallel}R^*$ $P \perp \underline{P} \perp {}^{\parallel}R \| R$
10			*2P<u>P</u>RRR*-P<u>P</u>RR* (Fig. 3.59b)	*1*	

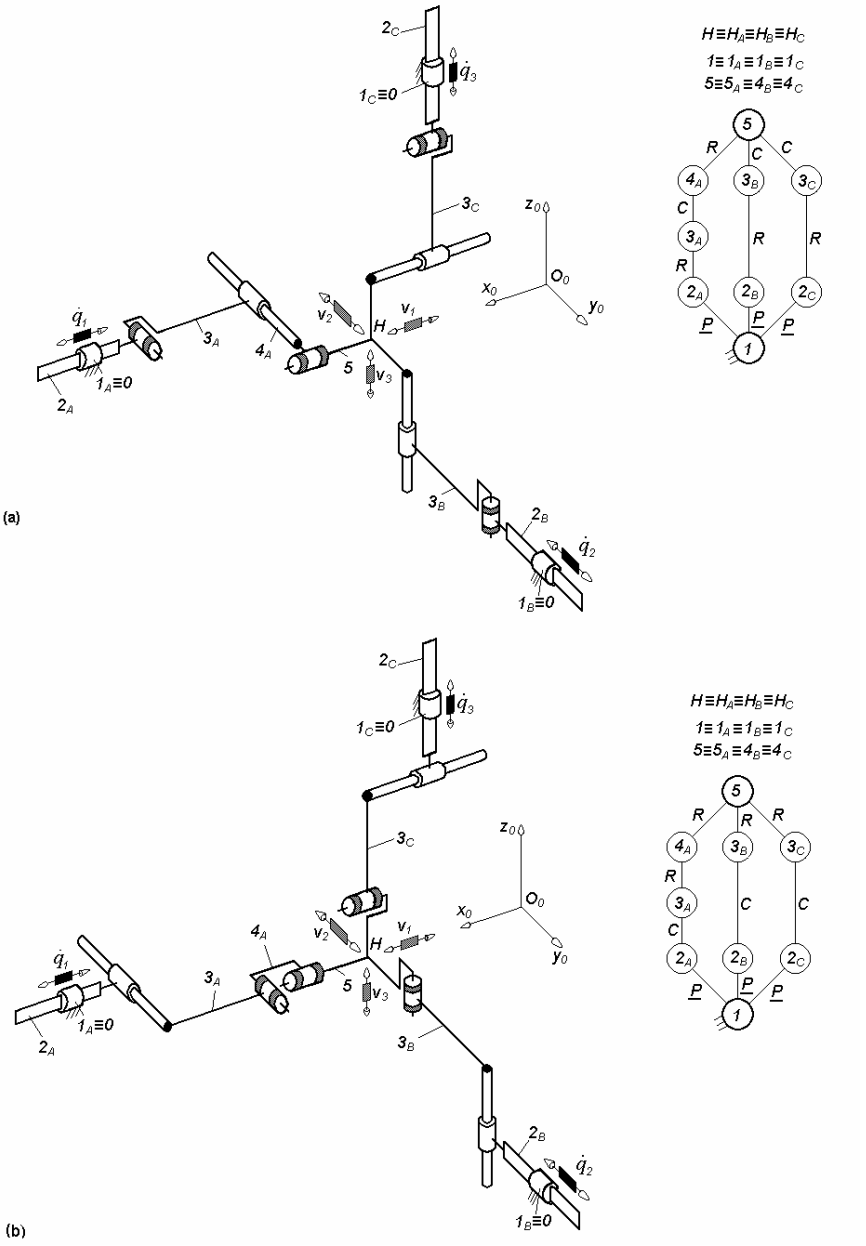

Fig. 3.43. Overconstrained TPMs of types $\underline{P}RCR^*$-$2\underline{P}RC$ (**a**) and $\underline{P}CRR^*$-$2\underline{P}CR$ (**b**) with coupled motions and linear actuators mounted on the fixed base, defined by $M_F = S_F = 3$, $(R_F) = (\boldsymbol{v}_1, \boldsymbol{v}_2, \boldsymbol{v}_3)$, $T_F = 0$, $N_F = 2$, limb toplogies $\underline{P} \perp R || C \perp {}^{||}R^*$ and $\underline{P} \perp R || C$ (**a**), $\underline{P} \perp C || R \perp {}^{||}R^*$ and $\underline{P} \perp C || R$ (**b**)

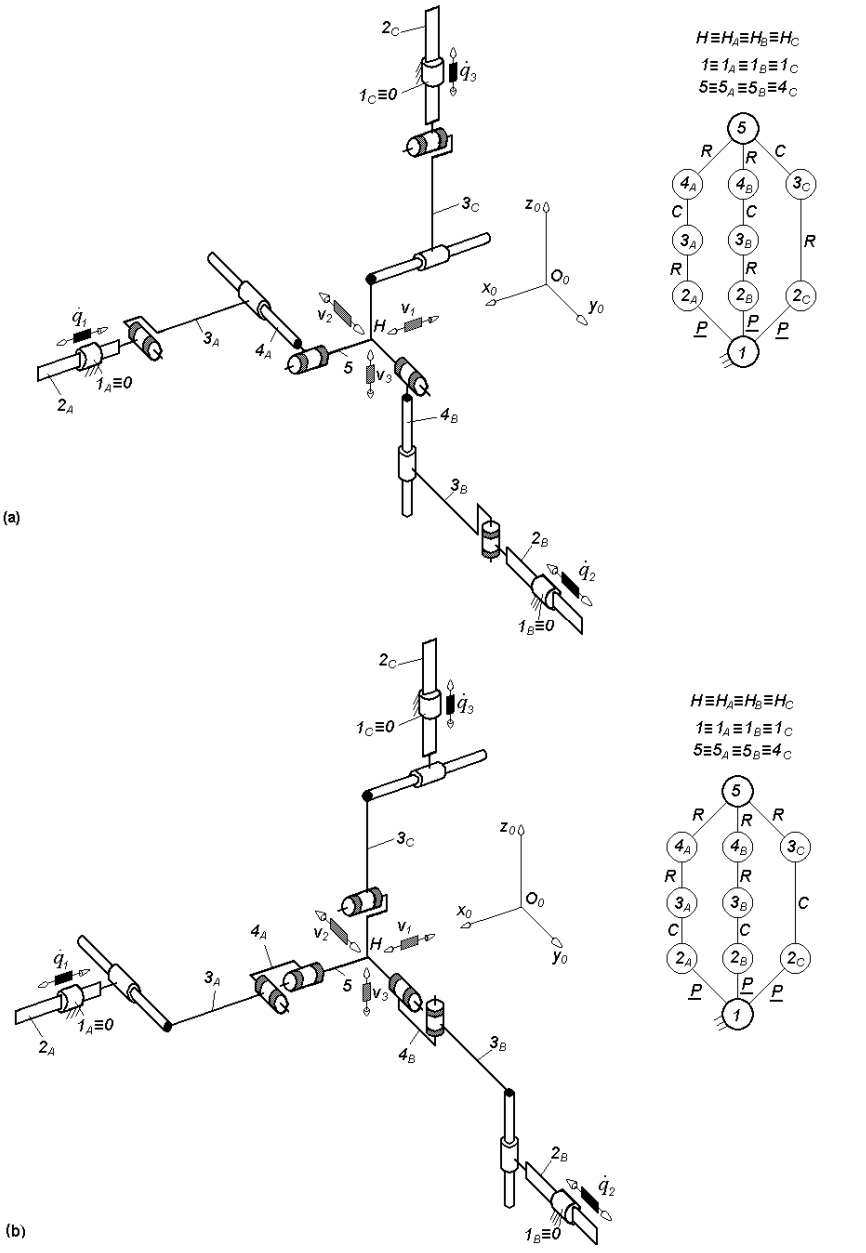

Fig. 3.44. Overconstrained TPMs of types *2*$\underline{P}$*RCR*-*$\underline{P}$*RC* (**a**) and *2*$\underline{P}$*CRR*-*$\underline{P}$*CR* (**b**) with coupled motions and linear actuators mounted on the fixed base, defined by $M_F = S_F = 3$, $(R_F) = (\boldsymbol{v}_1, \boldsymbol{v}_2, \boldsymbol{v}_3)$ $T_F = 0$, $N_F = 1$, limb topologies $\underline{P} \perp R || C \perp {}^{||}R^*$ and $\underline{P} \perp R || C$ (**a**), $\underline{P} \perp C || R \perp {}^{||}R^*$ and $\underline{P} \perp C || R$ (**b**)

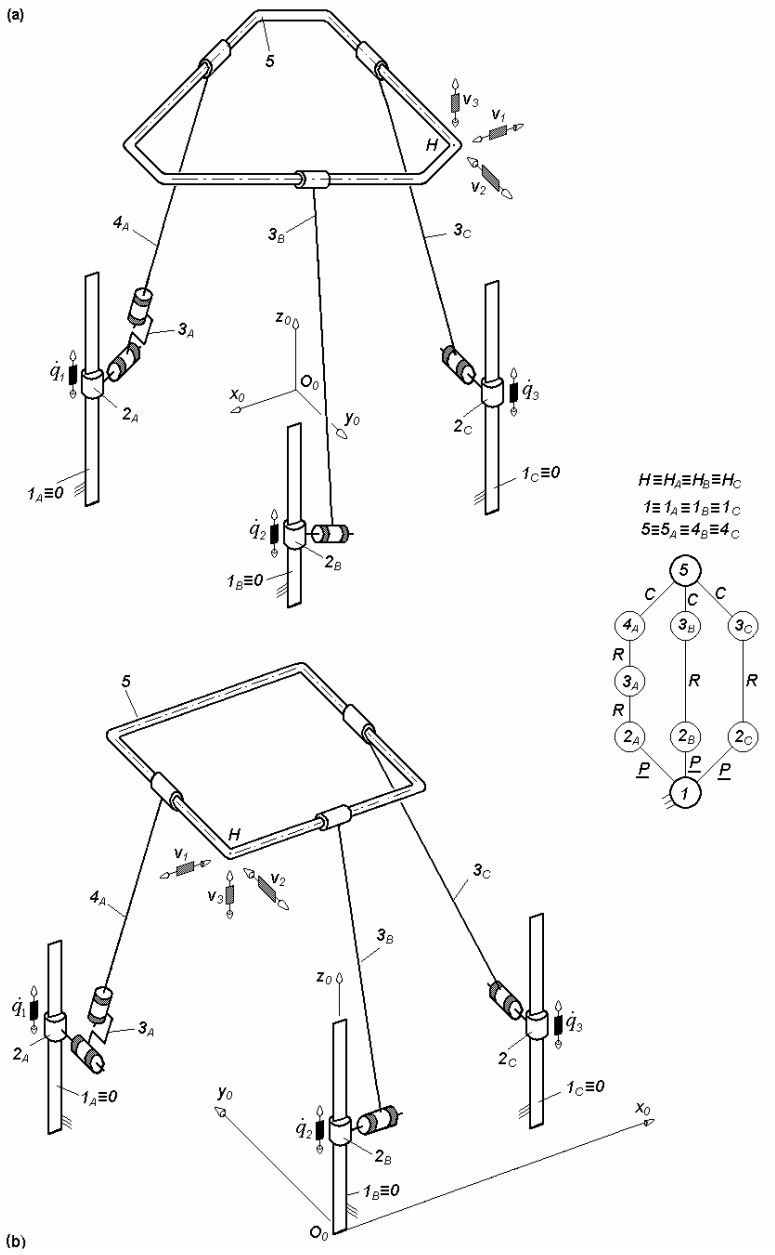

Fig. 3.45. *PRR*C-2PRC*-type overconstrained TPMs with coupled motions and parallel linear actuators mounted on the fixed base, defined by $M_F = S_F = 3$, $(R_F) = (\boldsymbol{v}_1, \boldsymbol{v}_2, \boldsymbol{v}_3)$ $T_F = 0$, $N_F = 2$, limb topologies $\underline{P} \perp R \perp R^* \perp {}^{||}C$ and $\underline{P} \perp R||C$

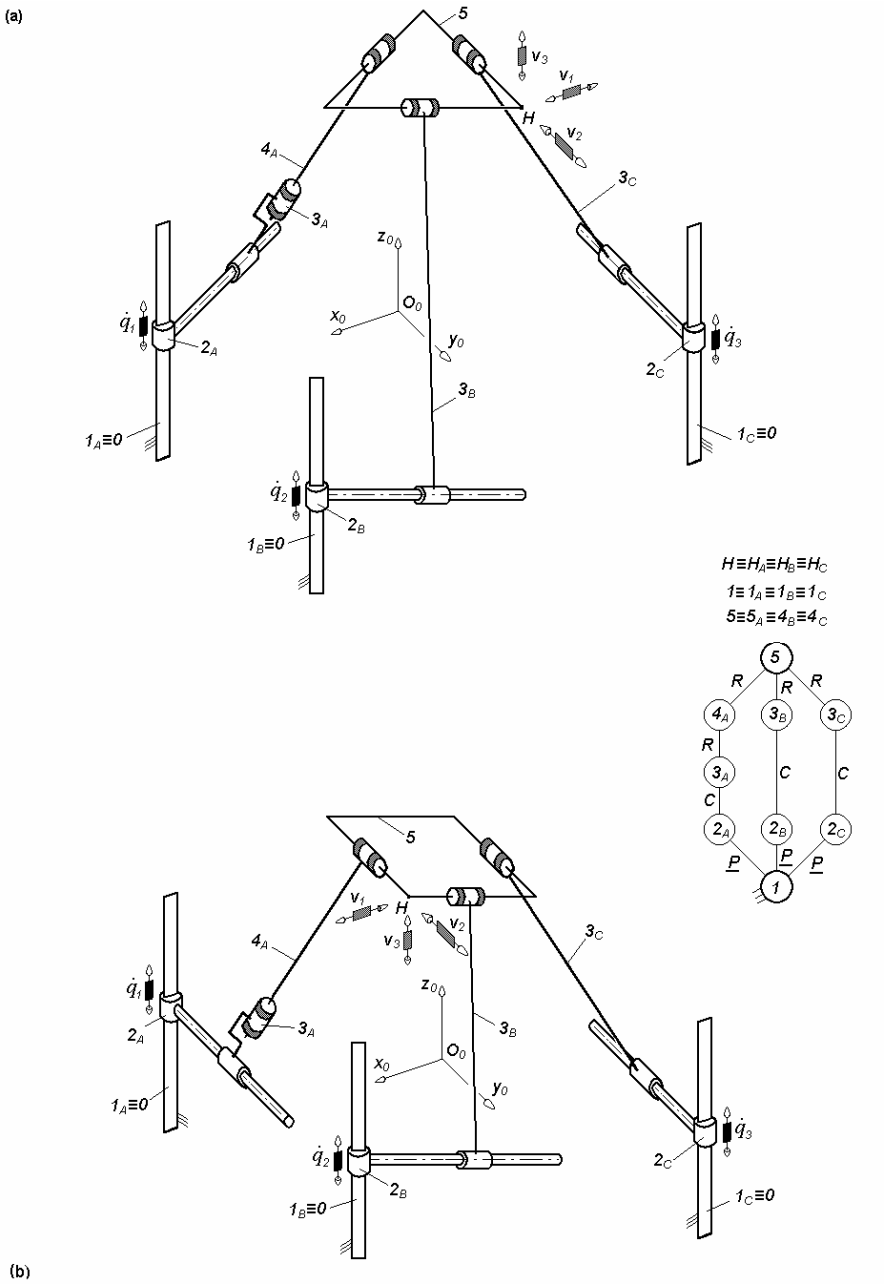

Fig. 3.46. *PCR*R-2PCR*-type overconstrained TPMs with coupled motions and parallel linear actuators mounted on the fixed base, defined by $M_F = S_F = 3$, $(R_F) = (\boldsymbol{v}_1, \boldsymbol{v}_2, \boldsymbol{v}_3)$ $T_F = 0$, $N_F = 2$, limb topologies $\underline{P} \perp C \perp R^* \perp {}^{\parallel}R$ and $\underline{P} \perp C \| R$

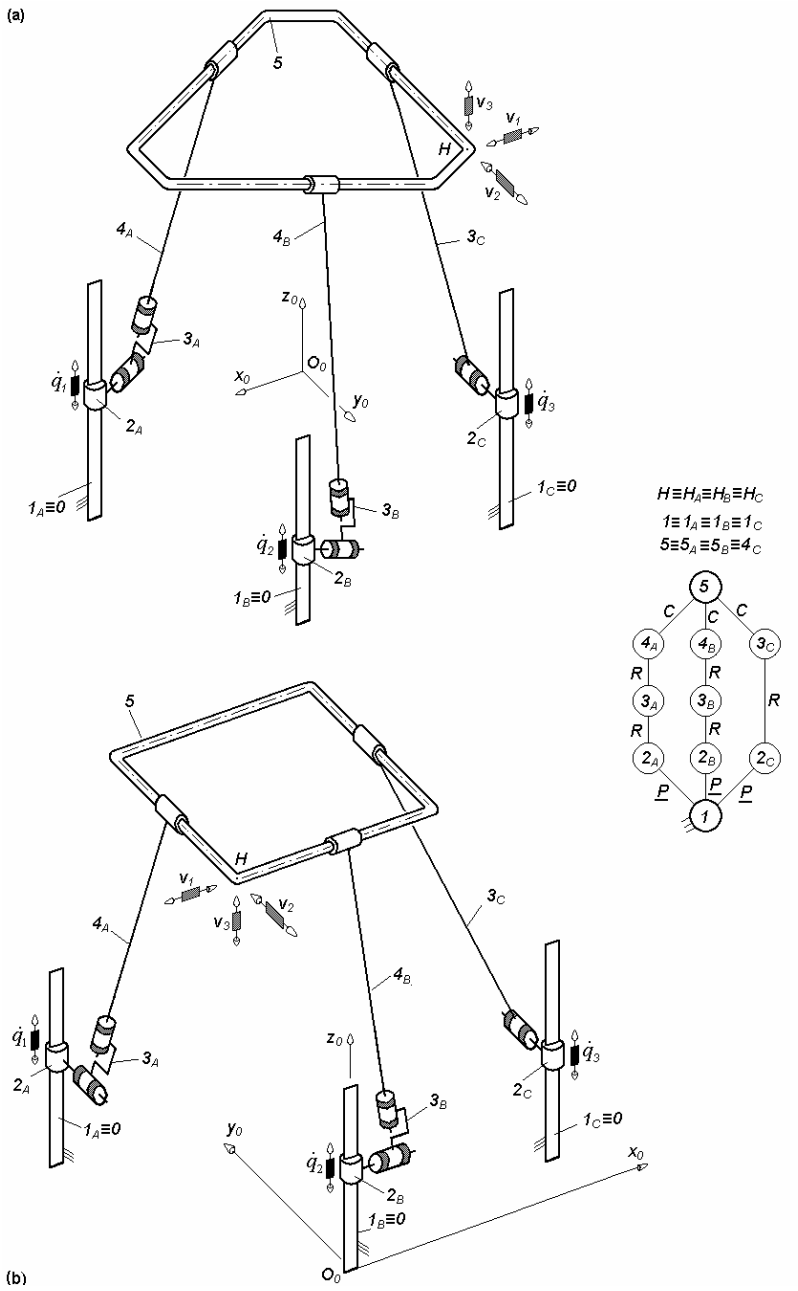

Fig. 3.47. *2PRR*C-PRC*-type overconstrained TPMs with coupled motions and parallel linear actuators mounted on the fixed base, defined by $M_F = S_F = 3$, $(R_F) = (\boldsymbol{v}_1, \boldsymbol{v}_2, \boldsymbol{v}_3)$ $T_F = 0$, $N_F = 1$, limb topologies $\underline{P} \perp R \perp R^* \perp {}^{\parallel}C$ and $\underline{P} \perp R \| C$

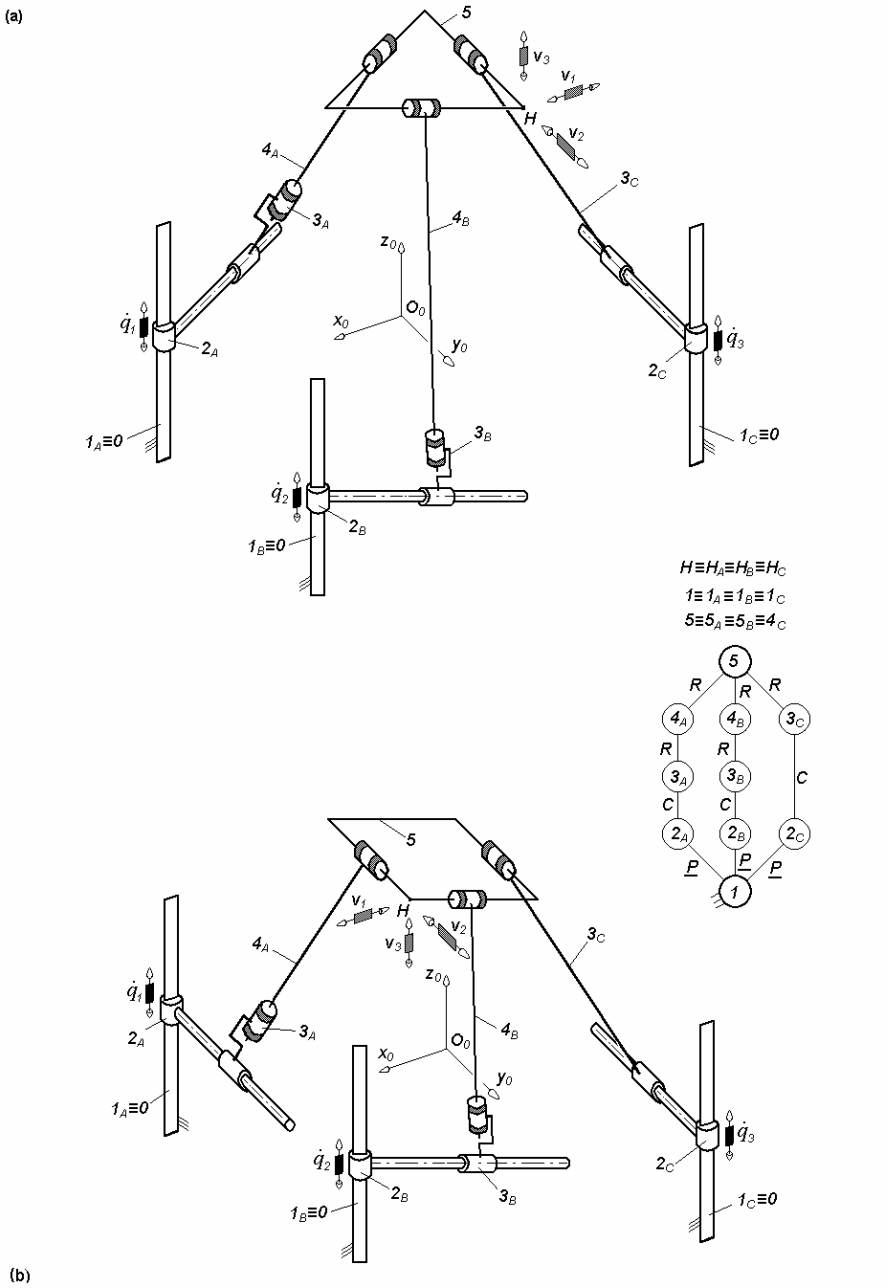

Fig. 3.48. *2PCR*R-PCR*-type overconstrained TPMs with coupled motions and parallel linear actuators mounted on the fixed base, defined by $M_F = S_F = 3$, $(R_F) = (\boldsymbol{v}_1, \boldsymbol{v}_2, \boldsymbol{v}_3)$ $T_F = 0$, $N_F = 1$, limb topologies $\underline{P} \perp C \perp R^* \perp {}^{||}R$ and $\underline{P} \perp C || R$

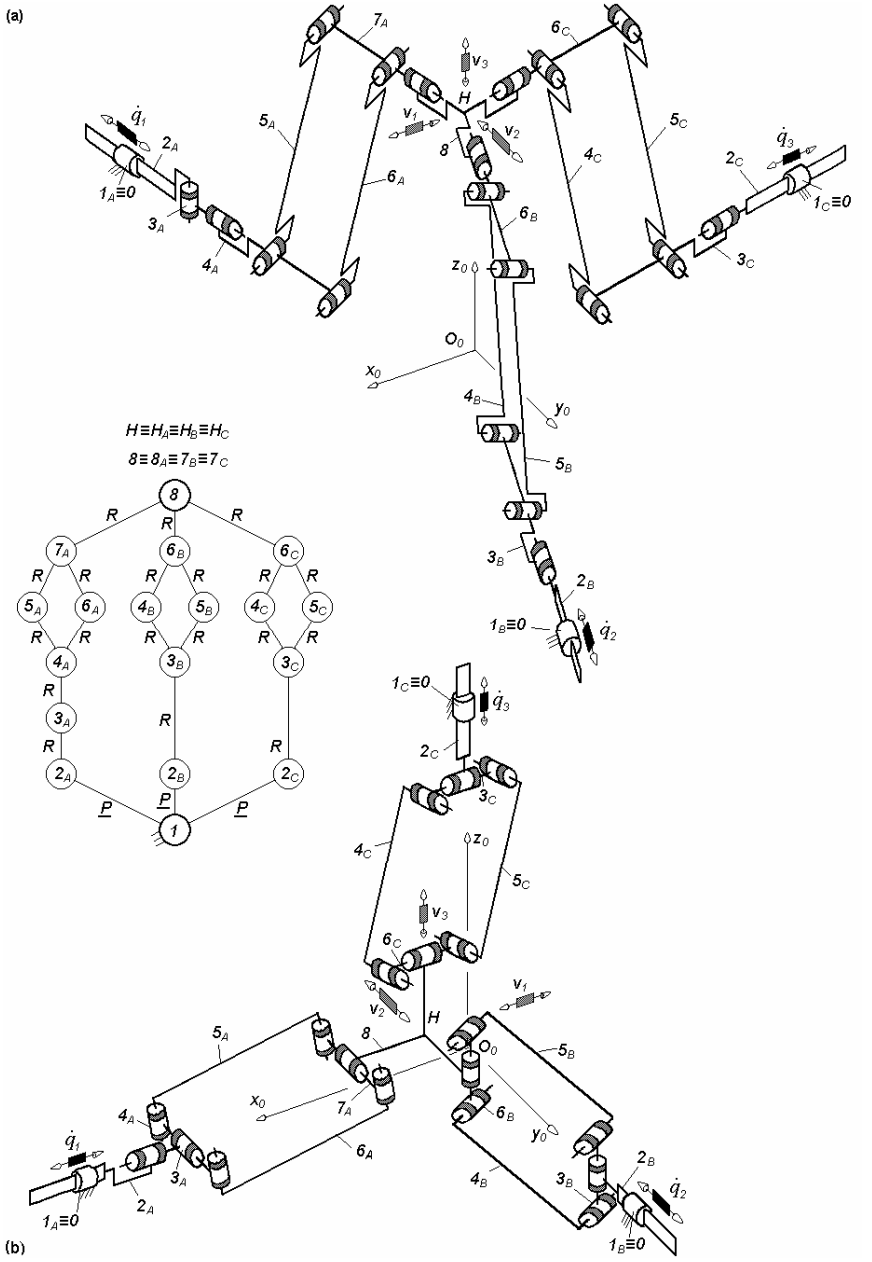

Fig. 3.49. $\underline{P}R^*RPaR$-$2\underline{P}RPaR$-type overconstrained TPMs with coupled motions and linear actuators mounted on the fixed base, defined by $M_F = S_F = 3$, $(R_F) = (\boldsymbol{v}_1, \boldsymbol{v}_2, \boldsymbol{v}_3)$ $T_F = 0$, $N_F = 11$, limb topologies $\underline{P} \perp R^* \perp {}^{\parallel}R \perp Pa \perp {}^{\parallel}R$ and $\underline{P}\|R \perp Pa \perp {}^{\parallel}R$ (**a**), $\underline{P}\|R^* \perp R \perp Pa \perp {}^{\parallel}R$ and $\underline{P} \perp R \perp Pa \perp {}^{\parallel}R$ (**b**)

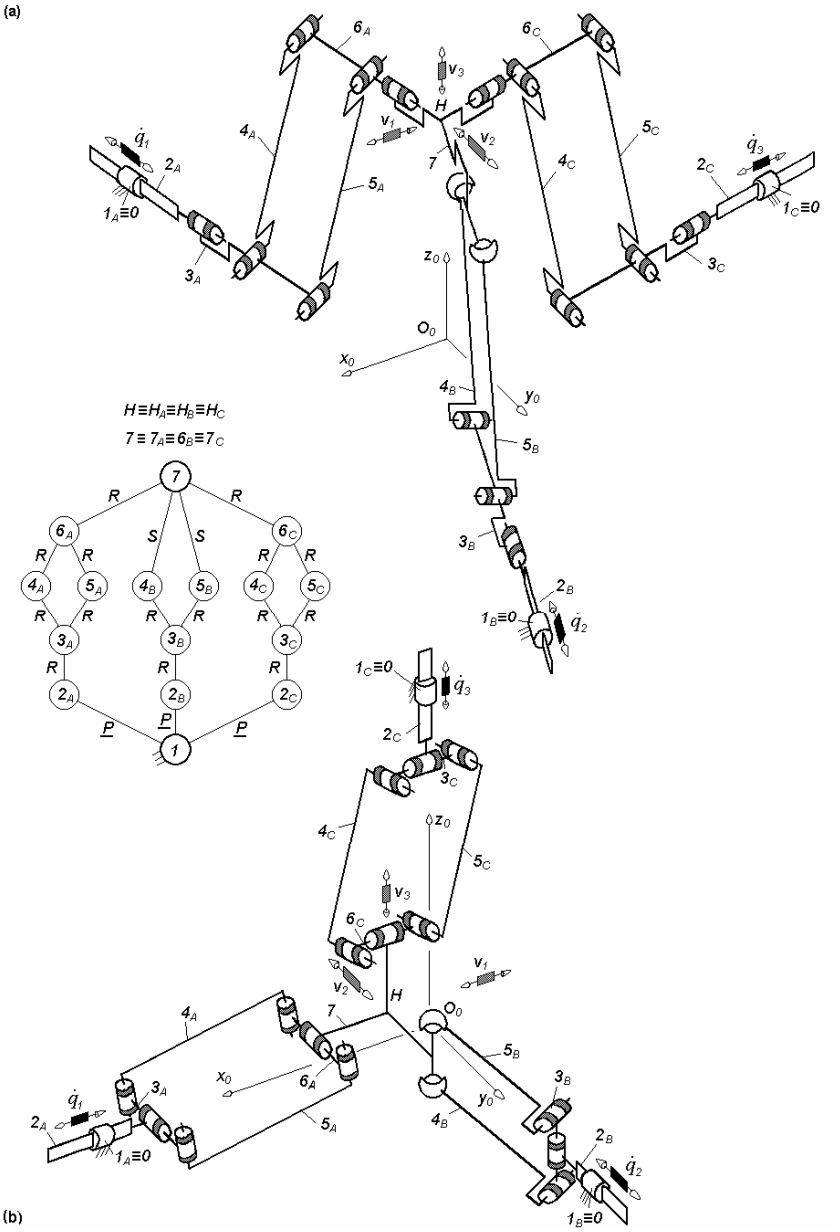

Fig. 3.50. $\underline{P}RPa^{ss}$-$2\underline{P}RPaR$-type overconstrained TPMs with coupled motions and linear actuators mounted on the fixed base, defined by $M_F = S_F = 3$, $(R_F) = (\boldsymbol{v}_1, \boldsymbol{v}_2, \boldsymbol{v}_3)$, $T_F = 0$, $N_F = 9$, limb topologies $\underline{P}||R \perp Pa^{ss}$ and $\underline{P}||R \perp Pa \perp {}^{||}R$ (**a**), $\underline{P} \perp R \perp Pa^{ss}$ and $\underline{P} \perp R \perp Pa \perp {}^{||}R$ (**b**)

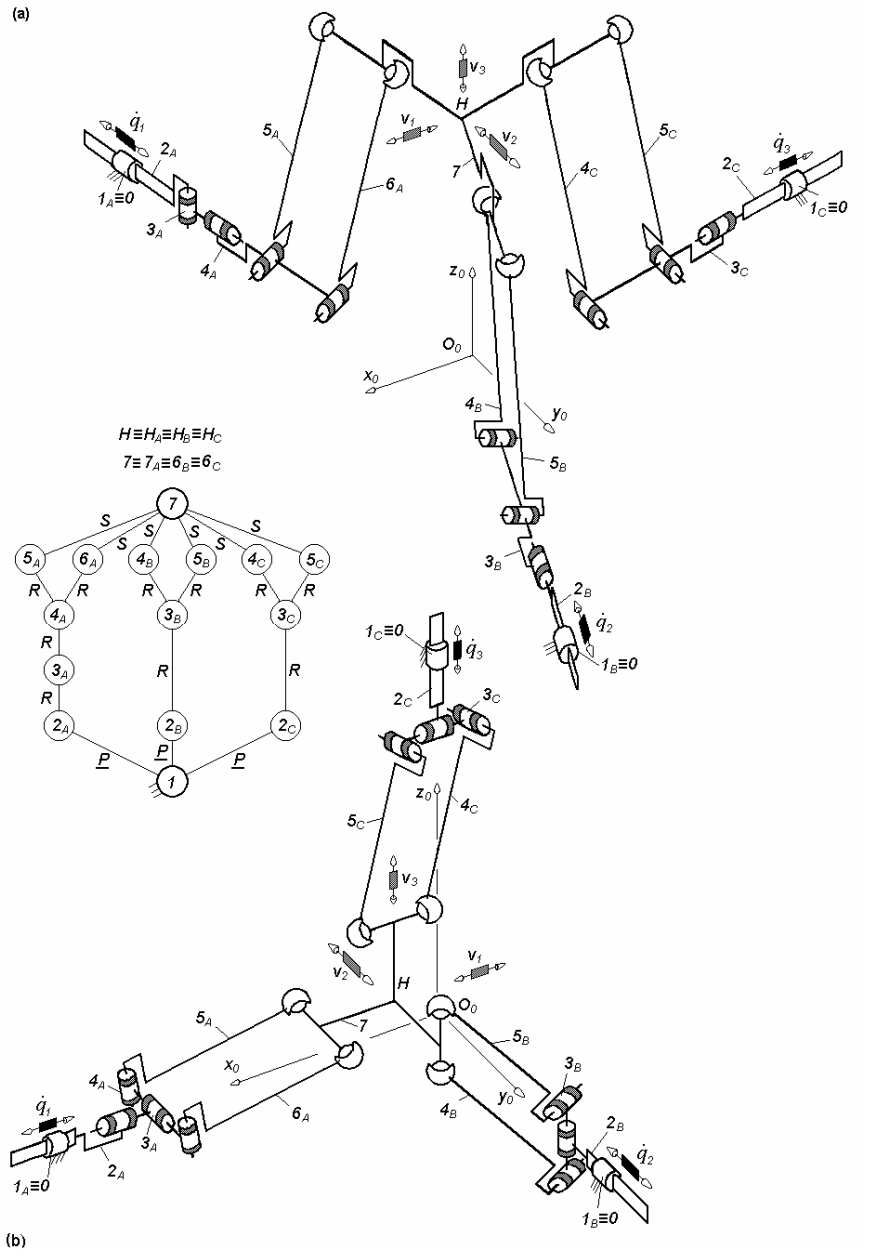

Fig. 3.51. $\underline{P}R^{*}RPa^{ss}$-$2\underline{P}RPa^{ss}$-type overconstrained TPMs with coupled motions and linear actuators mounted on the fixed base, defined by $M_F = S_F = 3$, $(R_F) = (\boldsymbol{v}_1, \boldsymbol{v}_2, \boldsymbol{v}_3)$, $T_F = 0$, $N_F = 2$, limb topologies $\underline{P} \perp R^{*} \perp {}^{||}R \perp Pa^{ss}$ and $\underline{P}||R \perp Pa^{ss}$ (**a**) and $\underline{P}||R^{*} \perp R \perp Pa^{ss}$ and $\underline{P} \perp R \perp Pa^{ss}$ (**b**)

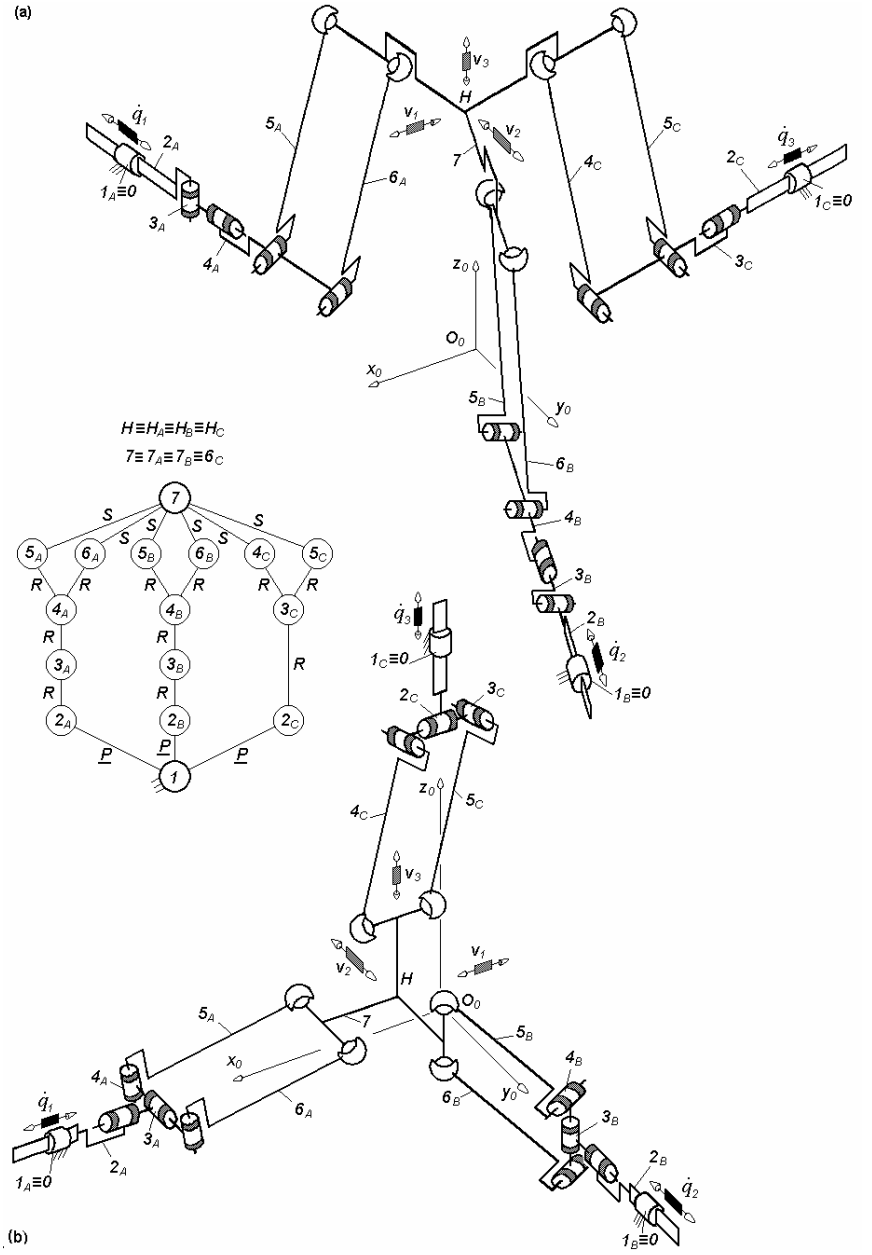

Fig. 3.52. *2PR*RPa*^{ss}-*PRPa*^{ss}-type overconstrained TPMs with coupled motions and linear actuators mounted on the fixed base, defined by $M_F = S_F = 3$, $(R_F) = (\boldsymbol{v}_1, \boldsymbol{v}_2, \boldsymbol{v}_3)$, $T_F = 0$, $N_F = 1$, limb topologies $\underline{P} \perp R^* \perp {}^{\parallel}R \perp Pa^{ss}$ and $\underline{P}||R \perp Pa^{ss}$ (**a**), $\underline{P}||R^* \perp R \perp Pa^{ss}$ and $\underline{P} \perp R \perp Pa^{ss}$ (**b**)

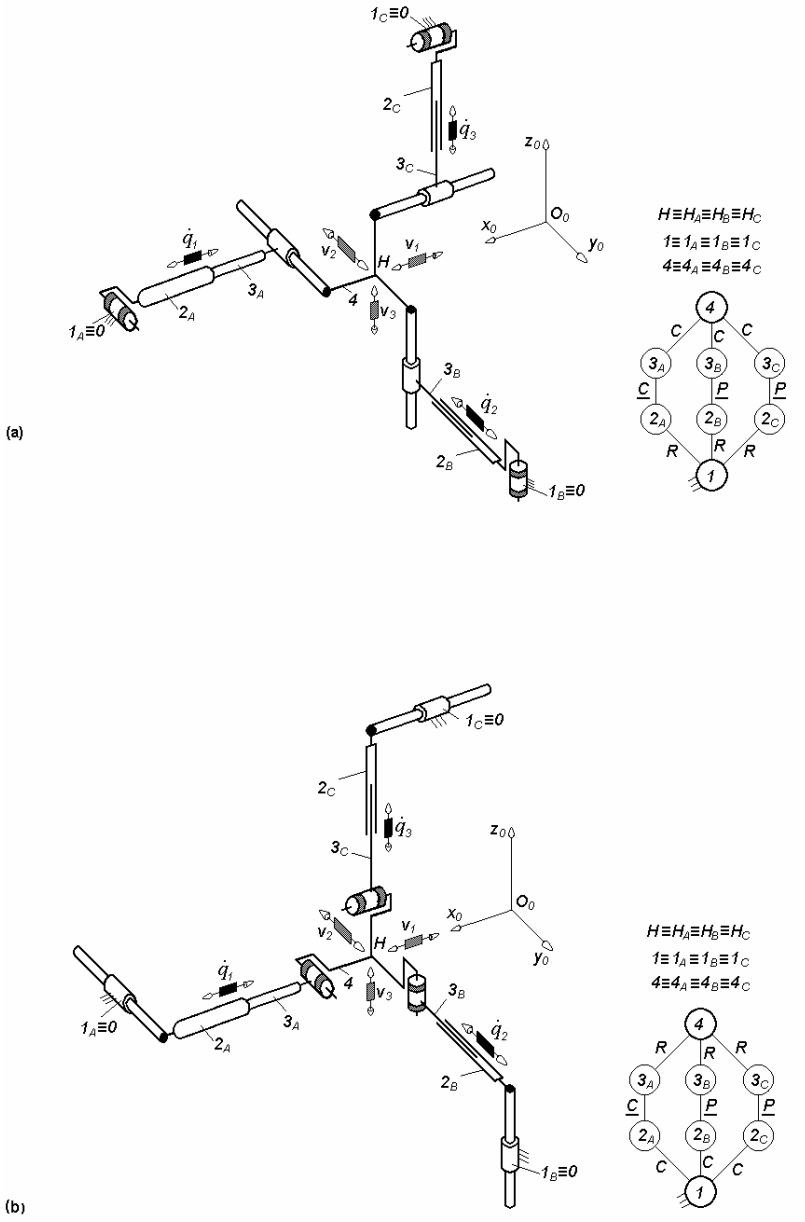

Fig. 3.53. Overconstrained TPMs of types $R\underline{C}$*C-$2R\underline{P}C$ (**a**) and $C\underline{C}$*R-$2C\underline{P}R$ (**b**) with coupled motions and linear actuators non adjacent to the fixed base, defined by $M_F = S_F = 3$, $(R_F) = (\boldsymbol{v}_1, \boldsymbol{v}_2, \boldsymbol{v}_3)$, $T_F = 0$, $N_F = 2$, limb topologies $R \perp \underline{C}^* \perp {}^{\|}C$ and $R \perp \underline{P} \perp {}^{\|}C$ (**a**), $C \perp \underline{C}^* \perp {}^{\|}R$ and $C \perp \underline{P} \perp {}^{\|}R$ (**b**)

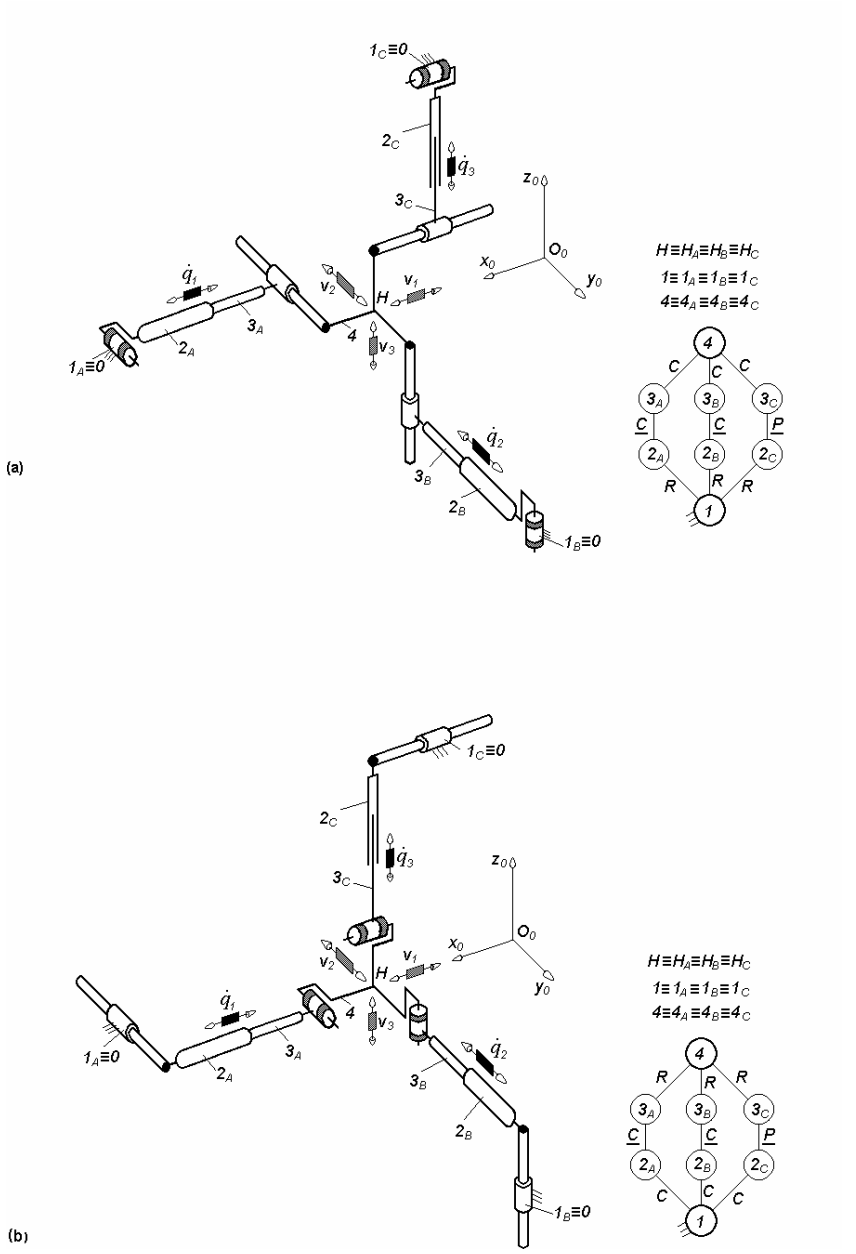

Fig. 3.54. Overconstrained TPMs of types *2R*$\underline{C}$**C-R*$\underline{P}$*C* (**a**) and *2C*$\underline{C}$**R-C*$\underline{P}$*R* (**b**) with coupled motions and linear actuators non adjacent to the fixed base, defined by $M_F = S_F = 3$, $(R_F) = (\boldsymbol{v}_1, \boldsymbol{v}_2, \boldsymbol{v}_3)$, $T_F = 0$, $N_F = 1$, limb topologies $R \perp \underline{C}^* \perp {}^{\|}C$ and $R \perp \underline{P} \perp {}^{\|}C$ (**a**), $C \perp \underline{C}^* \perp {}^{\|}R$ and $C \perp \underline{P} \perp {}^{\|}R$ (**b**)

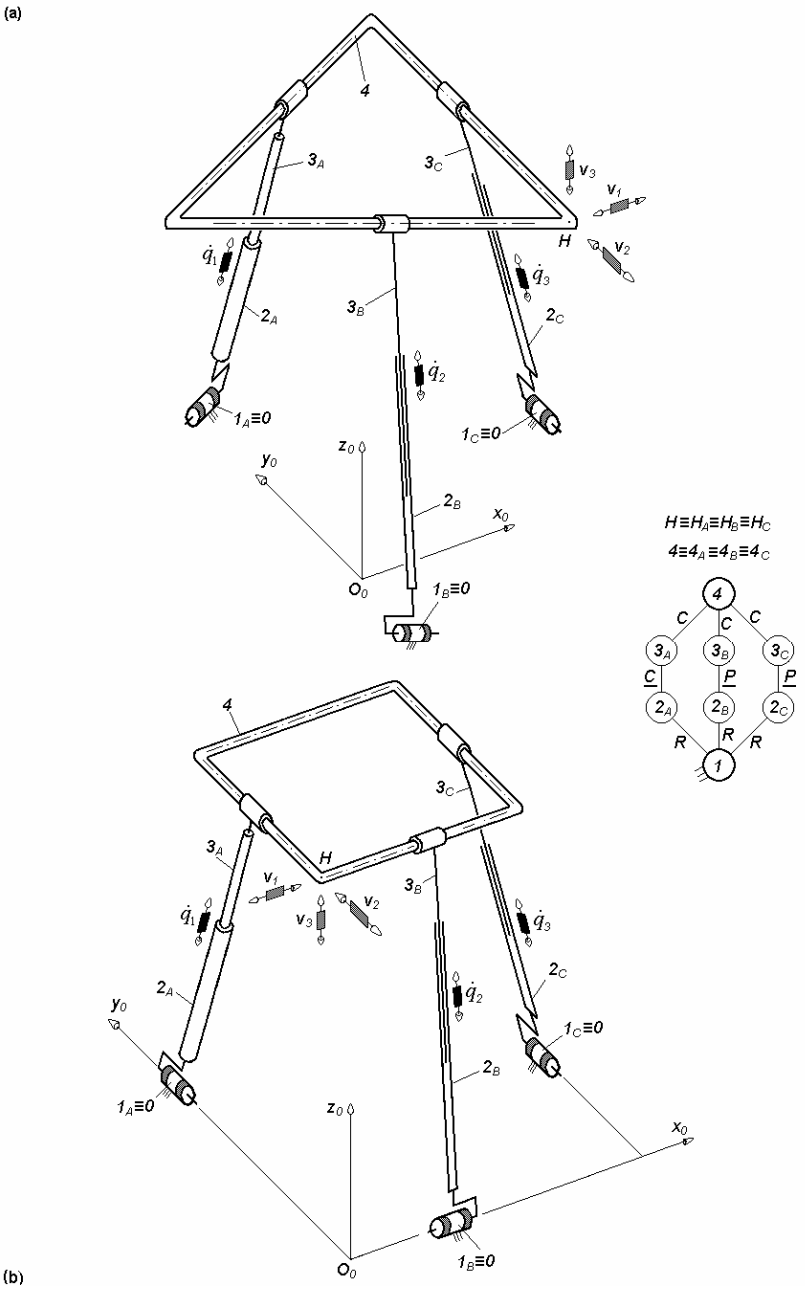

Fig. 3.55. *RC*C-2RPC*-type overconstrained TPMs with coupled motions and linear actuators non adjacent to the fixed base, defined by $M_F = S_F = 3$, $(R_F) = (\boldsymbol{v}_1, \boldsymbol{v}_2, \boldsymbol{v}_3)$, $T_F = 0$, $N_F = 2$, limb topologies $R \perp C^* \perp^{\parallel} C$ and $R \perp P \perp^{\parallel} C$

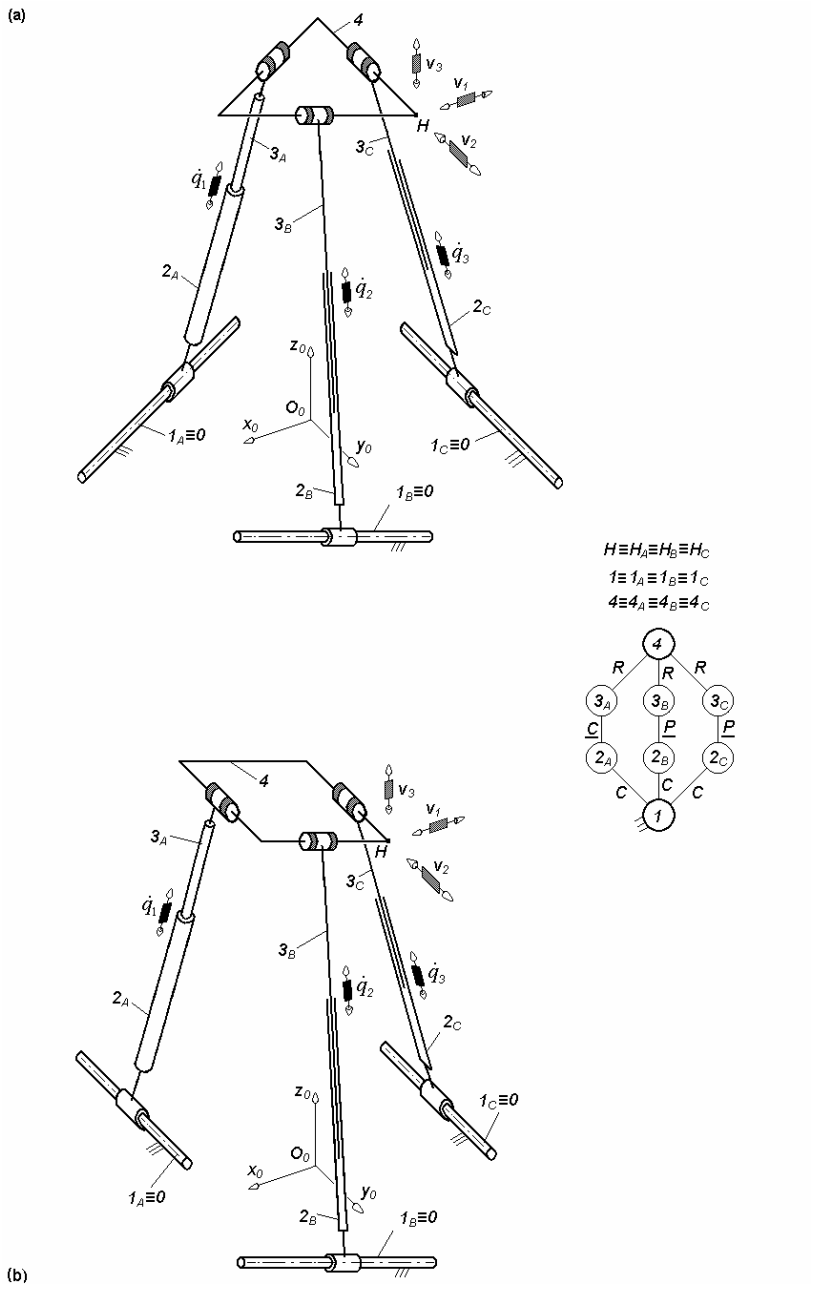

Fig. 3.56. *CC*R-2CPR*-type overconstrained TPMs with coupled motions and linear actuators non adjacent to the fixed base, defined by $M_F = S_F = 3$, $(R_F) = (\boldsymbol{v}_1, \boldsymbol{v}_2, \boldsymbol{v}_3)$, $T_F = 0$, $N_F = 2$, limb topologies $C \perp \underline{C}^* \perp {}^{\parallel}R$ and $C \perp \underline{P} \perp {}^{\parallel}R$

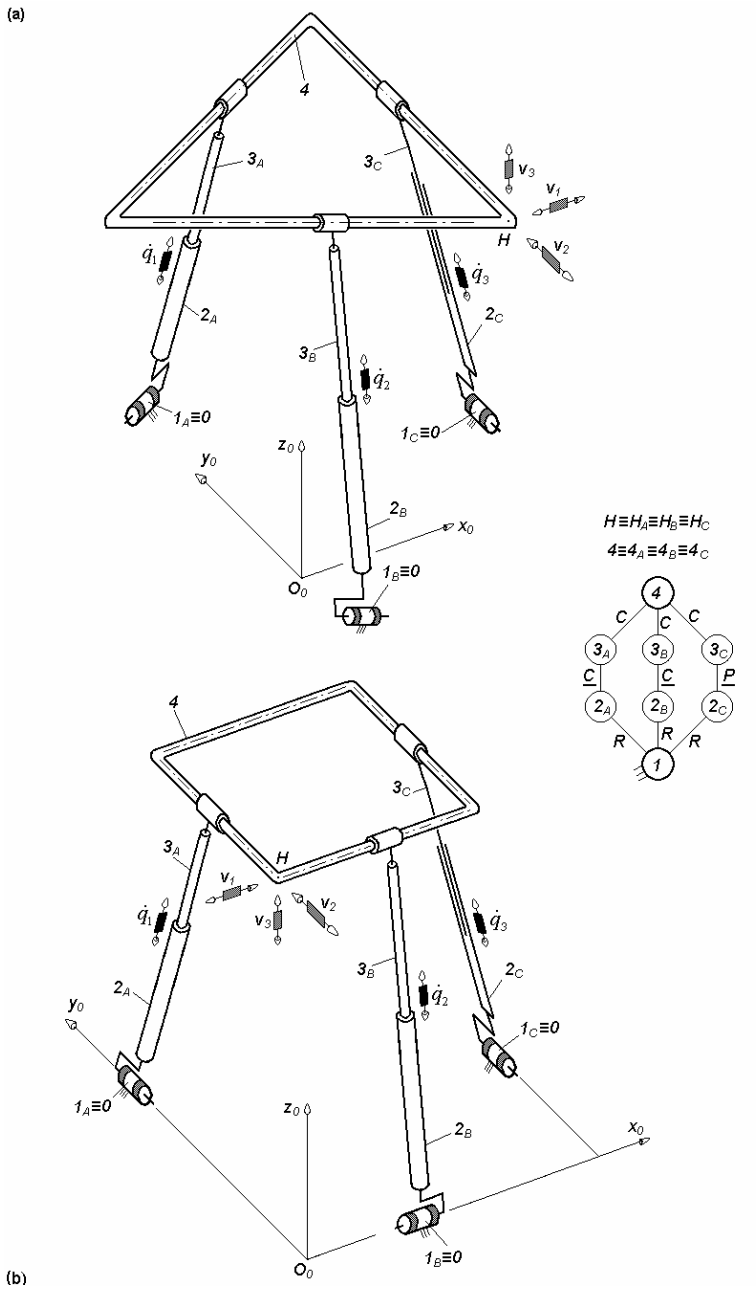

Fig. 3.57. *2RC*C-RPC*-type overconstrained TPMs with coupled motions and linear actuators non adjacent to the fixed base, defined by $M_F = S_F = 3$, $(R_F) = (\boldsymbol{v}_1, \boldsymbol{v}_2, \boldsymbol{v}_3)$, $T_F = 0$, $N_F = 1$, limb topologies $R \perp C^* \perp {}^{\parallel}C$ and $R \perp P \perp {}^{\parallel}C$

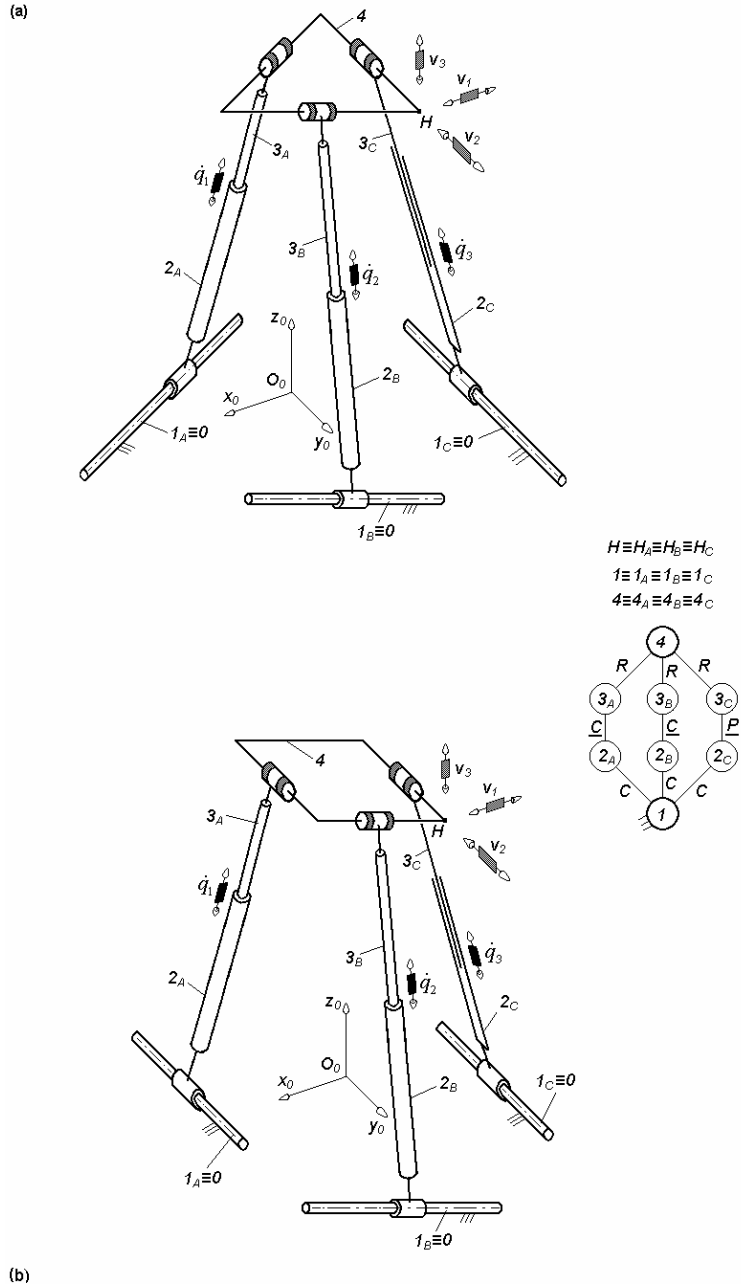

Fig. 3.58. *2C*$\underline{C}$**R-C*$\underline{P}$*R*-type overconstrained TPMs with coupled motions and linear actuators non adjacent to the fixed base, defined by $M_F = S_F = 3$, $(R_F) = (\boldsymbol{v}_1, \boldsymbol{v}_2, \boldsymbol{v}_3)$, $T_F = 0$, $N_F = 1$, limb topologies $C \perp \underline{C}^* \perp^{\parallel} R$ and $C \perp \underline{P} \perp^{\parallel} R$

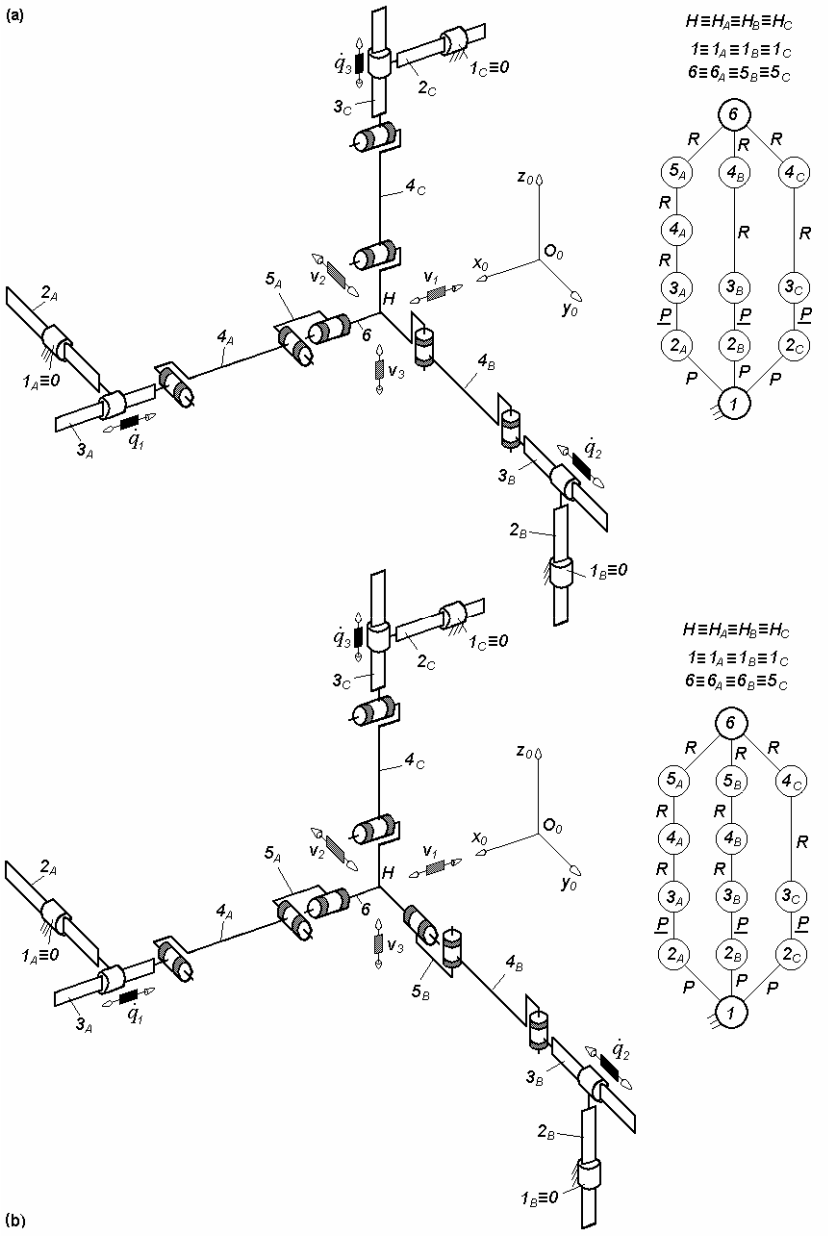

Fig. 3.59. Overconstrained TPMs of types *P*$\underline{P}$*RRR*-2P*$\underline{P}$*RR* (**a**) and *2P*$\underline{P}$*RRR*-P*$\underline{P}$*RR* (**b**) with coupled motions and linear actuators non adjacent to the fixed base, defined by $M_F = S_F = 3$, $(R_F) = (\boldsymbol{v}_1, \boldsymbol{v}_2, \boldsymbol{v}_3)$ $T_F = 0$, $N_F = 2$ (**a**), $N_F = 1$ (**b**), limb topologies $P \perp \underline{P} \perp {}^{\parallel}R \| R \perp {}^{\parallel}R^*$ and $P \perp \underline{P} \perp {}^{\parallel}R \| R$ (**a**), $P \perp \underline{P} \perp {}^{\parallel}R \| R \perp {}^{\parallel}R^*$ and $P \perp \underline{P} \perp {}^{\parallel}R \| R$ (**b**)

Table 3.20. Structural parameters[a] of translational parallel mechanisms in Figs. 3.43–3.48

No.	Structural parameter	Solution *P*RCR*-2*P*RC* (Fig. 3.43a) *P*CRR*-2*P*CR* (Fig. 3.43b) *P*RR*C-2*P*RC* (Fig. 3.45a, b) *P*CR*R-2*P*CR* (Fig. 3.46a, b)	 2*P*RCR*-*P*RC* (Fig. 3.44a) 2*P*CRR*-*P*CR* (Fig. 3.44b) 2*P*RR*C-*P*RC* (Fig. 3.47a, b) 2*P*CR*R-*P*CR* (Fig. 3.48a, b)
1	m	9	10
2	p_1	4	4
3	p_2	3	4
4	p_3	3	3
5	p	10	11
6	q	2	2
7	k_1	3	3
8	k_2	0	0
9	k	3	3
10	(R_{Gi}) (i = *1,2,3*)	See Table 3.24	See Table 3.24
11	S_{G1}	5	5
12	S_{G2}	4	5
13	S_{G3}	4	4
14	r_{G1}	0	0
15	r_{G2}	0	0
16	r_{G3}	0	0
17	M_{G1}	5	5
18	M_{G2}	4	5
19	M_{G3}	4	4
20	(R_F)	($\boldsymbol{v}_1, \boldsymbol{v}_2, \boldsymbol{v}_3$)	($\boldsymbol{v}_1, \boldsymbol{v}_2, \boldsymbol{v}_3$)
21	S_F	3	3
22	r_1	0	0
23	r_F	10	11
24	M_F	3	3
25	N_F	2	1
26	T_F	0	0
27	$\sum_{j=1}^{p_1} f_j$	5	5
28	$\sum_{j=1}^{p_2} f_j$	4	5
29	$\sum_{j=1}^{p_3} f_j$	4	4
30	$\sum_{j=1}^{p} f_j$	13	14

[a]See footnote of Table 2.1 for the nomenclature of structural parameters

Table 3.21. Structural parameters[a] of translational parallel mechanisms in Figs. 3.49–3.51

No.	Structural parameter	Solution $\underline{P}R^*RPaR$-2$\underline{P}RPaR$ (Fig. 3.49a, b)	$\underline{P}RPa^{ss}$-2$\underline{P}RPaR$ (Fig. 3.50a, b)	$\underline{P}R^*RPa^{ss}$-2$\underline{P}RPa^{ss}$ (Fig. 3.51a, b)
1	m	18	16	15
2	p_1	8	7	7
3	p_2	7	6	6
4	p_3	7	7	6
5	p	22	20	19
6	q	5	5	5
7	k_1	0	0	0
8	k_2	3	3	3
9	k	3	3	3
10	(R_{Gi}) $(i = 1,2,3)$	See Table 3.24	See Table 3.24	See Table 3.24
11	S_{G1}	5	4	5
12	S_{G2}	4	4	4
13	S_{G3}	4	4	4
14	r_{G1}	3	3	6
15	r_{G2}	3	6	6
16	r_{G3}	3	3	6
17	M_{G1}	5	4	5
18	M_{G2}	4	4	4
19	M_{G3}	4	4	4
20	(R_F)	$(\boldsymbol{v}_1, \boldsymbol{v}_2, \boldsymbol{v}_3)$	$(\boldsymbol{v}_1, \boldsymbol{v}_2, \boldsymbol{v}_3)$	$(\boldsymbol{v}_1, \boldsymbol{v}_2, \boldsymbol{v}_3)$
21	S_F	3	3	3
22	r_1	9	12	18
23	r_F	19	21	28
24	M_F	3	3	3
25	N_F	11	9	2
26	T_F	0	0	0
27	$\sum_{j=1}^{p_1} f_j$	8	7	11
28	$\sum_{j=1}^{p_2} f_j$	7	10	10
29	$\sum_{j=1}^{p_3} f_j$	7	7	10
30	$\sum_{j=1}^{p} f_j$	22	24	31

[a]See footnote of Table 2.1 for the nomenclature of structural parameters

Table 3.22. Structural parameters[a] of translational parallel mechanisms in Figs. 3.52–3.58

No.	Structural parameter	Solution *2PR*RPa^{ss}-PRPa^{ss}* (Fig. 3.52a, b)	*RC*C-2RPC* (Figs. 3.53a, 3.55a, b) *CC*R-2CPR* (Figs. 3.53b, 3.56a, b)	*2RC*C-RPC* (Figs. 3.54a, 3.57a, b) *2CC*R-CPR* (Figs. 3.54b, 3.58a, b)
1	m	16	8	8
2	p_1	7	3	3
3	p_2	7	3	3
4	p_3	6	3	3
5	p	20	9	9
6	q	5	2	2
7	k_1	0	3	3
8	k_2	3	0	0
9	k	3	3	3
10	(R_{Gi}) (i = 1,2,3)	See Table 3.24	See Table 3.24	See Table 3.24
11	S_{G1}	5	5	5
12	S_{G2}	5	4	5
13	S_{G3}	4	4	4
14	r_{G1}	6	0	0
15	r_{G2}	6	0	0
16	r_{G3}	6	0	0
17	M_{G1}	5	5	5
18	M_{G2}	5	4	5
19	M_{G3}	4	4	4
20	(R_F)	($\boldsymbol{v}_1,\boldsymbol{v}_2,\boldsymbol{v}_3$)	($\boldsymbol{v}_1,\boldsymbol{v}_2,\boldsymbol{v}_3$)	($\boldsymbol{v}_1,\boldsymbol{v}_2,\boldsymbol{v}_3$)
21	S_F	3	3	3
22	r_1	18	0	0
23	r_F	29	10	11
24	M_F	3	3	3
25	N_F	1	2	1
26	T_F	0	0	0
27	$\sum_{j=1}^{p_1} f_j$	11	5	5
28	$\sum_{j=1}^{p_2} f_j$	11	4	5
29	$\sum_{j=1}^{p_3} f_j$	10	4	4
30	$\sum_{j=1}^{p} f_j$	32	13	14

[a]See footnote of Table 2.1 for the nomenclature of structural parameters

Table 3.23. Structural parameters[a] of translational parallel mechanisms in Fig. 3.59

No.	Structural parameter	Solution *PPRRR*-2PPRR* (Fig. 3.59a)	*2PPRRR*-PPRR* (Fig. 3.59b)
1	m	12	13
2	p_1	5	5
3	p_2	4	5
4	p_3	4	4
5	p	13	14
6	q	2	2
7	k_1	3	3
8	k_2	0	0
9	k	3	3
10	(R_{Gi}) $(i = 1,2,3)$	See Table 3.24	See Table 3.24
11	S_{G1}	5	5
12	S_{G2}	4	5
13	S_{G3}	4	4
14	r_{G1}	0	0
15	r_{G2}	0	0
16	r_{G3}	0	0
17	M_{G1}	5	5
18	M_{G2}	4	5
19	M_{G3}	4	4
20	(R_F)	$(\boldsymbol{v}_1, \boldsymbol{v}_2, \boldsymbol{v}_3)$	$(\boldsymbol{v}_1, \boldsymbol{v}_2, \boldsymbol{v}_3)$
21	S_F	3	3
22	r_1	0	0
23	r_F	10	11
24	M_F	3	3
25	N_F	2	1
26	T_F	0	0
27	$\sum_{j=1}^{p_1} f_j$	5	5
28	$\sum_{j=1}^{p_2} f_j$	4	5
29	$\sum_{j=1}^{p_3} f_j$	4	4
30	$\sum_{j=1}^{p} f_j$	13	14

[a]See footnote of Table 2.1 for the nomenclature of structural parameters

Table 3.24. Bases of the operational velocities spaces of the limbs isolated from the parallel mechanisms presented in Figs. 3.43–3.59

No.	Parallel mechanism	Basis (R_{G1})	(R_{G2})	(R_{G3})
1	Figs. 3.43, 3.49b, 3.51b, 3.53, 3.59a	$(\boldsymbol{v}_1,\boldsymbol{v}_2,\boldsymbol{v}_3,\boldsymbol{\omega}_\alpha,\boldsymbol{\omega}_\beta)$	$(\boldsymbol{v}_1,\boldsymbol{v}_2,\boldsymbol{v}_3,\boldsymbol{\omega}_\delta)$	$(\boldsymbol{v}_1,\boldsymbol{v}_2,\boldsymbol{v}_3,\boldsymbol{\omega}_\alpha)$
2	Figs. 3.44, 3.52b, 3.54, 3.59b	$(\boldsymbol{v}_1,\boldsymbol{v}_2,\boldsymbol{v}_3,\boldsymbol{\omega}_\alpha,\boldsymbol{\omega}_\beta)$	$(\boldsymbol{v}_1,\boldsymbol{v}_2,\boldsymbol{v}_3,\boldsymbol{\omega}_\beta,\boldsymbol{\omega}_\delta)$	$(\boldsymbol{v}_1,\boldsymbol{v}_2,\boldsymbol{v}_3,\boldsymbol{\omega}_\alpha)$
3	Figs. 3.45, 3.46, 3.55, 3.56	$(\boldsymbol{v}_1,\boldsymbol{v}_2,\boldsymbol{v}_3,\boldsymbol{\omega}_\beta,\boldsymbol{\omega}_\delta)$	$(\boldsymbol{v}_1,\boldsymbol{v}_2,\boldsymbol{v}_3,\boldsymbol{\omega}_\alpha)$	$(\boldsymbol{v}_1,\boldsymbol{v}_2,\boldsymbol{v}_3,\boldsymbol{\omega}_\beta)$
4	Figs. 3.47, 3.48	$(\boldsymbol{v}_1,\boldsymbol{v}_2,\boldsymbol{v}_3,\boldsymbol{\omega}_\alpha,\boldsymbol{\omega}_\beta)$	$(\boldsymbol{v}_1,\boldsymbol{v}_2,\boldsymbol{v}_3,\boldsymbol{\omega}_\alpha,\boldsymbol{\omega}_\delta)$	$(\boldsymbol{v}_1,\boldsymbol{v}_2,\boldsymbol{v}_3,\boldsymbol{\omega}_\beta)$
5	Figs. 3.49a, 3.51a	$(\boldsymbol{v}_1,\boldsymbol{v}_2,\boldsymbol{v}_3,\boldsymbol{\omega}_\alpha,\boldsymbol{\omega}_\delta)$	$(\boldsymbol{v}_1,\boldsymbol{v}_2,\boldsymbol{v}_3,\boldsymbol{\omega}_\beta)$	$(\boldsymbol{v}_1,\boldsymbol{v}_2,\boldsymbol{v}_3,\boldsymbol{\omega}_\alpha)$
6	Fig. 3.50a	$(\boldsymbol{v}_1,\boldsymbol{v}_2,\boldsymbol{v}_3,\boldsymbol{\omega}_\alpha)$	$(\boldsymbol{v}_1,\boldsymbol{v}_2,\boldsymbol{v}_3,\boldsymbol{\omega}_\beta)$	$(\boldsymbol{v}_1,\boldsymbol{v}_2,\boldsymbol{v}_3,\boldsymbol{\omega}_\alpha)$
7	Fig. 3.50b	$(\boldsymbol{v}_1,\boldsymbol{v}_2,\boldsymbol{v}_3,\boldsymbol{\omega}_\alpha,\boldsymbol{\omega}_\beta)$	$(\boldsymbol{v}_1,\boldsymbol{v}_2,\boldsymbol{v}_3,\boldsymbol{\omega}_\beta,\boldsymbol{\omega}_\delta)$	$(\boldsymbol{v}_1,\boldsymbol{v}_2,\boldsymbol{v}_3,\boldsymbol{\omega}_\alpha,\boldsymbol{\omega}_\delta)$
8	Fig. 3.52a	$(\boldsymbol{v}_1,\boldsymbol{v}_2,\boldsymbol{v}_3,\boldsymbol{\omega}_\alpha,\boldsymbol{\omega}_\delta)$	$(\boldsymbol{v}_1,\boldsymbol{v}_2,\boldsymbol{v}_3,\boldsymbol{\omega}_\alpha,\boldsymbol{\omega}_\beta)$	$(\boldsymbol{v}_1,\boldsymbol{v}_2,\boldsymbol{v}_3,\boldsymbol{\omega}_\alpha)$
9	Figs. 3.57, 3.58	$(\boldsymbol{v}_1,\boldsymbol{v}_2,\boldsymbol{v}_3,\boldsymbol{\omega}_\beta,\boldsymbol{\omega}_\delta)$	$(\boldsymbol{v}_1,\boldsymbol{v}_2,\boldsymbol{v}_3,\boldsymbol{\omega}_\alpha,\boldsymbol{\omega}_\delta)$	$(\boldsymbol{v}_1,\boldsymbol{v}_2,\boldsymbol{v}_3,\boldsymbol{\omega}_\beta)$

3.3 Basic solutions with rotating actuators

In the *basic solutions* with *rotating actuators* and coupled motions $F \leftarrow G_1$-G_2, the moving platform $n \equiv n_{Gi}$ ($i = 1, 2, 3$) is connected to the reference platform $1 \equiv 1_{Gi} \equiv 0$ by three limbs with three, four or five degrees of connectivity. No idle mobilities exist in these basic solutions and the rotating actuator is associated with a revolute pair in each limb.

The various types of limbs with three degrees of connectivity are systematized in Figs. 3.60–3.62. They combine two (Figs. 3.60 and 3.61) or three (Fig. 3.62) parallelogram loops of types *Pa* (Figs. 3.60 and 3.62) or Pa^{cc} (Fig. 3.61). We recall that *Pa*-type parallelogram loop has one degree of mobility and Pa^{cc}-type parallelogram loop has two degrees of mobility. These limbs are actuated by rotating motors mounted on the fixed base and integrated in a parallelogram loop.

The limbs with four degrees of connectivity are systematized in Figs. 3.63–3.68. They can be simple (Fig. 3.63) or complex (Figs. 3.64–3.68) kinematic chains. The complex limbs combine parallelogram loops of types *Pa* (Figs. 3.64, 3.65, 3.67 and 3.68) and Pa^{cc} (Fig. 3.66a–c) or a prism mechanism *Pr* (Fig. 3.66d). The complex limbs are actuated by rotating motors mounted on the fixed base and combined in the kinematic chain of the parallelogram loop (Figs. 3.64, 3.65 and 3.66a) or outside the parallelogram loop (Figs. 3.66b–d, 3.67 and 3.68).

The limbs with five degrees of connectivity are systematized in Figs. 3.69 and 3.70. They are complex kinematic chains combining a *Pa*-type parallelogram loop. These limbs are actuated by rotating motors mounted on the fixed base and combined in the parallelogram loop (Fig. 3.69a–e) or outside the parallelogram loop (Figs. 3.69f and 3.70).

Various solutions of translational parallel robots with coupled motions and no idle mobilities can be obtained by using three limbs with identical or different topologies presented in Figs. 3.60–3.70. We only show solutions with identical limb type as illustrated in Figs. 3.71–3.118. The limb topology and connecting conditions in these solutions with no idle mobilities are systematized in Table 3.25.

The axes of the three actuated revolute joints adjacent to the fixed base can be in one of the following configurations (see Table 3.25): (i) reciprocally orthogonal in space, (ii) parallel to two orthogonal directions or (iii) parallel to a plane. The axes of the unactuated revolute or cylindrical joints adjacent to the moving platform can be orthogonal in space or parallel to a plane. In the latter case, the axes can form a triangle or can be situated on three sides of a rectangle. These axes form a configuration called spatial star, if they are orthogonal in space, and Δ or $\amalg$-type if they are parallel to a plane (see Table 3.25). The structural parameters of the solutions presented in Figs. 3.71–3.118 are systematized in Tables 3.26–3.31.

Table 3.25. Limb topology and connecting conditions of the TPMs with no idle mobilities and rotating actuators mounted on the fixed base presented in Figs. 3.71–3.118

No.	TPM type	Limb topology	Connecting conditions
1	*3-*$\underline{Pa}$*PaP* (Fig. 3.71a)	$\underline{Pa} \perp Pa \| \| P$ (Fig. 3.60a)	Axes of the actuated joints are reciprocally orthogonal and the moving platform in a spatial star configuration
2	*3-*$\underline{Pa}$*PaP* (Fig. 3.71b)	$\underline{Pa} \perp Pa \| \| P$ (Fig. 3.60a)	Axes of the actuated joints are parallel to two orthogonal directions and the moving platform in a $\amalg$ configuration
3	*3-*$\underline{Pa}$*PPa* (Fig. 3.72a)	$\underline{Pa} \| \| Pa \| \| P$ (Fig. 3.60b)	Idem No. 1
4	*3-*$\underline{Pa}$*PaPa* (Fig. 3.72b)	$\underline{Pa} \| \| Pa \| \| P$ (Fig. 3.60b)	Idem No. 2
5	*3-*$\underline{Pa}$*PPa* (Fig. 3.73a)	$\underline{Pa} \perp P \| \| Pa$ (Fig. 3.60c)	Idem No. 1
6	*3-*$\underline{Pa}$*PPa* (Fig. 3.73b)	$\underline{Pa} \perp P \| \| Pa$ (Fig. 3.60c)	Axes of the actuated joints are parallel to two orthogonal directions and the moving platform in a star configuration
7	*3-*$\underline{Pa}$*PPa* (Fig. 3.74a)	$\underline{Pa} \| \| P \| \| Pa$ (Fig. 3.60d)	Idem No. 1
8	*3-*$\underline{Pa}$*PPa* (Fig. 3.74b)	$\underline{Pa} \| \| P \| \| Pa$ (Fig. 3.60d)	Idem No. 6
9	*3-*$\underline{Pa}Pa^{cc}$ (Fig. 3.75a)	$\underline{Pa} \perp Pa^{cc}$ (Fig. 3.61a)	Idem No. 1
10	*3-*$\underline{Pa}Pa^{cc}$ (Fig. 3.75b)	$\underline{Pa} \perp Pa^{cc}$ (Fig. 3.61a)	Idem No. 2
11	*3-*$\underline{Pa}Pa^{cc}$ (Fig. 3.76a)	$\underline{Pa} \perp Pa^{cc}$ (Fig. 3.61b)	Idem No. 1
12	*3-*$\underline{Pa}Pa^{cc}$ (Fig. 3.76b)	$\underline{Pa} \perp Pa^{cc}$ (Fig. 3.61b)	Idem No. 6
13	*3-*$\underline{Pa}Pa^{cc}$ (Fig. 3.77a)	$\underline{Pa} \| \| Pa^{cc}$ (Fig. 3.61c)	Idem No. 1
14	*3-*$\underline{Pa}Pa^{cc}$ (Fig. 3.77b)	$\underline{Pa} \| \| Pa^{cc}$ (Fig. 3.61c)	Idem No. 2
15	*3-*$\underline{Pa}Pa^{cc}$ (Fig. 3.78a)	$\underline{Pa} \| \| Pa^{cc}$ (Fig. 3.61d)	Idem No. 1
16	*3-*$\underline{Pa}Pa^{cc}$ (Fig. 3.78b)	$\underline{Pa} \| \| Pa^{cc}$ (Fig. 3.61d)	Idem No. 6
17	*3-*$\underline{Pa^{cc}}Pa$ (Fig. 3.79a)	$\underline{Pa^{cc}} \| \| Pa$ (Fig. 3.61e)	Idem No. 1
18	*3-*$\underline{Pa^{cc}}Pa$ (Fig. 3.79b)	$\underline{Pa^{cc}} \| \| Pa$ (Fig. 3.61e)	Idem No. 6
19	*3-*$\underline{Pa}PaPa$ (Fig. 3.80)	$\underline{Pa} \perp Pa \perp {}^{\|\|}Pa$ (Fig. 3.62a)	Idem No. 1
20	*3-*$\underline{Pa}PaPa$ (Fig. 3.81)	$\underline{Pa} \perp Pa \perp^{\perp} Pa$ (Fig. 3.62b)	Idem No. 1

Table 3.25. (cont.)

21	*3-PaPaPa* (Fig. 3.82)	$\underline{Pa}\|\|Pa \perp Pa$ (Fig. 3.62c)	Idem No. 1
22	*3-RRC* (Fig. 3.83a)	$\underline{R}\|\|R\|\|C$ (Fig. 3.63c)	Axes of the actuated joints parallel to a plane and the moving platform in a Δ configuration
23	*3-RRC* (Fig. 3.83b, 3.84a)	$\underline{R}\|\|R\|\|C$ (Fig. 3.63c)	Idem No. 2
24	*3-RRC* (Fig. 3.84b)	$\underline{R}\|\|R\|\|C$ (Fig. 3.63c)	Idem No. 1
25	*3-RCR* (Fig. 3.85a)	$\underline{R}\|\|C\|\|R$ (Fig. 3.63f)	Idem No. 1
26	*RPRR* (Fig. 3.85b)	$\underline{R}\|\|P\|\|R\|\|R$ (Fig. 3.63j)	Idem No. 1
27	*3-RPC* (Fig. 3.86a)	$\underline{R} \perp P \perp^{\|\|} C$ (Fig. 3.63i)	Idem No. 1
28	*3-RPPR* (Fig. 3.86b)	$\underline{R}\|\|P \perp P \perp^{\|\|} R$ (Fig. 3.63k)	Idem No. 1
29	*3-PaRC* (Fig. 3.87a)	$\underline{Pa}\|\|R\|\|C$ (Fig. 3.64c)	Idem No. 1
30	*3-PaRC* (Fig. 3.87b)	$\underline{Pa}\|\|R\|\|C$ (Fig. 3.64c)	Idem No. 2
31	*3-PaCR* (Fig. 3.88a)	$\underline{Pa}\|\|C\|\|R$ (Fig. 3.64f)	Idem No. 1
32	*3-PaCR* (Fig. 3.88b)	$\underline{Pa}\|\|C\|\|R$ (Fig. 3.64f)	Idem No. 2
33	*3-PaPaRR* (Fig. 3.89)	$\underline{Pa}\|\|Pa \perp R\|\|R$ (Fig. 3.65a)	Idem No. 1
34	*3-PaPaRR* (Fig. 3.90)	$\underline{Pa} \perp Pa \perp^{\|\|} R\|\|R$ (Fig. 3.65b)	Idem No. 1
35	*3-PaPaRR* (Fig. 3.91)	$\underline{Pa} \perp Pa \perp^{\perp} R\|\|R$ (Fig. 3.65c)	Idem No. 1
36	*3-PaRRPa* (Fig. 3.92)	$\underline{Pa}\|\|R\|\|R \perp Pa$ (Fig. 3.65d)	Idem No. 1
37	*3-PaRRPa* (Fig. 3.93)	$\underline{Pa} \perp R\|\|R \perp^{\perp} Pa$ (Fig. 3.65e)	Idem No. 1
38	*3-PaRRPa* (Fig. 3.94)	$\underline{Pa} \perp R\|\|R \perp^{\|\|} Pa$ (Fig. 3.65f)	Idem No. 1
39	*3-PaRPaR* (Fig. 3.95)	$\underline{Pa} \perp R \perp Pa \perp^{\|\|} R$ (Fig. 3.65g)	Idem No. 1
40	*3-PaRPaR-* (Fig. 3.96)	$\underline{Pa}\|\|R \perp Pa \perp^{\|\|} R$ (Fig. 3.65h)	Idem No. 1
41	*3-RRPaP* (Fig. 3.97a)	$\underline{R}\|\|R\|\|Pa\|\|P$ (Fig. 3.67a)	Idem No. 1

Table 3.25. (cont.)

42	*3-<u>R</u>RPaP* (Fig. 3.97b)	$\underline{R}\|\|R\|\|Pa\|\|P$ (Fig. 3.67a)	Idem No. 2
43	*3-<u>R</u>PRPa* (Fig. 3.98a)	$\underline{R}\|\|P\|\|R\|\|Pa$ (Fig. 3.67b)	Idem No. 1
44	*3-<u>R</u>PRPa* (Fig. 3.98b)	$\underline{R}\|\|P\|\|R\|\|Pa$ (Fig. 3.67b)	Idem No. 6
45	*3-<u>R</u>CPa* (Fig. 3.99a)	$\underline{R}\|\|C\|\|Pa$ (Fig. 3.67e)	Idem No. 1
46	*3-<u>R</u>CPa* (Fig. 3.99b)	$\underline{R}\|\|C\|\|Pa$ (Fig. 3.67e)	Idem No. 6
47	*3-<u>R</u>PaRR* (Fig. 3.100a)	$\underline{R} \perp Pa \perp {}^{\|\|}R\|\|R$ (Fig. 3.67f)	Idem No. 1
48	*3-<u>R</u>PaRR* (Fig. 3.100b)	$\underline{R} \perp Pa \perp {}^{\|\|}R\|\|R$ (Fig. 3.67f)	Idem No. 22
49	*3-<u>R</u>RPaR* (Fig. 3.101a)	$\underline{R}\|\|R \perp Pa \perp {}^{\|\|}R$ (Fig. 3.68a)	Idem No. 1
50	*3-<u>R</u>RPaR* (Fig. 3.101b)	$\underline{R}\|\|R \perp Pa \perp {}^{\|\|}R$ (Fig. 3.68a)	Idem No. 22
51	*3-<u>R</u>PaPaR* (Fig. 3.102a)	$\underline{R} \perp Pa\|\|Pa \perp {}^{\|\|}R$ (Fig. 3.68b)	Idem No. 1
52	*3-<u>R</u>PaPaR* (Fig. 3.102b)	$\underline{R} \perp Pa\|\|Pa \perp {}^{\|\|}R$ (Fig. 3.68b)	Axes of the actuated joints are parallel to two orthogonal directions
53	*3-<u>R</u>PaRPa* (Fig. 3.103a)	$\underline{R} \perp Pa \perp {}^{\|\|}R \perp Pa$ (Fig. 3.68c)	Idem No. 1
54	*3-<u>R</u>PaRPa* (Fig. 3.103b)	$\underline{R} \perp Pa \perp {}^{\|\|}R \perp Pa$ (Fig. 3.68c)	Idem No. 52
55	*3-<u>R</u>PaRPa* (Fig. 3.104a)	$\underline{R} \perp Pa \perp {}^{\|\|}R \perp Pa$ (Fig. 3.68d)	Idem No. 1
56	*3-<u>R</u>PaRPa* (Fig. 3.104b)	$\underline{R} \perp Pa \perp {}^{\|\|}R \perp Pa$ (Fig. 3.68d)	Idem No. 52
57	*3-<u>R</u>PaPaR* (Fig. 3.105a)	$\underline{R} \perp Pa\|\|Pa \perp {}^{\|\|}R$ (Fig. 3.68e)	Idem No. 1
58	*3-<u>R</u>PaPaR* (Fig. 3.105b)	$\underline{R} \perp Pa\|\|Pa \perp {}^{\|\|}R$ (Fig. 3.68e)	Idem No. 52
59	*3-<u>R</u>RPa^{cc}* (Fig. 3.106a)	$\underline{R}\|\|R\|\|Pa^{cc}$ (Fig. 3.66b)	Idem No. 1
60	*3-<u>R</u>RPa^{cc}* (Fig. 3.106b)	$\underline{R}\|\|R\|\|Pa^{cc}$ (Fig. 3.66b)	Idem No. 6
61	*3-<u>R</u>RPa^{cc}* (Fig. 3.107a)	$\underline{R}\|\|R\|\|Pa^{cc}$ (Fig. 3.66c)	Idem No. 1
62	*3-<u>R</u>RPa^{cc}* (Fig. 3.107b)	$\underline{R}\|\|R\|\|Pa^{cc}$ (Fig. 3.66c)	Idem No. 2
63	*3-<u>Pa^{cc}</u>RR* (Fig. 3.108a)	$\underline{Pa^{cc}}\|\|R\|\|R$ (Fig. 3.66a)	Idem No. 1

Table 3.25. (cont.)

64	*3-$\underline{Pa}^{cc}RR$* (Fig. 3.108b)	$\underline{Pa}^{cc}\|\|R\|\|R$ (Fig. 3.66a)	Idem No. 2
65	*3-$\underline{Pa}Pr$* (Fig. 3.109a)	*$\underline{Pa}$-Pr* (Fig. 3.62d)	Idem No. 1
66	*3-$\underline{R}RPr$* (Fig. 3.109b)	$\underline{R}\|\|R$-*Pr* (Fig. 3.66d)	Idem No. 1
67	*3-$\underline{Pa}RRRR$* (Fig. 3.110a)	$\underline{Pa}\|\|R\|\|R \perp R\|\|R$ (Fig. 3.69a)	Idem No. 1
68	*3-$\underline{Pa}RRRR$* (Fig. 3.110b)	$\underline{Pa} \perp R \perp R\|\|R \perp R$ (Fig. 3.69b)	Idem No. 1
69	*3-$\underline{Pa}RRRR$* (Fig. 3.111a)	$\underline{Pa} \perp R\|\|R \perp {}^{\|\|}R\|\|R$ (Fig. 3.69c)	Idem No. 1
70	*3-$\underline{Pa}RRRR$* (Fig. 3.111b)	$\underline{Pa} \perp R \perp R\|\|R \perp {}^{\|\|}R$ (Fig. 3.69d)	Idem No. 1
71	*3-$\underline{Pa}RRRR$* (Fig. 3.112a)	$\underline{Pa}\|\|R \perp R\|\|R \perp {}^{\|\|}R$ (Fig. 3.69e)	Idem No. 1
72	*3-$\underline{R}RPaRR$* (Fig. 3.112b)	$\underline{R} \perp R \perp {}^{\|\|}Pa \perp {}^{\|\|}R \perp R$ (Fig. 3.69f)	Idem No. 1
73	*3-$\underline{R}PaRRR$* (Fig. 3.113a)	$\underline{R} \perp Pa\|\|R\|\|R \perp {}^{\|\|}R$ (Fig. 3.70a)	Idem No. 1
74	*3-$\underline{R}PaRRR$* (Fig. 3.113b)	$\underline{R} \perp Pa \perp^{\perp} R\|\|R \perp^{\perp} R$ (Fig. 3.70b)	Idem No. 1
75	*3-$\underline{R}PaRRR$* (Fig. 3.114a)	$\underline{R} \perp Pa \perp {}^{\|\|}R \perp R\|\|R$ (Fig. 3.70c)	Idem No. 1
76	*3-$\underline{R}PaRRR$* (Fig. 3.114b)	$\underline{R} \perp Pa\|\|R\|\|R \perp {}^{\|\|}R$ (Fig. 3.70d)	Idem No. 1
77	*3-$\underline{R}RPaRR$* (Fig. 3.115a)	$\underline{R}\|\|R\|\|Pa \perp R\|\|R$ (Fig. 3.70g)	Idem No. 1
78	*3-$\underline{R}RPaRR$* (Fig. 3.115b)	$\underline{R}\|\|R \perp Pa \perp^{\perp} R\|\|R$ (Fig. 3.70i)	Idem No. 1
79	*3-$\underline{R}RRRPa$* (Fig. 3.116a)	$\underline{R}\|\|R \perp R\|\|R \perp^{\perp} Pa$ (Fig. 3.70h)	Idem No. 1
80	*3-$\underline{R}RRRPa$* (Fig. 3.116b)	$\underline{R}\|\|R \perp R\|\|R \perp^{\perp} Pa$ (Fig. 3.70j)	Idem No. 1
81	*3-$\underline{R}RRPaR$* (Fig. 3.117a)	$\underline{R}\|\|R \perp R \perp Pa \perp {}^{\|\|}R$ (Fig. 3.70k)	Idem No. 1
82	*3-$\underline{R}RRRPa$* (Fig. 3.117b)	$\underline{R} \perp R\|\|R \perp {}^{\|\|}R \perp Pa$ (Fig. 3.70l)	Idem No. 1
83	*3-$\underline{R}RRPaR$* (Fig. 3.118a, b)	$\underline{R} \perp R\|\|R\|\|Pa \perp {}^{\|\|}R$ (Fig. 3.69e, f)	Idem No. 1

Table 3.26. Bases of the operational velocities spaces of the limbs isolated from the parallel mechanisms presented in Figs. 3.71–3.118

No.	Parallel mechanism	Basis (R_{G1})	(R_{G2})	(R_{G3})
1	Figs. 3.71–3.82, 3.109a	$(\boldsymbol{v}_1,\boldsymbol{v}_2,\boldsymbol{v}_3)$	$(\boldsymbol{v}_1,\boldsymbol{v}_2,\boldsymbol{v}_3)$	$(\boldsymbol{v}_1,\boldsymbol{v}_2,\boldsymbol{v}_3)$
2	Figs. 3.83, 3.84a, 3.100b, 3.101b	$(\boldsymbol{v}_1,\boldsymbol{v}_2,\boldsymbol{v}_3,\boldsymbol{\omega}_\beta)$	$(\boldsymbol{v}_1,\boldsymbol{v}_2,\boldsymbol{v}_3,\boldsymbol{\omega}_\alpha)$	$(\boldsymbol{v}_1,\boldsymbol{v}_2,\boldsymbol{v}_3,\boldsymbol{\omega}_\beta)$
3	Figs. 3.84b, 3.85, 3.86	$(\boldsymbol{v}_1,\boldsymbol{v}_2,\boldsymbol{v}_3,\boldsymbol{\omega}_\beta)$	$(\boldsymbol{v}_1,\boldsymbol{v}_2,\boldsymbol{v}_3,\boldsymbol{\omega}_\alpha)$	$(\boldsymbol{v}_1,\boldsymbol{v}_2,\boldsymbol{v}_3,\boldsymbol{\omega}_\delta)$
4	Figs. 3.87a, 3.88a, 3.89, 3.92, 3.93, 3.102a, 3.104a, 3.109b,	$(\boldsymbol{v}_1,\boldsymbol{v}_2,\boldsymbol{v}_3,\boldsymbol{\omega}_\delta)$	$(\boldsymbol{v}_1,\boldsymbol{v}_2,\boldsymbol{v}_3,\boldsymbol{\omega}_\alpha)$	$(\boldsymbol{v}_1,\boldsymbol{v}_2,\boldsymbol{v}_3,\boldsymbol{\omega}_\beta)$
5	Figs. 3.87b, 3.88b, 3.97b, 3.98b, 3.99b, 3.106b, 3.107b, 3.108b	$(\boldsymbol{v}_1,\boldsymbol{v}_2,\boldsymbol{v}_3,\boldsymbol{\omega}_\delta)$	$(\boldsymbol{v}_1,\boldsymbol{v}_2,\boldsymbol{v}_3,\boldsymbol{\omega}_\delta)$	$(\boldsymbol{v}_1,\boldsymbol{v}_2,\boldsymbol{v}_3,\boldsymbol{\omega}_\alpha)$
6	Fig. 3.94	$(\boldsymbol{v}_1,\boldsymbol{v}_2,\boldsymbol{v}_3,\boldsymbol{\omega}_\alpha)$	$(\boldsymbol{v}_1,\boldsymbol{v}_2,\boldsymbol{v}_3,\boldsymbol{\omega}_\beta)$	$(\boldsymbol{v}_1,\boldsymbol{v}_2,\boldsymbol{v}_3,\boldsymbol{\omega}_\delta)$
7	Figs. 3.90, 3.91, 3.95, 3.96, 3.97a, 3.98a, 3.99a, 3.100a, 3.101a, 3.103a, 3.105a, 3.106a, 3.107a, 3.108a	$(\boldsymbol{v}_1,\boldsymbol{v}_2,\boldsymbol{v}_3,\boldsymbol{\omega}_\beta)$	$(\boldsymbol{v}_1,\boldsymbol{v}_2,\boldsymbol{v}_3,\boldsymbol{\omega}_\delta)$	$(\boldsymbol{v}_1,\boldsymbol{v}_2,\boldsymbol{v}_3,\boldsymbol{\omega}_\alpha)$
8	Fig. 3.102b	$(\boldsymbol{v}_1,\boldsymbol{v}_2,\boldsymbol{v}_3,\boldsymbol{\omega}_\alpha)$	$(\boldsymbol{v}_1,\boldsymbol{v}_2,\boldsymbol{v}_3,\boldsymbol{\omega}_\delta)$	$(\boldsymbol{v}_1,\boldsymbol{v}_2,\boldsymbol{v}_3,\boldsymbol{\omega}_\beta)$
9	Fig. 3.103b, 3.105b	$(\boldsymbol{v}_1,\boldsymbol{v}_2,\boldsymbol{v}_3,\boldsymbol{\omega}_\beta)$	$(\boldsymbol{v}_1,\boldsymbol{v}_2,\boldsymbol{v}_3,\boldsymbol{\omega}_\alpha)$	$(\boldsymbol{v}_1,\boldsymbol{v}_2,\boldsymbol{v}_3,\boldsymbol{\omega}_\alpha)$
10	Fig. 3.104b	$(\boldsymbol{v}_1,\boldsymbol{v}_2,\boldsymbol{v}_3,\boldsymbol{\omega}_\delta)$	$(\boldsymbol{v}_1,\boldsymbol{v}_2,\boldsymbol{v}_3,\boldsymbol{\omega}_\delta)$	$(\boldsymbol{v}_1,\boldsymbol{v}_2,\boldsymbol{v}_3,\boldsymbol{\omega}_\beta)$
11	Figs. 3.110a, 3.111, 3.114b, 3.118b	$(\boldsymbol{v}_1,\boldsymbol{v}_2,\boldsymbol{v}_3,\boldsymbol{\omega}_\alpha,\boldsymbol{\omega}_\beta)$	$(\boldsymbol{v}_1,\boldsymbol{v}_2,\boldsymbol{v}_3,\boldsymbol{\omega}_\beta,\boldsymbol{\omega}_\delta)$	$(\boldsymbol{v}_1,\boldsymbol{v}_2,\boldsymbol{v}_3,\boldsymbol{\omega}_\alpha,\boldsymbol{\omega}_\delta)$
12	Figs. 3.110b, 3.112[a], 3.113a, 3.114a, 3.115, 3.116a, 3.117a	$(\boldsymbol{v}_1,\boldsymbol{v}_2,\boldsymbol{v}_3,\boldsymbol{\omega}_\beta,\boldsymbol{\omega}_\delta)$	$(\boldsymbol{v}_1,\boldsymbol{v}_2,\boldsymbol{v}_3,\boldsymbol{\omega}_\alpha,\boldsymbol{\omega}_\delta)$	$(\boldsymbol{v}_1,\boldsymbol{v}_2,\boldsymbol{v}_3,\boldsymbol{\omega}_\alpha,\boldsymbol{\omega}_\beta)$
13	Figs. 3.112b, 3.113b, 3.116b, 3.117b, 3.118a	$(\boldsymbol{v}_1,\boldsymbol{v}_2,\boldsymbol{v}_3,\boldsymbol{\omega}_\alpha,\boldsymbol{\omega}_\delta)$	$(\boldsymbol{v}_1,\boldsymbol{v}_2,\boldsymbol{v}_3,\boldsymbol{\omega}_\alpha,\boldsymbol{\omega}_\beta)$	$(\boldsymbol{v}_1,\boldsymbol{v}_2,\boldsymbol{v}_3,\boldsymbol{\omega}_\beta,\boldsymbol{\omega}_\delta)$

Table 3.27. Structural parameters[a] of translational parallel mechanisms in Figs. 3.71–3.82

No.	Structural parameter	Solution *3-PaPaP* (Figs. 3.71, 3.72) *3-PaPPa* (Figs. 3.73, 3.74)	*3-PaPa^{cc}* (Figs. 3.75–3.78) *3-Pa^{cc}Pa* (Fig. 3.79)	*3-PaPaPa* (Figs. 3.80–3.82)
1	m	20	17	26
2	p_1	9	8	12
3	p_2	9	8	12
4	p_3	9	8	12
5	p	27	24	36
6	q	8	8	11
7	k_1	0	0	0
8	k_2	3	3	3
9	k	3	3	3
10	(R_{Gi}) $(i = 1,2,3)$	See Table 3.26	See Table 3.26	See Table 3.26
11	S_{G1}	3	3	3
12	S_{G2}	3	3	3
13	S_{G3}	3	3	3
14	r_{G1}	6	7	9
15	r_{G2}	6	7	9
16	r_{G3}	6	7	9
17	M_{G1}	3	3	3
18	M_{G2}	3	3	3
19	M_{G3}	3	3	3
20	(R_F)	$(\boldsymbol{v}_1, \boldsymbol{v}_2, \boldsymbol{v}_3)$	$(\boldsymbol{v}_1, \boldsymbol{v}_2, \boldsymbol{v}_3)$	$(\boldsymbol{v}_1, \boldsymbol{v}_2, \boldsymbol{v}_3)$
21	S_F	3	3	3
22	r_1	18	21	27
23	r_F	24	27	33
24	M_F	3	3	3
25	N_F	24	21	33
26	T_F	0	0	0
27	$\sum_{j=1}^{p_1} f_j$	9	10	12
28	$\sum_{j=1}^{p_2} f_j$	9	10	12
29	$\sum_{j=1}^{p_3} f_j$	9	10	12
30	$\sum_{j=1}^{p} f_j$			

[a]See footnote of Table 2.1 for the nomenclature of structural parameters

Table 3.28. Structural parameters[a] of translational parallel mechanisms in Figs. 3.83–3.88

No.	Structural parameter	Solution *3-RRC* (Figs. 3.83, 3.84) *3-RCR, 3-RPC* (Figs. 3.85a, 3.86a)	*3-RPRR* (Fig. 3.85b) *3-RPPR* (Fig. 3.86b)	*3-PaRC* (Fig. 3.87) *3-PaCR* (Fig. 3.88)
1	m	8	11	14
2	p_1	3	4	6
3	p_2	3	4	6
4	p_3	3	4	6
5	p	9	12	18
6	q	2	2	5
7	k_1	3	3	3
8	k_2	0	0	0
9	k	3	3	3
10	(R_{Gi}) $(i = 1,2,3)$	See Table 3.26	See Table 3.26	See Table 3.26
11	S_{G1}	4	4	4
12	S_{G2}	4	4	4
13	S_{G3}	4	4	4
14	r_{G1}	0	0	3
15	r_{G2}	0	0	3
16	r_{G3}	0	0	3
17	M_{G1}	4	4	4
18	M_{G2}	4	4	4
19	M_{G3}	4	4	4
20	(R_F)	$(\boldsymbol{v}_1,\boldsymbol{v}_2,\boldsymbol{v}_3)$	$(\boldsymbol{v}_1,\boldsymbol{v}_2,\boldsymbol{v}_3)$	$(\boldsymbol{v}_1,\boldsymbol{v}_2,\boldsymbol{v}_3)$
21	S_F	3	3	3
22	r_1	0	0	9
23	r_F	9	9	18
24	M_F	3	3	3
25	N_F	3	3	12
26	T_F	0	0	0
27	$\sum_{j=1}^{p_1} f_j$	4	4	7
28	$\sum_{j=1}^{p_2} f_j$	4	4	7
29	$\sum_{j=1}^{p_3} f_j$	4	4	7
30	$\sum_{j=1}^{p} f_j$	12	12	21

[a]See footnote of Table 2.1 for the nomenclature of structural parameters

Table 3.29. Structural parameters[a] of translational parallel mechanisms in Figs. 3.89–3.99

No.	Structural parameter	Solution *3-PaPaRR* (Figs. 3.89–3.91) *3-PaRRPa* (Figs. 3.92–3.94) *3-PaRPaR* (Figs. 3.95, 3.96)	*3-RRPaP* (Fig. 3.97) *3-RPRPa* (Fig. 3.98)	*3-RCPa* (Fig. 3.99)
1	m	23	17	14
2	p_1	10	7	6
3	p_2	10	7	6
4	p_3	10	7	6
5	p	30	21	18
6	q	8	5	5
7	k_1	0	0	3
8	k_2	3	3	0
9	k	3	3	3
10	(R_{Gi}) $(i = 1,2,3)$	See Table 3.26	See Table 3.26	See Table 3.26
11	S_{G1}	4	4	4
12	S_{G2}	4	4	4
13	S_{G3}	4	4	4
14	r_{G1}	6	3	3
15	r_{G2}	6	3	3
16	r_{G3}	6	3	3
17	M_{G1}	4	4	4
18	M_{G2}	4	4	4
19	M_{G3}	4	4	4
20	(R_F)	$(\boldsymbol{v}_1, \boldsymbol{v}_2, \boldsymbol{v}_3)$	$(\boldsymbol{v}_1, \boldsymbol{v}_2, \boldsymbol{v}_3)$	$(\boldsymbol{v}_1, \boldsymbol{v}_2, \boldsymbol{v}_3)$
21	S_F	3	3	3
22	r_1	18	9	9
23	r_F	27	18	18
24	M_F	3	3	3
25	N_F	21	12	12
26	T_F	0	0	0
27	$\sum_{j=1}^{p_1} f_j$	10	7	7
28	$\sum_{j=1}^{p_2} f_j$	10	7	7
29	$\sum_{j=1}^{p_3} f_j$	10	7	7
30	$\sum_{j=1}^{p} f_j$	30	21	21

[a]See footnote of Table 2.1 for the nomenclature of structural parameters

Table 3.30. Structural parameters[a] of translational parallel mechanisms in Figs. 3.100–3.108

No.	Structural parameter	Solution *3-RPaRR* (Fig. 3.100) *3-RRPaR* (Fig. 3.101)	*3-RPaPaR* (Figs. 3.102, 3.105) *3-RPaRPa* (Figs. 3.103, 3.104)	*3-RRPa^{cc}* (Figs. 3.106, 3.107) *3-Pa^{cc}RR* (Fig. 3.108)
1	m	17	23	14
2	p_1	7	10	6
3	p_2	7	10	6
4	p_3	7	10	6
5	p	21	30	18
6	q	5	8	5
7	k_1	0	0	3
8	k_2	3	3	0
9	k	3	3	3
10	(R_{Gi}) (i = *1,2,3*)	See Table 3.26	See Table 3.26	See Table 3.26
11	S_{G1}	4	4	4
12	S_{G2}	4	4	4
13	S_{G3}	4	4	4
14	r_{G1}	3	6	4
15	r_{G2}	3	6	4
16	r_{G3}	3	6	4
17	M_{G1}	4	4	4
18	M_{G2}	4	4	4
19	M_{G3}	4	4	4
20	(R_F)	($\boldsymbol{v}_1,\boldsymbol{v}_2,\boldsymbol{v}_3$)	($\boldsymbol{v}_1,\boldsymbol{v}_2,\boldsymbol{v}_3$)	($\boldsymbol{v}_1,\boldsymbol{v}_2,\boldsymbol{v}_3$)
21	S_F	3	3	3
22	r_1	9	18	12
23	r_F	18	27	21
24	M_F	3	3	3
25	N_F	12	21	9
26	T_F	0	0	0
27	$\sum_{j=1}^{p_1} f_j$	7	10	8
28	$\sum_{j=1}^{p_2} f_j$	7	10	8
29	$\sum_{j=1}^{p_3} f_j$	7	10	8
30	$\sum_{j=1}^{p} f_j$	21	10	24

[a]See footnote of Table 2.1 for the nomenclature of structural parameters

Table 3.31. Structural parameters[a] of translational parallel mechanisms in Figs. 3.109–3.118

No.	Structural parameter	Solution *3-PaPr* (Fig. 3.109a)	*3-RRPr* (Fig. 3.109b)	*3-PaRRRR, 3-RPaRRR, 3-RRPaRR, 3-RRRRPa, 3-RRRPaR* Figs. 3.110–3.118
1	m	20	17	20
2	p_1	10	8	8
3	p_2	10	8	8
4	p_3	10	8	8
5	p	30	24	24
6	q	11	8	5
7	k_1	0	0	0
8	k_2	3	3	3
9	k	3	3	3
10	(R_{Gi}) $(i = 1,2,3)$	See Table 3.26	See Table 3.26	See Table 3.26
11	S_{G1}	3	4	5
12	S_{G2}	3	4	5
13	S_{G3}	3	4	5
14	r_{G1}	13	10	3
15	r_{G2}	13	10	3
16	r_{G3}	13	10	3
17	M_{G1}	3	4	5
18	M_{G2}	3	4	5
19	M_{G3}	3	4	5
20	(R_F)	$(\boldsymbol{v}_1, \boldsymbol{v}_2, \boldsymbol{v}_3)$	$(\boldsymbol{v}_1, \boldsymbol{v}_2, \boldsymbol{v}_3)$	$(\boldsymbol{v}_1, \boldsymbol{v}_2, \boldsymbol{v}_3)$
21	S_F	3	3	3
22	r_1	39	30	9
23	r_F	45	39	21
24	M_F	3	3	3
25	N_F	21	9	9
26	T_F	0	0	0
27	$\sum_{j=1}^{p_1} f_j$	16	14	8
28	$\sum_{j=1}^{p_2} f_j$	16	14	8
29	$\sum_{j=1}^{p_3} f_j$	16	14	8
30	$\sum_{j=1}^{p} f_j$	48	42	24

[a]See footnote of Table 2.1 for the nomenclature of structural parameters

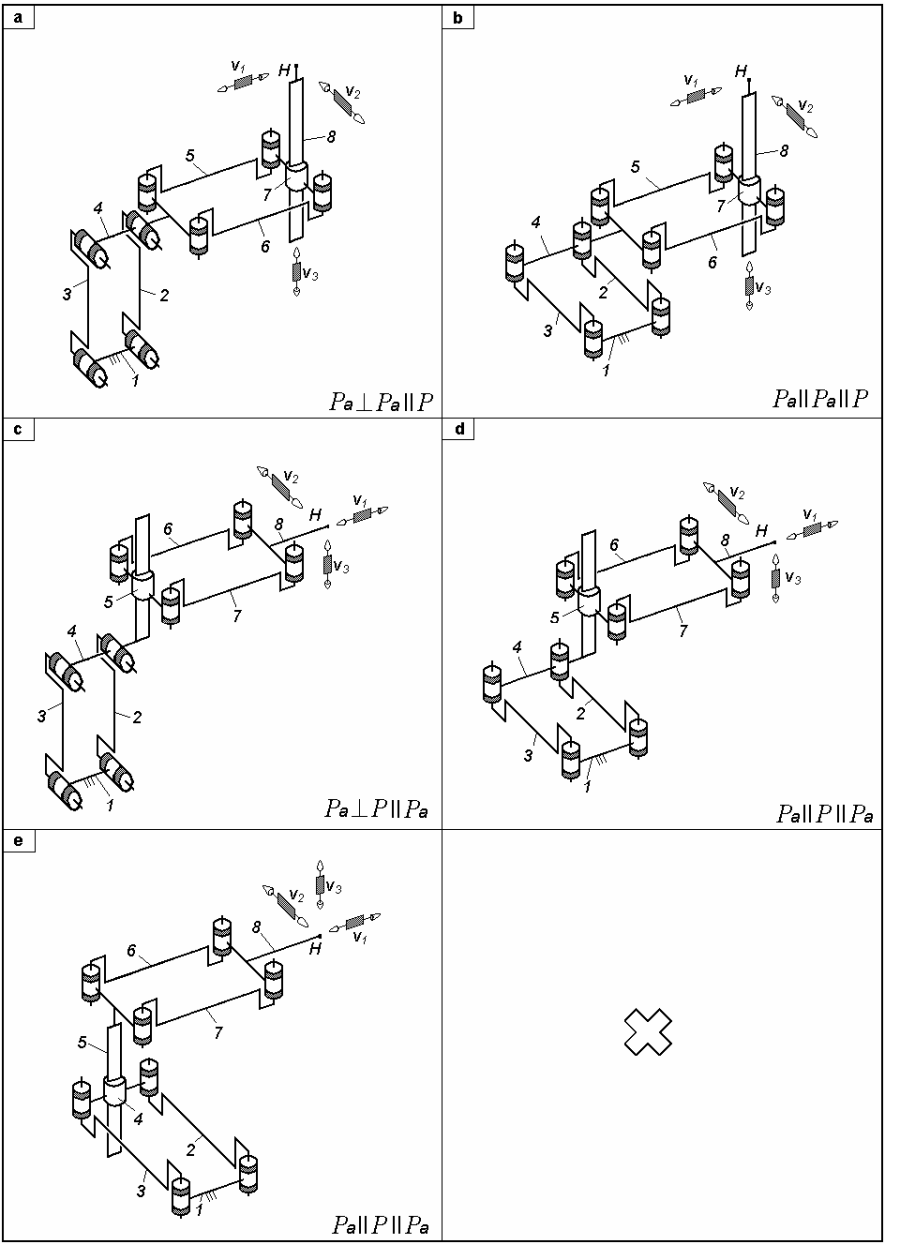

Fig. 3.60. Complex limbs for TPMs with coupled motions defined by $M_G = S_G = 3$, $(R_G) = (\boldsymbol{v}_1,\boldsymbol{v}_2,\boldsymbol{v}_3)$, combining two *Pa*-type parallelogram loops and actuated by rotating motors mounted on the fixed base

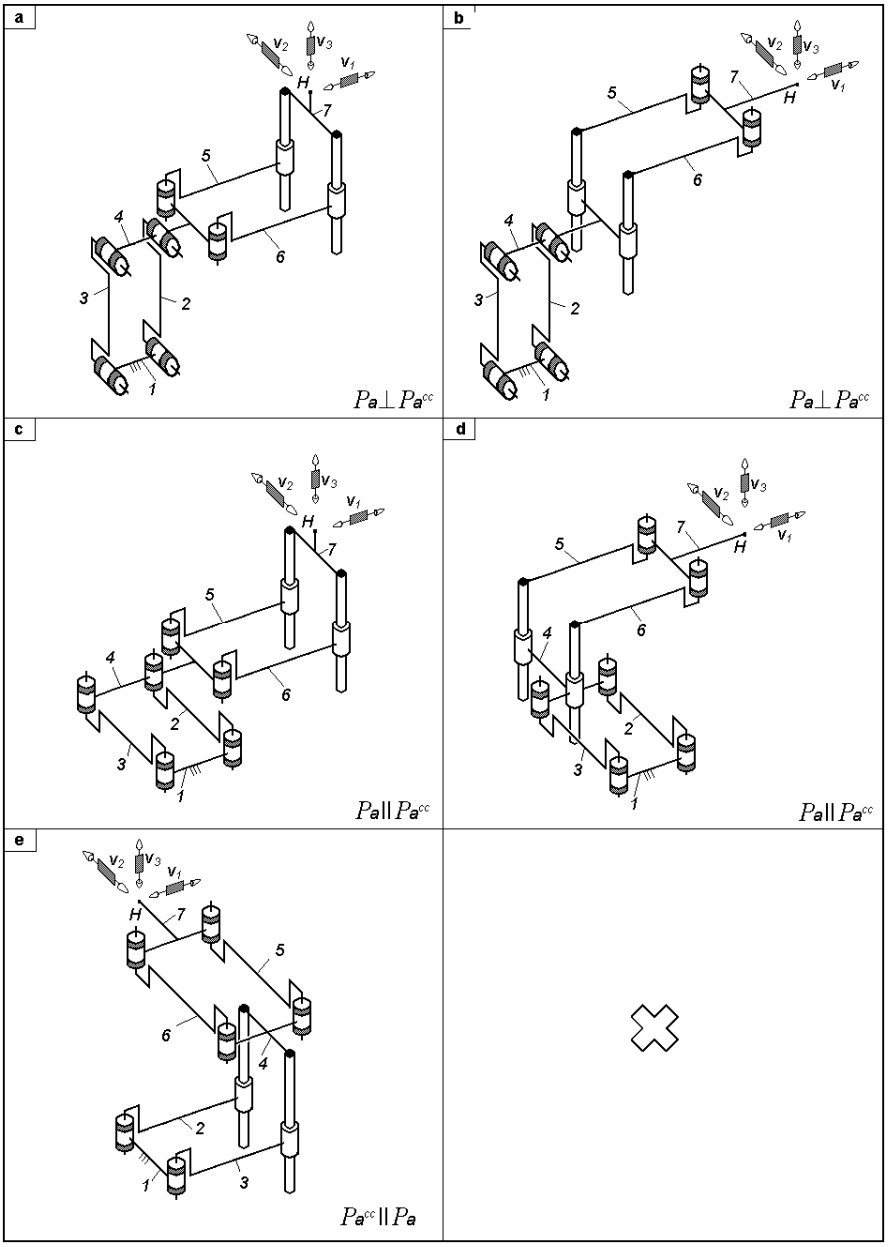

Fig. 3.61. Complex limbs for TPMs with coupled motions defined by $M_G = S_G = 3$, $(R_G) = (\boldsymbol{v}_1,\boldsymbol{v}_2,\boldsymbol{v}_3)$, combining parallelogram loops of types Pa and Pa^{cc} and actuated by rotating motors mounted on the fixed base

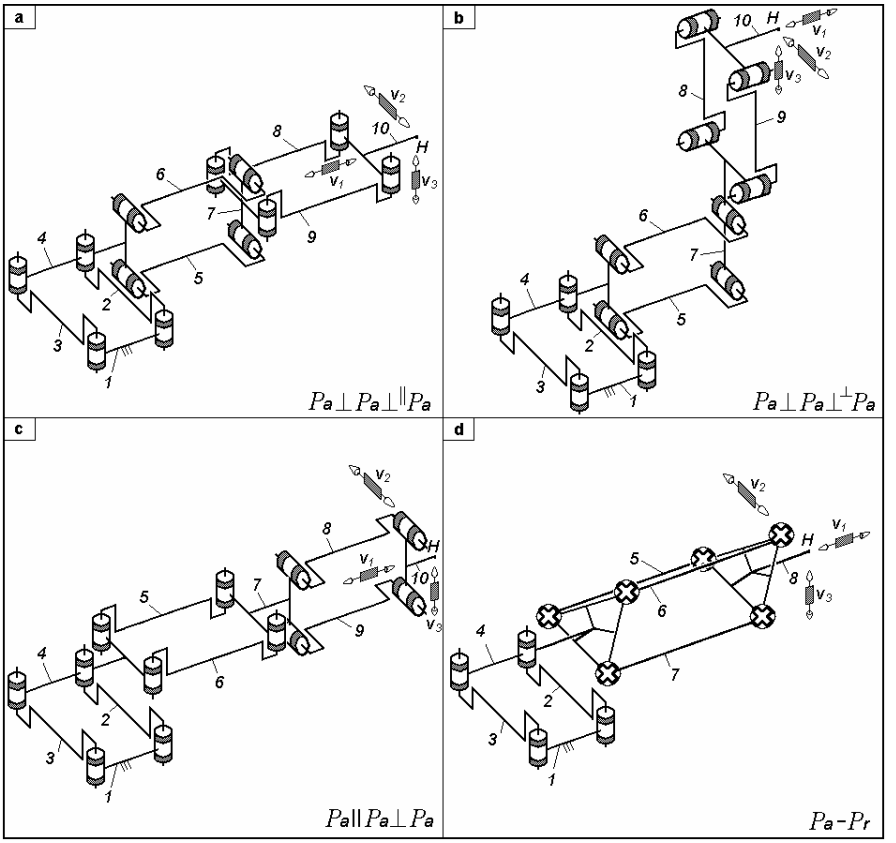

Fig. 3.62. Complex limbs for TPMs with coupled motions defined by $M_G = S_G = 3$, $(R_G) = (\boldsymbol{v}_1,\boldsymbol{v}_2,\boldsymbol{v}_3)$, combining three *Pa*-type parallelogram loops (**a**–**c**) or one *Pa*-type parallelogram loop and one *Pr*-type prism mechanism (**d**) and actuated by rotating motors mounted on the fixed base

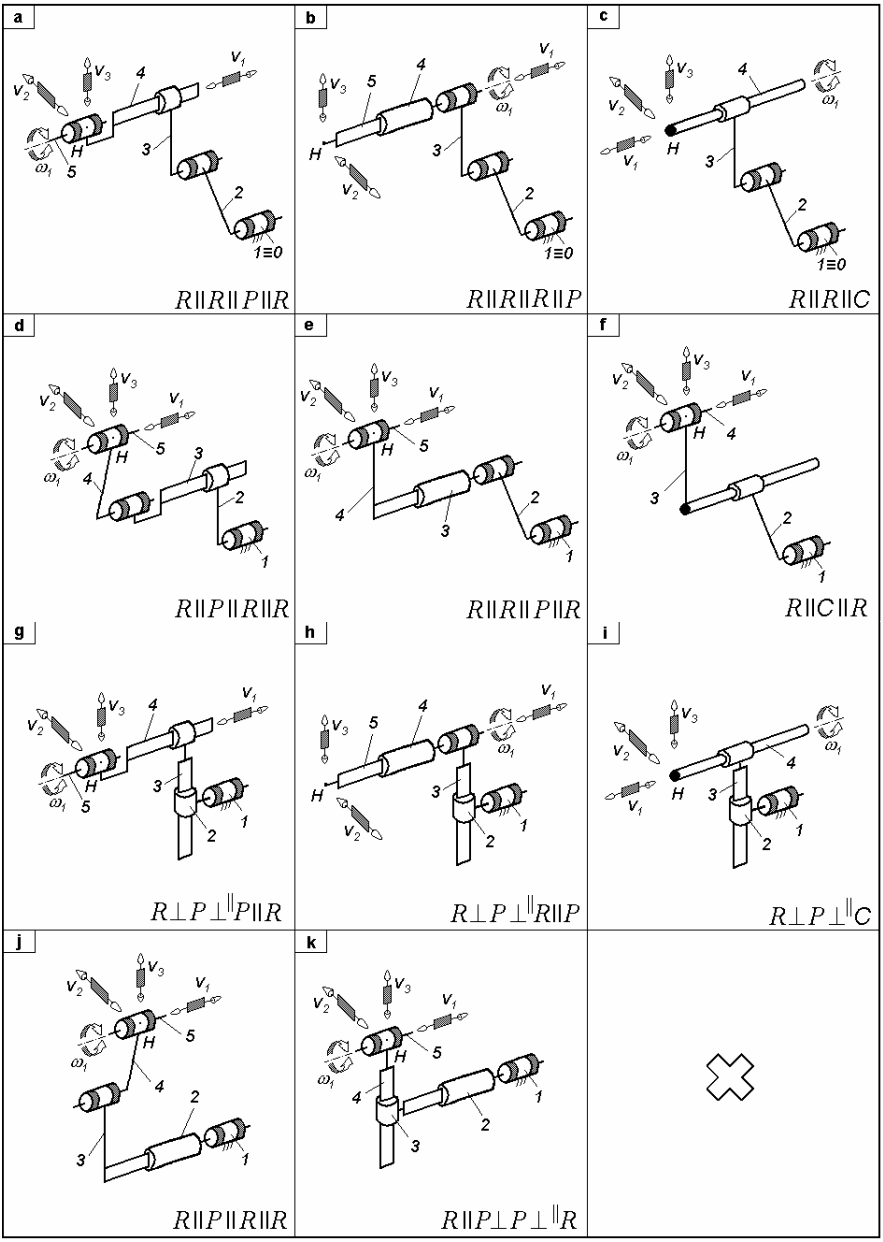

Fig. 3.63. Simple limbs for TPMs with coupled motions defined by $M_G = S_G = 4$, $(R_G) = (\boldsymbol{v}_1, \boldsymbol{v}_2, \boldsymbol{v}_3, \boldsymbol{\omega}_1)$ and actuated by rotating motors mounted on the fixed base

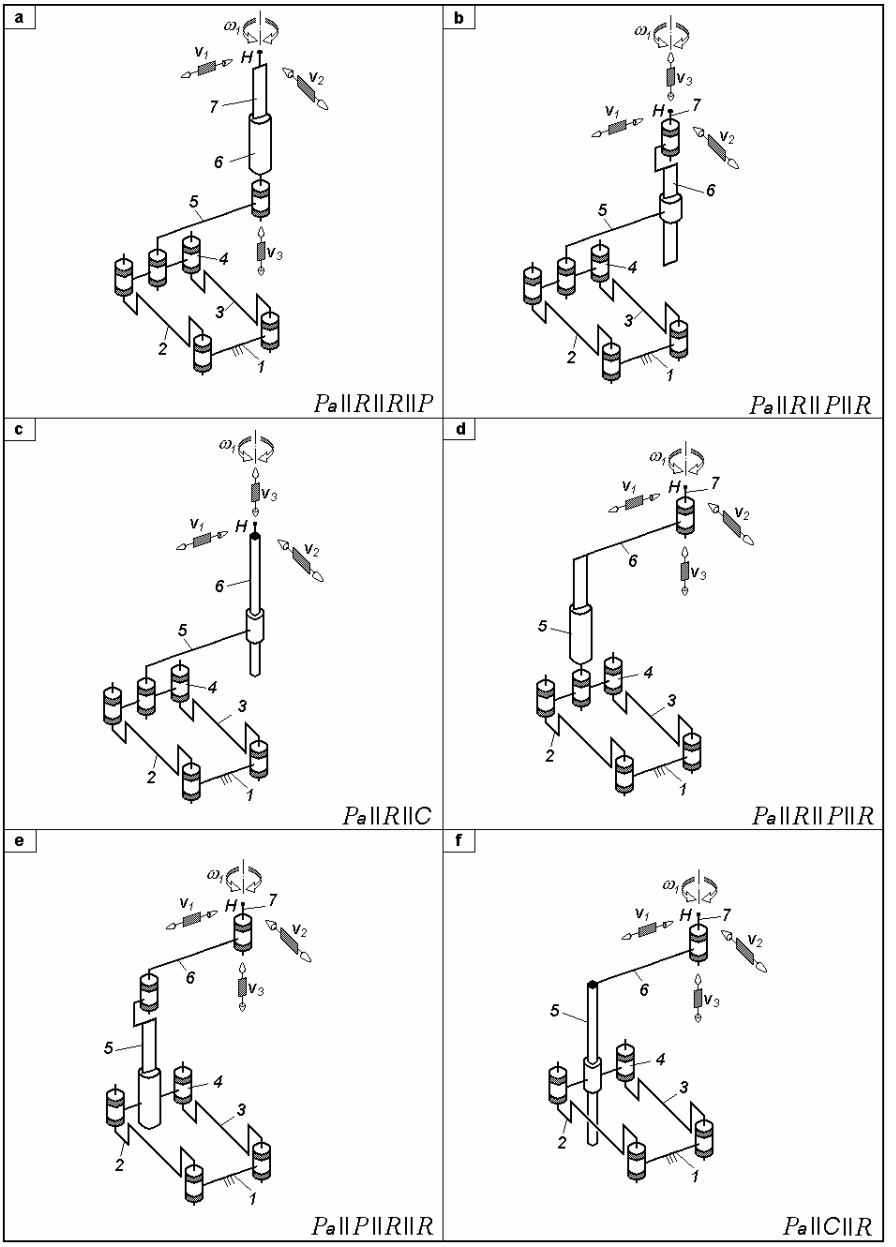

Fig. 3.64. Complex limbs for TPMs with coupled motions defined by $M_G = S_G = 4$, $(R_G) = (\boldsymbol{v}_1, \boldsymbol{v}_2, \boldsymbol{v}_3, \boldsymbol{\omega}_1)$, combining one *Pa*-type parallelogram loop and actuated by rotating motors mounted on the fixed base in the parallelogram loop

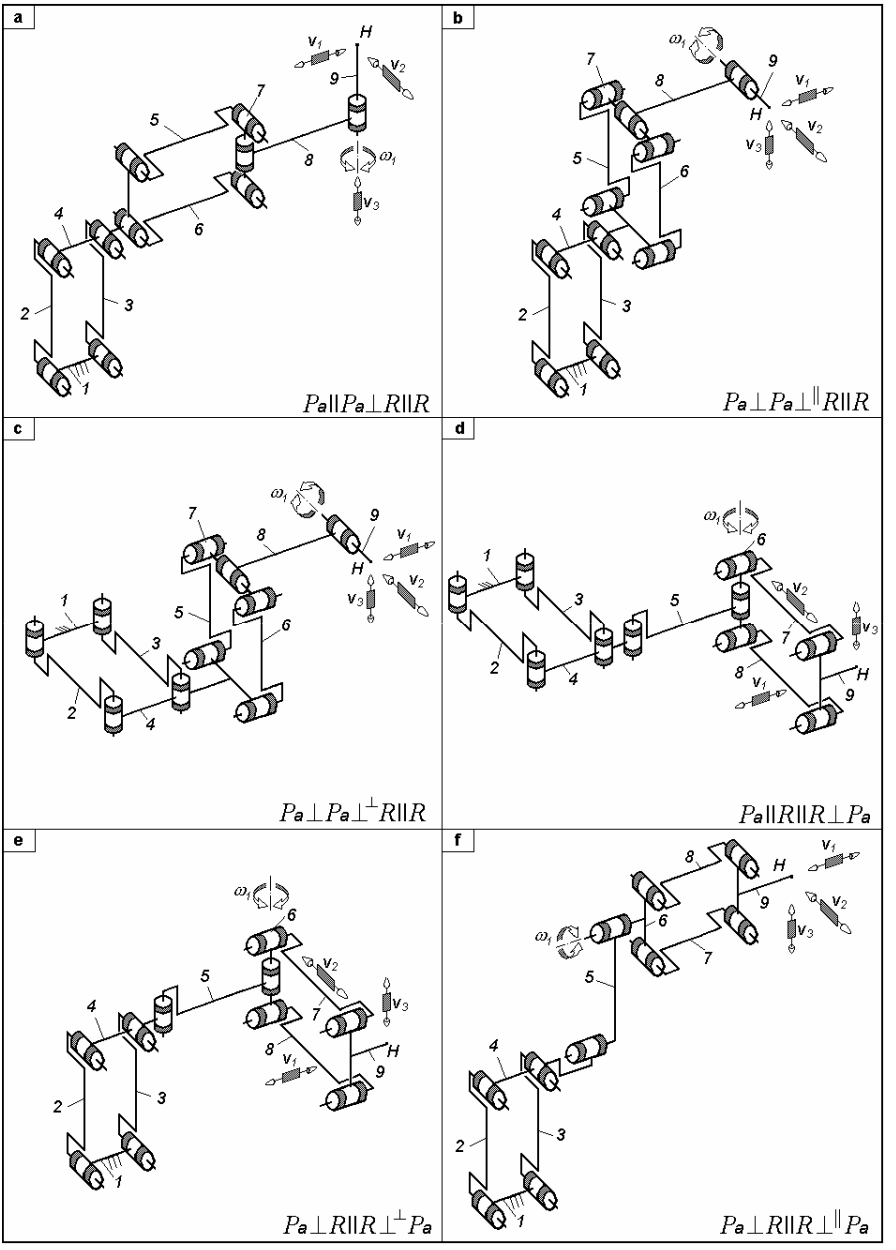

Fig. 3.65. Complex limbs for TPMs with coupled motions defined by $M_G = S_G = 4$, $(R_G) = (\boldsymbol{v}_1, \boldsymbol{v}_2, \boldsymbol{v}_3, \boldsymbol{\omega}_1)$, combining two *Pa*-type parallelogram loop and actuated by rotating motors mounted on the fixed base in a parallelogram loop

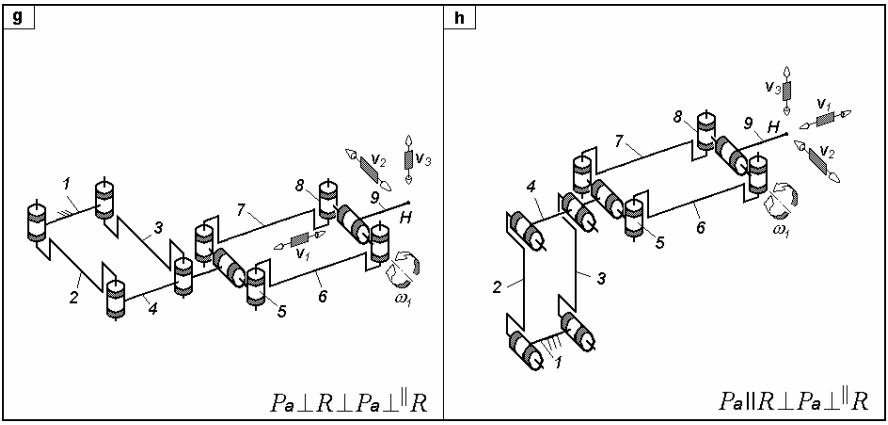

Fig. 3.65. (cont.)

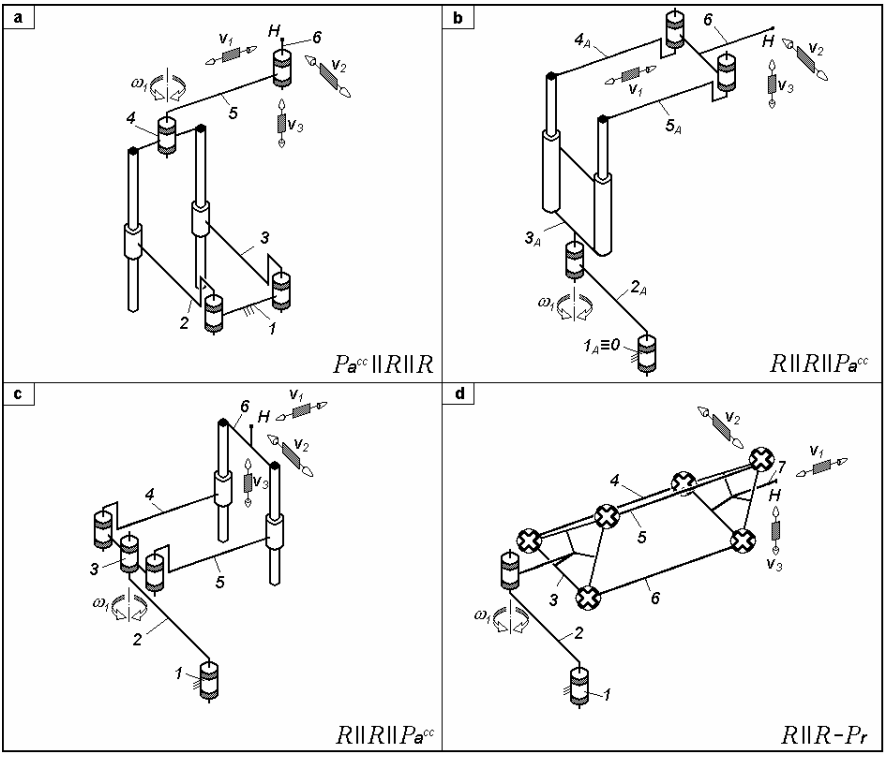

Fig. 3.66. Complex limbs for TPMs with coupled motions defined by $M_G = S_G = 4$, $(R_G) = (\boldsymbol{v}_1, \boldsymbol{v}_2, \boldsymbol{v}_3, \boldsymbol{\omega}_1)$, combining a Pa^{cc}-type parallelogram loop (**a**–**c**) or a *Pr*-type prism mechanism (**d**) and actuated by rotating motors mounted on the fixed base

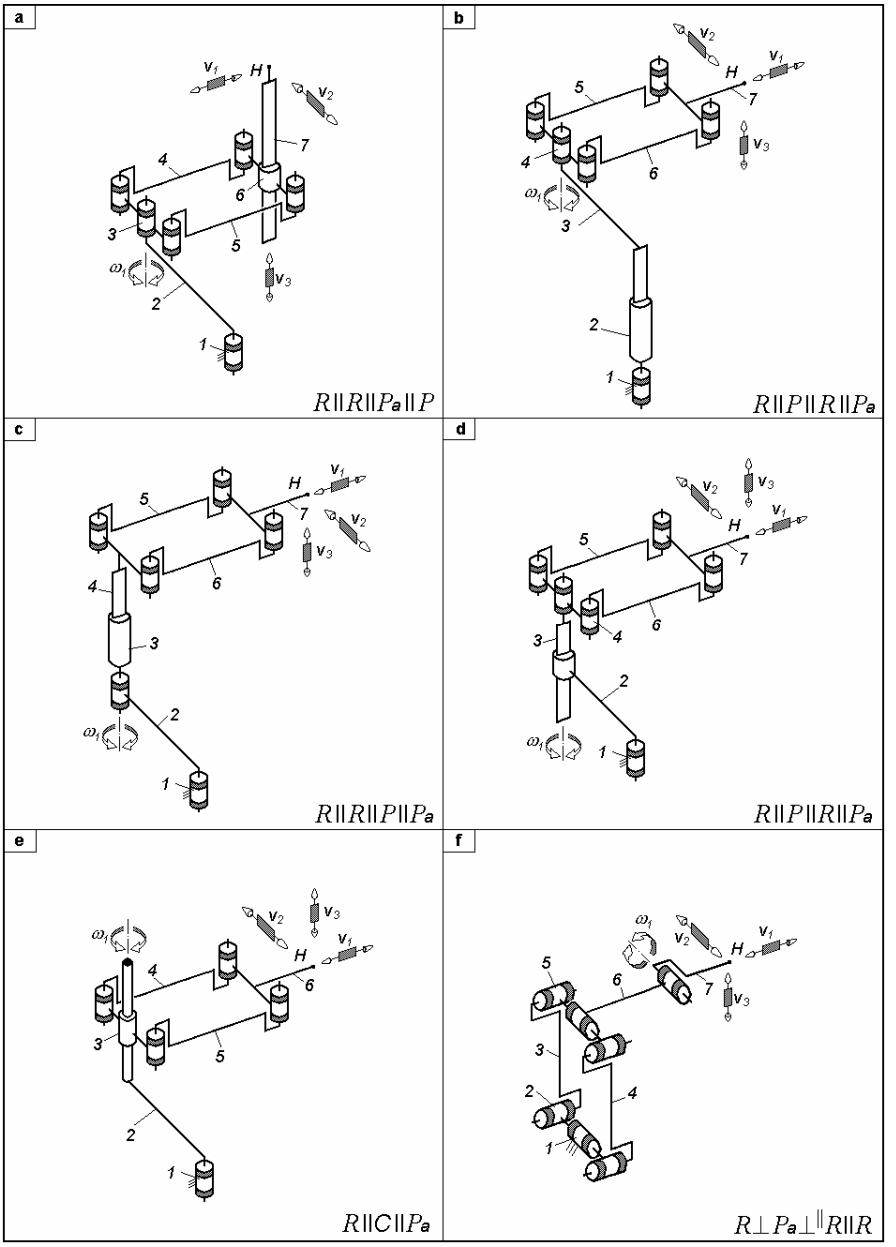

Fig. 3.67. Complex limbs for TPMs with coupled motions defined by $M_G = S_G = 4$, $(R_G) = (\boldsymbol{v}_1, \boldsymbol{v}_2, \boldsymbol{v}_3, \boldsymbol{\omega}_1)$, combining one *Pa*-type parallelogram loop and actuated by rotating motors mounted on the fixed base

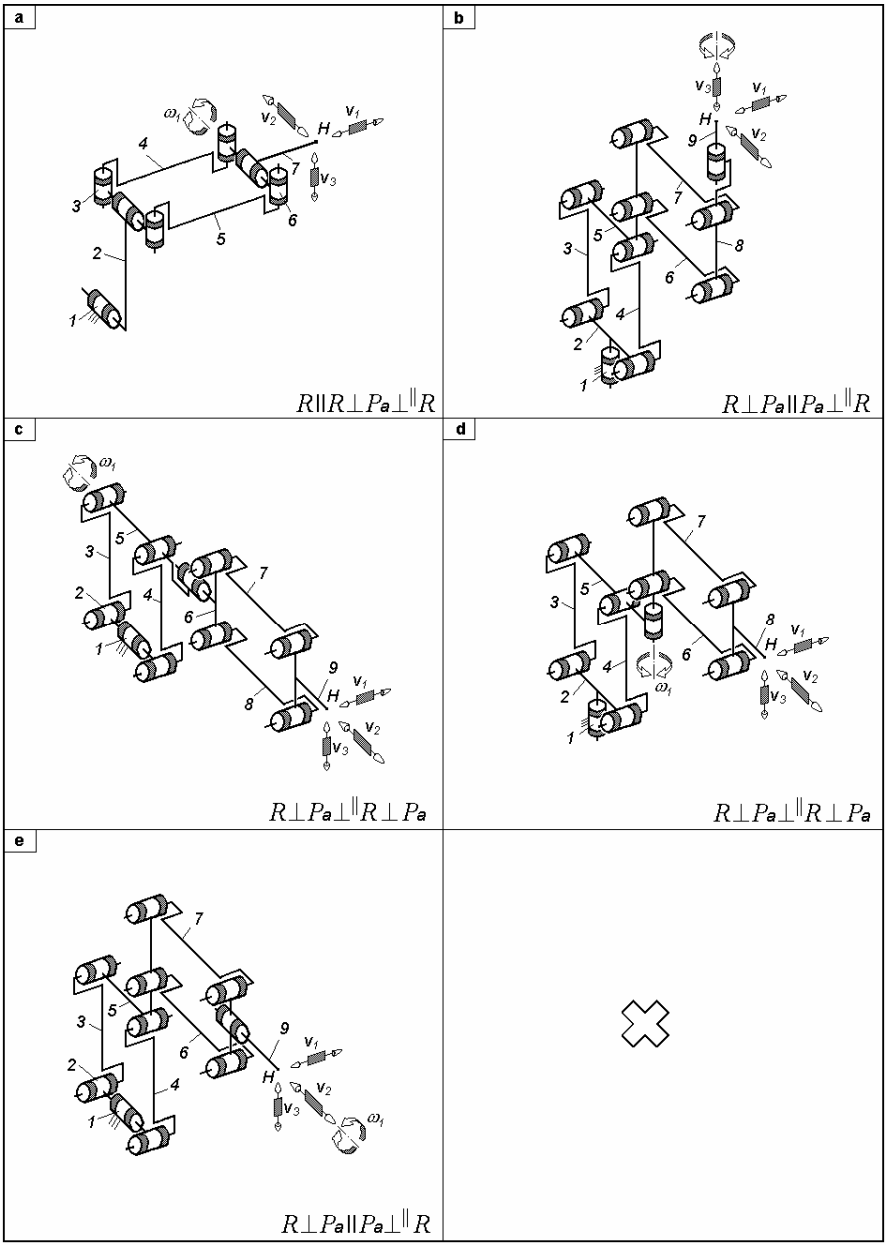

Fig. 3.68. Complex limbs for TPMs with coupled motions defined by $M_G = S_G = 4$, $(R_G) = (\boldsymbol{v}_1, \boldsymbol{v}_2, \boldsymbol{v}_3, \boldsymbol{\omega}_1)$, combining one (**a**) or two (**b**–**e**) *Pa*-type parallelogram loop and actuated by rotating motors mounted on the fixed base

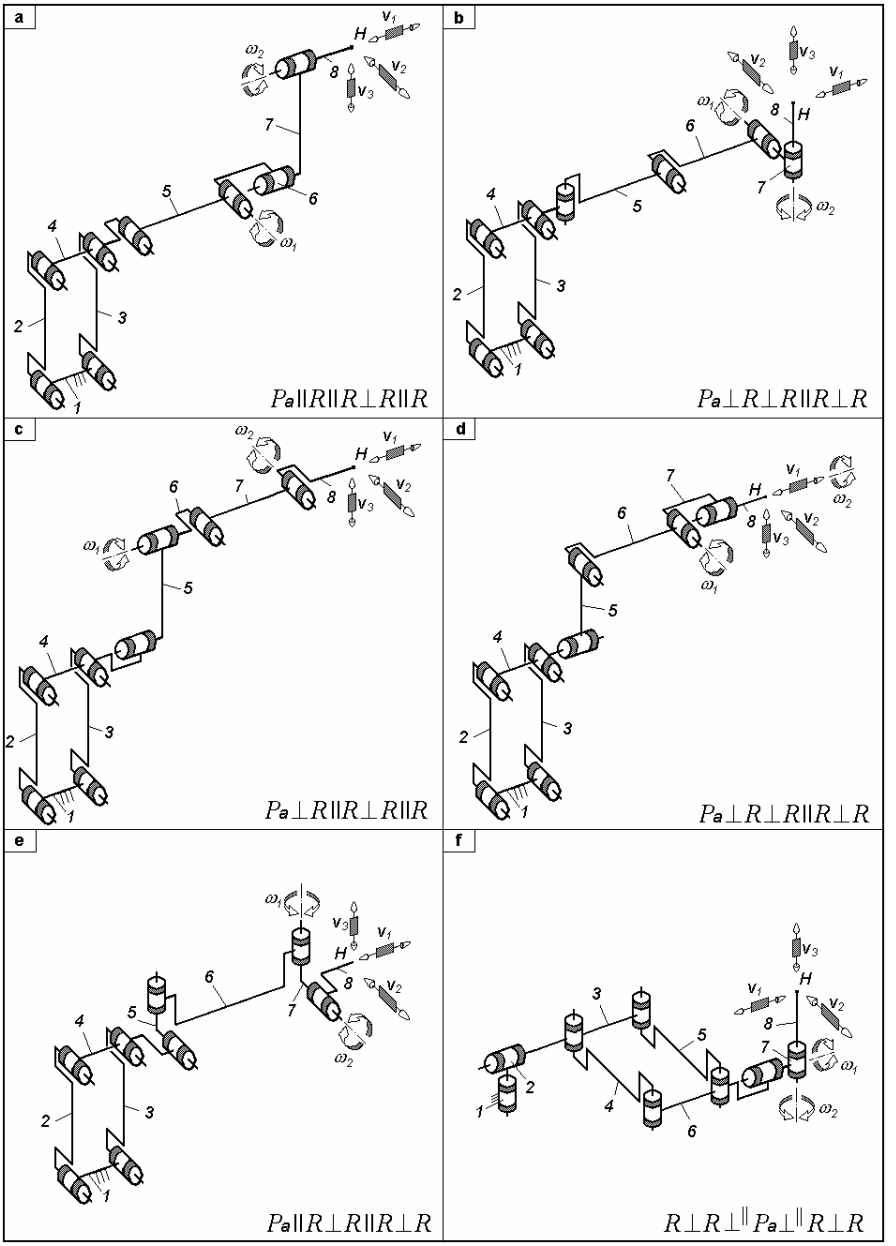

Fig. 3.69. Complex limbs for TPMs with coupled motions defined by $M_G = S_G = 5$, $(R_G) = (\boldsymbol{v}_1, \boldsymbol{v}_2, \boldsymbol{v}_3, \boldsymbol{\omega}_1, \boldsymbol{\omega}_2)$, combining one parallelogram loop and actuated by rotating motors mounted on the fixed base inside (**a**–**e**) or outside (**f**) the parallelogram loop

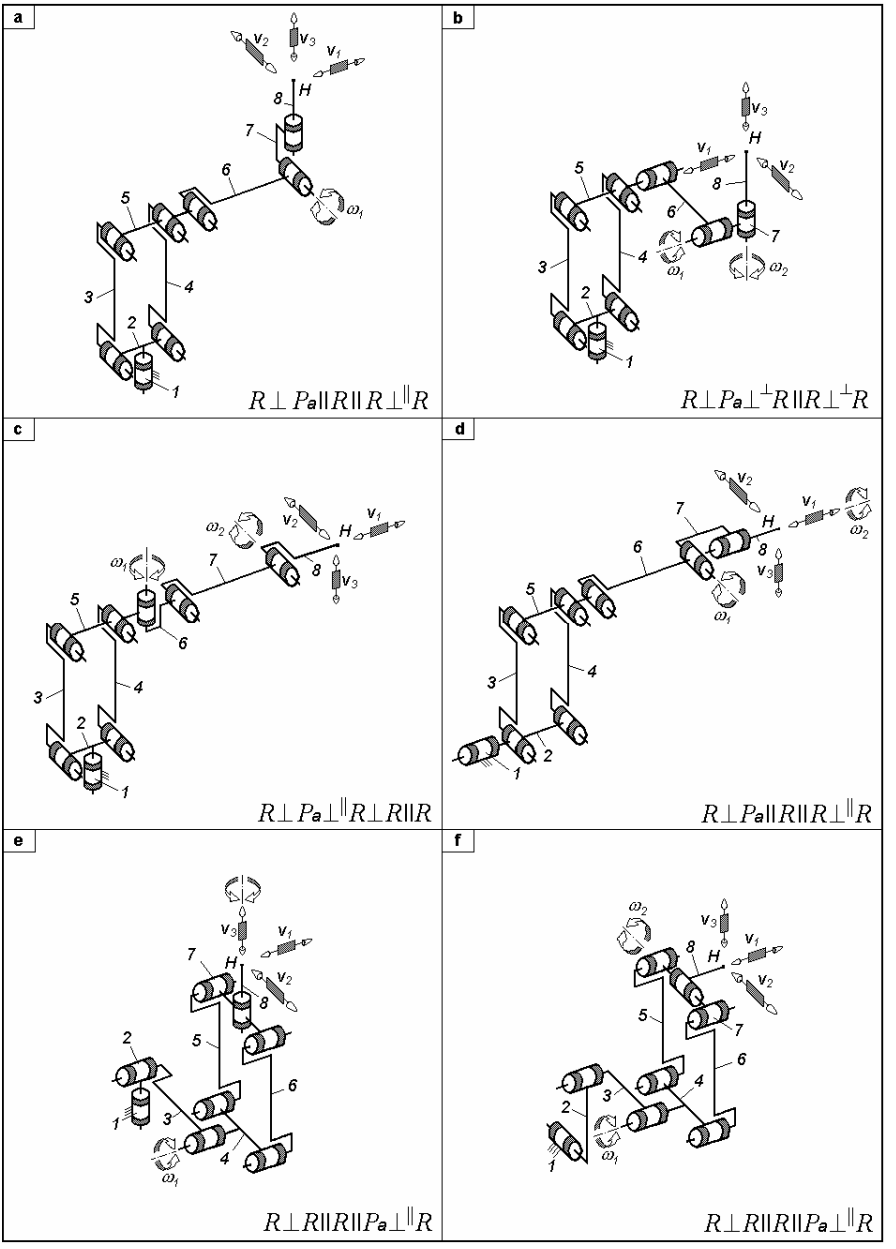

Fig. 3.70. Complex limbs for TPMs with coupled motions combining one parallelogram loop, defined by $M_G = S_G = 5$, $(R_G) = (\boldsymbol{v}_1, \boldsymbol{v}_2, \boldsymbol{v}_3, \boldsymbol{\omega}_1, \boldsymbol{\omega}_2)$ and actuated by rotating motors mounted on the fixed base

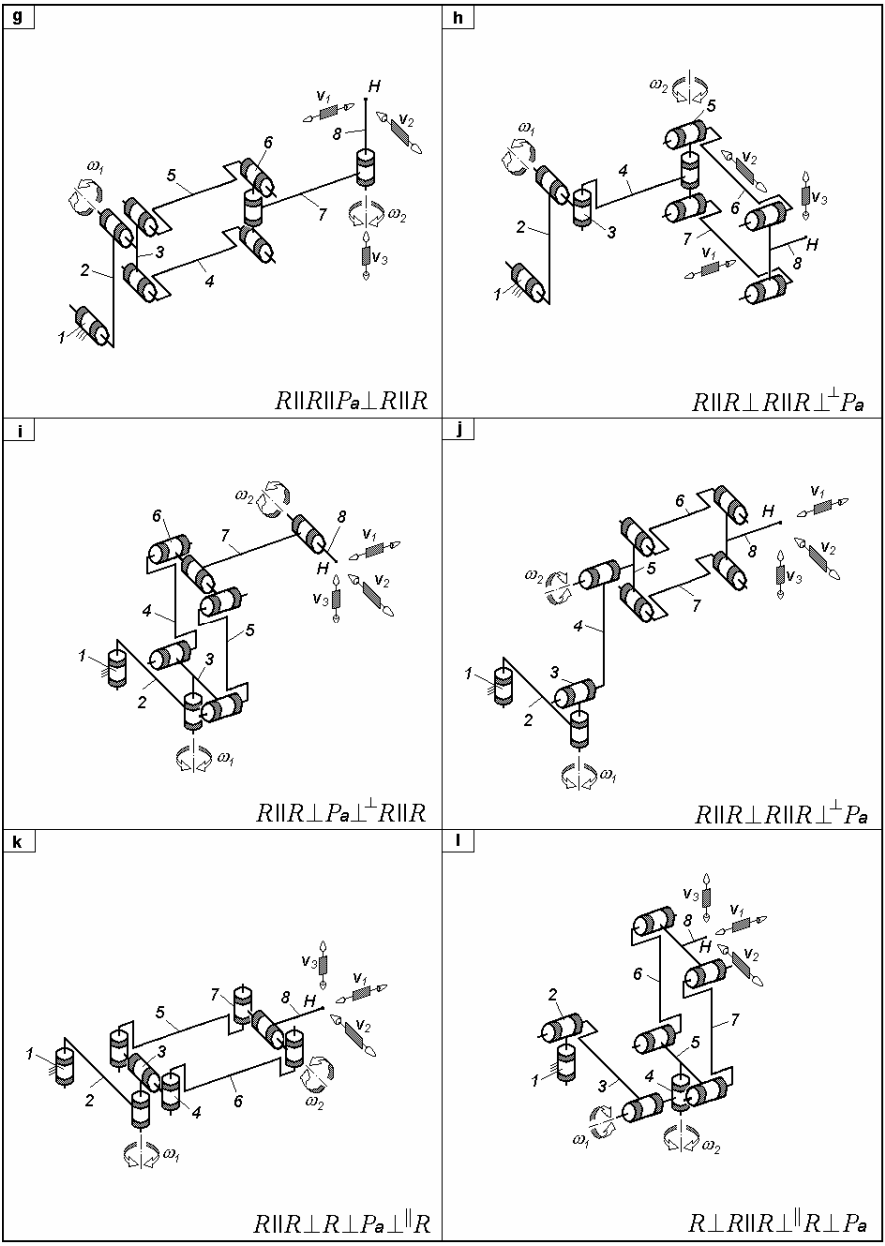
g
h
i
j
k
l
$R \| R \| Pa \perp R \| R$
$R \| R \perp R \| R \perp^{\perp} Pa$
$R \| R \perp Pa \perp^{\perp} R \| R$
$R \| R \perp R \| R \perp^{\perp} Pa$
$R \| R \perp R \perp Pa \perp^{\parallel} R$
$R \perp R \| R \perp^{\parallel} R \perp Pa$

Fig. 3.70. (cont.)

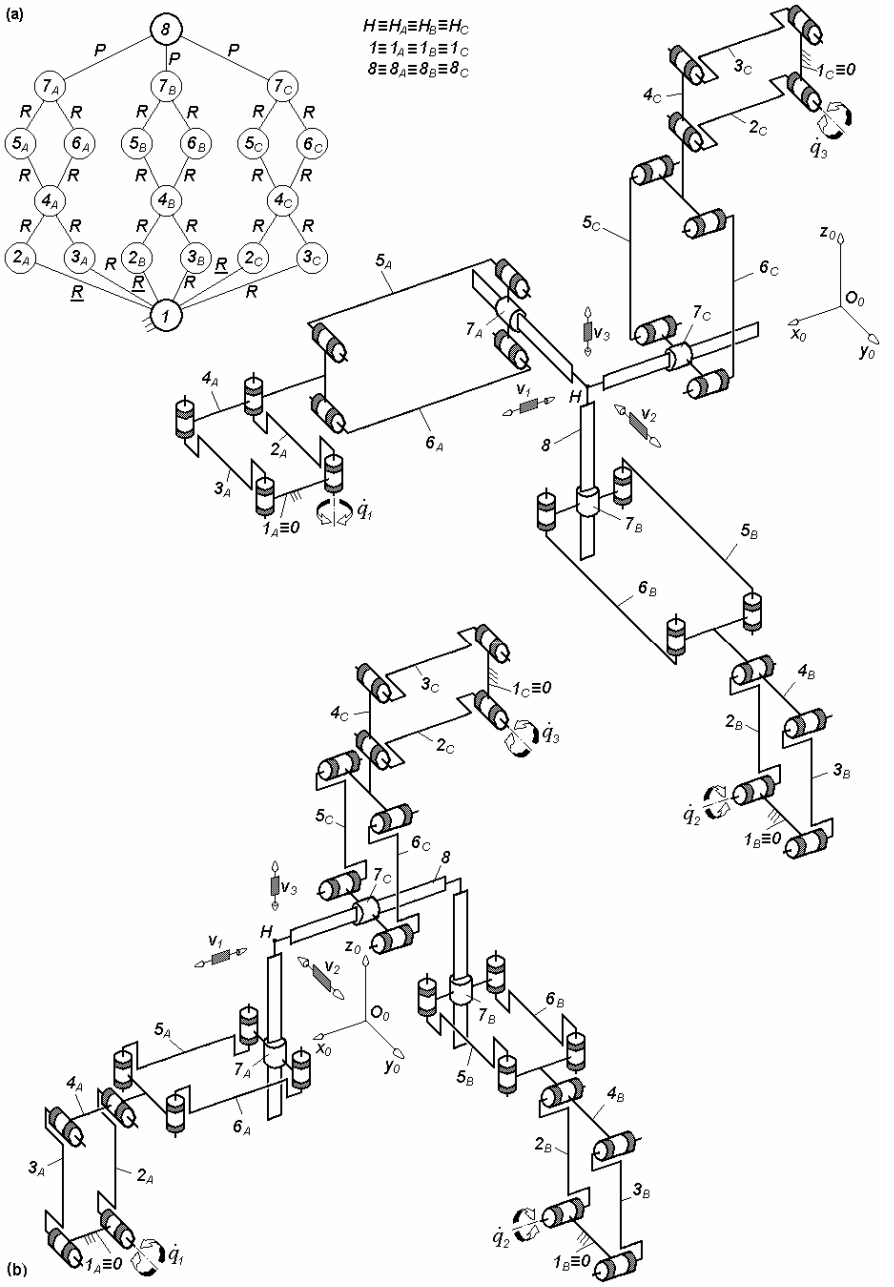

Fig. 3.71. *3-PaPaP*-type overconstrained TPMs with coupled motions and rotating actuators mounted on the fixed base, defined by $M_F = S_F = 3$, $(R_F) = (\boldsymbol{v}_1, \boldsymbol{v}_2, \boldsymbol{v}_3)$, $T_F = 0$, $N_F = 24$, limb topology $\underline{Pa} \perp Pa||P$

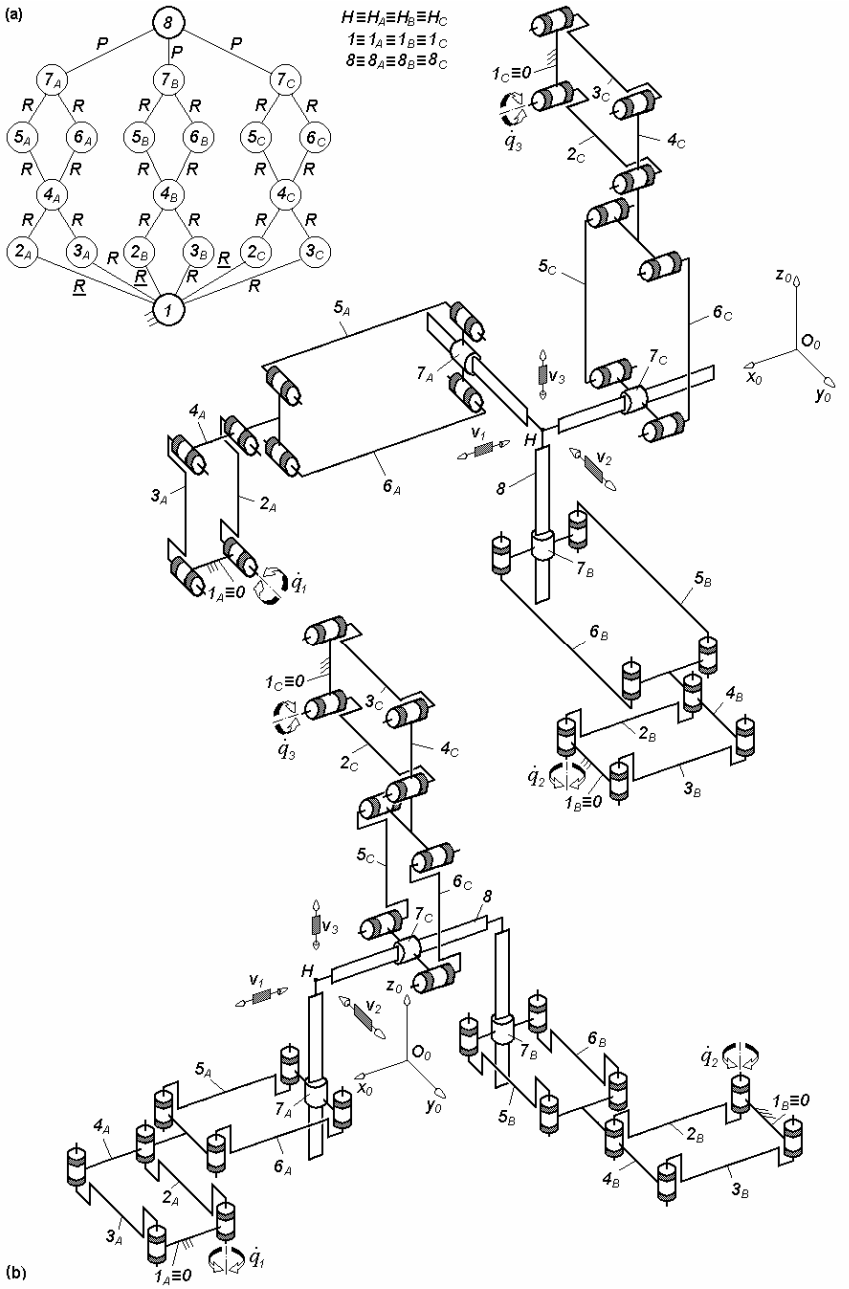

Fig. 3.72. *3-PaPaP*-type overconstrained TPMs with coupled motions and rotating actuators mounted on the fixed base, defined by $M_F = S_F = 3$, $(R_F) = (\boldsymbol{v}_1, \boldsymbol{v}_2, \boldsymbol{v}_3)$, $T_F = 0$, $N_F = 24$, limb topology $\underline{Pa}||Pa||P$

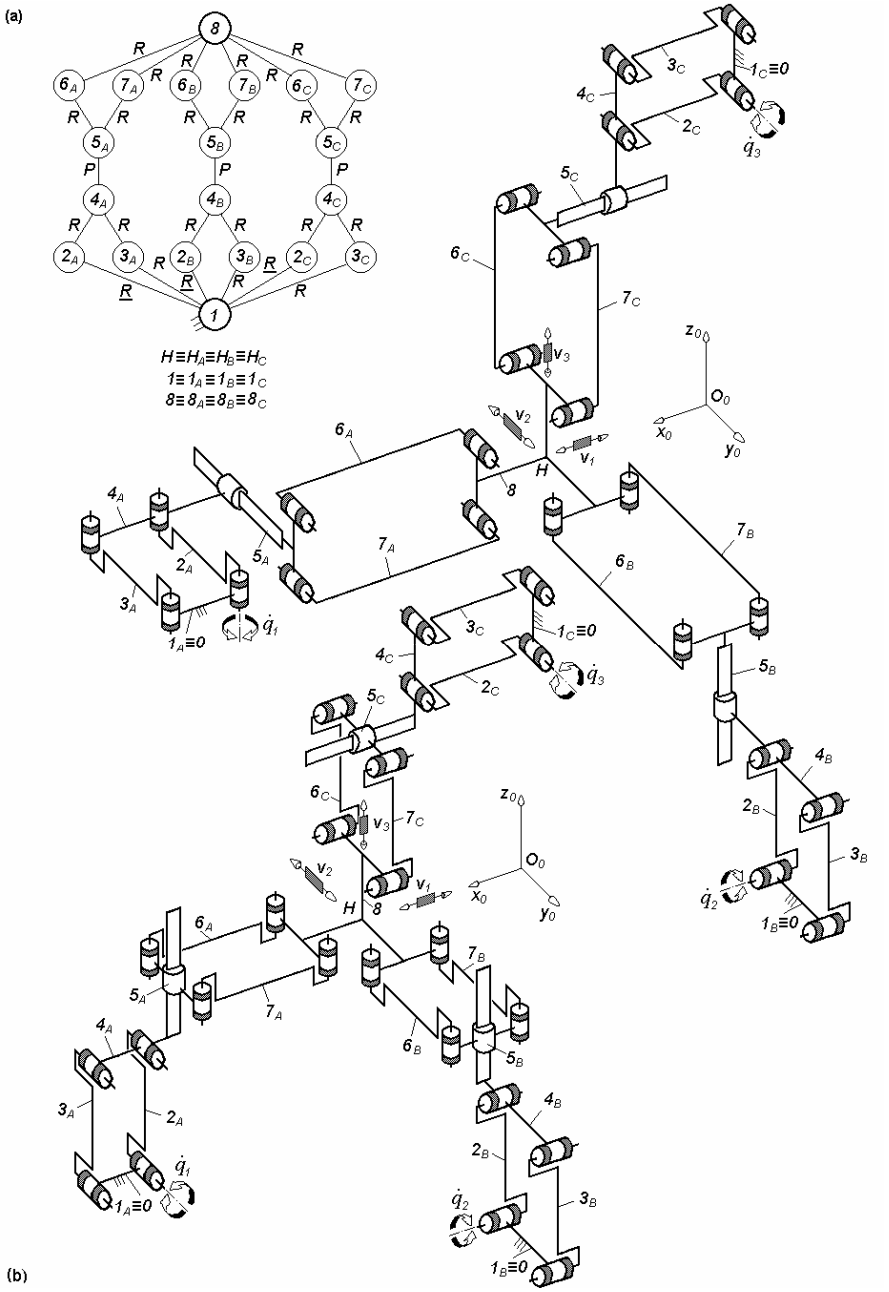

Fig. 3.73. *3-<u>Pa</u>PPa*-type overconstrained TPMs with coupled motions and rotating actuators mounted on the fixed base, defined by $M_F = S_F = 3$, $(R_F) = (\boldsymbol{v}_1, \boldsymbol{v}_2, \boldsymbol{v}_3)$, $T_F = 0$, $N_F = 24$, limb topology $\underline{Pa} \perp P || Pa$

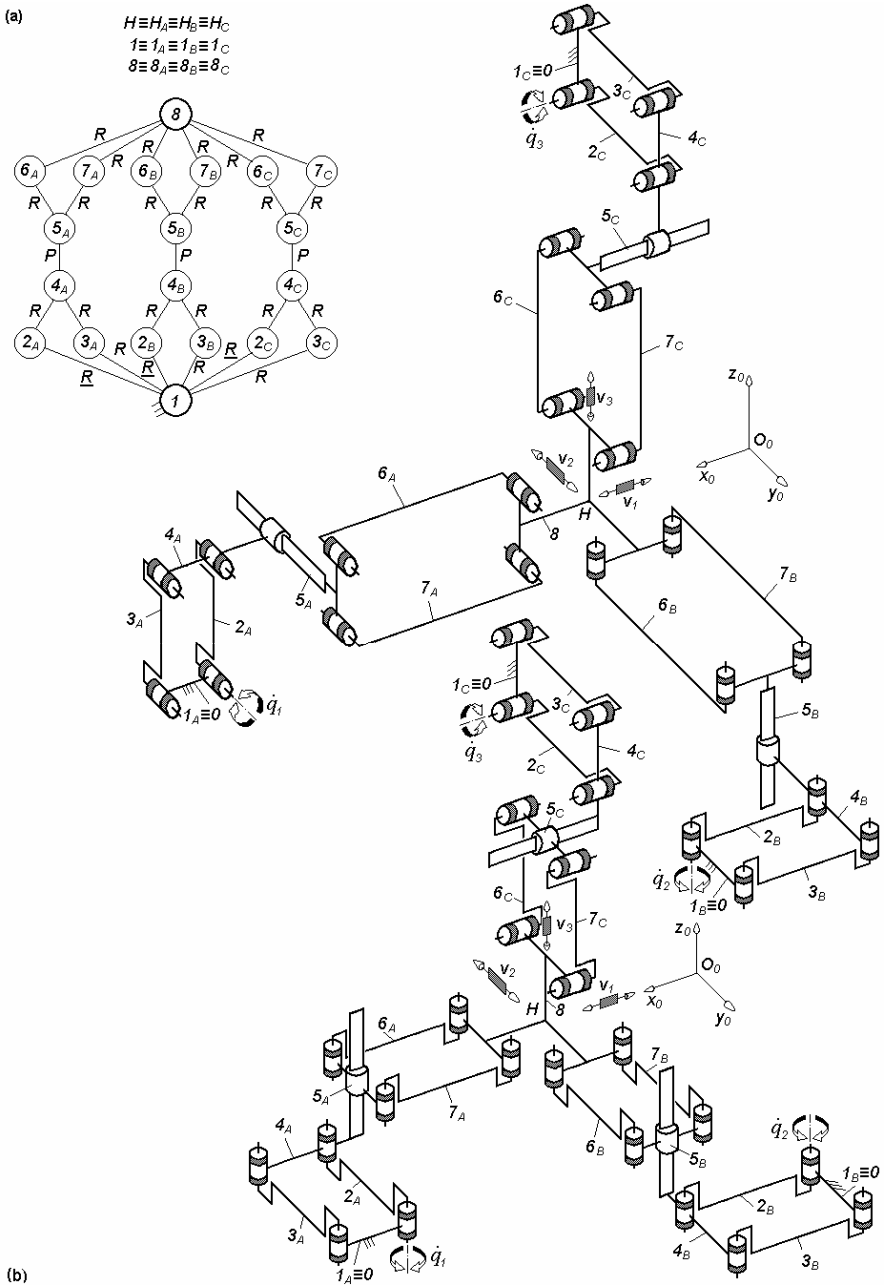

Fig. 3.74. *3-PaPPa*-type overconstrained TPMs with coupled motions and rotating actuators mounted on the fixed base, defined by $M_F = S_F = 3$, $(R_F) = (\boldsymbol{v}_1, \boldsymbol{v}_2, \boldsymbol{v}_3)$, $T_F = 0$, $N_F = 24$, limb topology *Pa*||*P*||*Pa*

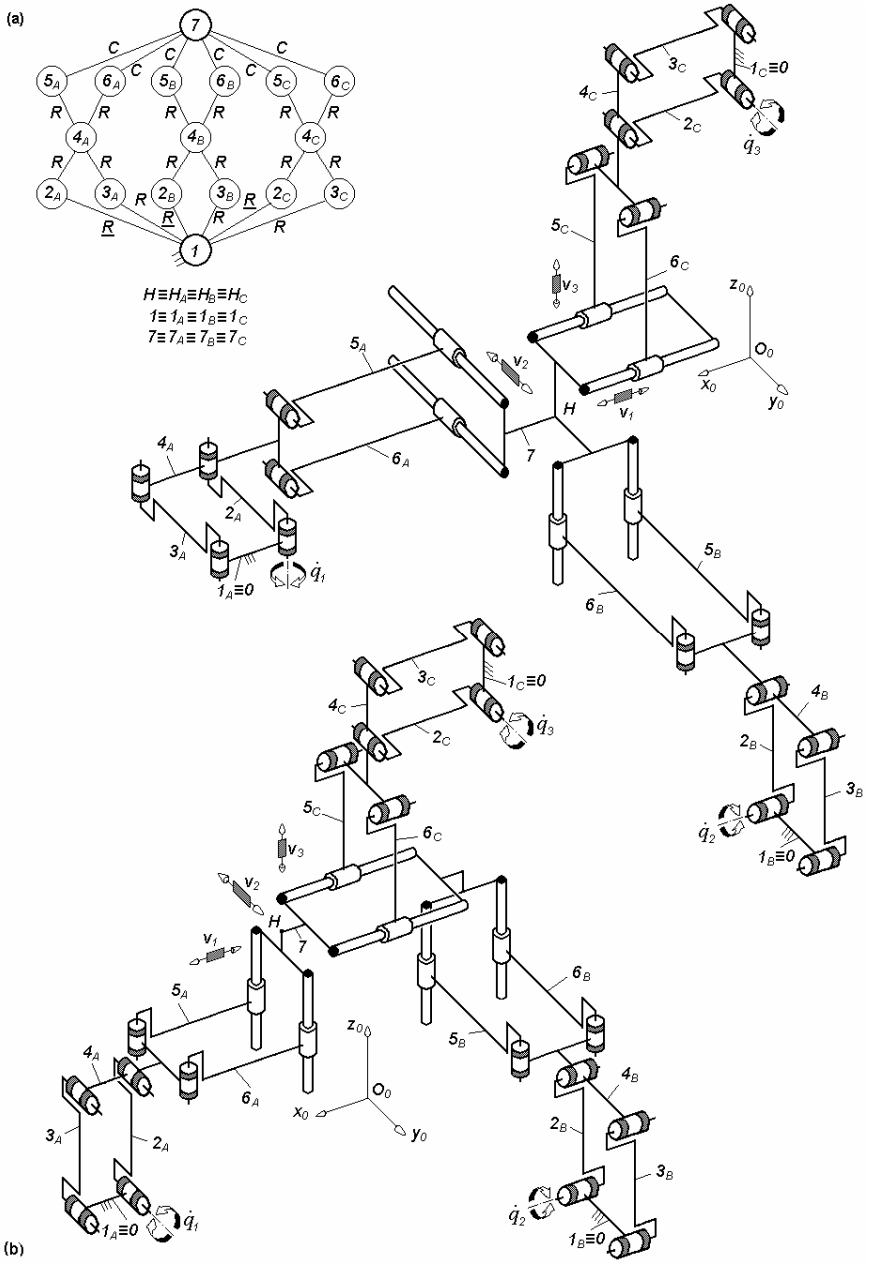

Fig. 3.75. *3-PaPa*^{cc} overconstrained TPMs with coupled motions, rotating actuators on the fixed base and six cylindrical joints adjacent to the moving platform, defined by $M_F = S_F = 3$, $(R_F) = (\boldsymbol{v}_1, \boldsymbol{v}_2, \boldsymbol{v}_3)$, $T_F = 0$, $N_F = 21$, limb topology $Pa \perp Pa^{cc}$

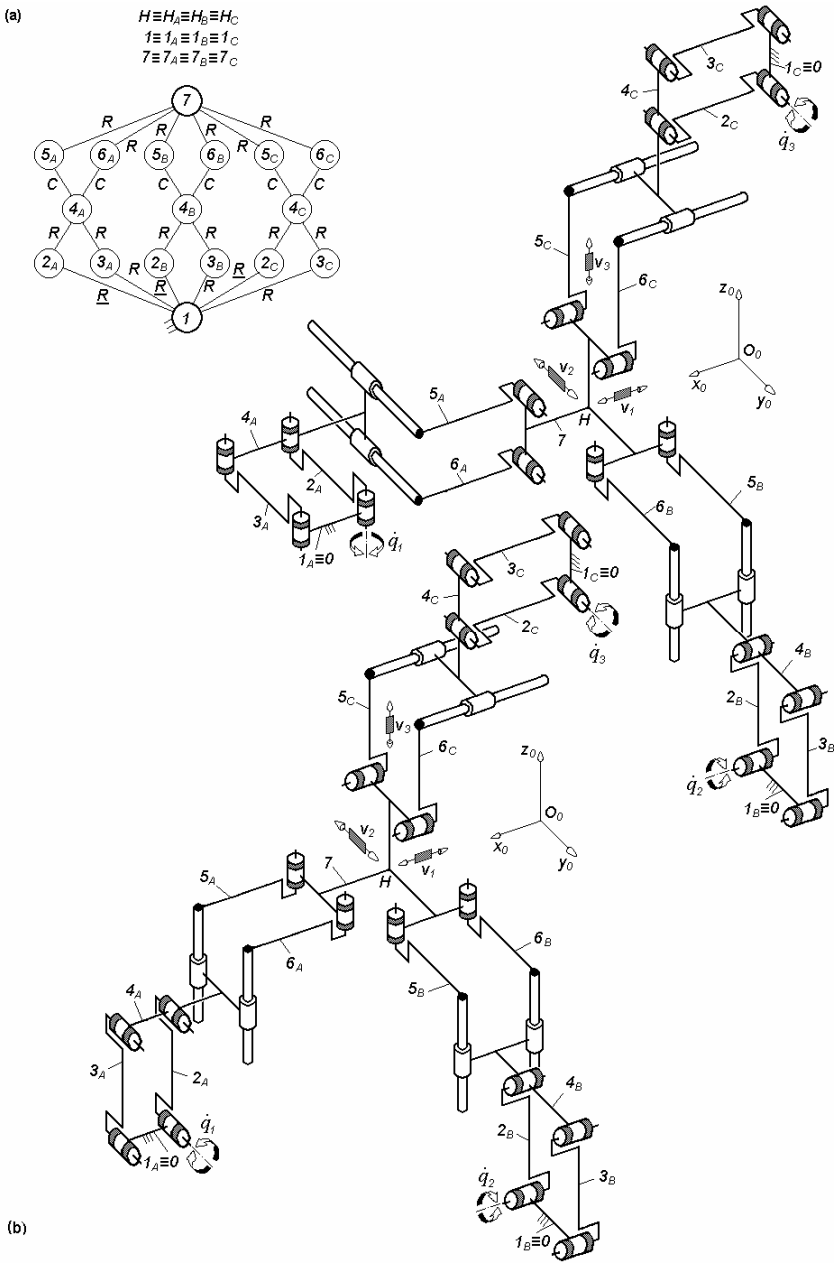

Fig. 3.76. *3-<u>Pa</u>Pa*^{cc}-type overconstrained TPMs with coupled motions, rotating actuators on the fixed base and six revolute joints adjacent to the moving platform, defined by $M_F = S_F = 3$, $(R_F) = (\boldsymbol{v}_1, \boldsymbol{v}_2, \boldsymbol{v}_3)$, $T_F = 0$, $N_F = 21$, limb topology $\underline{Pa} \perp Pa^{cc}$

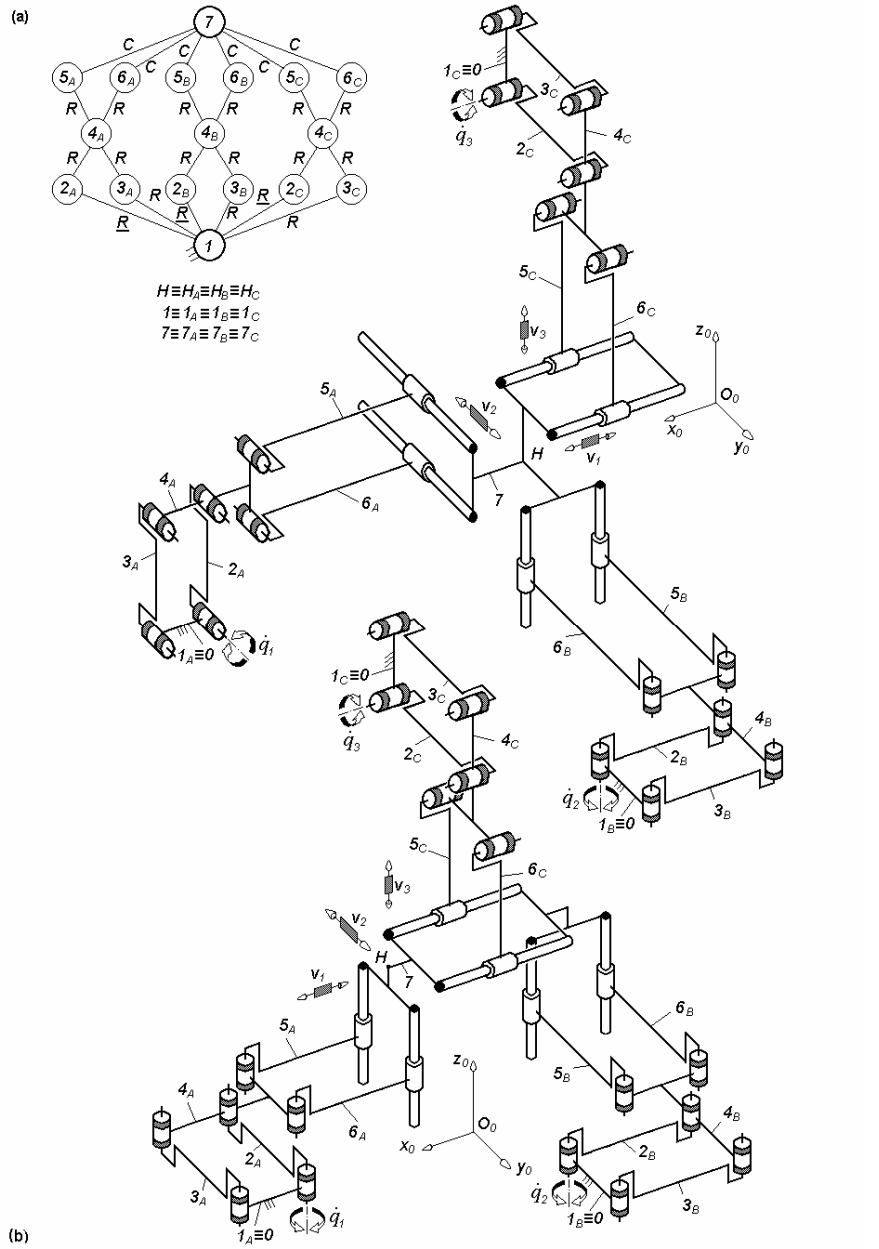

Fig. 3.77. *3-*$\underline{Pa}Pa^{cc}$-type overconstrained TPMs with coupled motions, rotating actuators mounted on the fixed base and six cylindrical joints adjacent to the moving platform, defined by $M_F = S_F = 3$, $(R_F) = (\boldsymbol{v}_1, \boldsymbol{v}_2, \boldsymbol{v}_3)$, $T_F = 0$, $N_F = 21$, limb topology $\underline{Pa}||Pa^{cc}$

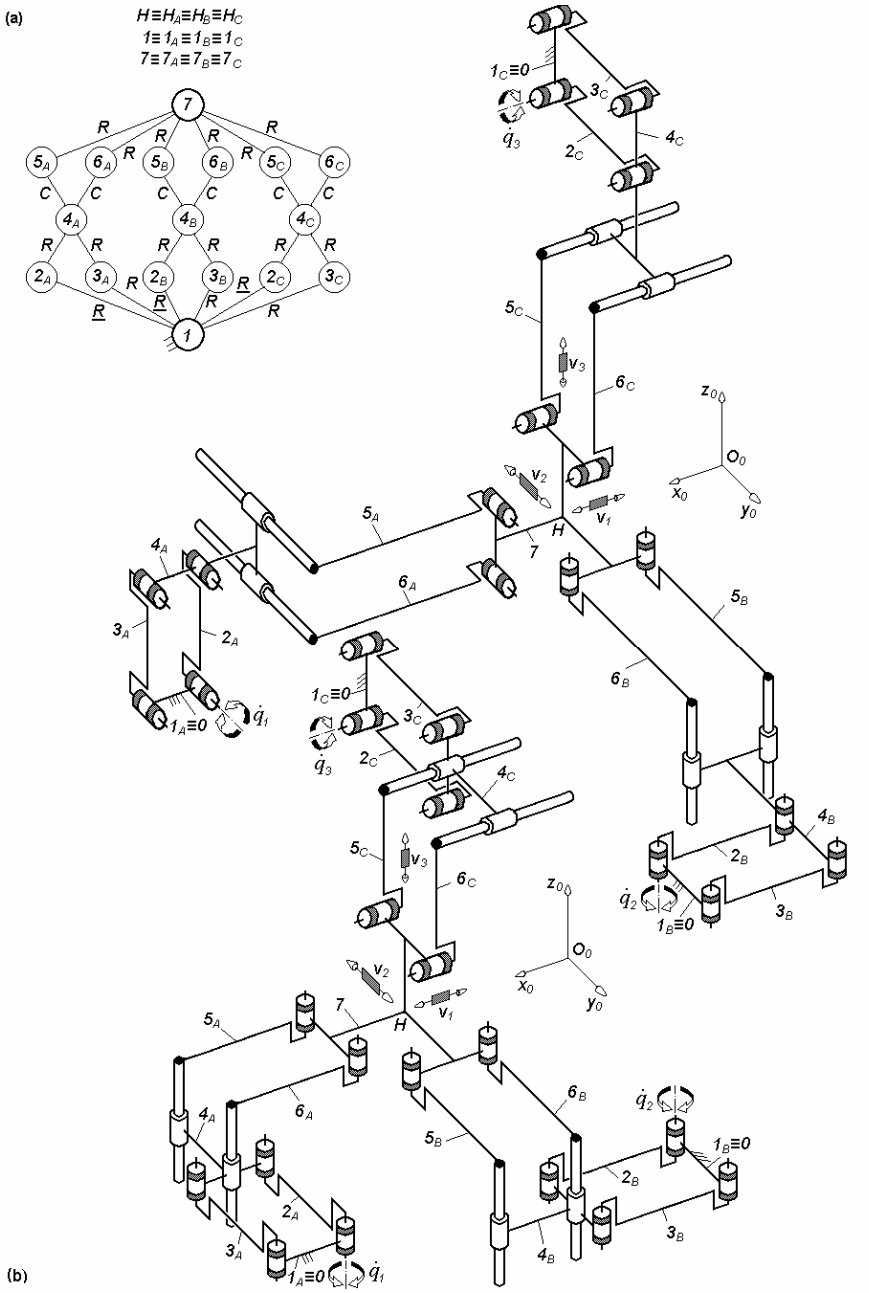

Fig. 3.78. *3-PaPa^cc*-type overconstrained TPMs with coupled motions, rotating actuators on the fixed base and six revolute joints adjacent to the moving platform, defined by $M_F = S_F = 3$, $(R_F) = (\boldsymbol{v}_1, \boldsymbol{v}_2, \boldsymbol{v}_3)$, $T_F = 0$, $N_F = 21$, limb topology $\underline{Pa}||Pa^{cc}$

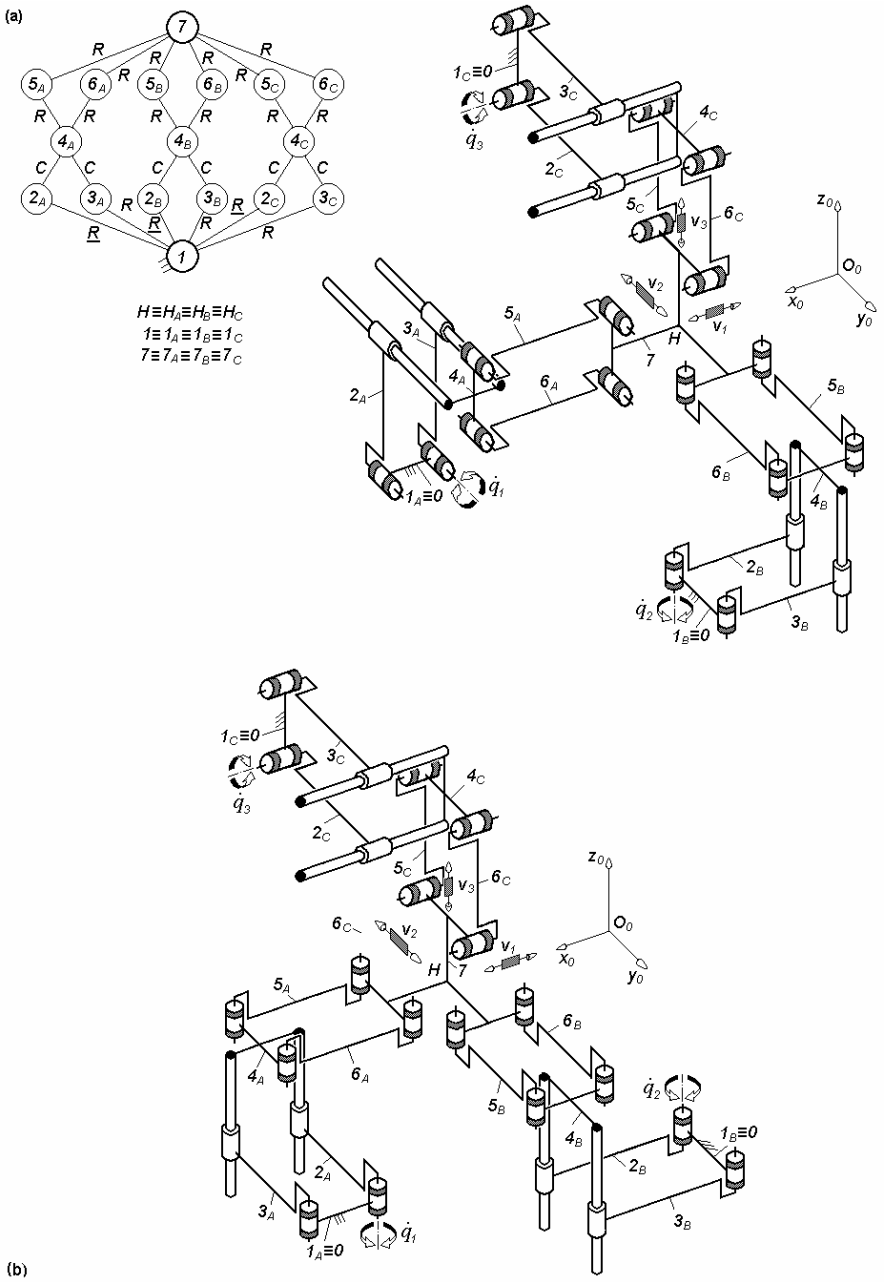

Fig. 3.79. *3-*$\underline{Pa}^{cc}Pa$*-*type overconstrained TPMs with coupled motions, rotating actuators on the fixed base and six revolute joints adjacent to the moving platform, defined by $M_F = S_F = 3$, $(R_F) = (\boldsymbol{v}_1, \boldsymbol{v}_2, \boldsymbol{v}_3)$, $T_F = 0$, $N_F = 21$, limb topology $\underline{Pa}^{cc}||Pa$

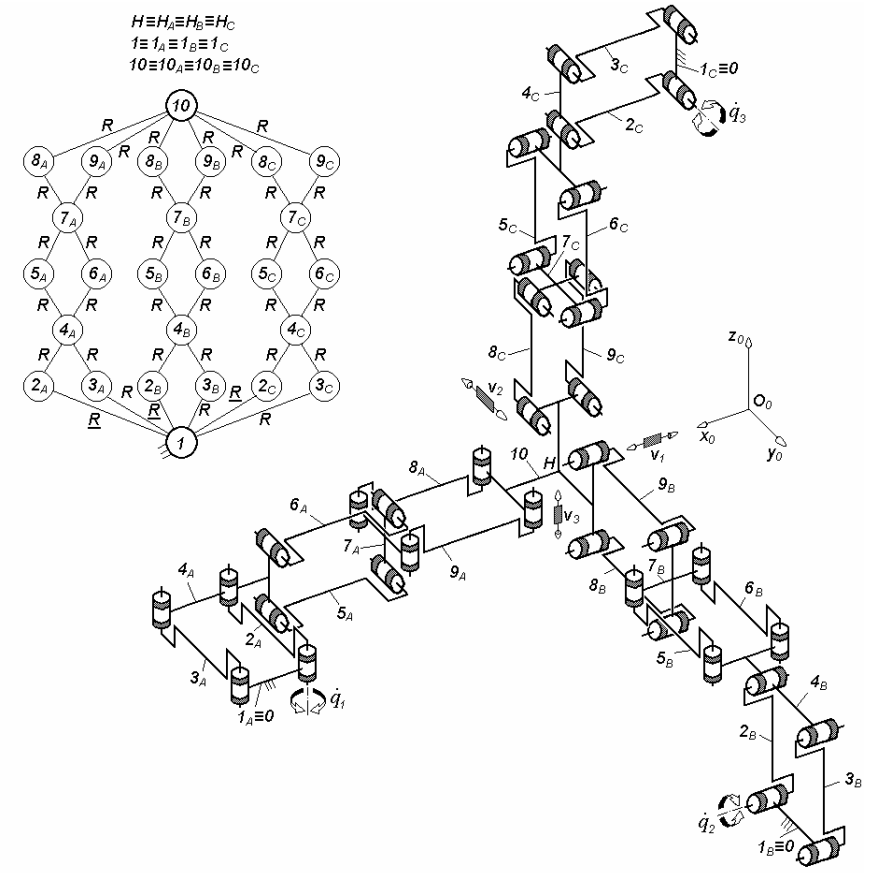

Fig. 3.80. *3-PaPaPa*-type overconstrained TPM with coupled motions and rotating actuators mounted on the fixed base, defined by $M_F = S_F = 3$, $(R_F) = (\boldsymbol{v}_1, \boldsymbol{v}_2, \boldsymbol{v}_3)$, $T_F = 0$, $N_F = 33$, limb topology $\underline{Pa} \perp Pa \perp {}^{\parallel}Pa$

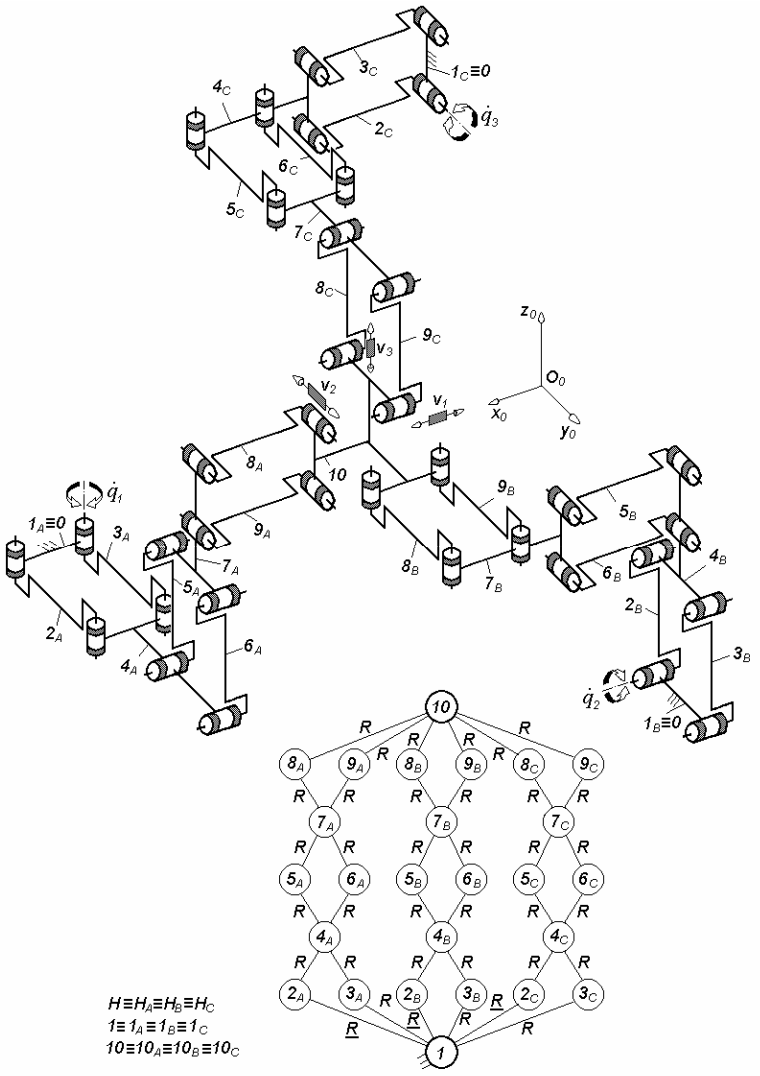

Fig. 3.81. *3-<u>Pa</u>PaPa*-type overconstrained TPM with coupled motions and rotating actuators mounted on the fixed base, defined by $M_F = S_F = 3$, $(R_F) = (\boldsymbol{v}_1, \boldsymbol{v}_2, \boldsymbol{v}_3)$, $T_F = 0$, $N_F = 33$, limb topology $\underline{Pa} \perp Pa \perp^{\perp} Pa$

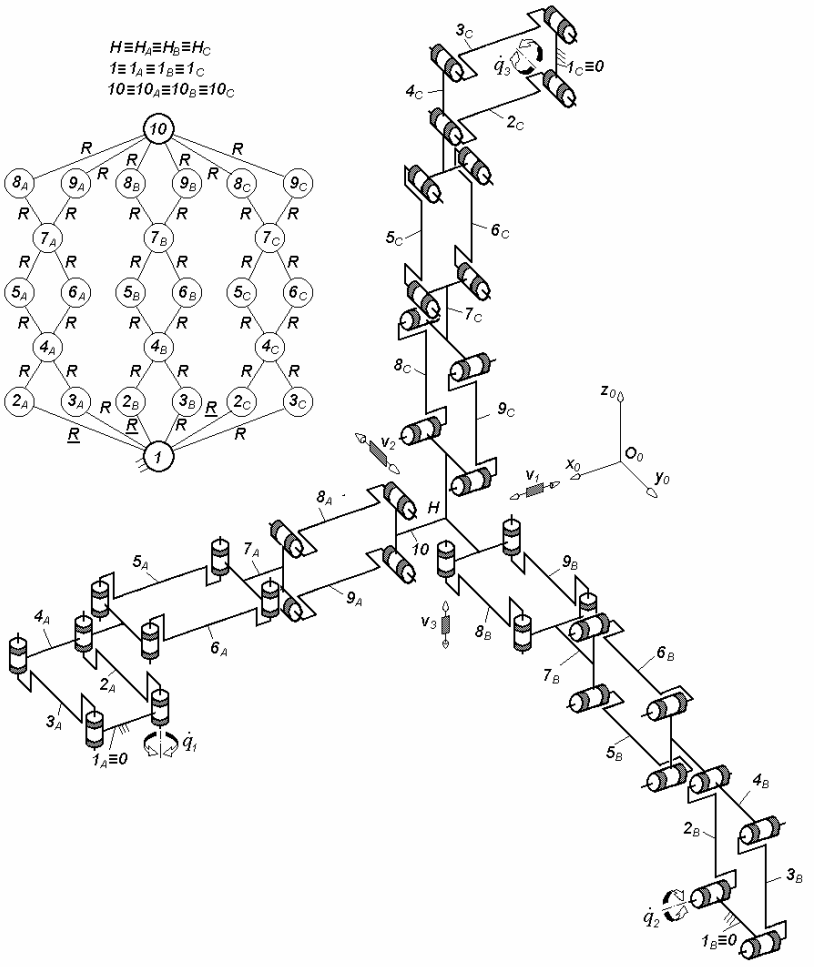

Fig. 3.82. *3-PaPaPa*-type overconstrained TPM with coupled motions and rotating actuators mounted on the fixed base, defined by $M_F = S_F = 3$, $(R_F) = (\boldsymbol{v}_1, \boldsymbol{v}_2, \boldsymbol{v}_3)$, $T_F = 0$, $N_F = 33$, limb topology $\underline{Pa}||Pa \perp Pa$

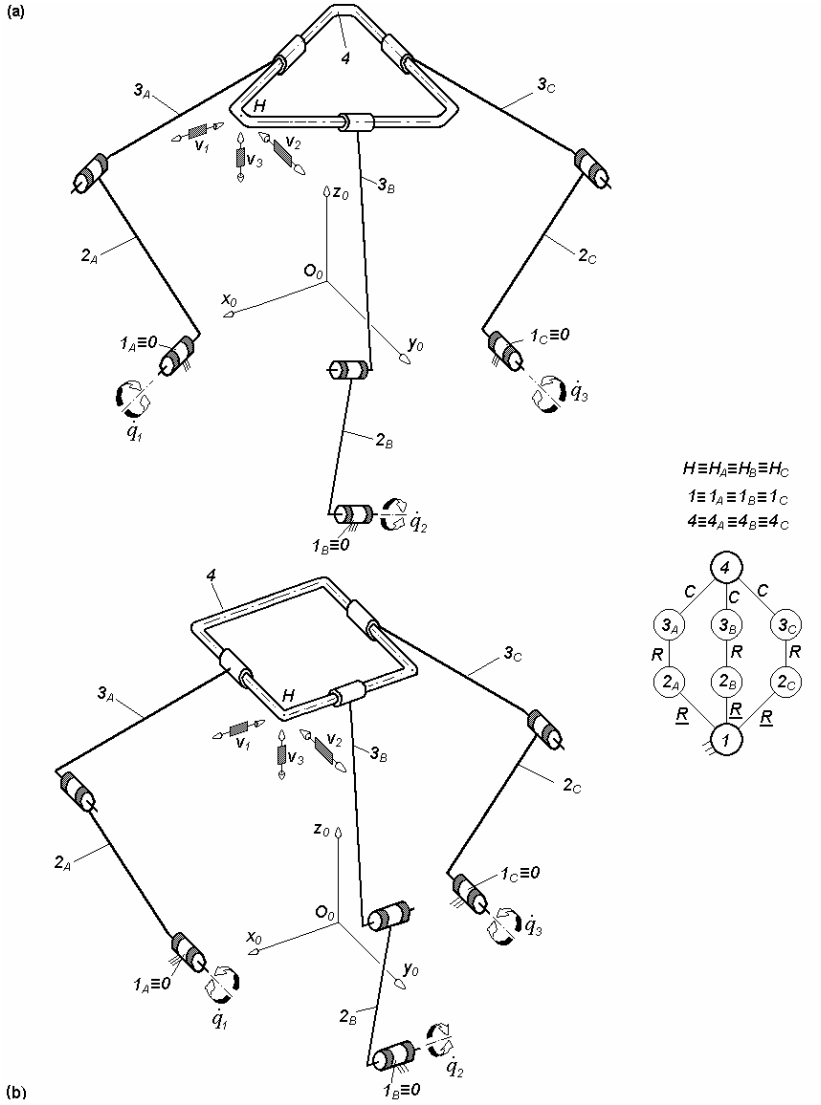

Fig. 3.83. *3-*$\underline{R}$*RRC*-type overconstrained TPMs with coupled motions and rotating actuators mounted on the fixed base (no isotropic position), defined by $M_F = S_F = 3$, $(R_F) = (\boldsymbol{v}_1, \boldsymbol{v}_2, \boldsymbol{v}_3)$, $T_F = 0$, $N_F = 3$, limb topology $\underline{R}||R||C$

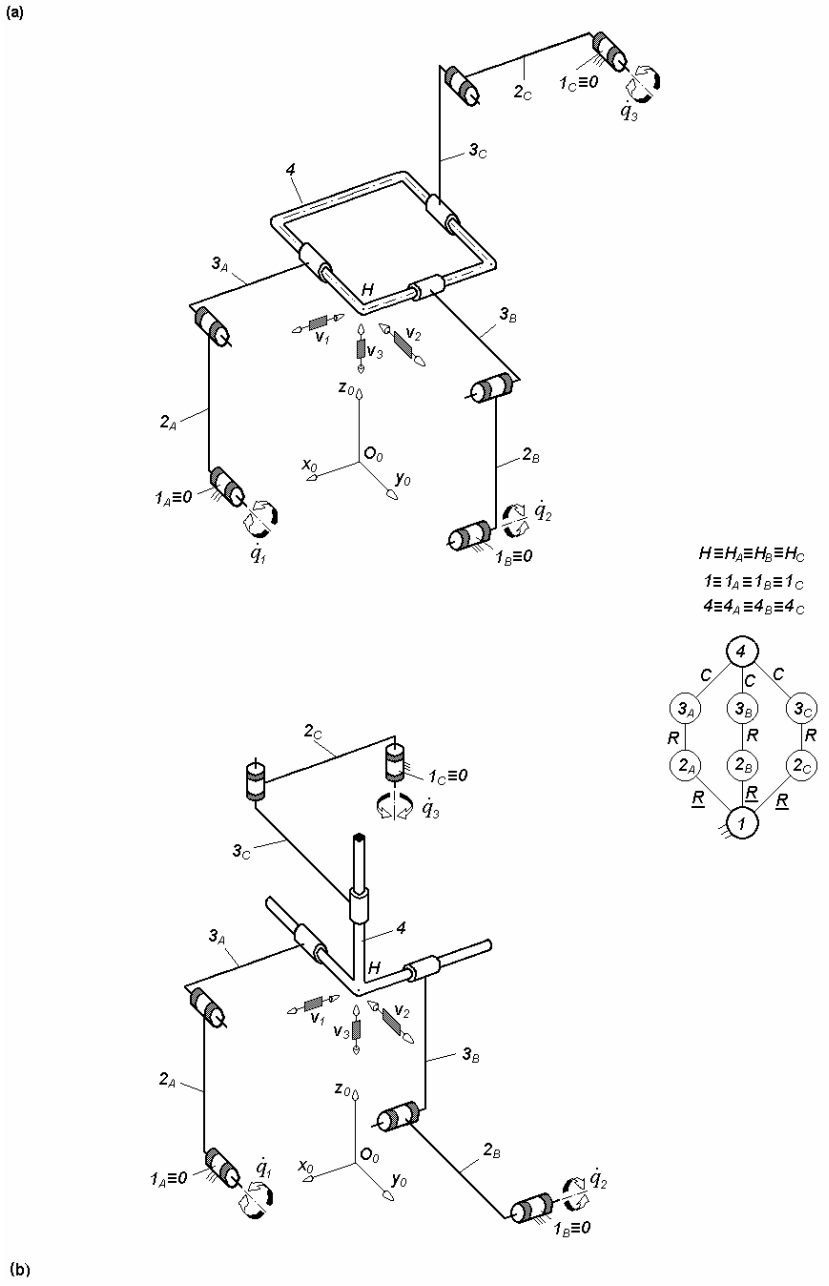

Fig. 3.84. *3-RRC*-type overconstrained TPMs with coupled motions and rotating actuators mounted on the fixed base (with an isotropic position), defined by $M_F = S_F = 3$, $(R_F) = (\boldsymbol{v}_1, \boldsymbol{v}_2, \boldsymbol{v}_3)$, $T_F = 0$, $N_F = 3$, limb topology $\underline{R}||R||C$

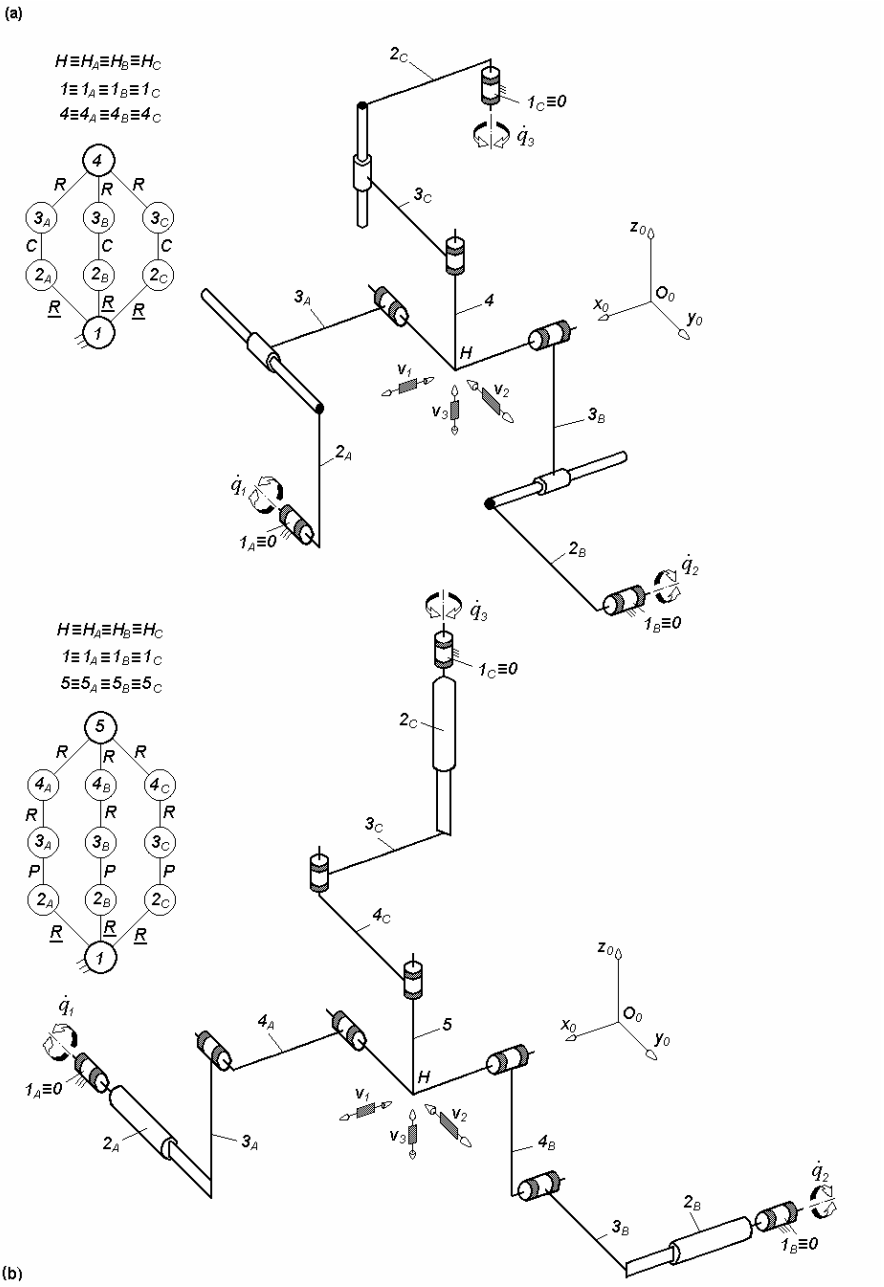

Fig. 3.85. Overconstrained TPMs with coupled motions of types *3-RCR* (**a**) and *3-RPRR* (**b**) defined by $M_F = S_F = 3$, $(R_F) = (\boldsymbol{v}_1, \boldsymbol{v}_2, \boldsymbol{v}_3)$, $T_F = 0$, $N_F = 3$, limb topology $\underline{R}||C||R$ (**a**) and $\underline{R}||P||R||R$ (**b**)

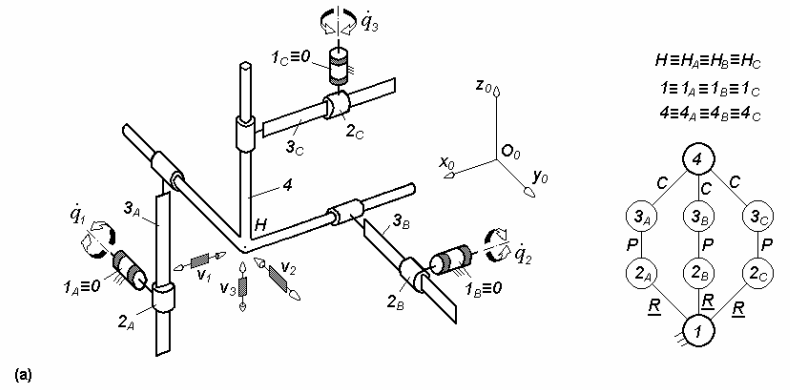

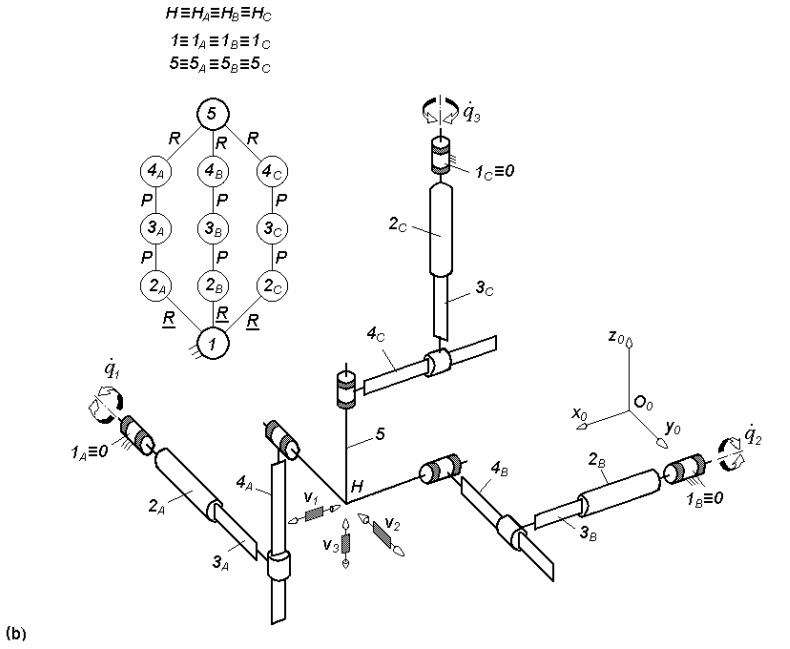

Fig. 3.86. Overconstrained TPMs with coupled motions of types *3-RPC* (**a**) and *3-RPPR* (**b**) defined by $M_F = S_F = 3$, $(R_F) = (\boldsymbol{v}_1, \boldsymbol{v}_2, \boldsymbol{v}_3)$, $T_F = 0$, $N_F = 3$, limb topology $\underline{R} \perp P \perp^{\parallel} C$ (**a**) and $\underline{R} \| P \perp P \perp^{\parallel} R$ (**b**)

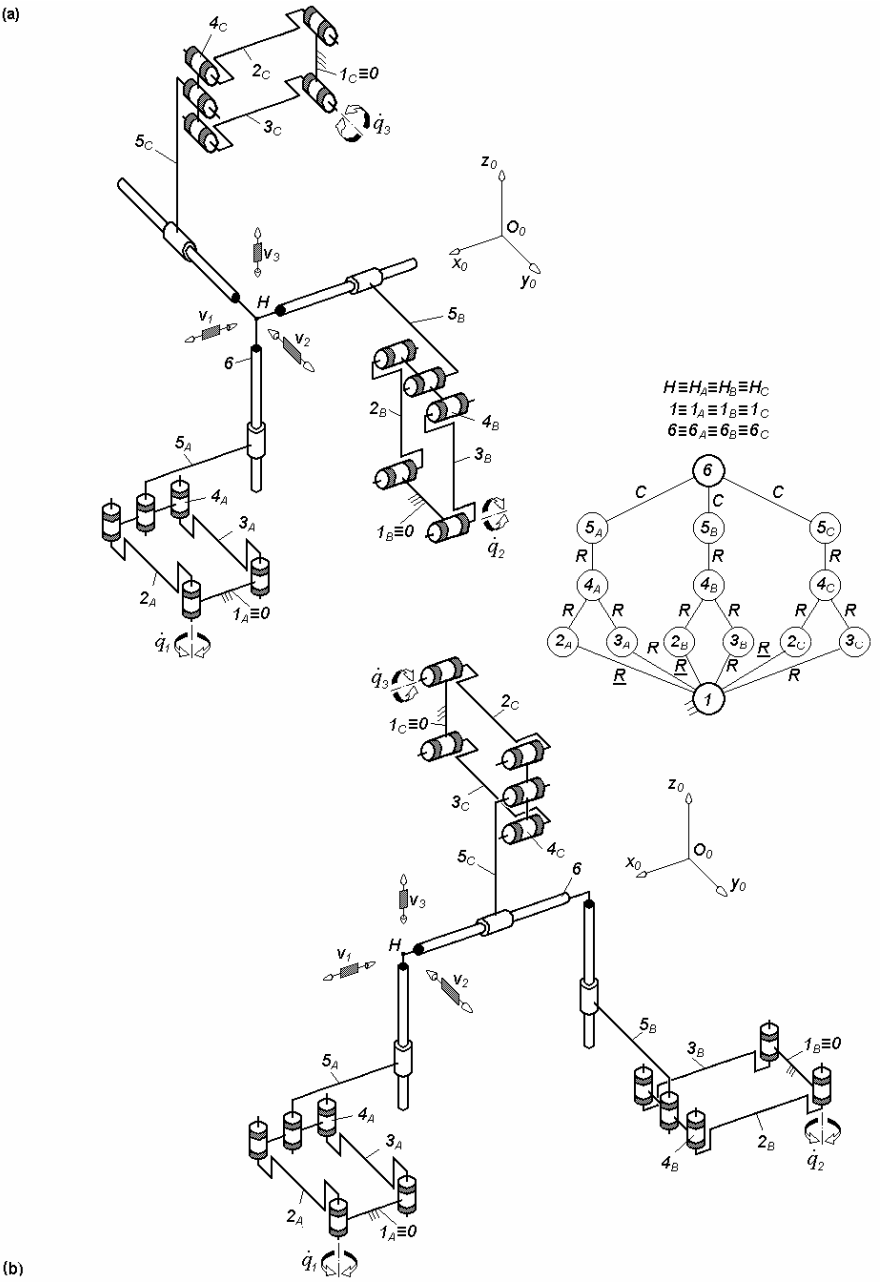

Fig. 3.87. *3-PaRC*-type overconstrained TPMs with coupled motions and rotating actuators mounted on the fixed base, defined by $M_F = S_F = 3$, $(R_F) = (\boldsymbol{v}_1, \boldsymbol{v}_2, \boldsymbol{v}_3)$, $T_F = 0$, $N_F = 12$, limb topology $\underline{Pa}||R||C$

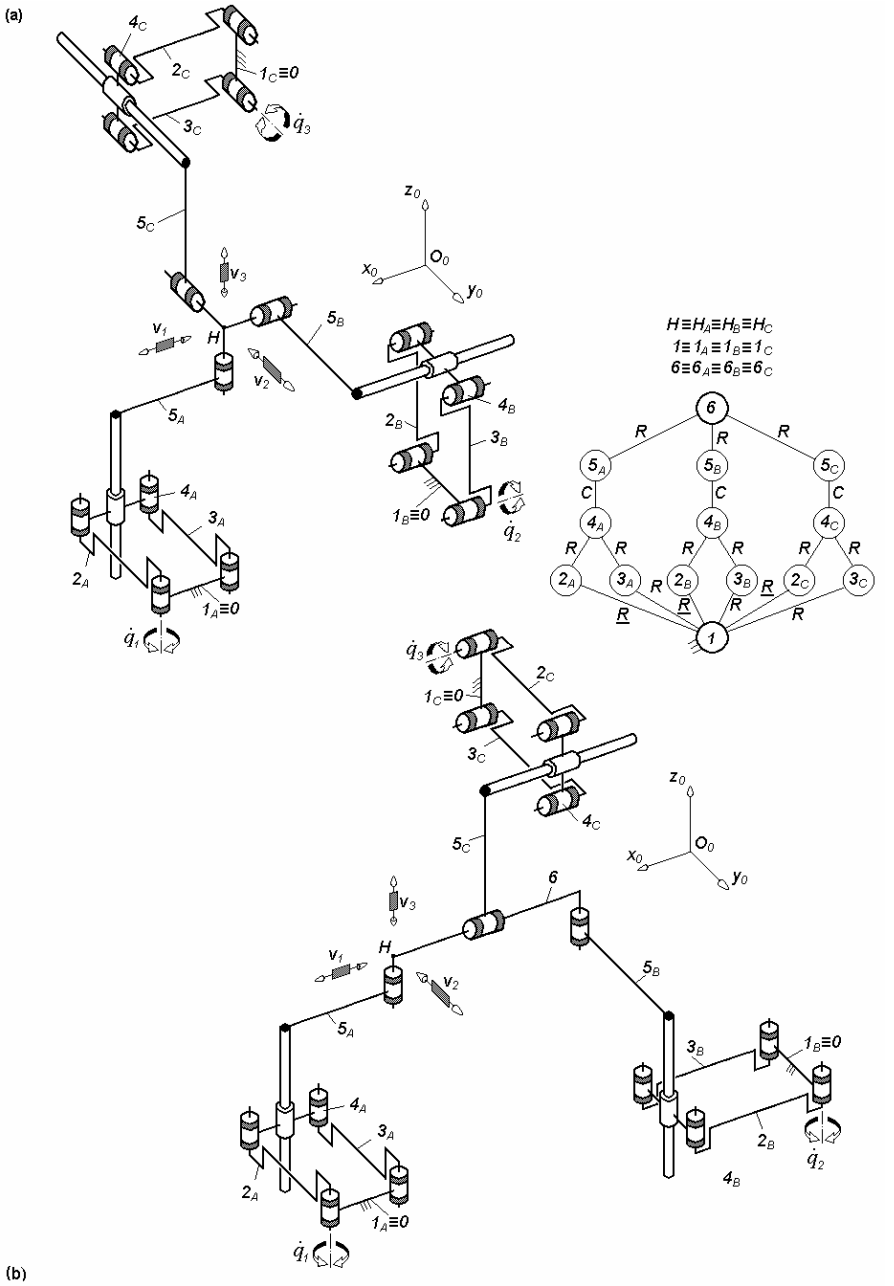

Fig. 3.88. *3-PaCR*-type overconstrained TPMs with coupled motions and rotating actuators mounted on the fixed base, defined by $M_F = S_F = 3$, $(R_F) = (\boldsymbol{v}_1, \boldsymbol{v}_2, \boldsymbol{v}_3)$, $T_F = 0$, $N_F = 12$, limb topology *Pa*||*C*||*R*

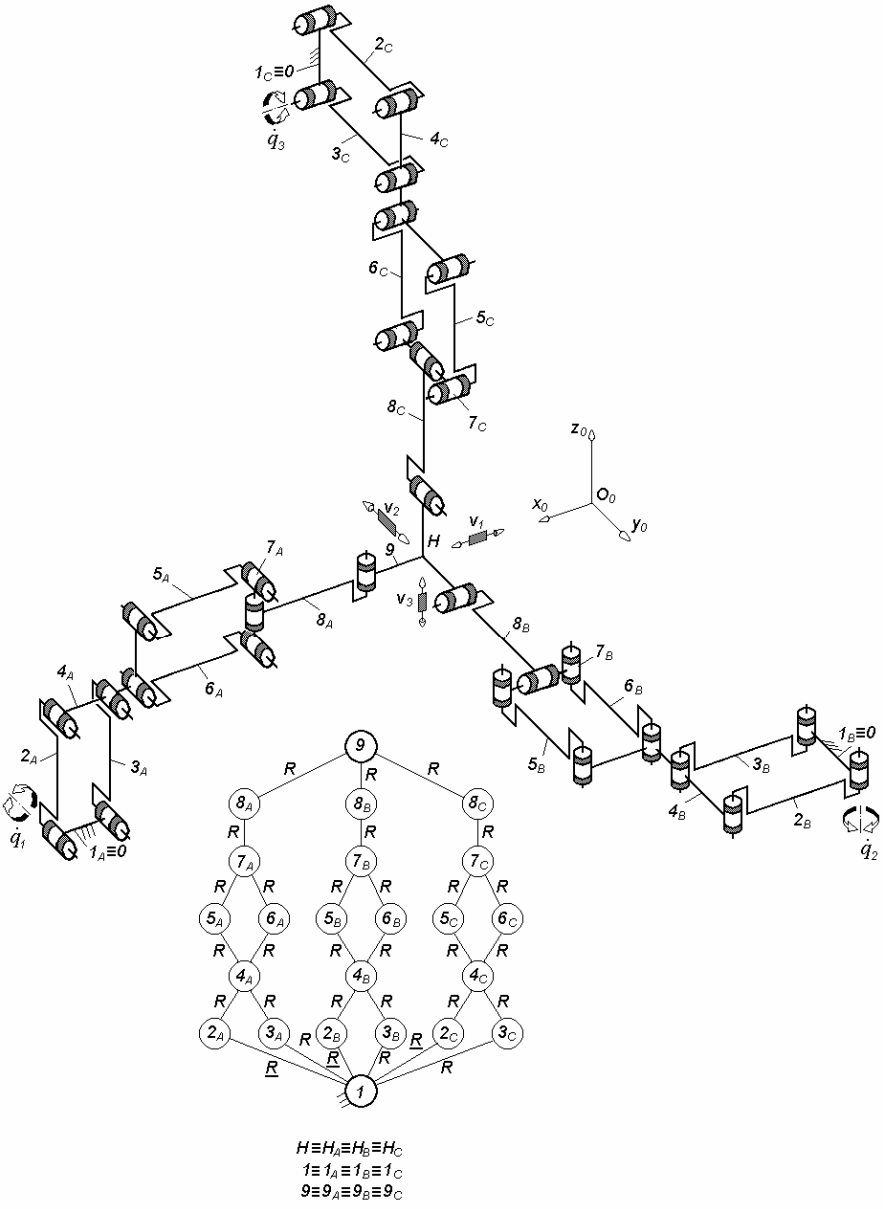

Fig. 3.89. *3-<u>Pa</u>PaRR*-type overconstrained TPMs with coupled motions and rotating actuators mounted on the fixed base defined by $M_F = S_F = 3$, $(R_F) = (\boldsymbol{v}_1, \boldsymbol{v}_2, \boldsymbol{v}_3)$, $T_F = 0$, $N_F = 21$, limb topology $\underline{Pa}||Pa \perp R||R$

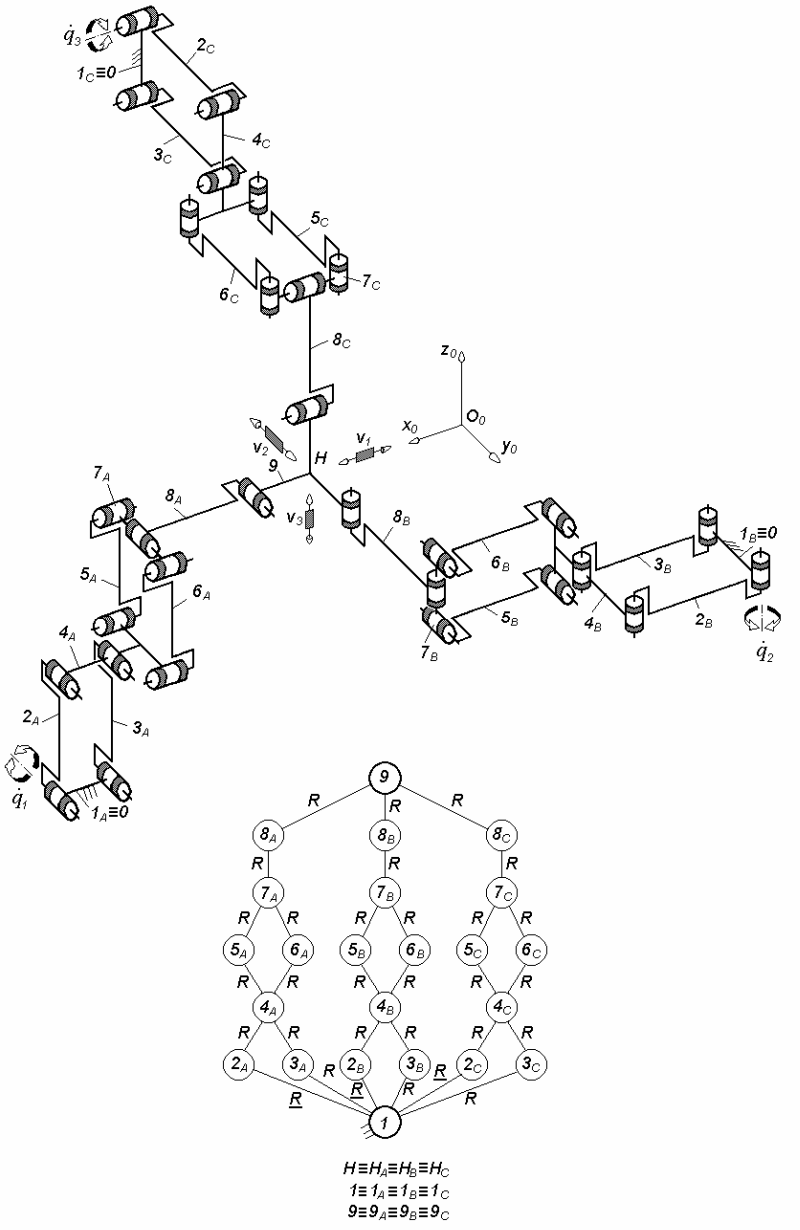

Fig. 3.90. *3-*$\underline{Pa}$*PaRR*-type overconstrained TPMs with coupled motions and rotating actuators mounted on the fixed base, defined by $M_F = S_F = 3$, $(R_F) = (\boldsymbol{v}_1, \boldsymbol{v}_2, \boldsymbol{v}_3)$, $T_F = 0$, $N_F = 21$, limb topology $\underline{Pa} \perp Pa \perp {}^{\parallel}R\|R$

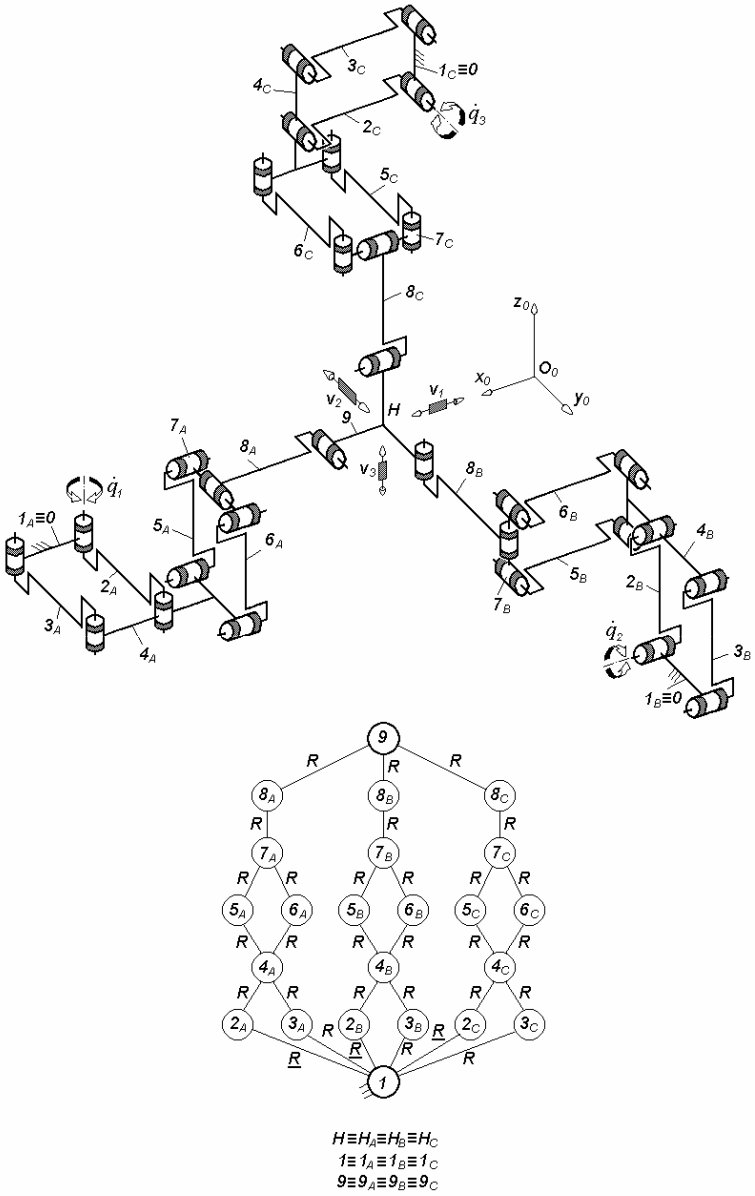

Fig. 3.91. *3-*$\underline{Pa}$*PaRR*-type overconstrained TPMs with coupled motions and rotating actuators mounted on the fixed base, defined by $M_F = S_F = 3$, $(R_F) = (\boldsymbol{v}_1, \boldsymbol{v}_2, \boldsymbol{v}_3)$, $T_F = 0$, $N_F = 21$, limb topology $\underline{Pa} \perp Pa \perp^{\perp} R||R$

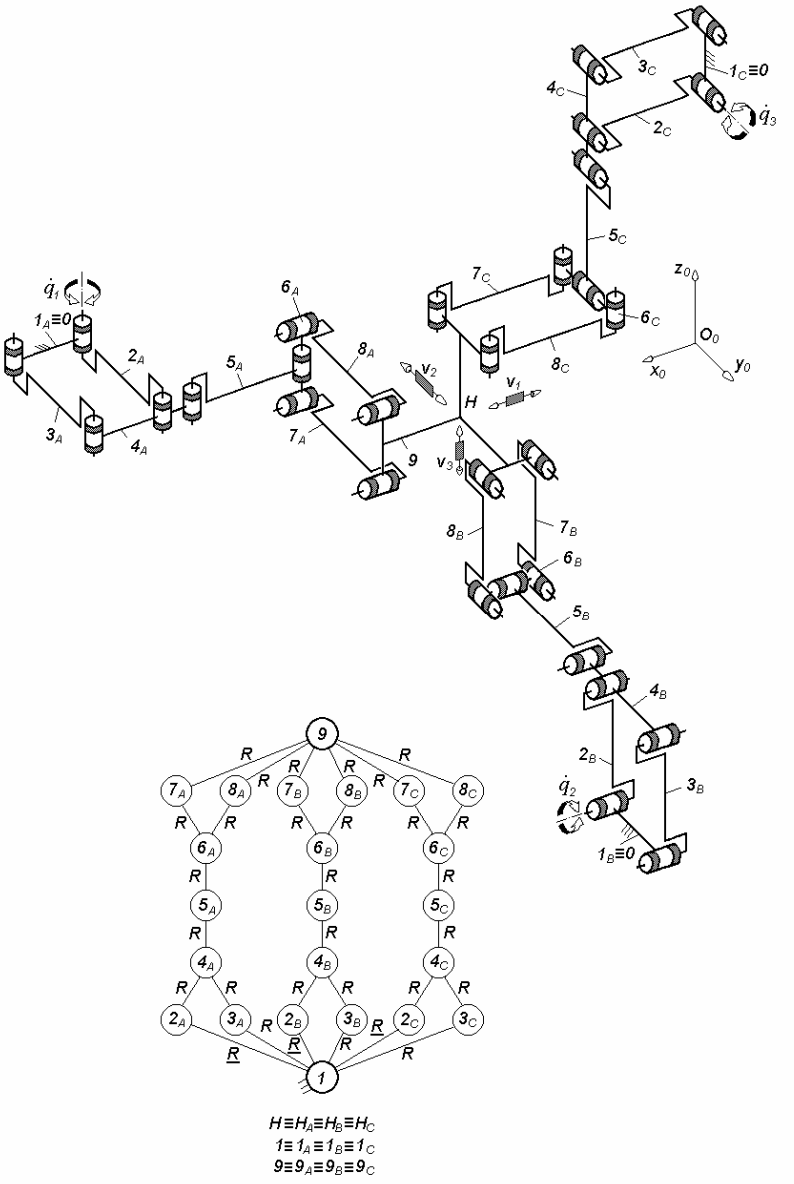

Fig. 3.92. *3-PaRRPa*-type overconstrained TPMs with coupled motions and rotating actuators mounted on the fixed base, defined by $M_F = S_F = 3$, $(R_F) = (\boldsymbol{v}_1, \boldsymbol{v}_2, \boldsymbol{v}_3)$, $T_F = 0$, $N_F = 21$, limb topology $\underline{Pa}||R||R \perp Pa$

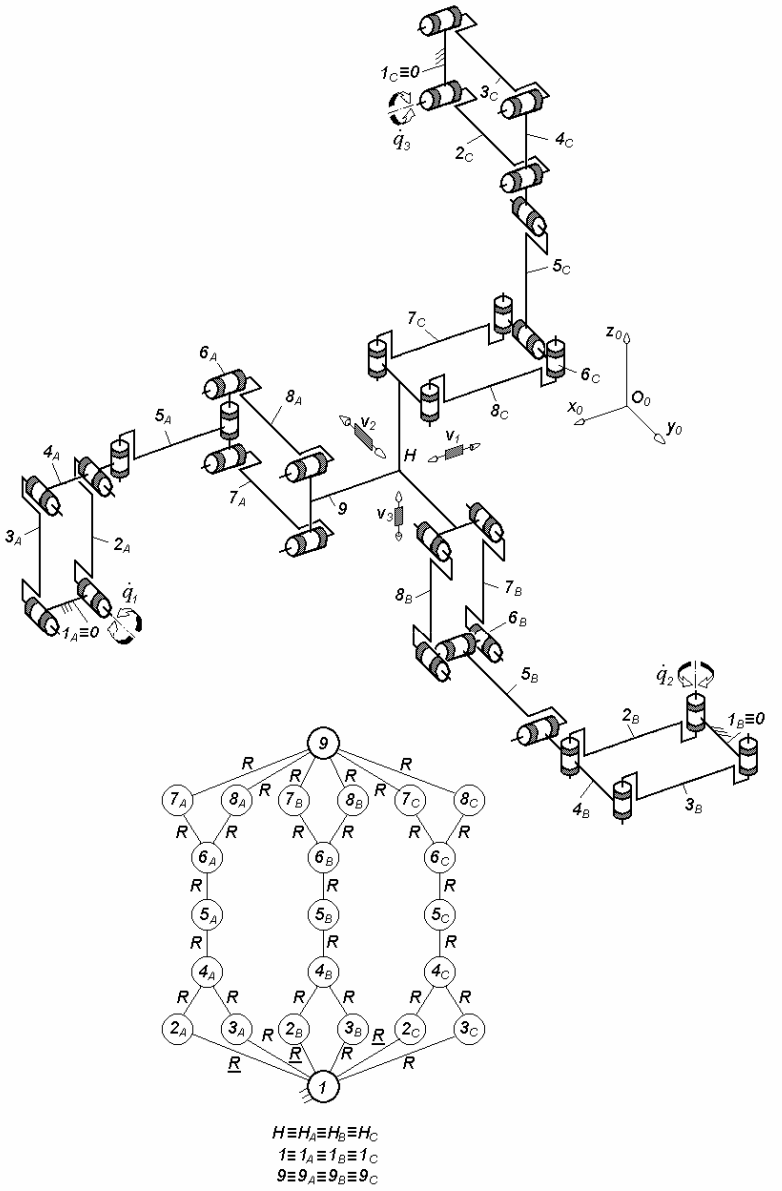

Fig. 3.93. *3-PaRRPa*-type overconstrained TPMs with coupled motions and rotating actuators mounted on the fixed base, defined by $M_F = S_F = 3$, $(R_F) = (\boldsymbol{v}_1, \boldsymbol{v}_2, \boldsymbol{v}_3)$, $T_F = 0$, $N_F = 21$, limb topology $\underline{Pa} \perp R || R \perp^{\perp} Pa$

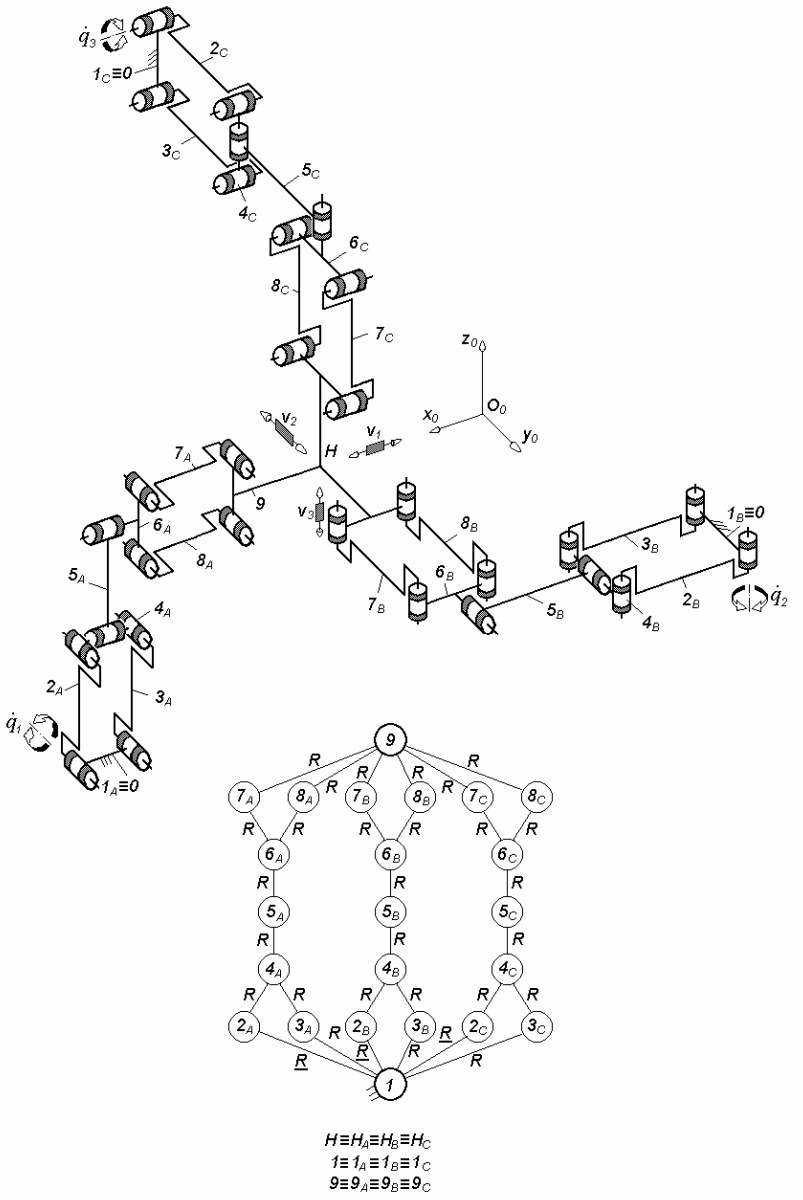

Fig. 3.94. *3-PaRRPa*-type overconstrained TPMs with coupled motions and rotating actuators mounted on the fixed base, defined by $M_F = S_F = 3$, $(R_F) = (\boldsymbol{v}_1, \boldsymbol{v}_2, \boldsymbol{v}_3)$, $T_F = 0$, $N_F = 21$, limb topology $\underline{Pa} \perp R \| R \perp \| Pa$

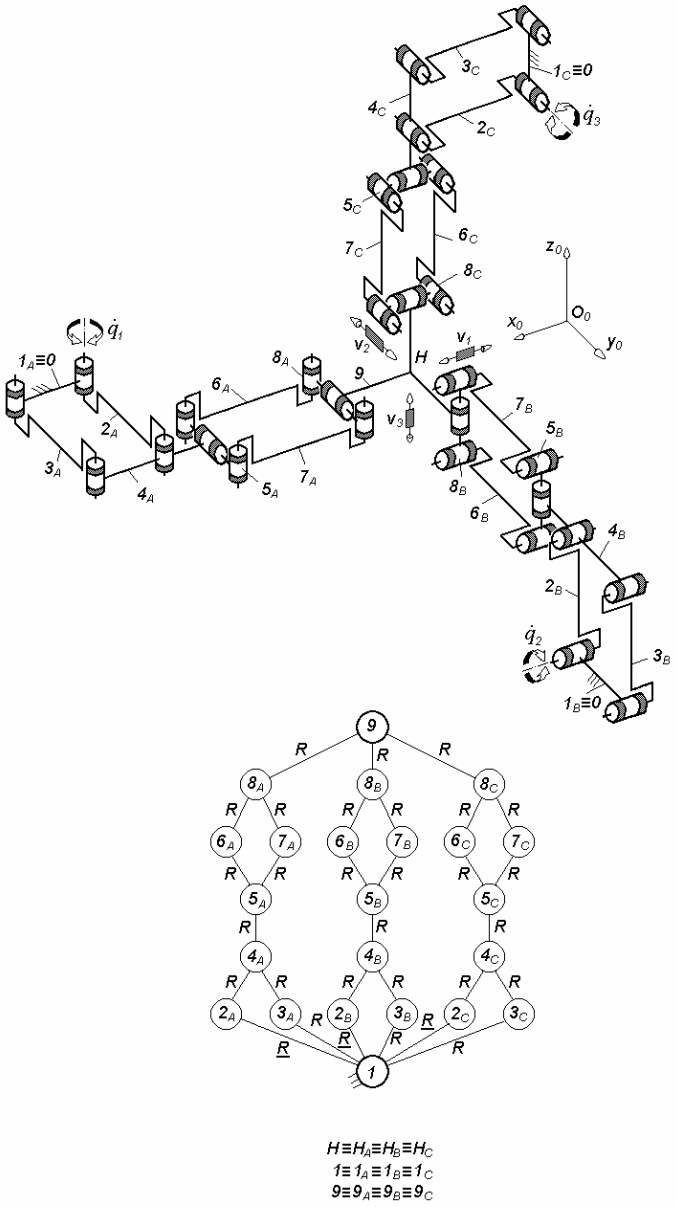

Fig. 3.95. *3-PaRPaR*-type overconstrained TPMs with coupled motions and rotating actuators mounted on the fixed base defined by $M_F = S_F = 3$, $(R_F) = (\boldsymbol{v}_1, \boldsymbol{v}_2, \boldsymbol{v}_3)$, $T_F = 0$, $N_F = 21$, limb topology $\underline{Pa} \perp R \perp Pa \perp^{\parallel} R$

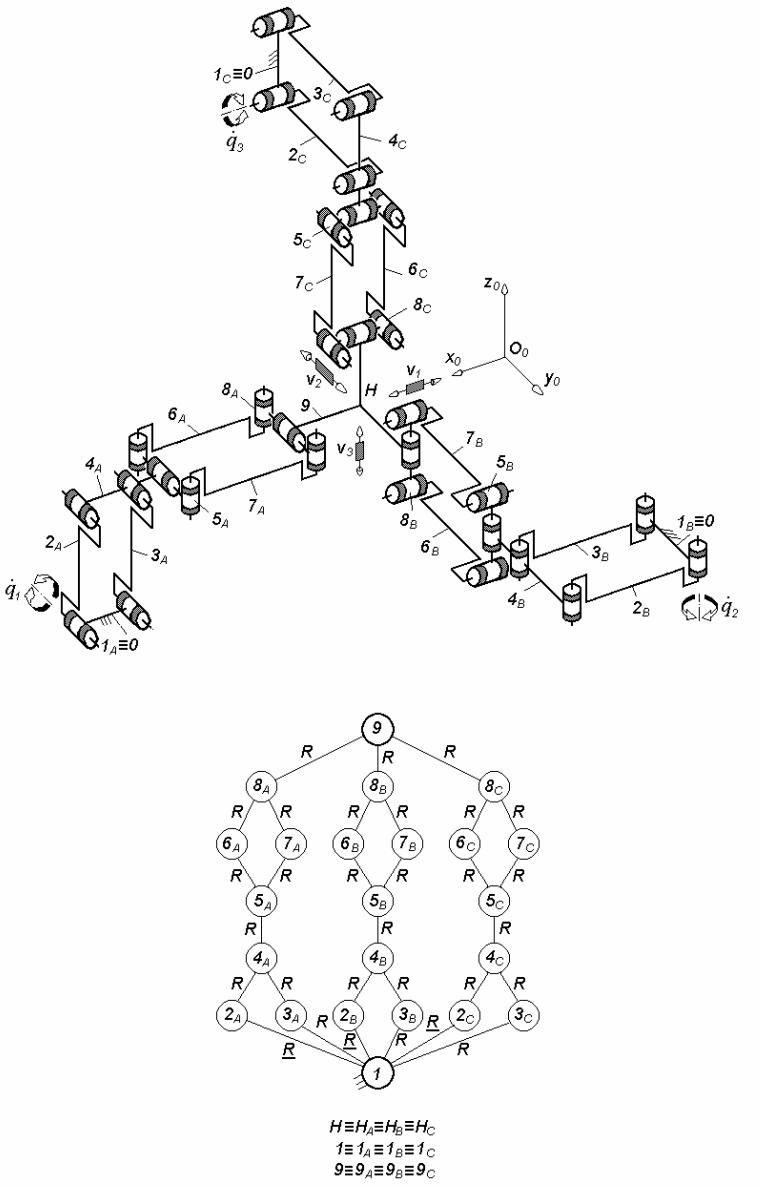

Fig. 3.96. *3-<u>Pa</u>RPaR*-type overconstrained TPMs with coupled motions and rotating actuators mounted on the fixed base, defined by $M_F = S_F = 3$, $(R_F) = (\boldsymbol{v}_1, \boldsymbol{v}_2, \boldsymbol{v}_3)$, $T_F = 0$, $N_F = 21$, limb topology $\underline{Pa}||R \perp Pa \perp {}^{||}R$

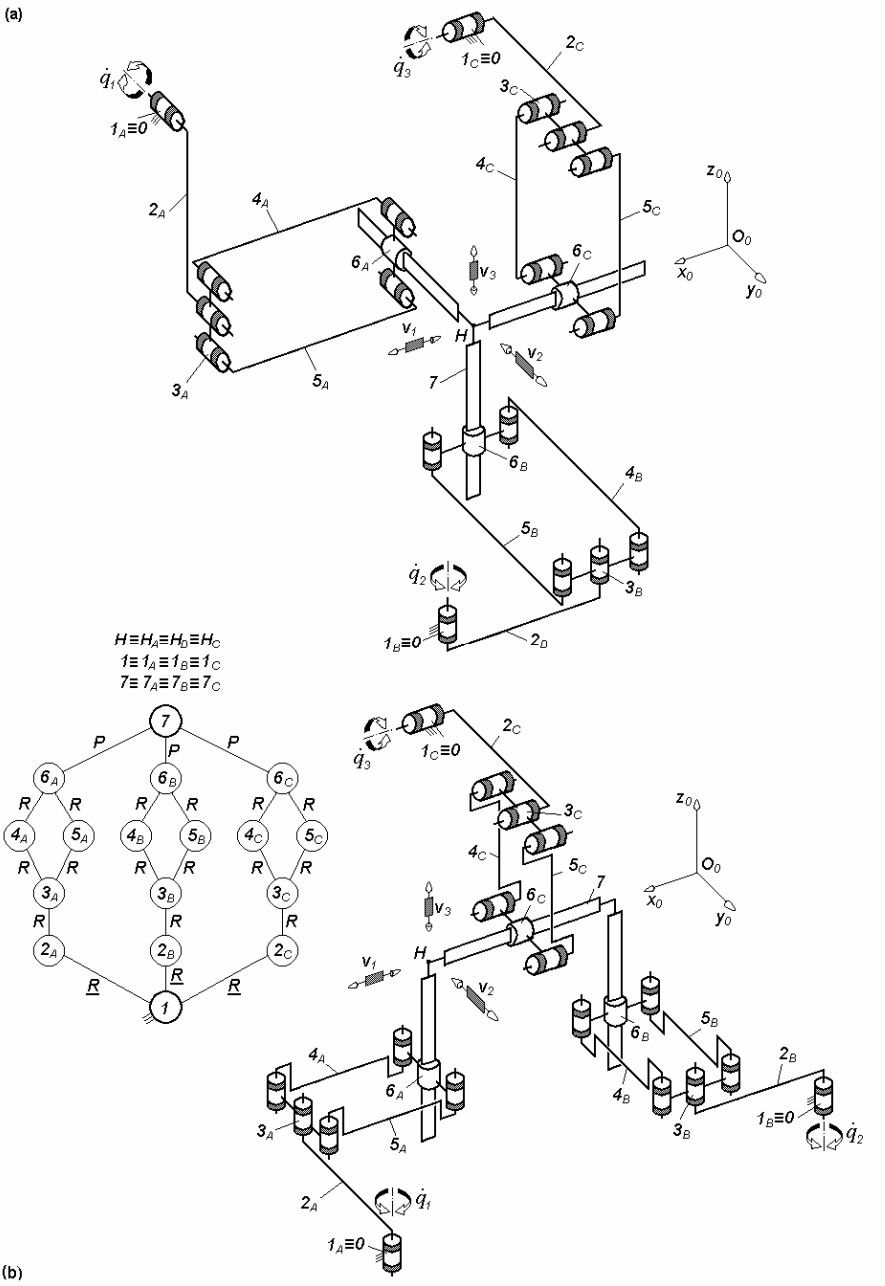

Fig. 3.97. *3-RRPaP*-type overconstrained TPMs with coupled motions and rotating actuators mounted on the fixed base, defined by $M_F = S_F = 3$, $(R_F) = (\boldsymbol{v}_1, \boldsymbol{v}_2, \boldsymbol{v}_3)$, $T_F = 0$, $N_F = 12$, limb topology $\underline{R}||R||Pa||P$

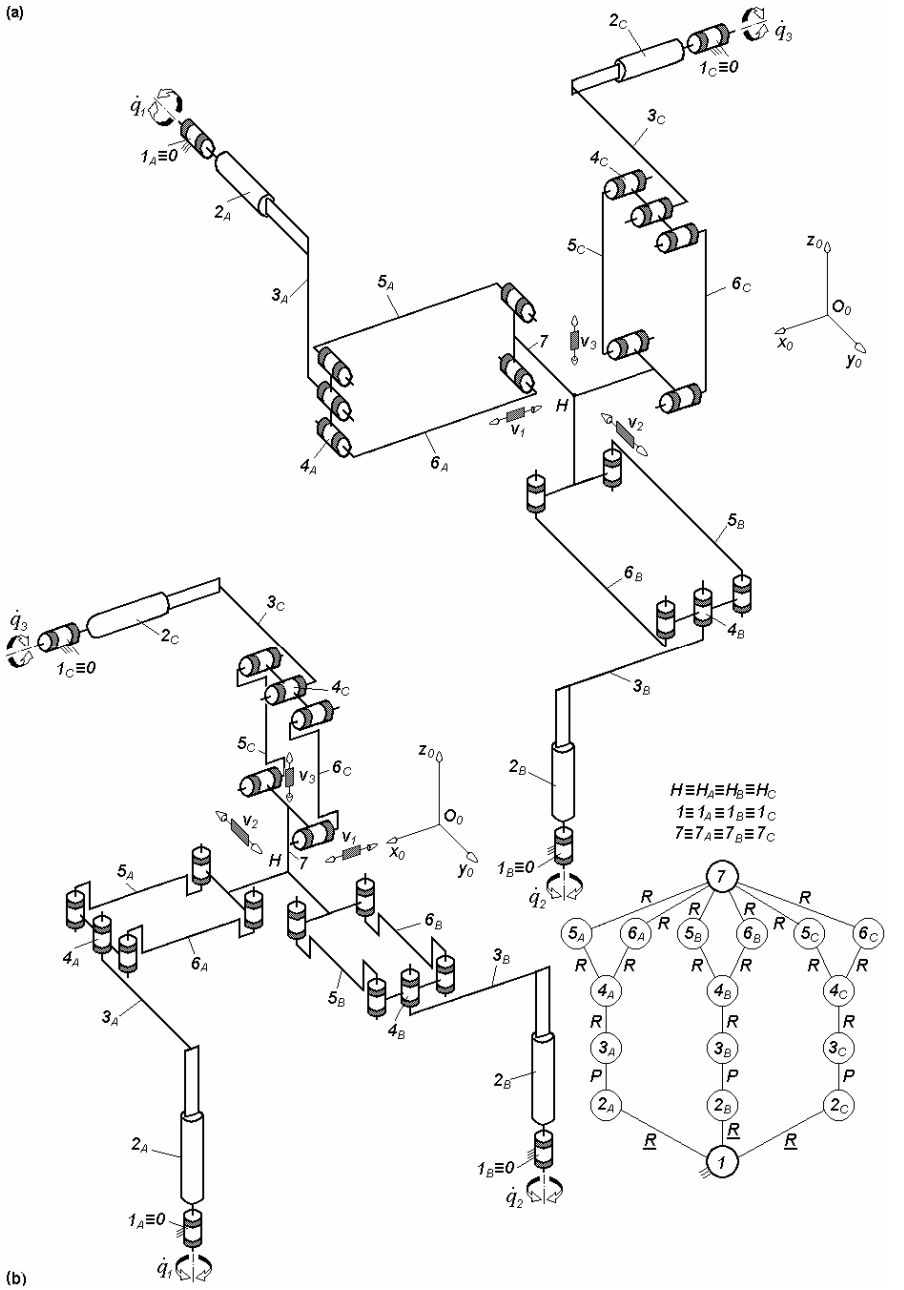

Fig. 3.98. *3-RPRPa*-type overconstrained TPMs with coupled motions and rotating actuators mounted on the fixed base, defined by $M_F = S_F = 3$, $(R_F) = (\boldsymbol{v}_1, \boldsymbol{v}_2, \boldsymbol{v}_3)$, $T_F = 0$, $N_F = 12$, limb topology $\underline{R}||P||R||Pa$

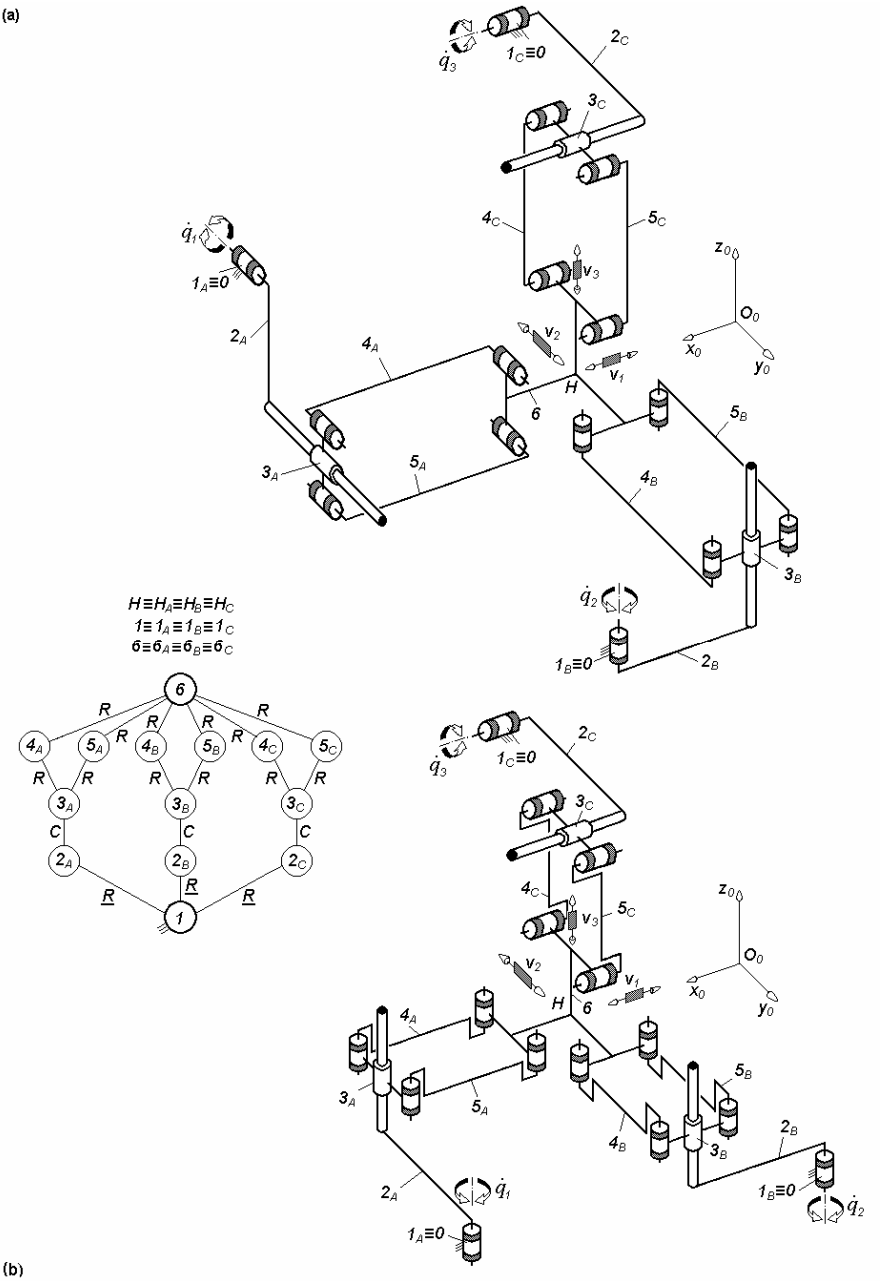

Fig. 3.99. *3-<u>R</u>CPa*-type overconstrained TPMs with coupled motions and rotating actuators mounted on the fixed base, defined by $M_F = S_F = 3$, $(R_F) = (\boldsymbol{v}_1, \boldsymbol{v}_2, \boldsymbol{v}_3)$, $T_F = 0$, $N_F = 12$, limb topology <u>R</u>||C||Pa

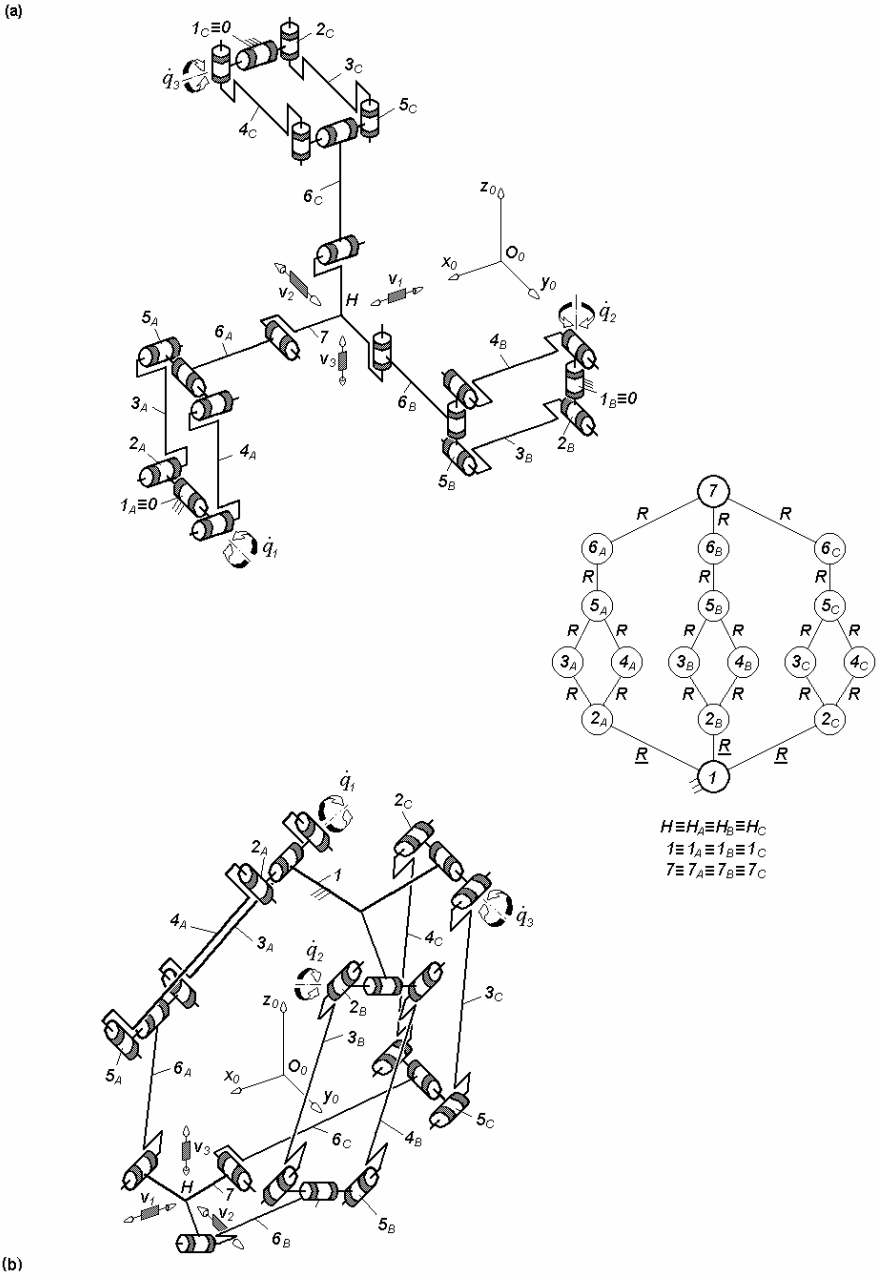

Fig. 3.100. *3-<u>R</u>PaRR*-type overconstrained TPMs with coupled motions and rotating actuators mounted on the fixed base, defined by $M_F = S_F = 3$, $(R_F) = (\boldsymbol{v}_1, \boldsymbol{v}_2, \boldsymbol{v}_3)$, $T_F = 0$, $N_F = 12$, limb topology $\underline{R} \perp Pa \perp {}^{\parallel}R||R$

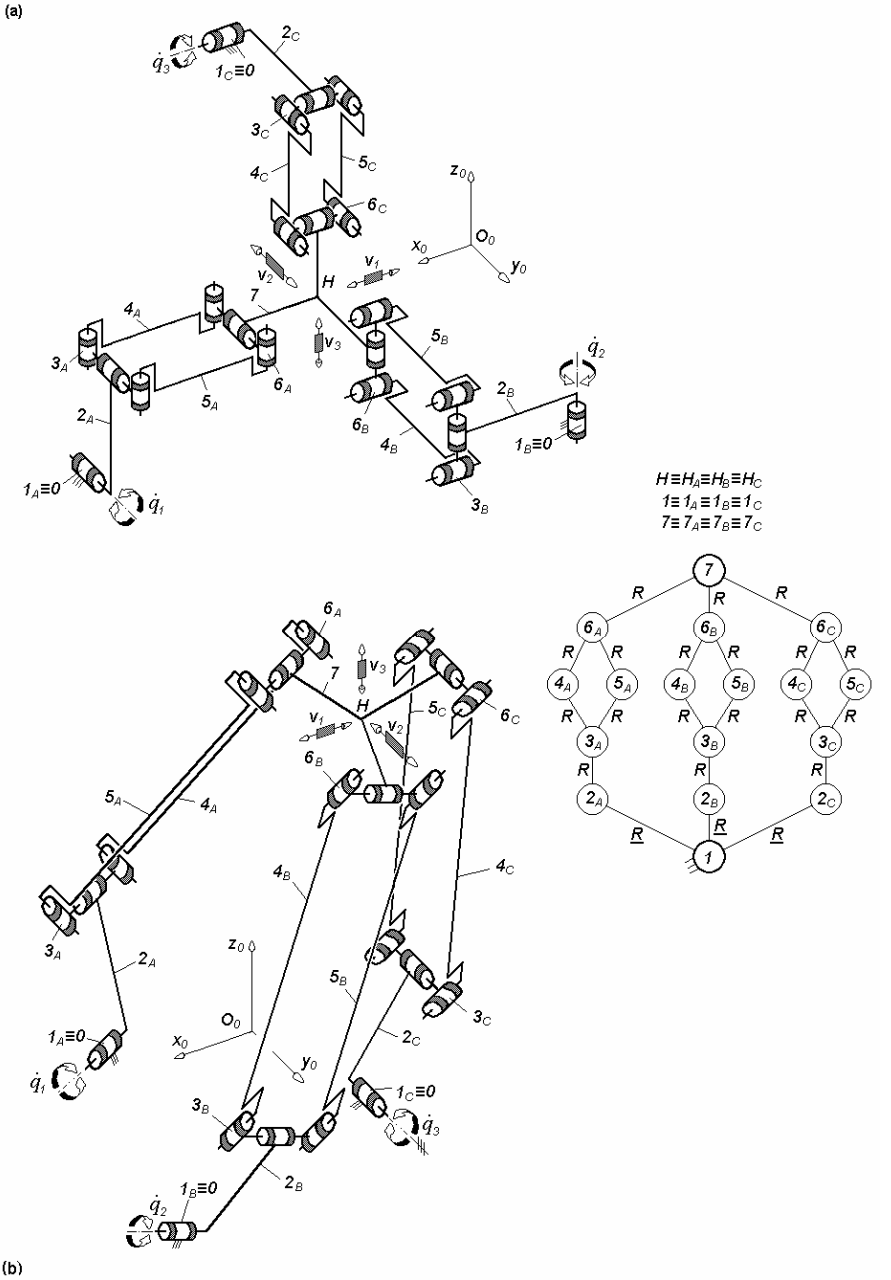

Fig. 3.101. *3-*$\underline{R}$*RRPaR*-type overconstrained TPMs with coupled motions and rotating actuators mounted on the fixed base, defined by $M_F = S_F = 3$, $(R_F) = (\boldsymbol{v}_1, \boldsymbol{v}_2, \boldsymbol{v}_3)$, $T_F = 0$, $N_F = 12$, limb topology $\underline{R} || R \perp Pa \perp {}^{||}R$

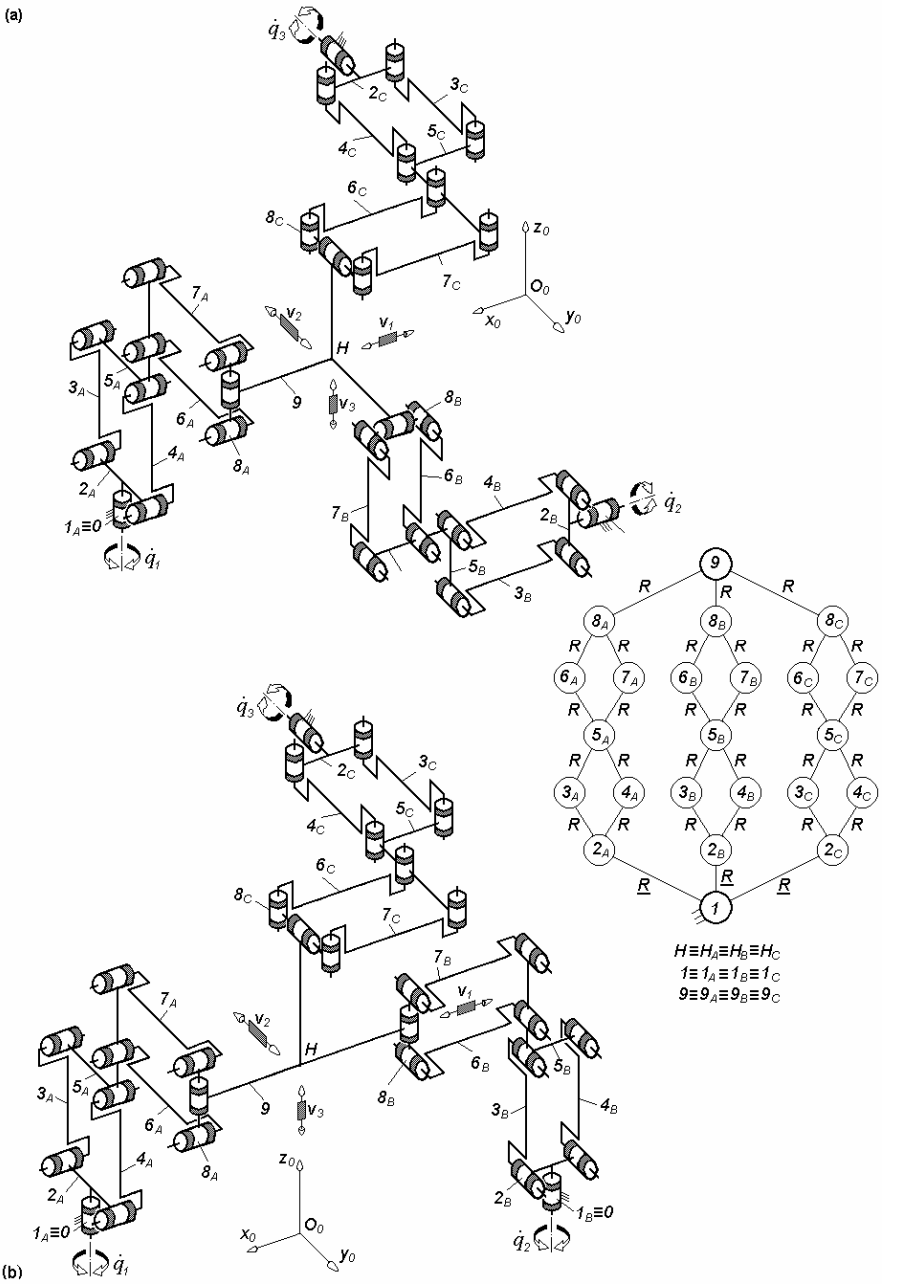

Fig. 3.102. *3-RPaPaR*-type overconstrained TPMs with coupled motions and rotating actuators mounted on the fixed base, defined by $M_F = S_F = 3$, $(R_F) = (\boldsymbol{v}_1, \boldsymbol{v}_2, \boldsymbol{v}_3)$, $T_F = 0$, $N_F = 21$, limb topology $\underline{R} \perp Pa \| Pa \perp \| R$

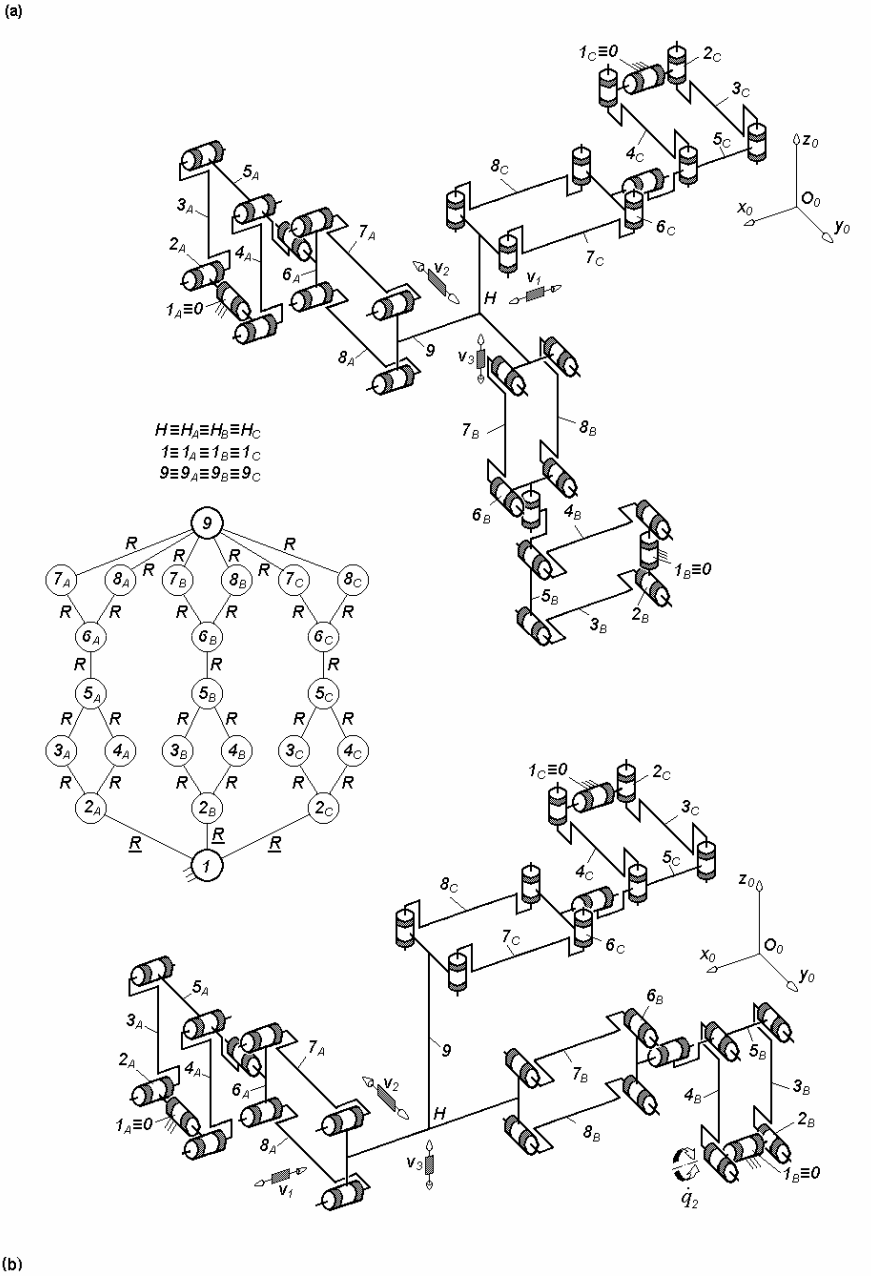

Fig. 3.103. *3-*$\underline{R}$*PaRPa*-type overconstrained TPMs with coupled motions and rotating actuators mounted on the fixed base, defined by $M_F = S_F = 3$, $(R_F) = (\boldsymbol{v}_1, \boldsymbol{v}_2, \boldsymbol{v}_3)$, $T_F = 0$, $N_F = 21$, limb topology $\underline{R} \perp Pa \perp {}^{\parallel}R \perp Pa$

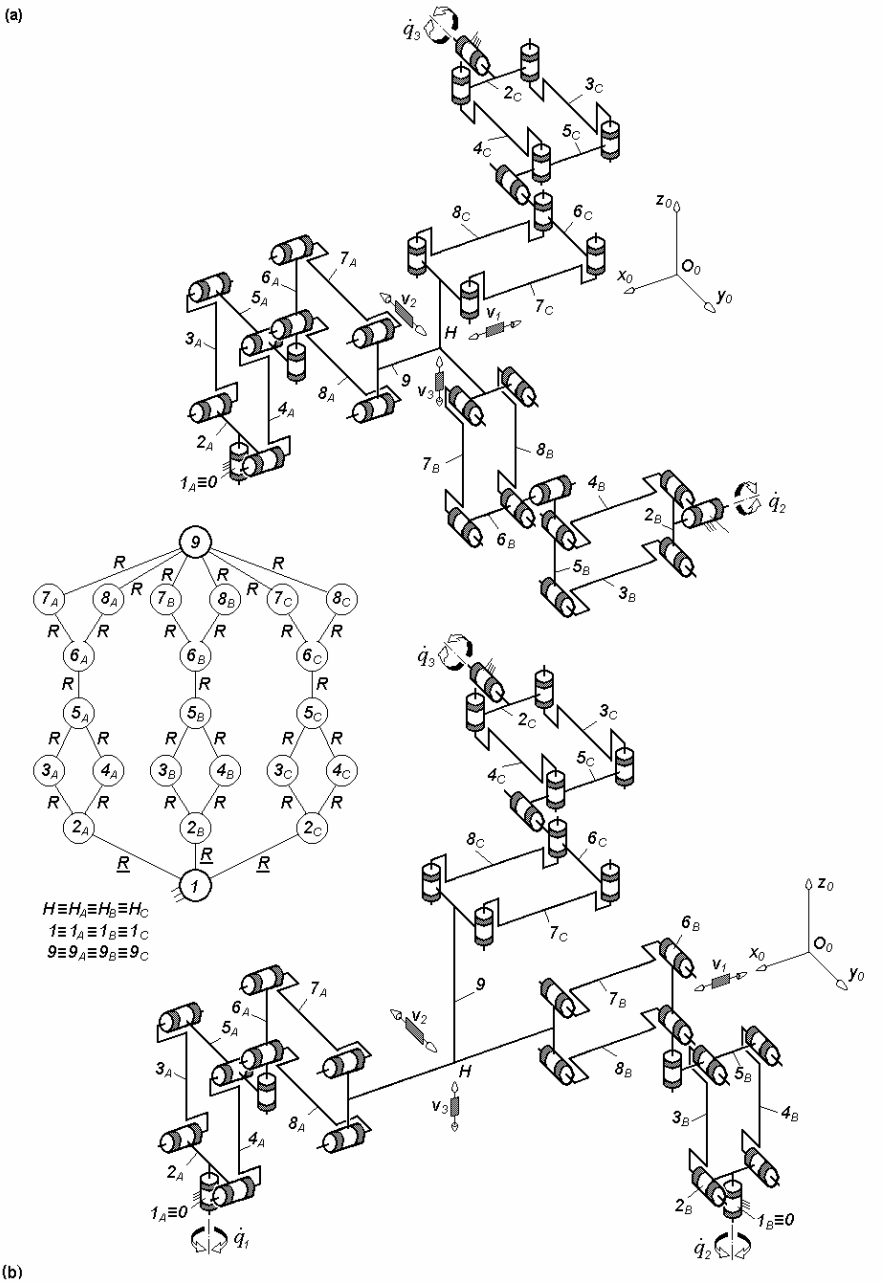

Fig. 3.104. *3-<u>R</u>PaRPa*-type overconstrained TPMs with coupled motions and rotating actuators mounted on the fixed base, defined by $M_F = S_F = 3$, $(R_F) = (\boldsymbol{v}_1, \boldsymbol{v}_2, \boldsymbol{v}_3)$, $T_F = 0$, $N_F = 21$, limb topology $\underline{R} \perp Pa \perp {}^{\parallel}R \perp Pa$

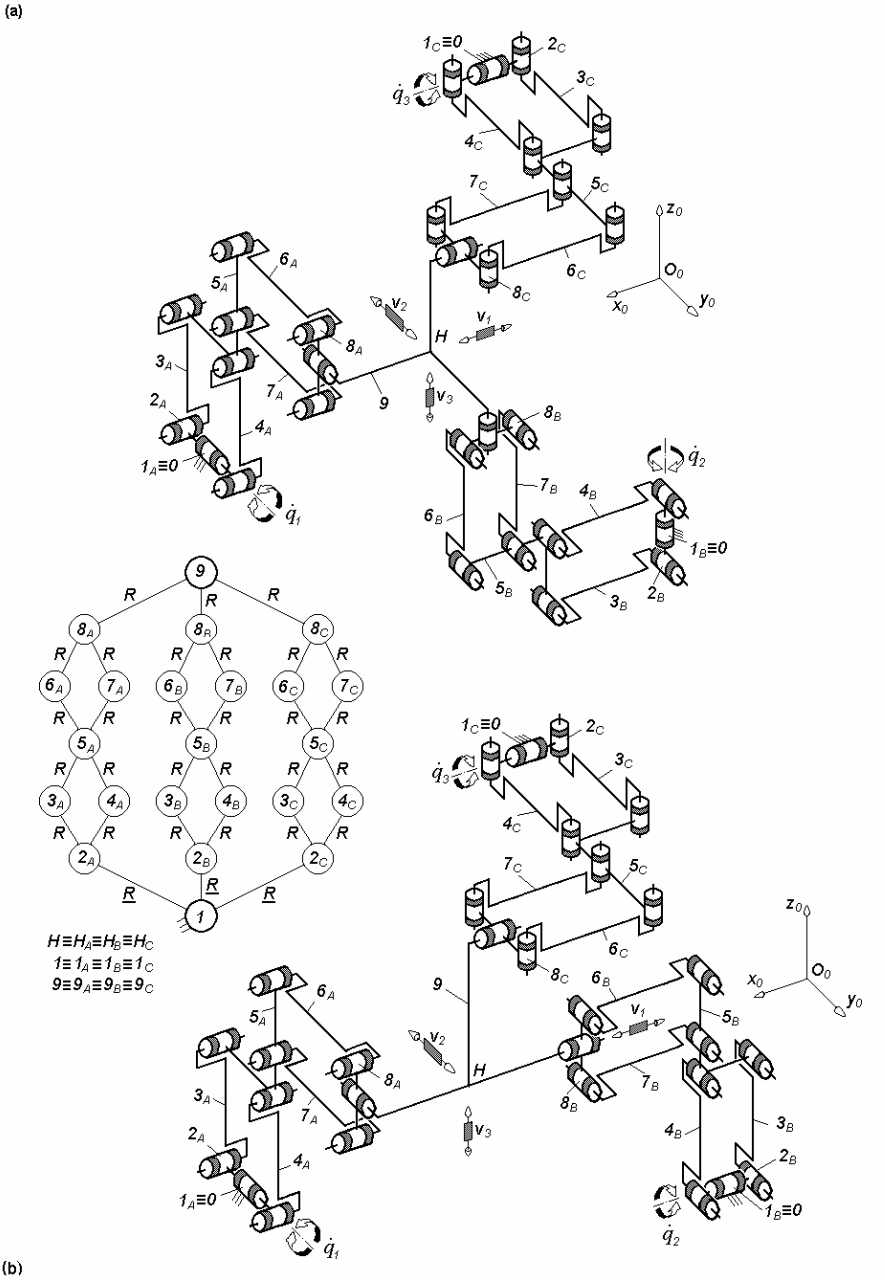

Fig. 3.105. *3-*$\underline{R}$*PaPaR*-type overconstrained TPMs with coupled motions and rotating actuators mounted on the fixed base, defined by $M_F = S_F = 3$, $(R_F) = (\boldsymbol{v}_1, \boldsymbol{v}_2, \boldsymbol{v}_3)$, $T_F = 0$, $N_F = 21$, limb topology $\underline{R} \perp Pa || Pa \perp {}^{||}R$

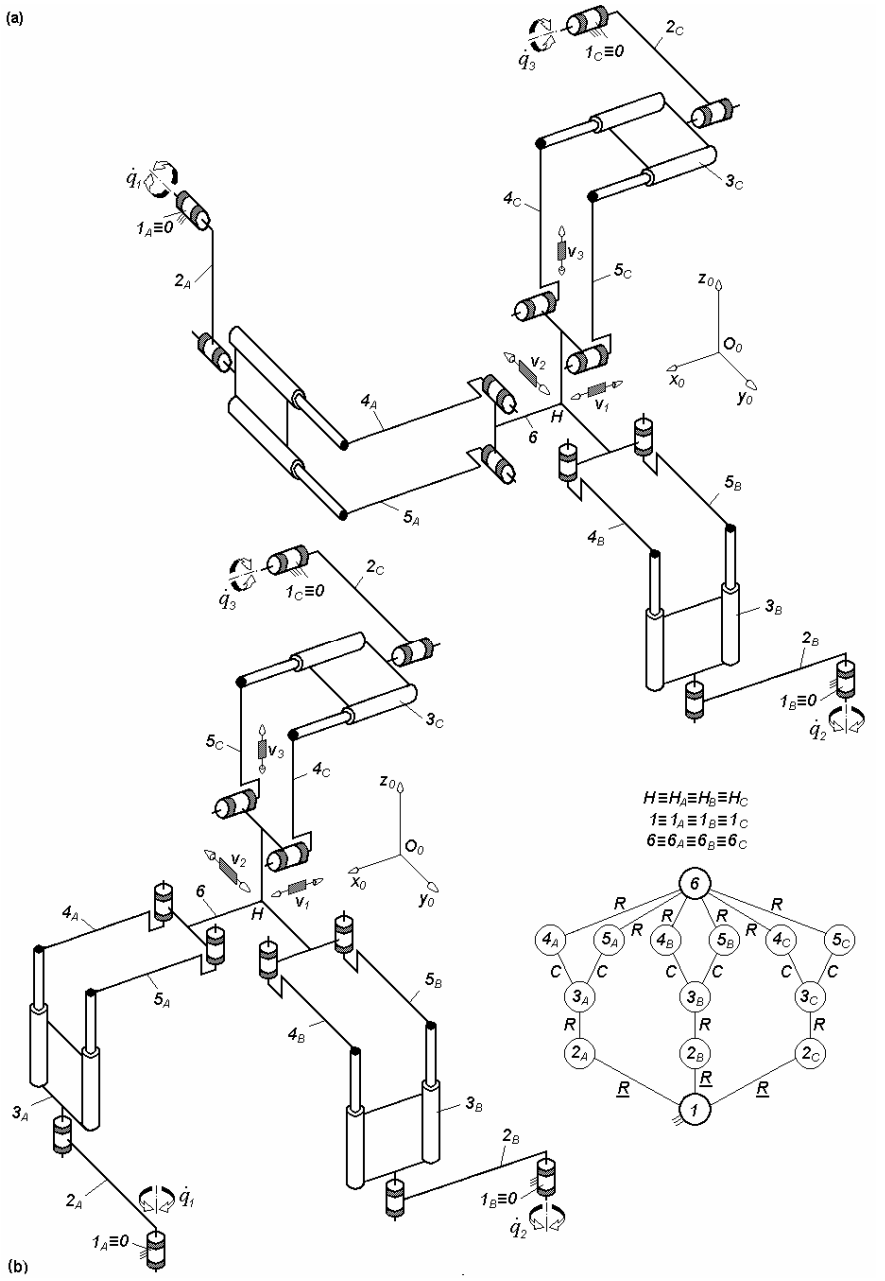

Fig. 3.106. *3-<u>R</u>RPa^{cc}*-type overconstrained TPMs with coupled motions, rotating actuators on the fixed base and six revolute joints adjacent to the moving platform, defined by $M_F = S_F = 3$, $(R_F) = (\boldsymbol{v}_1, \boldsymbol{v}_2, \boldsymbol{v}_3)$, $T_F = 0$, $N_F = 9$, limb topology <u>R</u>$||R||Pa^{cc}$

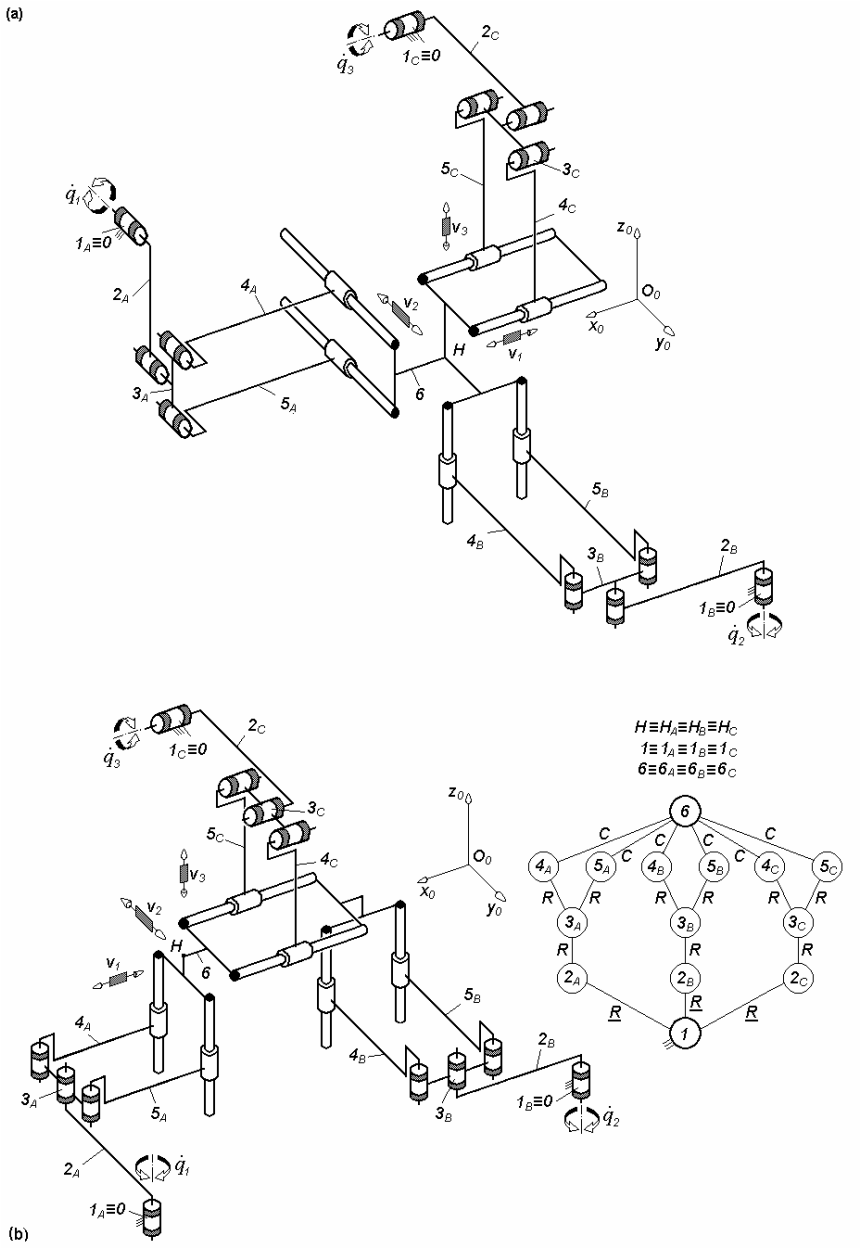

Fig. 3.107. *3-*$\underline{R}RPa^{cc}$-type overconstrained TPMs with coupled motions, rotating actuators mounted on the fixed base and six cylindrical joints adjacent to the moving platform, defined by $M_F = S_F = 3$, $(R_F) = (\boldsymbol{v}_1, \boldsymbol{v}_2, \boldsymbol{v}_3)$, $T_F = 0$, $N_F = 9$, limb topology $\underline{R}||R||Pa^{cc}$

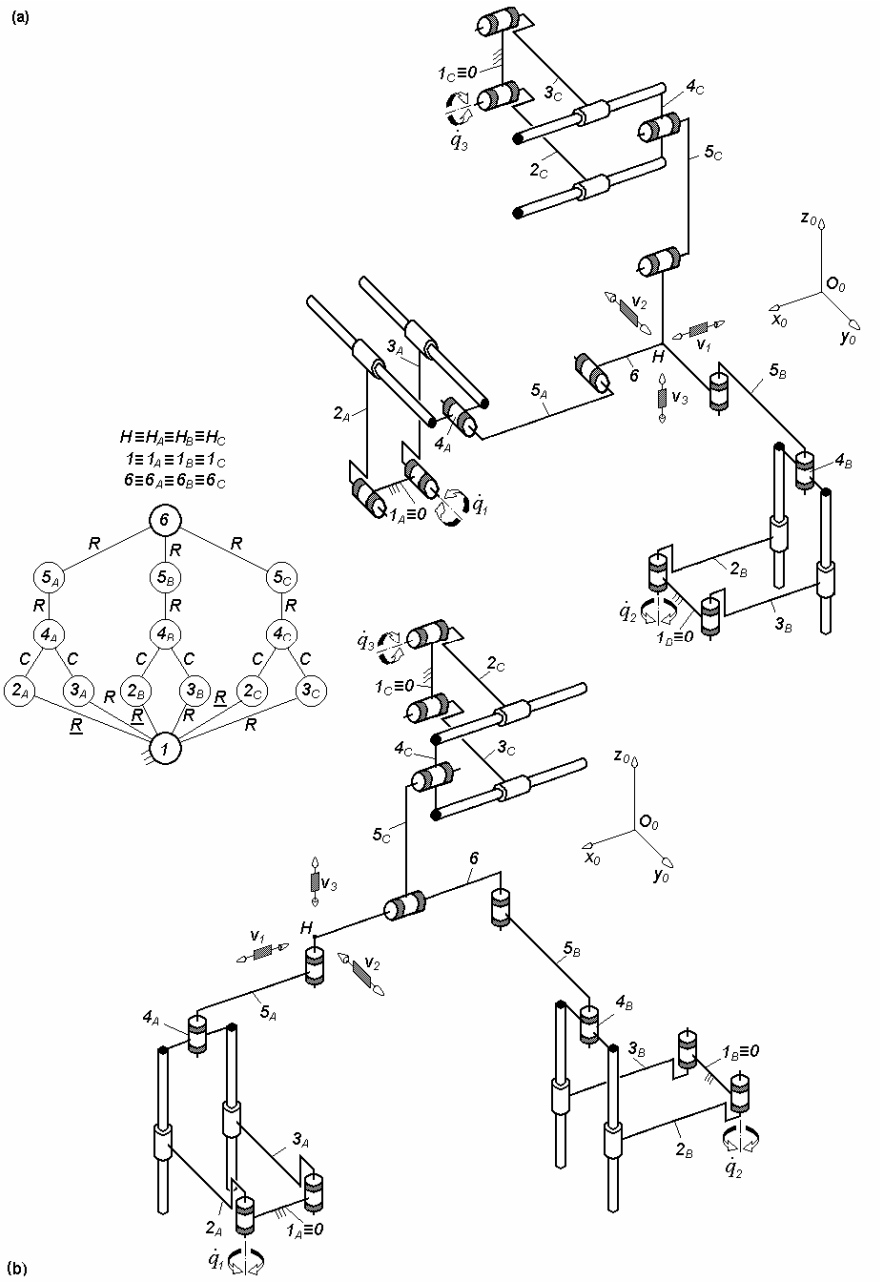

Fig. 3.108. *3-*$\underline{Pa}^{cc}$*RR*-type overconstrained TPMs with coupled motions and rotating actuators mounted on the fixed base, defined by $M_F = S_F = 3$, $(R_F) = (\boldsymbol{v}_1, \boldsymbol{v}_2, \boldsymbol{v}_3)$, $T_F = 0$, $N_F = 9$, limb topology $\underline{Pa}^{cc}||R||R$

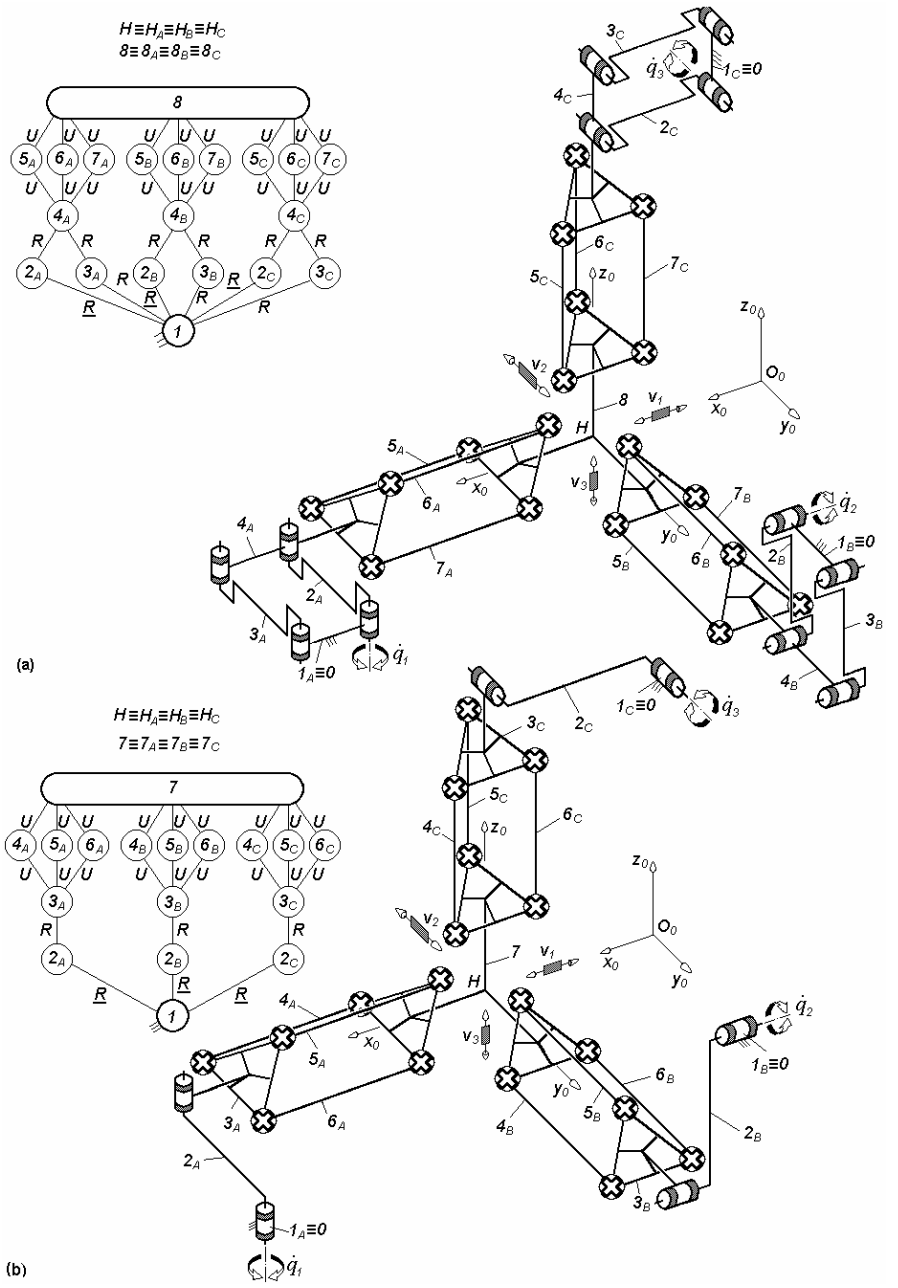

Fig. 3.109. Overconstrained TPMs with coupled motions of types *3-PaPr* (**a**) and *3-RRPr* (**b**) defined by $M_F = S_F = 3$, $(R_F) = (\boldsymbol{v}_1, \boldsymbol{v}_2, \boldsymbol{v}_3)$, $T_F = 0$, $N_F = 21$ (**a**), $N_F = 9$ (**b**), limb topology *Pa-Pr* (**a**) and *3-R||R-Pr* (**b**)

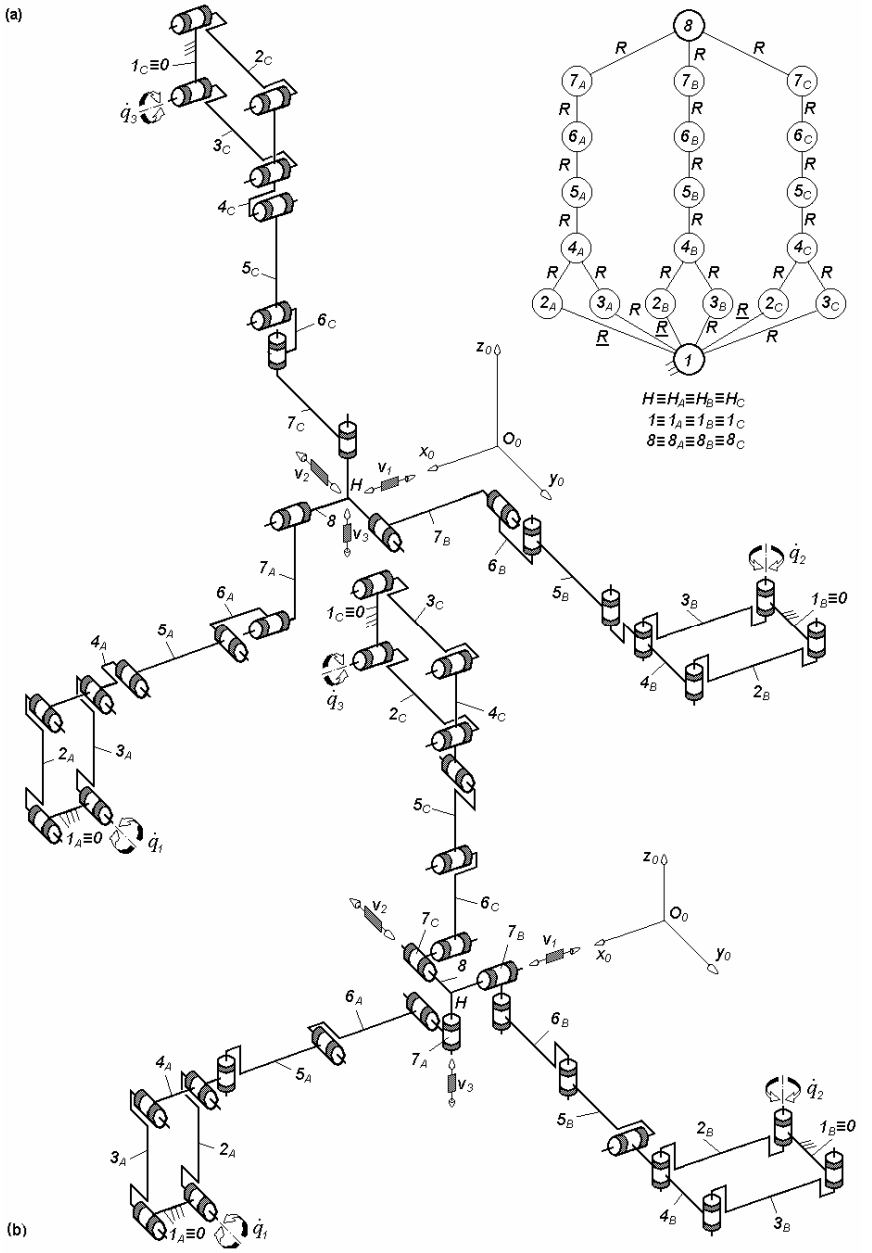

Fig. 3.110. *3-PaRRRR* -type overconstrained TPMs with coupled motions and rotating actuators mounted on the fixed base, defined by $M_F = S_F = 3$, $(R_F) = (\boldsymbol{v}_1, \boldsymbol{v}_2, \boldsymbol{v}_3)$, $T_F = 0$, $N_F = 9$, limb topology $\underline{Pa}||R||R \perp R||R$ (**a**) and $\underline{Pa} \perp R \perp R||R \perp R$ (**b**)

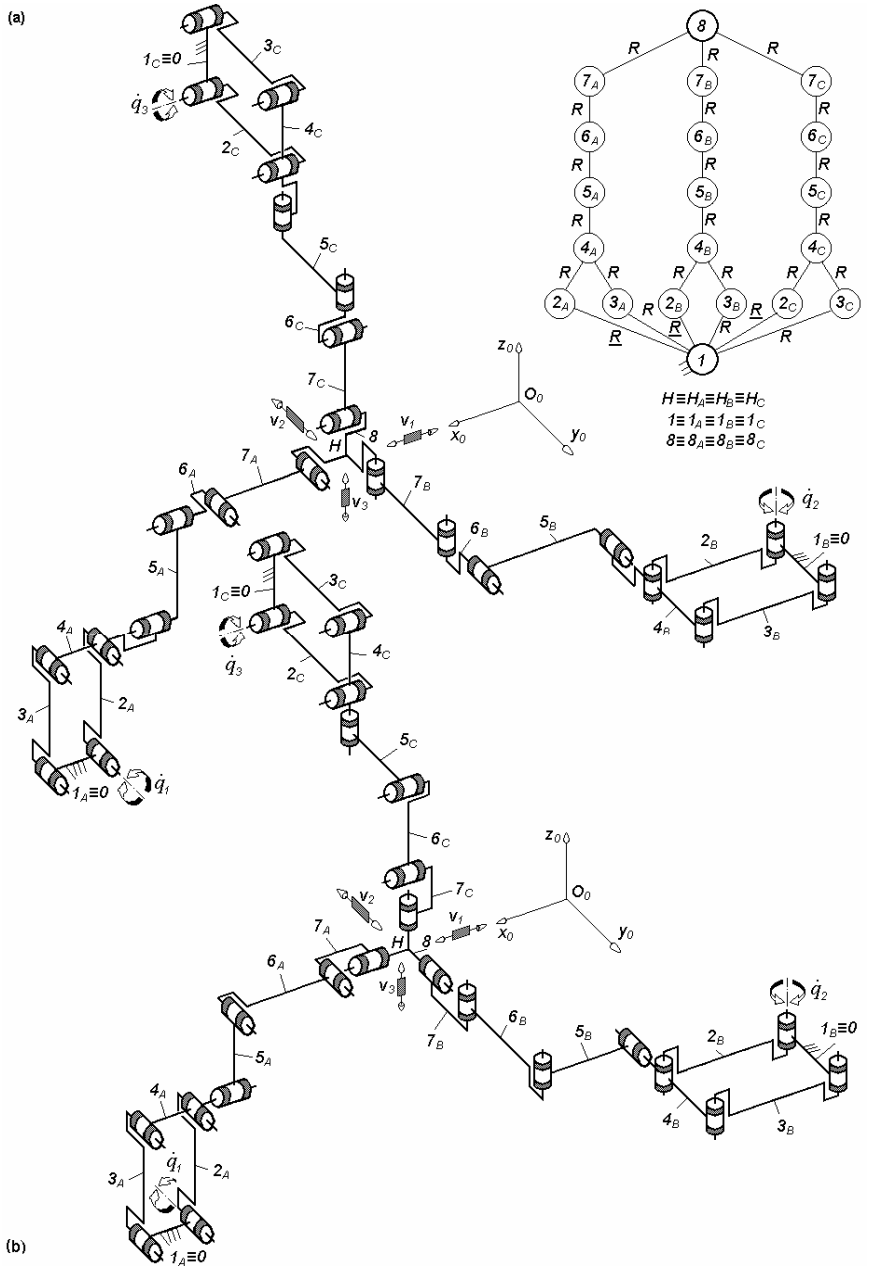

Fig. 3.111. *3-PaRRRR*-type overconstrained TPMs with coupled motions and rotating actuators mounted on the fixed base, defined by $M_F = S_F = 3$, $(R_F) = (\boldsymbol{v}_1, \boldsymbol{v}_2, \boldsymbol{v}_3)$, $T_F = 0$, $N_F = 9$, limb topology $\underline{Pa} \perp R || R \perp {}^{||}R || R$ (**a**) and $\underline{Pa} \perp R \perp R || R \perp {}^{||}R$ (**b**)

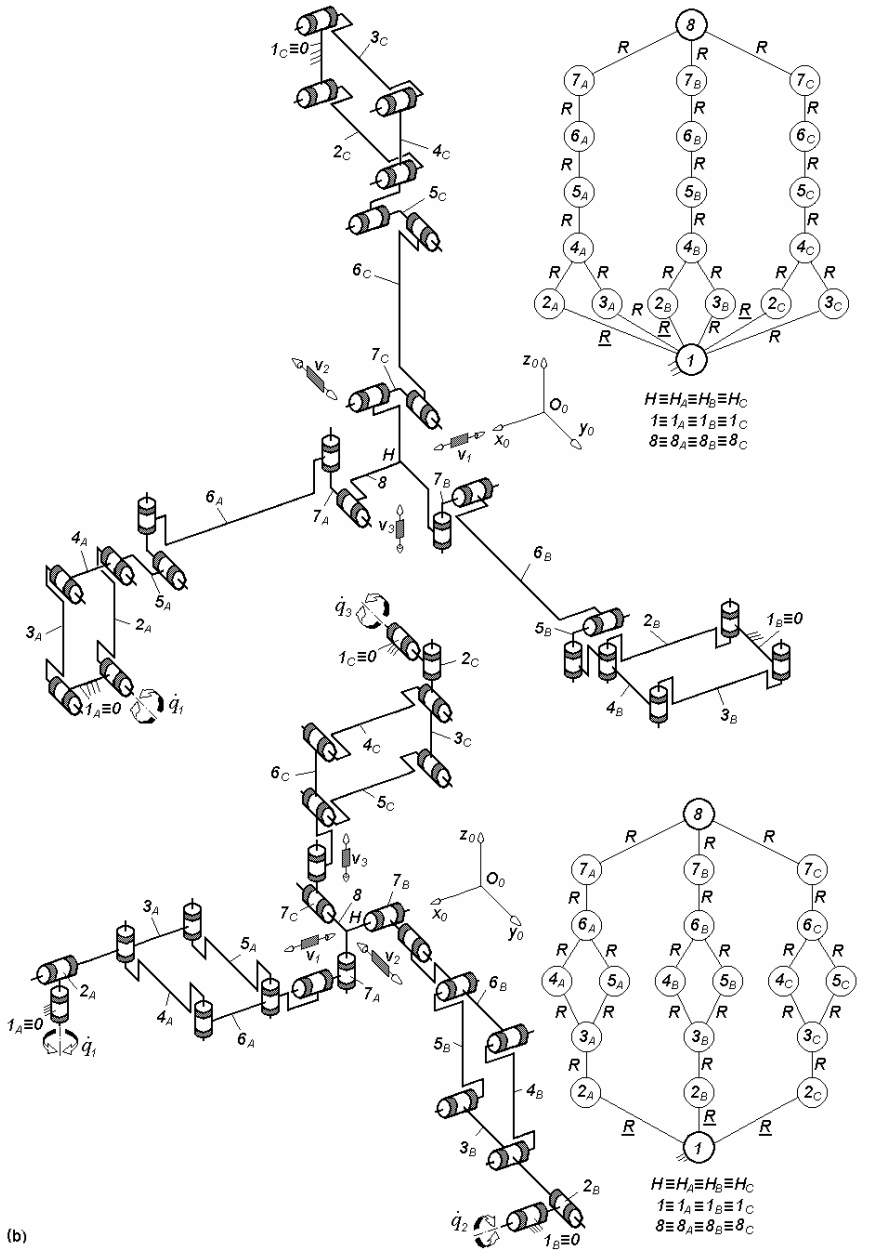

Fig. 3.112. Overconstrained TPMs of types *3-*$\underline{Pa}$*RRRR* (**a**) and *3-*$\underline{R}$*RPaRR* (**b**) with coupled motions defined by $M_F = S_F = 3$, $(R_F) = (\boldsymbol{v}_1, \boldsymbol{v}_2, \boldsymbol{v}_3)$, $T_F = 0$, $N_F = 9$, limb topology $\underline{Pa}||R \perp R||R \perp {}^{||}R$ (**a**) and $\underline{R} \perp R \perp {}^{||}Pa \perp {}^{||}R \perp R$ (**b**)

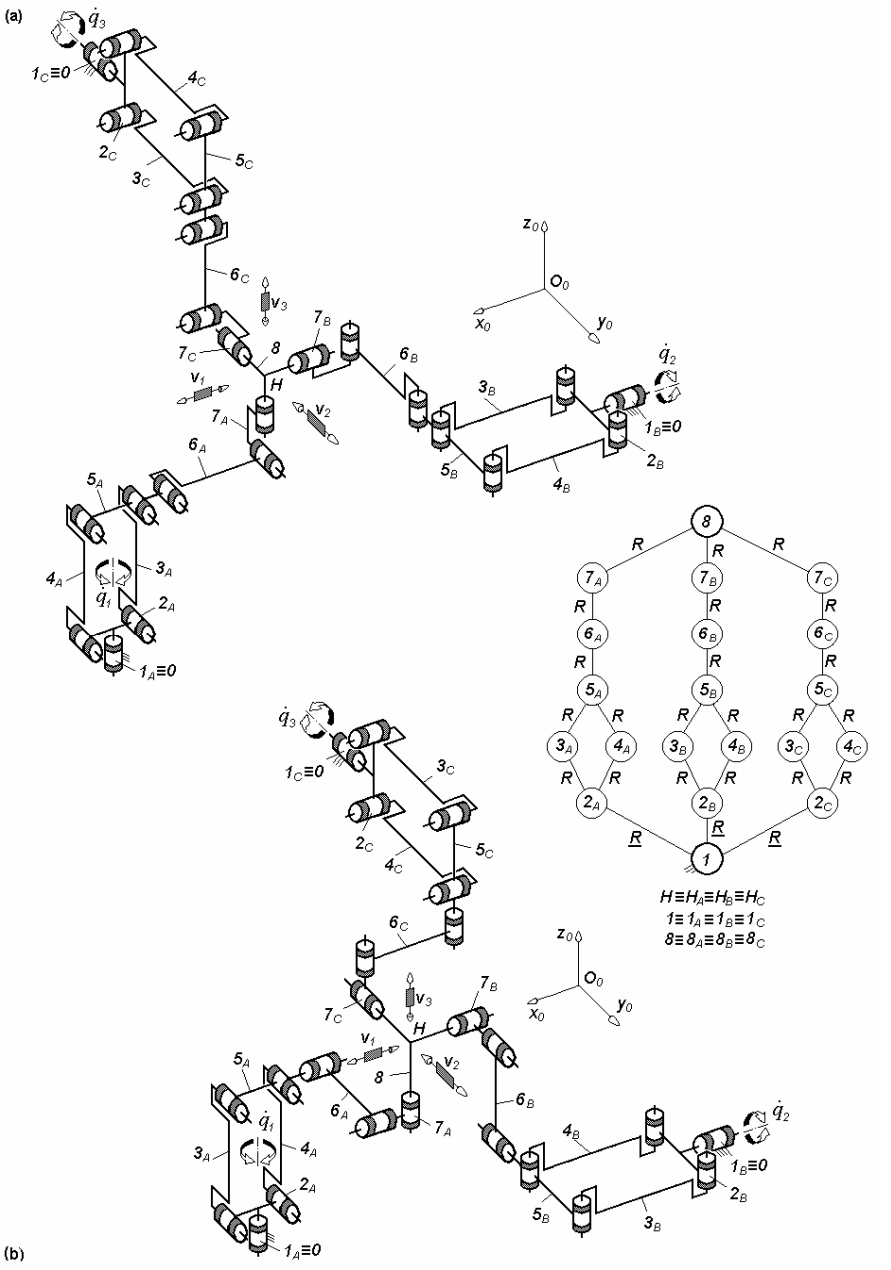

Fig. 3.113. *3-RPaRRR*-type overconstrained TPMs with coupled motions and rotating actuators mounted on the fixed base, defined by $M_F = S_F = 3$, $(R_F) = (\boldsymbol{v}_1, \boldsymbol{v}_2, \boldsymbol{v}_3)$, $T_F = 0$, $N_F = 9$, limb topology $\underline{R} \perp Pa || R || R \perp^{||} R$ (**a**) and $\underline{R} \perp Pa \perp^{\perp} R || R \perp^{\perp} R$ (**b**)

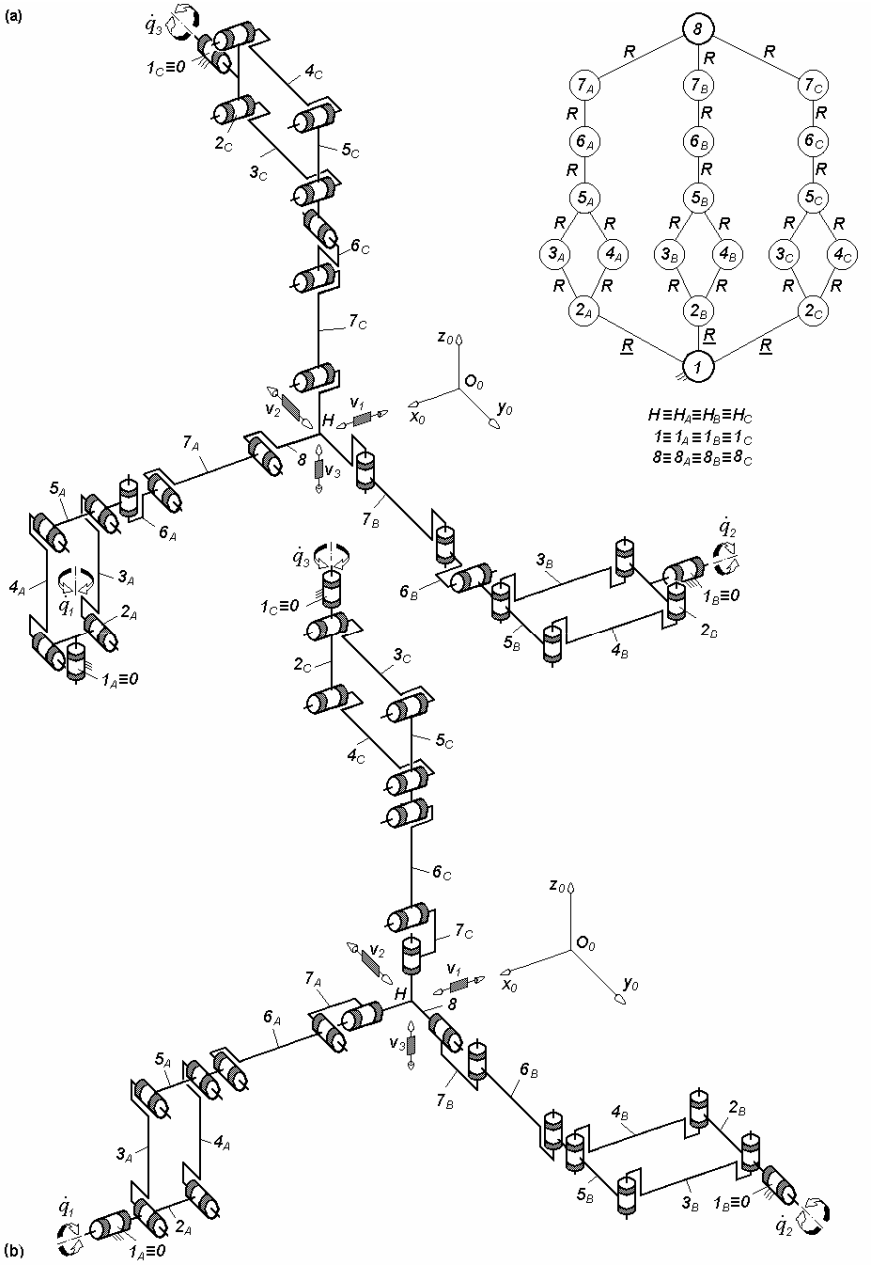

Fig. 3.114. *3-RPaRRR* -type overconstrained TPMs with coupled motions and rotating actuators mounted on the fixed base, defined by $M_F = S_F = 3$, $(R_F) = (\boldsymbol{v}_1, \boldsymbol{v}_2, \boldsymbol{v}_3)$, $T_F = 0$, $N_F = 9$, limb topology $\underline{R} \perp Pa \perp^{\parallel} R \perp R \| R$ (**a**) and $\underline{R} \perp Pa \| R \| R \perp^{\parallel} R$ (**b**)

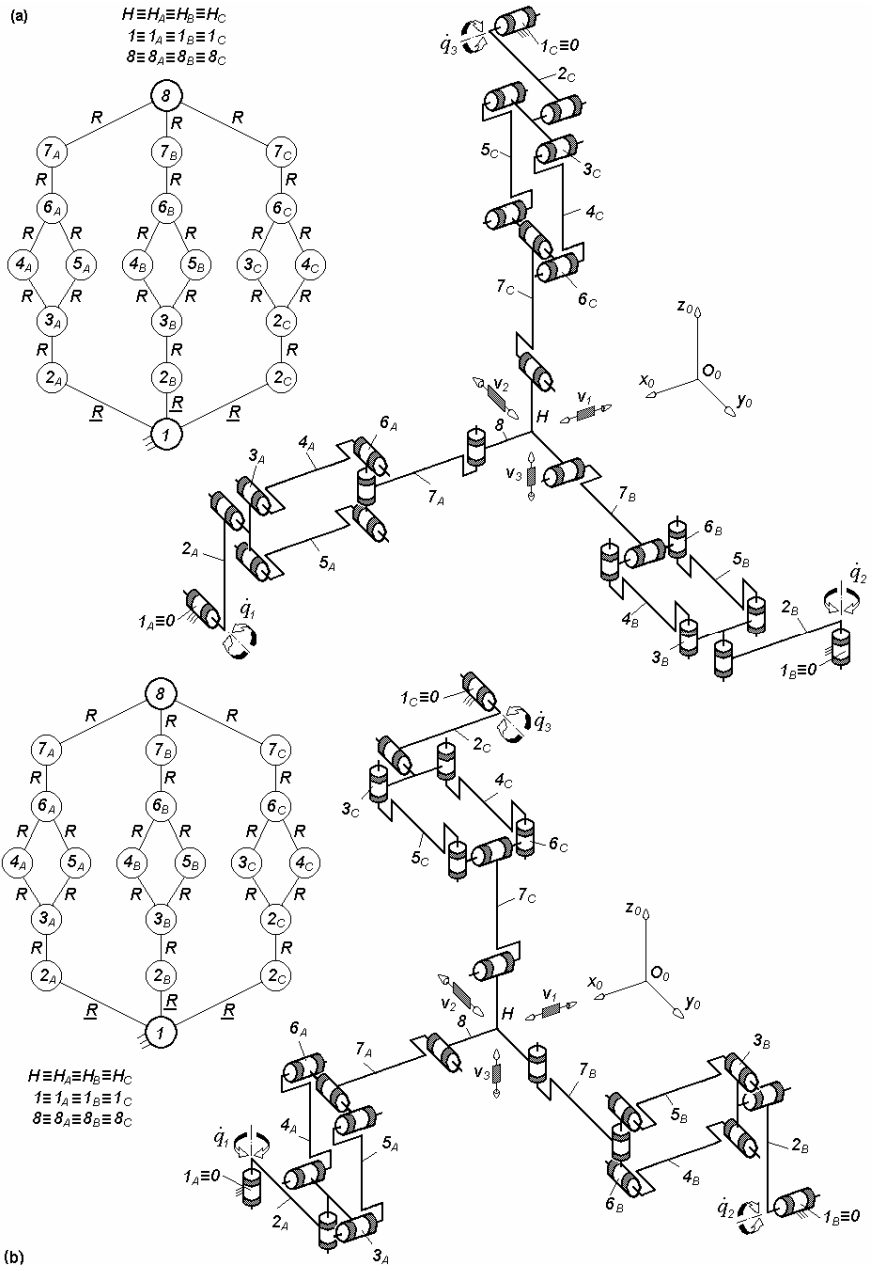

Fig. 3.115. *3-RRPaRR* -type overconstrained TPMs with coupled motions and rotating actuators mounted on the fixed base, defined by $M_F = S_F = 3$, $(R_F) = (\boldsymbol{v}_1, \boldsymbol{v}_2, \boldsymbol{v}_3)$, $T_F = 0$, $N_F = 9$, limb topology $\underline{R}||R||Pa \perp R||R$ (**a**) and $\underline{R}||R \perp Pa \perp^{\perp} R||R$ (**b**)

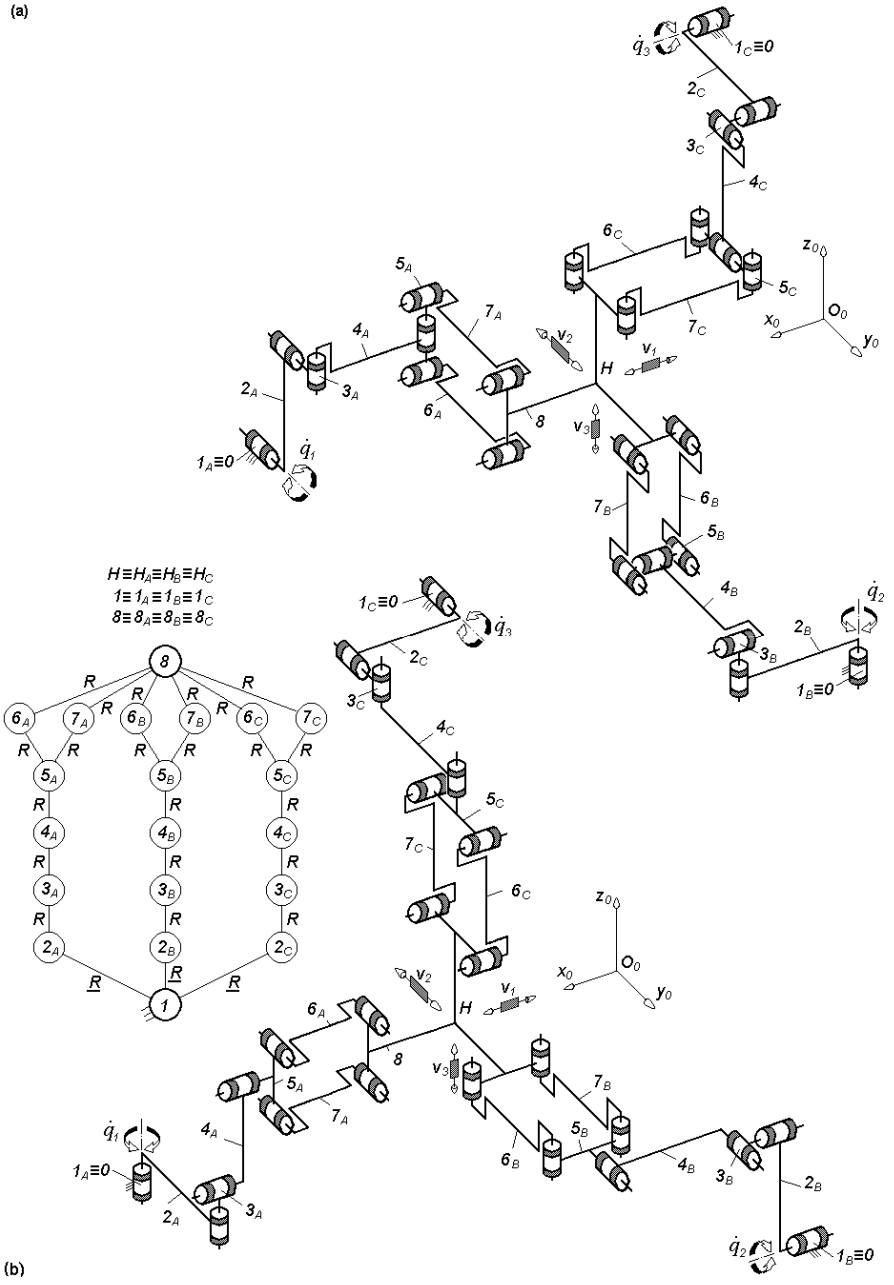

Fig. 3.116. *3-RRRRPa*-type overconstrained TPMs with coupled motions and rotating actuators mounted on the fixed base, defined by $M_F = S_F = 3$, $(R_F) = (\boldsymbol{v}_1, \boldsymbol{v}_2, \boldsymbol{v}_3)$, $T_F = 0$, $N_F = 9$, limb topology $\underline{R}||R \perp R||R \perp^{\perp} Pa$

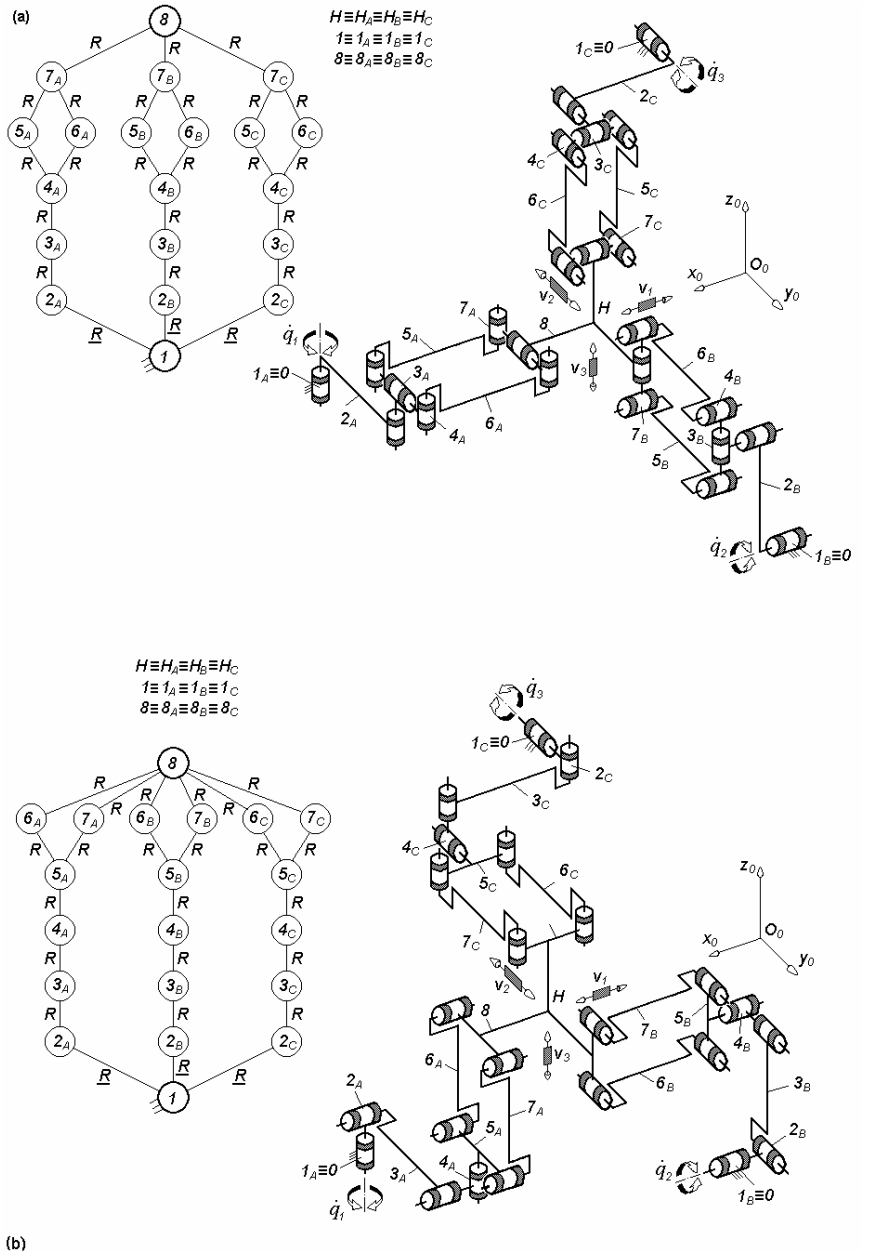

Fig. 3.117. Overconstrained TPMs of types *3-*$\underline{R}$*RRPaR* (**a**) and *3-*$\underline{R}$*RRRPa* (**b**) with coupled motions and rotating actuators mounted on the fixed base, defined by $M_F = S_F = 3$, $(R_F) = (\boldsymbol{v}_1, \boldsymbol{v}_2, \boldsymbol{v}_3)$, $T_F = 0$, $N_F = 9$, limb topology $\underline{R}||R \perp R \perp Pa \perp {}^{||}R$ (**a**) and $\underline{R} \perp R||R \perp R \perp Pa$ (**b**)

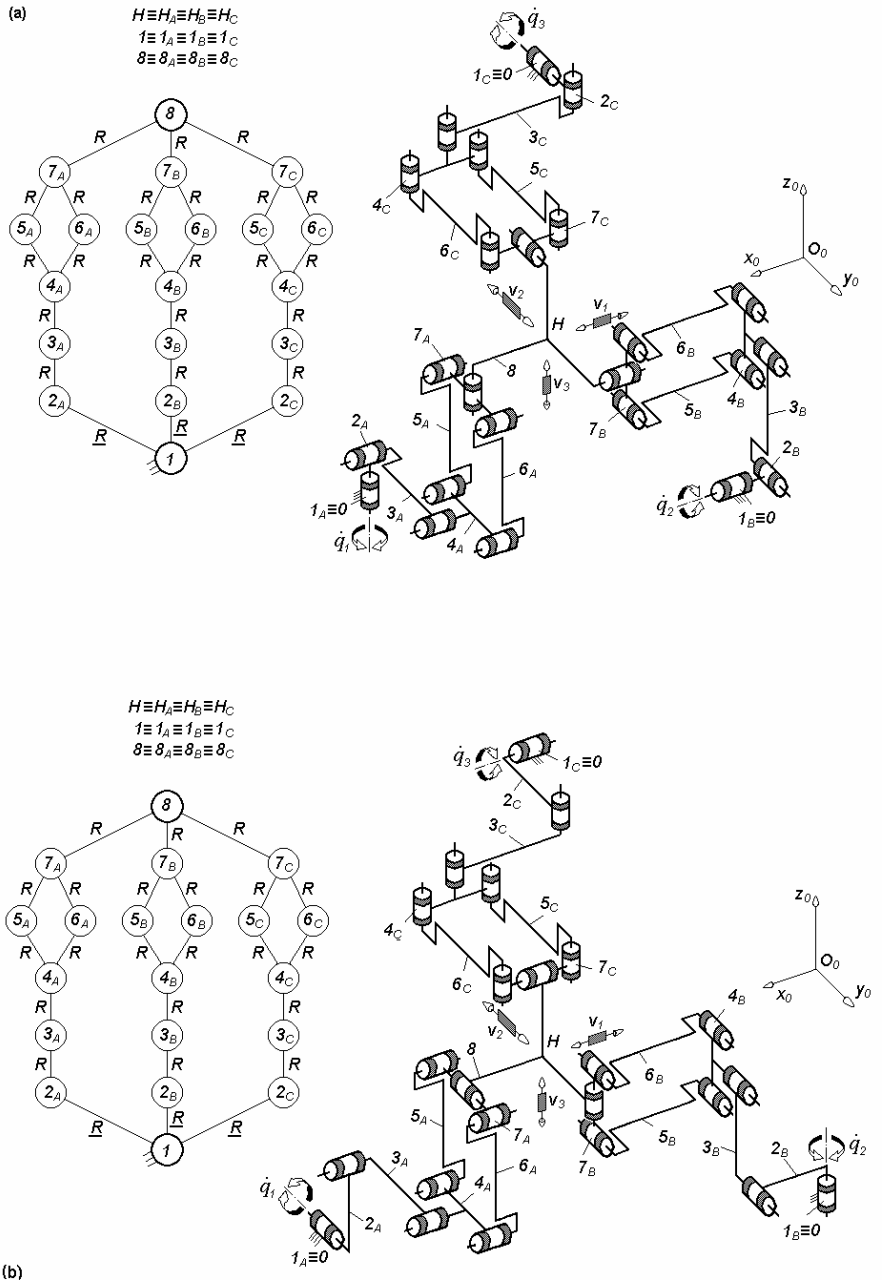

Fig. 3.118. *3-<u>R</u>RRPaR*-type overconstrained TPMs with coupled motions and rotating actuators mounted on the fixed base, defined by $M_F = S_F = 3$, $(R_F) = (\boldsymbol{v}_1, \boldsymbol{v}_2, \boldsymbol{v}_3)$, $T_F = 0$, $N_F = 9$, limb topology $\underline{R} \perp R || R || Pa \perp {}^{||}R$

3.4 Derived solutions with rotating actuators

Solutions with lower degrees of overconstraint can be derived from the basic solutions in Figs. 3.71–3.118 by using joints with idle mobilities. A large set of solutions can be obtained by introducing adequate idle mobilities inside and/or outside the parallelogram loops.

For example, the solution *3-PaPaC**-type in Fig. 3.119 is derived from the solution *3-PaPaP*-type in Fig. 3.71 by replacing in each leg the prismatic joint *P* by a cylindrical joint *C** combining one rotational idle mobility.

We recall that the joints combining idle mobilities are denoted by an asterisk. The idle mobilities that can be combined in a parallelogram loop (see Fig. 6.3 – Part 1) are systematized in Table 3.7. One rotational idle mobility is combined in each cylindrical joint *C** outside the parallelogram loop. The rotational mobility of the revolute joint denoted by *R** is an idle mobility. Two idle rotational mobilities are introduced in the spherical joint of the parallelogram loops denoted by Pa^{ccs} and Pa^{scc} which combines two cylindrical, one revolute and one spherical joint (see Figs. 3.147–3.151 and 3.194–3.196).

Examples of solutions with identical limbs and 3–30 degrees of overconstraint derived from the basic solutions in Figs. 3.71–3.82 and 3.87–3.109 are illustrated in Figs. 3.119–3.198. The limb topology and the number of overconstraints of these solutions are systematized in Table 3.32, and their structural parameters in Tables 3.33–3.44.

Table 3.32. Limb topology and the number of overconstraints N_F of the derived TPMs with idle mobilities and rotating actuators mounted on the fixed base presented in Figs. 3.119–3.198

No.	Basic TPM Type	N_F	Derived TPM Type	N_F	Limb topology
1	*3-<u>Pa</u>PaP* (Fig. 3.71)	*24*	*3-<u>Pa</u>PaC** (Fig. 3.119)	*21*	$\underline{Pa} \perp Pa \| \| C^*$
2			*3-<u>Pa</u>R*PaC** (Fig. 3.131)	*18*	$\underline{Pa} \| \| R \perp Pa \| \| C^*$
3			*3-<u>Pa</u>*Pa^{ss}P* (Fig. 3.143)	*3*	$\underline{Pa}^* \perp Pa^{ss} \| \| P$
4	*3-<u>Pa</u>PaP* (Fig. 3.72)	*24*	*3-<u>Pa</u>PaC** (Fig. 3.120)	*21*	$\underline{Pa} \| \| Pa \| \| C^*$
5			*3-<u>Pa</u>R*PaC** (Fig. 3.132)	*18*	$\underline{Pa} \perp R^* \perp {}^{\|\|}Pa \| \| C^*$
6			*3-<u>Pa</u>*Pa^{ss}P* (Fig. 3.144)	*3*	$\underline{Pa}^* \| \| Pa^{ss} \| \| P$
7	*3-<u>Pa</u>PPa* (Fig. 3.73)	*24*	*3-<u>Pa</u>C*Pa* (Fig. 3.121)	*21*	$\underline{Pa} \perp C^* \| \| Pa$
8			*3-<u>Pa</u>C*PaR** (Fig. 3.133)	*18*	$\underline{Pa} \perp C^* \| \| Pa \perp {}^{\|\|}R^*$
9			*3-<u>Pa</u>*PPa^{ss}* (Fig. 3.145)	*3*	$\underline{Pa}^* \perp P \| \| Pa^{ss}$
10	*3-<u>Pa</u>PPa* (Fig. 3.74)	*24*	*3-<u>Pa</u>C*Pa* (Fig. 3.122)	*21*	$\underline{Pa} \| \| C^* \| \| Pa$
11			*3-<u>Pa</u>C*PaR** (Fig. 3.134)	*18*	$\underline{Pa} \| \| C^* \| \| Pa \perp R^*$
12			*3-<u>Pa</u>*PPa^{ss}* (Fig. 3.146)	*3*	$\underline{Pa}^* \| \| P \| \| Pa^{ss}$
13	*3-<u>Pa</u>Pa^{cc}* (Fig. 3.75)	*21*	*3-<u>Pa</u>R*Pa^{cc}* (Fig. 3.123)	*18*	$\underline{Pa} \perp R^* \| \| Pa^{cc}$
14			*3-<u>Pa</u>R*R*Pa^{cc}* (Fig. 3.135)	*15*	$\underline{Pa} \| \| R^* \perp R^* \| \| Pa^{cc}$
15			*3-<u>Pa</u>*Pa^{scc}* (Fig. 3.147)	*6*	$\underline{Pa}^* \perp Pa^{scc}$
16	*3-<u>Pa</u>Pa^{cc}* (Fig. 3.76)	*21*	*3-<u>Pa</u>R*Pa^{cc}* (Fig. 3.124)	*18*	$\underline{Pa} \perp R^* \perp^{\perp} Pa^{cc}$
17			*3-<u>Pa</u>R*Pa^{cc}R** (Fig. 3.136)	*15*	$\underline{Pa} \perp R^* \| \| Pa^{cc} \perp {}^{\|\|}R^*$
18			*3-<u>Pa</u>*Pa^{ccs}* (Fig. 3.148)	*6*	$\underline{Pa}^* \perp Pa^{ccs}$
19	*3-<u>Pa</u>Pa^{cc}* (Fig. 3.77)	*21*	*3-<u>Pa</u>R*Pa^{cc}* (Fig. 3.125)	*18*	$\underline{Pa} \| \| R^* \| \| Pa^{cc}$
20			*3-<u>Pa</u>R*R*Pa^{cc}* (Fig. 3.137)	*15*	$\underline{Pa} \perp R^* \perp {}^{\|\|}R^* \| \| Pa^{cc}$

Table 3.32. (cont.)

21			3-$\underline{Pa}$*Pa^{scc} (Fig. 3.149)	*6*	$\underline{Pa}$*$\|\|Pa^{scc}$
22	3-$\underline{Pa}Pa^{cc}$ (Fig. 3.78)	*21*	3-$\underline{Pa}$R*Pa^{cc} (Fig. 3.126)	*18*	$\underline{Pa} \perp R^* \perp {}^{\|}Pa^{cc}$
23			3-$\underline{Pa}$R*Pa^{cc}R* (Fig. 3.138)	*15*	$\underline{Pa}\|\|R^*\|\|Pa^{cc} \perp R^*$
24			3-$\underline{Pa}$*Pa^{ccs} (Fig. 3.150)	*6*	$\underline{Pa}^*\|\|Pa^{ccs}$
25	3-$\underline{Pa}^{cc}Pa$ (Fig. 3.79)	*21*	3-$\underline{Pa}^{cc}$R*Pa (Fig. 3.127)	*18*	$\underline{Pa}^{cc} \perp R^* \perp {}^{\|}Pa$
26			3-$\underline{Pa}^{cc}$R*PaR* (Fig. 3.139)	*15*	$\underline{Pa}^{cc} \perp R^* \perp {}^{\|}Pa\|\|R^*$
27			3-$\underline{Pa}^{scc}Pa^{ss}$ (Fig. 3.151)	*3*	$\underline{Pa}^{scc}\|\|Pa^{ss}$
28	3-$\underline{Pa}$PaPa (Fig. 3.80)	*33*	3-$\underline{Pa}$R*PaPa (Fig. 3.128)	*30*	$\underline{Pa} \perp R^* \perp^{\perp} Pa \perp^{\perp} Pa$
29			3-$\underline{Pa}$R*PaPaR* (Fig. 3.140)	*27*	$\underline{Pa} \perp R^* \perp^{\perp} Pa \perp^{\perp} Pa \perp {}^{\|}R^*$
30			3-$\underline{Pa}^{ss}PaPa^{ss}$ (Fig. 3.152)	*9*	$\underline{Pa}^{ss} \perp Pa \perp {}^{\|}Pa^{ss}$
31	3-$\underline{Pa}$PaPa (Fig. 3.81)	*33*	3-$\underline{Pa}$R*PaPa (Fig. 3.129)	*30*	$\underline{Pa} \perp R^* \perp^{\perp} Pa \perp {}^{\|}Pa$
32			3-$\underline{Pa}$R*PaPaR* (Fig. 3.141)	*27*	$\underline{Pa} \perp R^* \perp^{\perp} Pa \perp {}^{\|}Pa \perp^{\perp} R^*$
33			3-$\underline{Pa}Pa^{ss}Pa^{ss}$ (Fig. 3.153)	*9*	$\underline{Pa} \perp Pa^{ss} \perp^{\perp} Pa^{ss}$
34	3-$\underline{Pa}$PaPa (Fig. 3.82)	*33*	3-$\underline{Pa}$R*PaPa (Fig. 3.130)	*30*	$\underline{Pa} \perp R \perp {}^{\|}Pa \perp^{\perp} Pa$
35			3-$\underline{Pa}$R*PaPaR* (Fig. 3.142)	*27*	$\underline{Pa} \perp R^* \perp {}^{\|}Pa \perp^{\perp} Pa \perp {}^{\|}R^*$
36			3-$\underline{Pa}^{ss}PaPa^{ss}$ (Fig. 3.154)	*9*	$\underline{Pa}^{ss}\|\|Pa \perp Pa^{ss}$
37	3-$\underline{Pa}$RC (Fig. 3.87)	*12*	3-$\underline{Pa}$R*RC (Fig. 3.155)	*9*	$\underline{Pa} \perp R^* \perp {}^{\|}R\|\|C$
38			3-$\underline{Pa}$*RC (Fig. 3.157)	*3*	$\underline{Pa}^*\|\|R\|\|C$
39	3-$\underline{Pa}$CR (Fig. 3.88)	*12*	3-$\underline{Pa}$R*CR (Fig. 3.156)	*9*	$\underline{Pa} \perp R^* \perp {}^{\|}C\|\|R$
40			3-$\underline{Pa}$*CR (Fig. 3.158)	*3*	$\underline{Pa}^*\|\|C\|\|R$
41	3-$\underline{Pa}$PaRR (Fig. 3.89)	*21*	3-$\underline{Pa}Pa^{ss}$R (Fig. 3.159)	*12*	$\underline{Pa}\|\|Pa^{ss} \perp R$
42			3-$\underline{Pa}^{ss}$PaRR (Fig. 3.166)	*9*	$\underline{Pa}^{ss}\|\|Pa \perp R\|\|R$

Table 3.32. (cont.)

43	*3-<u>Pa</u>PaRR* (Fig. 3.90)	*21*	*3-<u>Pa</u>Pa^{ss}R* (Fig. 3.160)	*12*	$\underline{Pa} \perp Pa^{ss} \perp^{\parallel} R$
44			*3-<u>Pa</u>^{ss}PaRR* (Fig. 3.167)	*9*	$\underline{Pa}^{ss} \perp Pa \perp^{\parallel} R \| \| R$
45	*3-<u>Pa</u>PaRR* (Fig. 3.91)	*21*	*3-<u>Pa</u>Pa^{ss}R* (Fig. 3.161)	*12*	$\underline{Pa} \perp Pa^{ss} \perp^{\perp} R$
46			*3-<u>Pa</u>^{ss}PaRR* (Fig. 3.168)	*9*	$\underline{Pa}^{ss} \perp Pa \perp^{\perp} R \| \| R$
47	*3-<u>Pa</u>RRPa* (Fig. 3.92)	*21*	*3-<u>Pa</u>RPa^{ss}* (Fig. 3.162)	*12*	$\underline{Pa} \| \| R \perp Pa^{ss}$
48			*3-<u>Pa</u>^{ss}RRPa* (Fig. 3.169)	*9*	$\underline{Pa}^{ss} \| \| R \| \| R \perp Pa$
49	*3-<u>Pa</u>RRPa* (Fig. 3.93)	*21*	*3-<u>Pa</u>RPa^{ss}* (Fig. 3.163)	*12*	$\underline{Pa} \perp R \perp^{\perp} Pa^{ss}$
50			*3-<u>Pa</u>^{ss}RRPa* (Fig. 3.170)	*9*	$\underline{Pa}^{ss} \perp R \| \| R \perp^{\perp} Pa$
51	*3-<u>Pa</u>RRPa* (Fig. 3.94)	*21*	*3-<u>Pa</u>^{ss}RPa* (Fig. 3.164)	*12*	$\underline{Pa}^{ss} \perp R \perp^{\parallel} Pa$
52			*3-<u>Pa</u>RRPa^{ss}* (Fig. 3.171)	*9*	$\underline{Pa} \perp R \| \| R \perp^{\parallel} Pa^{ss}$
53	*3-<u>Pa</u>RPaR* (Fig. 3.95)	*21*	*3-<u>Pa</u>RPa^{ss}* (Fig. 3.165a)	*12*	$\underline{Pa} \perp R \perp Pa^{ss}$
54			*3-<u>Pa</u>^{ss}RPaR* (Fig. 3.172a)	*9*	$\underline{Pa}^{ss} \perp R \perp Pa \perp^{\parallel} R$
55	*3-<u>Pa</u>RPaR* (Fig. 3.96)	*21*	*3-<u>Pa</u>RPa^{ss}* (Fig. 3.165b)	*12*	$\underline{Pa} \| \| R \perp Pa^{ss}$
56			*3-<u>Pa</u>^{ss}RPaR* (Fig. 3.172b)	*9*	$\underline{Pa}^{ss} \| \| R \perp Pa \perp^{\parallel} R$
57	*3-<u>R</u>RPaP* (Fig. 3.97)	*12*	*3-<u>R</u>R*RPaP* (Fig. 3.173)	*9*	$\underline{R} \perp R^{*} \perp^{\parallel} R \| \| Pa \| \| R$
58			*3-<u>R</u>RPa*P* (Fig. 3.176)	*3*	$\underline{R} \| \| R \| \| Pa^{*} \| \| P$
59	*3-<u>R</u>PRPa* (Fig. 3.98)	*12*	*3-<u>R</u>PR*RPa* (Fig. 3.174)	*9*	$\underline{R} \| \| P \perp R^{*} \perp^{\parallel} R \| \| Pa$
60			*3-<u>R</u>PRPa** (Fig. 3.177)	*3*	$\underline{R} \| \| P \| \| R \| \| Pa^{*}$
61	*3-<u>R</u>CPa* (Fig. 3.99)	*12*	*3-<u>R</u>R*CPa* (Fig. 3.175)	*9*	$\underline{R} \perp R^{*} \perp^{\parallel} C \| \| Pa$
62			*3-<u>R</u>CPa** (Fig. 3.178)	*3*	$\underline{R} \| \| C \| \| Pa^{*}$
63	*3-<u>R</u>PaRR* (Fig. 3.100a)	*12*	*3-<u>R</u>PaRRR** (Fig. 3.179a)	*9*	$\underline{R} \perp Pa \perp^{\parallel} R \| \| R \perp R^{*}$
64			*3-<u>R</u>Pa^{ss}R* (Fig. 3.185a)	*3*	$\underline{R} \perp Pa^{ss} \perp^{\parallel} R$

Table 3.32. (cont.)

65	3-$\underline{R}$PaRR (Fig. 3.100b)	12	3-$\underline{R}$PaRR*R (Fig. 3.179b)	9	$\underline{R} \perp Pa \perp {}^{\parallel}R \perp R^* \perp {}^{\parallel}R$
66			3-$\underline{R}Pa^{ss}R$ (Fig. 3.185b)	3	$\underline{R} \perp Pa^{ss} \perp {}^{\parallel}R$
67	3-$\underline{R}$RPaR (Fig. 3.101a)	12	3-$\underline{R}$RPaRR* (Fig. 3.180a)	9	$\underline{R} \parallel R \perp Pa \perp {}^{\parallel}R \perp R^*$
68			3-$\underline{R}RPa^{ss}$ (Fig. 3.186a)	3	$\underline{R} \parallel R \perp Pa^{ss}$
69	3-$\underline{R}$RPaR (Fig. 3.101b)	12	3-$\underline{R}$R*RPaR (Fig. 3.180b)	9	$\underline{R} \perp R^* \perp {}^{\parallel}R \perp Pa \perp {}^{\parallel}R$
70			3-$\underline{R}RPa^{ss}$ (Fig. 3.186b)	3	$\underline{R} \parallel R \perp Pa^{ss}$
71	3-$\underline{R}$PaPaR (Fig. 3.102)	21	3-$\underline{R}PaPa^{ss}$ (Fig. 3.181)	12	$\underline{R} \perp Pa \parallel Pa^{ss}$
72			3-$\underline{R}Pa^{ss}$PaR (Fig. 3.187)	9	$\underline{R} \perp Pa^{ss} \parallel Pa \perp {}^{\parallel}R$
73	3-$\underline{R}$PaRPa (Fig. 3.103)	21	3-$\underline{R}Pa^{ss}Pa$ (Fig. 3.182)	12	$\underline{R} \perp Pa^{ss} \parallel Pa$
73			3-$\underline{R}$PaRPa^{ss} (Fig. 3.188)	9	$\underline{R} \perp Pa \perp {}^{\parallel}R \perp Pa^{ss}$
75	3-$\underline{R}$PaRPa (Fig. 3.104)	21	3-$\underline{R}PaPa^{ss}$ (Fig. 3.183)	12	$\underline{R} \perp Pa \perp^{\perp} Pa^{ss}$
76			3-$\underline{R}Pa^{ss}$RPa (Fig. 3.189)	9	$\underline{R} \perp Pa^{ss} \perp {}^{\parallel}R \perp {}^{\parallel}Pa$
77	3-$\underline{R}$PaPaR (Fig. 3.105)	21	3-$\underline{R}Pa^{cs}PaR^*$ (Fig. 3.184)	9	$\underline{R} \perp Pa^{cs} \parallel Pa \perp {}^{\parallel}R^*$
78			3-$\underline{R}PaPa^{ss}R$ (Fig. 3.190)	9	$\underline{R} \perp Pa \parallel Pa^{ss} \perp {}^{\parallel}R$
79	3-$\underline{R}RPa^{cc}$ (Fig. 3.106)	9	3-$\underline{R}$R*RPa^{cc} (Fig. 3.191)	6	$\underline{R} \perp R^* \perp {}^{\parallel}R \parallel Pa^{cc}$
80			3-$\underline{R}RPa^{ccs}$ (Fig. 3.194)	3	$\underline{R} \parallel R \parallel Pa^{ccs}$
81	3-$\underline{R}RPa^{cc}$ (Fig. 3.107)	9	3-$\underline{R}$R*RPa^{cc} (Fig. 3.192)	6	$\underline{R} \perp R^* \perp {}^{\parallel}R \parallel Pa^{cc}$
82			3-$\underline{R}RPa^{scc}$ (Fig. 3.195)	3	$\underline{R} \parallel R \parallel Pa^{scc}$
83	3-$\underline{Pa}^{cc}$RR (Fig. 3.108)	9	3-$\underline{Pa}^{cc}$RRR*R (Fig. 3.193)	6	$\underline{Pa}^{cc} \parallel R \perp R^* \perp {}^{\parallel}R$
84			3-$\underline{Pa}^{scc}$RR (Fig. 3.196)	3	$\underline{Pa}^{scc} \parallel R \parallel R$
85	3-$\underline{Pa}$Pr (Fig. 3.109a)	21	3-$\underline{Pa}$Pr* (Fig. 3.197a)	15	$\underline{Pa}$-Pr*
86			3-$\underline{Pa}^{ss}$PrR* (Fig. 3.198a)	6	$\underline{Pa}^{ss}$-Pr-R*

Table 3.32. (cont.)

87	*3-<u>R</u>RPr* (Fig. 3.109b)	*9*	*3-<u>R</u>RPrR** (Fig. 3.197b)	*6*	*<u>R</u>||R-Pr-R**
88			*3-<u>R</u>RPr** (Fig. 3.198b)	*3*	*<u>R</u>||R-Pr**

Table 3.33. Bases of the operational velocities spaces of the limbs isolated from the parallel mechanisms presented in Figs. 3.119–3.198

No.	Parallel mechanism	Basis (R_{G1})	(R_{G2})	(R_{G3})
1	Figs. 3.119a, 3.120a, 3.121a, 3.122a, 3.123a, 3.125a, 3.129, 3.160, 3.161, 3.165, 3.176a, 3.177a, 3.178a, 3.182a, 3.184a, 3.185a, 3.186a, 3.194a, 3.195a, 3.196a,	$(\boldsymbol{v}_1, \boldsymbol{v}_2, \boldsymbol{v}_3, \boldsymbol{\omega}_\beta)$	$(\boldsymbol{v}_1, \boldsymbol{v}_2, \boldsymbol{v}_3, \boldsymbol{\omega}_\delta)$	$(\boldsymbol{v}_1, \boldsymbol{v}_2, \boldsymbol{v}_3, \boldsymbol{\omega}_\alpha)$
2	Figs. 3.119b, 3.120b, 3.121b, 3.122b, 3.123b, 3.125b, 3.157b, 3.158b, 3.176b, 3.177b, 3.178b, 3.181b, 3.194b, 3.195b, 3.196b	$(\boldsymbol{v}_1, \boldsymbol{v}_2, \boldsymbol{v}_3, \boldsymbol{\omega}_\delta)$	$(\boldsymbol{v}_1, \boldsymbol{v}_2, \boldsymbol{v}_3, \boldsymbol{\omega}_\delta)$	$(\boldsymbol{v}_1, \boldsymbol{v}_2, \boldsymbol{v}_3, \boldsymbol{\omega}_\alpha)$
3	Figs. 3.124, 3.126, 3.128, 3.130, 3.164	$(\boldsymbol{v}_1, \boldsymbol{v}_2, \boldsymbol{v}_3, \boldsymbol{\omega}_\alpha)$	$(\boldsymbol{v}_1, \boldsymbol{v}_2, \boldsymbol{v}_3, \boldsymbol{\omega}_\beta)$	$(\boldsymbol{v}_1, \boldsymbol{v}_2, \boldsymbol{v}_3, \boldsymbol{\omega}_\delta)$
4	Figs. 3.127a, 3.198b, 3.151a, 3.157a, 3.158a, 3.159, 3.162, 3.163, 3. 181a, 3.183a,	$(\boldsymbol{v}_1, \boldsymbol{v}_2, \boldsymbol{v}_3, \boldsymbol{\omega}_\delta)$	$(\boldsymbol{v}_1, \boldsymbol{v}_2, \boldsymbol{v}_3, \boldsymbol{\omega}_\alpha)$	$(\boldsymbol{v}_1, \boldsymbol{v}_2, \boldsymbol{v}_3, \boldsymbol{\omega}_\beta)$
5	Figs. 3.127b, 3.151b, 3.185b, 3.186b, 3.198b	$(\boldsymbol{v}_1, \boldsymbol{v}_2, \boldsymbol{v}_3, \boldsymbol{\omega}_\beta)$	$(\boldsymbol{v}_1, \boldsymbol{v}_2, \boldsymbol{v}_3, \boldsymbol{\omega}_\alpha)$	$(\boldsymbol{v}_1, \boldsymbol{v}_2, \boldsymbol{v}_3, \boldsymbol{\omega}_\beta)$

Table 3.33. (cont.)

6	Fig. 3.131–3.139, 3.141, 3.153, 3.155, 3.156, 3.173–3.175	$(\boldsymbol{v}_1,\boldsymbol{v}_2,\boldsymbol{v}_3,\boldsymbol{\omega}_\alpha)$	$(\boldsymbol{v}_1,\boldsymbol{v}_2,\boldsymbol{v}_3,\boldsymbol{\omega}_\beta)$	$(\boldsymbol{v}_1,\boldsymbol{v}_2,\boldsymbol{v}_3,\boldsymbol{\omega}_\delta)$
7	Fig. 3.140, 3.152, 3.167, 3.168, 3.172, 3.179, 3.180, 3.197b, 3.197b, 3.198a	$(\boldsymbol{v}_1,\boldsymbol{v}_2,\boldsymbol{v}_3,\boldsymbol{\omega}_\beta,\boldsymbol{\omega}_\delta)$	$(\boldsymbol{v}_1,\boldsymbol{v}_2,\boldsymbol{v}_3,\boldsymbol{\omega}_\alpha,\boldsymbol{\omega}_\delta)$	$(\boldsymbol{v}_1,\boldsymbol{v}_2,\boldsymbol{v}_3,\boldsymbol{\omega}_\alpha,\boldsymbol{\omega}_\beta)$
8	Fig. 3.142, 3.154, 3.166, 3.169, 3.170, 3.171	$(\boldsymbol{v}_1,\boldsymbol{v}_2,\boldsymbol{v}_3,\boldsymbol{\omega}_\alpha,\boldsymbol{\omega}_\delta)$	$(\boldsymbol{v}_1,\boldsymbol{v}_2,\boldsymbol{v}_3,\boldsymbol{\omega}_\alpha,\boldsymbol{\omega}_\beta)$	$(\boldsymbol{v}_1,\boldsymbol{v}_2,\boldsymbol{v}_3,\boldsymbol{\omega}_\beta,\boldsymbol{\omega}_\delta)$
9	Figs. 3.143a, 3.144a, 3.145a, 3.146a	$(\boldsymbol{v}_1,\boldsymbol{v}_2,\boldsymbol{v}_3,\boldsymbol{\omega}_\delta)$	$(\boldsymbol{v}_1,\boldsymbol{v}_2,\boldsymbol{v}_3,\boldsymbol{\omega}_\alpha)$	$(\boldsymbol{v}_1,\boldsymbol{v}_2,\boldsymbol{v}_3,\boldsymbol{\omega}_\beta)$
10	Figs. 3.147–3.150, 3.197a	$(\boldsymbol{v}_1,\boldsymbol{v}_2,\boldsymbol{v}_3)$	$(\boldsymbol{v}_1,\boldsymbol{v}_2,\boldsymbol{v}_3)$	$(\boldsymbol{v}_1,\boldsymbol{v}_2,\boldsymbol{v}_3)$
11	Figs. 3.182b, 3.184b	$(\boldsymbol{v}_1,\boldsymbol{v}_2,\boldsymbol{v}_3,\boldsymbol{\omega}_\beta)$	$(\boldsymbol{v}_1,\boldsymbol{v}_2,\boldsymbol{v}_3,\boldsymbol{\omega}_\alpha)$	$(\boldsymbol{v}_1,\boldsymbol{v}_2,\boldsymbol{v}_3,\boldsymbol{\omega}_\alpha)$
12	Fig. 3.183b	$(\boldsymbol{v}_1,\boldsymbol{v}_2,\boldsymbol{v}_3,\boldsymbol{\omega}_\delta)$	$(\boldsymbol{v}_1,\boldsymbol{v}_2,\boldsymbol{v}_3,\boldsymbol{\omega}_\delta)$	$(\boldsymbol{v}_1,\boldsymbol{v}_2,\boldsymbol{v}_3,\boldsymbol{\omega}_\beta)$
13	Figs. 3.187–3.193	$(\boldsymbol{v}_1,\boldsymbol{v}_2,\boldsymbol{v}_3,\boldsymbol{\omega}_\beta,\boldsymbol{\omega}_\delta)$	$(\boldsymbol{v}_1,\boldsymbol{v}_2,\boldsymbol{v}_3,\boldsymbol{\omega}_\alpha,\boldsymbol{\omega}_\delta)$	$(\boldsymbol{v}_1,\boldsymbol{v}_2,\boldsymbol{v}_3,\boldsymbol{\omega}_\alpha,\boldsymbol{\omega}_\beta)$

Table 3.34. Structural parameters[a] of translational parallel mechanisms in Figs. 3.119–3.130

No.	Structural parameter	Solution *3-PaPaC** (Figs. 3.119, 3.120) *3-PaC*Pa* (Figs. 3.121, 3.122)	*3-PaR*Pa^{cc}* (Figs. 3.123–3.126) *3-Pa^{cc}R*Pa* (Fig. 3.127)	*3-PaR*PaPa* (Figs. 3.128–3.130)
1	m	20	20	29
2	p_1	9	9	13
3	p_2	9	9	13
4	p_3	9	9	13
5	p	27	27	39
6	q	8	8	11
7	k_1	0	0	0
8	k_2	3	3	3
9	k	3	3	3
10	(R_{Gi}) $(i = 1,2,3)$	See Table 3.33	See Table 3.33	See Table 3.33
11	S_{G1}	4	4	4
12	S_{G2}	4	4	4
13	S_{G3}	4	4	4
14	r_{G1}	6	7	9
15	r_{G2}	6	7	9
16	r_{G3}	6	7	9
17	M_{G1}	4	4	4
18	M_{G2}	4	4	4
19	M_{G3}	4	4	4
20	(R_F)	$(\boldsymbol{v}_1,\boldsymbol{v}_2,\boldsymbol{v}_3)$	$(\boldsymbol{v}_1,\boldsymbol{v}_2,\boldsymbol{v}_3)$	$(\boldsymbol{v}_1,\boldsymbol{v}_2,\boldsymbol{v}_3)$
21	S_F	3	3	3
22	r_1	18	21	27
23	r_F	27	30	36
24	M_F	3	3	3
25	N_F	21	18	30
26	T_F	0	0	0
27	$\sum_{j=1}^{p_1} f_j$	10	11	13
28	$\sum_{j=1}^{p_2} f_j$	10	11	13
29	$\sum_{j=1}^{p_3} f_j$	10	11	13
30	$\sum_{j=1}^{p} f_j$	30	33	39

[a]See footnote of Table 2.1 for the nomenclature of structural parameters

Table 3.35. Structural parameters[a] of translational parallel mechanisms in Figs. 3.131–3.142

No.	Structural parameter	Solution *3-PaR*PaC** (Figs. 3.131, 3.132) *3-PaC*PaR** (Figs. 3.133, 3.134)	*3-PaR*R*Pa^{cc}* (Figs. 3.135, 3.137) *3-PaR*Pa^{cc}R** (Fig. 3.136, 3.138) *3-Pa^{cc}R*PaR** (Fig. 3.139)	*3-PaR*PaPaR** (Figs. 3.140–3.142)
1	m	23	23	32
2	p_1	10	10	14
3	p_2	10	10	14
4	p_3	10	10	14
5	p	30	30	42
6	q	8	8	11
7	k_1	0	0	0
8	k_2	3	3	3
9	k	3	3	3
10	(R_{Gi}) $(i = 1,2,3)$	See Table 3.33	See Table 3.33	See Table 3.33
11	S_{G1}	5	5	5
12	S_{G2}	5	5	5
13	S_{G3}	5	5	5
14	r_{G1}	6	7	9
15	r_{G2}	6	7	9
16	r_{G3}	6	7	9
17	M_{G1}	5	5	5
18	M_{G2}	5	5	5
19	M_{G3}	5	5	5
20	(R_F)	$(\boldsymbol{v}_1, \boldsymbol{v}_2, \boldsymbol{v}_3)$	$(\boldsymbol{v}_1, \boldsymbol{v}_2, \boldsymbol{v}_3)$	$(\boldsymbol{v}_1, \boldsymbol{v}_2, \boldsymbol{v}_3)$
21	S_F	3	3	3
22	r_1	18	21	27
23	r_F	30	33	39
24	M_F	3	3	3
25	N_F	18	15	27
26	T_F	0	0	0
27	$\sum_{j=1}^{p_1} f_j$	11	12	14
28	$\sum_{j=1}^{p_2} f_j$	11	12	14
29	$\sum_{j=1}^{p_3} f_j$	11	12	14
30	$\sum_{j=1}^{p} f_j$	33	36	42

[a]See footnote of Table 2.1 for the nomenclature of structural parameters

Table 3.36. Structural parameters[a] of translational parallel mechanisms in Figs. 3.143–3.151

No.	Structural parameter	Solution 3-$\underline{Pa}$*$Pa^{ss}P$ (Figs. 3.143, 3.144) 3-$\underline{Pa}$*PPa^{ss} (Figs. 3.145, 3.146)	3-$\underline{Pa}$*Pa^{scc} (Figs. 3.147, 3.149) 3-$\underline{Pa}$*Pa^{ccs} (Figs. 3.148, 3.150)	3-$\underline{Pa}^{scc}Pa^{ss}$ (Fig. 3.151)
1	m	20	17	17
2	p_1	9	8	8
3	p_2	9	8	8
4	p_3	9	8	8
5	p	27	24	24
6	q	8	8	8
7	k_1	0	0	0
8	k_2	3	3	3
9	k	3	3	3
10	(R_{Gi}) $(i = 1,2,3)$	See Table 3.33	See Table 3.33	See Table 3.33
11	S_{G1}	4	3	4
12	S_{G2}	4	3	4
13	S_{G3}	4	3	4
14	r_{G1}	12	12	12
15	r_{G2}	12	12	12
16	r_{G3}	12	12	12
17	M_{G1}	4	3	4
18	M_{G2}	4	3	4
19	M_{G3}	4	3	4
20	(R_F)	$(\boldsymbol{v}_1,\boldsymbol{v}_2,\boldsymbol{v}_3)$	$(\boldsymbol{v}_1,\boldsymbol{v}_2,\boldsymbol{v}_3)$	$(\boldsymbol{v}_1,\boldsymbol{v}_2,\boldsymbol{v}_3)$
21	S_F	3	3	3
22	r_1	36	36	36
23	r_F	45	42	45
24	M_F	3	3	3
25	N_F	3	6	3
26	T_F	0	0	0
27	$\sum_{j=1}^{p_1} f_j$	16	15	16
28	$\sum_{j=1}^{p_2} f_j$	16	15	16
29	$\sum_{j=1}^{p_3} f_j$	16	15	16
30	$\sum_{j=1}^{p} f_j$	48	45	48

[a]See footnote of Table 2.1 for the nomenclature of structural parameters

Table 3.37. Structural parameters[a] of translational parallel mechanisms in Figs. 3.152–3.158

No.	Structural parameter	Solution *3-Pa^{ss}PaPa^{ss}* (Figs. 3.152, 3.154) *3-PaPa^{ss}Pa^{ss}* (Fig. 3.153)	*3-PaR*RC* (Fig. 3.155) *3-PaR*CR* (Fig. 3.156)	*3-Pa*RC* (Fig. 3.157) *3-Pa*CR* (Fig. 3.158)
1	m	26	17	14
2	p_1	12	7	6
3	p_2	12	7	6
4	p_3	12	7	6
5	p	36	21	18
6	q	11	5	5
7	k_1	0	0	0
8	k_2	3	3	3
9	k	3	3	3
10	(R_{Gi}) (i = *1,2,3*)	See Table 3.33	See Table 3.33	See Table 3.33
11	S_{G1}	5	5	4
12	S_{G2}	5	5	4
13	S_{G3}	5	5	4
14	r_{G1}	15	3	6
15	r_{G2}	15	3	6
16	r_{G3}	15	3	6
17	M_{G1}	5	5	4
18	M_{G2}	5	5	4
19	M_{G3}	5	5	4
20	(R_F)	($\boldsymbol{v}_1,\boldsymbol{v}_2,\boldsymbol{v}_3$)	($\boldsymbol{v}_1,\boldsymbol{v}_2,\boldsymbol{v}_3$)	($\boldsymbol{v}_1,\boldsymbol{v}_2,\boldsymbol{v}_3$)
21	S_F	3	3	3
22	r_1	45	9	18
23	r_F	57	21	27
24	M_F	3	3	3
25	N_F	9	9	3
26	T_F	0	0	0
27	$\sum_{j=1}^{p_1} f_j$	20	8	10
28	$\sum_{j=1}^{p_2} f_j$	20	8	10
29	$\sum_{j=1}^{p_3} f_j$	20	8	10
30	$\sum_{j=1}^{p} f_j$	60	24	

[a]See footnote of Table 2.1 for the nomenclature of structural parameters

Table 3.38. Structural parameters[a] of translational parallel mechanisms in Figs. 3.159–3.172

No.	Structural parameter	Solution *3-PaPa^{ss}R* (Figs. 3.159–3.161) *3-PaRPa^{ss}* (Figs. 3.162, 3.163) *3-Pa^{ss}RPa* (Fig. 3.164) *3-PaRPa^{ss}* (Fig. 3.165)	 *3-Pa^{ss}PaRR* (Figs. 3.166–3.168) *3-Pa^{ss}RRPa* (Figs. 3.169, 3.170) *3-PaRRPa^{ss}* (Fig. 3.171) *3-Pa^{ss}RPaR* (Fig. 3.172)
1	m	20	23
2	p_1	9	10
3	p_2	9	10
4	p_3	9	10
5	p	27	30
6	q	8	8
7	k_1	0	0
8	k_2	3	3
9	k	3	3
10	(R_{Gi}) (i = *1,2,3*)	See Table 3.33	See Table 3.33
11	S_{G1}	4	5
12	S_{G2}	4	5
13	S_{G3}	4	5
14	r_{G1}	9	9
15	r_{G2}	9	9
16	r_{G3}	9	9
17	M_{G1}	4	5
18	M_{G2}	4	5
19	M_{G3}	4	5
20	(R_F)	($\boldsymbol{v}_1,\boldsymbol{v}_2,\boldsymbol{v}_3$)	($\boldsymbol{v}_1,\boldsymbol{v}_2,\boldsymbol{v}_3$)
21	S_F	3	3
22	r_l	27	27
23	r_F	36	39
24	M_F	3	3
25	N_F	12	9
26	T_F	0	0
27	$\sum_{j=1}^{p_1} f_j$	13	14
28	$\sum_{j=1}^{p_2} f_j$	13	14
29	$\sum_{j=1}^{p_3} f_j$	13	14
30	$\sum_{j=1}^{p} f_j$	39	42

[a]See footnote of Table 2.1 for the nomenclature of structural parameters

Table 3.39. Structural parameters[a] of translational parallel mechanisms in Figs. 3.173–3.177

No.	Structural parameter	Solution *3-RR*RPaP* (Fig. 3.173) *3-RPR*RPa* (Fig. 3.174)	*3-RR*CPa* (Fig. 3.175)	*3-RRPa*P* (Fig. 3.176) *3-RPRPa** (Fig. 3.177)
1	m	20	17	17
2	p_1	8	7	7
3	p_2	8	7	7
4	p_3	8	7	7
5	p	24	21	21
6	q	5	5	5
7	k_1	0	0	0
8	k_2	3	3	3
9	k	3	3	3
10	(R_{Gi}) $(i = 1,2,3)$	See Table 3.33	See Table 3.33	See Table 3.33
11	S_{G1}	5	5	4
12	S_{G2}	5	5	4
13	S_{G3}	5	5	4
14	r_{G1}	3	3	6
15	r_{G2}	3	3	6
16	r_{G3}	3	3	6
17	M_{G1}	5	5	4
18	M_{G2}	5	5	4
19	M_{G3}	5	5	4
20	(R_F)	$(\boldsymbol{v}_1,\boldsymbol{v}_2,\boldsymbol{v}_3)$	$(\boldsymbol{v}_1,\boldsymbol{v}_2,\boldsymbol{v}_3)$	$(\boldsymbol{v}_1,\boldsymbol{v}_2,\boldsymbol{v}_3)$
21	S_F	3	3	3
22	r_1	9	9	18
23	r_F	21	21	27
24	M_F	3	3	3
25	N_F	9	9	3
26	T_F	0	0	0
27	$\sum_{j=1}^{p_1} f_j$	8	8	10
28	$\sum_{j=1}^{p_2} f_j$	8	8	10
29	$\sum_{j=1}^{p_3} f_j$	8	8	10
30	$\sum_{j=1}^{p} f_j$	24	24	30

[a]See footnote of Table 2.1 for the nomenclature of structural parameters

Table 3.40. Structural parameters[a] of translational parallel mechanisms in Figs. 3.178–3.180

No.	Structural parameter	Solution *3-<u>R</u>CPa** (Fig. 3.178)	*3-<u>R</u>PaRRR*,3-<u>R</u>PaRR*R* (Fig. 3.179) *3-<u>R</u>RPaRR*, 3-<u>R</u>R*RPaR* (Fig. 3.180)
1	m	14	20
2	p_1	6	8
3	p_2	6	8
4	p_3	6	8
5	p	18	24
6	q	5	5
7	k_1	0	0
8	k_2	3	3
9	k	3	3
10	(R_{Gi}) (i = 1,2,3)	See Table 3.33	See Table 3.33
11	S_{G1}	4	5
12	S_{G2}	4	5
13	S_{G3}	4	5
14	r_{G1}	6	3
15	r_{G2}	6	3
16	r_{G3}	6	3
17	M_{G1}	4	5
18	M_{G2}	4	5
19	M_{G3}	4	5
20	(R_F)	($\boldsymbol{v}_1,\boldsymbol{v}_2,\boldsymbol{v}_3$)	($\boldsymbol{v}_1,\boldsymbol{v}_2,\boldsymbol{v}_3$)
21	S_F	3	3
22	r_1	18	9
23	r_F	27	21
24	M_F	3	3
25	N_F	3	9
26	T_F	0	0
27	$\sum_{j=1}^{p_1} f_j$	10	8
28	$\sum_{j=1}^{p_2} f_j$	10	8
29	$\sum_{j=1}^{p_3} f_j$	10	8
30	$\sum_{j=1}^{p} f_j$	30	24

[a]See footnote of Table 2.1 for the nomenclature of structural parameters

Table 3.41. Structural parameters[a] of translational parallel mechanisms in Figs. 3.181–3.186

No.	Structural parameter	Solution 3-$\underline{R}PaPa^{ss}$ (Figs. 3.181, 3.183) 3-$\underline{R}Pa^{ss}Pa$ (Fig. 3.182)	3-$\underline{R}Pa^{cs}PaR$* (Fig. 3.184)	3-$\underline{R}Pa^{ss}R$ (Fig. 3.185) 3-$\underline{R}RPa^{ss}$ (Fig. 3.186)
1	m	20	23	14
2	p_1	9	10	6
3	p_2	9	10	6
4	p_3	9	10	6
5	p	27	30	18
6	q	8	8	5
7	k_1	0	0	0
8	k_2	3	3	3
9	k	3	3	3
10	(R_{Gi}) (i = *1,2,3*)	See Table 3.33	See Table 3.33	See Table 3.33
11	S_{G1}	4	4	4
12	S_{G2}	4	4	4
13	S_{G3}	4	4	4
14	r_{G1}	9	9	6
15	r_{G2}	9	9	6
16	r_{G3}	9	9	6
17	M_{G1}	4	4	4
18	M_{G2}	4	4	4
19	M_{G3}	4	4	4
20	(R_F)	($\boldsymbol{v}_1,\boldsymbol{v}_2,\boldsymbol{v}_3$)	($\boldsymbol{v}_1,\boldsymbol{v}_2,\boldsymbol{v}_3$)	($\boldsymbol{v}_1,\boldsymbol{v}_2,\boldsymbol{v}_3$)
21	S_F	3	3	3
22	r_1	27	27	18
23	r_F	36	36	27
24	M_F	3	3	3
25	N_F	12	12	3
26	T_F	0	0	0
27	$\sum_{j=1}^{p_1} f_j$	13	13	10
28	$\sum_{j=1}^{p_2} f_j$	13	13	10
29	$\sum_{j=1}^{p_3} f_j$	13	13	10
30	$\sum_{j=1}^{p} f_j$	39	39	30

[a]See footnote of Table 2.1 for the nomenclature of structural parameters

Table 3.42. Structural parameters[a] of translational parallel mechanisms in Figs. 3.187–3.193

No.	Structural parameter	Solution 3-$\underline{R}Pa^{ss}PaR$ (Fig. 3.187) 3-$\underline{R}PaRPa^{ss}$ (Fig. 3.188) 3-$\underline{R}Pa^{ss}RPa$ (Fig. 3.189) 3-$\underline{R}PaPa^{ss}R$ (Fig. 3.190)	3-$\underline{RR}$*RPa^{cc} (Figs. 3.191, 3.192) 3-$\underline{Pa}^{cc}RR$*R (Fig. 3.193)
1	m	23	17
2	p_1	10	7
3	p_2	10	7
4	p_3	10	7
5	p	30	21
6	q	8	5
7	k_1	0	0
8	k_2	3	3
9	k	3	3
10	(R_{Gi}) $(i = 1,2,3)$	See Table 3.33	See Table 3.33
11	S_{G1}	5	5
12	S_{G2}	5	5
13	S_{G3}	5	5
14	r_{G1}	9	4
15	r_{G2}	9	4
16	r_{G3}	9	4
17	M_{G1}	5	5
18	M_{G2}	5	5
19	M_{G3}	5	5
20	(R_F)	$(\boldsymbol{v}_1, \boldsymbol{v}_2, \boldsymbol{v}_3)$	$(\boldsymbol{v}_1, \boldsymbol{v}_2, \boldsymbol{v}_3)$
21	S_F	3	3
22	r_l	39	12
23	r_F	21	24
24	M_F	3	3
25	N_F	9	6
26	T_F	0	0
27	$\sum_{j=1}^{p_1} f_j$	14	9
28	$\sum_{j=1}^{p_2} f_j$	14	9
29	$\sum_{j=1}^{p_3} f_j$	14	9
30	$\sum_{j=1}^{p} f_j$	42	27

[a]See footnote of Table 2.1 for the nomenclature of structural parameters

Table 3.43. Structural parameters[a] of translational parallel mechanisms in Figs. 3.194–3.197

No.	Structural parameter	*3-RRPa*^{ccs} (Fig. 3.194) *3-RRPa*^{scc} (Fig. 3.195) *3-Pa*^{scc}*RR* (Fig. 3.196)	*3-PaPr** (Fig. 3.197a)	*3-RRPrR** (Fig. 3.197b)
1	m	14	20	20
2	p_1	6	10	9
3	p_2	6	10	9
4	p_3	6	10	9
5	p	18	30	27
6	q	5	11	8
7	k_1	0	0	0
8	k_2	3	3	3
9	k	3	3	3
10	(R_{Gi}) (i = *1,2,3*)	See Table 3.33	See Table 3.33	See Table 3.33
11	S_{G1}	4	3	5
12	S_{G2}	4	3	5
13	S_{G3}	4	3	5
14	r_{G1}	6	15	10
15	r_{G2}	6	15	10
16	r_{G3}	6	15	10
17	M_{G1}	4	3	5
18	M_{G2}	4	3	5
19	M_{G3}	4	3	5
20	(R_F)	($\boldsymbol{v}_1,\boldsymbol{v}_2,\boldsymbol{v}_3$)	($\boldsymbol{v}_1,\boldsymbol{v}_2,\boldsymbol{v}_3$)	($\boldsymbol{v}_1,\boldsymbol{v}_2,\boldsymbol{v}_3$)
21	S_F	3	3	3
22	r_1	18	45	30
23	r_F	27	51	42
24	M_F	3	3	3
25	N_F	3	15	6
26	T_F	0	0	0
27	$\sum_{j=1}^{p_1} f_j$	10	18	15
28	$\sum_{j=1}^{p_2} f_j$	10	18	15
29	$\sum_{j=1}^{p_3} f_j$	10	18	15
30	$\sum_{j=1}^{p} f_j$	30	54	45

[a]See footnote of Table 2.1 for the nomenclature of structural parameters

Table 3.44. Structural parameters[a] of translational parallel mechanisms in Fig. 3.198

No.	Structural parameter	Solution *3-<u>Pa</u>^{ss}PrR** (Fig. 3.198a)	*3-<u>R</u>RPr** (Fig. 3.198b)
1	m	23	17
2	p_1	11	8
3	p_2	11	8
4	p_3	11	8
5	p	33	24
6	q	11	8
7	k_1	0	0
8	k_2	3	3
9	k	3	3
10	(R_{Gi}) (i = *1,2,3*)	See Table 3.33	See Table 3.33
11	S_{G1}	5	4
12	S_{G2}	5	4
13	S_{G3}	5	4
14	r_{G1}	16	12
15	r_{G2}	16	12
16	r_{G3}	16	12
17	M_{G1}	5	4
18	M_{G2}	5	4
19	M_{G3}	5	4
20	(R_F)	($\boldsymbol{v}_1,\boldsymbol{v}_2,\boldsymbol{v}_3$)	($\boldsymbol{v}_1,\boldsymbol{v}_2,\boldsymbol{v}_3$)
21	S_F	3	3
22	r_1	48	36
23	r_F	60	45
24	M_F	3	3
25	N_F	6	3
26	T_F	0	0
27	$\sum_{j=1}^{p_1} f_j$	21	16
28	$\sum_{j=1}^{p_2} f_j$	21	16
29	$\sum_{j=1}^{p_3} f_j$	21	16
30	$\sum_{j=1}^{p} f_j$	63	48

[a]See footnote of Table 2.1 for the nomenclature of structural parameters

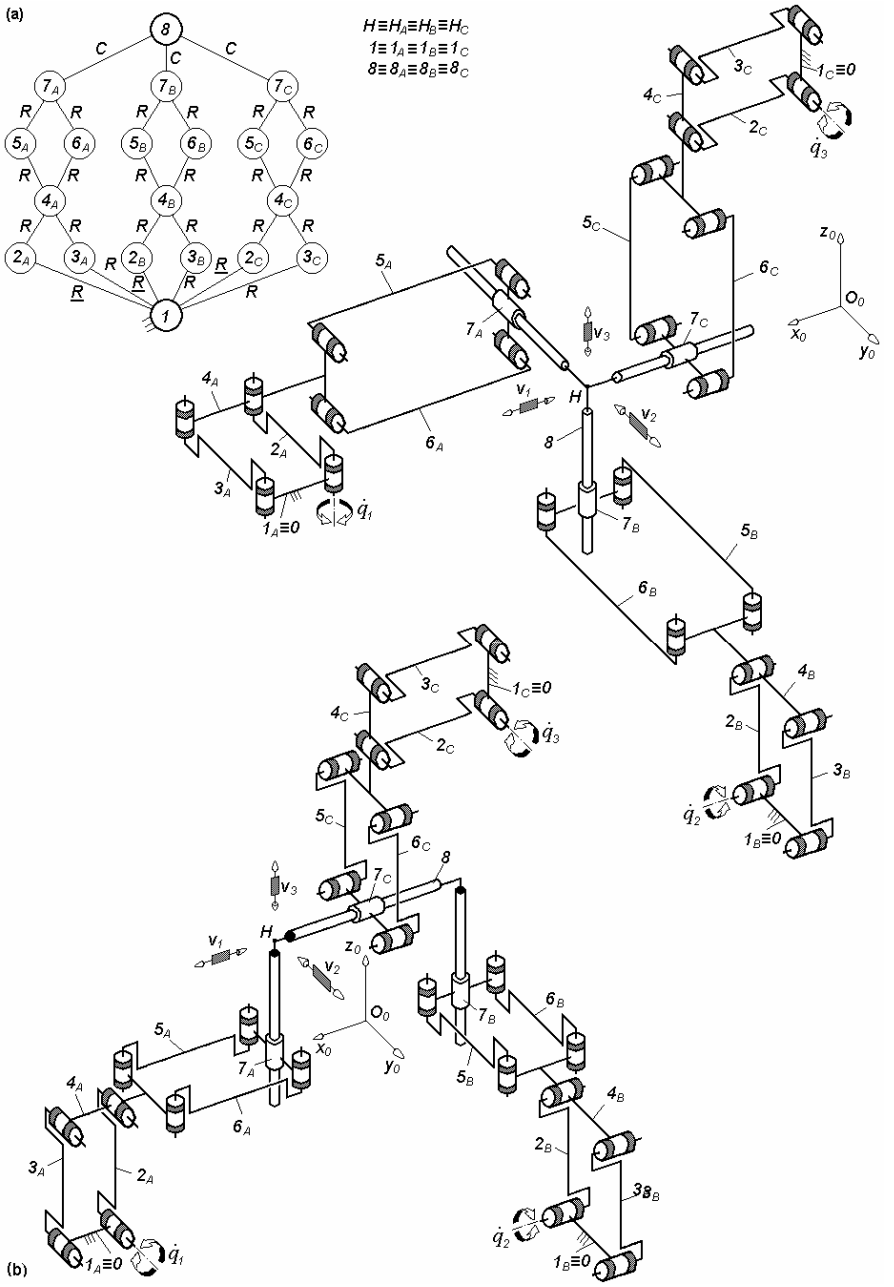

Fig. 3.119. *3-PaPaC**-type overconstrained TPMs with coupled motions and rotating actuators mounted on the fixed base, defined by $M_F = S_F = 3$, $(R_F) = (\boldsymbol{v}_1, \boldsymbol{v}_2, \boldsymbol{v}_3)$, $T_F = 0$, $N_F = 21$, limb topology $\underline{Pa} \perp Pa || C^*$

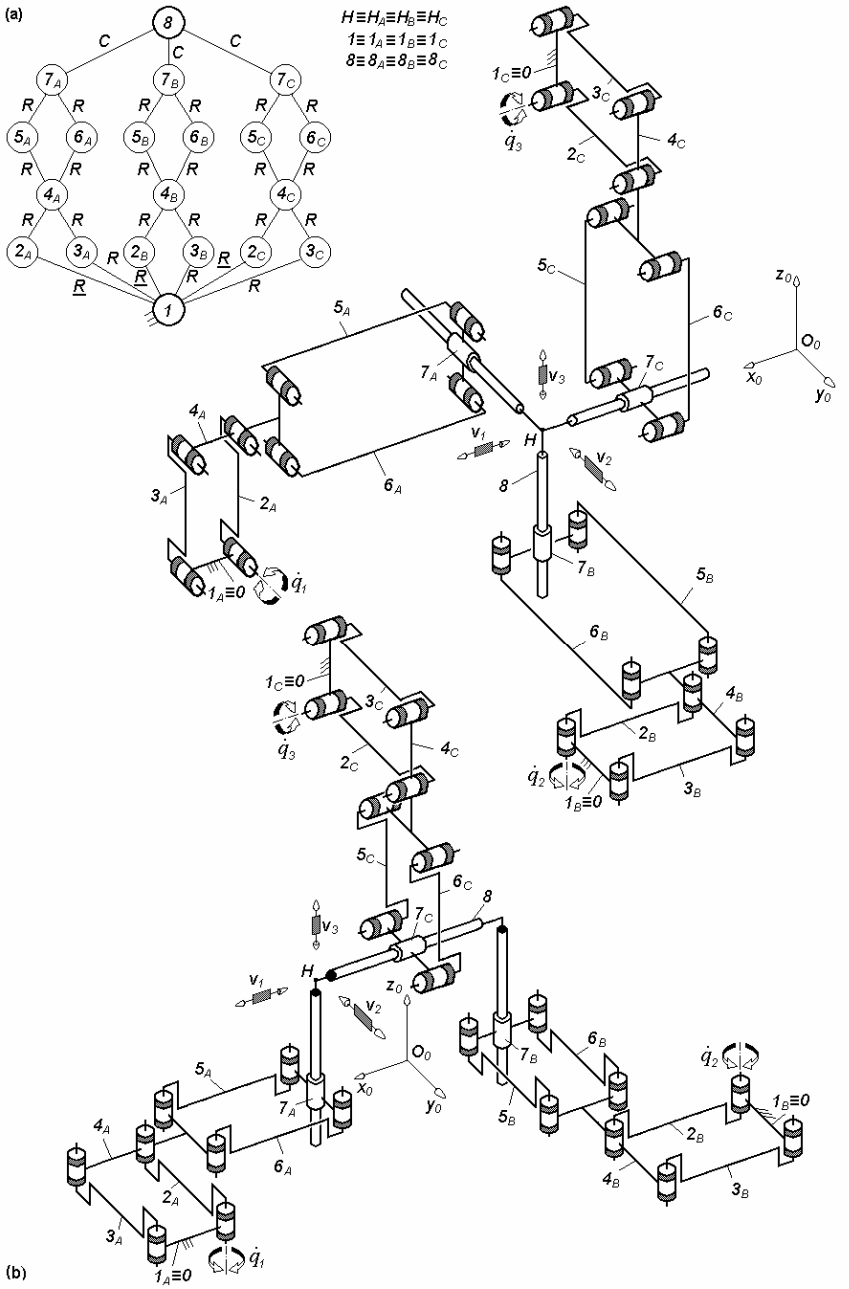

Fig. 3.120. *3-<u>Pa</u>PaC**-type overconstrained TPMs with coupled motions and rotating actuators mounted on the fixed base, defined by $M_F = S_F = 3$, $(R_F) = (\boldsymbol{v}_1, \boldsymbol{v}_2, \boldsymbol{v}_3)$, $T_F = 0$, $N_F = 21$*, limb topology *<u>Pa</u>||Pa||C**

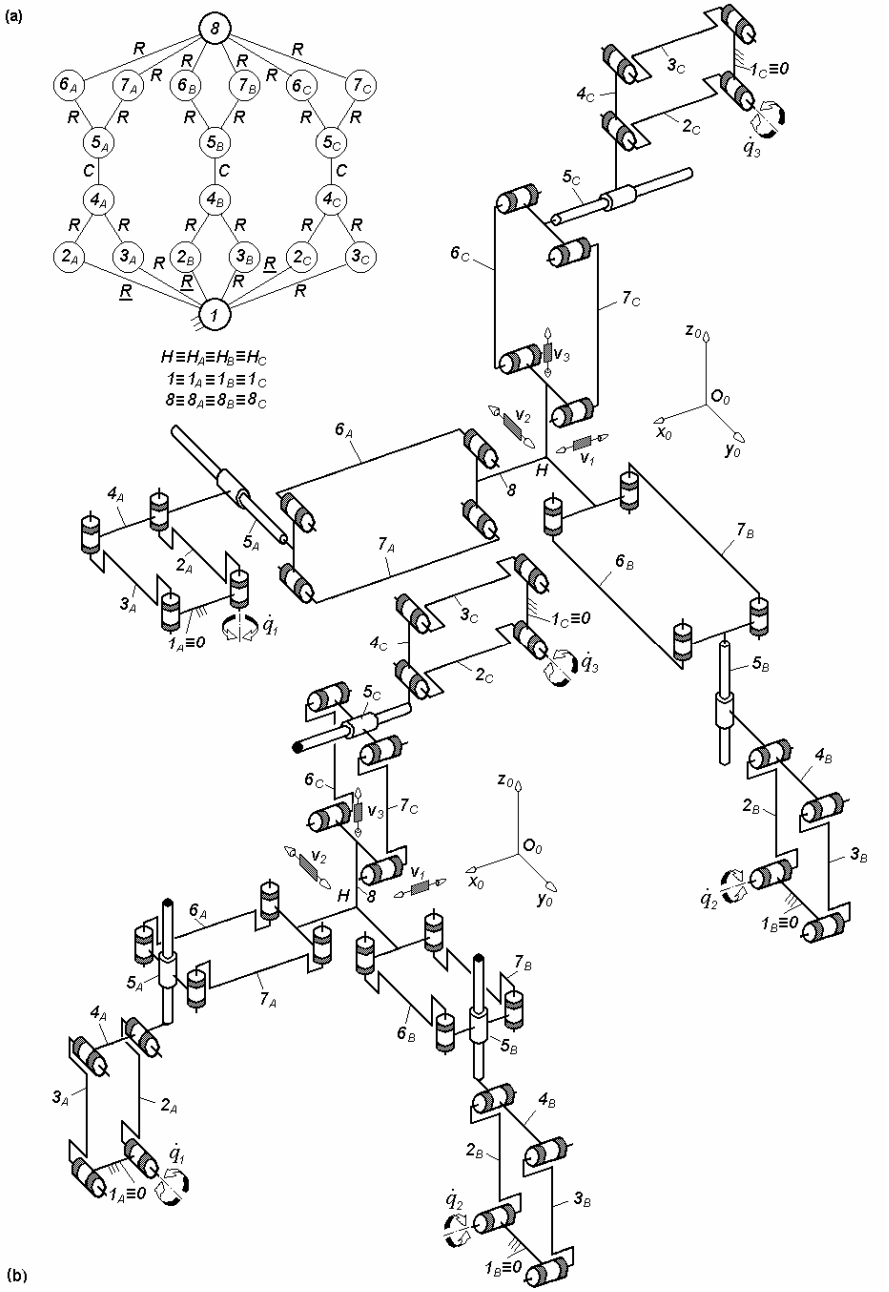

Fig. 3.121. *3-PaC*Pa*-type overconstrained TPMs with coupled motions and rotating actuators mounted on the fixed base, defined by $M_F = S_F = 3$, $(R_F) = (\boldsymbol{v}_1, \boldsymbol{v}_2, \boldsymbol{v}_3)$, $T_F = 0$, $N_F = 21$, limb topology $\underline{Pa} \perp C^* || Pa$

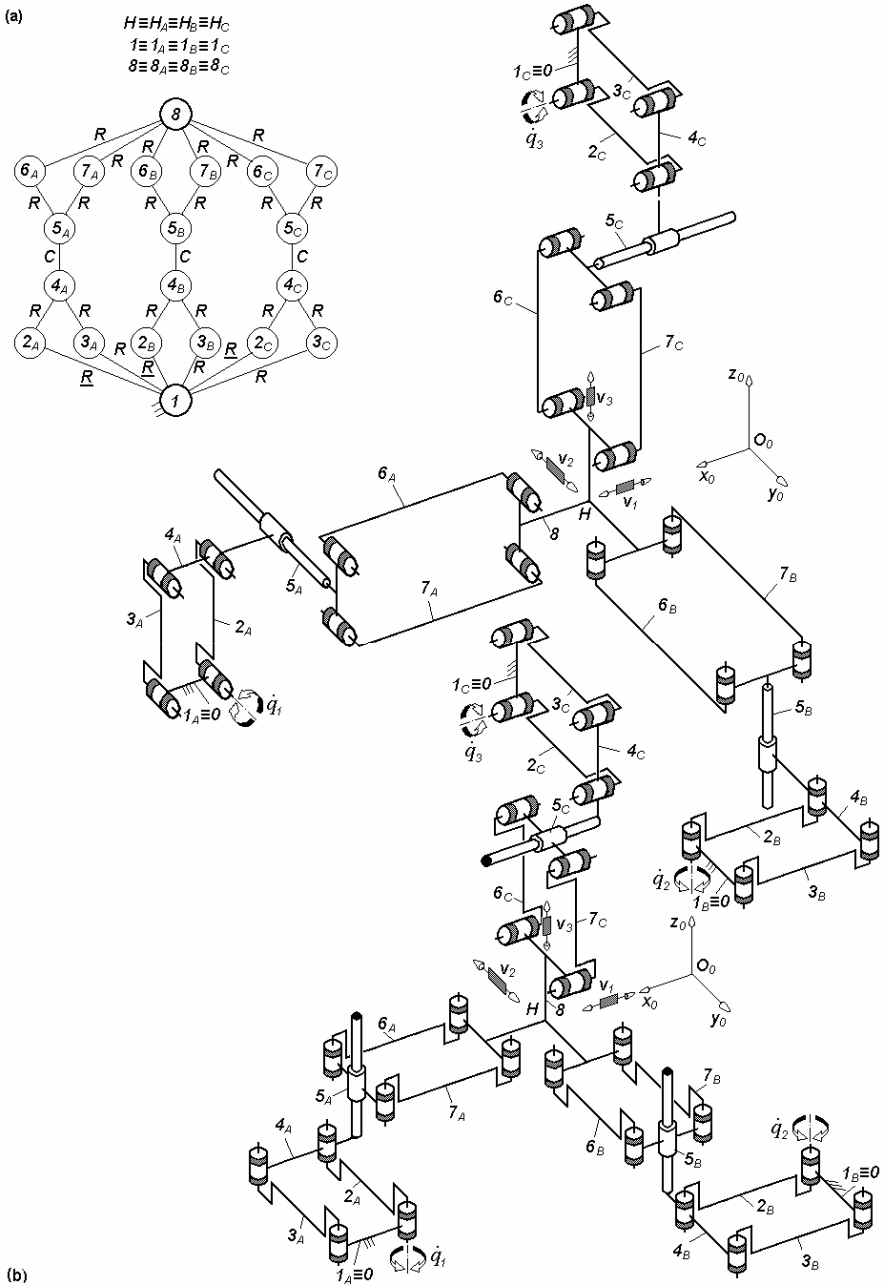

Fig. 3.122. *3-PaC*Pa*-type overconstrained TPMs with coupled motions and rotating actuators mounted on the fixed base, defined by $M_F = S_F = 3$, $(R_F) = (\boldsymbol{v}_1, \boldsymbol{v}_2, \boldsymbol{v}_3)$, $T_F = 0$ and $N_F = 21$, limb topology *Pa*||*C**||*Pa*

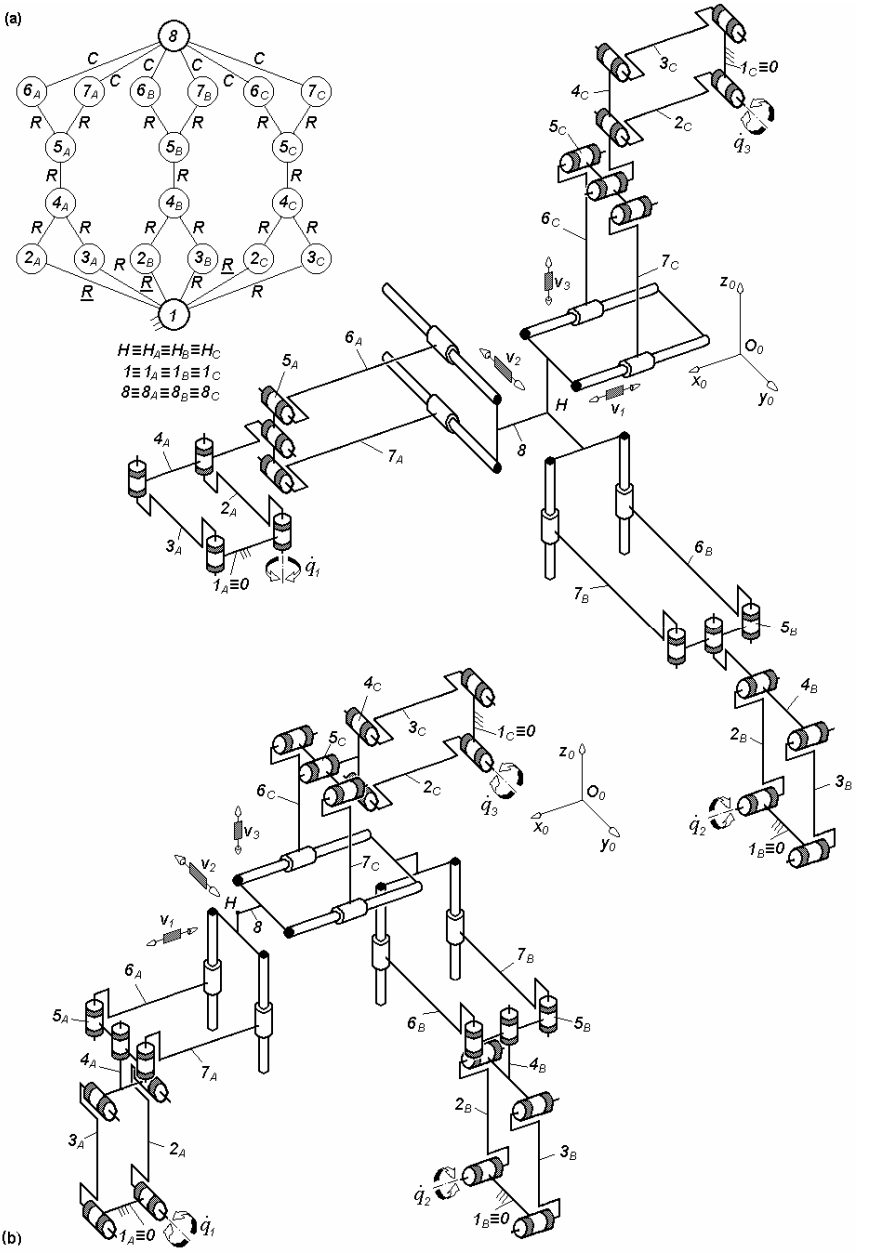

Fig. 3.123. *3-<u>Pa</u>R*Pa*^{cc} overconstrained TPMs with coupled motions, rotating actuators mounted on the fixed base and six cylindrical joints adjacent to the moving platform, defined by $M_F = S_F = 3$, $(R_F) = (\boldsymbol{v}_1, \boldsymbol{v}_2, \boldsymbol{v}_3)$, $T_F = 0$, $N_F = 18$, limb topology $\underline{Pa} \perp R^* || Pa^{cc}$

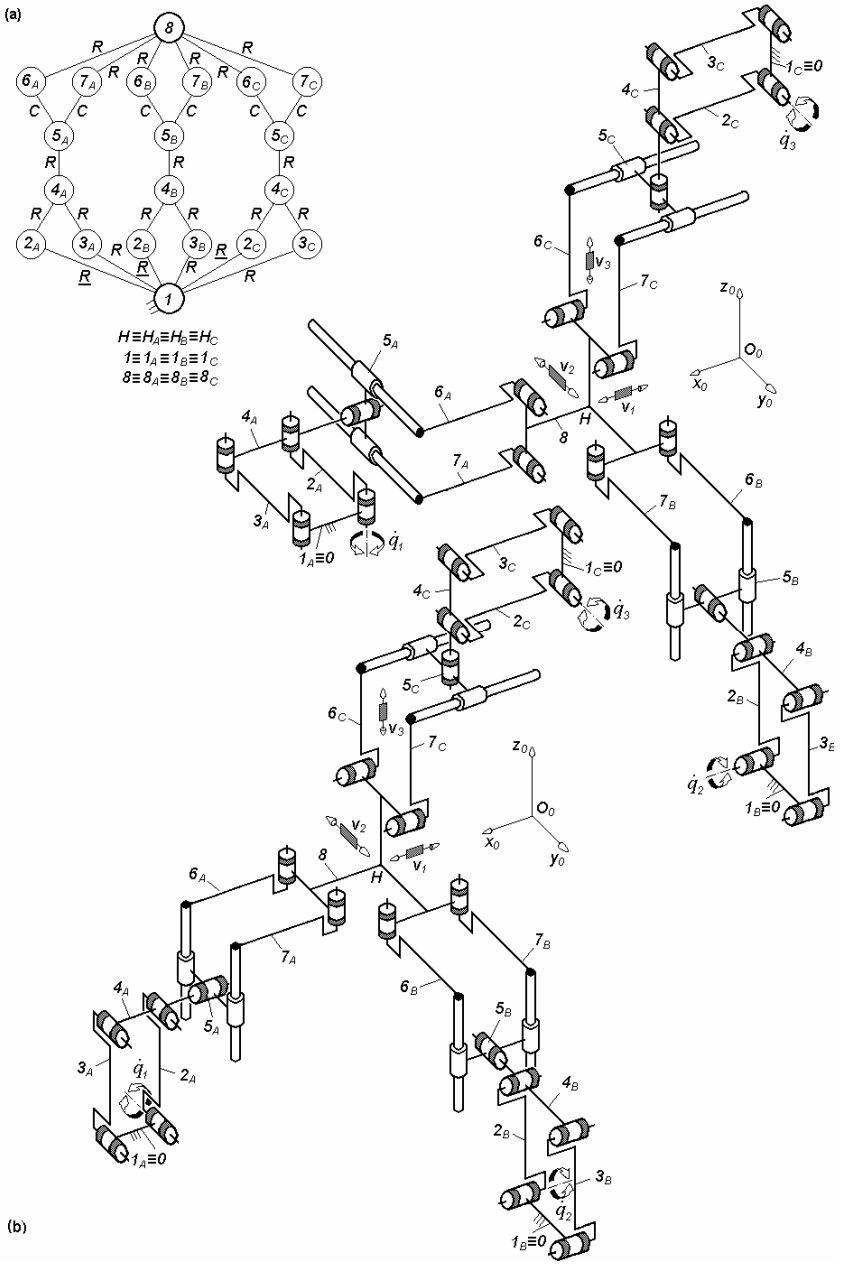

Fig. 3.124. *3-PaR*Pa*^{cc}-type overconstrained TPMs with coupled motions, rotating actuators mounted on the fixed base and six revolute joints adjacent to the moving platform, defined by $M_F = S_F = 3$, $(R_F) = (\boldsymbol{v}_1, \boldsymbol{v}_2, \boldsymbol{v}_3)$, $T_F = 0$, $N_F = 18$, limb topology $\underline{Pa} \perp R^* \perp^{\perp} Pa^{cc}$

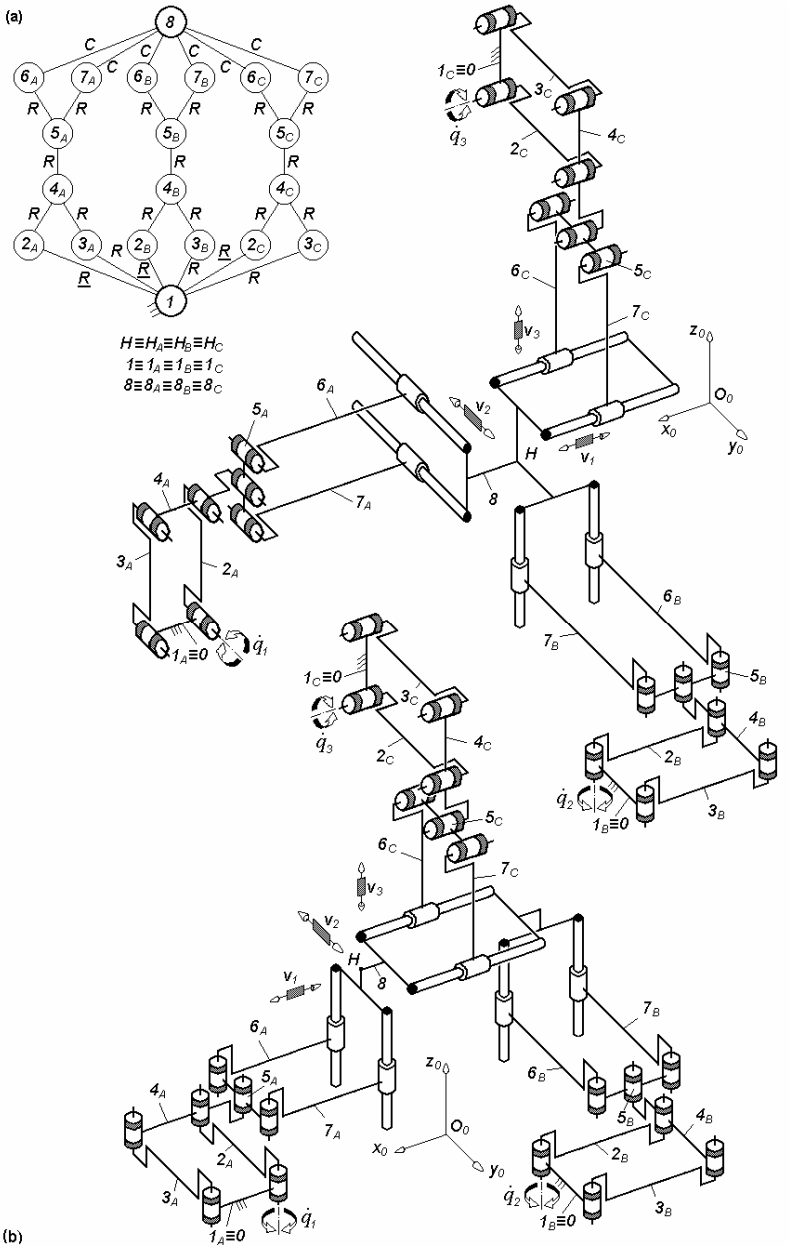

Fig. 3.125. *3-PaR*Pa*^{cc}-type overconstrained TPMs with coupled motions, rotating actuators mounted on the fixed base and six cylindrical joints adjacent to the moving platform, defined by $M_F = S_F = 3$, $(R_F) = (\boldsymbol{v}_1, \boldsymbol{v}_2, \boldsymbol{v}_3)$, $T_F = 0$, $N_F = 18$, limb topology $Pa||R^*||Pa^{cc}$

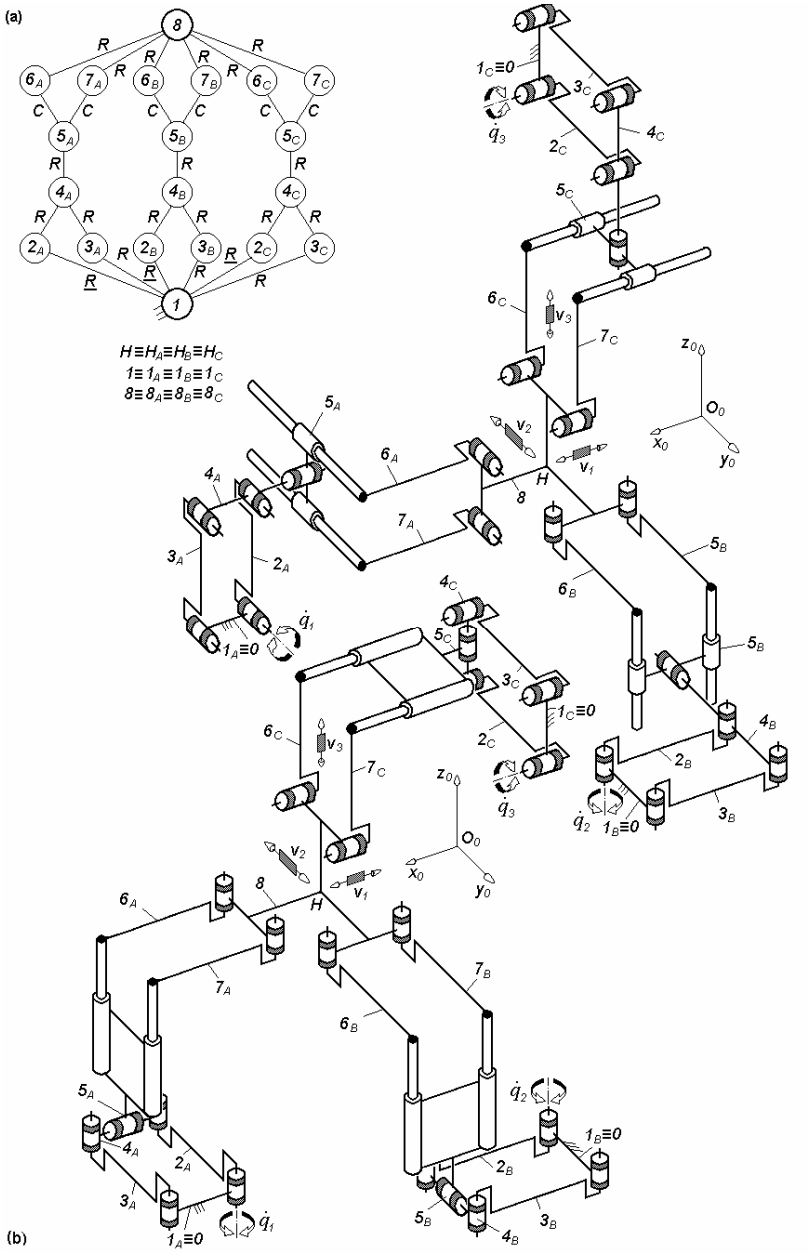

Fig. 3.126. *3-*$\underline{Pa}$*R*Pa*^{cc}-type overconstrained TPMs with coupled motions, rotating actuators mounted on the fixed base and six revolute joints adjacent to the moving platform, defined by $M_F = S_F = 3$, $(R_F) = (\boldsymbol{v}_1, \boldsymbol{v}_2, \boldsymbol{v}_3)$, $T_F = 0$, $N_F = 18$, limb topology* $\underline{Pa} \perp R^* \perp {}^{||}Pa^{cc}$

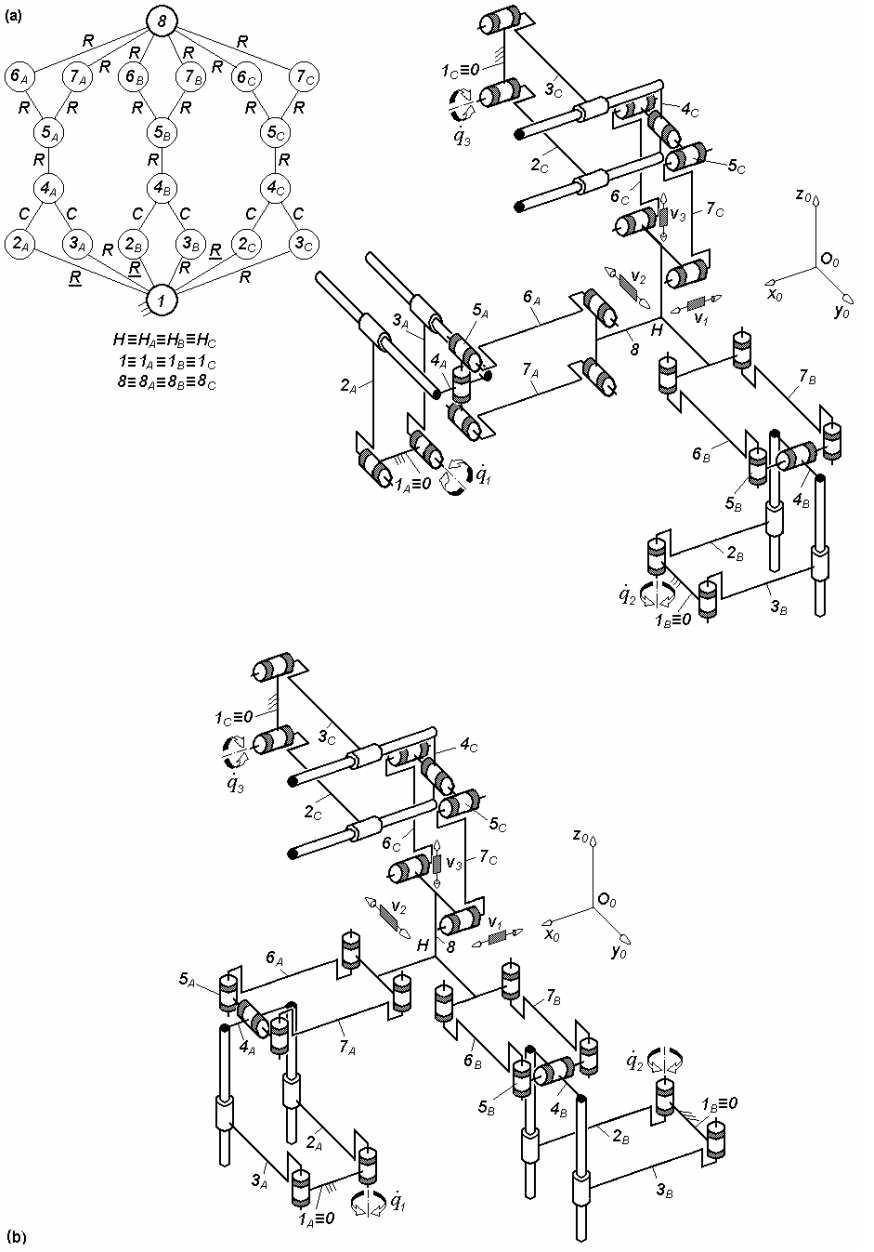

Fig. 3.127. *3-*$\underline{Pa}^{cc}$*R*Pa*-type overconstrained TPMs with coupled motions, rotating actuators mounted on the fixed base and six revolute joints adjacent to the moving platform, defined by $M_F = S_F = 3$, $(R_F) = (\boldsymbol{v}_1, \boldsymbol{v}_2, \boldsymbol{v}_3)$, $T_F = 0$, $N_F = 18$, limb topology $\underline{Pa}^{cc} \perp R^* \perp^{\parallel} Pa$

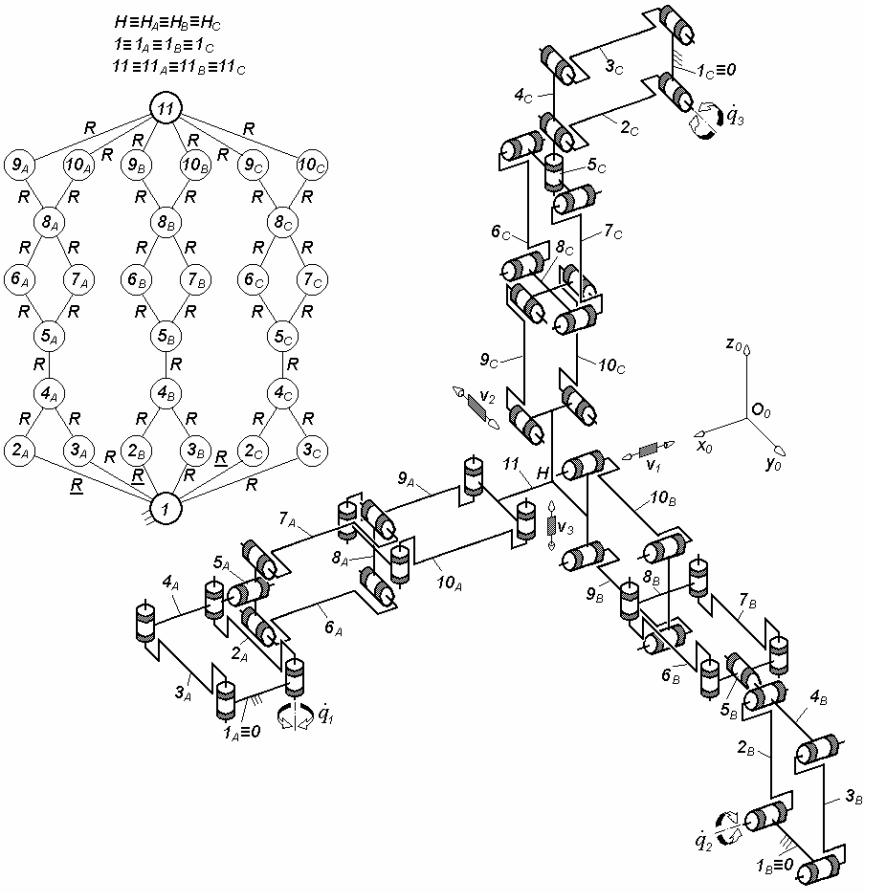

Fig. 3.128. *3-PaR*PaPa*-type overconstrained TPM with coupled motions and rotating actuators mounted on the fixed base, defined by $M_F = S_F = 3$, $(R_F) = (\boldsymbol{v}_1, \boldsymbol{v}_2, \boldsymbol{v}_3)$, $T_F = 0$, $N_F = 30$, limb topology $\underline{Pa} \perp R^* \perp^{\perp} Pa \perp^{\perp} Pa$

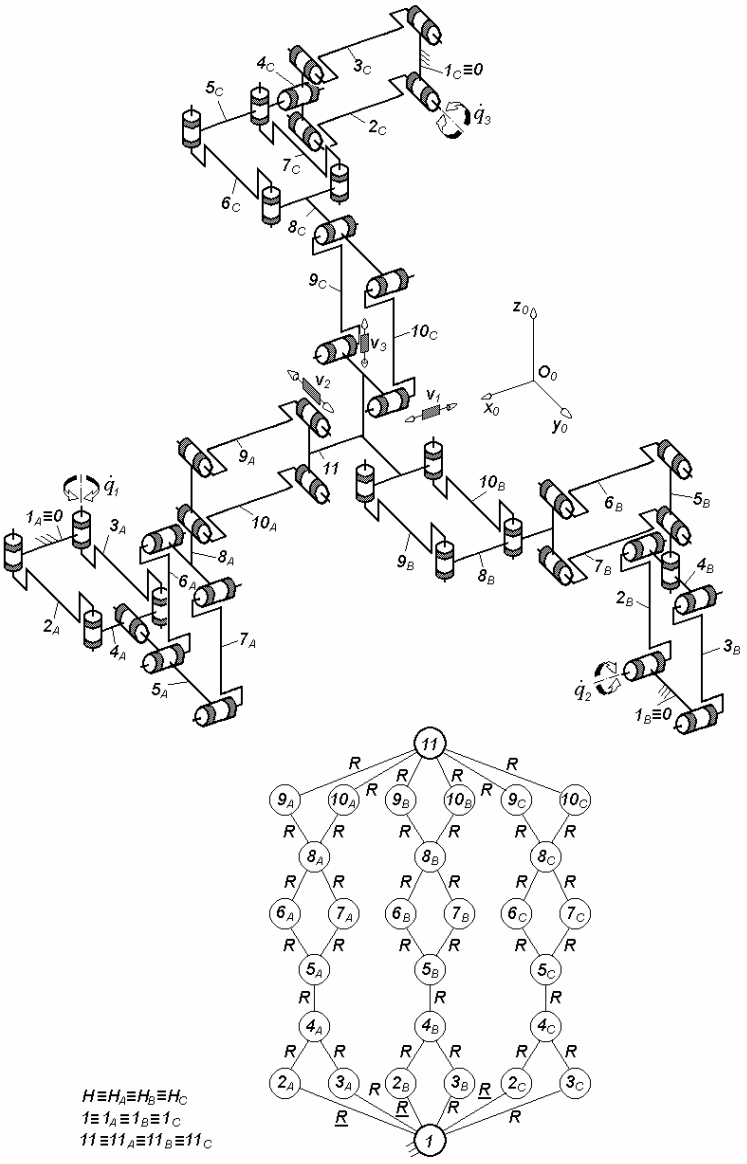

Fig. 3.129. *3-PaR*PaPa*-type overconstrained TPM with coupled motions and rotating actuators mounted on the fixed base, defined by $M_F = S_F = 3$, $(R_F) = (\boldsymbol{v}_1, \boldsymbol{v}_2, \boldsymbol{v}_3)$, $T_F = 0$, $N_F = 30$, limb topology $\underline{Pa} \perp R^* \perp^{\perp} Pa \perp^{\parallel} Pa$

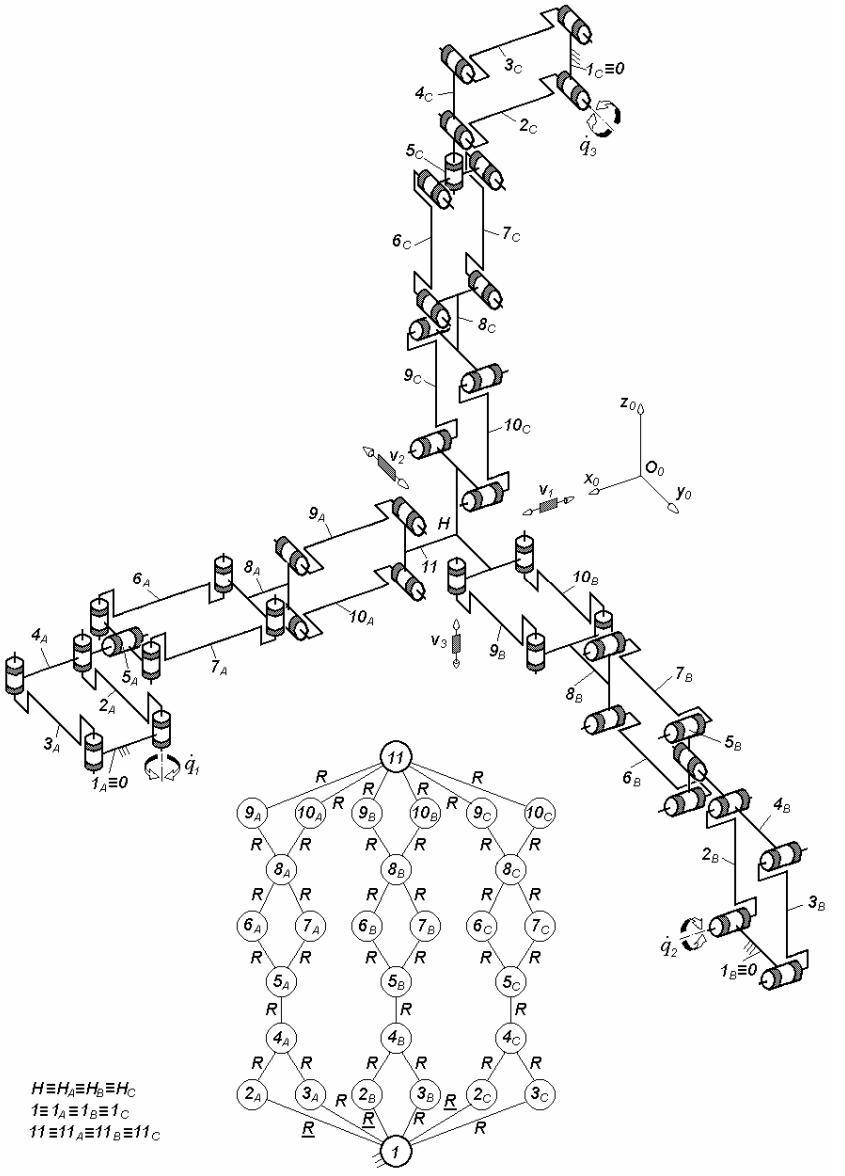

Fig. 3.130. *3-PaR*PaPa*-type overconstrained TPM with coupled motions and rotating actuators mounted on the fixed base, defined by $M_F = S_F = 3$, $(R_F) = (\boldsymbol{v}_1, \boldsymbol{v}_2, \boldsymbol{v}_3)$, $T_F = 0$, $N_F = 30$, limb topology $\underline{Pa} \perp R^* \perp {}^{\parallel}Pa \perp^{\perp} Pa$

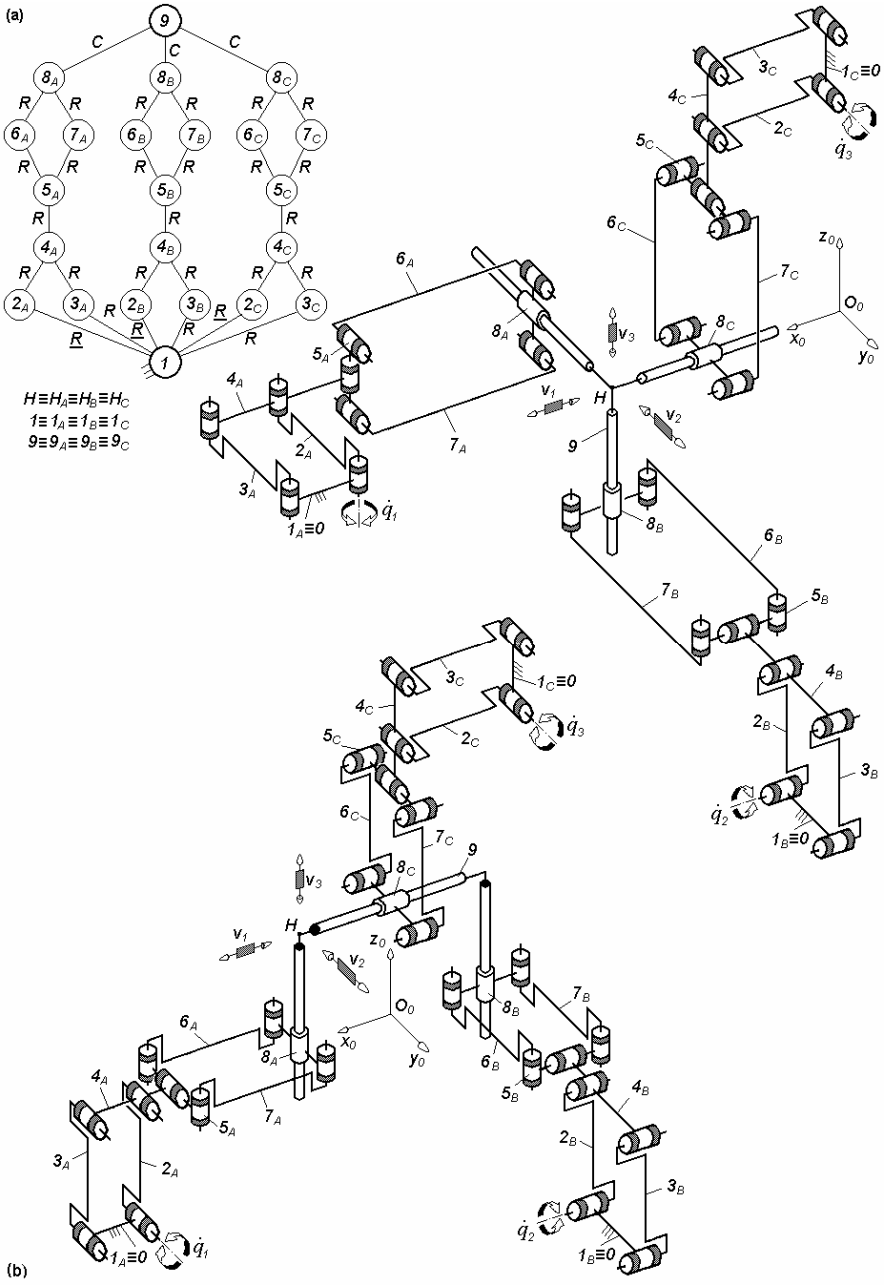

Fig. 3.131. *3-<u>Pa</u>R*PaC**-type overconstrained TPMs with coupled motions and rotating actuators mounted on the fixed base, defined by $M_F = S_F = 3$, $(R_F) = (\boldsymbol{v}_1, \boldsymbol{v}_2, \boldsymbol{v}_3)$, $T_F = 0$, $N_F = 18$, limb topology <u>Pa</u>||R* ⊥ Pa||C**

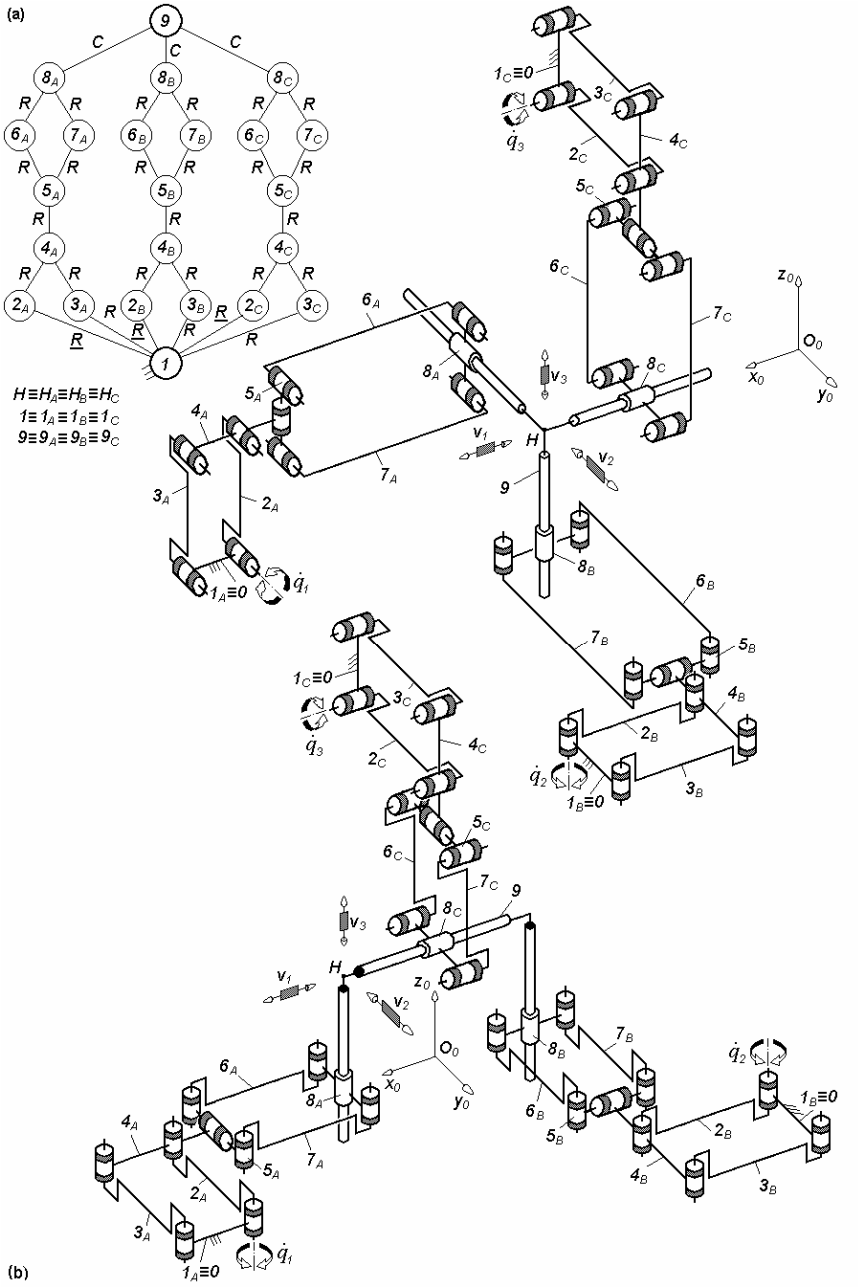

Fig. 3.132. *3-PaR*PaC**-type overconstrained TPMs with coupled motions and rotating actuators mounted on the fixed base, defined by $M_F = S_F = 3$, $(R_F) = (\boldsymbol{v}_1, \boldsymbol{v}_2, \boldsymbol{v}_3)$, $T_F = 0$, $N_F = 18$, limb topology $\underline{Pa} \perp R^* \perp {}^{\parallel}Pa \| C^*$

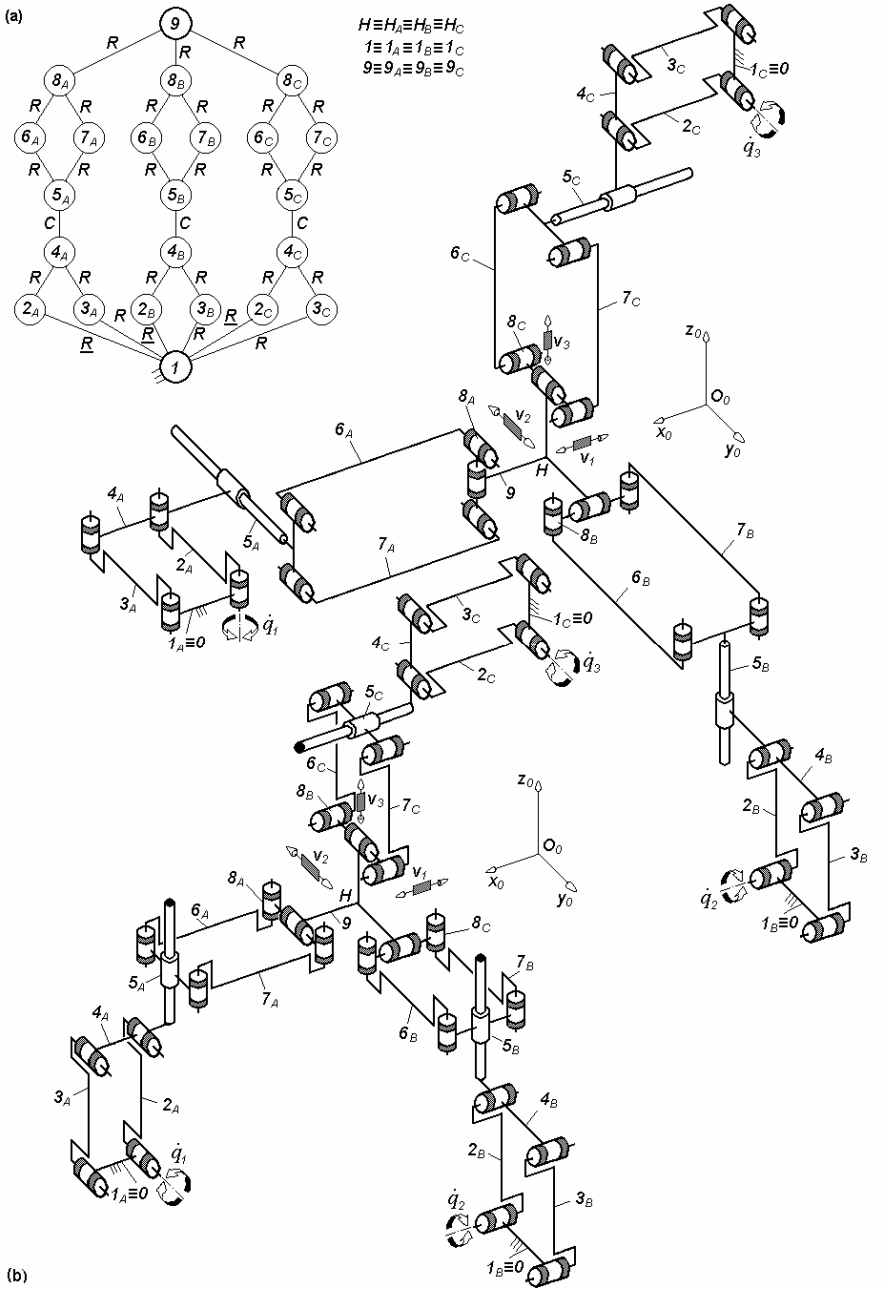

Fig. 3.133. *3-PaC*PaR**-type overconstrained TPMs with coupled motions and rotating actuators mounted on the fixed base, defined by $M_F = S_F = 3$, $(R_F) = (\boldsymbol{v}_1, \boldsymbol{v}_2, \boldsymbol{v}_3)$, $T_F = 0$, $N_F = 18$, limb topology $\underline{Pa} \perp C^* || Pa \perp {}^{||}R^*$

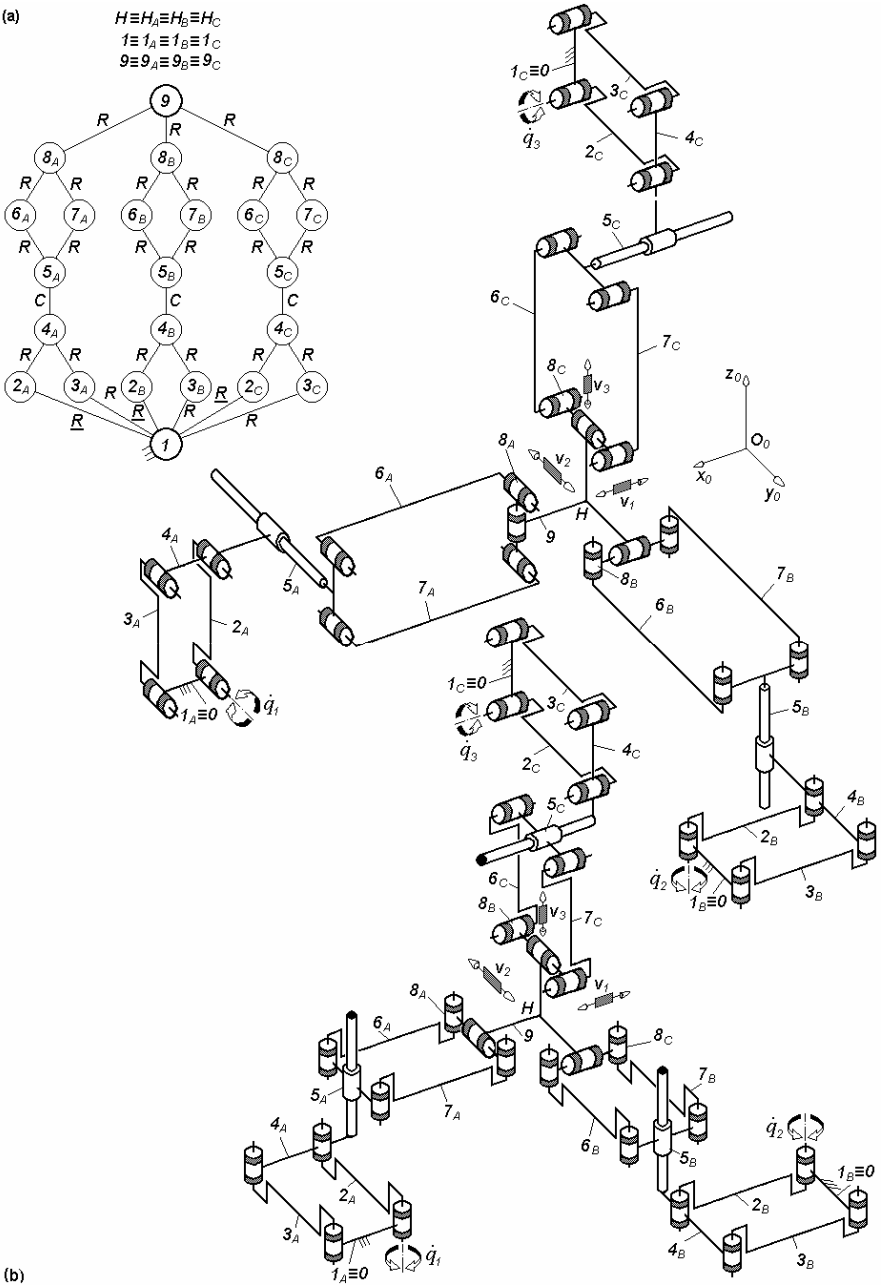

Fig. 3.134. *3-PaC*PaR*-type overconstrained TPMs with coupled motions and rotating actuators mounted on the fixed base, defined by $M_F = S_F = 3$, $(R_F) = (\boldsymbol{v}_1, \boldsymbol{v}_2, \boldsymbol{v}_3)$, $T_F = 0$, $N_F = 18$, limb topology Pa\|\|C*\|\|Pa ⊥ R**

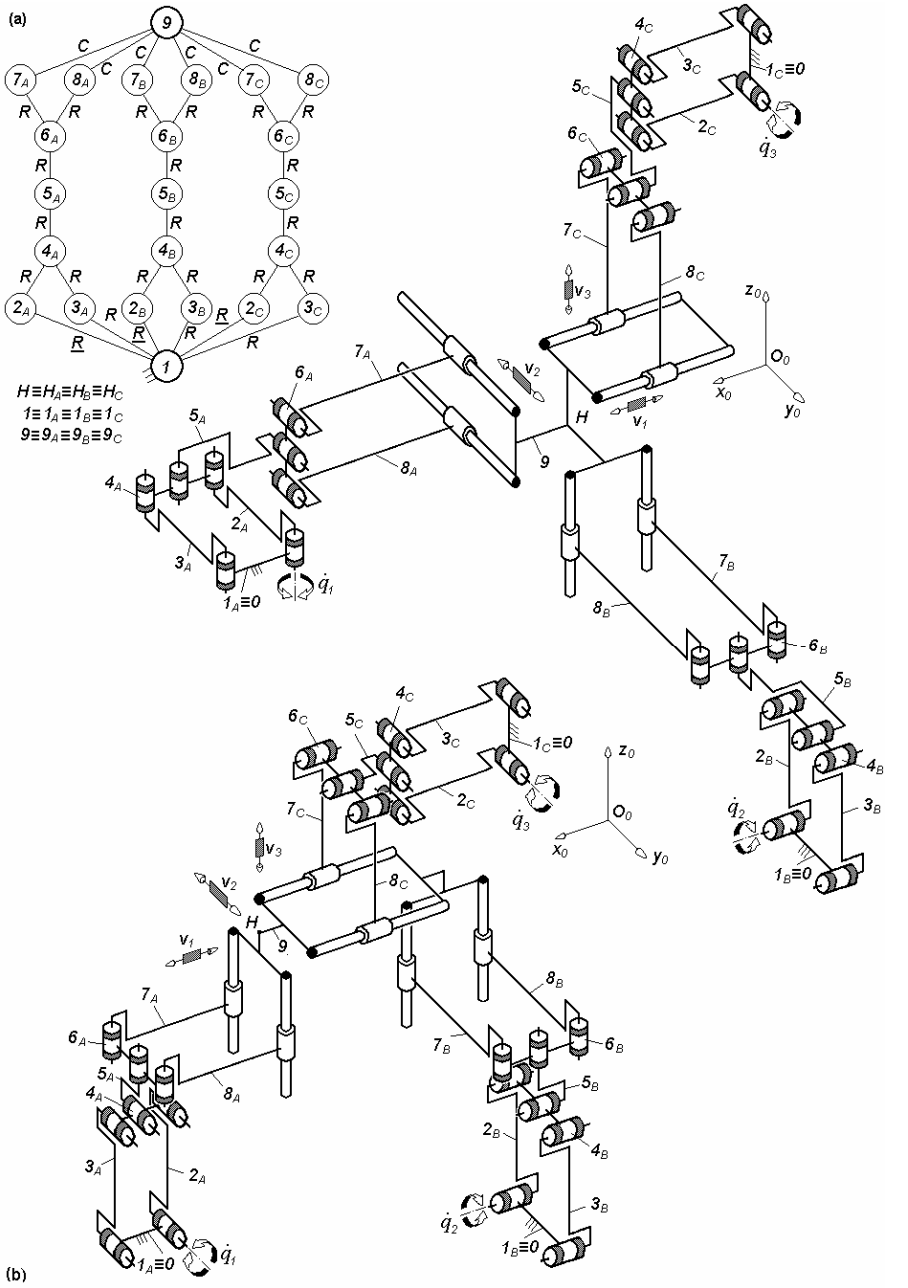

Fig. 3.135. *3-<u>Pa</u>R*R*Pa*^{cc}-type overconstrained TPMs with coupled motions and rotating actuators mounted on the fixed base, defined by $M_F = S_F = 3$, $(R_F) = (\boldsymbol{v}_1, \boldsymbol{v}_2, \boldsymbol{v}_3)$, $T_F = 0$, $N_F = 15$, limb topology <u>Pa</u>||R*⊥R*||Pa^{cc}

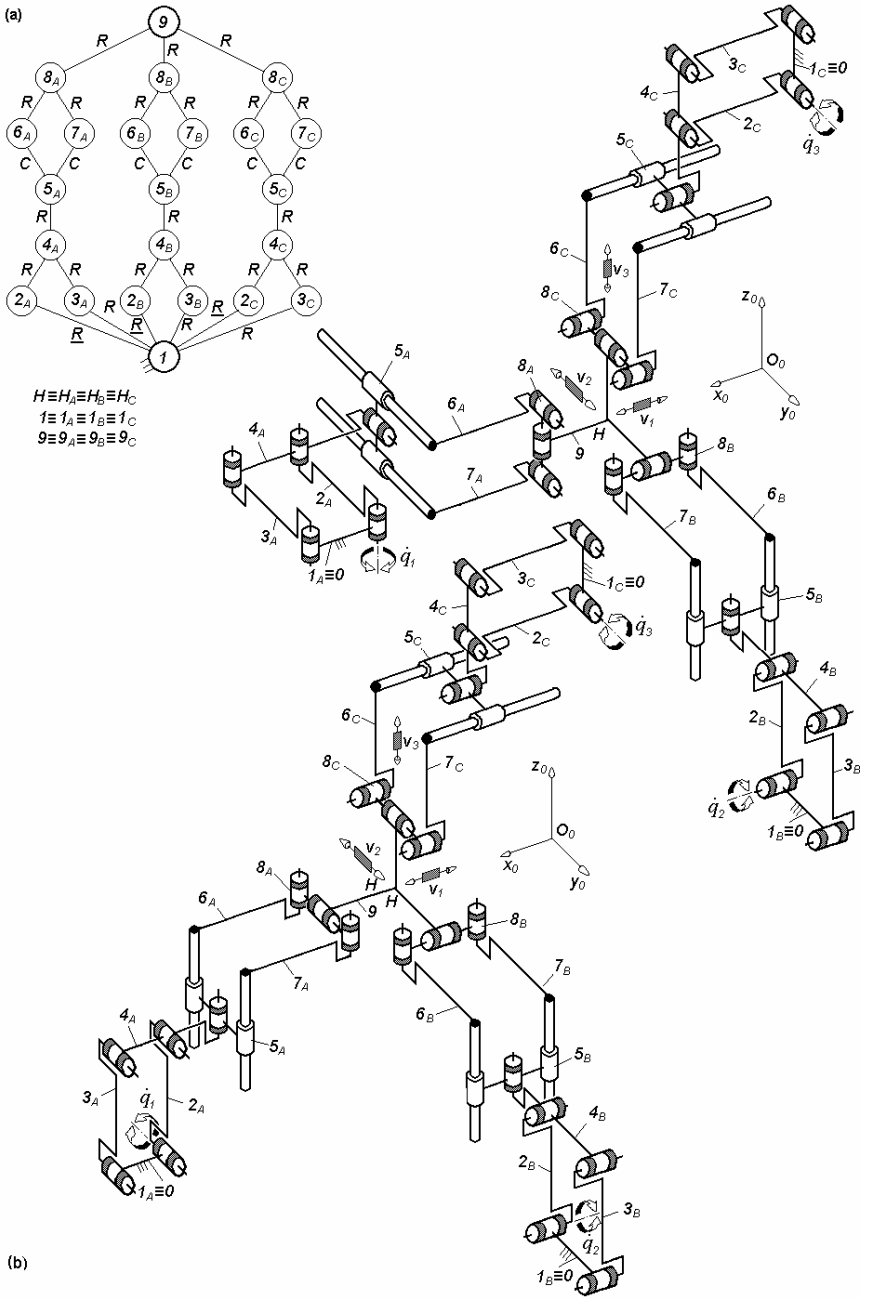

Fig. 3.136. *3-<u>Pa</u>R*Pa^cc R**-type overconstrained TPMs with coupled motions and rotating actuators mounted on the fixed base, defined by $M_F = S_F = 3$, $(R_F) = (\boldsymbol{v}_1, \boldsymbol{v}_2, \boldsymbol{v}_3)$, $T_F = 0$, $N_F = 15$, limb topology $\underline{Pa} \perp R^* || Pa^{cc} \perp {}^{||}R^*$*

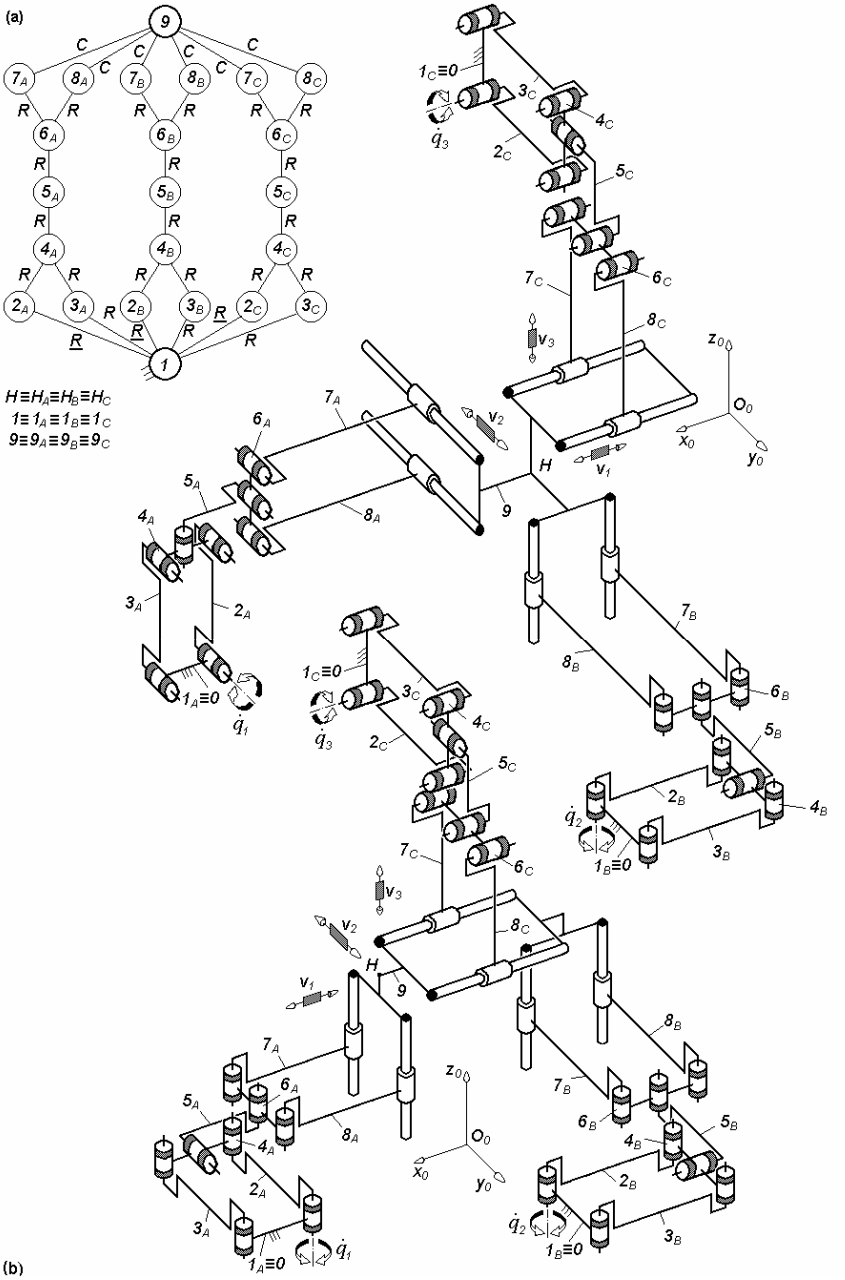

Fig. 3.137. *3-*$\underline{Pa}R^*R^*Pa^{cc}$-type overconstrained TPMs with coupled motions and rotating actuators mounted on the fixed base, defined by $M_F = S_F = 3$, $(R_F) = (\boldsymbol{v}_1, \boldsymbol{v}_2, \boldsymbol{v}_3)$, $T_F = 0$, $N_F = 15$, limb topology $\underline{Pa} \perp R^* \perp {}^{||}R^* || Pa^{cc}$

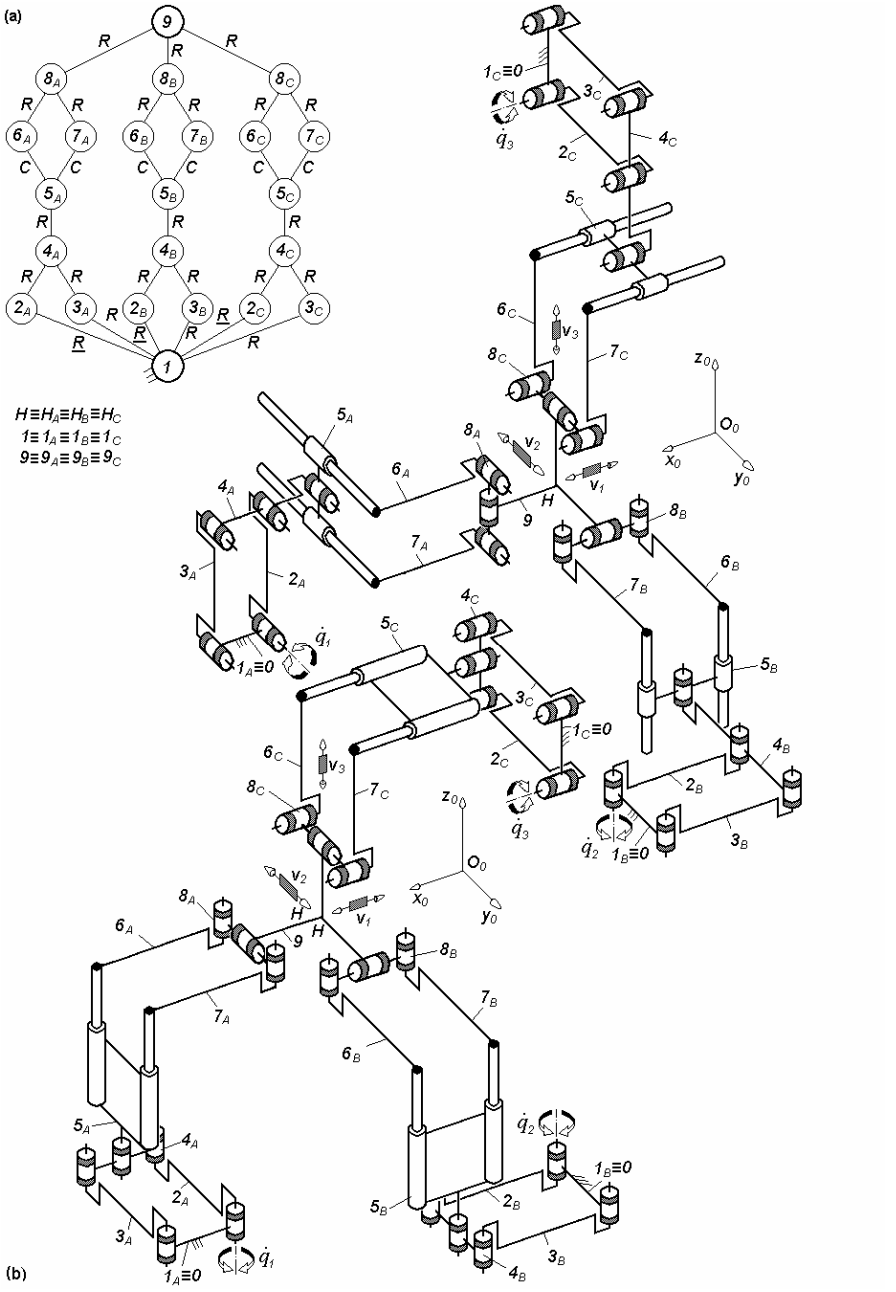

Fig. 3.138. *3-<u>Pa</u>R*Pa^cc R**-type overconstrained TPMs with coupled motions and rotating actuators mounted on the fixed base, defined by $M_F = S_F = 3$, $(R_F) = (\boldsymbol{v}_1, \boldsymbol{v}_2, \boldsymbol{v}_3)$, $T_F = 0$, $N_F = 15$, limb topology <u>Pa</u>||R*||Pa^cc ⊥ R**

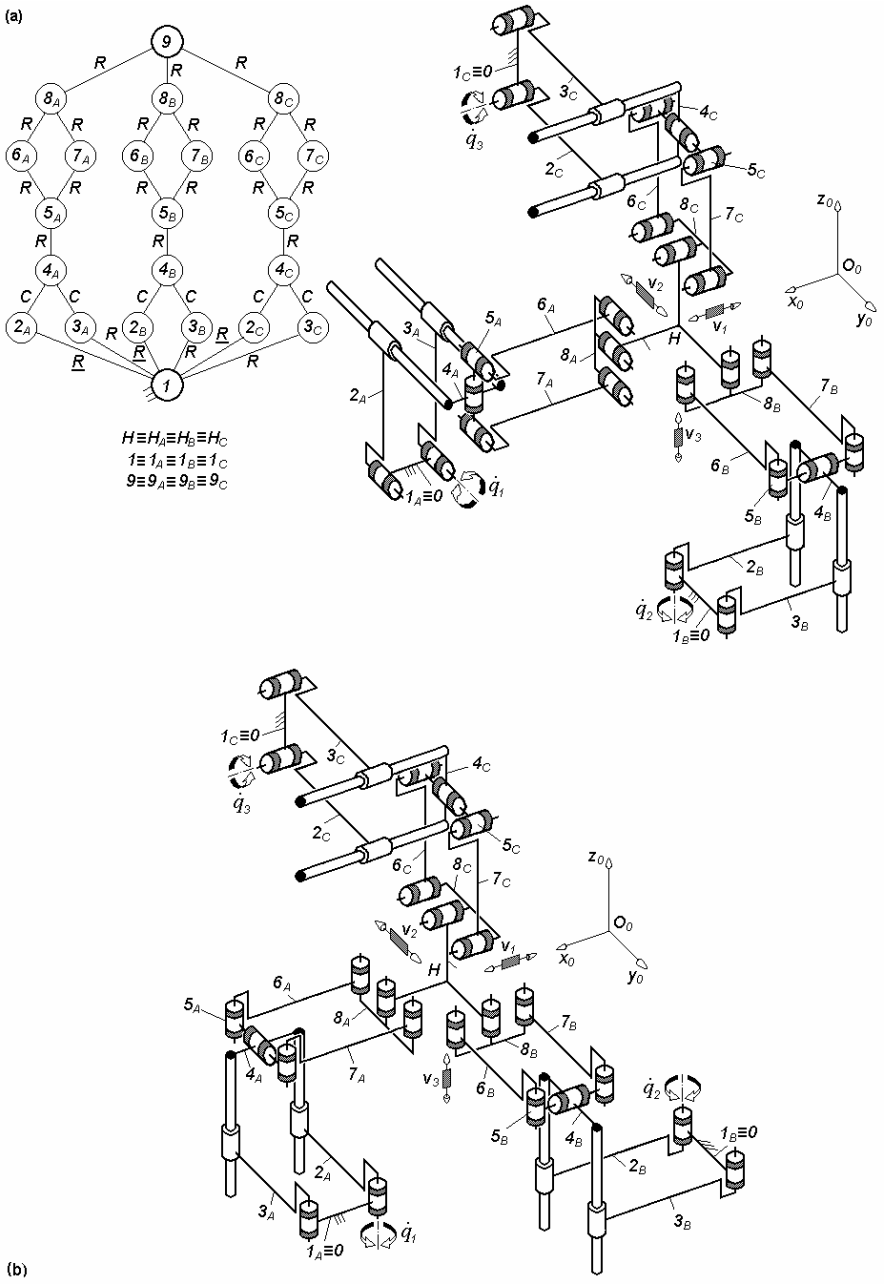

Fig. 3.139. *3-*$\underline{Pa}^{cc}$*R*PaR*-*type overconstrained TPMs with coupled motions and rotating actuators mounted on the fixed base, defined by $M_F = S_F = 3$, $(R_F) = (\boldsymbol{v}_1, \boldsymbol{v}_2, \boldsymbol{v}_3)$, $T_F = 0$, $N_F = 15$, limb topology $\underline{Pa}^{cc} \perp R^* \perp {}^{\parallel}Pa \| R^*$

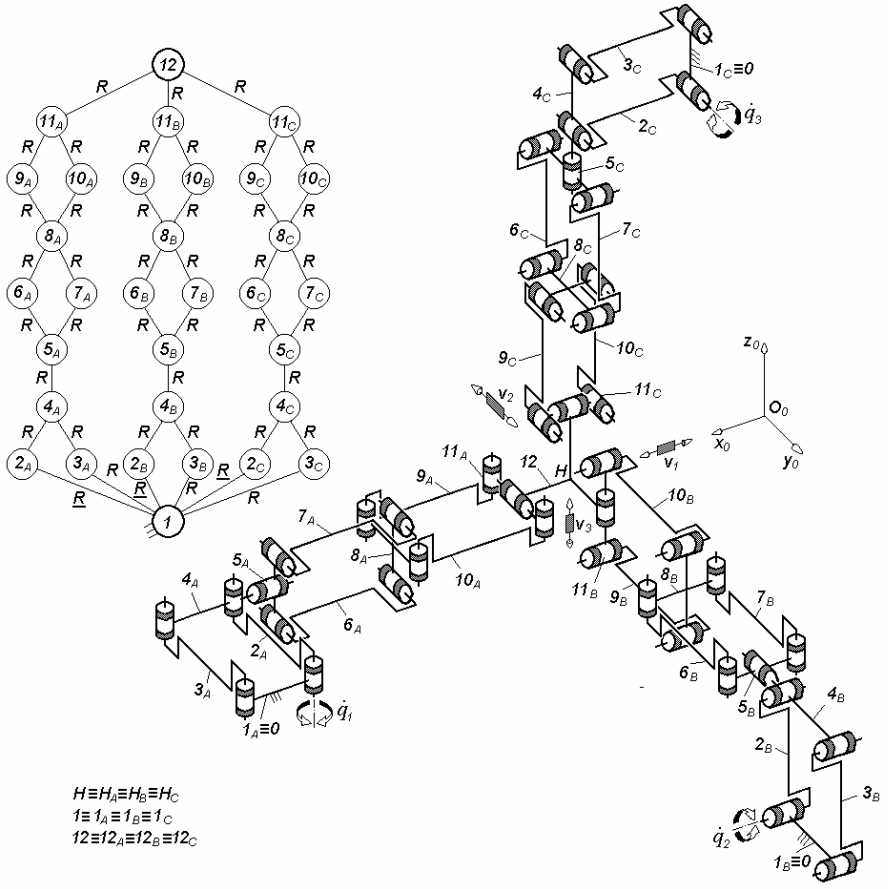

Fig. 3.140. *3-<u>Pa</u>R*PaPaR**-type overconstrained TPM with coupled motions and rotating actuators mounted on the fixed base, defined by $M_F = S_F = 3$, $(R_F) = (\boldsymbol{v}_1, \boldsymbol{v}_2, \boldsymbol{v}_3)$, $T_F = 0$, $N_F = 27$, limb topology <u>Pa</u>* $\perp$ *R** $\perp^{\perp}$ *Pa* $\perp^{\perp}$ *Pa* $\perp$ $^{\parallel}$*R**

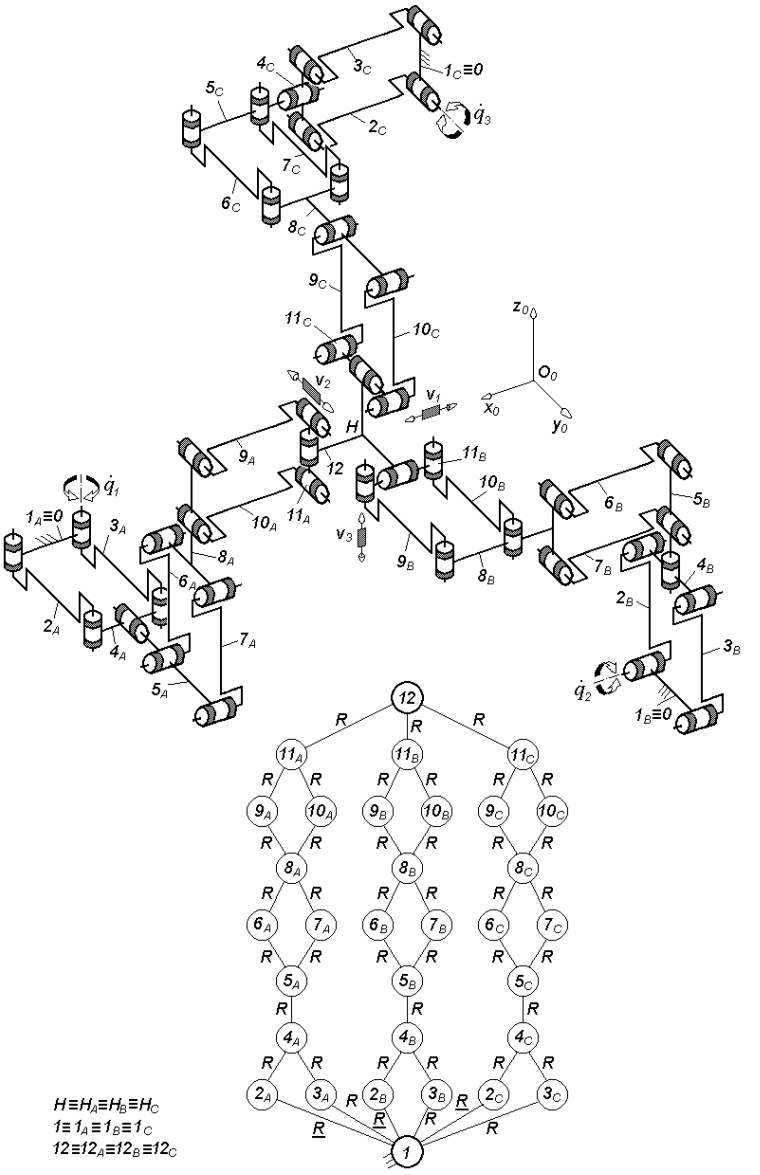

Fig. 3.141. *3-PaR*PaPaR**-type overconstrained TPM with coupled motions and rotating actuators mounted on the fixed base, defined by $M_F = S_F = 3$, $(R_F) = (\boldsymbol{v}_1, \boldsymbol{v}_2, \boldsymbol{v}_3)$, $T_F = 0$, $N_F = 27$, limb topology $\underline{Pa} \perp R^* \perp^{\perp} Pa \perp^{\parallel} Pa \perp^{\perp} R^*$

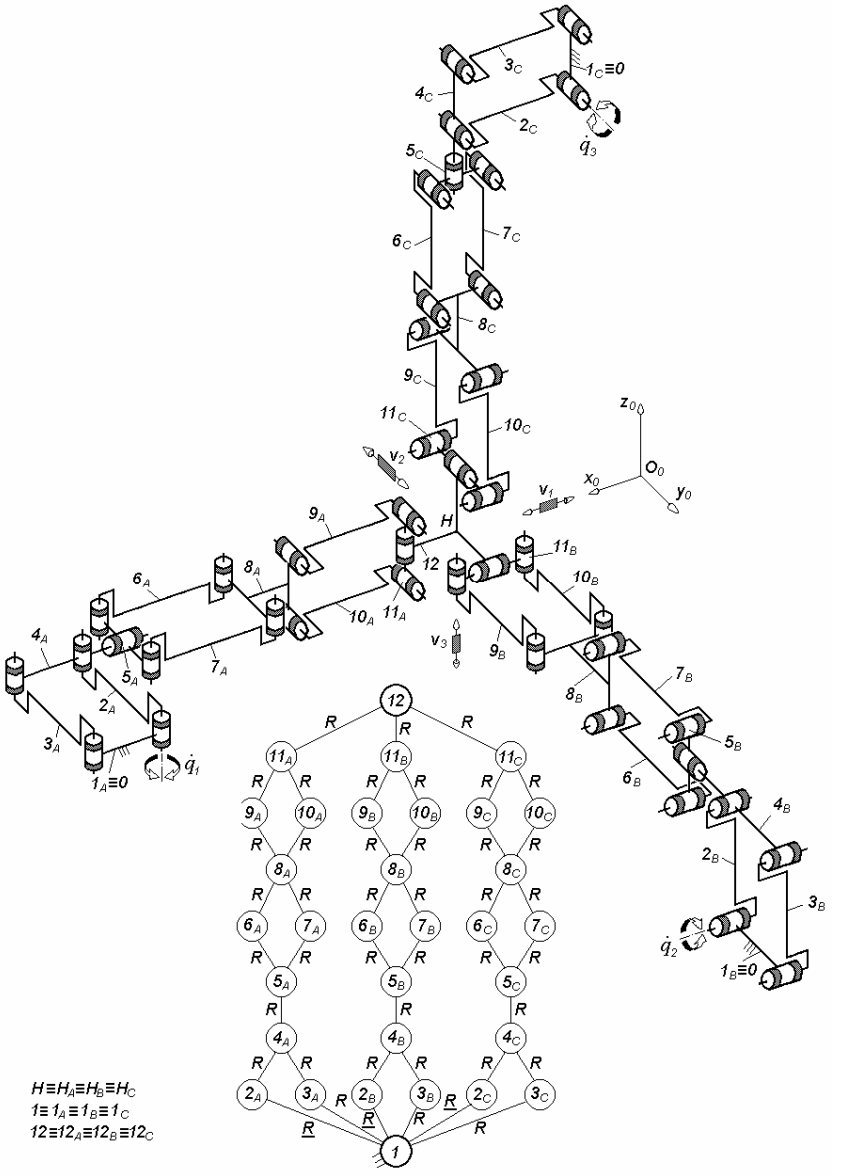

Fig. 3.142. *3-PaR*PaPaR**-type overconstrained TPM with coupled motions and rotating actuators mounted on the fixed base, defined by $M_F = S_F = 3$, $(R_F) = (\boldsymbol{v}_1, \boldsymbol{v}_2, \boldsymbol{v}_3)$, $T_F = 0$, $N_F = 27$, limb topology $\underline{Pa} \perp R^* \perp {}^{\parallel}Pa \perp^{\perp} Pa \perp {}^{\parallel}R^*$

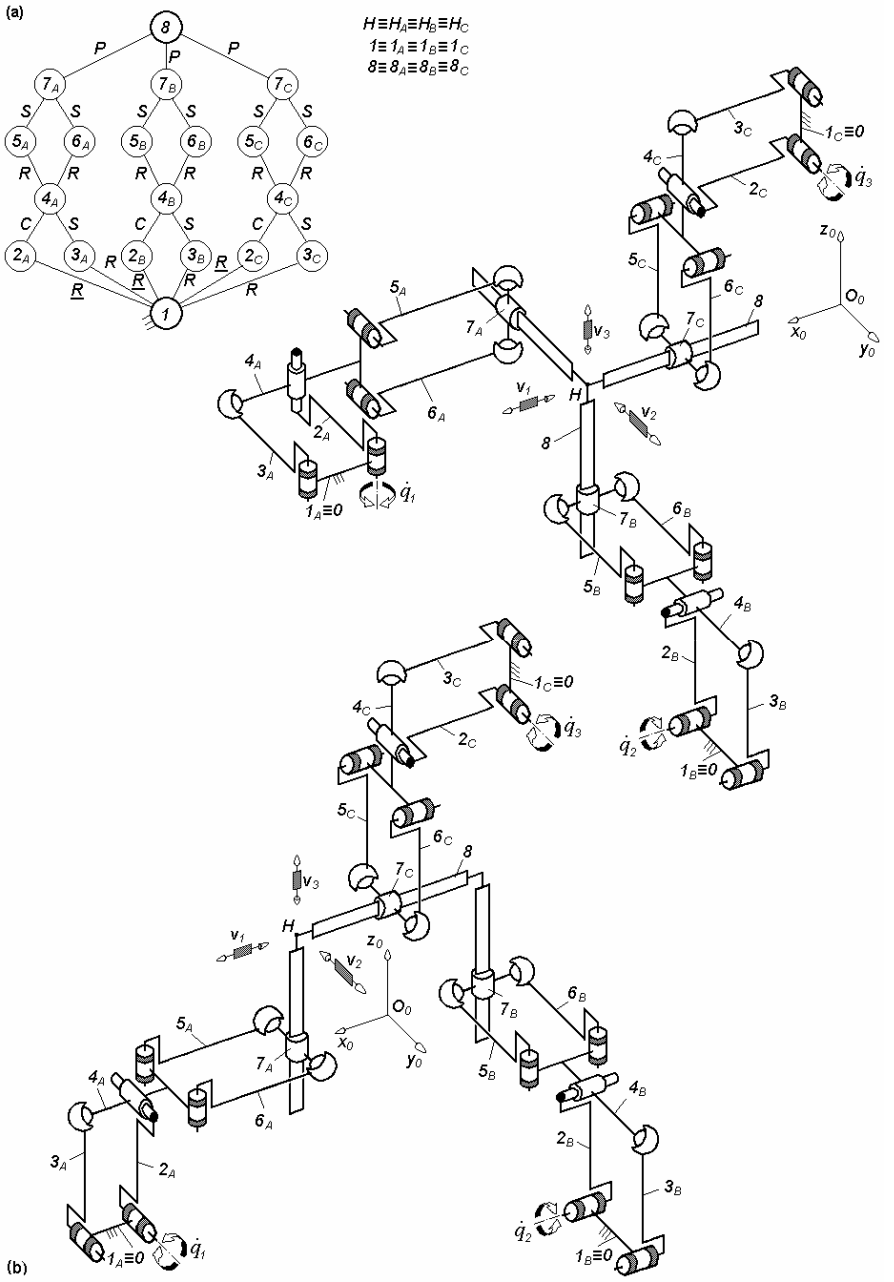

Fig. 3.143. *3-Pa*Pa^{ss}P*-type overconstrained TPMs with coupled motions and rotating actuators mounted on the fixed base, defined by $M_F = S_F = 3$, $(R_F) = (\boldsymbol{v}_1, \boldsymbol{v}_2, \boldsymbol{v}_3)$, $T_F = 0$, $N_F = 3$, limb topology $Pa^* \perp Pa^{ss} || P$

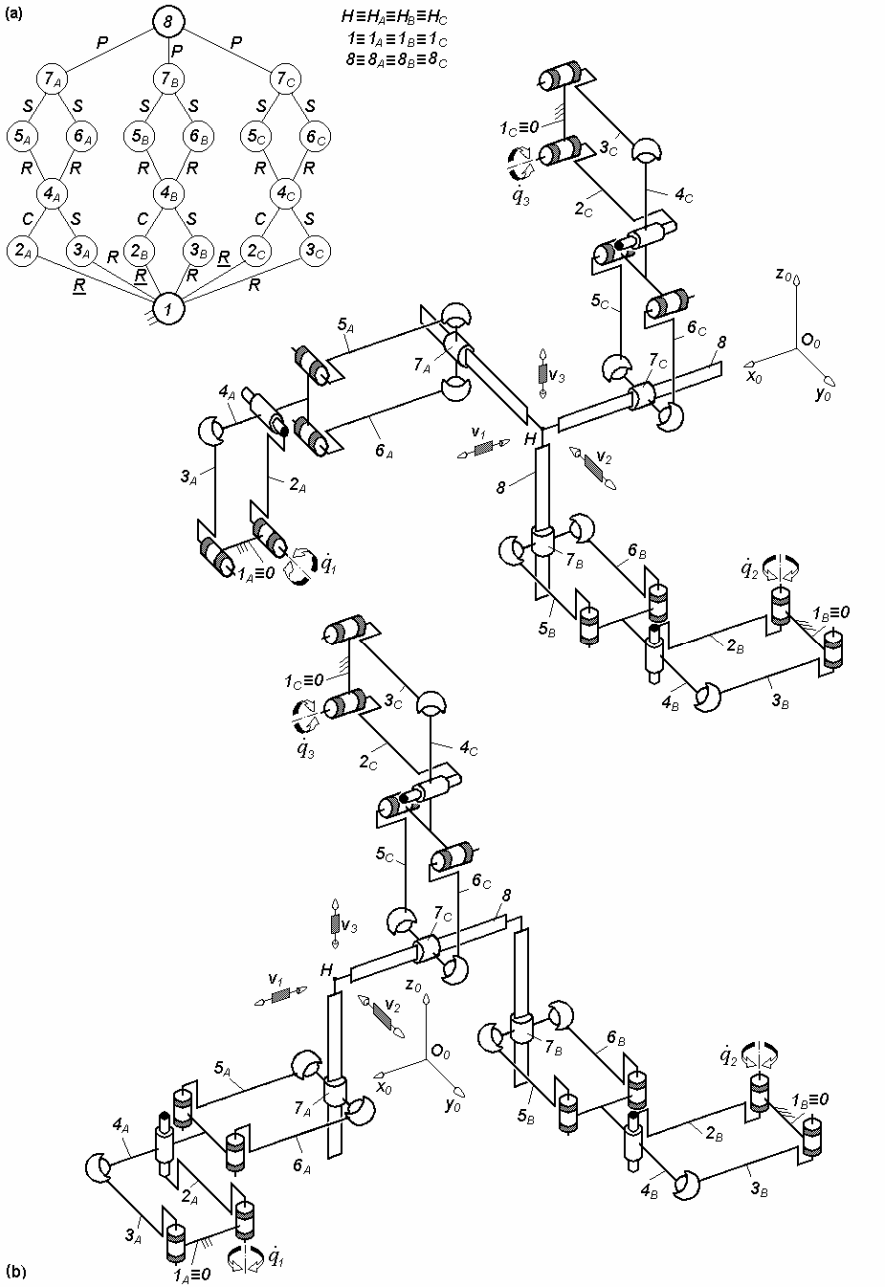

Fig. 3.144. *3-<u>Pa</u>*Pa^ssP*-type overconstrained TPMs with coupled motions and rotating actuators mounted on the fixed base, defined by $M_F = S_F = 3$, $(R_F) = (\boldsymbol{v}_1, \boldsymbol{v}_2, \boldsymbol{v}_3)$ $T_F = 0$, $N_F = 3$, limb topology <u>Pa</u>*||Pa^ss||P

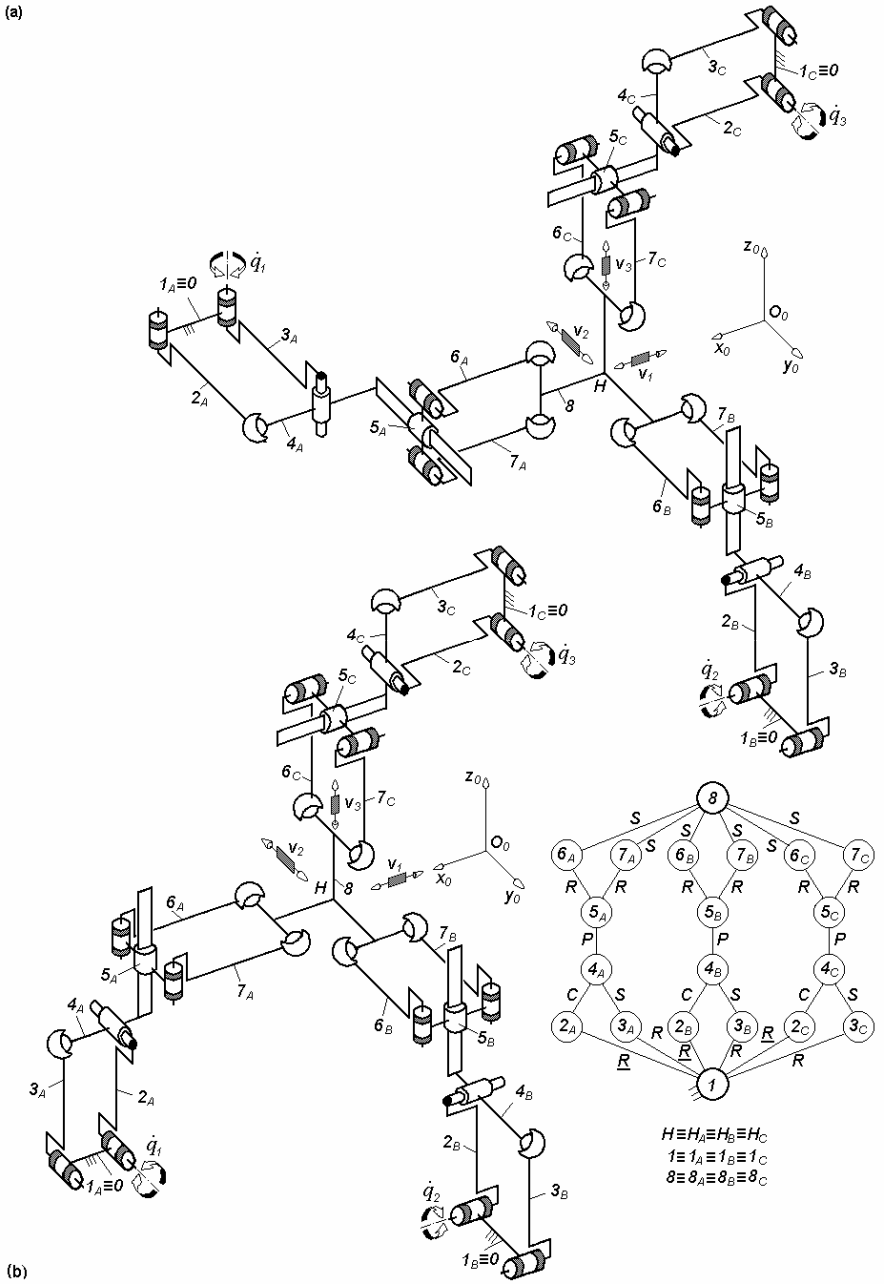

Fig. 3.145. *3-<u>Pa</u>*PPa*^{ss}-type overconstrained TPMs with coupled motions and rotating actuators mounted on the fixed base, defined by $M_F = S_F = 3$, $(R_F) = (\boldsymbol{v}_1, \boldsymbol{v}_2, \boldsymbol{v}_3)$, $T_F = 0$, $N_F = 3$, limb topology $\underline{Pa}^* \perp P || Pa^{ss}$

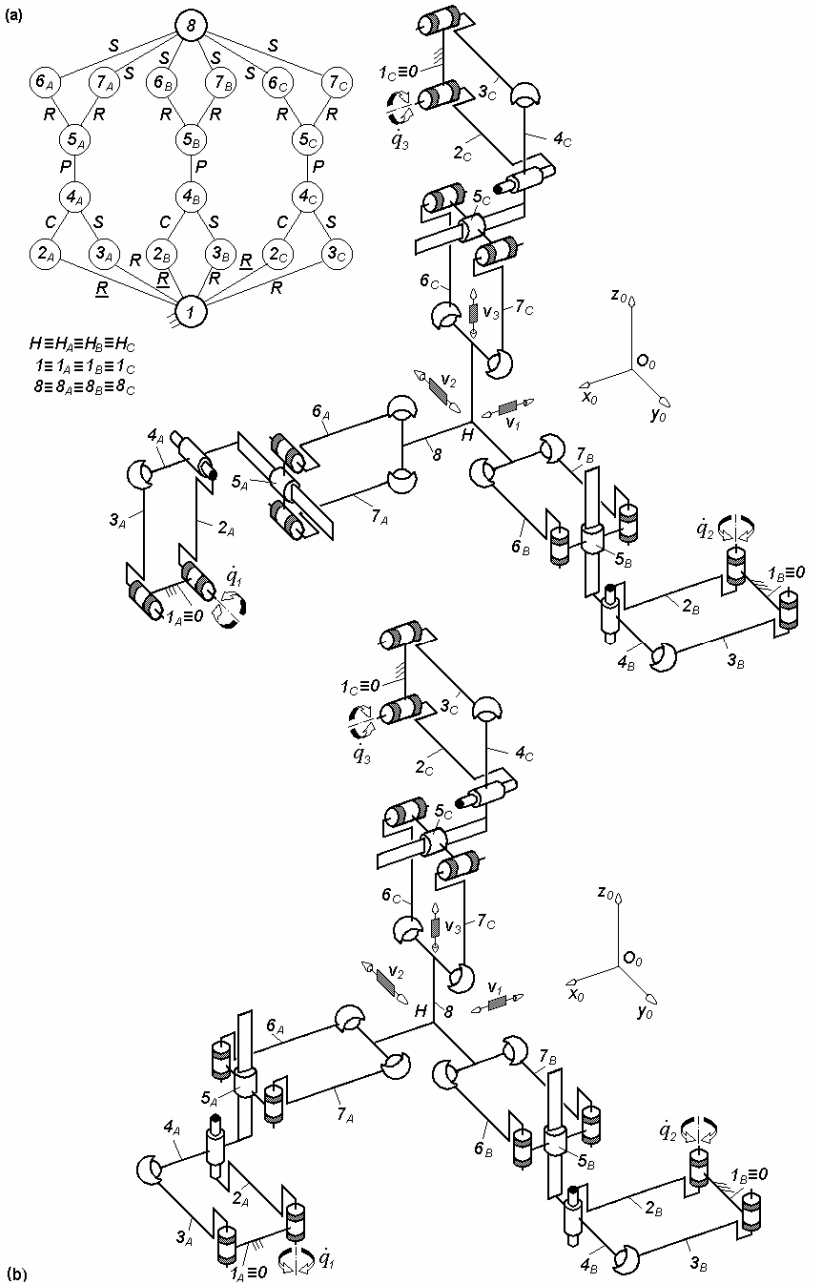

Fig. 3.146. *3-Pa*PPa*^{ss}-type overconstrained TPMs with coupled motions and rotating actuators mounted on the fixed base, defined by $M_F = S_F = 3$, $(R_F) = (\boldsymbol{v}_1, \boldsymbol{v}_2, \boldsymbol{v}_3)$, $T_F = 0$, $N_F = 3$, limb topology $\underline{Pa}^*||P||Pa^{ss}$

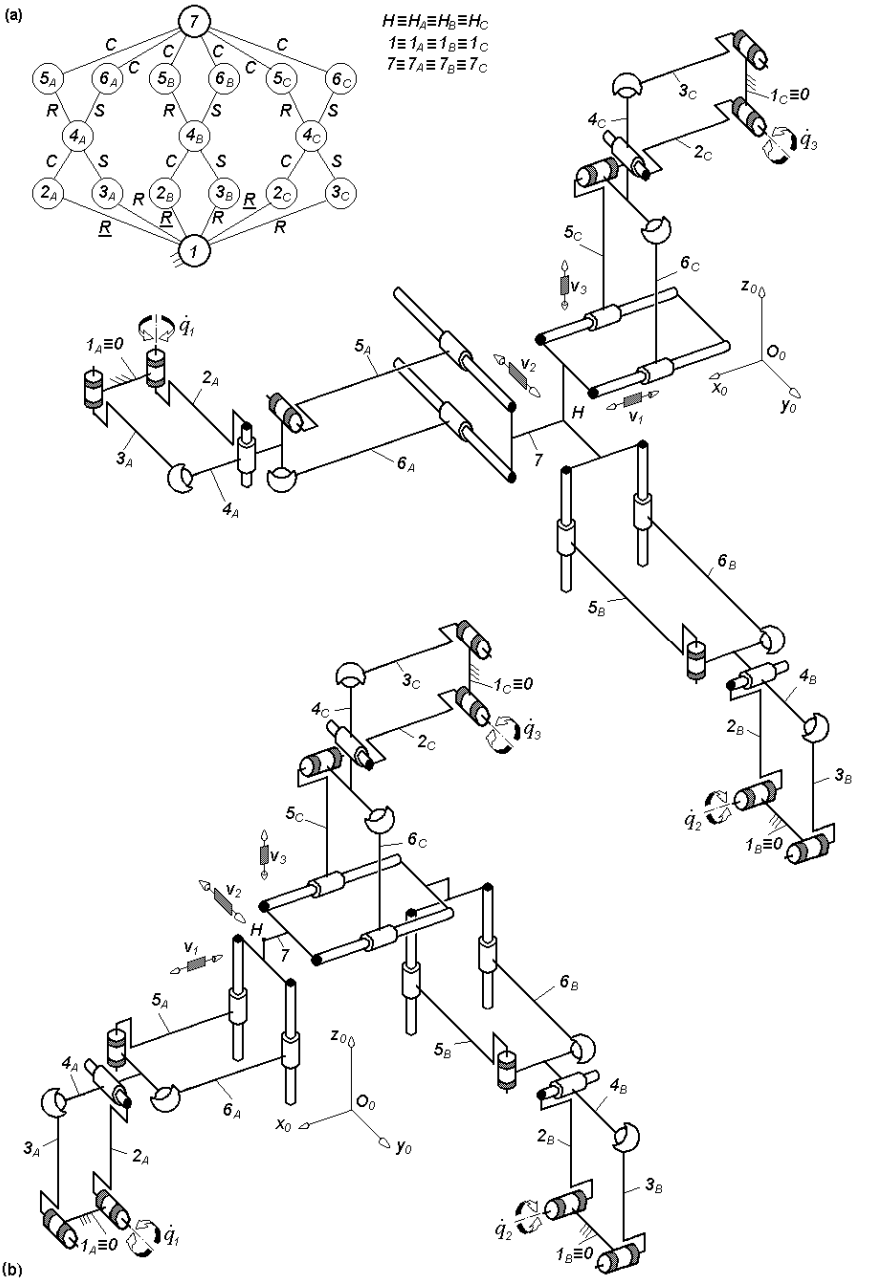

Fig. 3.147. *3-*$\underline{Pa}$*Pa^{scc}-type overconstrained TPMs with coupled motions and rotating actuators mounted on the fixed base, defined by $M_F = S_F = 3$, $(R_F) = (\boldsymbol{v}_1, \boldsymbol{v}_2, \boldsymbol{v}_3)$, $T_F = 0$, $N_F = 6$, limb topology $\underline{Pa}^* \perp Pa^{scc}$

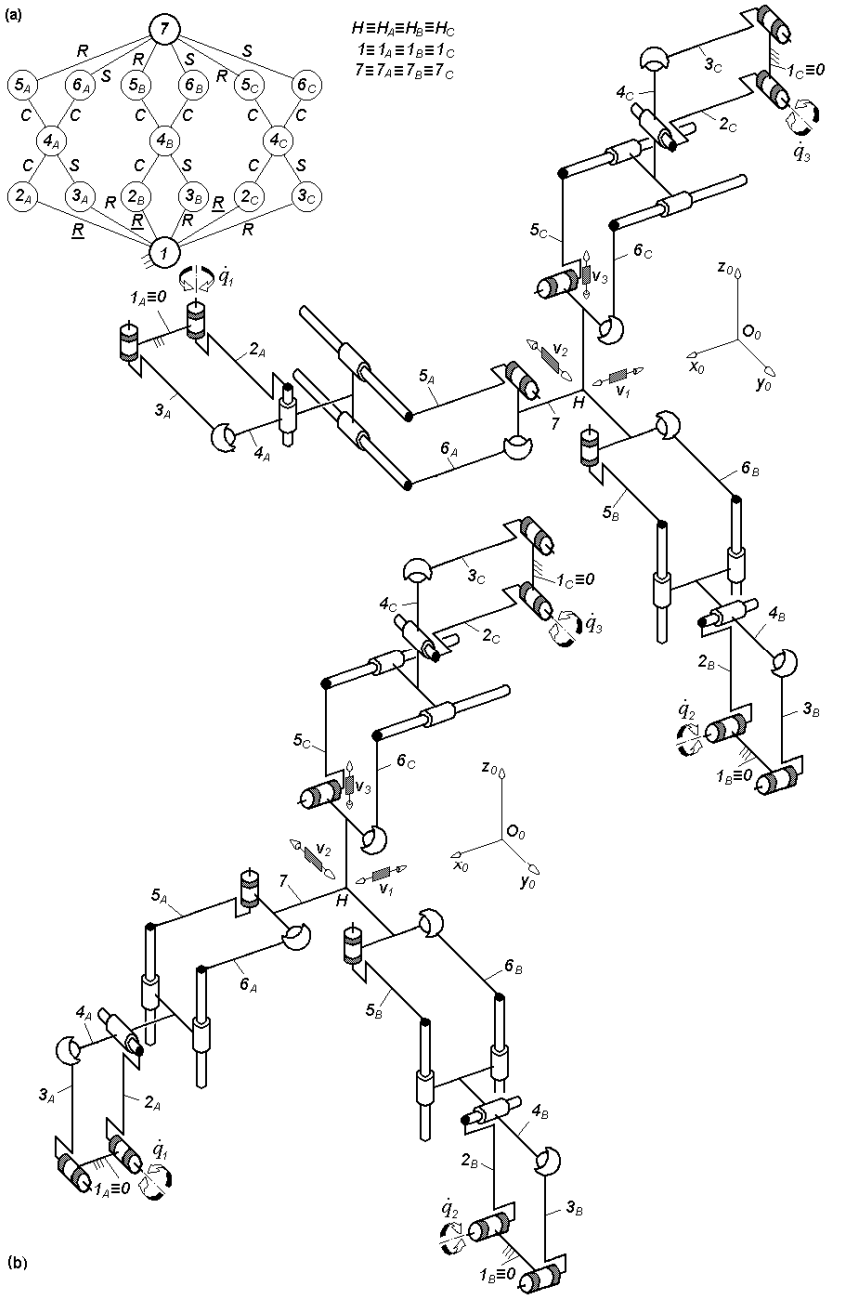

Fig. 3.148. *3-<u>Pa</u>*Pa*^{ccs}-type overconstrained TPMs with coupled motions and rotating actuators mounted on the fixed base, defined by $M_F = S_F = 3$, $(R_F) = (\boldsymbol{v}_1, \boldsymbol{v}_2, \boldsymbol{v}_3)$, $T_F = 0$, $N_F = 6$, limb topology <u>Pa</u>* ⊥ Pa^{ccs}

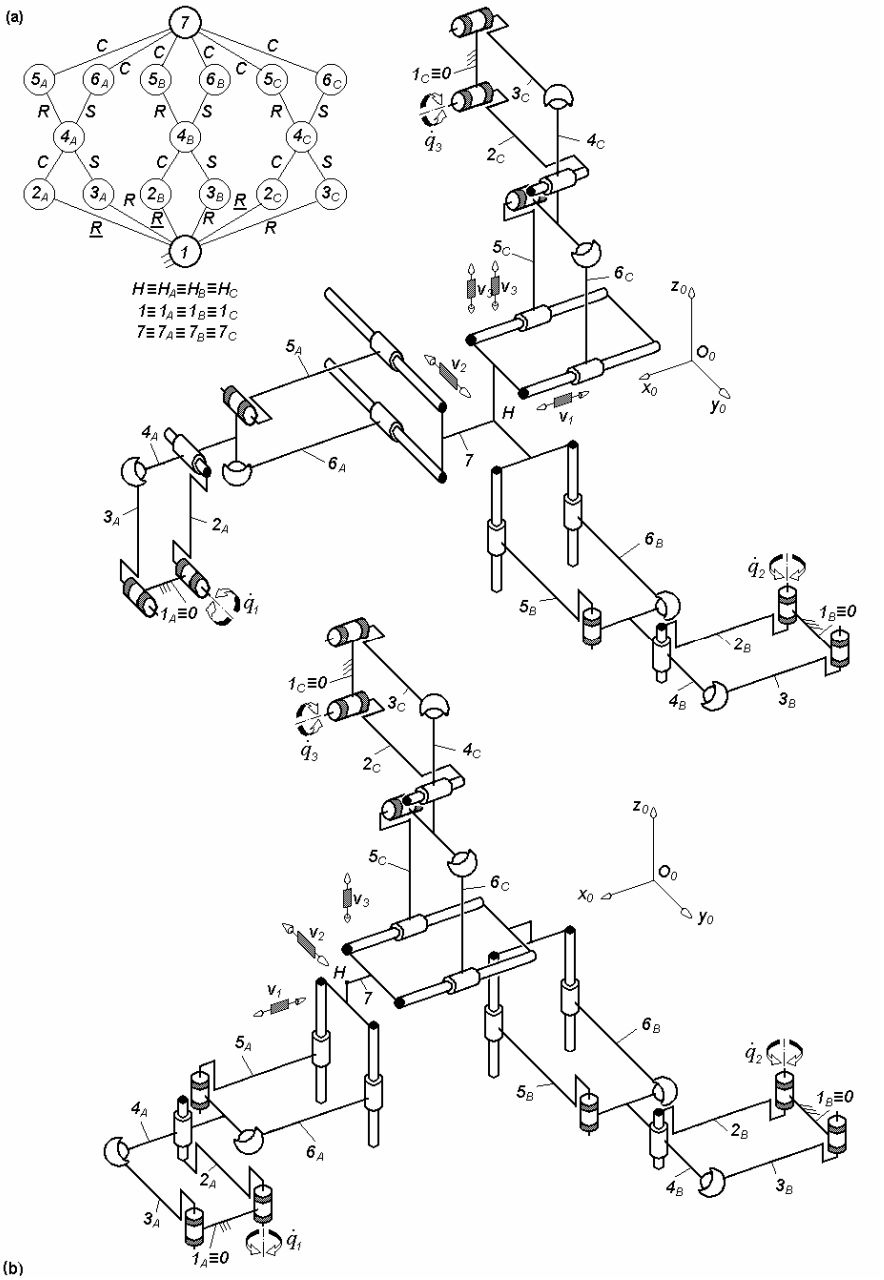

Fig. 3.149. *3-*<u>*Pa*</u>**Pa*^{scc}-type overconstrained TPMs with coupled motions and rotating actuators mounted on the fixed base, defined by $M_F = S_F = 3$, $(R_F) = (\boldsymbol{v}_1, \boldsymbol{v}_2, \boldsymbol{v}_3)$, $T_F = 0$, $N_F = 6$, limb topology <u>*Pa*</u>**||*Pa*^{scc}

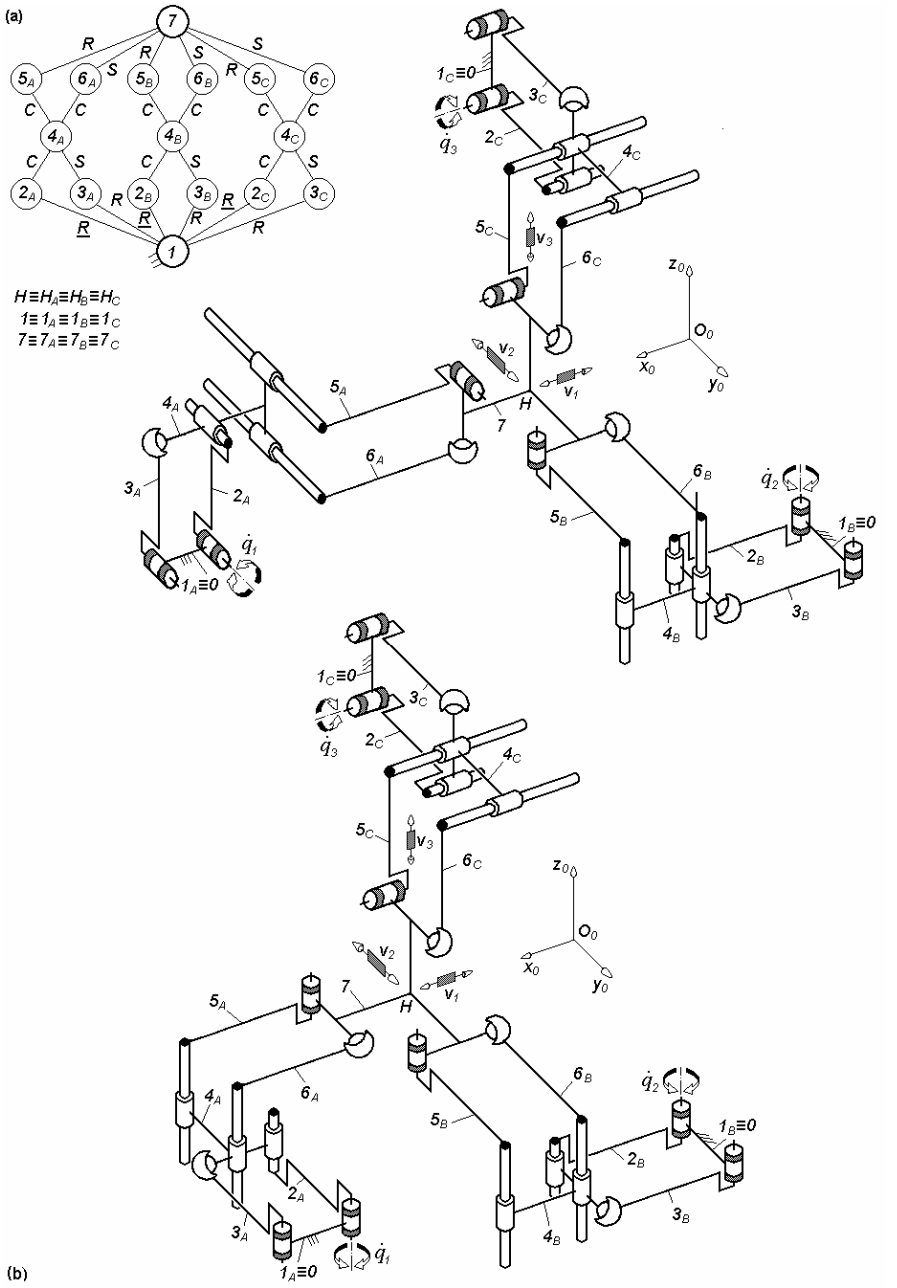

Fig. 3.150. *3-<u>Pa</u>*Pa*^{ccs}-type overconstrained TPMs with coupled motions and rotating actuators mounted on the fixed base, defined by $M_F = S_F = 3$, $(R_F) = (\boldsymbol{v}_1, \boldsymbol{v}_2, \boldsymbol{v}_3)$, $T_F = 0$, $N_F = 6$, limb topology <u>Pa</u>*||*Pa*^{ccs}

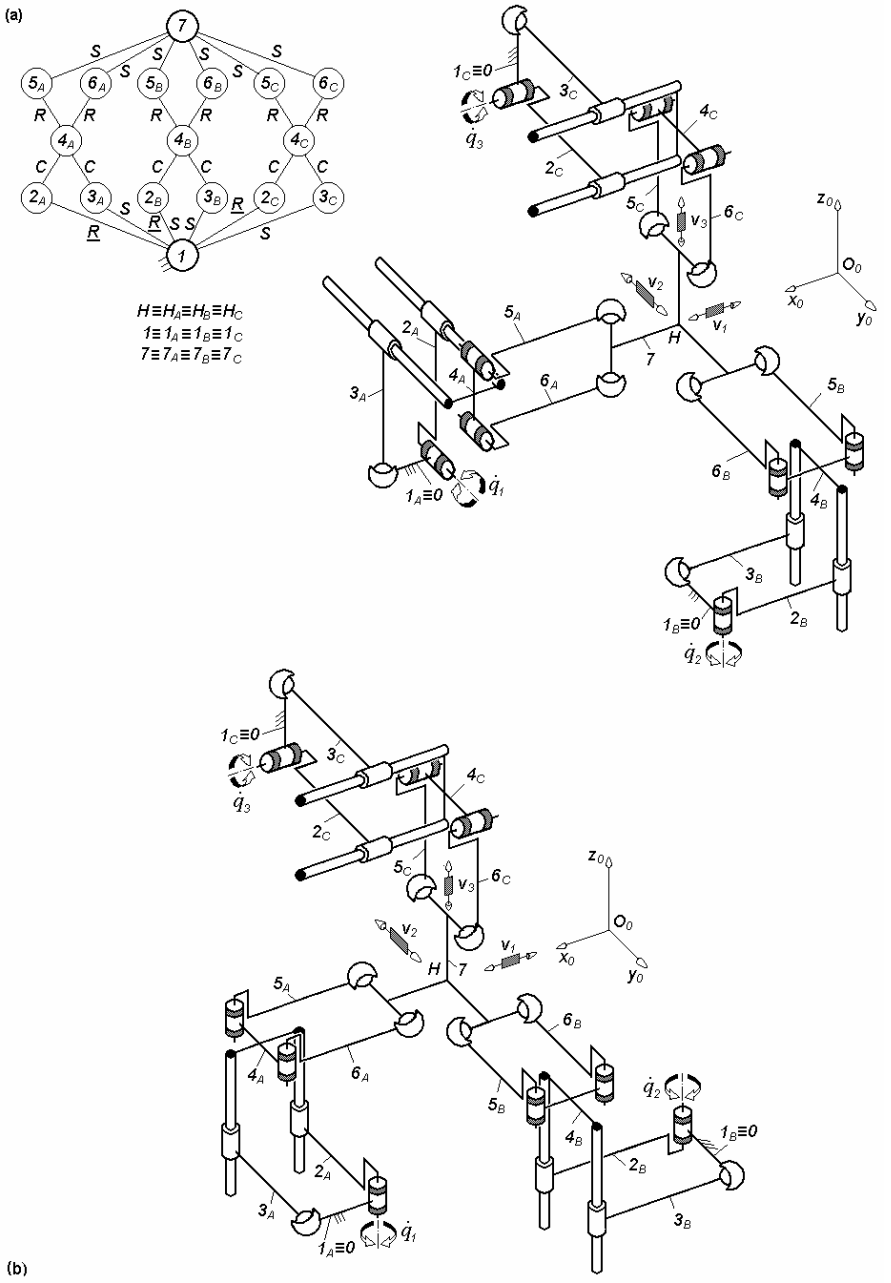

Fig. 3.151. *3-*$\underline{Pa}^{scc}Pa^{ss}$-type overconstrained TPMs with coupled motions and rotating actuators mounted on the fixed base, defined by $M_F = S_F = 3$, $(R_F) = (\boldsymbol{v}_1, \boldsymbol{v}_2, \boldsymbol{v}_3)$, $T_F = 0$, $N_F = 3$, limb topology $\underline{Pa}^{scc}||Pa^{ss}$

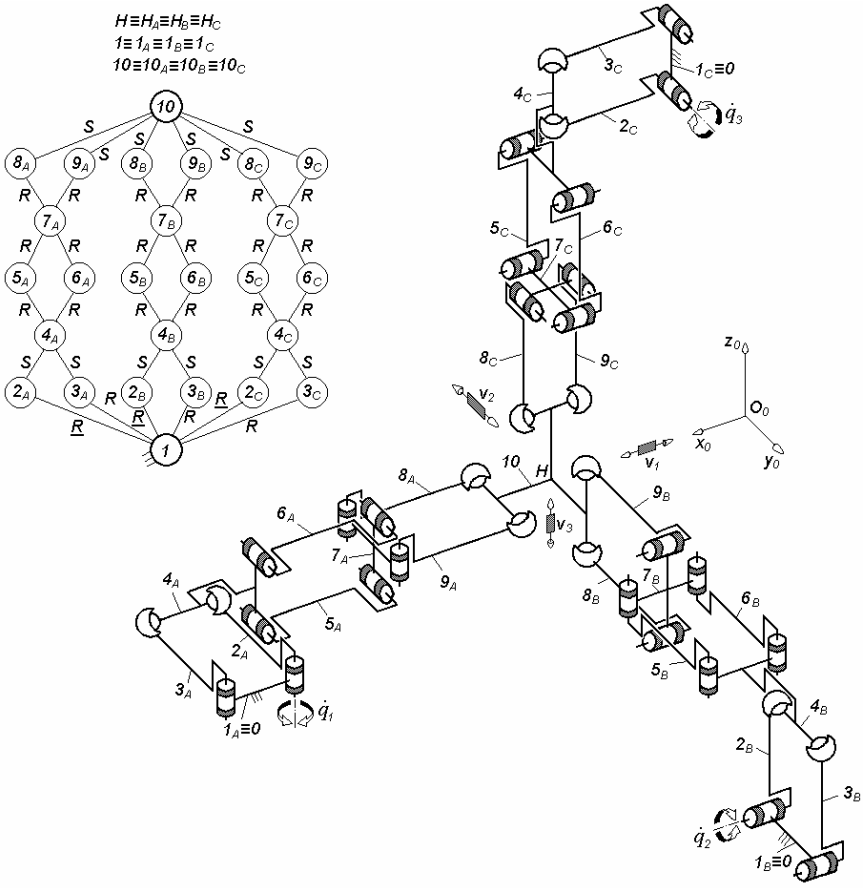

Fig. 3.152. *3-*$\underline{Pa}^{ss}PaPa^{ss}$-type overconstrained TPM with coupled motions and rotating actuators mounted on the fixed base, defined by $M_F = S_F = 3$, $(R_F) = (\boldsymbol{v}_1, \boldsymbol{v}_2, \boldsymbol{v}_3)$, $T_F = 0$, $N_F = 9$, limb topology $\underline{Pa}^{ss} \perp Pa \perp {}^{\parallel}Pa^{ss}$

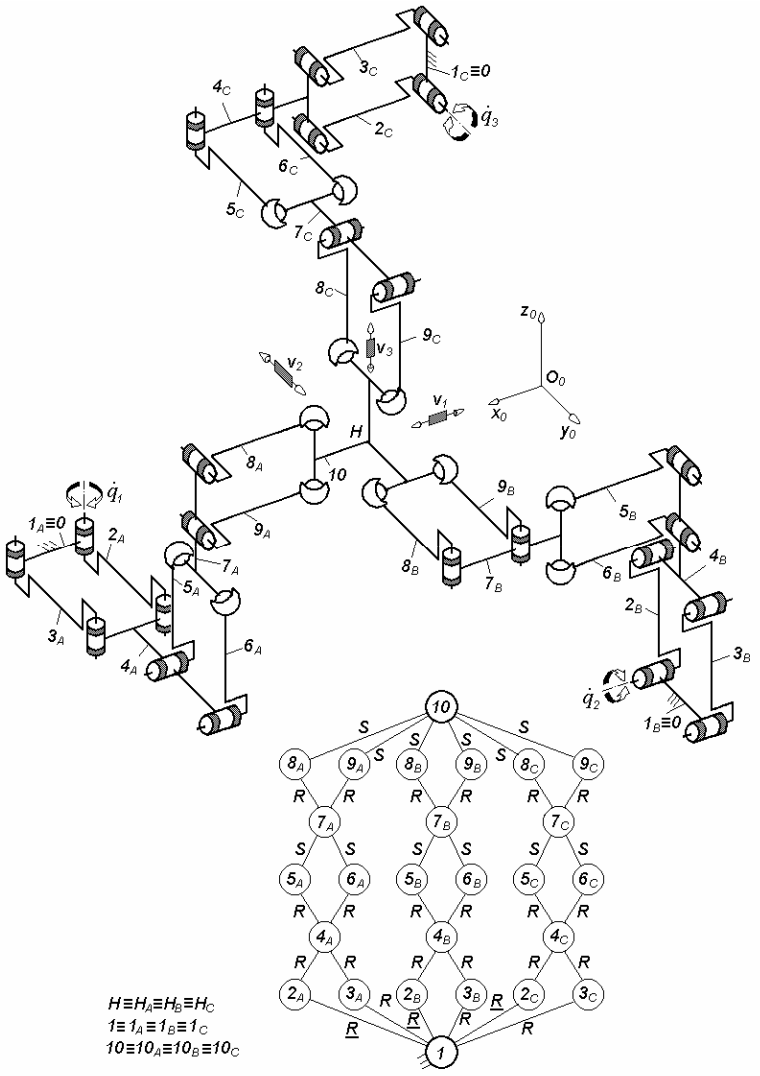

Fig. 3.153. *3-*$\underline{Pa}Pa^{ss}Pa^{ss}$-type overconstrained TPM with coupled motions and rotating actuators mounted on the fixed base, defined by $M_F = S_F = 3$, $(R_F) = (\boldsymbol{v}_1, \boldsymbol{v}_2, \boldsymbol{v}_3)$, $T_F = 0$, $N_F = 9$, limb topology $\underline{Pa} \perp Pa^{ss} \perp^{\perp} Pa^{ss}$

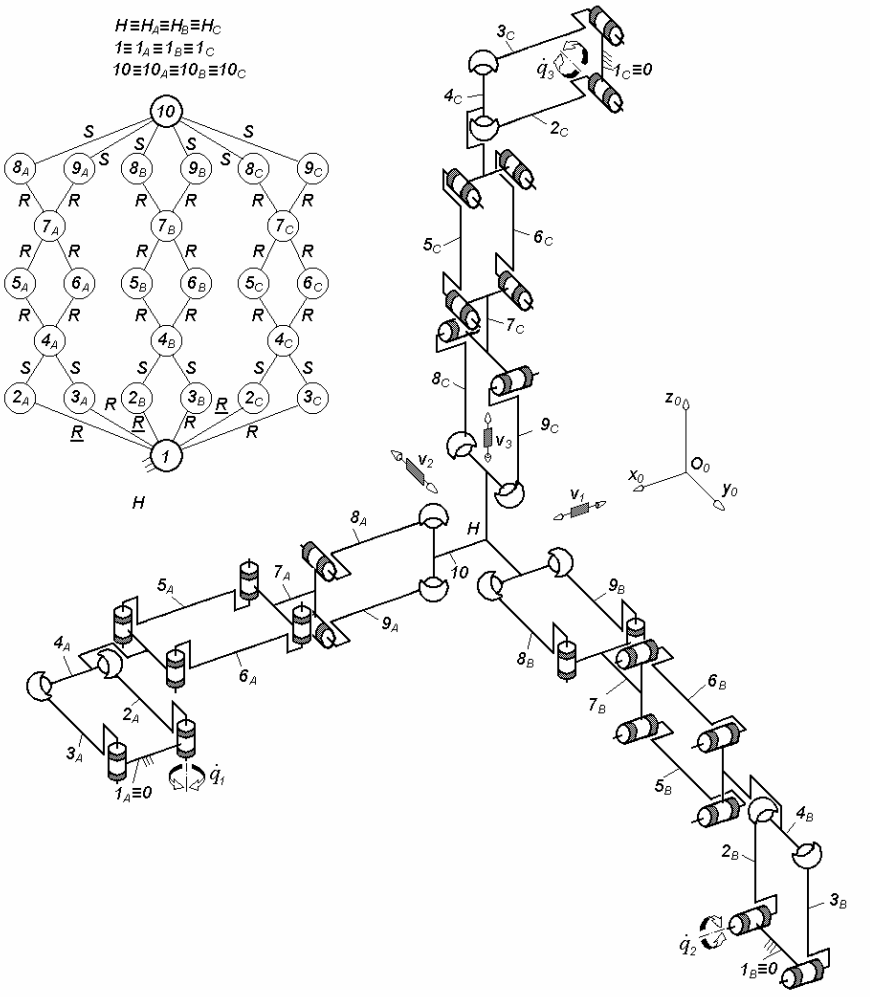

Fig. 3.154. *3-$\underline{Pa}^{ss}PaPa^{ss}$*-type overconstrained TPM with coupled motions and rotating actuators mounted on the fixed base, defined by $M_F = S_F = 3$, $(R_F) = (\boldsymbol{v}_1, \boldsymbol{v}_2, \boldsymbol{v}_3)$, $T_F = 0$, $N_F = 9$, limb topology $\underline{Pa}^{ss} || Pa \perp Pa^{ss}$

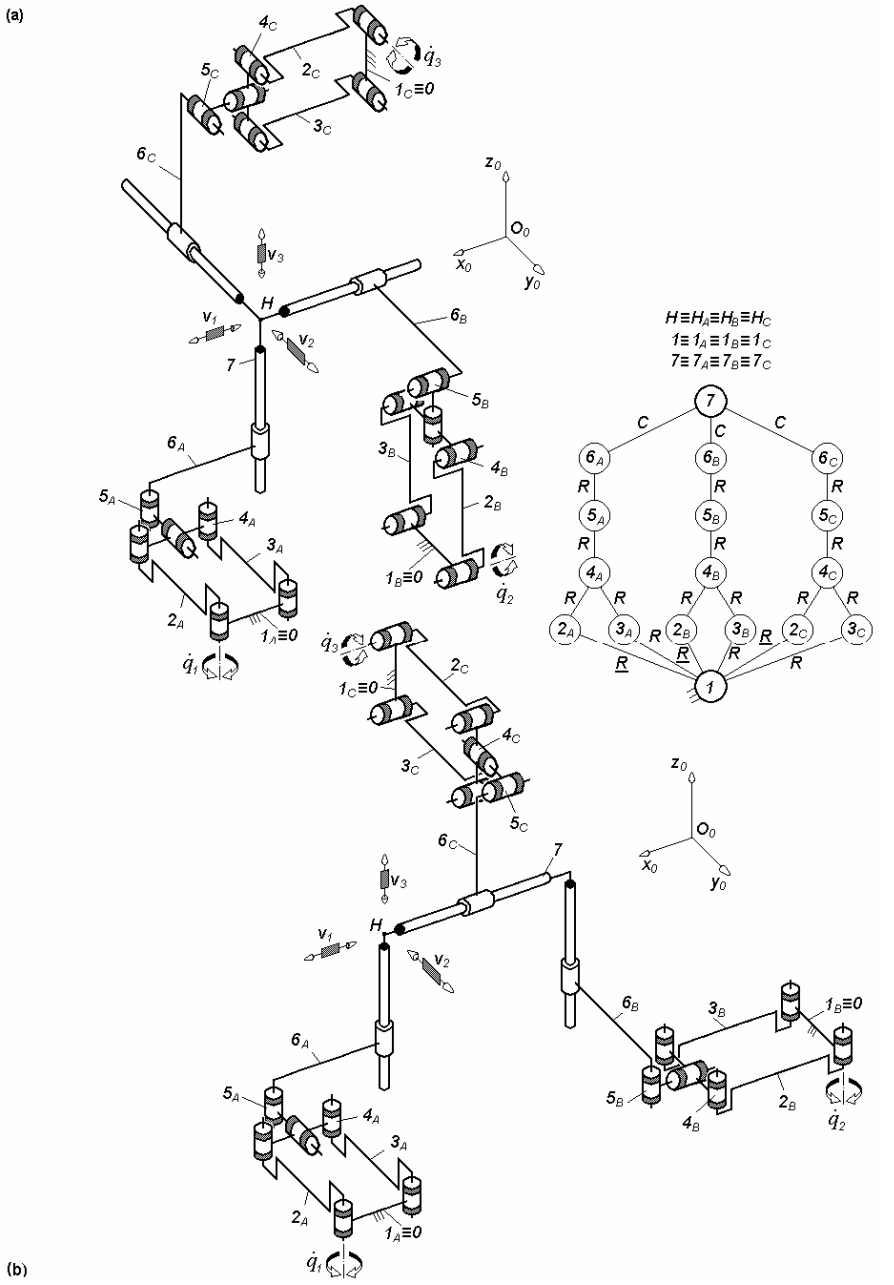

Fig. 3.155. *3-PaR*RC*-type overconstrained TPMs with coupled motions and rotating actuators mounted on the fixed base, defined by $M_F = S_F = 3$, $(R_F) = (\boldsymbol{v}_1, \boldsymbol{v}_2, \boldsymbol{v}_3)$, $T_F = 0$, $N_F = 9$, limb topology $\underline{Pa} \perp R^* \perp {}^{||}R||C$

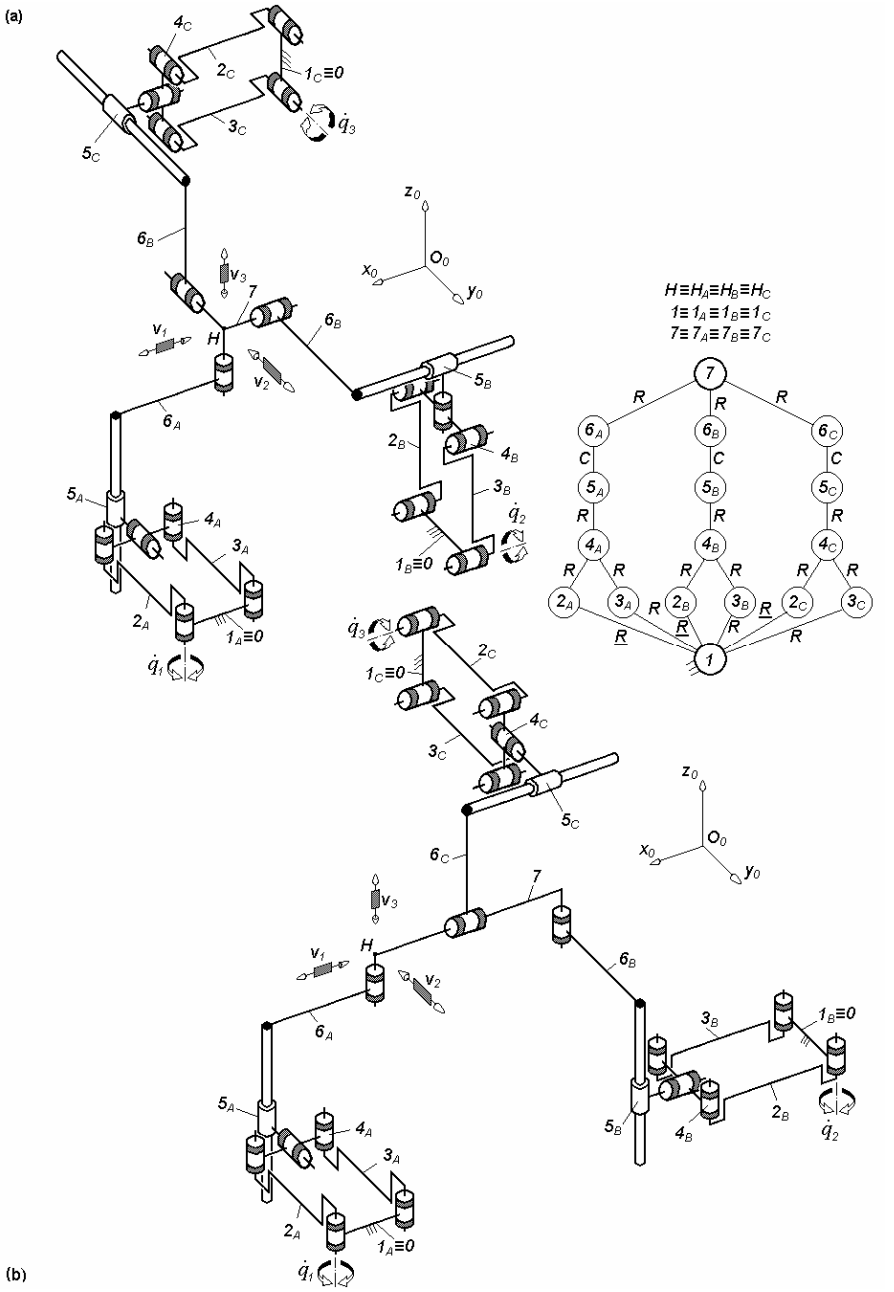

Fig. 3.156. *3-PaR*CR*-type overconstrained TPMs with coupled motions and rotating actuators mounted on the fixed base, defined by $M_F = S_F = 3$, $(R_F) = (\boldsymbol{v}_1, \boldsymbol{v}_2, \boldsymbol{v}_3)$, $T_F = 0$, $N_F = 9$, limb topology $\underline{Pa} \perp R^* \perp {}^{||}C||R$

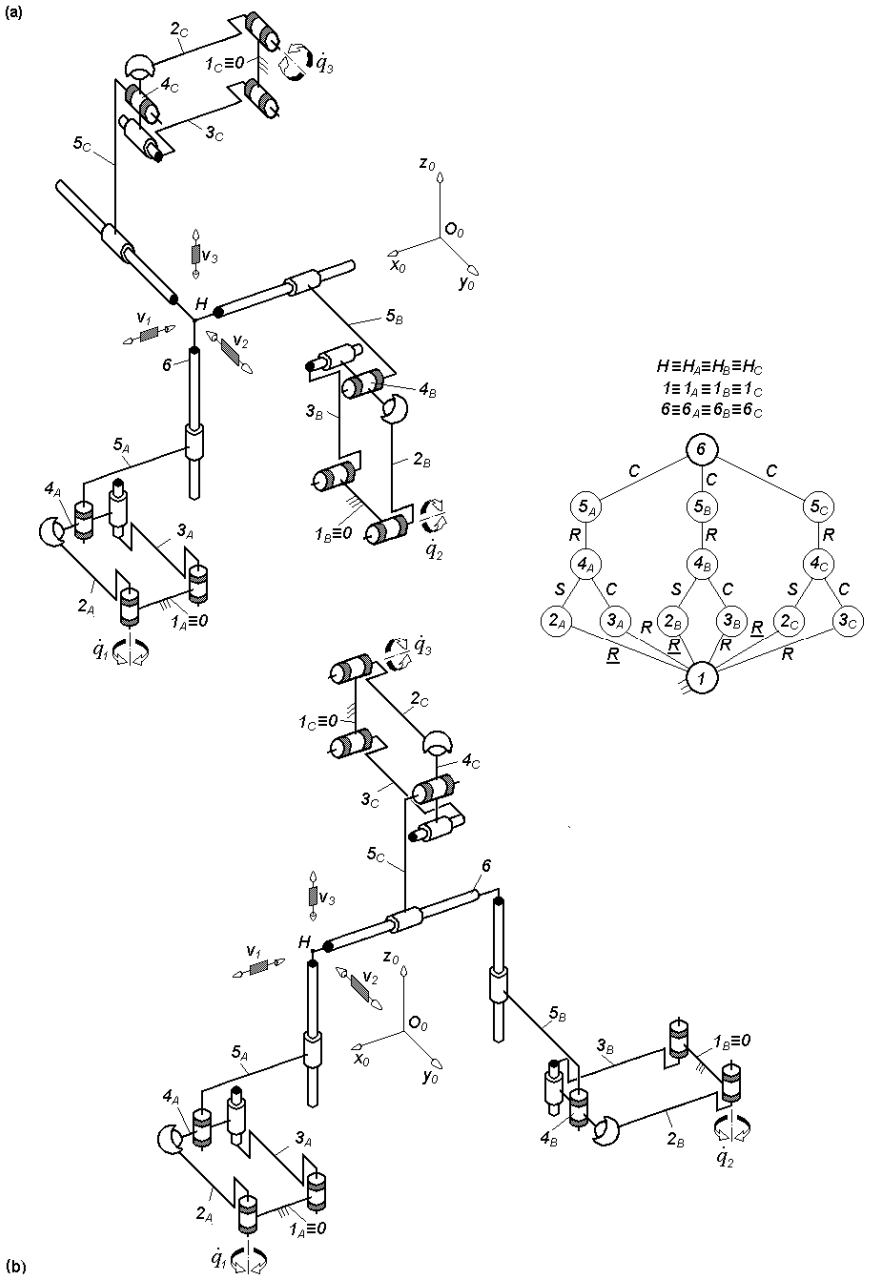

Fig. 3.157. *3-<u>Pa</u>*RC*-type overconstrained TPMs with coupled motions and rotating actuators mounted on the fixed base, defined by $M_F = S_F = 3$, $(R_F) = (\boldsymbol{v}_1, \boldsymbol{v}_2, \boldsymbol{v}_3)$, $T_F = 0$, $N_F = 3$, limb topology <u>*Pa*</u>*||*R*||*C*

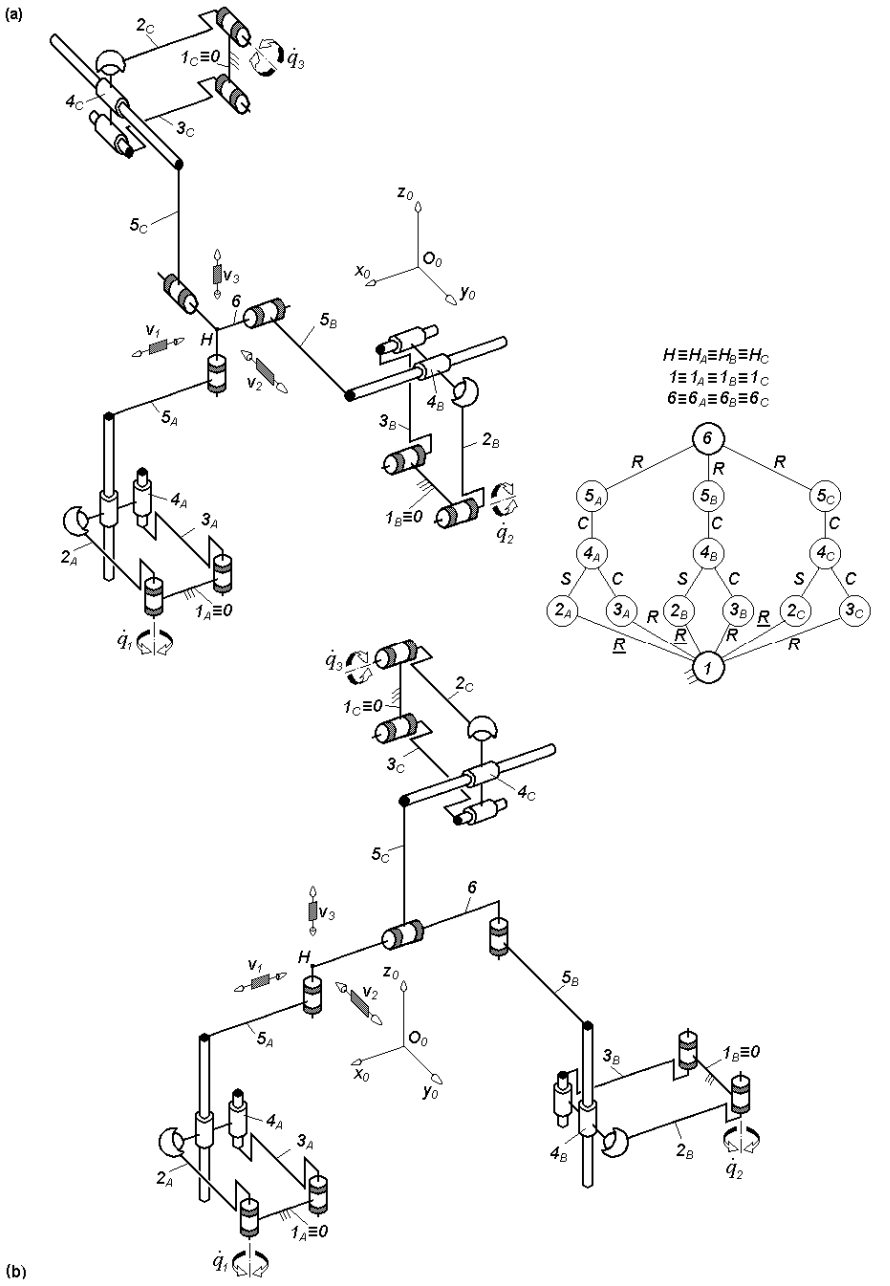

Fig. 3.158. *3-Pa*CR*-type overconstrained TPMs with coupled motions and rotating actuators mounted on the fixed base, defined by $M_F = S_F = 3$, $(R_F) = (\boldsymbol{v}_1, \boldsymbol{v}_2, \boldsymbol{v}_3)$, $T_F = 0$, $N_F = 3$, limb topology *Pa*||C||R*

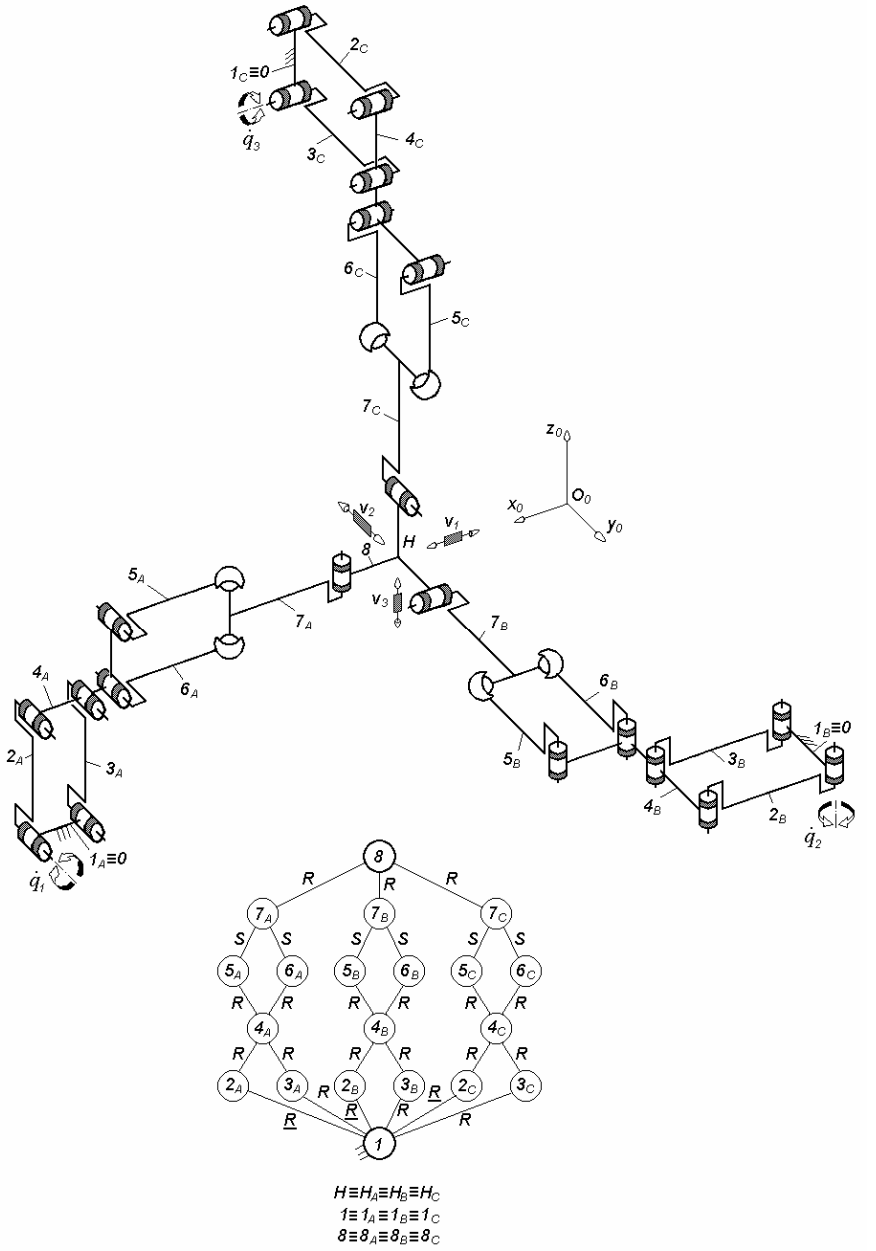

Fig. 3.159. *3-*$\underline{Pa}Pa^{ss}R$-type overconstrained TPM with coupled motions and rotating actuators mounted on the fixed base, defined by $M_F = S_F = 3$, $(R_F) = (\boldsymbol{v}_1, \boldsymbol{v}_2, \boldsymbol{v}_3)$, $T_F = 0$, $N_F = 12$, limb topology $\underline{Pa}||Pa^{ss} \perp R$

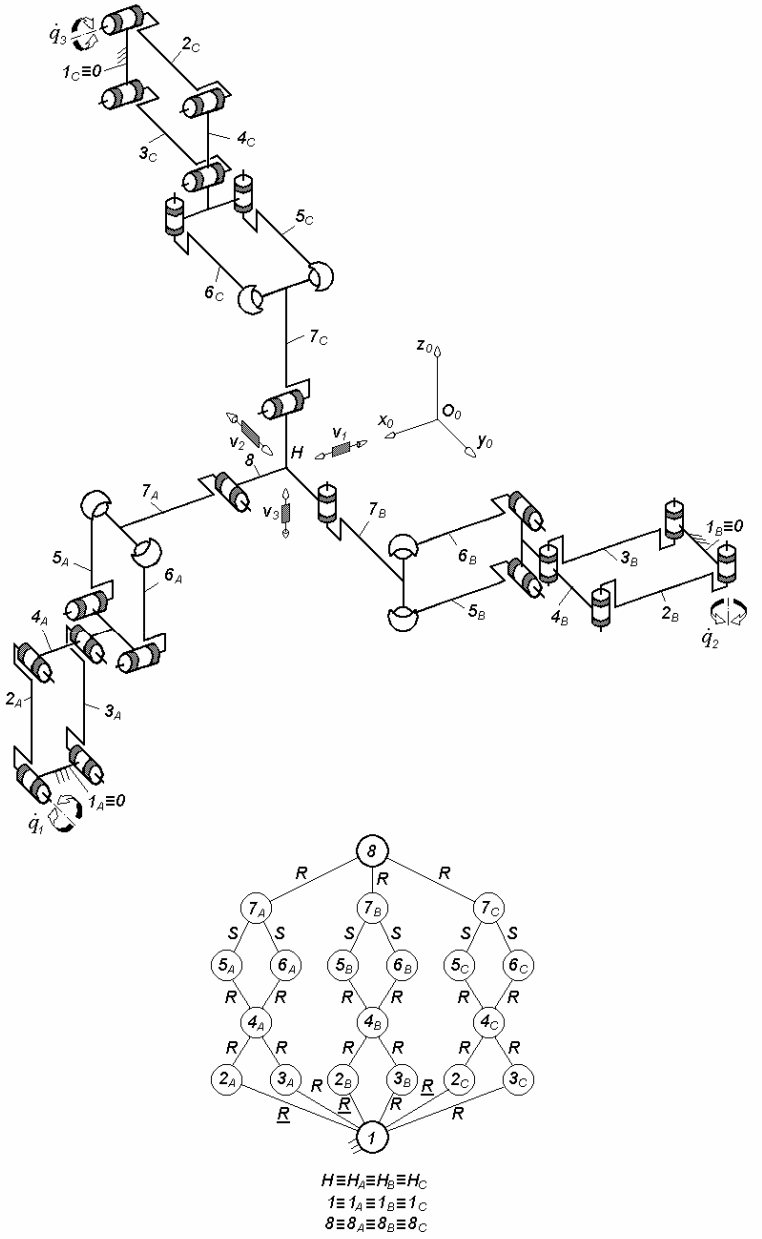

Fig. 3.160. *3-<u>Pa</u>Pa^{ss}R*-type overconstrained TPM with coupled motions and rotating actuators mounted on the fixed base, defined by $M_F = S_F = 3$, $(R_F) = (\boldsymbol{v}_1, \boldsymbol{v}_2, \boldsymbol{v}_3)$, $T_F = 0$, $N_F = 12$, limb topology $\underline{Pa} \perp Pa^{ss} \perp {}^{\|}R$

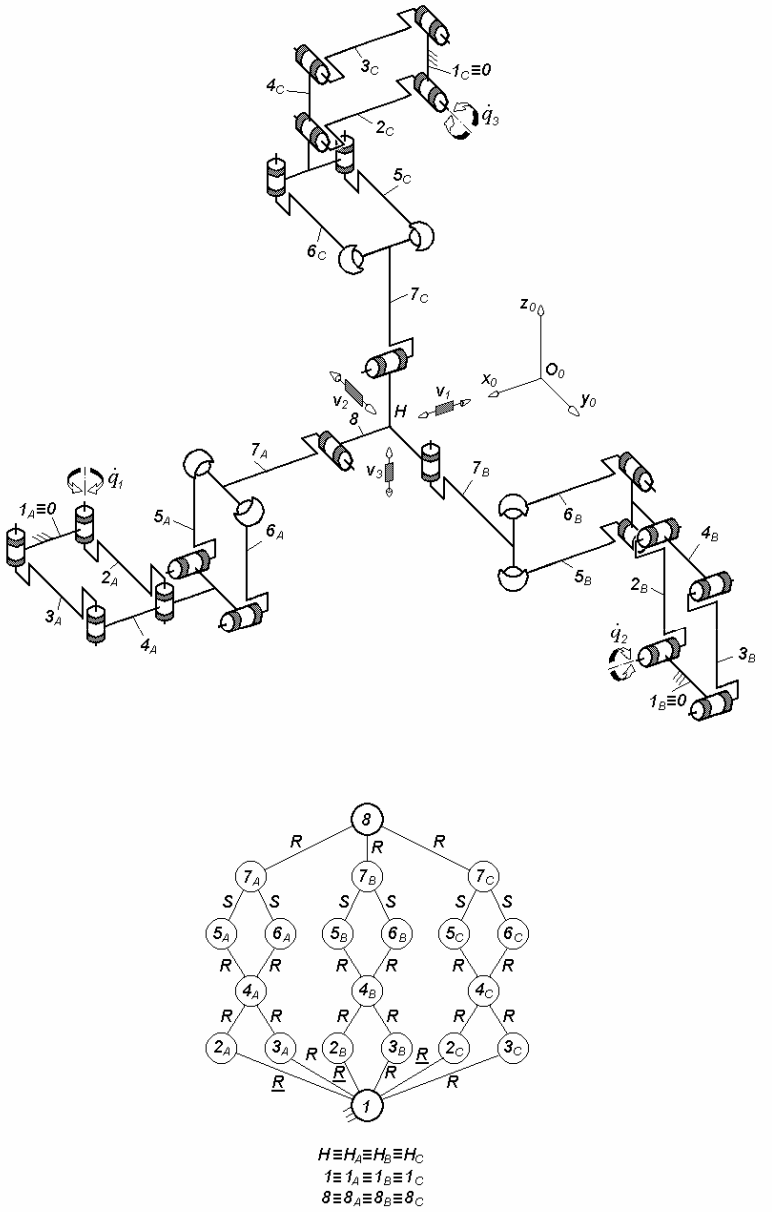

Fig. 3.161. *3-*$\underline{Pa}Pa^{ss}R$-type overconstrained TPM with coupled motions and rotating actuators mounted on the fixed base, defined by $M_F = S_F = 3$, $(R_F) = (\boldsymbol{v}_1, \boldsymbol{v}_2, \boldsymbol{v}_3)$, $T_F = 0$, $N_F = 12$, limb topology $\underline{Pa} \perp Pa^{ss} \perp^{\perp} R$

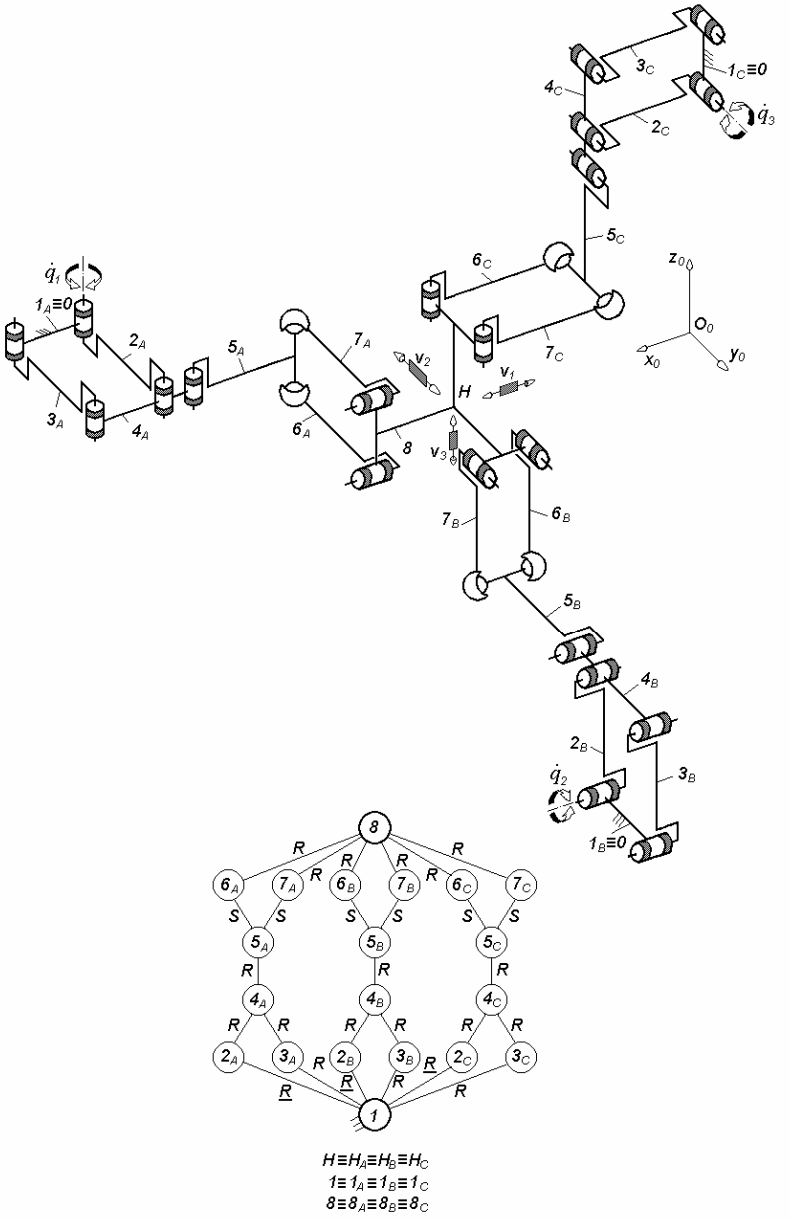

Fig. 3.162. *3-*$\underline{Pa}RPa^{ss}$-type overconstrained TPM with coupled motions and rotating actuators mounted on the fixed base, defined by $M_F = S_F = 3$, $(R_F) = (\boldsymbol{v}_1, \boldsymbol{v}_2, \boldsymbol{v}_3)$, $T_F = 0$, $N_F = 12$, limb topology $\underline{Pa}||R \perp Pa^{ss}$

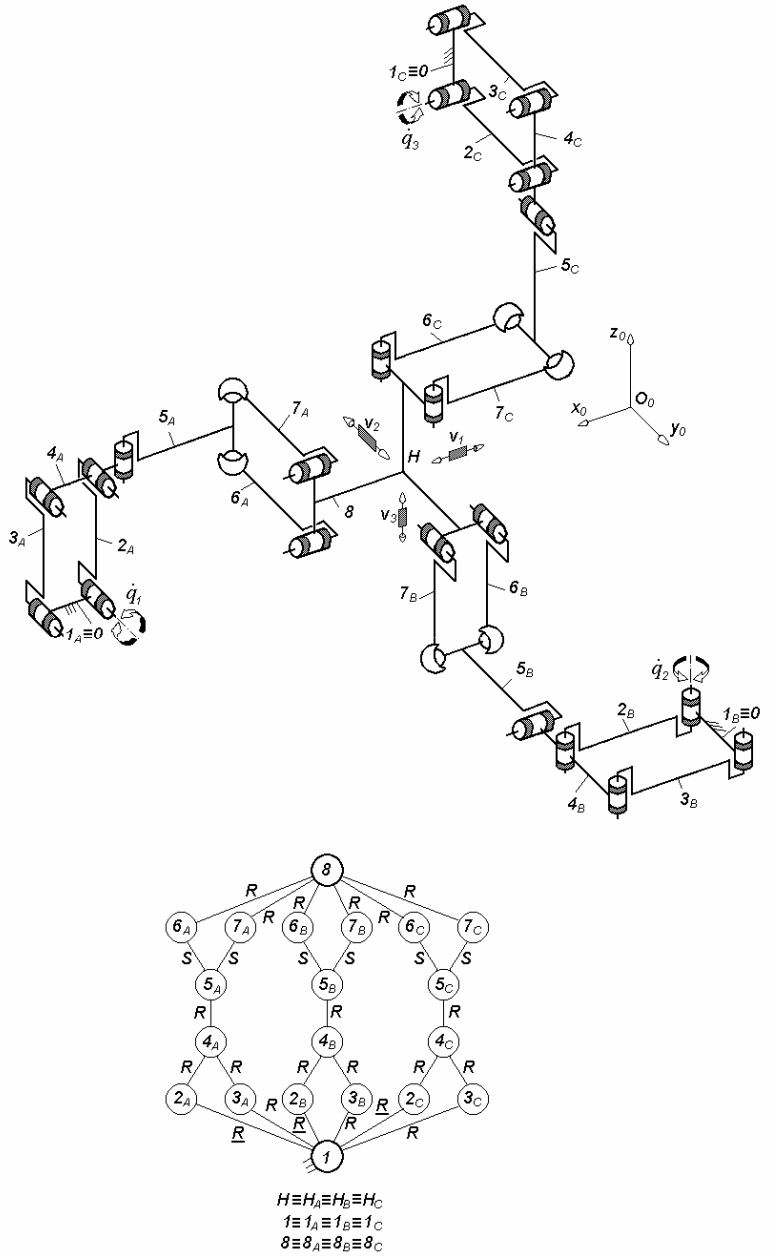

Fig. 3.163. *3-*$\underline{Pa}$*RPa*^{ss}-type overconstrained TPM with coupled motions and rotating actuators mounted on the fixed base, defined by $M_F = S_F = 3$, $(R_F) = (\boldsymbol{v}_1, \boldsymbol{v}_2, \boldsymbol{v}_3)$, $T_F = 0$, $N_F = 12$, limb topology $\underline{Pa} \perp R \perp^{\perp} Pa^{ss}$

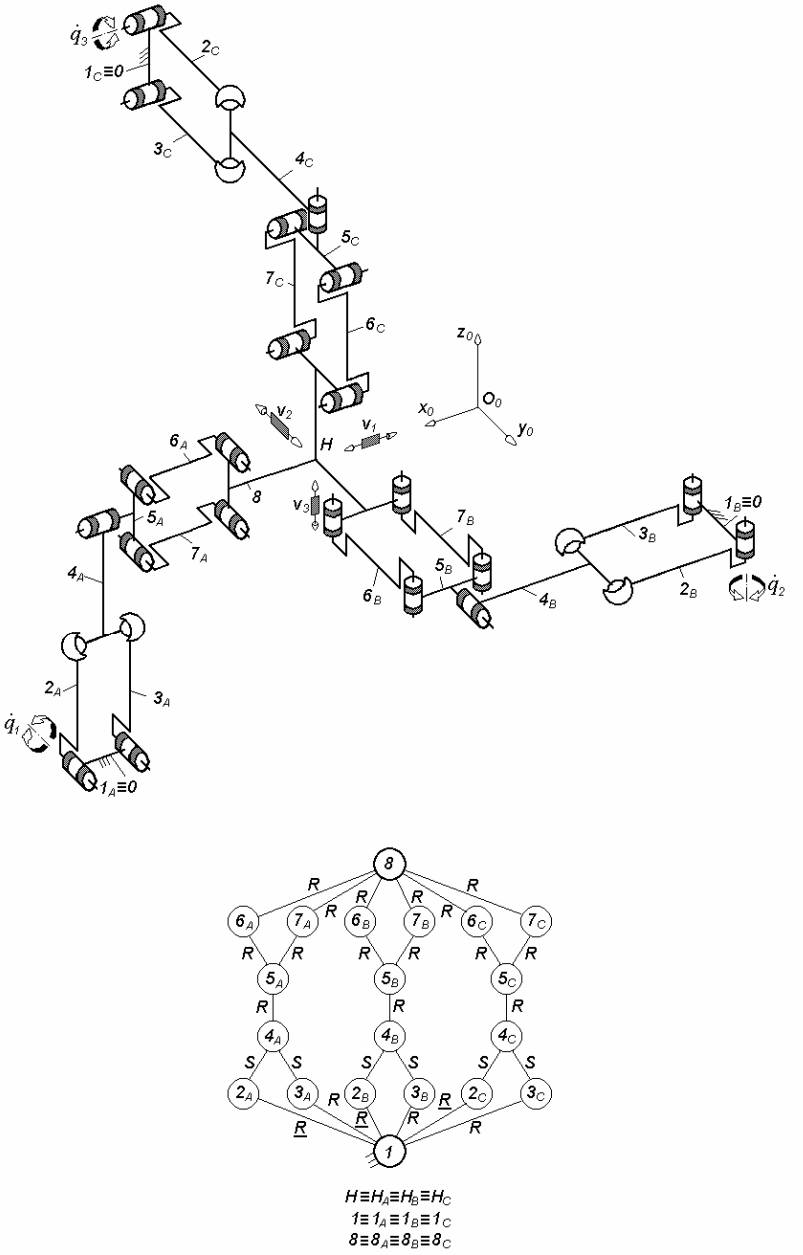

Fig. 3.164. *3-<u>Pa</u>^{ss}RPa*-type overconstrained TPM with coupled motions and rotating actuators mounted on the fixed base, defined by $M_F = S_F = 3$, $(R_F) = (\boldsymbol{v}_1, \boldsymbol{v}_2, \boldsymbol{v}_3)$, $T_F = 0$, $N_F = 12$, limb topology <u>*Pa*</u>$^{ss} \perp R \perp {}^{\parallel}Pa$

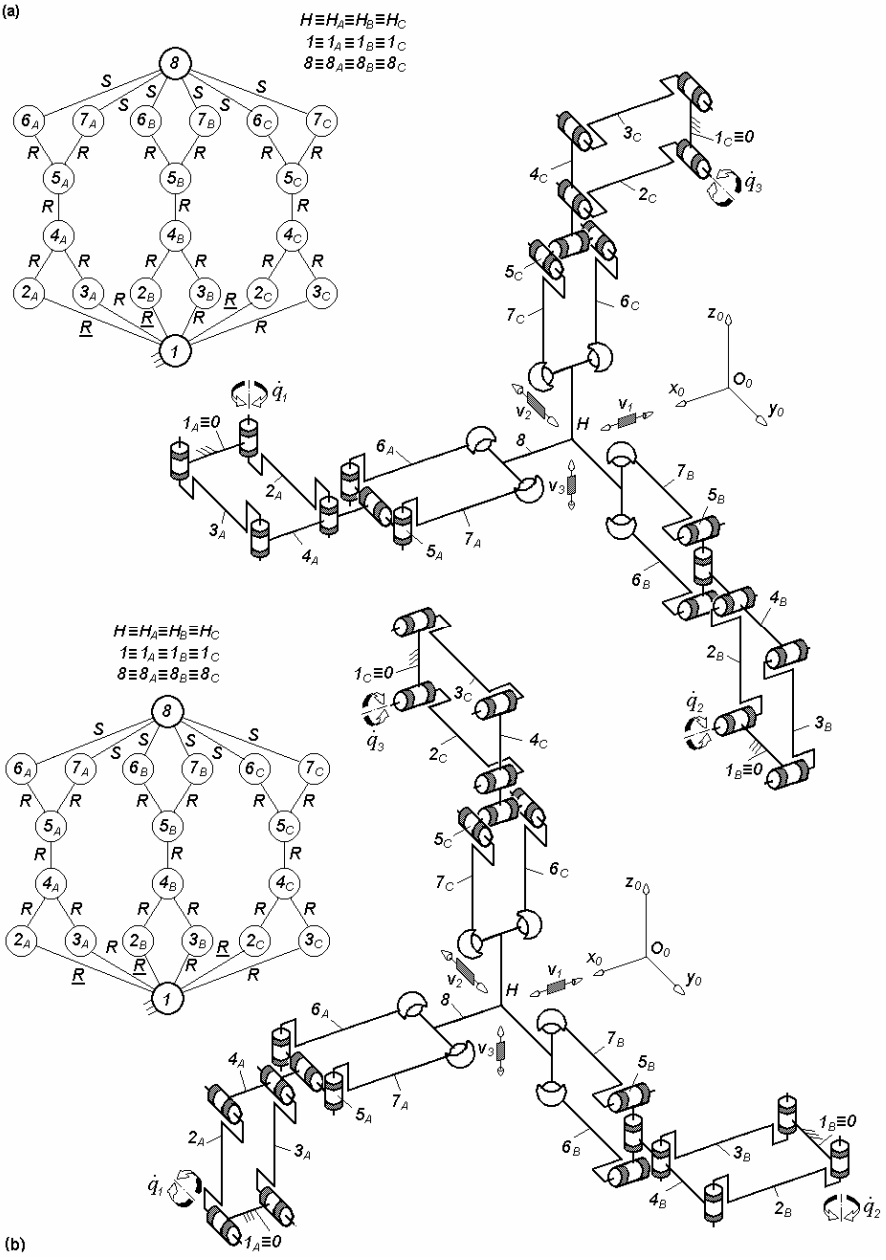

Fig. 3.165. *3-PaRPa*^{ss}-type overconstrained TPMs with coupled motions and rotating actuators mounted on the fixed base, defined by $M_F = S_F = 3$, $(R_F) = (\boldsymbol{v}_1, \boldsymbol{v}_2, \boldsymbol{v}_3)$ $T_F = 0$, $N_F = 12$, limb topology $\underline{Pa} \perp R \perp Pa^{ss}$ (**a**) and $\underline{Pa} \| R \perp Pa^{ss}$ (**b**)

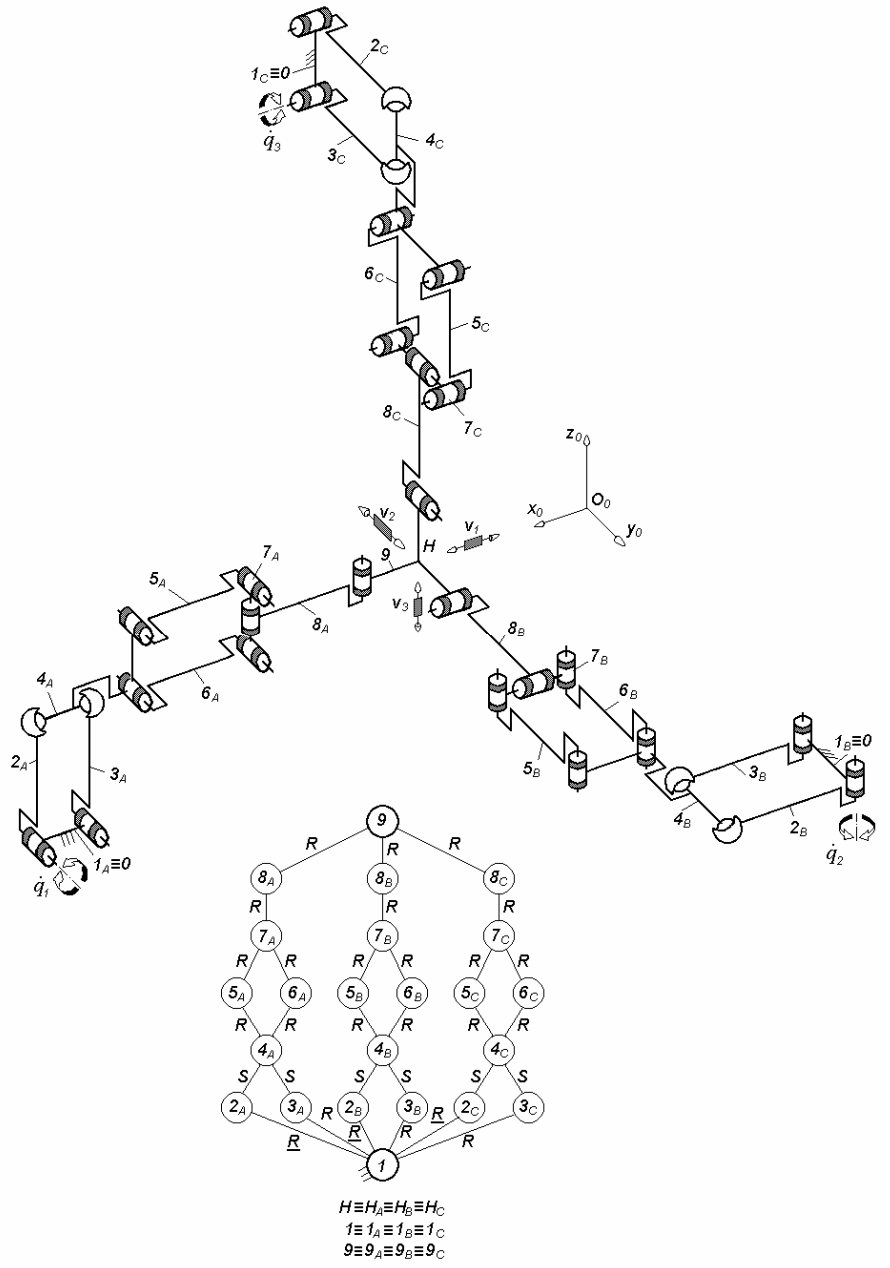

Fig. 3.166. *3-*$\underline{Pa}^{ss}$*PaRR*-type ($\underline{Pa}^{ss}||Pa \perp R||R$) overconstrained TPM with coupled motions and rotating actuators mounted on the fixed base, defined by $M_F = S_F = 3$, $(R_F) = (\boldsymbol{v}_1, \boldsymbol{v}_2, \boldsymbol{v}_3)$ $T_F = 0$ and $N_F = 9$

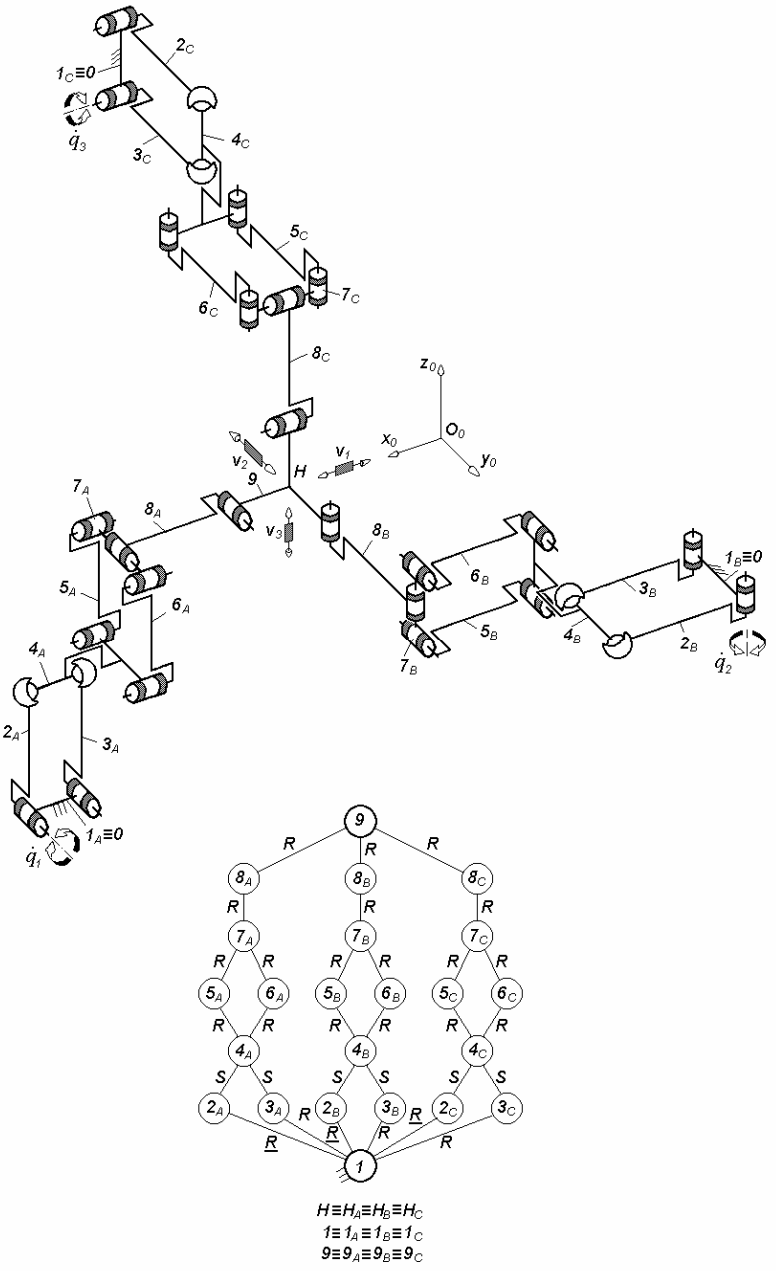

Fig. 3.167. *3-*$\underline{Pa}^{ss}$*PaRR*-type overconstrained TPM with coupled motions and rotating actuators mounted on the fixed base, defined by $M_F = S_F = 3$, $(R_F) = (\boldsymbol{v}_1, \boldsymbol{v}_2, \boldsymbol{v}_3)$, $T_F = 0$, $N_F = 9$, limb topology $\underline{Pa}^{ss} \perp Pa \perp {}^{\parallel}R \| R$

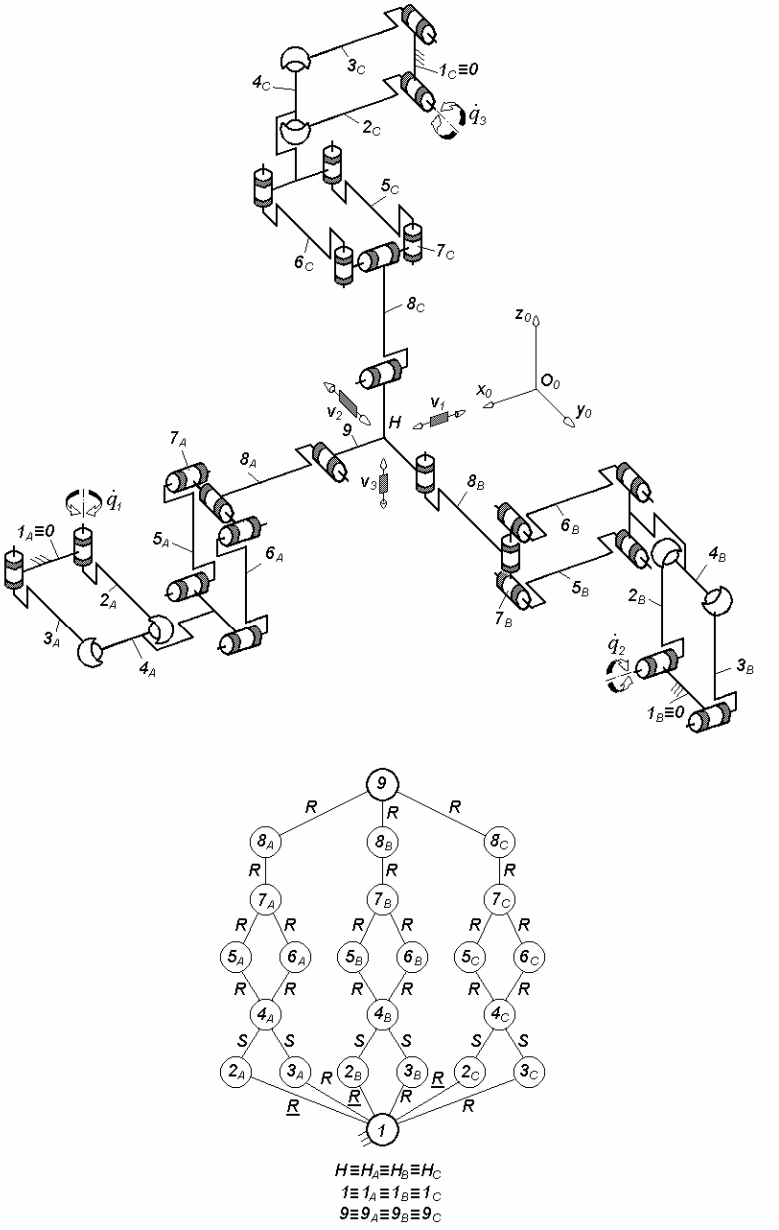

Fig. 3.168. *3-*$\underline{Pa}^{ss}$*PaRR*-type overconstrained TPM with coupled motions and rotating actuators mounted on the fixed base, defined by $M_F = S_F = 3$, $(R_F) = (\boldsymbol{v}_1, \boldsymbol{v}_2, \boldsymbol{v}_3)$, $T_F = 0$, $N_F = 9$, limb topology $\underline{Pa}^{ss} \perp Pa \perp^{\perp} R||R$

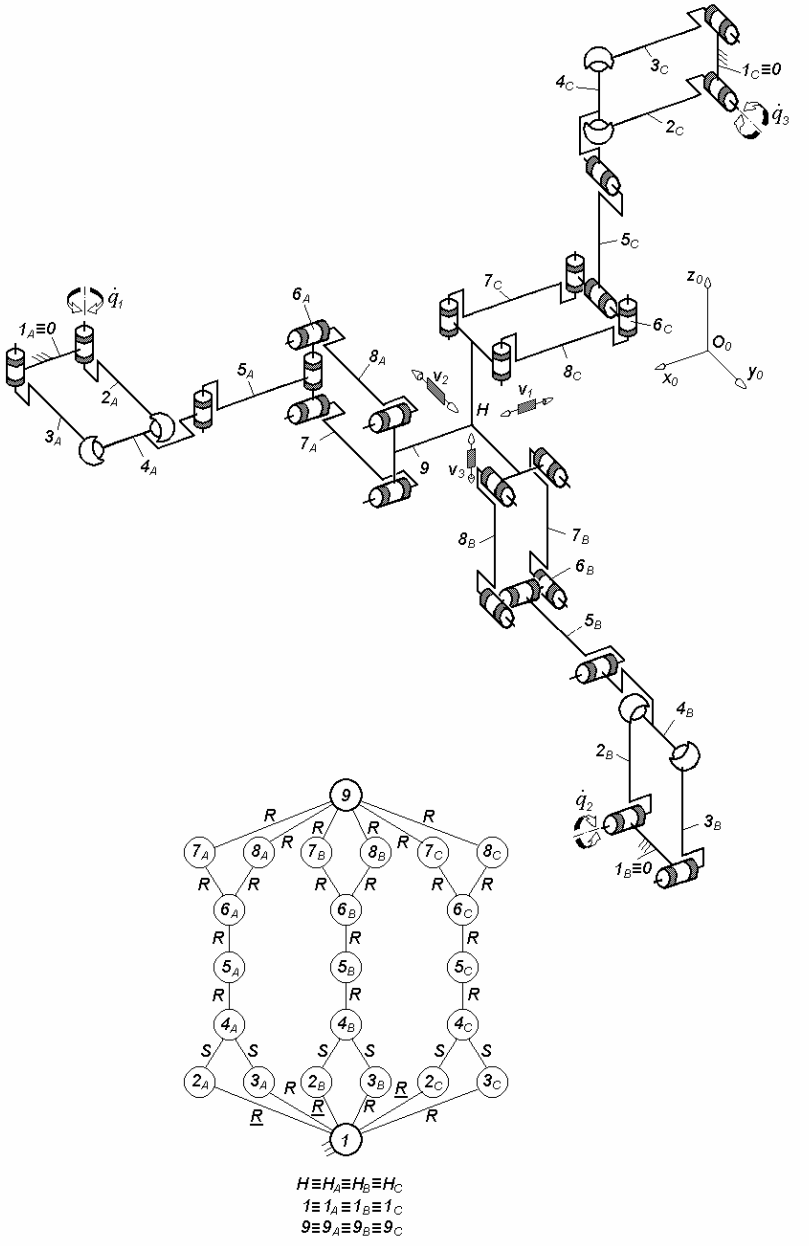

Fig. 3.169. *3-*$\underline{Pa}^{ss}$*RRPa*-type overconstrained TPM with coupled motions and rotating actuators mounted on the fixed base, defined by $M_F = S_F = 3$, $(R_F) = (\boldsymbol{v}_1, \boldsymbol{v}_2, \boldsymbol{v}_3)$, $T_F = 0$, $N_F = 9$, limb topology $\underline{Pa}^{ss}||R||R \perp Pa$

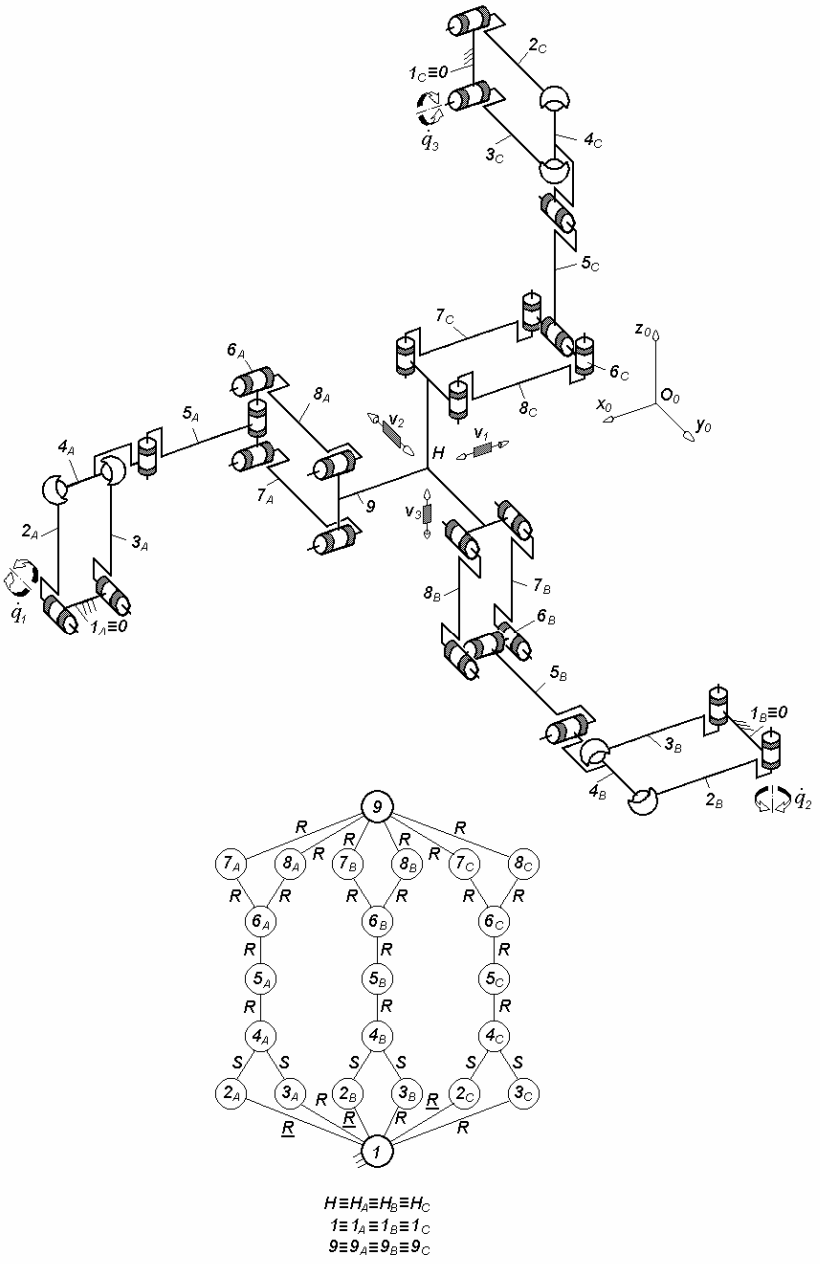

Fig. 3.170. *3-*$\underline{Pa}^{ss}$*RRPa*-type overconstrained TPM with coupled motions and rotating actuators mounted on the fixed base, defined by $M_F = S_F = 3$, $(R_F) = (\boldsymbol{v}_1, \boldsymbol{v}_2, \boldsymbol{v}_3)$, $T_F = 0$, $N_F = 9$, limb topology $\underline{Pa}^{ss} \perp R || R \perp^{\perp} Pa$

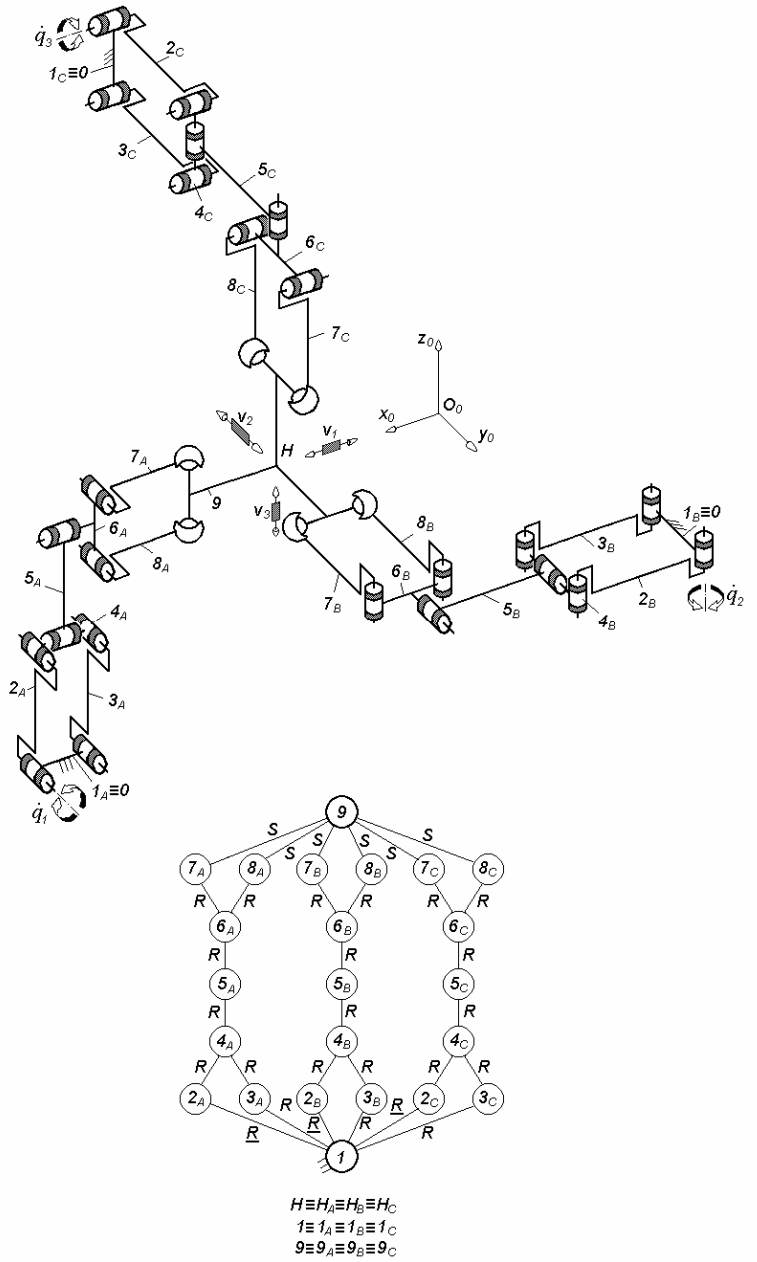

Fig. 3.171. *3-*$\underline{Pa}$*RRPa*^{ss}-type overconstrained TPM with coupled motions and rotating actuators mounted on the fixed base, defined by $M_F = S_F = 3$, $(R_F) = (\boldsymbol{v}_1, \boldsymbol{v}_2, \boldsymbol{v}_3)$, $T_F = 0$, $N_F = 9$, limb topology $\underline{Pa} \perp R || R \perp {}^{||}Pa^{ss}$

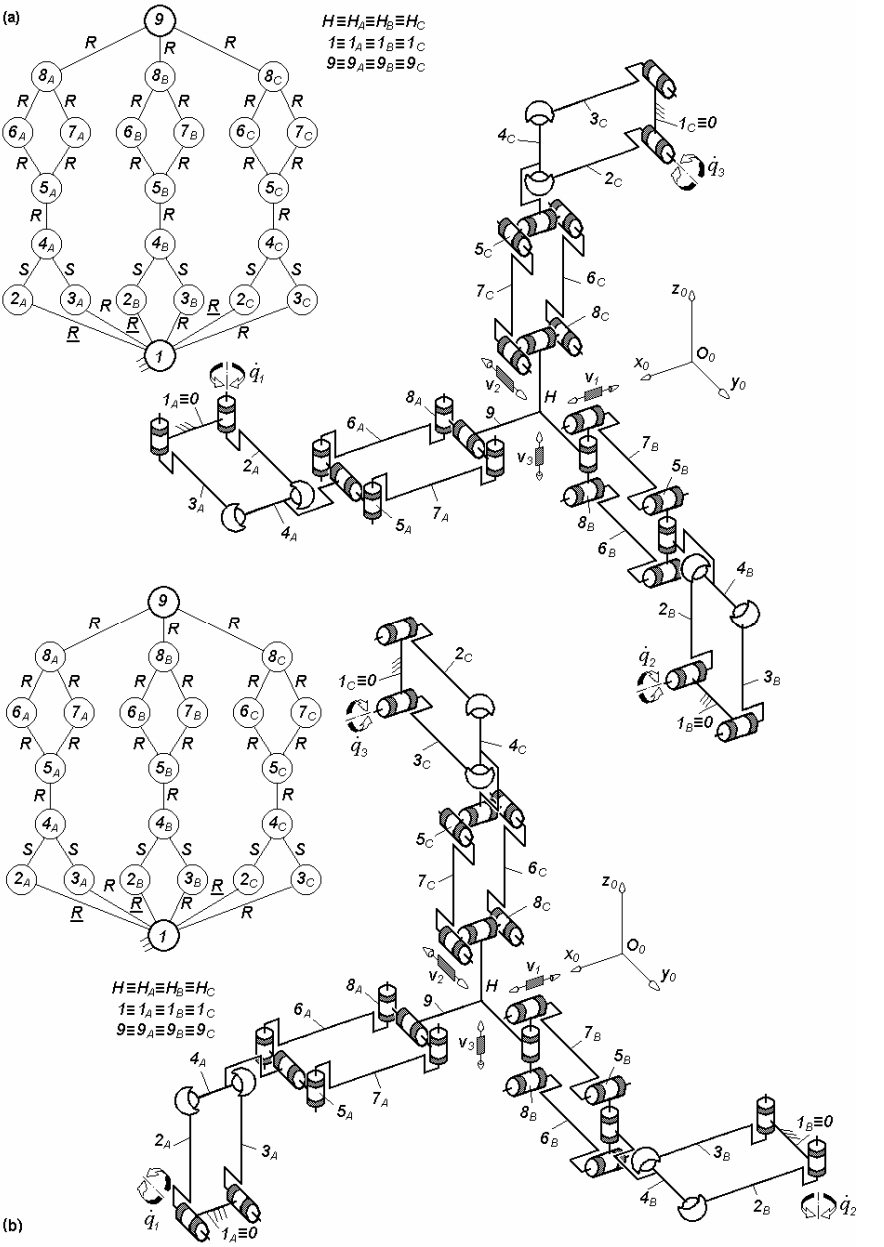

Fig. 3.172. *3-*$\underline{Pa}^{ss}$*RPaR*-type overconstrained TPMs with coupled motions and rotating actuators mounted on the fixed base, defined by $M_F = S_F = 3$, $(R_F) = (\boldsymbol{v}_1, \boldsymbol{v}_2, \boldsymbol{v}_3)$ $T_F = 0$, $N_F = 9$, limb topology $\underline{Pa}^{ss} \perp R \perp Pa \perp {}^{\parallel}R$ (**a**) and $\underline{Pa}^{ss} \| R \perp Pa \perp {}^{\parallel}R$ (**b**)

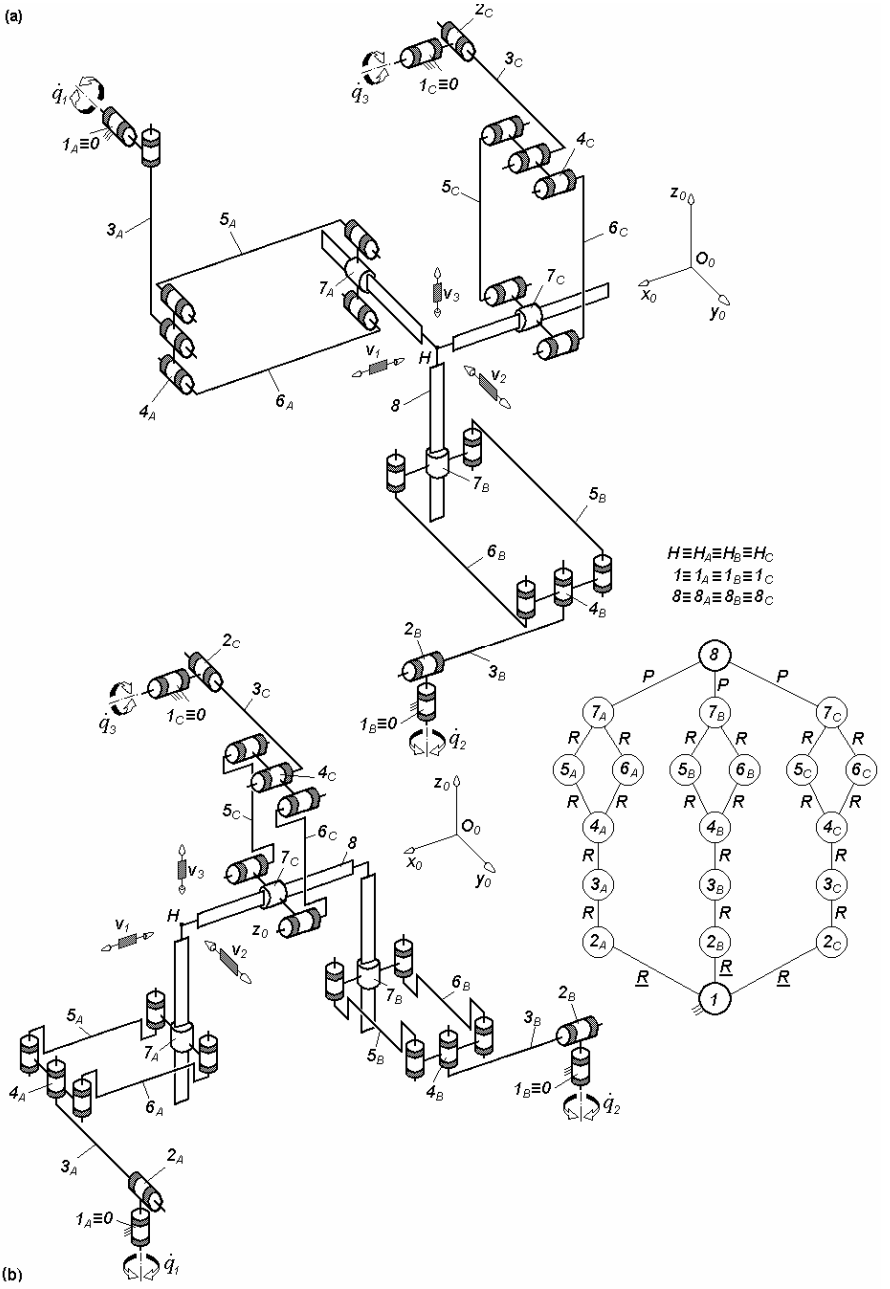

Fig. 3.173. *3-<u>R</u>R*RPaP*-type overconstrained TPMs with coupled motions and rotating actuators mounted on the fixed base, defined by $M_F = S_F = 3$, $(R_F) = (\boldsymbol{v}_1, \boldsymbol{v}_2, \boldsymbol{v}_3)$, $T_F = 0$, $N_F = 9$, limb topology $\underline{R} \perp R^* \perp {}^{\|}R||Pa||P$

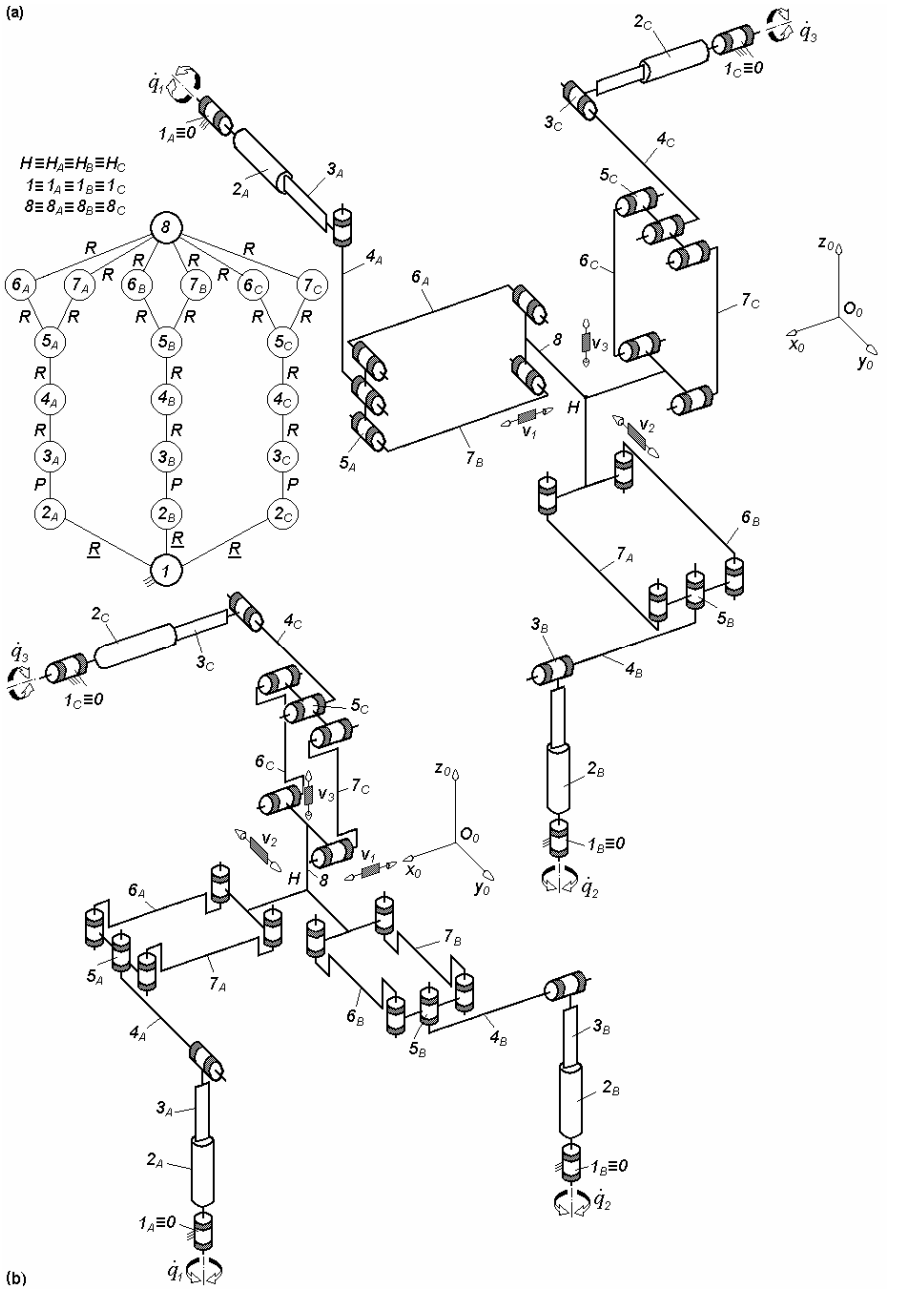

Fig. 3.174. *3-<u>R</u>PR*RPa*-type overconstrained TPMs with coupled motions and rotating actuators mounted on the fixed base, defined by $M_F = S_F = 3$, $(R_F) = (\boldsymbol{v}_1, \boldsymbol{v}_2, \boldsymbol{v}_3)$, $T_F = 0$, $N_F = 9$, limb topology $\underline{R}||P \perp R^* \perp {}^{||}R||Pa$

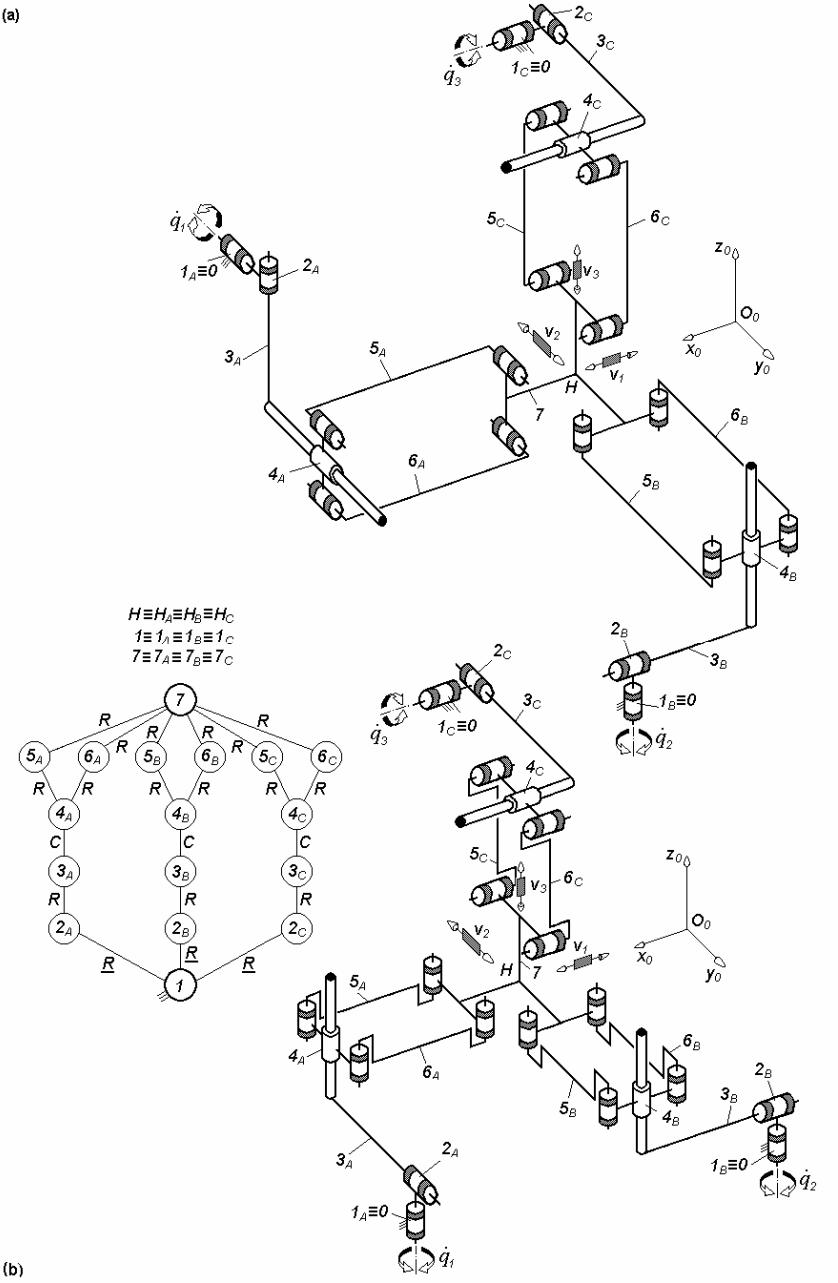

Fig. 3.175. *3-RR*CPa*-type overconstrained TPMs with coupled motions and rotating actuators mounted on the fixed base, defined by $M_F = S_F = 3$, $(R_F) = (\boldsymbol{v}_1, \boldsymbol{v}_2, \boldsymbol{v}_3)$, $T_F = 0$, $N_F = 9$, limb topology $\underline{R} \perp R^* \perp {}^{\parallel}C \| Pa$

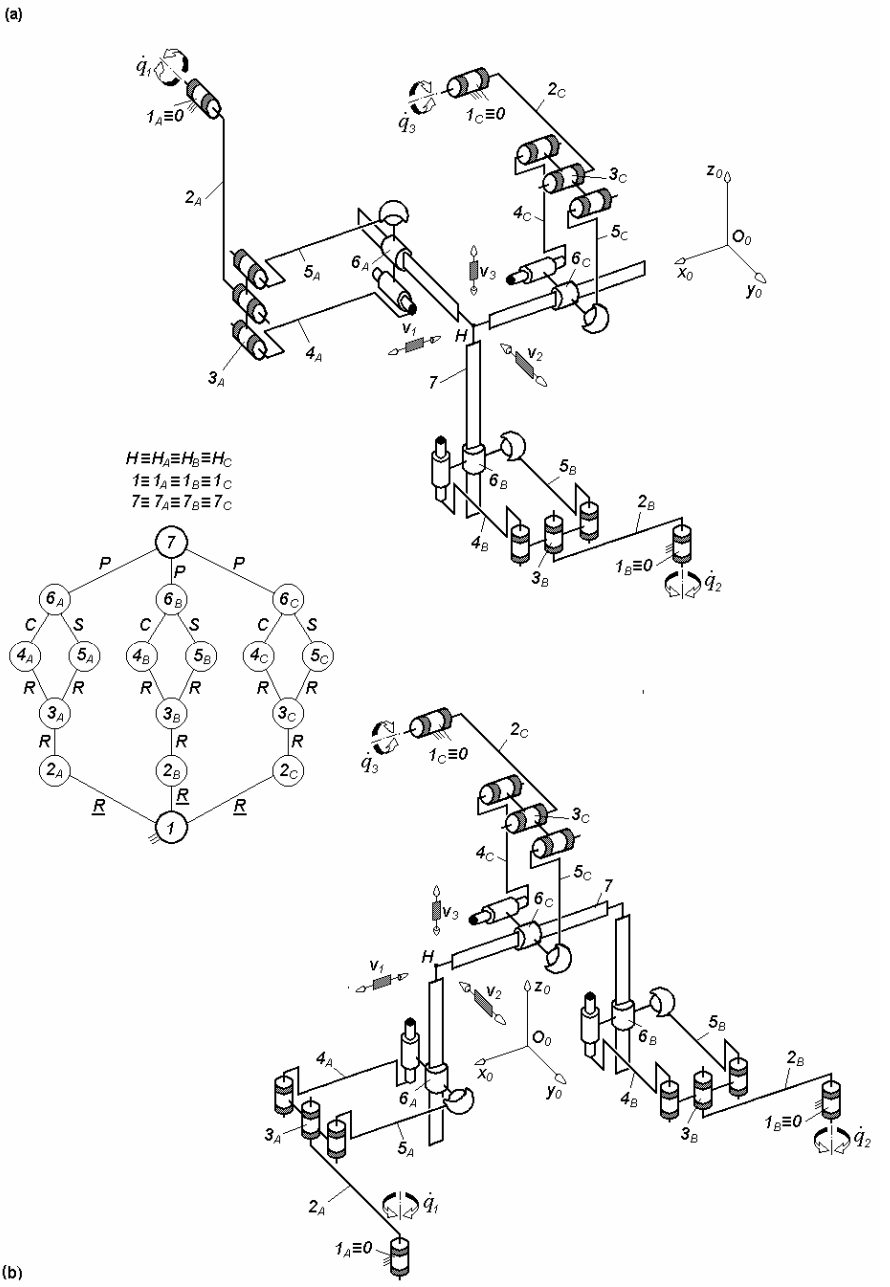

Fig. 3.176. *3-RRPa*P*-type overconstrained TPMs with coupled motions and rotating actuators mounted on the fixed base, defined by $M_F = S_F = 3$, $(R_F) = (\boldsymbol{v}_1, \boldsymbol{v}_2, \boldsymbol{v}_3)$, $T_F = 0$, $N_F = 3$, limb topology $\underline{R}||R||Pa^*||P$

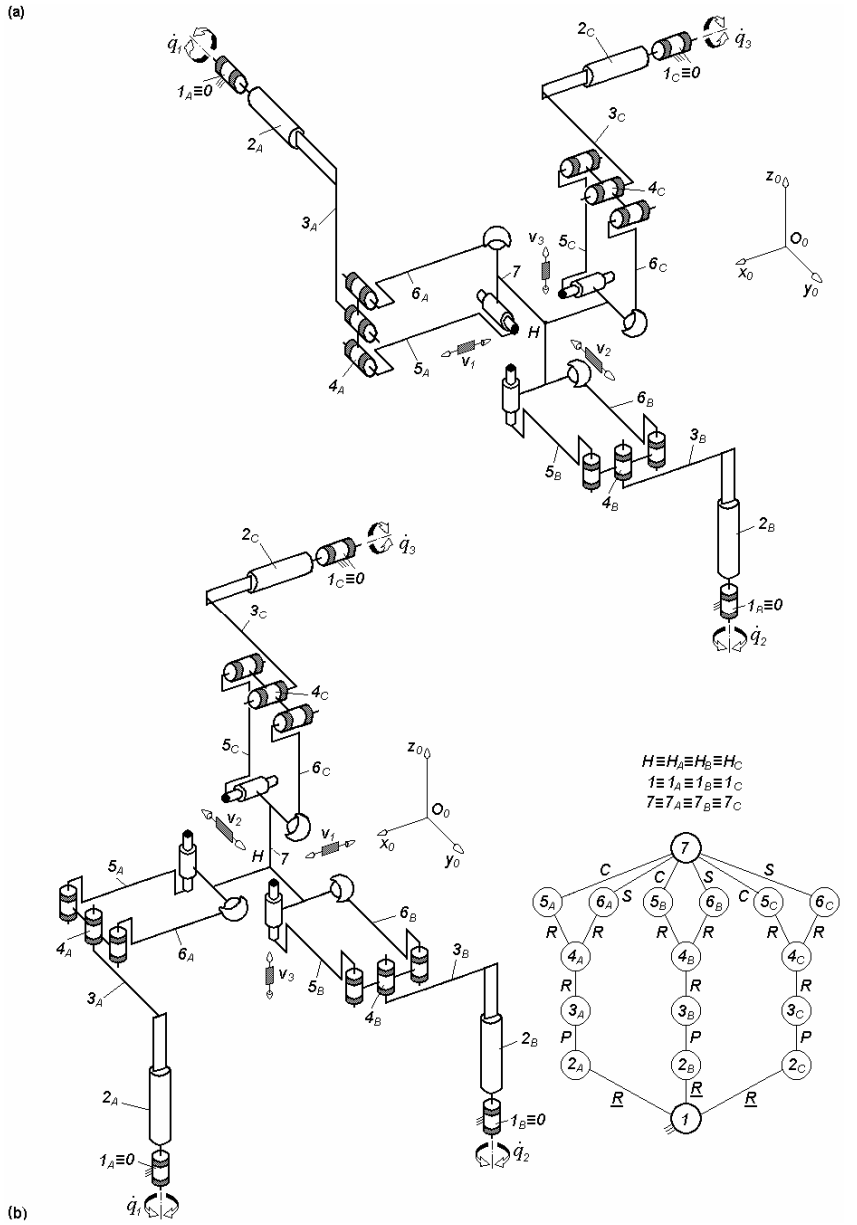

Fig. 3.177. *3-<u>R</u>PRPa**-type overconstrained TPMs with coupled motions and rotating actuators mounted on the fixed base, defined by $M_F = S_F = 3$, $(R_F) = (\boldsymbol{v}_1, \boldsymbol{v}_2, \boldsymbol{v}_3)$, $T_F = 0$, $N_F = 3$, limb topology <u>R</u>||P||R||Pa**

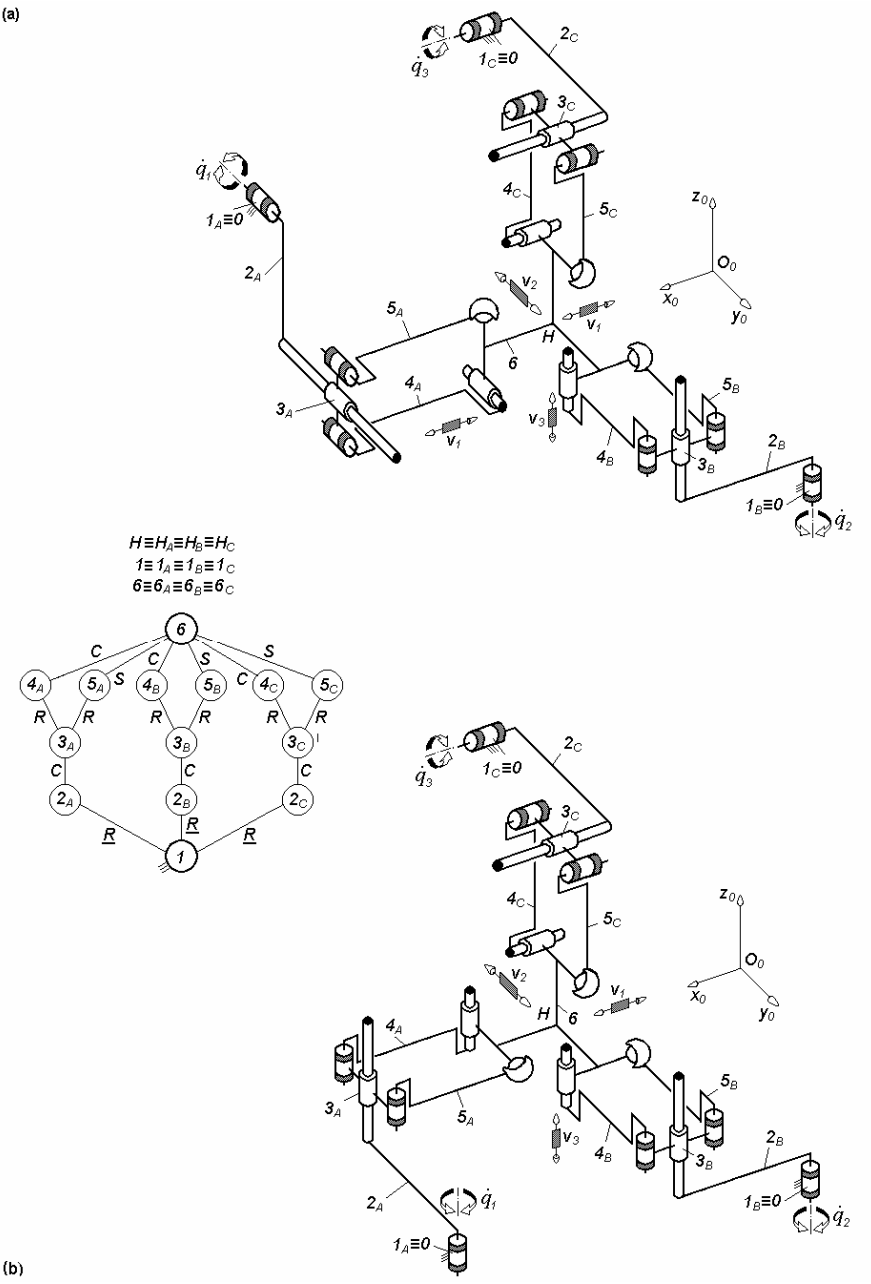

Fig. 3.178. *3-<u>R</u>CPa**-type overconstrained TPMs with coupled motions and rotating actuators mounted on the fixed base, defined by $M_F = S_F = 3$, $(R_F) = (\boldsymbol{v}_1, \boldsymbol{v}_2, \boldsymbol{v}_3)$, $T_F = 0$, $N_F = 3$*, limb topology *<u>R</u>||C||Pa**

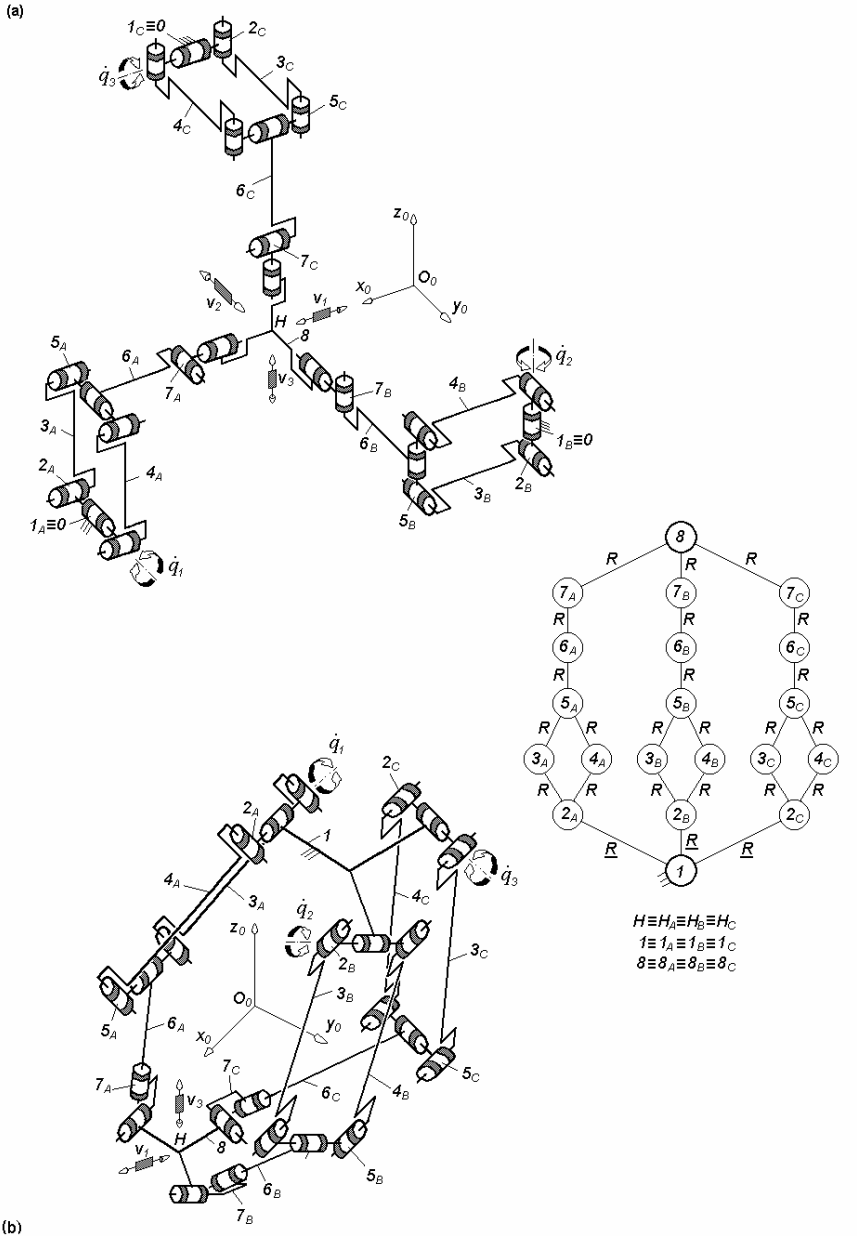

Fig. 3.179. Overconstrained TPMs of types *3-*$\underline{R}$*PaRRR** (**a**) and *3-*$\underline{R}$*PaRR*R* (**b**) with coupled motions and rotating actuators mounted on the fixed base, defined by $M_F = S_F = 3$, $(R_F) = (\boldsymbol{v}_1, \boldsymbol{v}_2, \boldsymbol{v}_3)$, $T_F = 0$, $N_F = 9$, limb topology $\underline{R} \perp Pa \perp {}^{||}R||R \perp R^*$ (**a**) and $\underline{R} \perp Pa \perp {}^{||}R \perp R^* \perp {}^{||}R$ (**b**)

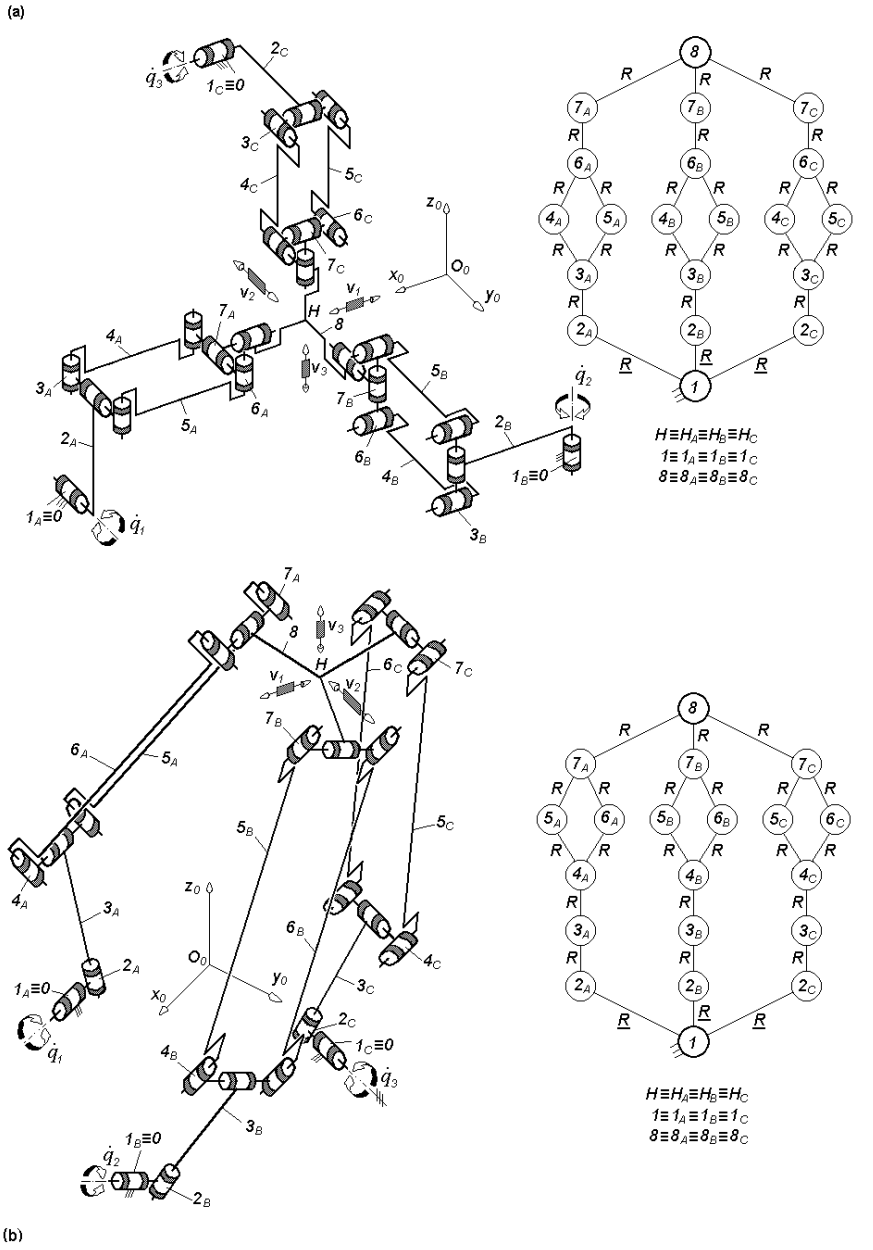

Fig. 3.180. Overconstrained TPMs of types *3-RRPaRR** (**a**) and *3-RR*RPaR* (**b**) with coupled motions and rotating actuators mounted on the fixed base, defined by $M_F = S_F = 3$, $(R_F) = (\boldsymbol{v}_1, \boldsymbol{v}_2, \boldsymbol{v}_3)$ $T_F = 0$, $N_F = 9$, limb topology $\underline{R}||R \perp Pa \perp {}^{||}R \perp R^*$ (**a**) and $\underline{R} \perp R^* \perp {}^{||}R \perp Pa \perp {}^{||}R$ (**b**)

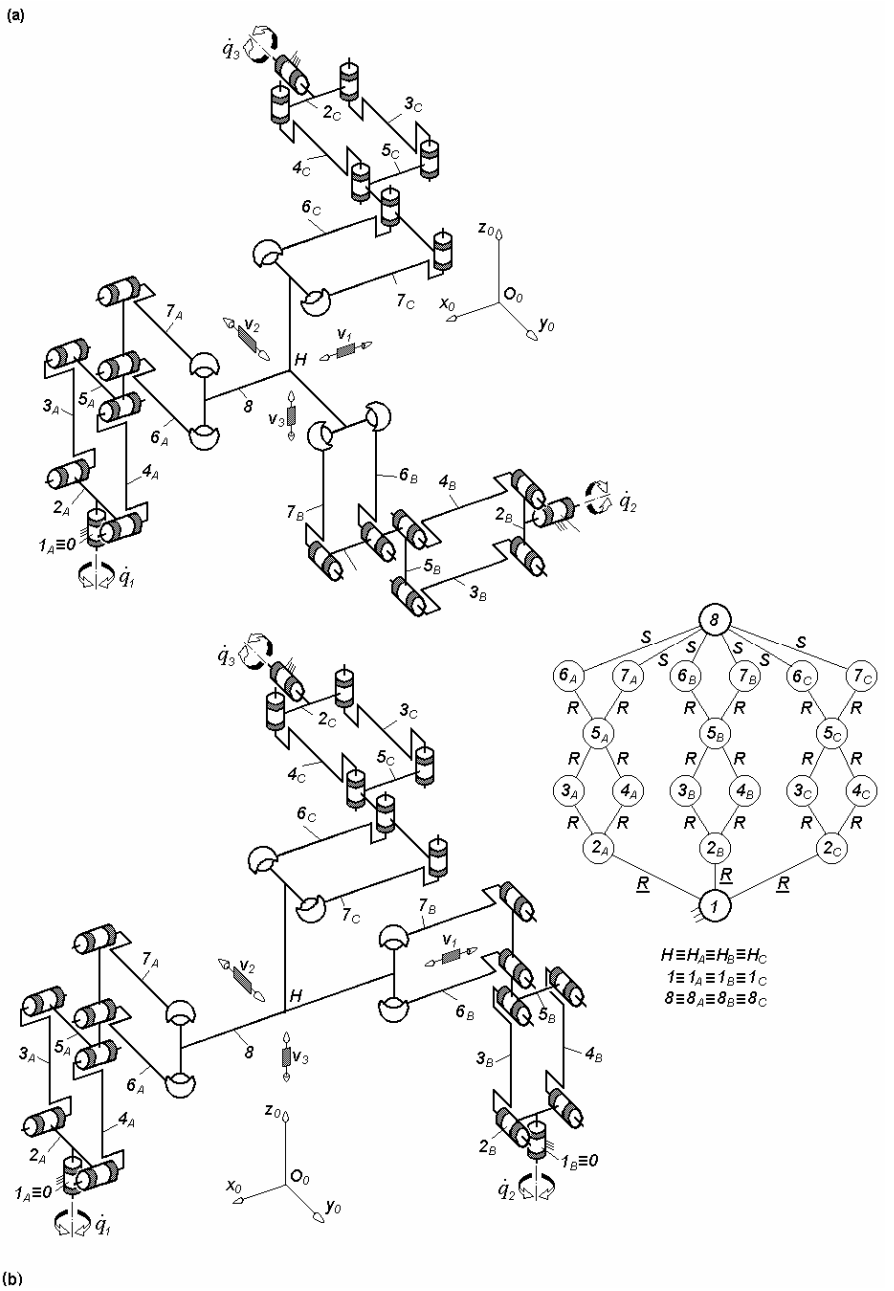

Fig. 3.181. *3-*$\underline{R}$*PaPa*^{ss}-type TPMs with coupled motions and rotating actuators mounted on the fixed base, defined by $M_F = S_F = 3$, $(R_F) = (\boldsymbol{v}_1, \boldsymbol{v}_2, \boldsymbol{v}_3)$, $T_F = 0$, $N_F = 12$, limb topology $\underline{R} \perp Pa || Pa^{ss}$

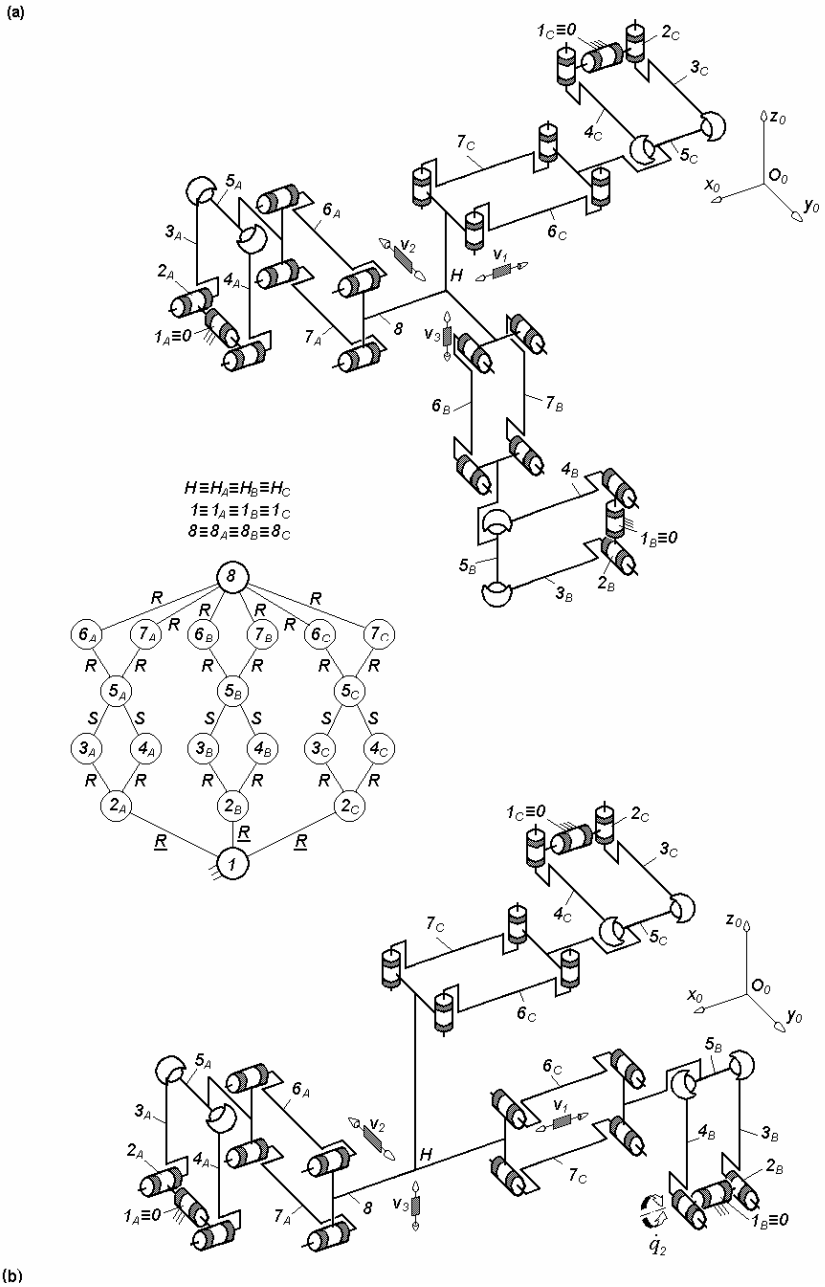

Fig. 3.182. *3-<u>R</u>Pa^{ss}Pa*-type TPMs with coupled motions and rotating actuators mounted on the fixed base, defined by $M_F = S_F = 3$, $(R_F) = (\boldsymbol{v}_1, \boldsymbol{v}_2, \boldsymbol{v}_3)$, $T_F = 0$, $N_F = 12$, limb topology $\underline{R} \perp Pa^{ss} || Pa$

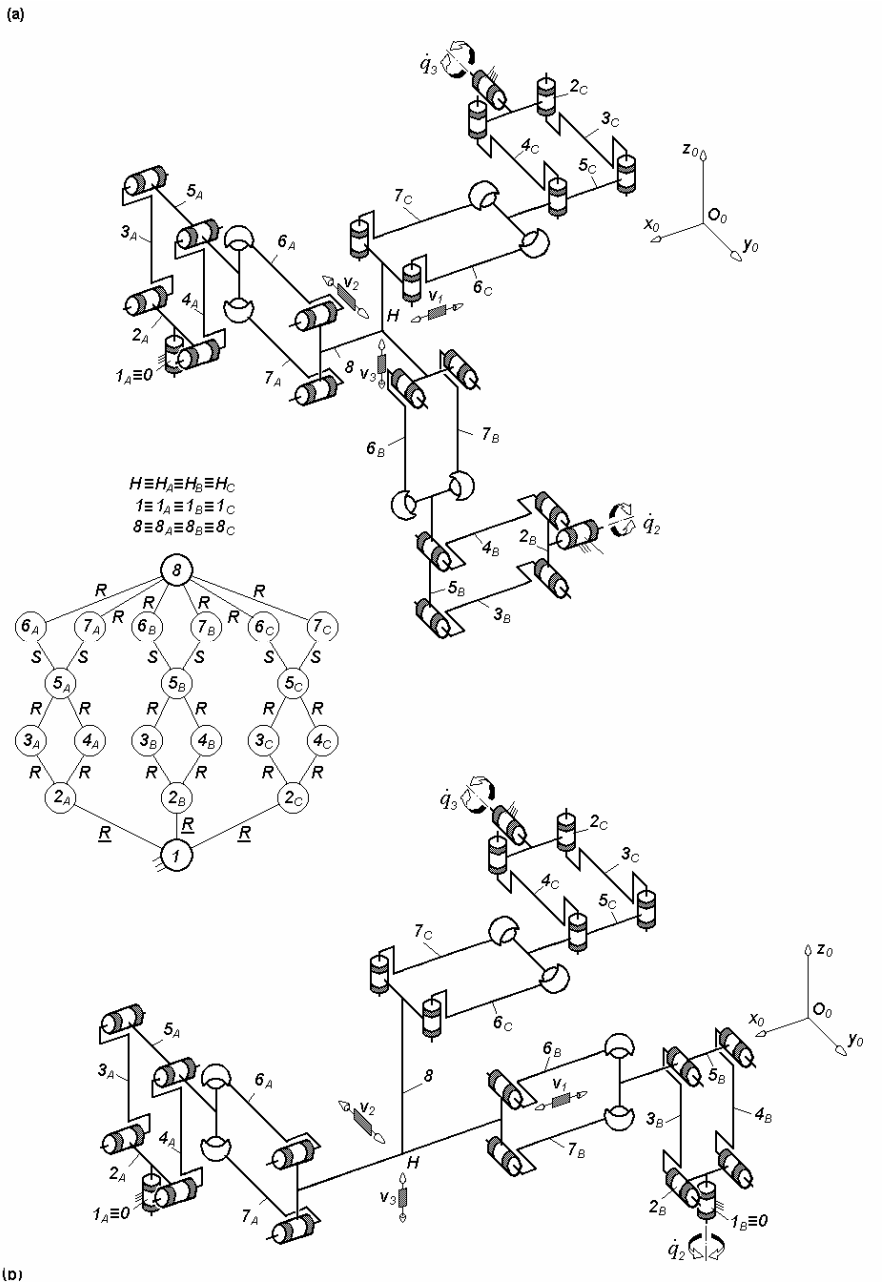

Fig. 3.183. *3-<u>R</u>PaPa^{ss}*-type TPMs with coupled motions and rotating actuators mounted on the fixed base, defined by $M_F = S_F = 3$, $(R_F) = (\boldsymbol{v}_1, \boldsymbol{v}_2, \boldsymbol{v}_3)$, $T_F = 0$, $N_F = 12$, limb topology $\underline{R} \perp Pa \perp^{\perp} Pa^{ss}$

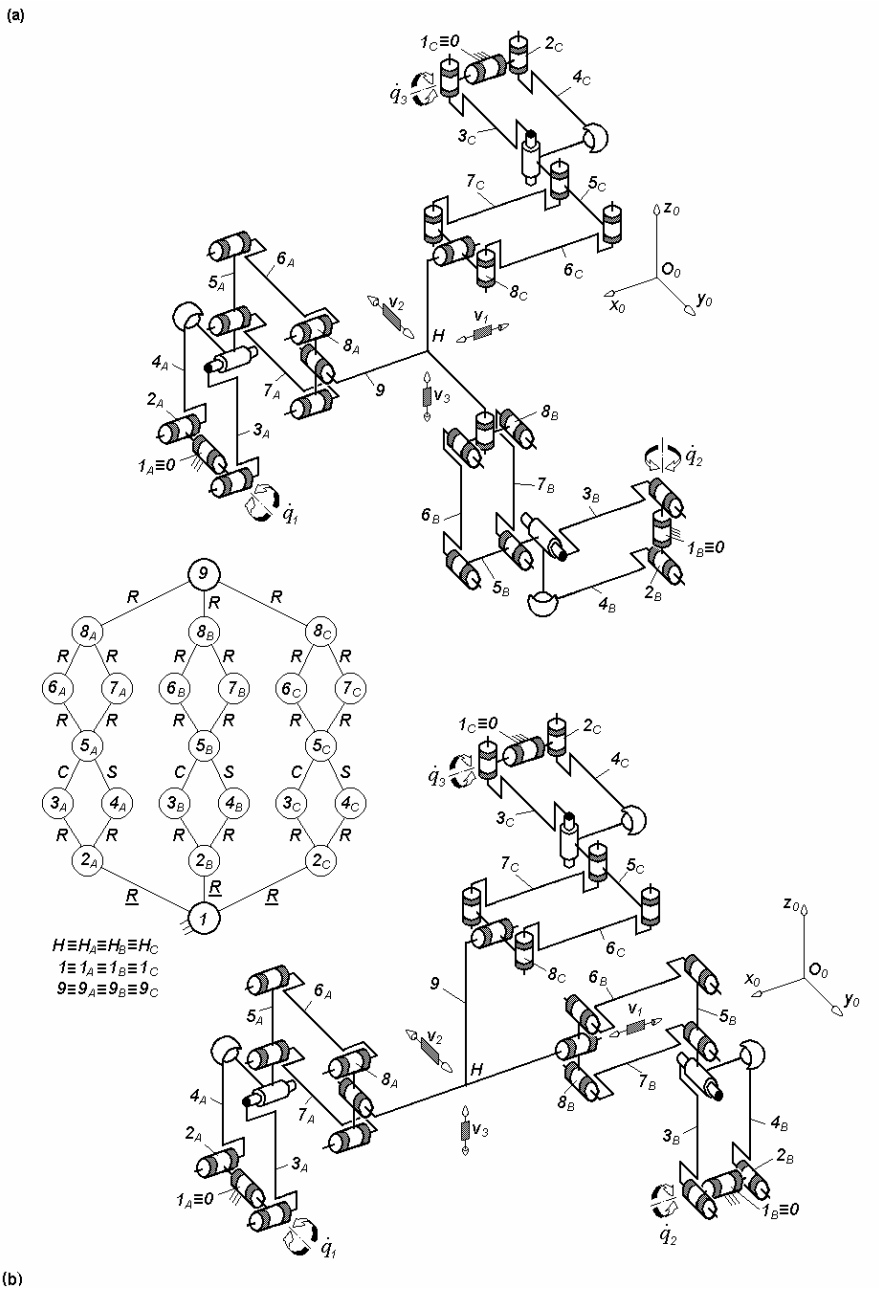

Fig. 3.184. *3-$\underline{R}Pa^{cs}PaR$**-type TPMs with coupled motions and rotating actuators mounted on the fixed base, defined by $M_F = S_F = 3$, $(R_F) = (\boldsymbol{v}_1, \boldsymbol{v}_2, \boldsymbol{v}_3)$, $T_F = 0$, $N_F = 9$, limb topology $\underline{R} \perp Pa^{cs} || Pa \perp {}^{||}R$**

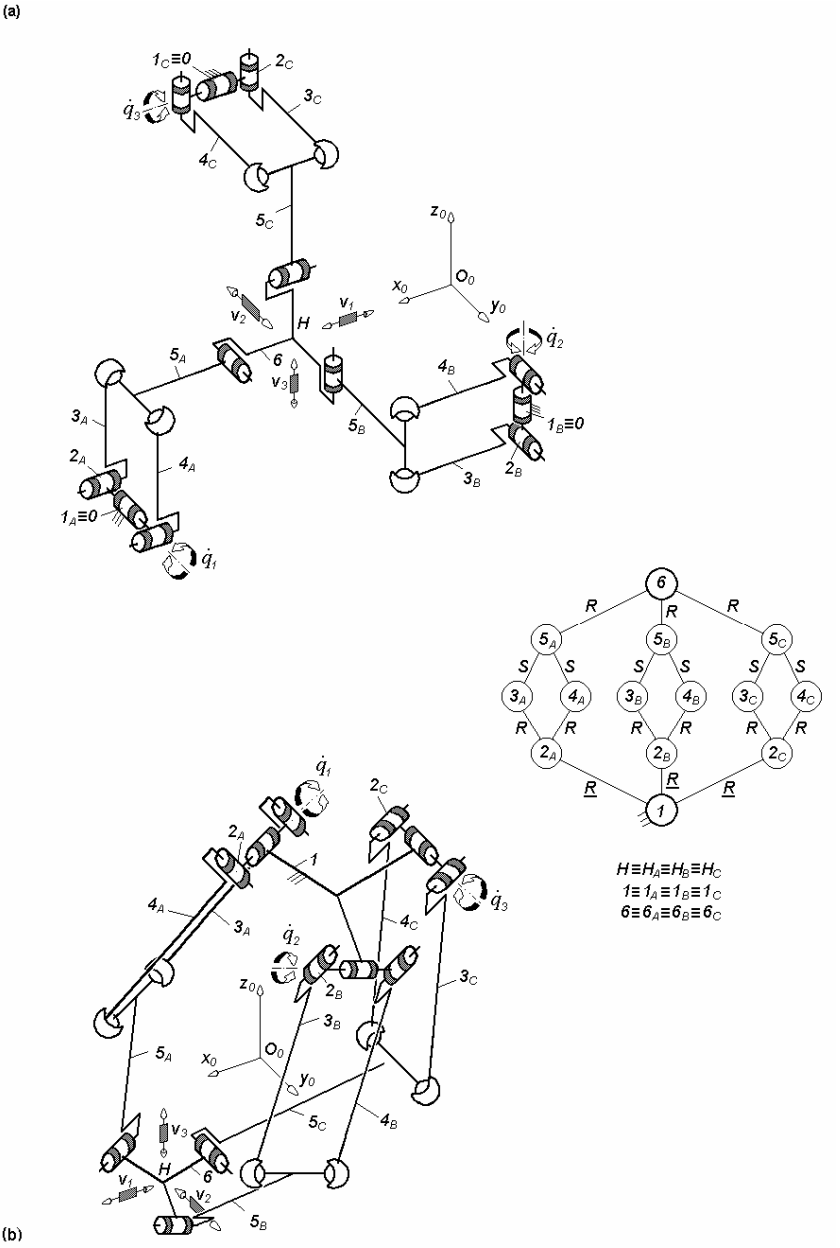

Fig. 3.185. *3-*$\underline{R}$*P*a^{ss}*R*-type TPMs with coupled motions and rotating actuators mounted on the fixed base, defined by $M_F = S_F = 3$, $(R_F) = (\boldsymbol{v}_1, \boldsymbol{v}_2, \boldsymbol{v}_3)$, $T_F = 0$, $N_F = 3$, limb topology $\underline{R} \perp Pa^{ss} \perp {}^{\parallel}R$

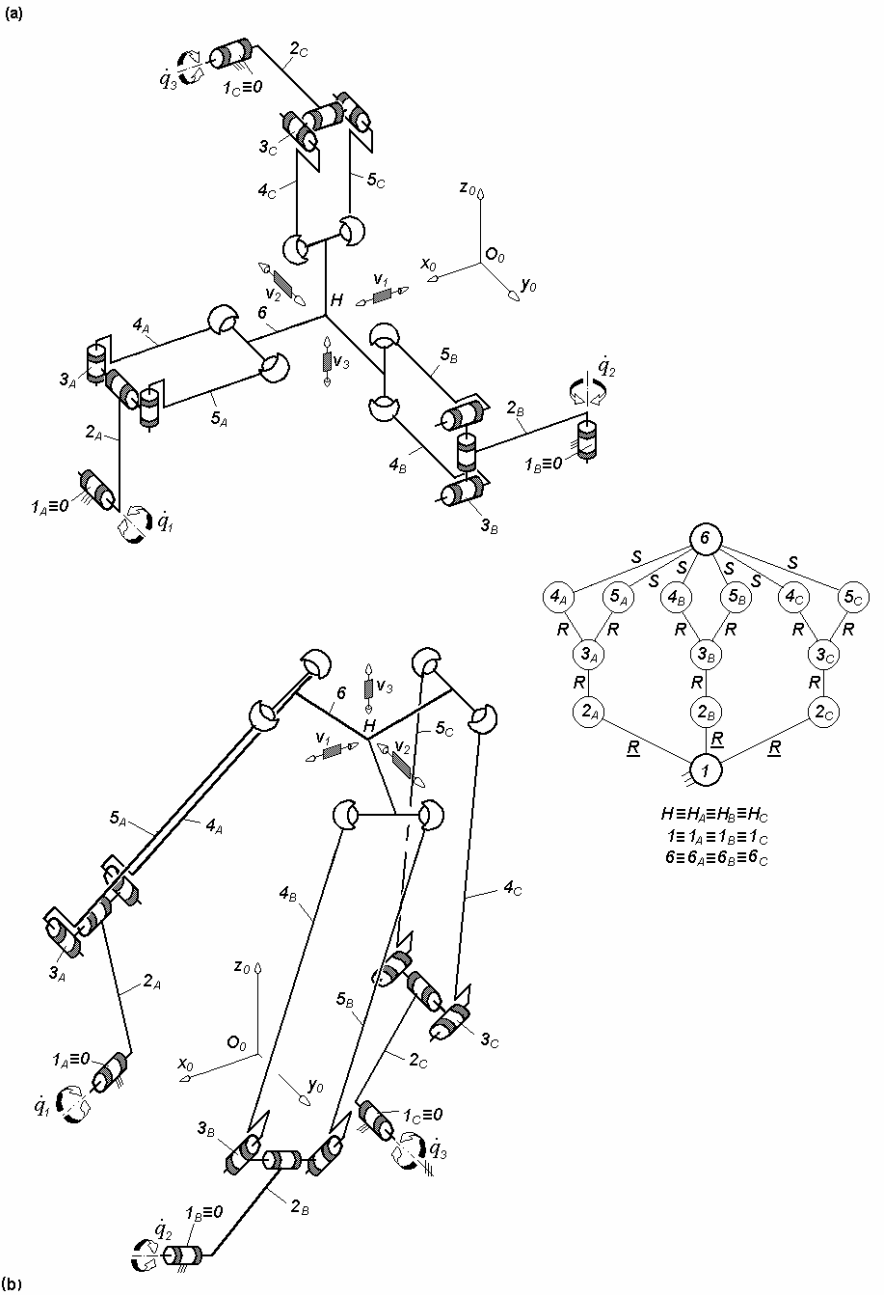

Fig. 3.186. *3-<u>R</u>RPa*^{ss}-type TPMs with coupled motions and rotating actuators mounted on the fixed base, defined by $M_F = S_F = 3$, $(R_F) = (\boldsymbol{v}_1, \boldsymbol{v}_2, \boldsymbol{v}_3)$, $T_F = 0$, $N_F = 3$, limb topology $\underline{R}||R \perp Pa^{ss}$

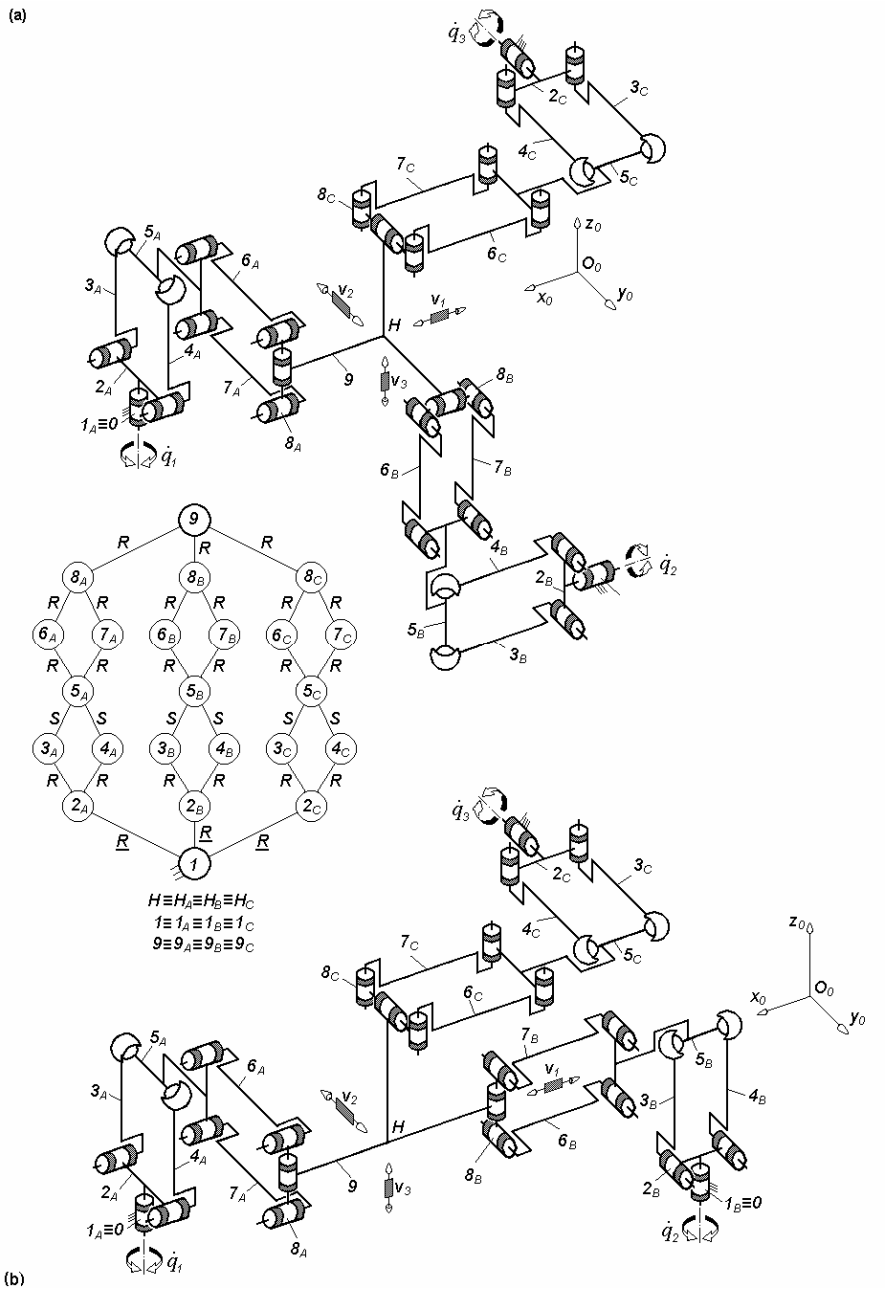

Fig. 3.187. *3-*$\underline{R}Pa^{ss}PaR$*-type TPMs with coupled motions and rotating actuators mounted on the fixed base, defined by* $M_F = S_F = 3$, $(R_F) = (\boldsymbol{v}_1, \boldsymbol{v}_2, \boldsymbol{v}_3)$, $T_F = 0$, $N_F = 9$, limb topology $\underline{R} \perp Pa^{ss} || Pa \perp^{||} R$

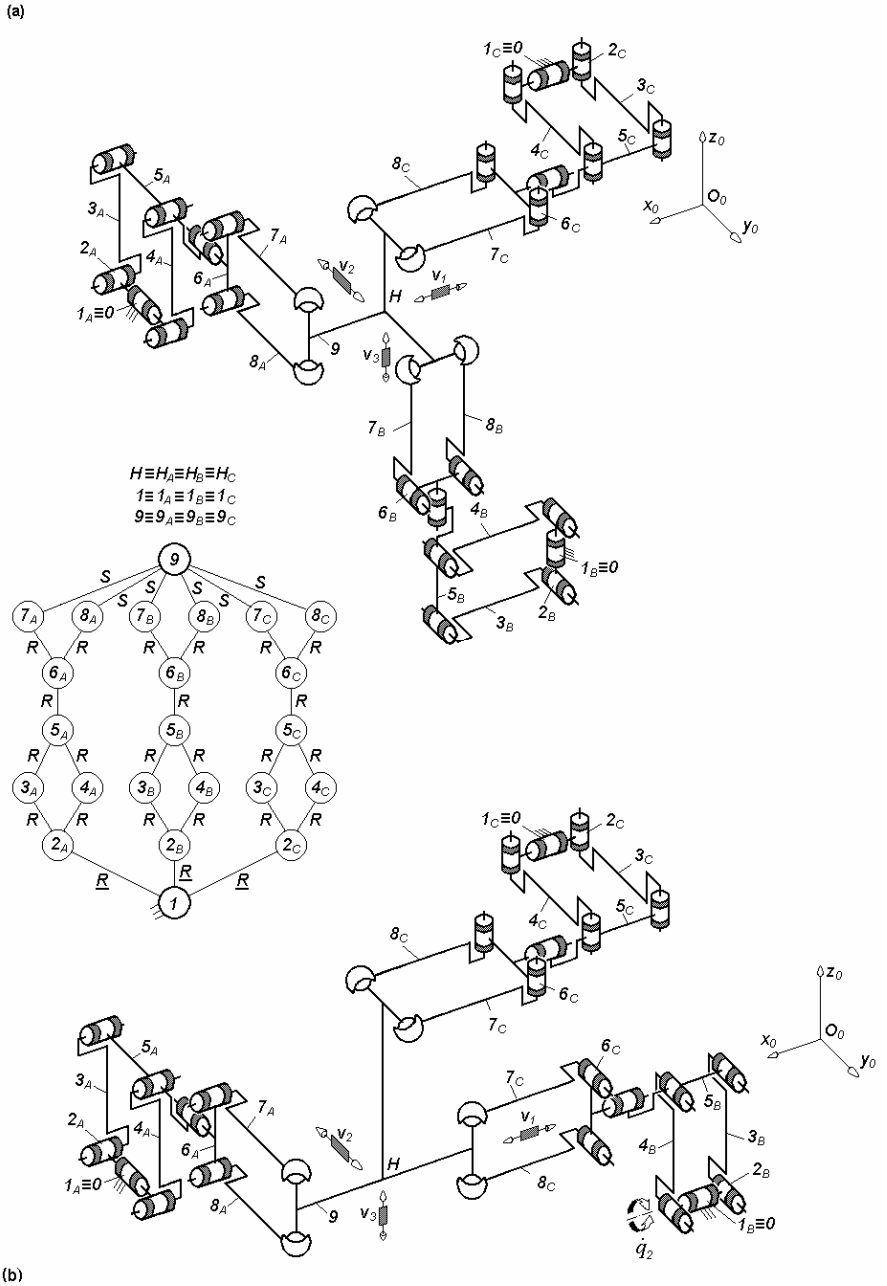

Fig. 3.188. *3-$\underline{R}PaRPa^{ss}$*-type TPMs with coupled motions and rotating actuators mounted on the fixed base, defined by $M_F = S_F = 3$, $(R_F) = (\boldsymbol{v}_1, \boldsymbol{v}_2, \boldsymbol{v}_3)$, $T_F = 0$, $N_F = 9$, limb topology $\underline{R} \perp Pa \perp {}^{\parallel}R \perp Pa^{ss}$

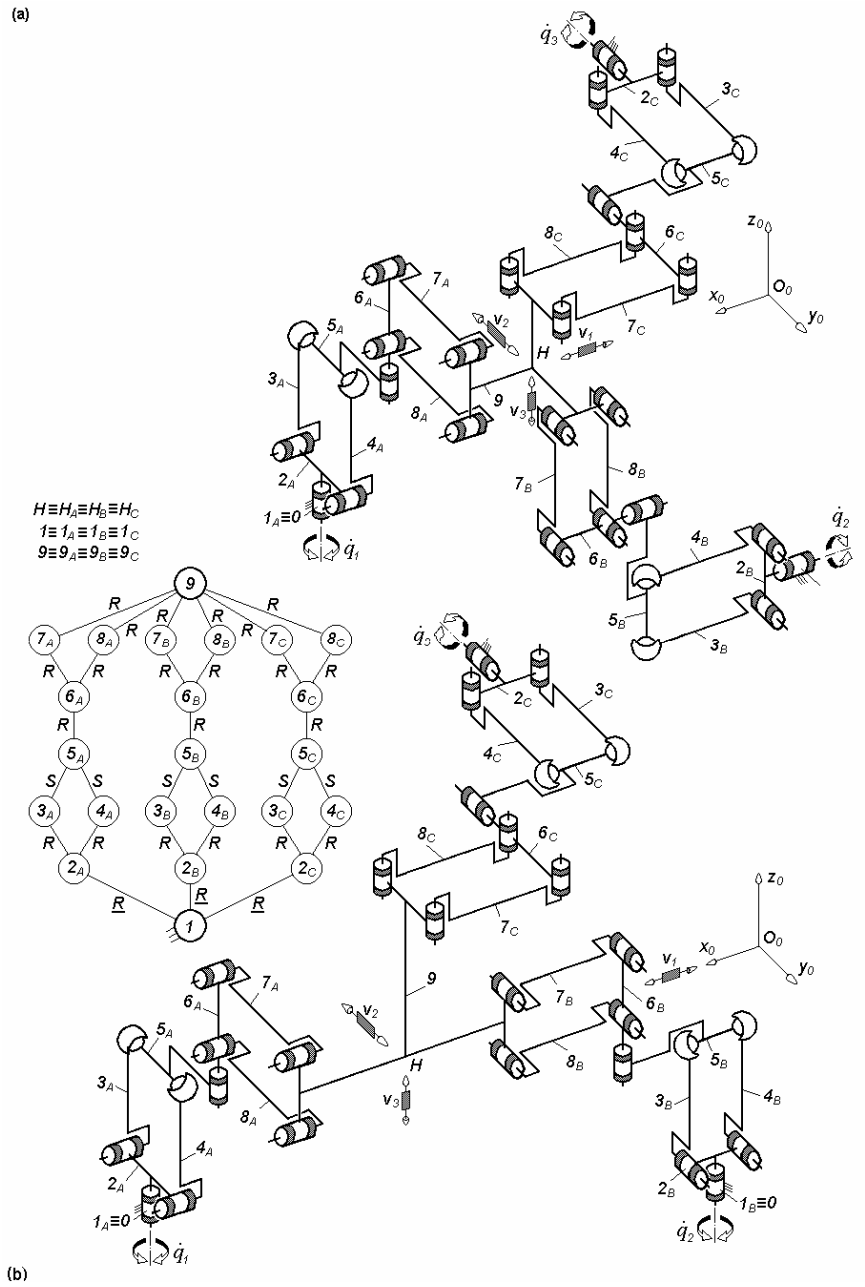

Fig. 3.189. *3-*$\underline{R}$*Pa*^{ss}*RPa*-type TPMs with coupled motions and rotating actuators mounted on the fixed base, defined by $M_F = S_F = 3$, $(R_F) = (\boldsymbol{v}_1, \boldsymbol{v}_2, \boldsymbol{v}_3)$, $T_F = 0$, $N_F = 9$, limb topology $\underline{R} \perp Pa^{ss} \perp {}^{\parallel}R \perp {}^{\parallel}Pa$

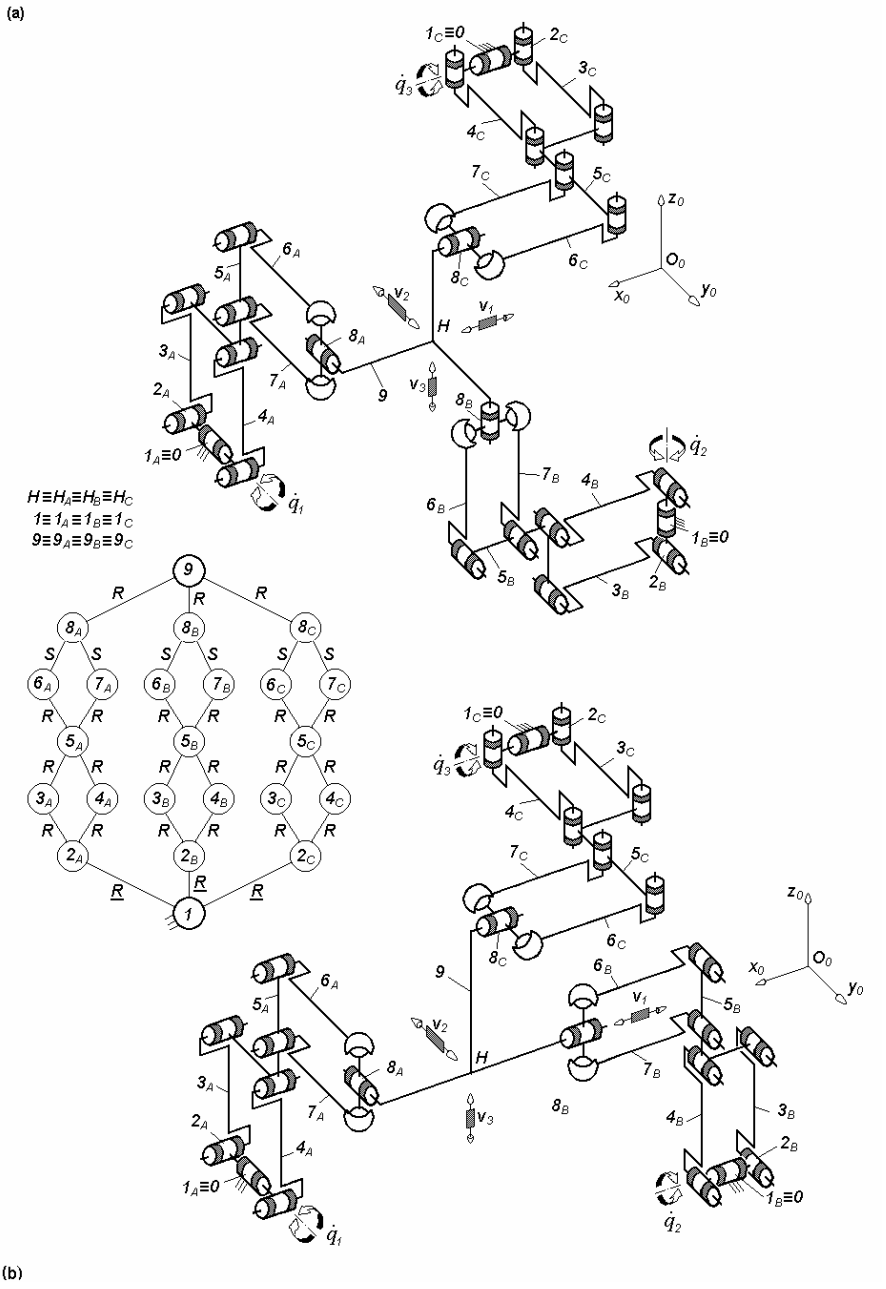

Fig. 3.190. *3-<u>R</u>PaPa^{ss}R*-type TPMs with coupled motions and rotating actuators mounted on the fixed base, defined by $M_F = S_F = 3$, $(R_F) = (\boldsymbol{v}_1, \boldsymbol{v}_2, \boldsymbol{v}_3)$, $T_F = 0$, $N_F = 9$, limb topology $\underline{R} \perp Pa \| Pa^{ss} \perp {}^{\|}R$

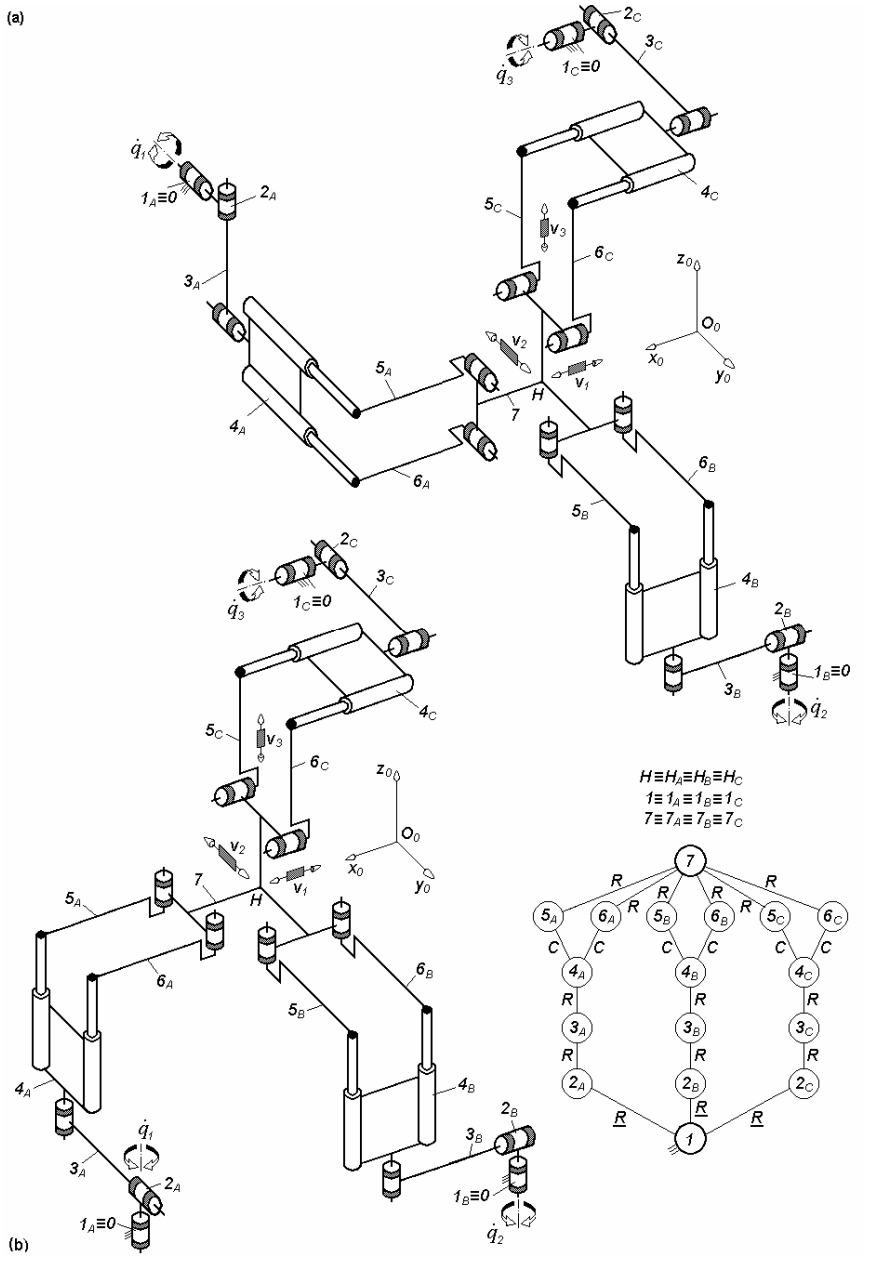

Fig. 3.191. *3-*$\underline{R}R$*RPa^{cc}-type overconstrained TPMs with coupled motions, rotating actuators mounted on the fixed base and six revolute joints adjacent to the moving platform, defined by $M_F = S_F = 3$, $(R_F) = (\boldsymbol{v}_1, \boldsymbol{v}_2, \boldsymbol{v}_3)$, $T_F = 0$, $N_F = 6$, limb topology $\underline{R} \perp R^* \perp {}^{\parallel}R||Pa^{cc}$

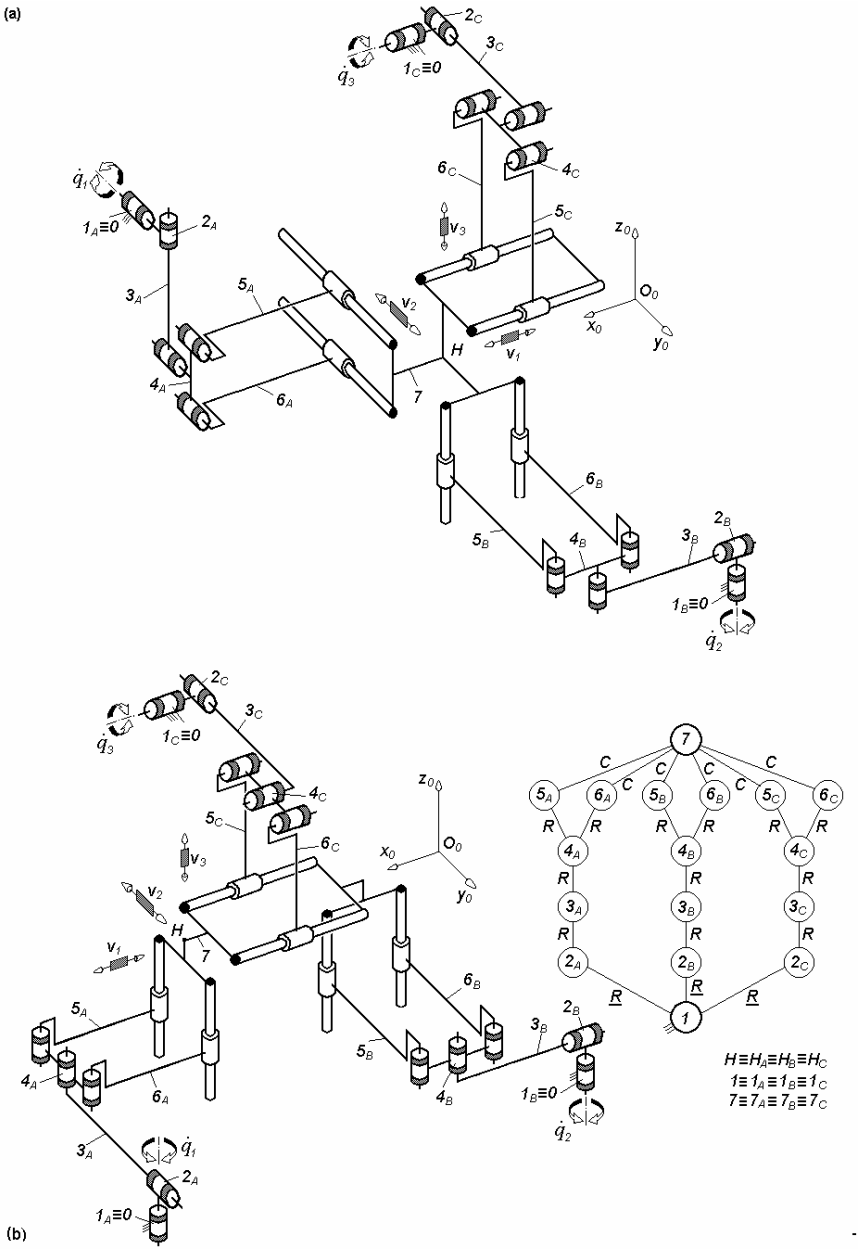

Fig. 3.192. *3-<u>R</u>R*RPa*^{cc}-type overconstrained TPMs with coupled motions, rotating actuators mounted on the fixed base and six cylindrical joints adjacent to the moving platform, defined by $M_F = S_F = 3$, $(R_F) = (\boldsymbol{v}_1, \boldsymbol{v}_2, \boldsymbol{v}_3)$, $T_F = 0$, $N_F = 6$, limb topology $\underline{R} \perp R^* \perp {}^{\parallel}R \| Pa^{cc}$

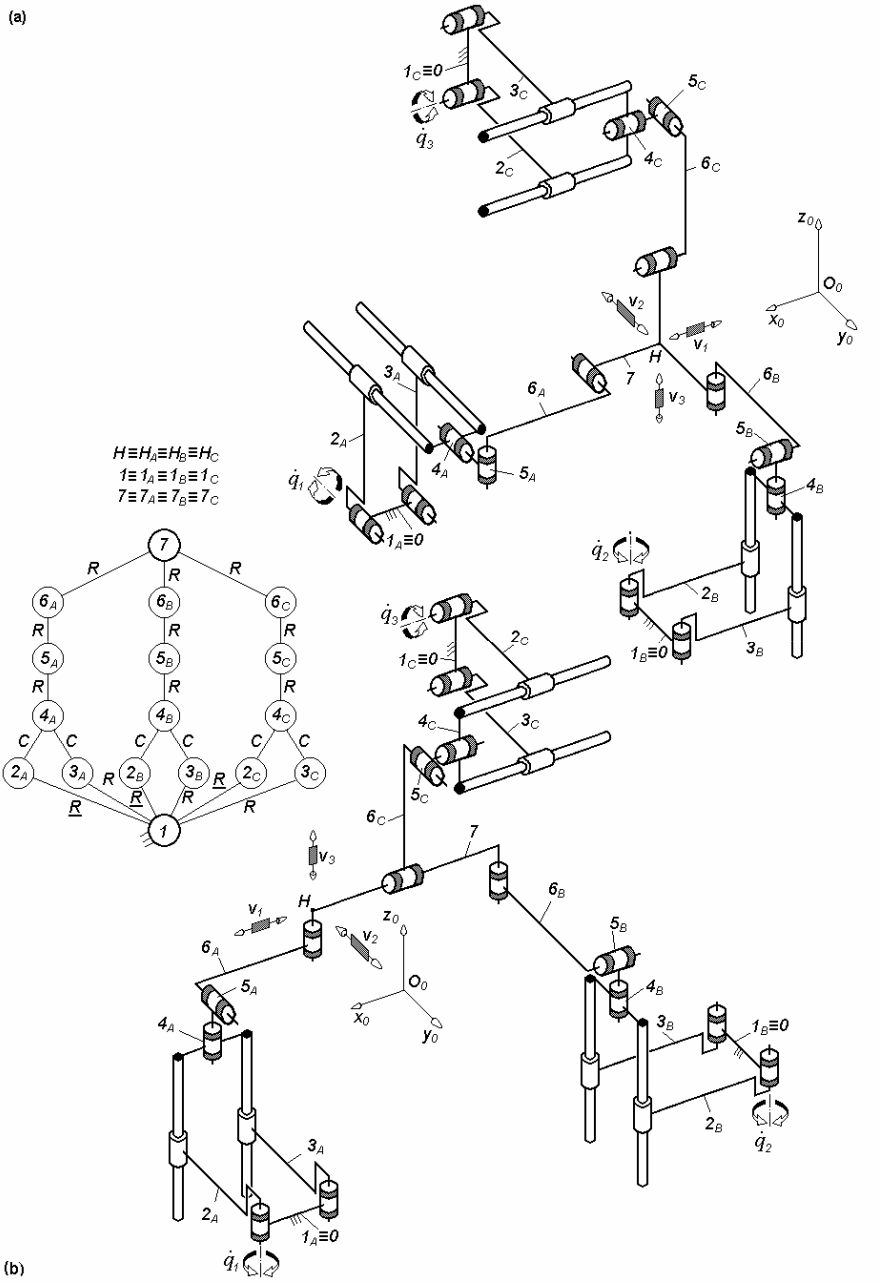

Fig. 3.193. *3-*$\underline{Pa}^{cc}$*RR*R*-type overconstrained TPMs with coupled motions and rotating actuators mounted on the fixed base, defined by $M_F = S_F = 3$, $(R_F) = (\boldsymbol{v}_1, \boldsymbol{v}_2, \boldsymbol{v}_3)$, $T_F = 0$, $N_F = 6$, limb topology $\underline{Pa}^{cc}||R \perp R^* \perp {}^{||}R$

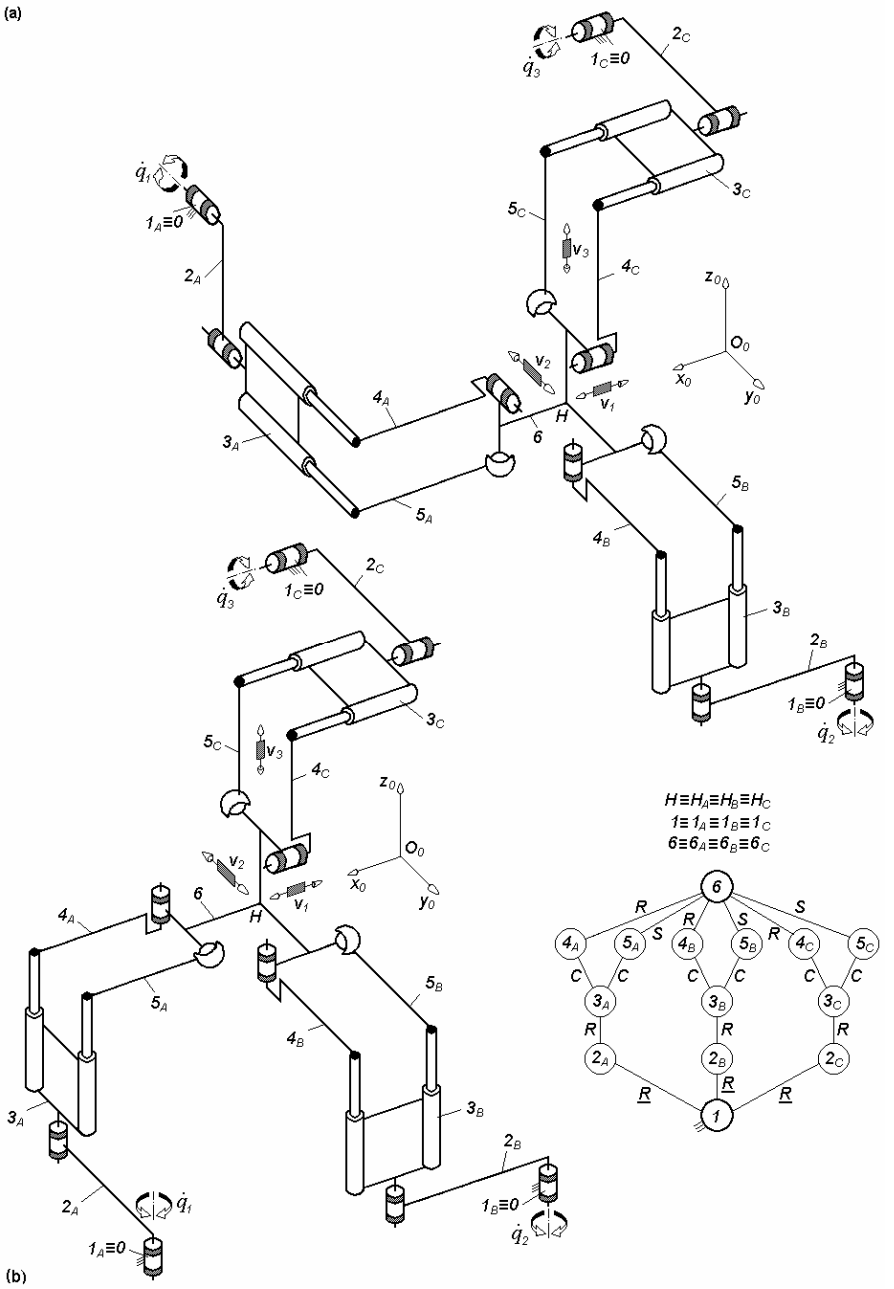

Fig. 3.194. *3-<u>R</u>RPa*^{ccs}-type overconstrained TPMs with coupled motions and rotating actuators mounted on the fixed base, defined by $M_F = S_F = 3$, $(R_F) = (\boldsymbol{v}_1, \boldsymbol{v}_2, \boldsymbol{v}_3)$, $T_F = 0$, $N_F = 3$, limb topology <u>R</u>||R||Pa^{ccs}

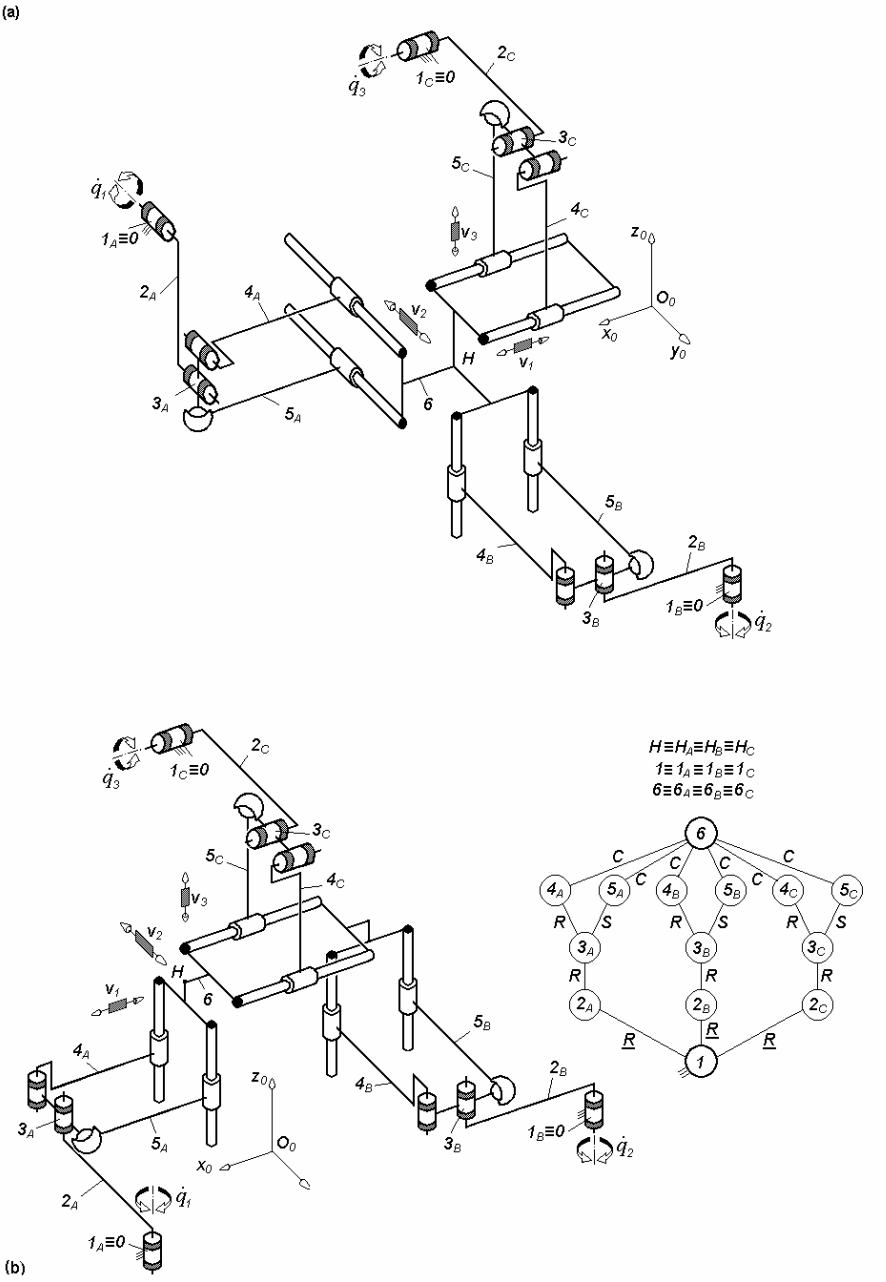

Fig. 3.195. *3-<u>R</u>RPa*^{scc}-type overconstrained TPMs with coupled motions and rotating actuators mounted on the fixed base, defined by $M_F = S_F = 3$, $(R_F) = (\boldsymbol{v}_1, \boldsymbol{v}_2, \boldsymbol{v}_3)$, $T_F = 0$, $N_F = 3$, limb topology $\underline{R}||R||Pa^{scc}$

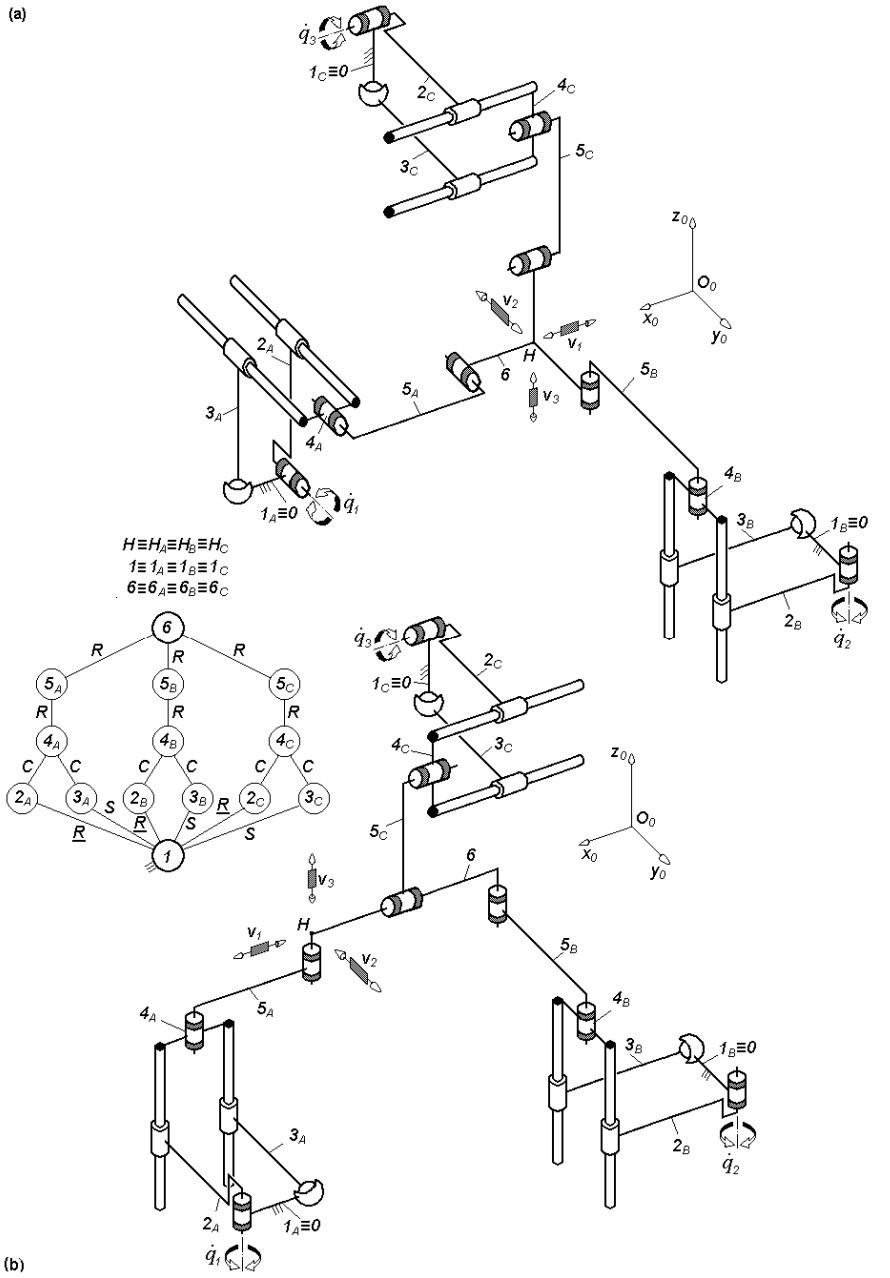

Fig. 3.196. *3-*$\underline{Pa}^{scc}$*RR*-type overconstrained TPMs with coupled motions and rotating actuators mounted on the fixed base, defined by $M_F = S_F = 3$, $(R_F) = (\boldsymbol{v}_1, \boldsymbol{v}_2, \boldsymbol{v}_3)$, $T_F = 0$, $N_F = 3$, limb topology $\underline{Pa}^{scc}||R||R$

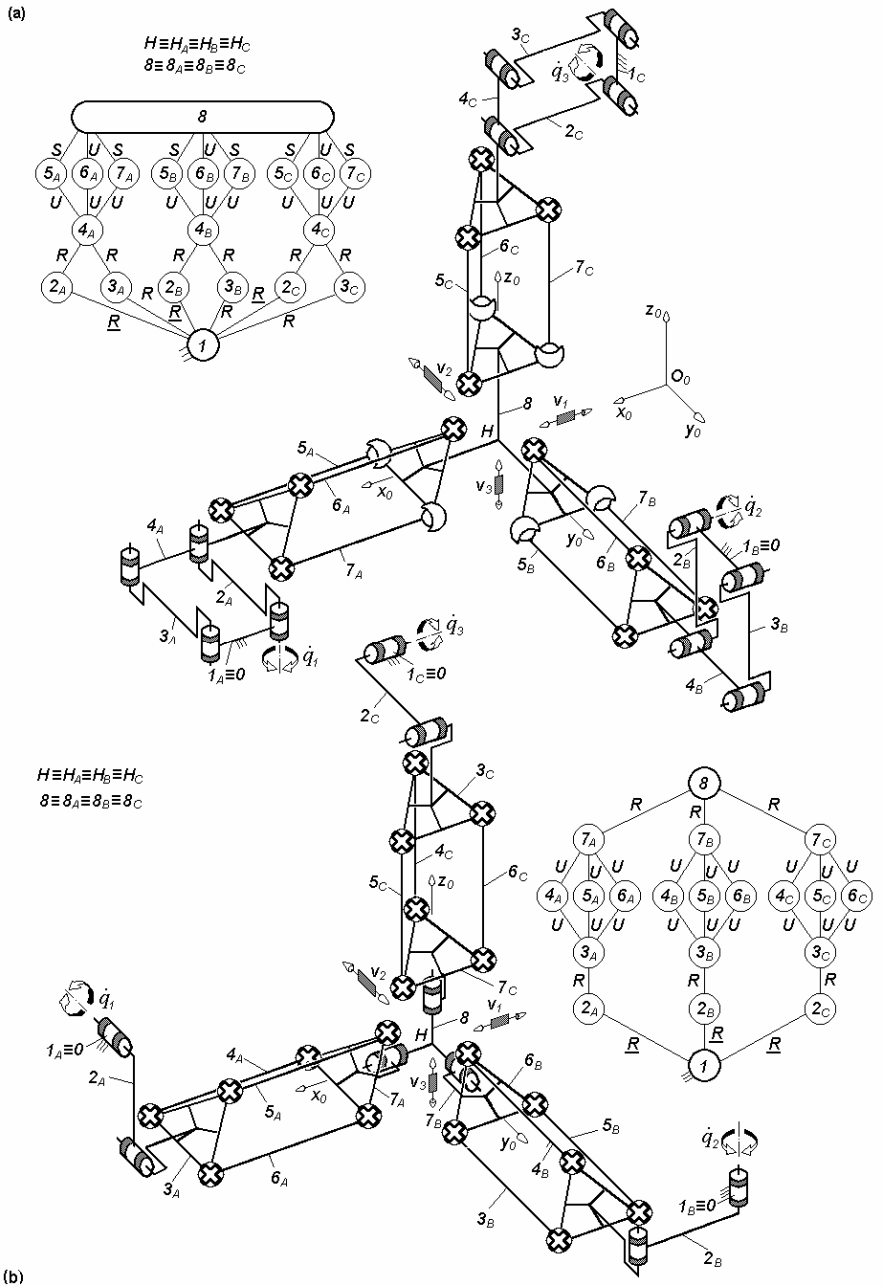

Fig. 3.197. Overconstrained TPMs with coupled motions of types *3-PaPr** (**a**) and *3-RRPrR** (**b**) defined by $M_F = S_F = 3$, $(R_F) = (\boldsymbol{v}_1, \boldsymbol{v}_2, \boldsymbol{v}_3)$, $T_F = 0$, $N_F = 15$ (**a**), $N_F = 6$ (**b**), limb topology *Pa-Pr** (**a**) and *3-R||RPr-R** (**b**)

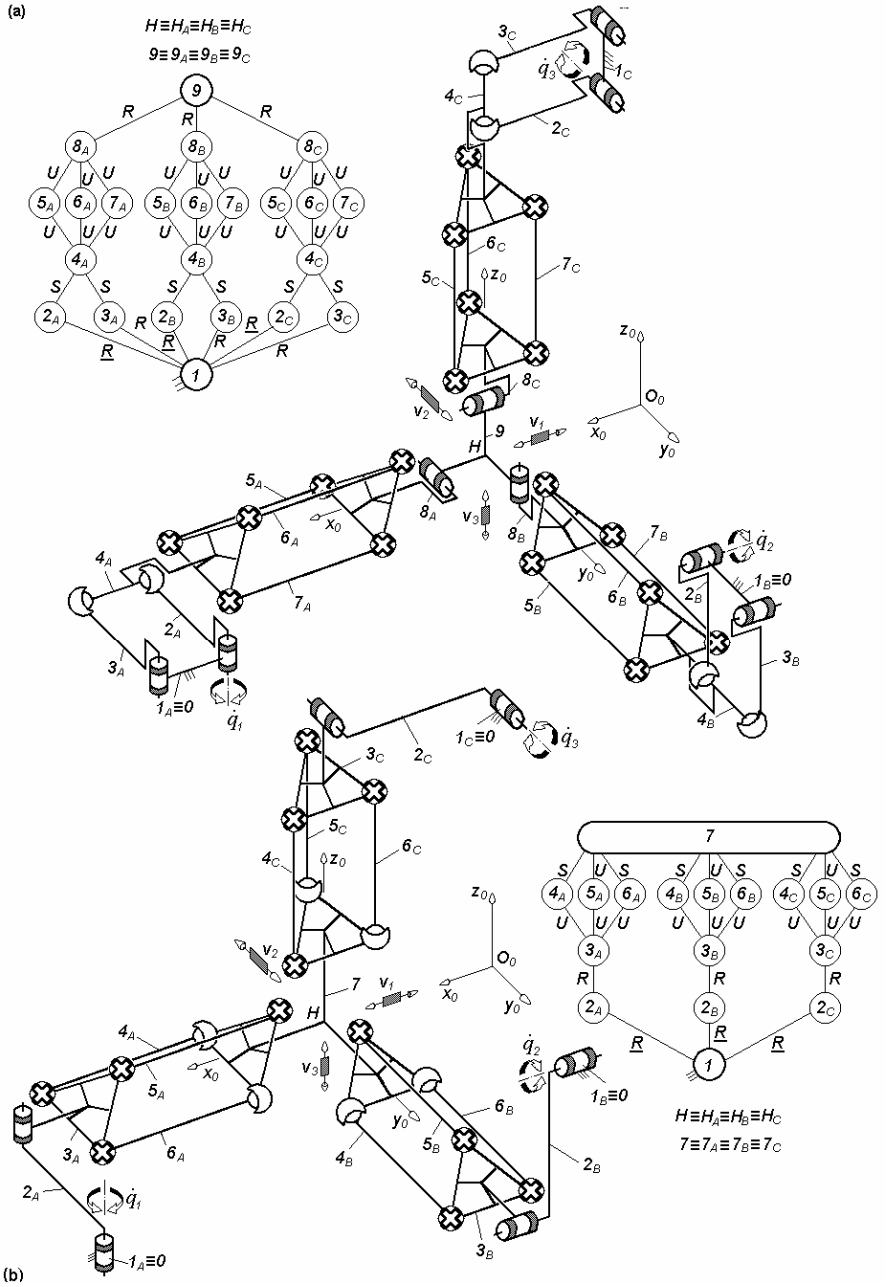

Fig. 3.198. Overconstrained TPMs with coupled motions of types *3-*$\underline{Pa}^{ss}$*PrR** (**a**) and *3-*$\underline{R}$*RPr** (**b**) defined by $M_F = S_F = 3$, $(R_F) = (\boldsymbol{v}_1, \boldsymbol{v}_2, \boldsymbol{v}_3)$, $T_F = 0$, $N_F = 6$ (**a**), $N_F = 3$ (**b**), limb topology $\underline{Pa}^{ss}$*-Pr-R** (**a**) and $\underline{R}||$*R-Pr** (**b**)